AD-A238 040

DTIC
ELECTE
JUL 02 1991
S D
C

DOT/FAA/CT-88/8-2

FAA Technical Center
Atlantic City International Airport
N.J. 08405

Aircraft Icing Handbook
Volume 2 of 3

March 1991

This document is available to the U.S. public through the National Technical Information Service, Springfield, Virginia 22161

U.S. Department of Transportation
Federal Aviation Administration

91-03902

070

NOTICE

This document is disseminated under the sponsorship of the U. S. Department of Transportation in the interest of information exchange. The United States Government assumes no liability for the contents or use thereof.

The United States Government does not endorse products or manufacturers. Trade or manufacturers' names appear herein solely because they are considered essential to the objective of this report.

** NOTICE **

This Handbook is maintained by the:

FAA Technical Center
Aircraft Icing E&D Program
Flight Safety Research Branch, ACD-230
Atlantic City Int'l Airport, NJ 08405

Handbook changes will be transmitted in the form of either ERRATA or REVISIONS. ERRATA will be notices of pen & ink corrections and REVISIONS will consist of reprinted pages, sections, or chapters. Each revised page will contain the revision number and date. This page can be used to track changes made to each volume of the Handbook.

It would be appreciated if readers would notify the Aircraft Icing E&D Program Manager at the above address of any necessary corrections, or any other appropriate comments.

CHANGE No.	ERRATA No.	REVISION No.	APPLICABLE PAGES	DATE ENTERED

CHAPTER III
ICE PROTECTION METHODS

SECTION 1.0 - PNEUMATIC BOOT DE-ICING SYSTEMS
SECTION 2.0 - ELECTRO-THERMAL SYSTEMS
SECTION 3.0 - FLUID ICE PROTECTION SYSTEMS
SECTION 4.0 - ELECTRO-IMPULSE DE-ICING SYSTEMS
SECTION 5.0 - HOT AIR SYSTEMS
SECTION 6.0 - SYSTEM SELECTION

Accession For
NTIS GRA&I ☑
DTIC Tab ☐
Unannounced ☐
Justification
By
Distribution/
Availability Codes
Dist | Avail and/or Special
A-1

Technical Report Documentation Page

1. Report No.	2. Government Accession No.	3. Recipient's Catalog No.
DOT/FAA/CT-88/8-2		

4. Title and Subtitle	5. Report Date
Aircraft Icing Handbook - Volume 2 of 3	March 1991
	6. Performing Organization Code
7. Author(s) A. Heinrich, R. Ross, G. Zumwalt, J. Provorse, V. Padmanabhan, J. Thompson, J. Riley	8. Performing Organization Report No. DOT/FAA/CT-88/8-2
9. Performing Organization Name and Address	10. Work Unit No. (TRAIS)
Gates Learjet Corporation 8220 W. Harry Wichita, KS 67277	11. Contract or Grant No. DTFA03-85-C-00007
	13. Type of Report and Period Covered
12. Sponsoring Agency Name and Address Department of Transportation Federal Aviation Administration Technical Center Atlantic City International Airport, NJ 08405	Final Report February 1985-March 1991
	14. Sponsoring Agency Code ACD 230

15. Supplementary Notes

FAA Technical Monitor, E. E. Schlatter
Flight Safety Research Branch
ACD 230

16. Abstract

The design and validation of adequate aircraft ice protection has evolved into a specialized and technically complex area where many engineering disciplines are involved; namely, aeronautical, electrical, mechanical, electronics, chemical simulations, mathematical modeling, airframe/engine systems design, atmospheric physics, and meteorology. Research advances in any one discipline have a direct effect on updating the procedural technology used in the design and validation of ice protection configurations, equipment, and systems. Periodically the Federal Aviation Administration (FAA) provides documentation to assist regulatory certification teams and industry design engineers in standardizing testing and validating procedures. Examples of such documentation are "Engineering Summary of Airframe Icing Technical Data," FAA Report No. ADS-4 dated December 1968, and "Engineering Summary of Powerplant Icing Technical Data," FAA Report No. RD-77-76 dated July 1977. Although most of the information contained in these reports is still valid, some is outdated, and more usable information is now available through recent research and experience. Therefore, this work was directed towards developing an updated and more comprehensive combined version of Report ADS-4 and RD-77-76 that includes reference material on ground and airborne icing facilities, simulation procedures, and analytical techniques. This document represents all types and classes of aircraft and is intended as a working tool for the designer and analyst of ice protection systems.

17. Key Words		18. Distribution Statement
Aircraft Icing, Atmospheric Icing, Icing Measurements, Anti-Icing,	Ice Protection, Icing Certification, De-Icing Systems, Helicopter Icing.	Document is available to the U. S. public through National Technical Information Service, Springfield, Virginia.

19. Security Classif. (of this report)	20. Security Classif. (of this page)	21. No. of Pages	22. Price
Unclassified.	Unclassified.	612	

Form DOT F 1700.7 (8-72) Reproduction of completed page authorized

CHAPTER III
SECTION 1.0
PNEUMATIC BOOT DE-ICING SYSTEMS

CHAPTER III - ICE PROTECTION METHODS

CONTENTS

SECTION 1.0 PNEUMATIC BOOT DE-ICING SYSTEMS

	Page
LIST OF FIGURES	III 1-iii
SYMBOLS AND ABBREVIATIONS	III 1-iv
GLOSSARY	III 1-v
III.1.1 OPERATING CONCEPTS AND COMPONENTS	III 1-1
1.1.1 Conventional Pneumatic Boot De-icing Systems	III 1-1
1.1.2 Pneumatic Impulse Ice Protection	III 1-2
III.1.2 DESIGN GUIDANCE FOR CONVENTIONAL PNEUMATIC BOOT SYSTEM	III 1-3
1.2.1 Fixed Wing Aircraft	III 1-3
1.2.1.1 Turbine Engine Powered Aircraft	III 1-3
1.2.1.1 Reciprocating Engine Powered Aircraft	III 1-4
1.2.2 Rotorcraft	III 1-4
1.2.3 Other Applications	III 1-4
III.1.3 USAGES AND SPECIAL REQUIREMENTS	III 1-5
1.3.1 Airfoil and Leading Edge Requirements	III 1-5
1.3.2 Windshields	III 1-5
1.3.3 Engine Inlet Lips and Components	III 1-5
1.3.4 Turbofan Components	III 1-5
1.3.5 Propellers, Spinners, and Nose Cones	III 1-5
1.3.6 Helicopter Rotors and Hubs	III 1-5
1.3.7 Flight Sensors	III 1-5
1.3.8 Radomes	III 1-6
1.3.9 Miscellaneous Intakes and Vents	III 1-6
III.1.4 WEIGHT AND POWER REQUIREMENTS	III 1-6
III.1.5 ACTUATION, REGULATION, AND CONTROL	III 1-7
III.1.6 OPERATIONAL USE	III 1-7
III.1.7 MAINTENANCE, INSPECTION, AND RELIABILITY	III 1-8
III.1.8 PENALTIES	III 1-8
III.1.9 ADVANTAGES AND LIMITATIONS	III 1-8
III.1.10 CONCERNS	III 1-8
III.1.11 REFERENCES	III 1-9

LIST OF FIGURES

		Page
1-1	Inflatable De-Icing Tubes	III 1-10
1-2	Typical De-Icing Boot Installation	III 1-11
1-3	Pneumatic Boot Surface De-Icing System - Turbine Engine Powered Aircraft	III 1-12
1-4	Pneumatic Boot Surface De-Icing System - Reciprocating Engine Powered Aircraft	III 1-13
1-5	Rotorcraft Blade Pneumatic Boot De-Icing System	III 1-14
1-6	Rotorcraft Pneumatic Boot De-Icing System - Schematic	III 1-15
1-7	Pneumatic Boot De-Icing System - Nose Radomes	III 1-16
1-8	Typical Nose Radome De-Icing Boot Configuration	III 1-17

SYMBOLS AND ABBREVIATIONS

Symbol	Description
°C	Degrees Celsius
cm	Centimeter
°F	Degrees Fahrenheit
FAA	Federal Aviation Administration
ft	Feet or foot
gpm	Gallons per minute
HP	Horsepower
kg	Kilogram
kN	Kilonewton
lbf	Pounds force
lbs	Pounds
m	Meter
mm	Millimeter
PIIP	Pneumatic Impulse Ice Protection
psig	Pounds per square inch gauge (pressure)
scfm	Specific cubic feet per minute

GLOSSARY

bridging - The formation of an arch of ice over a pneumatic boot on an airfoil surface.

icephobic - A surface property exhibiting a reduced adhesion to ice; literally, "ice-hating."

light icing - The rate of accumulation that may create a hazard if flight is prolonged in this environment. Occasional use of de-icing/anti-icing equipment removes/prevents accumulation.

moderate icing - The rate of accumulation is such that even short encounters become potentially hazardous and use of de-icing/anti-icing equipment or diversion from the area/or altitude is necessary.

III.1.0 PNEUMATIC BOOT DE-ICING SYSTEMS

III.1.1 OPERATING CONCEPTS AND COMPONENTS

Pneumatic boot surface de-icing systems remove ice accumulations mechanically by alternately inflating and deflating tubes in a boot covering the surface to be de-iced. Inflation of the tubes under the accreted ice breaks the ice into particles and destroys the ice bond to the surface. Aerodynamic or centrifugal forces then remove the ice. This method of de-icing is designed to remove ice after it has accumulated rather than to prevent its accretion on the surface; thus, it cannot be used as an anti-icing device.

The tubes in the pneumatic boot are usually oriented spanwise but may be oriented chordwise if dictated by a particular design. Chordwise tubes have lower drag than spanwise tubes but may present manifolding complications. The inflatable tubes are manifolded together in a manner to permit alternate or simultaneous inflation as shown in figures 1-1 and 1-2, but alternate inflation is less commonly used. Chordwise boot coverage should be determined by analysis or test of droplet impingement limits (Section I.2.2.1.6). Spanwise coverage should be sufficient to protect the surface in question.

In addition to the boots, the primary components of a pneumatic system are a regulated pressure source, a vacuum source, and an air distribution system. Miscellaneous components include a solenoid, check and relief valves, air filters, control switches and timer, and electrical interfaces including fuses and circuit breakers. A regulated pressure source is required to insure expansion of all tubes in the system to design limits and within design rise times. If tube expansion is too slow, de-icing effectiveness is lessened. The vacuum source is essential to insure positive deflation and keep the tubes collapsed during non-icing flight conditions to minimize the aerodynamic penalty.

Air pumps generally multiply the atmospheric pressure by a fixed factor, so the pressure delivered becomes a function of altitude. Therefore, the pressure produced at service ceiling altitude is a design condition.

1.1.1 Conventional Pneumatic Boot De-icing Systems

Conventional pneumatic boots are constructed of fabric-reinforced synthetic rubber or other flexible material. The material is wrapped around and bonded to the leading edge surfaces to be de-iced on wings or empennage. Total thickness of typical pneumatic boots is usually less than 0.10 inch (2.54 mm).

Pneumatic boots have been the standard ice protection method for piston engine aircraft since the 1930's. Pneumatic boots are easily retrofitted, require very little power, and are a light weight system of reasonable cost.

1.1.2 Pneumatic Impulse Ice Protection

A Pneumatic Impulse Ice Protection System (PIIP) is currently in development (reference 1-1) with the principle goal of optimizing the performance of pneumatic de-icing systems. Specific goals are to (a) minimize boot intrusion into the airstream, (b) minimize threshold ice thickness required for removal while retaining the ability to remove ice of thickness 0.50 inches (12.7 mm) or more, and (c) maximize weatherability and erosion resistance of the outer surface ply material.

The pneumatic impulse system is a surface-mounted device which relies on surface distortion to break up and remove accumulated ice. With the PIIP systems, the surface is momentarily distorted through a pulsed inflation on the order of 10 milliseconds. Total surface deformation is approximately 0.09 inch (2.3 mm). The pneumatic impulse system consists of fabric-reinforced elastomeric coated tubes with a titanium outer cover which enhances the weatherability and erosion resistance. The maximum ice protector thickness is 0.075 inch (1.90 mm) nominal, tapering to 0.015 inch (0.38 mm) at the trailing edge. Tube orientation tested to date has been spanwise. An interstice, or non-bonded region consisting of two facing fabric layers, aids surface distortion.

A solenoid activated high pressure flow valve connected to a high pressure air source (1500 psig nominal) pulses air to the ice protector. Each flow valve contains a small accumulator sized to inflate the ice protector tubes to a maximum of less than 200 psig. One high pressure valve is required for approximately every 10 feet of surface protection. The high pressure flow valve is cycled via an electronic timer/controller configured to accept signals from ice detectors and/or temperature probes to initiate system sequencing.

Icing tunnel and limited flight testing to date has shown that ice layers as thin as 0.02 inch (0.50 mm) can he removed. However, a nominal ice thickness of 0.06 inch (1.50 mm) cold ice has been consistently removed. Wet ice existing at 25 °F or greater also has been consistently removed at a thickness of 0.10 inch (2.5 mm). Ice layers as thick as 1 inch (25.4 mm) have been successfully removed.

The weight of the pneumatic impulse ice protection system is similar to the conventional system, i.e., approximately 0.44 lbs/ft^2 (2.15 kg/m^2). A system designed for the wings of a typical twin-engine 100-passenger commercial transport is estimated to weigh 123 lbs (55.8 kg) total. This system includes eight ice protectors 10 feet (3.05 m) long, ten high pressure flow valves, two electronic controllers, a distribution network, and two hydraulic-driven air compressors. Total power requirements for this system were estimated as follows:

Electrical:	100 watts for 1 second
Power for one compressor:	1.9 hp based on fluid drive of 1.3 gpm @ 3000 psig. Power is consumed only during the system charge time.

A comparison of impulse and conventional pneumatic boot system characteristics follows:

	Pneumatic Impulse Ice Protector	Conventional Pneumatic De-Icer
Surface Ply Elongation	.1 to .25%	40 to 50%
Nominal Inflation Time	.010 Seconds	2 Seconds
Nominal Deflation Time	.100 Seconds	6 Seconds
Maximum Surface Distortion	.09 Inch (2.29 mm)	.375 Inch (9.53 mm)
Threshold Ice Removal Thickness	.06 Inch (1.52 mm)	.25 Inch (6.35 mm)
Surface Ply Material	Metallic	Elastomeric

III.1.2 DESIGN GUIDANCE FOR CONVENTIONAL PNEUMATIC BOOT SYSTEM

1.2.1 Fixed Wing Aircraft

Boot de-icing is strongly affected by the airfoil shape. It is not uncommon to find that several iterations of boot design are required to obtain the desired ice protection performance. The boot manufacturer's assistance is usually needed in the process of choosing tube size, sequencing order, pressure level, spanwise/chordwise tube combinations, etc.

The system should be operated to evaluate overall performance during dry air flight testing. Boot inflation pressure should reach the design pressure within the allowable inflation time (usually about six seconds). This pressure should be maintained up to the maximum icing altitude of 22,000 feet (6100 m) (see FAR 25, Appendix C) or the aircraft's service altitude, whichever is lower. Also, the vacuum used to deflate the boots should be adequate even at maximum operating airspeeds.

1.2.1.1 Turbine Engine Powered Aircraft

Gas turbine engines generally provide pressure directly from compressor bleed air and vacuum from a bleed air driven ejector.

Components of a typical pneumatic boot surface de-icing system for a turbine powered aircraft are shown schematically in figure 1-3. This typical system utilizes engine bleed air for the air pressure source, which is regulated to 18 lb_f/in^2 (124 KN/m^2) for boot inflation. As a safety feature, a relief valve is incorporated into the regulator valve design that will limit the over-pressure. For the dual cycle system shown, the wing and empennage boots may be alternately pressurized.

The regulated bleed air is routed to a venturi air ejector which provides vacuum for boot hold-down, as well as for flight instruments. A distributor valve applies pressure or vacuum to the boots in conformity with a selected cycle. Usually this valve has two boot distribution ports - one port is used to inflate and deflate the wing boots and the other port is used for the empennage boots. Air plumbing line sizes and system components are selected based on the functional requirements; namely,

maximum boot operating pressure and the pressure rise time. Installation of this type system requires only minor airframe modifications.

1.2.1.1 Reciprocating Engine Powered Aircraft

For piston engine aircraft, air pumps driven from the engine's geared accessory drive are usually used. Some manufacturers use the inlet and outlet sides of a single centrifugal air pump to provide both vacuum and pressure. Engine manifold vacuum is not suitable due to its extreme variability with engine load, and with turbo-charged engines, no manifold vacuum exists. Vacuum systems are often shared with vacuum-driven flight instruments.

Components of a typical pneumatic boot surface de-icing system for a reciprocating engine powered aircraft are shown in figure 1-4. Engine driven dry air pumps supply air pressure for boot inflation. A dual pressure regulator and relief valves control the pressure at a low pressure setting that is adequate for instrument operation. When the surface de-icing system is activated, the dual pressure regulators shift to the higher pressure required for pneumatic boot inflation. This two-stage pressure control provides extended pump life and less engine power extraction in normal flight without icing conditions. A timer operates the solenoids in the pressure regulators and the de-icing valve. A pressure switch operates a signal lamp to show boot operation.

The pressure regulator and relief valve system maintains pressure when the de-icing system is in use. The de-icing valve is a solenoid operated ON-OFF valve which applies pressure or vacuum to the boots. An air ejector is included in the system to provide vacuum to the boots in the OFF valve position. A single-cycle system where all boots are pressurized together is shown in figure 1-4.

1.2.2 Rotorcraft

An experimental pneumatic boot de-icing system has been successfully tested on helicopter rotor blades (references 1-2 and 1-3). A de-icing boot configuration was developed (figure 1-5) to minimize aerodynamic drag when the boot was inflated. In this test, the inflated boots caused a drag increase equivalent to about 3/8 inch (.95 cm) ice on the rotor blades. For a 9500 lb (4310 kg) 2-blade helicopter, full span de-icing boots were simultaneously inflated in less than two seconds to effectively remove accreted ice. Operating air pressure was obtained from a turbine engine bleed source. Figure 1-6 shows the operating schematic of this system. Improved ice shedding indicated that the boot rubber surface had a reduced surface adhesion to the ice. Boots therefore may provide some icephobic benefit.

1.2.3 Other Applications

Ice protection of some other components, such as radomes, with pneumatic boot de-icing systems is feasible (see Section 1.3.8).

III.1.3 USAGES AND SPECIAL REQUIREMENTS

1.3.1 Airfoil and Leading Edge Requirements

The airflow required for pneumatic boot operation is small compared with that for a hot gas ice protection system. Pneumatic boot de-icing systems may be added to an existing airplane with minor modification and expense. In areas of low static pressure on airfoils, auto-inflation of pneumatic boot tubes may occur and disrupt airflow over the surface. A vacuum source is used to prevent auto-inflation during the deflation period. During the inflation portion of the cycle, large drag increases and lift degradation can occur because of the spoiler action of inflated spanwise tubes. The use of chordwise tubes minimizes this problem.

Ice particles shed by pneumatic boots may be large enough to damage aft-mounted engines or propellers. Axial flow engines (turbojets and turbofans) are the most vulnerable, while turboprop engines with particle-separating inlet ducts are less likely to be damaged. For some airplanes, the wing section upstream of the engine may be provided with some form of anti-icing to avoid engine ice ingestion while the remainder of the wing is de-iced by pneumatic boots.

1.3.2 Windshields

The application of pneumatic boots for windshields is not possible.

1.3.3 Engine Inlet Lips and Components

The use of pneumatic boots has been limited to ice protection of turbine engines with bypass inlets.

1.3.4 Turbofan Components

The use of pneumatic boots for turbofan components has not been tried.

1.3.5 Propellers, Spinners, and Nose Cones

The use of pneumatic boot de-icing on propellers, spinners, and nose cones is feasible but has not been tried.

1.3.6 Helicopter Rotors and Hubs

Pneumatic boot de-icing systems have been tried on helicopters on an experimental basis using a 9500 lb (4310 kg) 2-blade helicopter (references 1-2 and 1-3) as discussed in Section 1.2.2. No application to rotor hubs is known.

1.3.7 Flight Sensors

Pneumatic boot systems are not suitable to de-ice flight sensors.

1.3.8 Radomes

Radar-designed pneumatic boot de-icers may be installed on the external contour of radomes; however, the boot may slightly increase transmission losses. A schematic of a pneumatic boot system applied to a radome is shown in figure 1-7. This system inflates all tubes at the same time. A combination valve provides deflation vacuum or inflation air as determined by a control timer. Installation details are shown in figure 1-8. The boot is about 0.075 inches (1.91 mm) thick except in the supply manifold area where it is 0.16 inches (4.1 mm) thick. Greater thickness will provide longer service life but will increase transmission losses.

1.3.9 Miscellaneous Intakes and Vents

Flush or recessed air scoops may not require ice protection. Pneumatic boot de-icing of air intakes and vents may be feasible, depending on the size of the intake or vent, but no application is known.

III.1.4 WEIGHT AND POWER REQUIREMENTS

The weight of a pneumatic boot ice protection system for a small, single-engine, FAR Part 23 airplane is approximately 25 lb (11 kg) and requires about one-third horsepower (250 watts). The distribution of the system weight should not significantly affect aircraft balance and the total weight should not cause an appreciable performance penalty. The power extracted to drive an air pump in a piston engine powered aircraft is small in relation to the total power available.

For a small twin-engine FAR Part 23 airplane, a pneumatic boot ice protection system will weigh approximately 28 lb (12.5 kg) and require about one-half HP (370 watts). The distribution of system weight should not significantly affect aircraft balance and the total weight should not cause an appreciable performance penalty.

For a small twin jet engine FAR Part 25 business jet airplane, a pneumatic boot ice protection system will weigh approximately 35 lb (16 kg) and require about one-half HP (370 watts). For a large FAR Part 25 transport category airplane, the system will weigh approximately 195 lb (90 kg) and require about 2.8 HP (2100 watts).

For a 9500 lb (4310 kg) FAR Part 27 helicopter, a pneumatic boot de-icing system (figure 1-6) will weigh approximately 40 lb (18 kg). The weight breakdown of this system: is inflatable boots 22 lb (10 kg), components 3.8 lb (1.7 kg), and plumbing 14.8 lb (6.7 kg). Operating air for a two-second inflation cycle is about 22 ft^3 per minute. Electrical power required for this cycle is about one-half HP (370 watts). For a larger FAR Part 29 transport category helicopter, the system weight and power required would be in proportion to aircraft weight.

III.1.5 ACTUATION, REGULATION, AND CONTROL

A pneumatic boot de-icing system is usually controlled by a three-position switch with OFF, MANUAL, and AUTO CYCLE modes of operation. When the switch is held in the MANUAL position, all boots will inflate and remain inflated until the switch is released. When the AUTO CYCLE position is selected, an electronic timer controls the inflation, deflation, timing, and sequence of the system.

III.1.6 OPERATIONAL USE

Preflight checkout of the pneumatic boot de-icing system pressure and boot inflation is recommended. Generally, a nominal ice thickness of 0.5 inches is allowed to accrete before the de-ice system is turned on. This thickness is determined by analysis and test and is dependent on the type of boots, leading edge contour, aircraft speed, atmospheric conditions, and drag characteristics of the surfaces that have accreted ice. Bridging is the formation of an arch of ice over the boot which is not removed by boot inflation. This can occur if the system is activated too early or too frequently, especially in glaze icing conditions. As icing encounters and severity of icing are difficult to forecast, the pilot should not depend upon marginal reserve power when ice protection is required and fly into an area where icing is predicted. Operation of a pneumatic boot ice protection system in ambient temperatures below -40 °F (-40 °C) may cause permanent damage to the de-icing boots.

Pneumatic boots should inflate and deflate rapidly to function effectively. To accomplish this, the time to reach full pressure should be about 5 to 6 seconds. During moderate icing a 60 second cycle is suggested, while for light icing, longer accretion times of 3 to 4 minutes should be permitted (reference 1-4).

In tests to date on rotorcraft, the pneumatic boot system is activated when ice growth reaches approximately a 0.25-inch (6 mm) thickness or when the indicated torque increases noticeably above the level with no ice accretion. Rotorcraft typically have smaller airfoils chords than fixed wing aircraft, so thick ice will result in high rotor power penalties, also thick ice may self-shed asymmetrically. The boot inflation time is approximately 2 seconds in rotorcraft applications.

An ice detection light is usually installed where it will illuminate a wing leading edge surface as an aid in observing ice accumulation during night operation. The location of the light and area illuminated must be such that the pilot can readily observe ice accretion and its thickness.

Icephobic liquids are available for spraying on the boots prior to a flight when an icing encounter is likely. These sprays reduce the adhesion of ice to the boot surface resulting in improved de-icing. However, the liquid erodes away so that its effectiveness is nearly gone after a few de-icing cycles or even after a few hours of flight in clear air.

III.1.7 MAINTENANCE, INSPECTION, AND RELIABILITY

Because pneumatic boot de-icing systems operate on clean turbine engine bleed or filtered air from dry air pumps, little is required in servicing the system. All vacuum and pressure filters used in the system should be periodically cleaned. Frequency of this cleaning will vary with the conditions under which the airplane is operated.

The pressure regulating valves in the system ordinarily should not require adjustment although the valve assembly will usually be equipped with adjusting screws to permit field adjustments.

The dry air pumps require no lubrication or maintenance but should be overhauled or replaced at engine overhaul.

Surfaces of the pneumatic boots should be inspected for engine oil after servicing and at the end of each flight. Any oil deposits should be removed with non-detergent soap and water solution. Care should be exercised during cleaning to avoid scuffing the boot surface. Pneumatic boots may he damaged if refueling hoses are dragged over the surface of the boots, or if ladders and platforms are rested against them. In any event, the hoot manufacturer's recommendations should be followed for maintenance and repair of cuts and scuff damage.

III.1.8 PENALTIES

Some aerodynamic drag penalty is to be expected with pneumatic boot de-icing systems on the wing, but it can be minimized by recessing the surface leading edge to offset the boot thickness.

III.1.9 ADVANTAGES AND LIMITATIONS

Pneumatic boot de-icing systems have been in use for many years and their repair, inspection, maintenance, and replacement are well understood (references 1-5 and 1-6). System weight and power requirements are minimal. Pneumatic boot material deteriorates with time and periodic inspection is recommended to determine need for replacement.

III.1.10 CONCERNS

A certain degree of pilot skill is required for safe and effective pneumatic boot operation. Actuation when accreted ice is too thin may result in "bridging" where the formation of ice over the boot is not cracked by boot inflation. Thus, attention is required to judge whether the cycle time continues to be correct as icing conditions change. Demands on the pilot increase during flight in darkness since observation of ice accretion rate and severity is more difficult.

III.1.11 REFERENCES

1-1 Sweet, David, "Pneumatic Impulse Ice Protection System," Private Communication for the B.F. Goodrich Company to Gates Learjet Corporation, April 14, 1987.

1-2 Blaha, B.J. and Evanich, P.L., "Pneumatic Boot for Helicopter Rotor De-icing," NASA CP-2170, November 1980.

1-3 Haworth, L.A. and Oliver, R.G., "JUH-1H Pneumatic Boot De-Icing System Flight Test Evaluation," USAAEFA Project No. 81-11, Final Report, May 1983.

1-4 Bowden, D.T.. Gensemer, A.E., and Skeen, C.A., "Engineering Summary of Airframe Icing Technical Data," FAA ADS-4, December 1963.

1-5 Bowden, D.T.. "Effect of Pneumatic De-Icers and Ice Formation on Aerodynamic Characteristics of an Airfoil," NACA TN 3564, February 1956.

1-6 Anon., "De-Icing System. Pneumatic Boot, Aircraft General Specification for," Military Specification MIL-D-8804A, September 26, 1958.

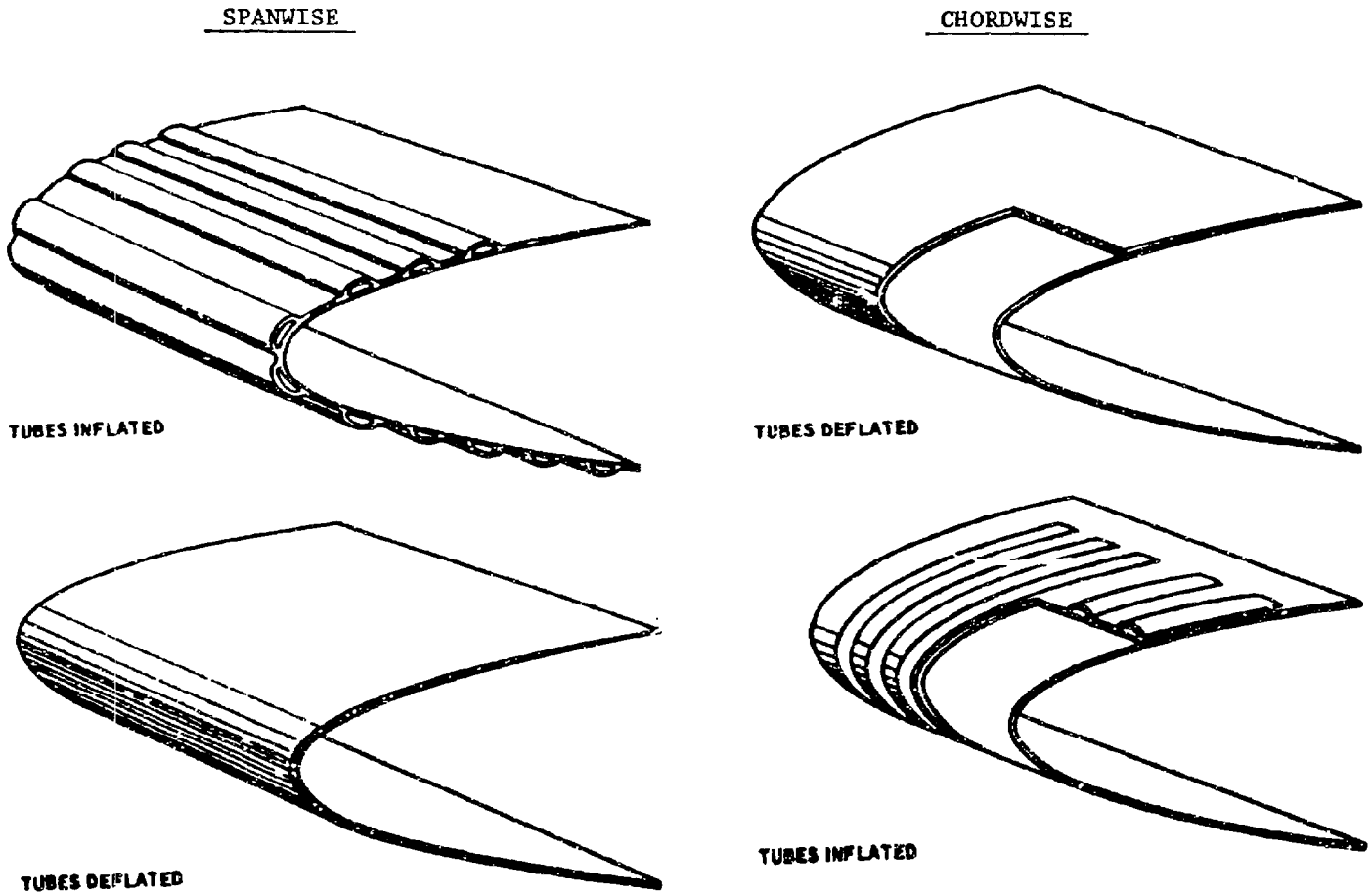

FIGURE 1-1. INFLATABLE DE-ICING TUBES

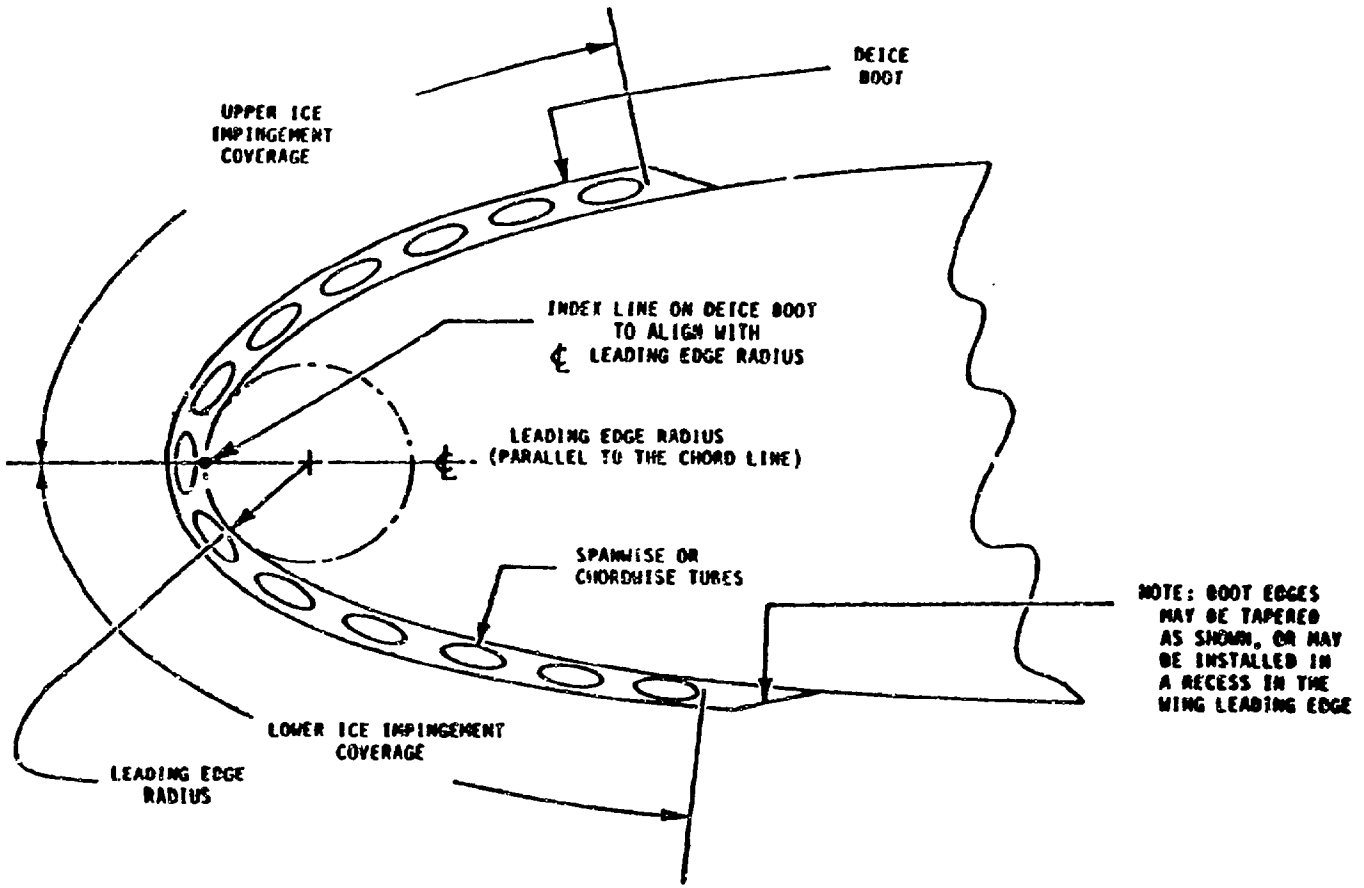

FIGURE 1-2. TYPICAL DE-ICING BOOT INSTALLATION

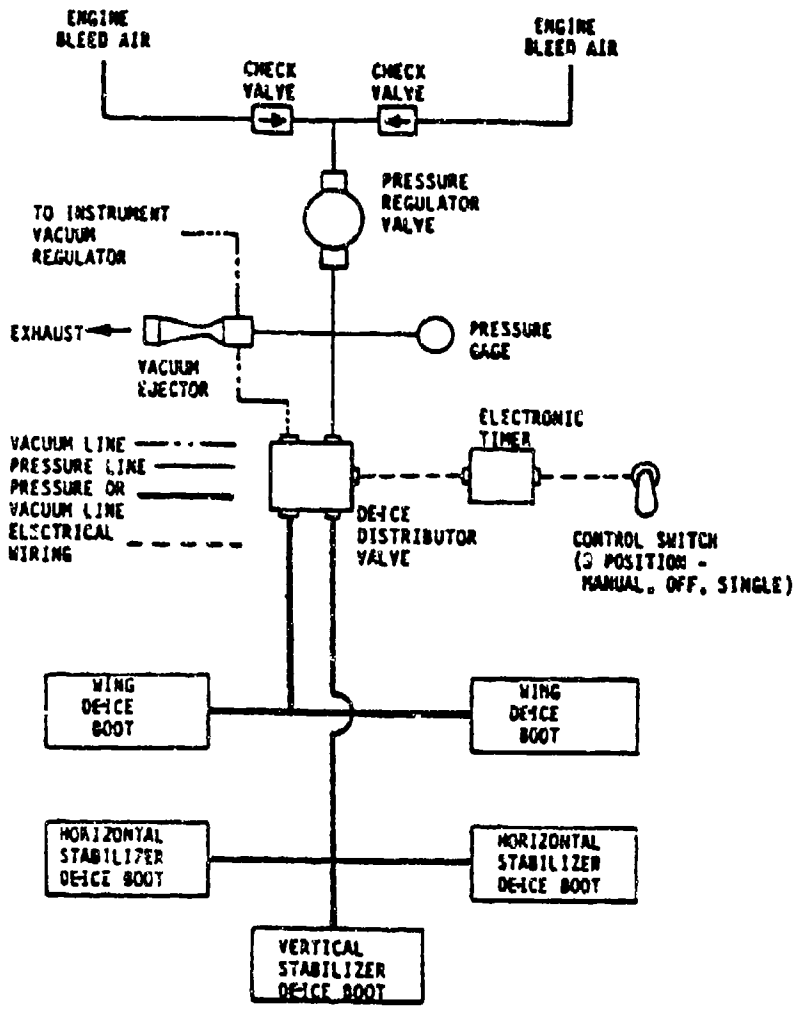

Dual Cycle System

FIGURE 1-3. PNEUMATIC BOOT SURFACE DE-ICING SYSTEM - TURBINE ENGINE POWERED AIRCRAFT

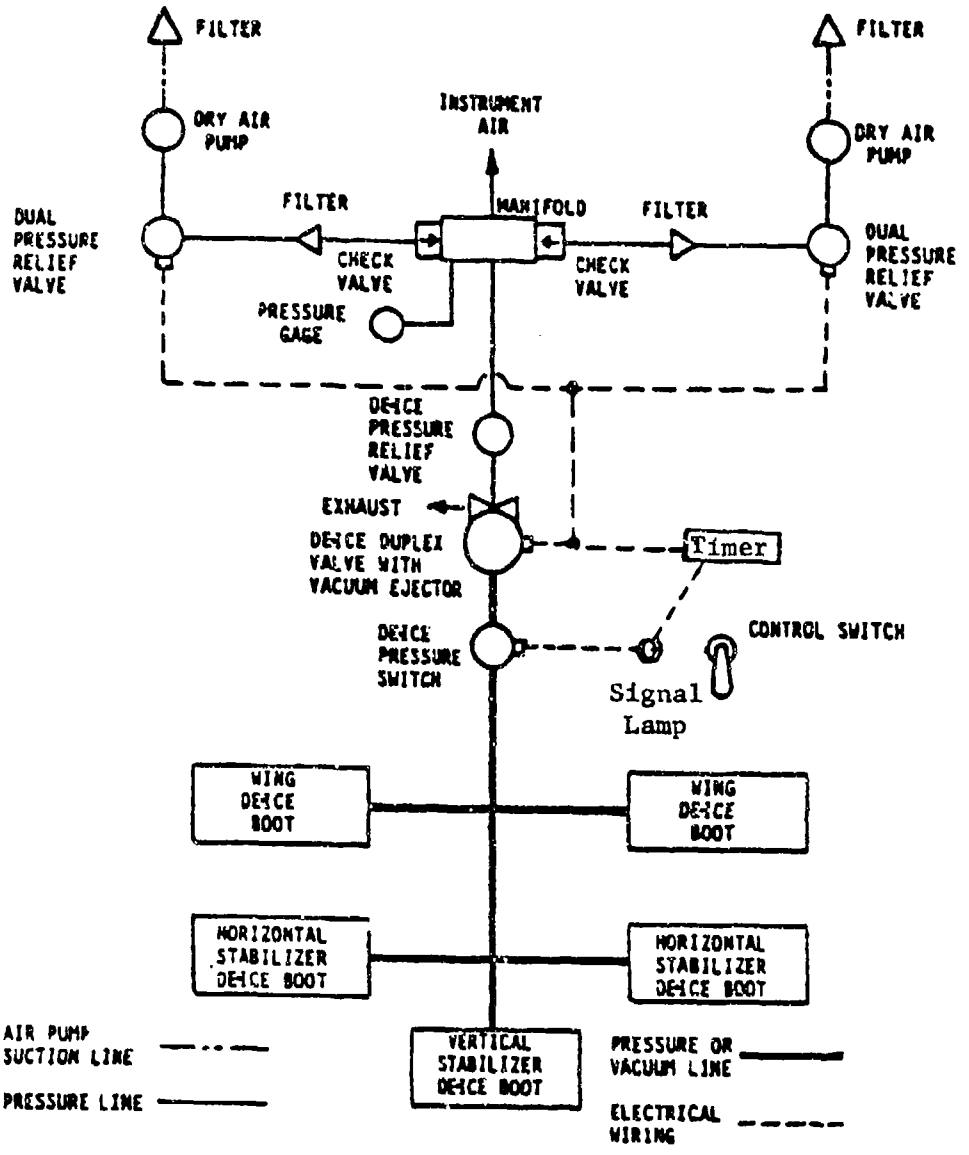

Single Cycle System

FIGURE 1-4. PNEUMATIC BOOT SURFACE DE-ICING SYSTEM - RECIPROCATING ENGINE POWERED AIRCRAFT

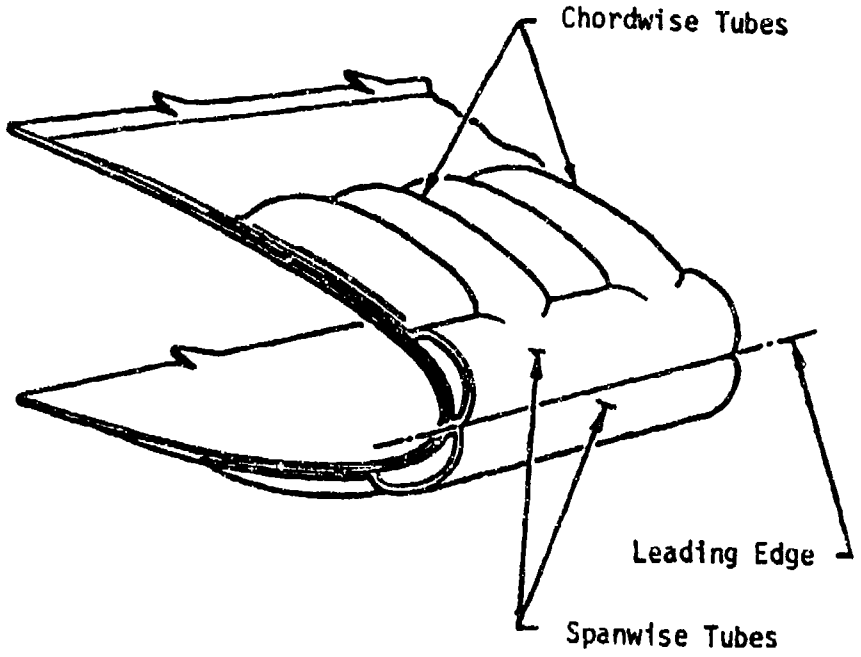

FIGURE 1-5. ROTORCRAFT BLADE PNEUMATIC BOOT DE-ICING SYSTEM

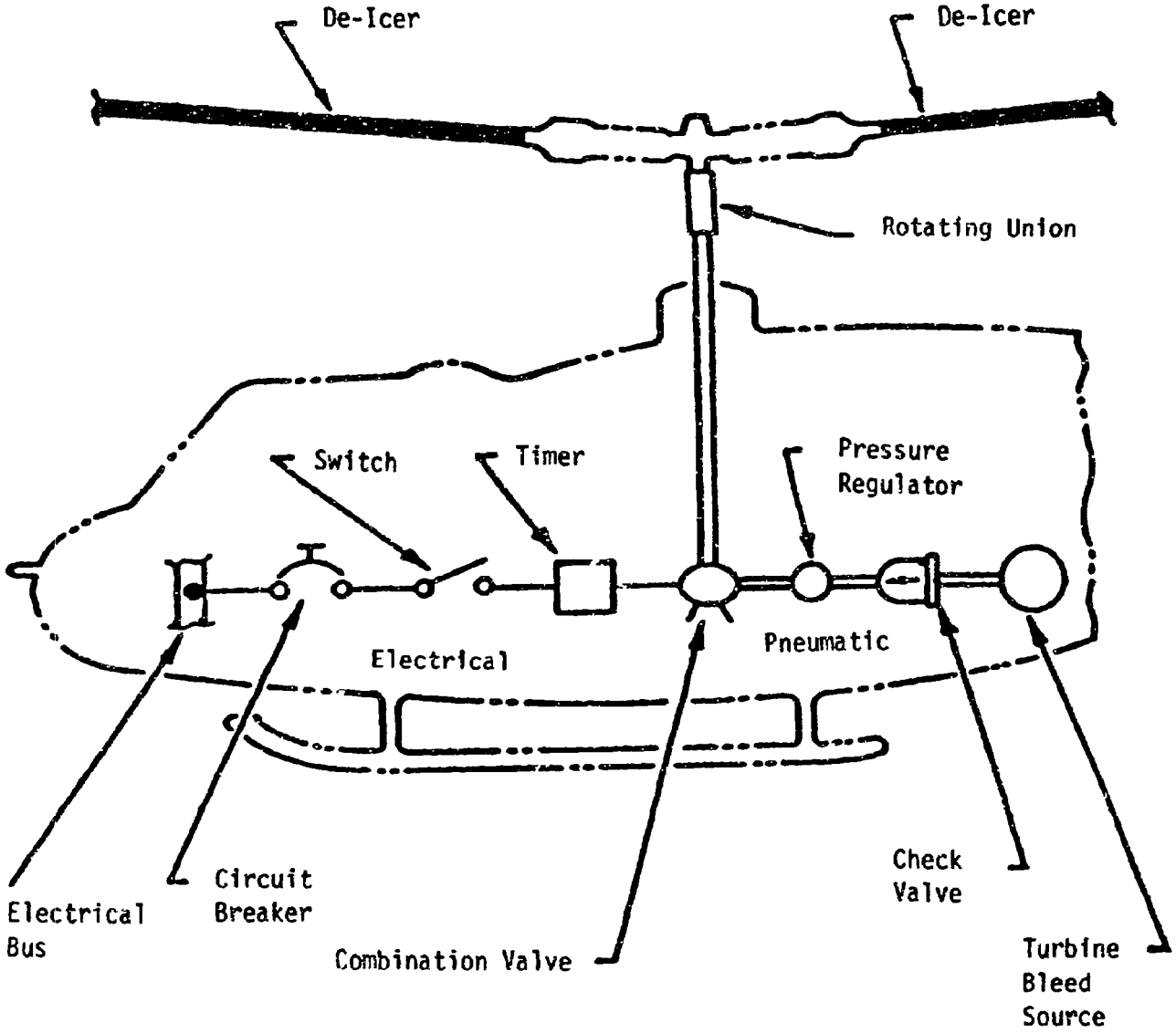

FIGURE 1-6. ROTORCRAFT PNEUMATIC BOOT DE-ICING SYSTEM - SCHEMATIC

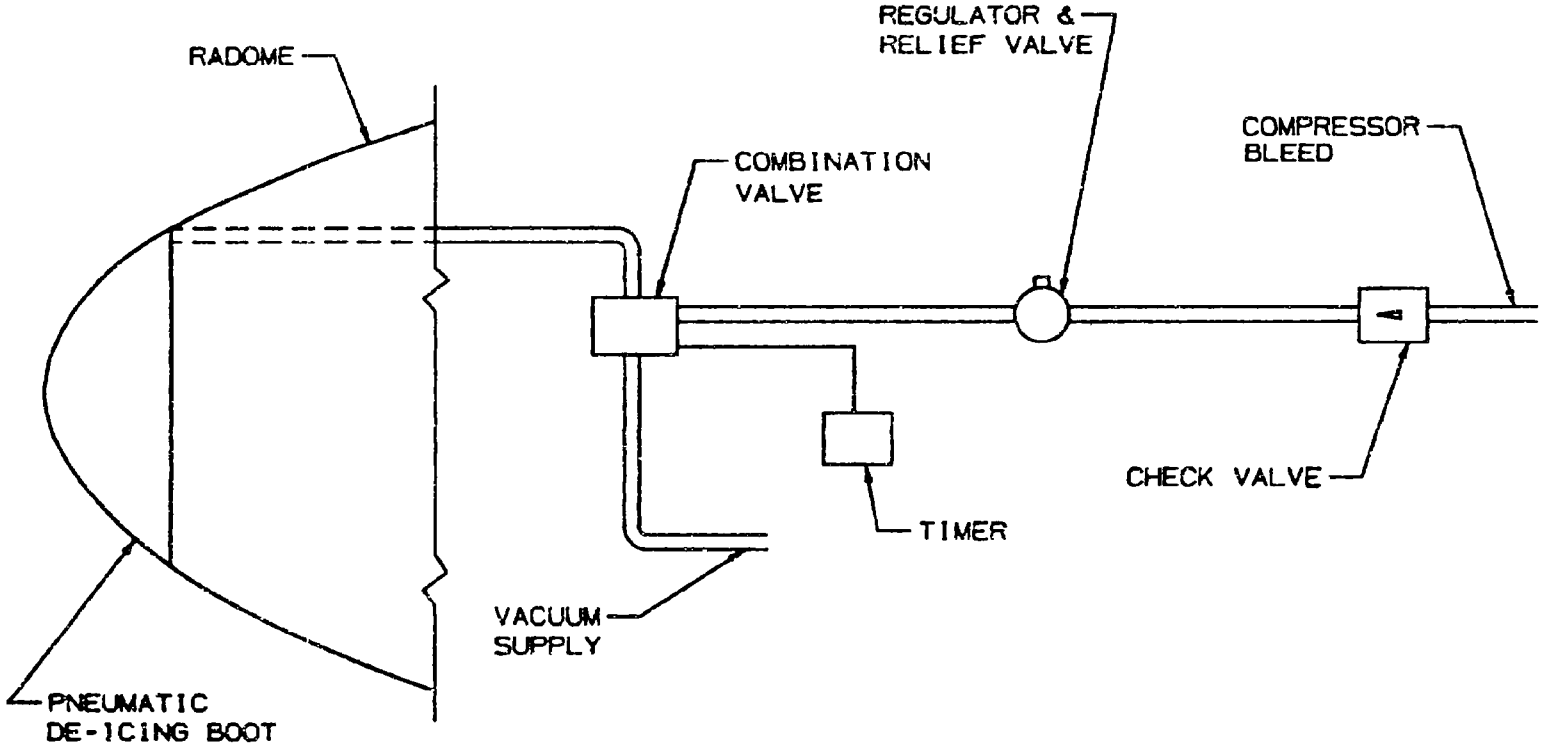

FIGURE 1-7. PNEUMATIC BOOT DE-ICING SYSTEM - NOSE RADOMES

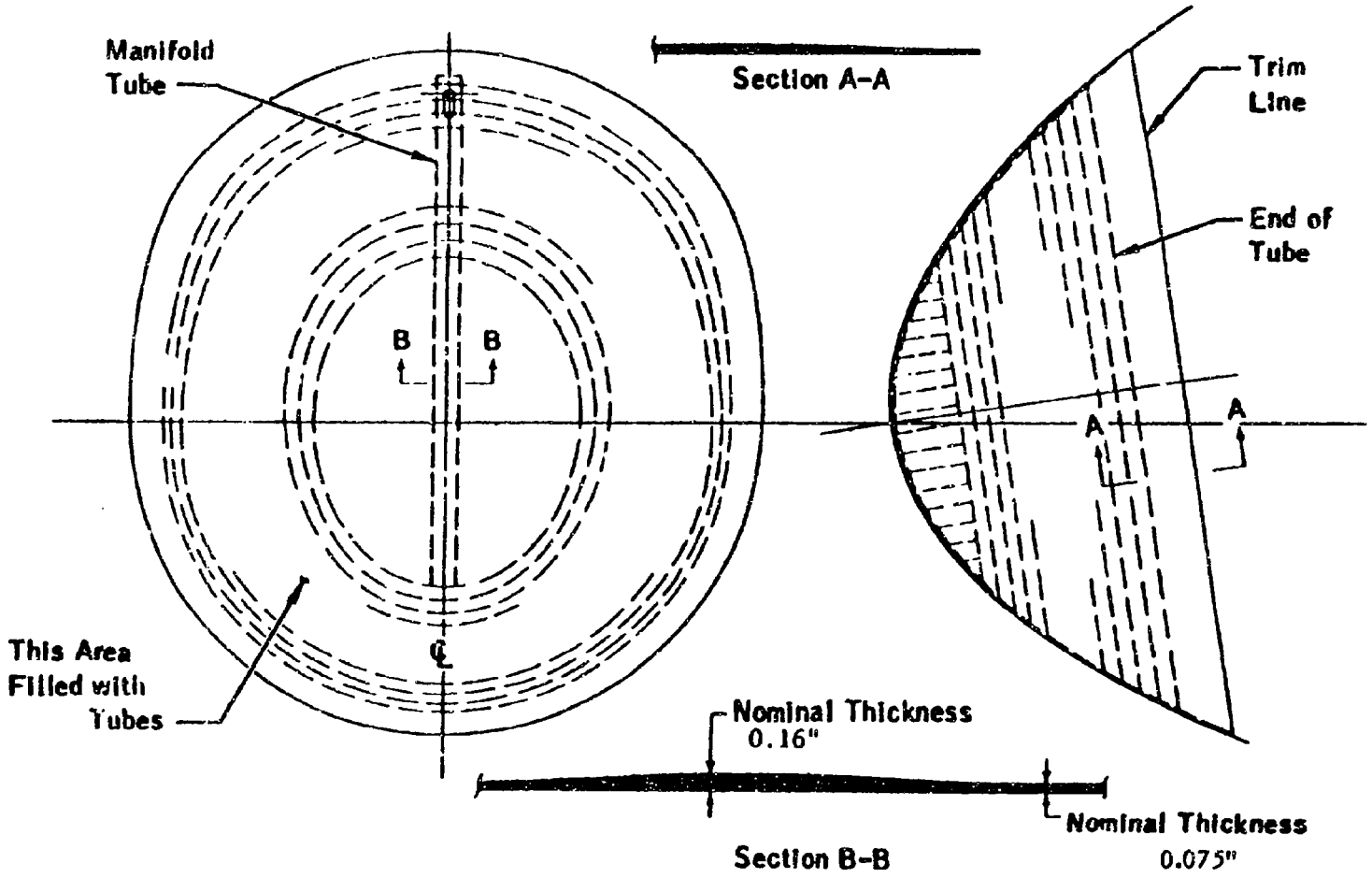

FIGURE 1-8. TYPICAL NOSE RADOME DE-ICING BOOT CONFIGURATION

CHAPTER III
SECTION 2.0
ELECTRO-THERMAL SYSTEMS

CHAPTER III - ICE PROTECTION METHODS

CONTENTS

SECTION 2.0 ELECTRO-THERMAL SYSTEMS

	Page
LIST OF TABLES	III 2-iv
LIST OF FIGURES	III 2-v
SYMBOLS AND ABBREVIATIONS	III 2-vi
GLOSSARY	III 2-vii
II.2.1 OPERATING CONCEPTS AND COMPONENTS	III 2-1
II.2.2 DESIGN GUIDANCE	III 2-1
2.2.1 Anti-Icing Systems	III 2-2
2.2.2 De-Icing Systems	III 2-2
III.2.3 USAGES AND SPECIAL REQUIREMENTS	III 2-2
2.3.1 Airfoil and Leading Edge Devices	III 2-5
2.3.1.1 Airfoils	III 2-5
2.3.1.2 Leading Edge Devices	III 2-5
2.3.2 Windshields	III 2-6
2.3.3 Engine Inlet Lips and Components	III 2-8
2.3.3.1 Inlet Types	III 2-8
2.3.3.2 Power and Cycling	III 2-9
2.3.3.3 Materials	III 2-9
2.3.4 Turbofan Components	III 2-10
2.3.5 Propellers and Spinners	III 2-10
2.3.6 Helicopter Rotors and Hubs	III 2-11
2.3.6.1 Heater Elements	III 2-11
2.3.6.2 De-ice Power Supply	III 2-13
2.3.6.3 Power Switching and Distribution	III 2-13
2.3.6.4 De-ice Controller	III 2-13
2.3.6.5 External Sensors	III 2-14
2.3.7 Flight Sensors	III 2-14
2.3.8 Radomes and Antennas	III 2-15
2.3.8.1 Radomes	III 2-15
2.3.8.2 Antennas	III 2-15
2.3.9 Miscellaneous Intakes and Vents	III 2-15
2.3.10 Other	III 2-15
III.2.4 WEIGHT AND POWER REQUIREMENTS	III 2-15
III.2.5 ACTUATION, REGULATION, AND CONTROL	III 2-16

CONTENTS (CONTINUED)

	Page
III.2.6 OPERATIONAL USE	III 2-16
2.6.1 Anti-Icing Systems	III 2-16
2.6.2 De-Icing Systems	III 2-16
2.6.2.1 Typical System Operation	III 2-17
2.6.2.2 Test Considerations	III 2-18
III.2.7 MAINTENANCE, INSPECTION, AND RELIABILITY	III 2-20
III.2.8 PENALTIES	III 2-21
III.2.9 ADVANTAGES AND LIMITATIONS	III 2-21
III.2.10 CONCERNS	III 2-21
III.2.11 REFERENCES	III 2-22

LIST OF TABLES

		Page
2-1	Weight and Power Requirements for Electro-Thermal Ice Protection Systems for Three Typical Aircraft	III 2-23

LIST OF FIGURES

		Page
2-1	Areas of Airframe That May Require Ice Protection	III 2-24
2-2	Cross Sections of Typical Electric Heaters	III 2-25
2-3	Electro-Thermal Wing Anti-Ice System	III 2-26
2-4	Typical Wing Leading Edge With Slat	III 2-27
2-5	Typical Wing Leading Edge Krueger Flap	III 2-28
2-6	Ice Accretion on Unprotected Extended Leading Edge Flap for Continuous Maximum Icing Conditions	III 2-29
2-7	Typical Electrically Heated Windshield Construction	III 2-30
2-8	Typical Windshield Areas to be Protected for Two Windshield Arrangements on Multi-Engine Transport	III 2-31
2-9	Typical Main Windshield Showing Construction and Location of Conductive Films and Sensing Elements	
	a. Five-ply, Non-rectangular, Birdproof Glass Windshield	III 2-32
	b. Three-ply, Nearly Rectangular Glass Windshield	III 2-33
	c. Five-ply, Nearly Rectangular, Birdproof Glass Windshield	III 2-34
2-10	Typical Anti-Icing Heat Requirements vs. Altitude for Center Windshield Panel	III 2-35
2-11	Electro-Thermal Propeller Deice System	III 2-36
2-12	Typical Propeller and Spinner Ice Protection for Turboprop Aircraft	III 2-37
2-13	Main Components for Rotor Deice System	III 2-38
2-14	Spanwise Heater Element Arrangement	III 2-39
2-15	Chordwise Heater Element Arrangement	III 2-40
2-16	De-icing System Optimization	III 2-41
2-17	Data and Control Function In-Flight Monitor	III 2-42

SYMBOLS AND ABBREVIATIONS

Symbol	Description
AC	Alternating Current
BTU	British Thermal Unit
°C	Degrees Celsius
CAR	Civil Air Regulation
cm	Centimeter
CRT	Cathode Ray Tube
DC	Direct Current
EMI	Electro Magnetic Interference
EOT	Element on Time
°F	Degrees Fahrenheit
ft	Feet or foot
HP	Horsepower
in	Inch
kg	Kilogram
kw	Kilowatt
lbf	Pounds force
lbm	Pounds mass
lbs	Pounds
LWC	Liquid Water Content
m	Meter
mm	Millimeter
MVD	Median Volume Diameter
NACA	National Advisory Committee for Aeronautics
OAT	Outside Air Temperature
sq	Square
S/R	Slip Ring
V	Velocity
VDC	Volts Direct Current
w	Watts

GLOSSARY

evaporative system - Any anti-icing system that supplies heat sufficient to evaporate all water droplets impinging on the heated surface.

light icing - The rate of accumulation that may create a hazard if flight is prolonged in this environment. Occasional use of de-icing/anti-icing equipment removes/prevents accumulation.

liquid water content (LWC) - The total mass of water contained in all the liquid cloud droplets within a unit volume of cloud. Units of LWC are usually grams of water per cubic meter of air (g/m^3).

median volumetric diameter (MVD) - The droplet diameter which divides the total water volume present in the droplet distribution in half; i.e., half the water volume will be in larger drops and half the volume in smaller drops. The value is obtained by actual drop size measurements.

micron (μm) - One millionth of a meter.

moderate icing - The rate of accumulation is such that even short encounters become potentially hazardous and use of de-icing/anti-icing equipment or diversion from the area and/or altitude is necessary.

running-wet system - Any anti-icing system that supplies only enough heat to prevent impinging water droplets from freezing on the heated surface.

severe icing - The rate of accumulation is such that de-icing/anti-icing fails to reduce or control the hazard requiring immediate diversion from the area and/or altitude.

stagnation point - The point on a surface where the local velocity is zero.

trace icing - Ice becomes perceptible. The rate of accumulation is slightly greater than the rate of sublimation. It is not hazardous, even though de-icing/anti-icing equipment is not used, unless encountered for an extended period of time.

III.2.0 ELECTRO-THERMAL SYSTEMS

III.2.1 OPERATING CONCEPTS AND COMPONENTS

All thermal ice protection systems operate on the same principle: Heat is applied to an area encompassing the water impingement region. The heat is used to evaporate or prevent impinging cloud droplets from freezing or to debond or melt an existing ice cap. The equipment required for electro-thermal systems is the same in either case: a source of electrically generated heat a distribution system, and a control system.

Two sources of the required electrical energy are considered in this section:

a. Extraction from the airplane's own electrical system.

b. A separate onboard generator with its own source of power.

The electrical energy is distributed to the areas requiring anti-icing or de-icing. It then flows through resistance heaters designed to provide the necessary heat for either anti-icing or de-icing of the surface.

Major components of an electro-thermal system are:

a. Source of electrical energy.

b. Wiring system to distribute energy to the surfaces to be heated.

c. Resistance heaters in the areas to be anti-iced or de-iced.

d. Temperature sensors at the heated surfaces.

e. Manual or automatic control unit to monitor icing conditions and heat supplied to the surface.

f. Cockpit panel mounted display to keep the crew advised of the system operation (e.g., warning lights, surface temperature indicator, icing condition warning, power consumption, etc.).

Provisions for redundant electrical energy sources are generally used to provide a high probability of being able to venture into known icing conditions and to ensure safe system operation when icing conditions are encountered.

Aircraft surface areas that may be afforded electro-thermal ice protection are shown in figure 2-1. Of these areas, the windshield is always given anti-ice protection while the remainder of the areas may be given anti-ice or de-ice protection, depending on the power available for ice protection and the effects of ice accretion on the component.

II.2.2 DESIGN GUIDANCE

Electro-thermal systems use electrical resistance heaters (foil, film, resistance wire, mesh, etc.) imbedded in fiberglass, plastic, rubber, or metal to heat the surface. Figure 2-2 shows cross-sections of typical electrical heaters.

Electro-thermal systems are classified as anti-icing or de-icing systems. An anti-icing system prevents the formation of ice in a specified area whereas a de-icing system allows ice to build up and then removes the ice cap.

2.2.1 Anti-Icing Systems

Electro-thermal anti-icing systems use electrical heaters to maintain the temperature of the surface to be protected above freezing throughout an icing encounter. Electro-thermal anti-icing systems are classified as evaporative or "running wet."

Evaporative systems, as the name implies, supply sufficient heat to evaporate all water droplets impinging upon the heated surface. The running wet systems, however, provide only enough heat to prevent freezing on the heated surface. Beyond the heated surface of a running wet system, the water can freeze, resulting in runback ice. For this reason, running wet systems must be used carefully so as not to permit buildup of runback ice in critical locations. For example, the heated surface of a running wet system on a turboprop or turbojet engine inlet should extend into the inlet to the compressor face so that the water runoff will combine with the intake air and not strike cold surfaces where it could refreeze, break off, and possibly damage the engine.

2.2.2 De-Icing Systems

In a de-icing system, ice is allowed to accrete on the surfaces to be protected and is then removed periodically. Electro-thermal de-icing systems function by rapidly applying sufficient heat to the ice-surface interface in order to melt the bonding layer of ice; aerodynamic or centrifugal forces then remove the bulk of the ice.

Parting strips may be used in the electrical de-icing system to divide the total protected area into smaller, sequentially heated areas. This reduces the total instantaneous power requirement and maintains a stable load on the electrical system. The size of the cycled shedding sections will depend upon the total wattage available and the wattage density required for efficient de-icing.

III.2.3 USAGES AND SPECIAL REQUIREMENTS

For anti-icing, the heat source must remain on throughout the icing encounter. The power requirements for completely anti-icing an airplane using an electrically powered heat source are usually prohibitive. Therefore, the areas generally anti-iced electrically are the windshield, small air inlets, instrument probes, leading edges forward of engine inlets and data probes, and areas remote from any hot air source.

For efficient de-icing protection, the correct amount of heat must be supplied where and when needed. If there is too little heat, the ice may not shed as required, perhaps causing large chunks of ice to shed or creating unbalanced rotors on a helicopter. If too much heat is supplied, there can be too much melting, resulting in undesirable amounts of runback ice. It has been found desirable to have the following characteristics in the cyclically heated shedding zones (reference 2-1):

a. A high specific heat input applied over a short period. This generally requires less total energy than a lower specific heat over a longer period of time. The high specific heat input reduces the convective heat losses from the exposed ice surface and conductive losses to the ice and structure, and to a lesser degree compensates for the uncertainty caused by the large variation in the bonding strength of ice. This requires that the deice system element-on-time (EOT) be optimized as a function of ambient or total air temperature to provide just the amount of heat necessary to melt the ice-to-surface bond layer. If the EOT is too short, de-icing will not occur. If the EOT is too long, the deicer will melt too much ice, resulting in runback ice.

b. Immediate cessation of heating and rapid cooling of the surface after shedding occurs (this is to greatly reduce runback ice).

c. The heated area should be the minimum necessary so that heat is applied only under the ice and not dissipated to the airstream. Good insulation between the heater and the supporting structure is required to direct the heat outward to the exposed surface.

e. To produce clean shedding and to avoid runback icing, the proper distribution of heat is required. It is desirable that melting of the ice bond should occur uniformly over the surface; this may require some chordwise gradient to the heat input.

f. The spanwise and chordwise parting strips must prevent any bridging from one shedding zone to another. Even a small strip of anchorage may delay ice from shedding until dangerously large pieces have formed.

g. The cycle "off time" should be controlled to permit adequate ice accretion for the best shedding characteristics.

The "off time" will depend upon the thermal capacity of the shedding zone and the rate at which the surface cools to 32°F (0°C). It will also depend upon the icing rate so that the ice thickness accumulated is the best for shedding when de-icing occurs. The "off time" may be from three to four minutes for a typical ice buildup, however, rotorcraft "off times" are as low as 60 seconds for high liquid water contents.

System requirements for de-icing must be considered in two parts: First, the parting strips and dividing strips, and second, the cycled shedding area. The heat input to the strips must provide at least running wet anti-icing to prevent ice from bridging. For electro-thermal de-icing, bridging means that an arch of ice remains over the heating element. The ice arch will be attached to a cool surface and the dividing strips can serve as attachment points if not heated. Control of the temperature of the strips is desirable both for economy and to prevent overheating. Overheating the

dividing strips encourages runback icing and detracts from shedding performance. Severe overheating may cause a burnout of the heating elements. Dividing strip widths should be sufficient to accommodate the change in stagnation point with changes in angle of attack. A parting strip width of from 1 to 1.25 inch (25 to 32 mm) should be adequate for most installations.

Aircraft wings with about 30° or more sweep-back will normally use only chordwise parting strips since aerodynamic forces will remove the ice from the shedding zones without the aid of stagnation line parting strips.

Shedding zone power requirements are difficult to determine. Heat transfer rates, aerodynamic forces, and bonding characteristics of the ice (to the surface material) are some of the factors affecting the power requirements. Heat-on times less than 10 seconds require heaters capable of withstanding very high power densities and a large number of cycled areas. Rotorcraft, with their smaller chord airfoils, have used element-on-times approaching one second for warm temperatures. Heat-on times longer than 40 seconds would not result in an appreciable reduction in power density. Shedding zone power density requirements are not appreciably affected by variations in heat-off times. To achieve an even melting of ice throughout the shedding zone it is desirable to have a uniform power distribution in the region of highest water collection, and a decreasing power requirement downstream.

Over-heat protection devices may be required for electrical de-icing systems. Inadvertent actuation of the electrical de-icing system during a period where little cooling takes place could cause burnout of the high wattage density heating pads. The over-heat protection device should be temperature sensing so that the systems may be used during ground operation to remove accumulated ice and during takeoff to prevent excessive ice formation.

An electro-thermal de-icing system may be installed on any existing aircraft by attaching flexible wrap-around heating pads to the structure with an adhesive. The heating pads are fairly thin and may not appreciably affect the aircraft performance. Another method of providing electro-thermal ice protection is to mold the heating elements into the leading edge structure. No aerodynamic performance loss is experienced by this construction method.

The electrical wiring supplying power for the heating pads requires little space and can normally be routed through existing passages within the structure. Generating equipment may be either engine-driven or auxiliary power source driven. The required power generator capacity will depend upon several factors: the efficiency of the heating pads, the wattage of the shedding sections, and the number of pads required to be on at any one time. Shedding section cycling should be scheduled to maintain an even power load upon the generating equipment.

In higher speed aircraft, the rubber heating pads are subject to rain erosion and hail damage. A metal overshoe (erosion shield) (figure 2-2) will protect the pads and help to even out the heat distribution and prevent surface cold spots. Detracting from the overshoe installation is the loss in heater efficiency and the added weight to the aircraft. The electro-thermal system for rotorcraft will generally be constructed in a composite, rather than in a rubber boot, but it will still require an erosion shield.

2.3.1 Airfoil and Leading Edge Devices

2.3.1.1 Airfoils

The use of electro-thermal boot systems for all wing and empennage surfaces is usually not feasible because of the amount of power required and the associated weights of the power generating equipment. Wing and empennage surfaces provided with electro-thermal systems are usually limited to those requiring special consideration such as surfaces forward of engine inlets. These applications are generally anti-icing, running wet systems.

The heater elements are molded into the boot assemblies which are bonded to the wing leading edge. The boot is usually divided into a number of independent heating elements. Each heating element is protected by a circuit breaker and a current sensor. The temperature of the boot is controlled by a thermal control switch attached to the leading edge wing skin. The thermal control switch senses the skin temperature and opens or closes the power circuit at pre-set skin temperatures. See figure 2-3 for a typical wiring diagram. This system is activated continuously when in icing conditions.

2.3.1.2 Leading Edge Devices

The preceding description of an electro-thermal ice protection system for a wing assumed a fixed leading edge. Wings with high lift leading edge devices will have the same ice protection requirements but methods of satisfying these requirements will differ and will be more complex.

Leading edge devices may consist of slats, slots, or flaps. A wing leading edge slat configuration is shown in figure 2-4. A slot is similar to an extended slat but is a fixed geometry, rather than being retractable for cruising flight. Leading edge flaps are hinged plates which are nested against the wing for cruise and played forward for low speed, high lift conditions: See figure 2-5. The fixed wing behind the slat may or may not require protection, depending on geometry, ice accretion characteristics, and time in icing. For each new aircraft, a study should be made of the need for heating this area.

Electro-thermal de-icing may be applied to leading-edge slats. Difficulty in retraction of the slats may be experienced if ice accretes on the fixed leading edge or if residual ice or runback ice occurs behind the flap.

Leading edge "Krueger" flaps may or may not be protected depending upon the effects of ice accretion on performance. Figure 2-5 illustrates an unprotected leading edge flap as might be installed on a transport aircraft. Ice protection requirements for the wing leading edge will remain the same but because of the leading edge flap installation there will be a reduction in the heated area on the lower surface. Water may runback from the heated leading edge and freeze behind the flap if the leading edge anti-icing system is not fully evaporative. Also, there will be a small amount of direct impingement. Evaluation of the need for heating the flaps must be made by either an aerodynamic analysis or by flight test.

Ice accretion can occur when the flap is extended during takeoff and approach. Figure 2-6 illustrates the amount of ice that may accumulate on extended flaps during a 30 minute hold in icing. However, no appreciable ice usually accumulates during takeoff, as flaps are retracted about 1-1/2 minutes after brake release. If the flap is unprotected, flight tests should be conducted to determine the effects of this ice accretion. One flight test method which may be employed is to simulate the critical predicted ice shapes with wood or plastic and attach them to the flap. The airplane performance then may be evaluated in clear air.

It should be noted that the extension of either leading or trailing devices changes the air flow around the wing, including sizeable changes in stagnation line location. This will alter the droplet impingement and ice accretion patterns. Trailing edge flaps sometimes accrete ice; This can generally be determined only from flight tests.

De-icing requirements would be similar to the requirements of a fixed leading edge. Shedding characteristics will probably be different because of the airfoil shape and the aerodynamic forces the ice will encounter. An icing tunnel test program may be required due to the difficulty in predicting shedding forces and impingement.

2.3.2 Windshields

Anti-icing protection is usually provided for the forward-facing windshield panels on both military and commercial aircraft that are required to operate in all-weather conditions. The most widely used system is electrical anti-icing whereby electric current is passed through a transparent conductive film or resistance that is part of the laminated windshield. The heat from the anti-icing film or resistance wire also prevents internal fogging for most configurations. Electrical heat may also be used to maintain the windshield interlayers (of a glass/plastic laminated windshield) at or near the optimum temperature for resistance to bird strikes (birdproofing).

Figure 2-7 shows a typical windshield construction. The thickness of the conductive film or the wire size can be varied to accommodate variation in heating requirements or to heat irregular shapes (reference 2-2 and 2-3).

The windshield arrangement of a typical multi-engine transport is shown in figure 2-8. Ice protection is needed for the forward facing windshields (main and center), but not for the side and aft windows which are at minimum angle to the airstream and probably do not collect ice. An alternate arrangement often used deletes the center windshield and increases the size of the main windshields. The center windshield for rotorcraft was considered at one time not to require anti-icing, but operational experience showed that this section should also be protected. In either case, the conductive anti-icing film or wire grid is applied to the inside of the outer ply of glass, as shown in figures 2-9a-c. The film usually covers only a roughly rectangular area of the windshield, as non-uniformity of heating and actual "hot spots" become a serious problem with the high power density heating needed for anti-icing (3 to 4 watts/sq. in. for glass or 5.25 watts/sq. in. for plexiglass). The exterior ply is usually limited to 0.18 inch (4.6 mm) thickness if the surface is glass, 0.06 inch (1.5

mm) if plastic, to avoid excessive internal temperatures. Power supply bus bars and the temperature control sensor are usually located as shown in figures 2-7 and 2-9a-c.

Anti-fog films, in contrast, are often applied to non-rectangular areas. The low power densities (1/2 to 1 watt/in^2) used for anti-fog tend to reduce the problem of "hot spots" and attendant glass breakage problems. For this reason, the arrangement of figure 2-9a has been used on at least one jet transport. Where the panel in question is nearly rectangular as in figure 2-9b, a single coating may meet the requirements for anti-icing, fog prevention, and maintenance of optimum vinyl temperature. In the configuration of figure 2-9c, the anti-fog and anti-ice films are never used simultaneously.

Typical heat requirements for a jet transport center windshield are shown in figure 2-10. For a typical flight profile, a maximum input of 1,800 BTU/hr-ft^2 was found to be adequate. Inward heat losses have not been considered here as analysis shows them to be less than 5%. Calculations were based on boundary layer buildup from the aircraft nose. For windshields that depart abruptly from the fuselage contour, a thickened boundary layer starts at the windshield's base and heat requirements will be higher.

One of the main problems associated with the use of electrically heated windshields is inflight breakage caused by thermal stress in the glass. Replacement rates for windshields often are several times as great in winter as in summer. There are two effective approaches to this problem. One is to design the heat input to the minimum possible value. Clear vision is essential at low altitude, but air temperatures associated with icing are not likely to be below 0 °F (see Chapter I). At higher altitudes where lower temperatures are found, flight through icing would be made on instruments and some partial obstruction of vision might be acceptable. The non-uniformity of the conductive coating would tend to prevent complete obscuring of the windshield even under marginal conditions. Some transports equipped with high (2,300 BTU/hr-ft^2) and low (1,500 BTU/hr-ft^2) control settings have found no need for the higher setting. However, conformity with FAR 25.773(b) must be observed:

> The airplane must have a means to maintain a clear portion of the windshield, during precipitation conditions, sufficient for both pilots to have a sufficiently extensive view along the flight path in normal flight attitudes of the airplane. This means must be designed to function, without continuous attention on the part of the crew, in... (ii) the icing conditions specified in para. 25.1419 if certification with ice protection provisions is requested."

The FAR 25.1419 atmospheric conditions are given in FAR Part 25, Appendix C. FAR 23 requirements are less specific, but FAR 29 requirements are essentially the same as for FAR 25.

A second approach (which can be used in conjunction with the first) is to employ a power modulating control. Recent advances in electronic switching devices have made this an attractive method of control. Mechanical switching (use of a transformer, relay, and power contactor) may result in large transient currents and temperature differentials that adversely affect windshield service life.

Power supply is normally from an AC generator; however, if only DC power is available, an inverter can be used to produce the required voltage. In several instances, windshields have used DC power directly. The temperature control is set at a value high enough to produce the design heat requirement without overheating the interlayer. Usually a setting of 100 to 110°F (38-43°C) will fulfill both the anti-icing and anti-fog temperature requirements. The most common control turns full power ON and OFF as necessary to maintain the set temperature within a 10°F (5.6°C) deadband. Controlling in this manner may result in cyclic thermal stresses that have adverse effects on windshield service life. Some current aircraft are using modulating controls that vary power as a function of temperature sensor demand to reduce thermal stresses (reference 2-4).

Successful design of a windshield having electrical heating requires careful integration of all factors involved. The most important are: providing good coating uniformity (use of nearly rectangular areas), limiting heat input to the minimum acceptable level and, if possible, using a modulating control to eliminate cyclic thermal stresses. Methods of calculating the heat required and temperature control setting are shown in Chapter V together with a calculation method to determine temperature of the interlayer.

2.3.3 Engine Inlet Lips and Components

2.3.3.1 Inlet Types

The method in which ice protection is used in turbine powered aircraft is dependent on inlet design. The major differences in ice protection system needs are due to the two inlet designs termed "contoured" and "non-contoured." A contoured inlet duct is defined here as a duct that has sufficient internal surface curvature, and causing sufficient redirecting of inflowing air such that water particles ingested will impinge directly on the duct surface. On the other hand, many inlet designs used for modern turbine powered aircraft have a mild contour such that the incoming air is not significantly redirected and the air travels straight into the engine. In this case, the inlet duct walls are not prone to direct water droplet impingement. These inlets will be defined as noncontoured, and ice protection against directly impinging water under icing conditions is not needed. A typical example of non-contoured inlets is the turbofan powered commercial transport aircraft with externally mounted engines. Contoured inlet aircraft are typically turboprop powered aircraft or aircraft with internally mounted engines. For many of these aircraft, the duct contour causes significant water droplet impingement, making ice protection a requirement for these areas. In many cases, electro-thermal de-icing provides the best combination of cost, weight, operational features, manufacturing ease, and power requirements for inlet duct ice protection, provided that the engine can tolerate the shed ice.

For most turbine powered aircraft, engine inlet leading edge surfaces require some type of ice protection. Electro-thermal de-icing provides effective inlet leading edge ice protection and usually draws a relatively low amount of electrical power. Electro-thermal anti-icing systems require more

power than de-icing systems but insure a minimum of engine ice ingestion, provided that runback icing is avoided.

2.3.3.2 Power and Cycling

Numerous power and timing combinations are available that can provide satisfactory ice protection. Alternating current obtained directly from aircraft alternators is typically routed through one or more electrical heating elements. Two fundamental parameters of electric power application are power density and duration. Typical power density ranges used in present day aircraft de-icing applications are from 10 to 30 watts per square inch (1.5 to 4.7 watts per square centimeter). Two different methods of applying power to the de-icing device are (1) holding power density constant and varying the duration - with the duration determined by ambient condition sensing - or (2) holding the time base constant and varying the power density (by varying the voltage or changing the total system resistance) - with power density determined by the ambient condition sensing. Regardless of which method is used, the success of a de-icing system in an inlet is heavily dependent on rapid heat-up and rapid cool-down. The desire to have rapid heat-up and cool-down grows out of the need to minimize the melting of ice and hence the forming of water during the de-icing cycle. By forcing the temperature of the surface to rise quickly, the ice will not gradually absorb heat, but instead, the frozen ice/surface interface will separate, allowing the ice particle to be swept away by the airflow, with the departing ice taking the small amount of melted water along with it. The more rapidly the surface cools to below freezing the sooner the reformation of ice will commence, preventing the runback of a significant amount of liquid water that could freeze onto unprotected areas. The potential problems of runback icing are dealt with in Section 2.10. A typical heating strategy to help alleviate the hazardous build-up of runback ice is to divide the deiced surface into several streamwise zones and apply power to each zone separately. By alternating the on-cycle from zone to zone and going from "front to back," runback water can be shed as ice or "chased back" to non-hazardous areas.

2.3.3.3 Materials

Electro-thermal de-icing heater elements are typically fabricated in one of several designs. The element may be built as an add-on pad type of device or it may be built in as an integral layer within the actual aerodynamic surface. If the heater is the bond-on pad type, it may be applied to either the front (air wetted) surface or on the backside of the aerodynamic surface, out of the air stream. If the heater is mounted on the external surface, consideration must be made for resistance to impact from foreign objects and from lightning strikes. Effects of changes in heat transfer characteristics should be accounted for when the decision is made to install a heater system externally, internally, or integrally. The installation location and consideration for impact resistance will usually have a bearing on whether the heater element is embedded in a flexible or a rigid material. In either case, the material must be electrically non-conductive and completely encase the heater element to insulate

the conductive element electrically. For embedded heaters, an overtemperature sensor may be placed behind the heater to provide thermostat control and avoid heater damage by overheating.

2.3.4 Turbofan Components

Ice protection for turbofan engine components is commonly provided by hot air methods (Section III.5.3.4).

2.3.5 Propellers and Spinners

Propeller and spinner (nose cone) ice protection is employed for three reasons: (1) leading edge ice formations may cause a propeller efficiency loss, (2) unsymmetrical shedding of ice may result in propeller unbalance, and (3) large pieces of ice shed from the propeller or spinner may be ingested by the engine on turboprop aircraft.

Electro-thermal de-icing may be installed on the external surface of a propeller without appreciably affecting its performance. Coverage should be approximately 15 percent of the chord on the suction surface and approximately 30 percent on the pressure surface. Protection is typically extended to only 30 percent radius because ice formations are negligible beyond that point. This is attributable to aerodynamic heating and centrifugal force effects. However, in some instances, ice may accrete farther outboard with very detrimental effects on propeller performance since the propeller is most heavily loaded in the tip region. Careful selection of the protection coverage extremes is warranted in these cases. The power to the heating pads is supplied through slip rings at the propeller hub. Installation of the heating element on the interior of the propeller would protect the heating elements from damage, but the loss of efficiency and the difficulty of repair make the external system more feasible. An example of the construction of an external electric heater for a propeller is shown in figure 2-11. The outer ply of the propeller heater must be of a material which is rain erosion resistant and not too vulnerable to hail damage.

Propeller thermal de-icing requirements will vary depending upon propeller diameter, rotational speed, and aircraft forward velocity. The watt density and coverage are usually determined by the boot manufacturer.

Shedding of ice from propellers should be equal from each blade of a propeller to prevent unbalance. Timing sequences are usually established so that only one propeller is heated at a time. Also, the frequency of shedding should be scheduled to prevent large pieces of ice from forming, as they may cause damage to the aircraft when they are shed. Fuselage skin damage due to ice shed in the propeller plane should be considered. In some cases, a protective shield may be desirable.

Ice protection for propellers and, to a limited extent, spinners of turboprop aircraft is commonly provided by the electro-thermal method. A typical system of this type is illustrated in figure 2-12 and is described in detail in reference 2-1. In this particular system, continuous (running wet) heating is provided for the forward portion of the spinner; cyclic heating is provided for the aft

portion of the spinner, the spinner islands, and the propeller blade leading edges (to 30 percent radius). These are the areas from which shed ice would have the greatest tendency to enter the engine.

In the system illustrated, the distribution of power to the forward (anti-ice) portion of the spinner is shown in figure 2-12. Power to this area is varied in steps from 3.5 to 8 watts/in^2. The watt densities supplied to the cycled areas are 11 watts/in^2 for the aft portion of the spinner and 13 watts/in^2 for the spinner islands and propeller blade "cuffs." Heat-on time for these cycled areas is 20 seconds and the total cycle time is 160 seconds (heat-off time is 140 seconds).

For other configurations, the same principles may be applied to obtain satisfactory protection. Other methods have been used in the past, such as fluid and hot-air ice protection, but have fallen into disuse because of installation difficulties, as compared to the electrical system.

2.3.6 Helicopter Rotors and Hubs

The main components of a typical rotorcraft rotor blade electro-thermal deice system are shown in figure 2-13. These include main and tail rotor blades with electro-thermal heaters embedded in the leading edges, a system controller, main and tail rotor sliprings, system power stepping, fault monitoring, ambient temperature sensor, and an ice detector rate meter subsystem.

The electro-thermal deice system installation for rotorcraft can be divided into the following subsystems:

- Electrical heaters
- Deice power supply
- Power distribution
- Deice system controller
- External environment sensors
- Ice detection
- Ambient temperature sensing

Tilt rotor aircraft spinner protection (shown in figure 2-13) and articulated rotor droop stop protection can also be provided by electro-thermal systems.

2.3.6.1 Heater Elements

Several variations in the design of electrical heating elements are in use today. Concepts for locating the heater elements are spanwise (elements from tip to root) or chordwise (around the leading edge), with power density variations in chordwise and/or spanwise directions. Figures 2-14 and 2-15 show examples of these element configurations. The chordwise heaters are generally activated in sections from tip to root while the spanwise heaters are generally activated around the chord starting at the stagnation region. Combinations of these two arrangements are in use.

The heaters may be constructed of wire conductors woven into a carrier, etched foil bonded to a carrier, conductive composite material, or sprayed metallic coating applied to a contoured surface. A suitable dielectric layer is incorporated on each side of the heater to provide electrical insulation

from the erosion cap or spar. The blade is generally fabricated with the heater embedded in the leading edge assembly. Some development aircraft have used add-on deice boots which are fabricated from a heater mat and suitable dielectric. These add-on boots are bonded to the exposed leading edge surface. This is a less expensive approach; however, it affects aerodynamic performance. Heater blanket materials must be evaluated for stress-strain properties, material temperature limits, fatigue limits, and repairability.

The extent of rotor blade coverage can be determined through analysis and test. Since the shedding G forces are much lower for a helicopter rotor than for propellers, coverage usually extends from 20% to 99% rotor span and to about 15% and 25% of the upper and lower chord, respectively. Once the area requiring protection is determined, the area is divided into zones to minimize the power necessary at a given time to provide effective protection. Most ice accretion occurs at the leading edge (around the stagnation region) along the span, with the largest proportion at the outboard areas, generally between 40 and 80% span. This is due to greater local collection efficiencies due to higher rates of impingement. Centrifugal force and kinetic heating effects tend to reduce the ice accretion rate near the rotor tip.

The rotor blade local heat requirements in each heater area can be determined by analysis and testing. Variations in the local blade heating can be accomplished by changing the heater resistance (this changes the local power density), and adjusting the length of time power is applied to a specific zone. Power to the rotor deice heaters can be supplied from the main aircraft generating system or from a dedicated electrical supply.

The following considerations need to be addressed when evaluating an electro-thermal deice installation:

- Reliability
- Overheat protection
- Power required/available
- Redundancy requirements
- Fault detection
- Repairability
- System check
- Ground check
- System saturation
- Electro-magnetic interference

In designing electro-thermal deice blankets for rotor blades, there are several flight occurrences that need to be considered such as erosion, lightning strike capability, impact of rain, hail, insects and varying airloads caused by centrifugal forces and blade bending and the cyclic expansion and contraction loads due to heating and cooling.

2.3.6.2 De-ice Power Supply

De-icing power is generally supplied from the aircraft main generator/alternator system. In some configurations, however, use of a dedicated power supply source may be a better choice, particularly where a decision on use of constant frequency vs. variable frequency may be an influencing factor. With any choice of power supply, however, the electrical system must be sized for the load demand of the de-icing system, which in many cases may be equal to or greater than the total of all other aircraft electrical load requirements. Additionally, the redundant power source requirement (if the requirement is specified) must be taken into account (i.e., does the rotor de-ice system continue to function with one generator/alternator out?).

2.3.6.3 Power Switching and Distribution

Deice power must be transferred from a stationary system (i.e., generators, alternators, power switching unit) to the rotating system (i.e., rotor head). The most common system employed to date is the rotor shaft slip-ring assembly. The power to individual heater element zones is generally directed by a mechanical or solid state switching device (or stepper), located in the rotor head. The device transmits a power pulse to each heater element in a predefined sequence and on-time determined by the main deice controller.

2.3.6.4 De-ice Controller

The de-icing system for main and tail rotors utilizes a deice controller which can be designed to provide automatic control, manual control, or both. Typically, an automatic controller processes signals from the outside air temperature (OAT) sensor (or from an icing rate sensor) to establish the heater element on-time, while the element off-time is determined via the signal from the icing rate system. The controller automatically sequences power to the blade, adjusting the cycle timing based on ambient conditions. The automatic controller may also examine deice system malfunctions and attempt to maintain system function for as long as possible by bypassing the failed element and signaling the cockpit.

A manual controller establishes element on-times and off-times based on pilot selected switch settings. Typically, as a minimum, the pilot selects the OAT range at which he is operating, (i.e., 0°C to -10°C), and his estimation of the icing severity (trace, light, moderate, severe). Changes in ambient conditions are reflected via changes in the switch settings. Manual control of element on-time is not recommended for composite rotor blades, to prevent possible overheating of blade resin.

Many controllers can operate in either an automatic or a manual mode, with the manual mode typically available as a backup to the automatic system. Additionally, protective circuitry can be incorporated into the controller. This circuitry can alter or shutdown the de-ice power sequence in the event of an electrical system failure while providing system status information to the helicopter instrument panel. A failure, as detected by the controller check circuitry, will result in automatic power sequence shutdown or alteration of the cycle sequence and the appropriate cockpit fail signal.

The controller can also include built-in test circuitry. This circuitry, when supplied with the proper signals, can verify correct system operation. Usually, the system is tested on the ground prior to flight and can be activated at any time by the pilot.

2.3.6.5 External Sensors

A signal from an outside air temperature (OAT) sensor is used, either independently or with other system parameters (i.e., icing rate or LWC) to control the heater element on-time schedule. To insure accurate temperature readings, the sensor should be protected from ice accumulations either thermally or through the use of shielding. Additionally, OAT sensor location must be selected so that fuselage skin temperatures or other external conditions cannot influence the temperature readings.

Icing information is obtained through the use of an ice detector or an ice accretion rate system.

One of the primary signals to the deice controller is the ice indication/ice rate input which is generally used to initiate the deice sequence and determine the heater on and off times when the deice controller is in the automatic mode. The trigger signal for the deice sequence is generally set to activate at a predetermined value of ice rate or at a reference ice accretion obtained from the ice detector rate or ice detector count. Helicopters have special problems in ice detection and rate measurement; see Section II.1.4.2. In determining the reference ice thickness for de-ice sequence initiation, several topics should be considered such as; the rate of torque rise, size of shed ice which impacts other aircraft components, and the ice thickness which results in satisfactory shedding (no runback).

Further information on ice detectors commonly used with electro-thermal ice protection systems is found in Sections II.1.3.3 and II.1.3.5. Visual means also exist for ice detection and ice thickness indication.

2.3.7 Flight Sensors

Any large aircraft has small components that accumulate ice if not protected. Typical examples are pitot tubes and angle of attack indicators. The need for ice protection of these components can be determined by answering the following questions:

a. Will ice accumulate on the object in question and in what amount?
b. Will this accumulation adversely affect the component's function?
c. If the component's function is affected, will this have an effect on safe flight of the aircraft?
d. What is the effect of ice shedding from the component on other components, such as the engine inlets? Will ice shedding affect engine operation?

The current practice for small, critical components is the application of electrical heat to the critical area.

Static ports located on the fuselage (if suitably far from the nose of the aircraft) usually have not needed protection. In any case, where ice protection is provided for small components, the effect of a single failure should be considered. In the case of pitot tubes, for example, if the pilot's pitot tube fails, the copilot's may be used.

2.3.8 Radomes and Antennas

2.3.8.1 Radomes

Electrical systems are not applicable to the ice protection of radomes because of the interference from the heating element (reference 2-5).

2.3.8.2 Antennas

Ice protection for antennas, if provided, can be of the electro-thermal type. General practice has been not to provide such protection, but large antennas such as those on the U. S. Army EH-60A helicopter are protected to avoid possible breakage due to large ice buildups. In some cases, flexible antennas improve the self-shedding of ice.

2.3.9 Miscellaneous Intakes and Vents

General practice has been to provide no protection for flush inlets and vents. Although detailed studies must be made for each new application, it is usually found that the flush inlets will not close completely in icing, therefore, protection is not provided. Static ports located on the fuselage (if suitably far from the nose of the aircraft) usually have not been protected. Inlets for air conditioning systems may or may not be protected depending on whether ice formed on the inlet would shed into the heat exchangers or turbo-compressors and cause damage. In any case, where ice protection is provided, it will probably be of the electro-thermal type.

2.3.10 Other

Other small components of an aircraft that accumulate ice if not protected are wing fences, stabilizer mass balance "horns," tip tanks, and wheel covers. The need for ice protection for these components can be assessed by answering the questions listed in Section 2.3.7. For many of these miscellaneous components, electro-thermal is the only practical ice protection method.

III.2.4 WEIGHT AND POWER REQUIREMENTS

The effect of an installed electro-thermal ice protection system on the weight and power requirements of some typical aircraft is presented in Table 2-1. From these data, the actual aircraft performance penalties can be predicted. These numbers are representative of what would be required; however, a more detailed analysis would be necessary to determine them more precisely for any particular airplane (reference 2-1).

III.2.5 ACTUATION, REGULATION, AND CONTROL

Automatic initial actuation of electro-thermal systems is discouraged for several reasons. First, automatic actuation decreases the reliability of the system. It could fail to be turned on, or be turned on when not required, reducing heating element life and wasting energy. Second, the pilot needs to determine if the system is functioning properly. His attention may not be drawn to a system that automatically actuates. Third, the complexity of the system is greater. If a manual backup is required, then an additional annunciator is required to show the primary system failure. More components require more frequent replacement and higher maintenance cost.

Having emphasized the dangers of automatic initiation, it must be stated that once activated, automatic regulation and control are very valuable in reducing crew workload. Annunciator lights or a CRT display should then be used to inform the pilot of system status or faults.

III.2.6 OPERATIONAL USE

2.6.1 Anti-Icing Systems

In most cases, anti-icing systems should be turned on as soon as icing conditions are encountered. If too much ice has accumulated, the system will be required to de-ice the surface. The watt density is usually too low to do this quickly and will likely produce an objectional amount of runback in the de-icing process.

These systems also need to be tested prior to flight into known icing conditions. In some cases, an annunciator light will indicate when the system is functioning properly. In other cases, the aircraft's ammeter or power meter are observed for reading changes when the system is turned on or off.

2.6.2 De-Icing Systems

De-icing systems do not have to be turned on until after ice has started to accumulate on the surface protected. The watt density is sufficiently high to remove accumulated ice. Of course, the system should be turned on before large amounts of ice accumulate or some undesirable secondary effects may occur. For example, if operation of the propeller de-icing system is delayed too long, the ice thrown from the propeller would be thicker than usual and could cause excessive fuselage skin damage.

The de-icing systems need to be tested prior to flight into known icing conditions. This is done by turning on the system and observing the system ammeter or power meter to ensure the proper power is being provided. A periodic flicker should be observed when the system cycles from one area to another. The system would then be turned off until required. This conserves energy, extends the life of the heating element, and in some cases, keeps an element from burning out on the ground.

2.6.2.1 Typical System Operation

The following is a description of a typical electro-thermal de-icing system in operation. When the aircraft flies into conditions where the outside air temperature is below a certain value, typically a value between 0°C and 4°C, the de-icing system becomes armed (prepared to start the deice sequence).

Once activated by input from the external sensors (i.e., ice detector, ice rate probe, outside air sensor) or from pilot manual control, the deice system will automatically sequence power to the propeller or rotor blades according to the programmed cycle schedule. In general, the deice heater element-on-time is set by the signal from the outside air sensor while the deice trigger (start of deice cycle) is controlled by the icing rate signal.

When the aircraft enters the icing environment, the ice detector is typically employed to sense the accumulation of ice and determine the rate of ice accretion. At a predetermined accretion (for helicopters it is generally based on a reference rotor ice thickness, or a rotor torque increase) the deice controller is activated and power is supplied in a predetermined sequence to the blade heater zones.

In this system, the off-time for a zone (i.e., delay time between deice cycles) is controlled by the icing rate indication system while the heater element on-time is controlled by the outside air temperature indication system. Manual on-time control can also be set by a pilot switch, however this would increase the potential for blade overheating if an incorrect switch position were selected by the pilot.

Once a de-ice cycle is initiated, the cycle will proceed in the programmed manner through each heater element, always starting with the same initial element. For helicopters, the number of blades on the rotor head generally determines the deice firing sequence from blade to blade. For example, on a four-bladed head, the first element on each of the four blades might be powered, or more probably the first element of opposing blades (i.e., blades 1 and 3) would be powered, with power being applied element-to-element on blades 1 and 3 until each element had been fired. The power sequence would then switch to blades 2 and 4, and the power sequence repeated. In the case of an odd number of blades, such as three, the elements of each blade are fired simultaneously so as to prevent asymmetric ice shedding.

The element heating sequence may also be varied to meet the de-icing requirements of changing icing conditions. For example, the power may be applied to an outboard rotor element or the stagnation region element more frequently to reduce the amount of ice build-up at a higher liquid water content.

During the heat-on portion of the deice cycle, the controller resets the ice rate accumulator to zero and begins the ice rate accumulation for the next cycle. Under severe icing conditions (i.e., high liquid water content), the next deice cycle may be ready to fire at the completion of the current cycle, thus the deice sequence will begin immediately. At lower icing rates, there may be a considerable time delay before the next cycle.

2.6.2.2 Test Considerations

Tests of components and subsystems during the design and development of an electro-thermal propeller or rotor de-icing system in simulated severe icing conditions are necessary as part of the overall certification/qualification process and should precede flight test of the complete aircraft ice protection system in natural icing conditions.

Heater Element Tests

Several types of tests are used to provide design data for electro-thermal heaters. Fatigue tests of candidate heater foils or wire matrices should be accomplished to establish fatigue life of the heater elements, especially for those bonded to structure with large cyclic loading or vibrations. Examples are rotor blades and leading edge slats. The heater elements should be fabricated in a sample which encloses the heater in the same structural elements which would surround it in the actual aircraft. The sample is then subjected to repetitive loads in a tensile fatigue test machine. While being subjected to the repetitive loads, the heater can be energized to simulate the effects of temperature variations.

The above described tests are useful for comparing the relative value of various heater element materials, but a more conclusive test may be devised. This test would use a structural segment fatigue test specimen exactly the same as used for normal qualification fatigue tests common to aircraft qualification programs. During such a test, the heater element should be energized to bring the heater element temperature up to the maximum permissible design values.

Another useful test is a bench test of a segment of the structures (rotor blade, propeller, inlet lip, etc.) to examine the heat transfer characteristics between the heater element and the surface. Variations in the thickness of materials and possible voids between the heater element and the surface, along with the spacing of the heater elements, can cause considerable inconsistency in surface temperatures. Since the de-icing method requires the surface to be heated and then allowed to cool rapidly, it is important to know the time required to heat and then cool the structure. Although the surface heating and cooling is affected considerably in flight by the air flow and cloud moisture, much can still be learned from laboratory tests of a heater in a sample structural segment. Temperature sensors located within the design specimen can provide valuable heat transfer data.

Power Transfer System Tests

For helicopters, all electro-thermal rotor blade de-icing systems to date use the same general method for electrical power transfer from fixed to rotating members. Propellers have similar power transfer methods. A two channel or three channel slip ring (DC or AC current, respectively) converts the fixed to rotating hardware and a solid state or mechanical stepping switch routes the electrical power to the appropriate blades heater elements. Slip rings and stepping switch systems should be laboratory tested, simulating actual flight conditions as closely as possible, including temperature effects. The controller should also be tested to evaluate system performance and determine the controllers operating characteristics.

Icing Wind Tunnel Tests

Icing wind tunnel tests are valuable to the extent that flight conditions can be simulated. The available facilities are given in Section IV.1. In general, large size and high speeds are difficult to simulate, but a wide range of temperature and icing cloud conditions are available.

Icing wind tunnel tests of helicopter airfoils have been conducted, but no icing wind tunnel facility at present is large enough to contain a full-scale rotating helicopter rotor. Although the cyclical variations in blade angle of attack can be simulated, the dominant effects of centrifugal force cannot be simulated without actually rotating the blade. For this, ground spray rigs are useful; see IV.1.3.2 and Table IV.1-4. An oscillating rig can be used to simulate some of the angle of attack variations and blade bending effects to assist in the evaluation of the rotor de-ice capability. The icing wind tunnel is very helpful in better defining the required power density distribution and to verify adequate coverage.

Dry Air Flight Tests

Prior to testing a blade electro-thermal de-icing system in simulated or natural icing conditions, flight tests in non-icing conditions can be used to determine system operating characteristics and internal blade temperature profiles under rotating conditions. EMI (Electro Magnetic Interference) tests should also be done at this time.

Icing Flight Tests

Flight tests in natural icing conditions are presently required as a major part of certification of an aircraft ice protection system for operational capability into known icing. Artificial icing tests, such as spray tankers, can also be used to supplement natural icing testing and expand the certification envelope. Flight in icing conditions is used to optimize heater on-times, deice sequencing, and heater off-times. Icing flights can also be used to study the effects of ice shedding and discover any problems in flight which did not appear during previous testing.

Aircraft and systems performance degradation limits are generally established for flight into icing conditions. These limits include:

- Range of operation
- Maximum forward speed
- Maneuvering capability
- Rate of climb performance
- Dynamic and fixed system component loads
- Engine Operation
- Aircraft systems and avionics system operation
- Vibration level

The test equipment required for an icing trials program using a real-time data acquisition system (i.e., on-board system or ground station telemetry system) includes:

- Master control unit
- Signal conditioners
- Pulse modulation unit
- On-board unit
- Trend recorder
- Leading edge cameras
- Rotor cameras
- Engine inlet cameras
- Leading edge ice thickness indicators
- Ground station data processing and ground interface
- Reference liquid water content (LWC)
- Reference outside air temperature (OAT)
- Water droplet measuring system

The flight data parameters necessary for a detailed evaluation of the aircraft performance characteristics during the icing flight include:

- Basic aircraft parameters (airspeed, altitude, rotor rpm, OAT, control positioning, attitude, actuator positions, load factor, gross weight, rate of climb, time, event, fuel used, etc.)
- Rotor system (shaft torque, bending, fixed link load, pitch link load, pitch shaft bending, blade temperatures, blade loads, etc.)
- Power plant (fuel flow, torque, gas generator speed, turbine inlet temp., etc.)
- Electrical system (current and voltage, LWC, icing rate, threshold signal, ice counts, and control discretes)
- Environmental (OAT, LWC, droplet size)

Figures 2-16 and 2-17 illustrate a typical de-icing system optimization flow and the inflight monitoring system, respectively.

III.2.7 MAINTENANCE, INSPECTION, AND RELIABILITY

The electro-thermal elements should be inspected periodically for damage. Broken elements are a common form of damage and should be replaced. If other damage is found, the system should be checked thoroughly to determine if it is functioning properly.

Sometimes deterioration of the exterior covering on surface leading edge boots, for example, may cause premature failures. These should be inspected periodically. They should be cleaned and a protective coating should be applied periodically per the manufacturer's recommendations.

There is little maintenance required for an electrically heated windshield except keeping it clean. Stone or gravel pitting on the outside layer may allow static electric discharges to occur to the heating element. This could cause the element to fail prematurely.

Slip rings must be kept clean to avoid sparking and the resulting pitting of the contact elements. If inspection of the slip rings is difficult, sealing of the slip rings from outside contamination must be done as well as possible.

III.2.8 PENALTIES

There are three primary areas of penalties due to electro-thermal de-icing installation: weight, electric power, and aerodynamic performance. The power required for a complete electro-thermal anti-icing system is very large and in many cases impractical. Typical weight and power requirements are given in Section 2.4. There are two primary methods of installing electro-thermal systems: attaching flexible wrap-around heating pads to the structure with adhesive and molding the heating element into the surface of the structural member. Typical weights involved in either installation are presented in Table 2-1.

The heating pads used in these installations are fairly thin and may not affect the aircraft's performance. Little, if any, performance degradation would be expected from molded heater installation. In higher speed aircraft and helicopter blades, rubber heating pads are subject to sand and rain erosion and hail damage. A metal overshoe will protect the pads and at the same time may even out the heat distribution and prevent cold spots on the surface. Detracting from the overshoe installation is the loss in heater efficiency and the degradation in rotor blade performance.

Electro-thermal ice protection may be applied to windshields with small or negligible loss in aircraft performance (Section 2.3.2).

Electro-thermal ice protection may be installed on the external surface of a propeller (III.2.3.5) without appreciably affecting its performance. All power to the heating pads is supplied through slip rings at the propeller hub resulting in added aircraft weight. Heating element installation on the propeller interior would protect the heating elements from damage, but the efficiency reduction and the repair difficulty make the external system more feasible.

III.2.9 ADVANTAGES AND LIMITATIONS

The advantages and limitations of the electro-thermal system will be discussed and compared with other candidate systems in Section III.6.

III.2.10 CONCERNS

Runback icing occurs when local heating of accumulated ice results in water running back from heated areas to unheated areas where refreezing then occurs.

For an anti-ice system, the entire surface may need to be heated to prevent runback or all the water droplets impinging on the leading edge surface may have to be evaporated. For engine inlets,

anti-ice protection is preferred to avoid accumulated ice from being ingested and possibly causing damage or engine flameout.

While using the deice system, the minimum time required to heat the critical surface area to release the ice with a minimum amount of water remaining must be found during test. Rotor blades are generally deiced due to power constraints. Runback on rotor blades may cause aerodynamic degradation and may cause residual rotor performance losses that cannot be eliminated by the de-icing system.

The impact of runback ice refreeze varies considerably with rotor geometry such as blade chord, thickness, and leading edge profile.

Element burnout is of concern since no redundancy exists and failure is total. No practical method is available for detecting incipient burnout.

Ice shedding is a concern for all ice protection systems, and the electro-thermal system does not give a fixed ice particle size under normal icing condition variations. Ice shed unsymmetrically can cause difficulty ranging from bothersome (inboard wing leading edges) to disastrous (helicopter rotors).

III.2.11 REFERENCES

2-1 Bowden, D.T., Gensemer, A.E., and Skeen, C.A., "Engineering Summary of Airframe Icing Technical Data," FAA ADS-4, December 1963.

2-2 Lawrence, Jr., J.H., "Guidelines for the Design of Aircraft Windshields/ Canopy Systems," USAF WADC-TR-80-3003, February 1980.

2-3 Hassard, R.S., "Plastics for Aerospace Vehicles. Part II, Transparent Glazing Materials," MIL-HDBK-17A, Part II, January 1973.

2-4 Anon., S.A.E. Aerospace Report, "Applied Thermodynamics Manual," SAE, ARP-1168, 1969.

2-5 Messinger, B.L. and Werner, J.R., "Design and Development of the Ice Protection Systems for the Lockheed Electra," paper presented at 1959 Aircraft Ice Protection Conference, D. Napier and Son, Ltd. (Also published in December 1959 issue of Space/Aeronautics.)

TABLE 2-1

Weight and Power Requirements for Electro-Thermal Ice Protection Systems For Three Typical Aircraft (Reference 2-1)

Aircraft	Aircraft Component	System Type	Weight Lb.		
"A"	Windshield	Elec. Anti-icing	10	1.5	2.0
(Twin-	Propeller	Elec. De-icing	10	0.8	1.1
Engine		Generator (a)	15		
Recip.)	Total		35	2.3	3.1
	Wing and Tail	Elec. De-icing	40	6.8	9.1
	Windshield Elec.	Anti-icing	10	1.5	2.0
	Propeller	Elec. De-icing	10	De-iced with	
		Alternator (b)	20	wing and tail	
	Total		80	8.3	11.1
"B"	Windshield	Elec. Anti-icing	10	1.4	2.0
(Single-	Propeller	Elec. De-icing	5	0.6	0.8
Engine		Generator (a)	15		
Recip.)	Total		30	2.0	2.8
	Wing and Tail	Elec. De-icing	45	9.3	12.5
	Windshield	Elec. Anti-icing	10	1.4	1.9
	Propeller	Elec. De-icing	5	Deiced with	
		Alternator (b)	20	wing and tail	
	Total		80	10.7	14.4
"C"	Wing and Tail	Elec. De-icing	45	11.7	15.7
(Light	Windshield	Elec. Anti-icing	10	1.5	2.0
Twin Jet)	Engine Inlet	Elec. Anti-icing	10	3.8	11.8
		Alternator	20		
	Total		85	22.0	29.5

(a) 15 lb. added for increase in generating capacity (28-volt generator + transformer).

(b) 20 lb. added for increase in generating capacity (115-volt alternator substituted).

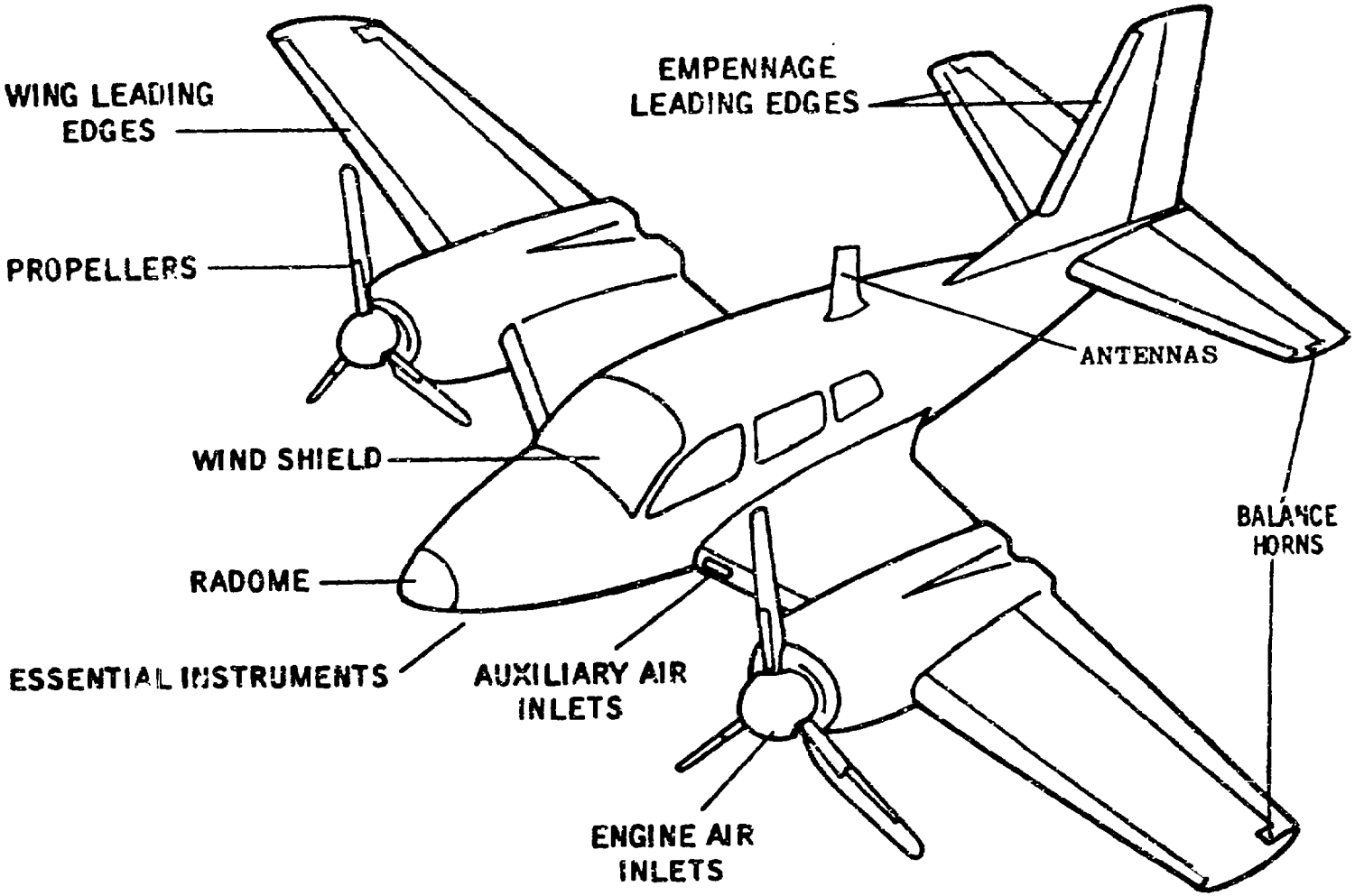

FIGURE 2-1. AREAS OF AIRFRAME THAT MAY REQUIRE ICE PROTECTION

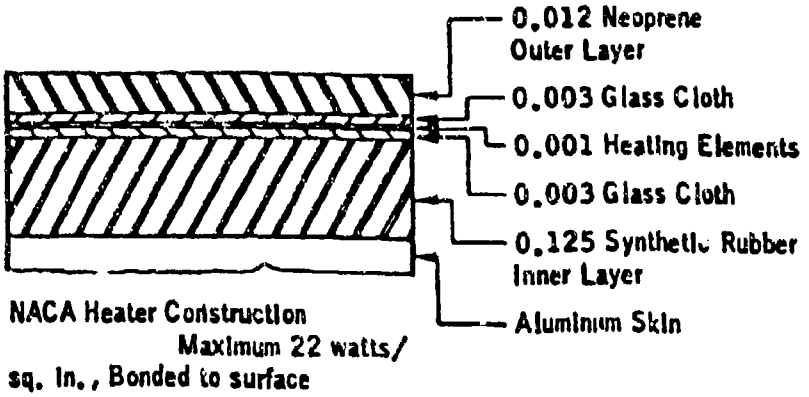

NACA Heater Construction
Maximum 22 watts/
sq. in., Bonded to surface

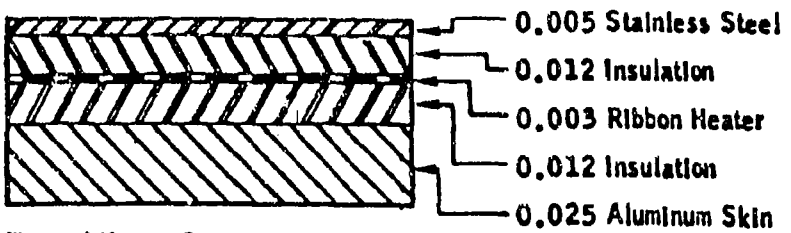

Typical Heater Construction with
Metal Overshoe - 18-22 watts/
sq. in. - Laminated to structure

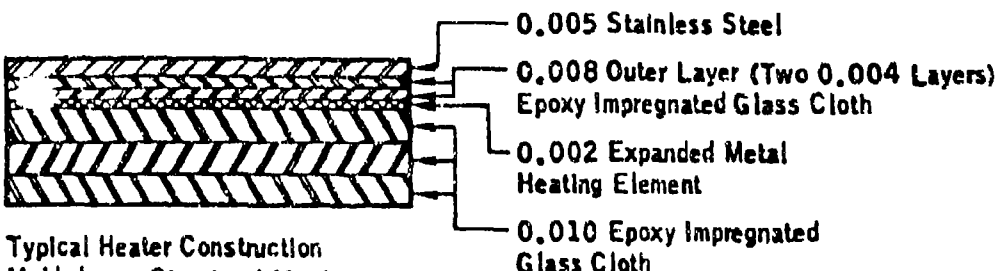

Typical Heater Construction
Molded as a Structural Member -
16-20 watts/sq. in.

FIGURE 2-2. CROSS SECTIONS OF TYPICAL ELECTRIC HEATERS

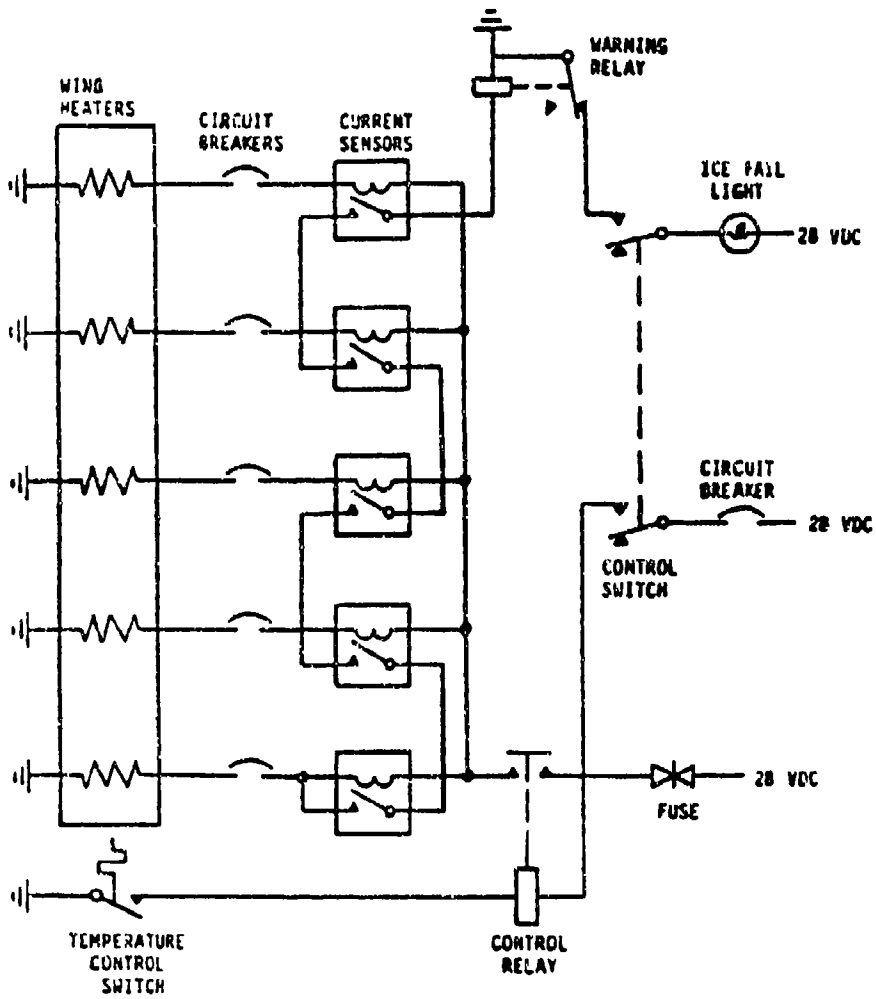

FIGURE 2-3. ELECTRO-THERMAL WING ANTI-ICE SYSTEM

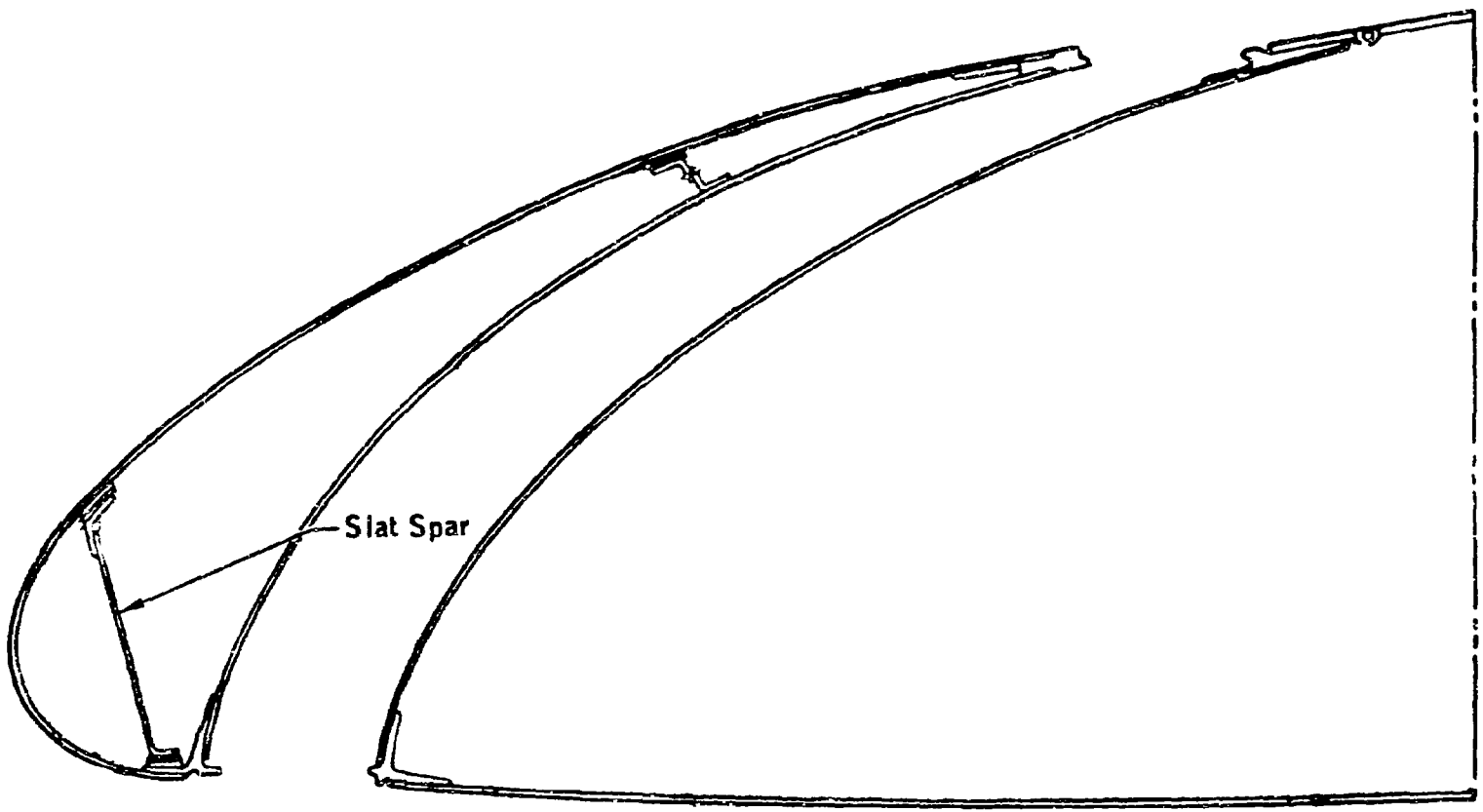

FIGURE 2-4. TYPICAL WING LEADING EDGE WITH SLAT

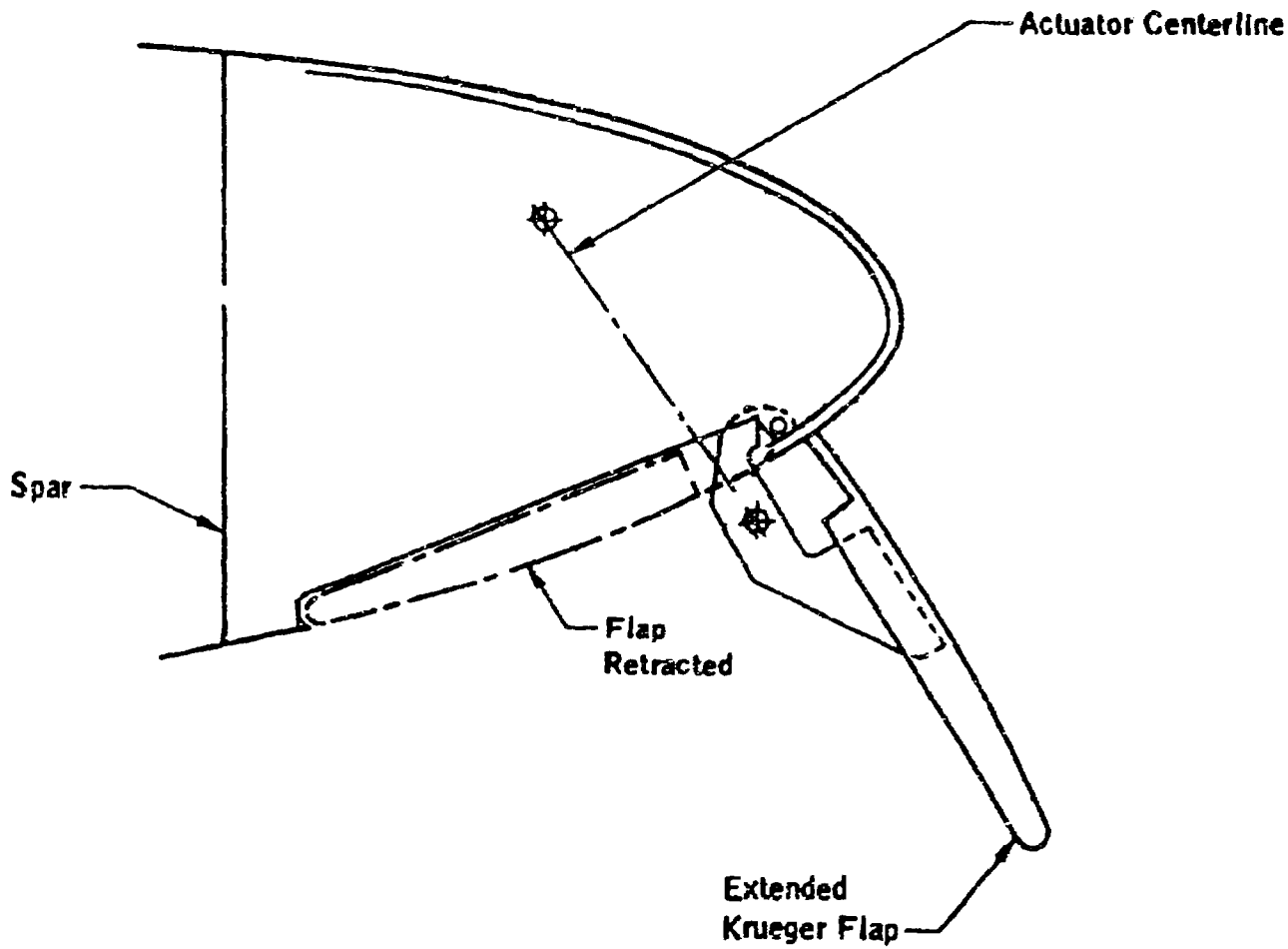

FIGURE 2-5. TYPICAL WING LEADING EDGE KRUEGER FLAP

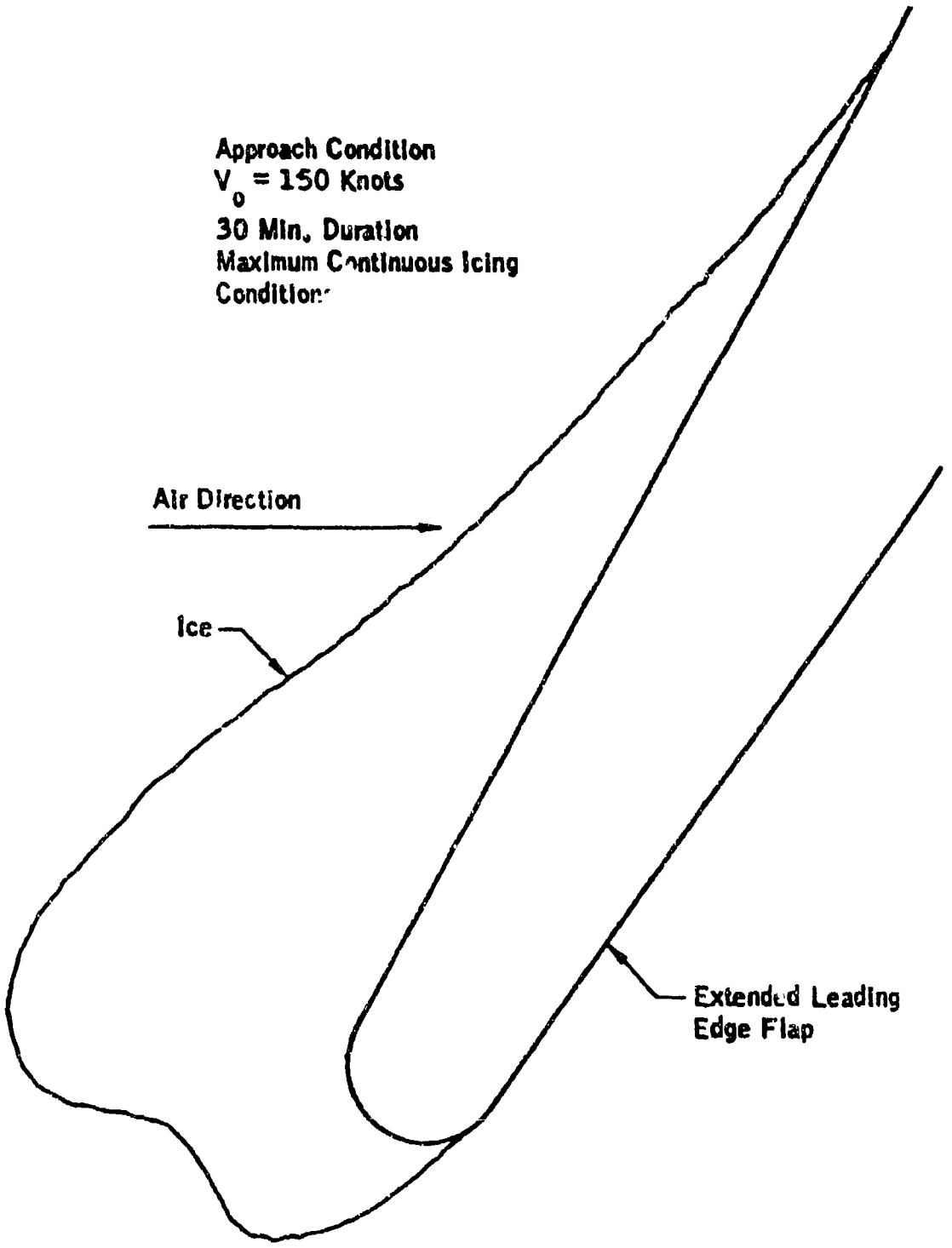

FIGURE 2-6. ICE ACCRETION ON UNPROTECTED EXTENDED LEADING EDGE FLAP FOR MAXIMUM CONTINUOUS ICING CONDITIONS

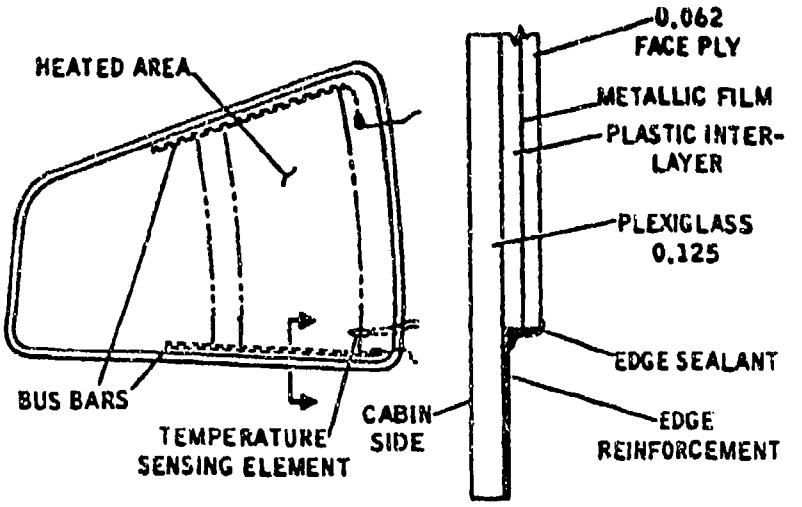

TYPICAL ELECTRICALLY HEATED PLASTIC WINDSHIELD

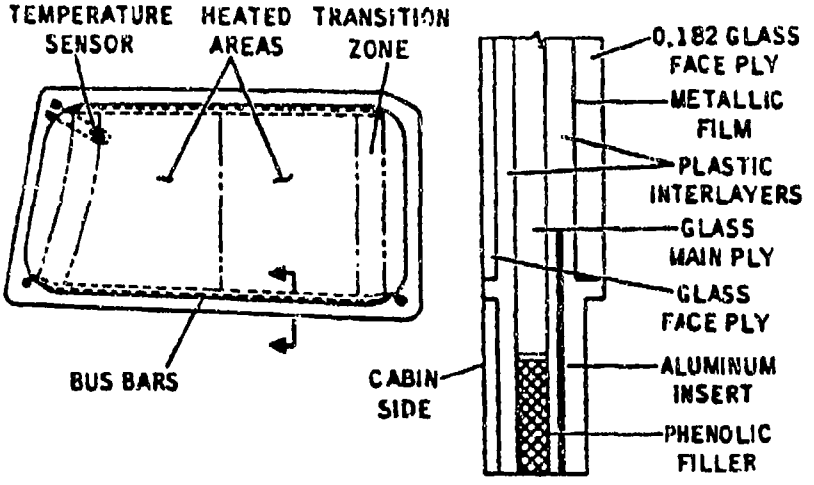

FIGURE 2-7. TYPICAL ELECTRICALLY HEATED WINDSHIELD CONSTRUCTION

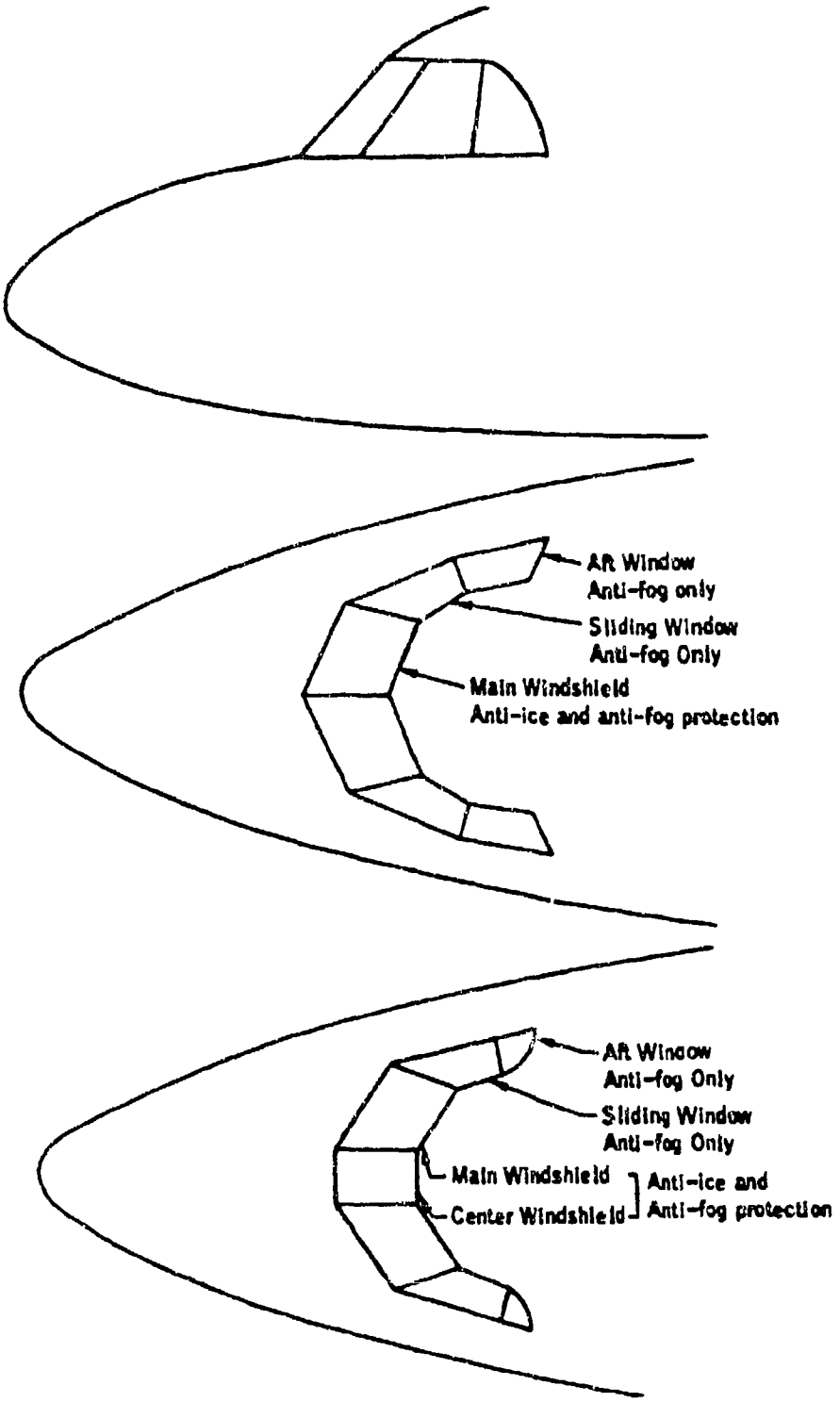

FIGURE 2-8. TYPICAL WINDSHIELD AREAS TO BE PROTECTED FOR TWO WINDSHIELD ARRANGEMENTS ON MULTI-ENGINE TRANSPORT

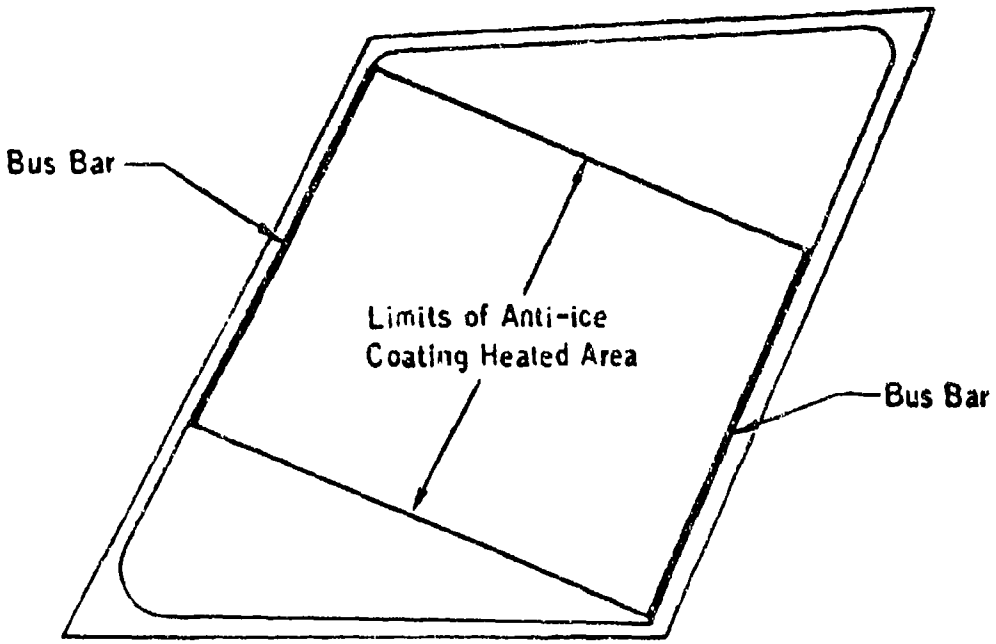

Note: Entire area of panel protected by anti-fog coating. Center windshield similar, except entire area had anti-ice and anti-fog protection.

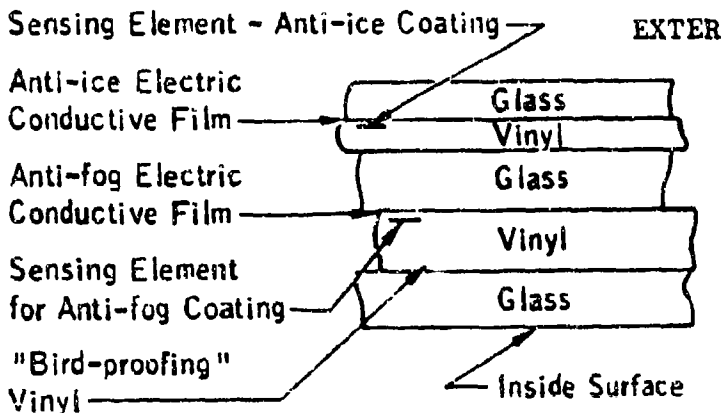

Section of Windshield
(a) Five Ply, Non-Rectangular, Birdproof Glass Windshield

FIGURE 2-9a. TYPICAL MAIN WINDSHIELD SHOWING CONSTRUCTION AND LOCATION OF CONDUCTIVE FILMS AND SENSING ELEMENTS

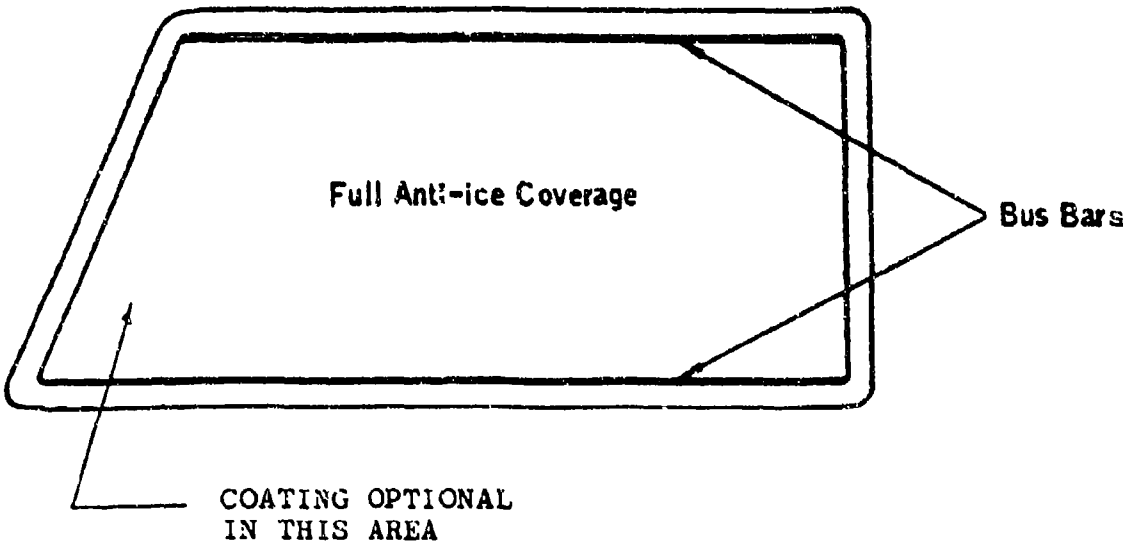

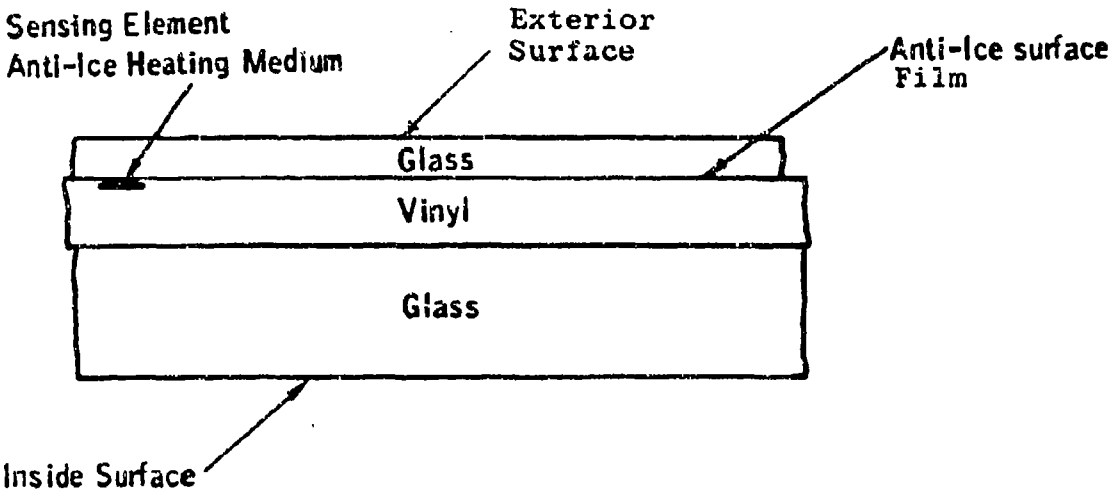

(b) Three Ply, Nearly Rectangular, Glass Windshield

FIGURE 2-9b. TYPICAL MAIN WINDSHIELD SHOWING CONSTRUCTION AND LOCATION OF CONDUCTIVE FILMS AND SENSING ELEMENTS

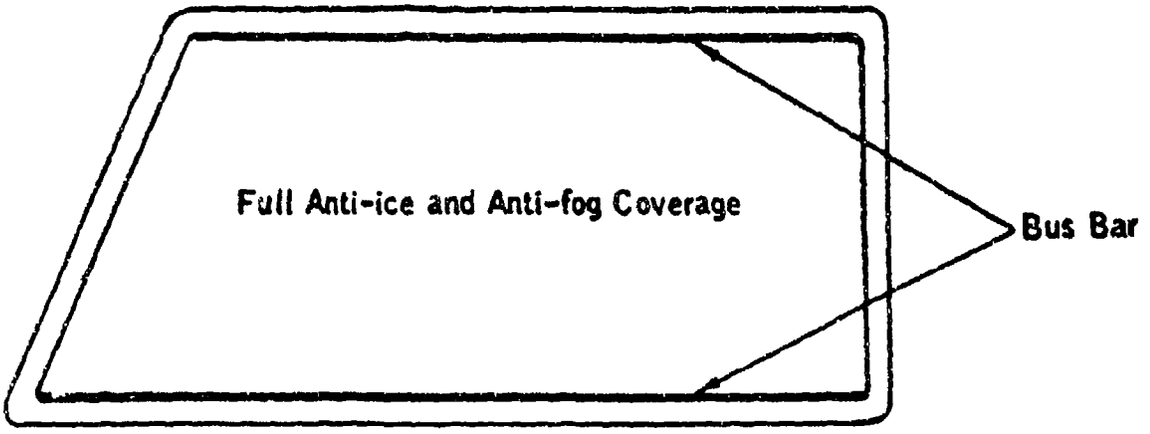

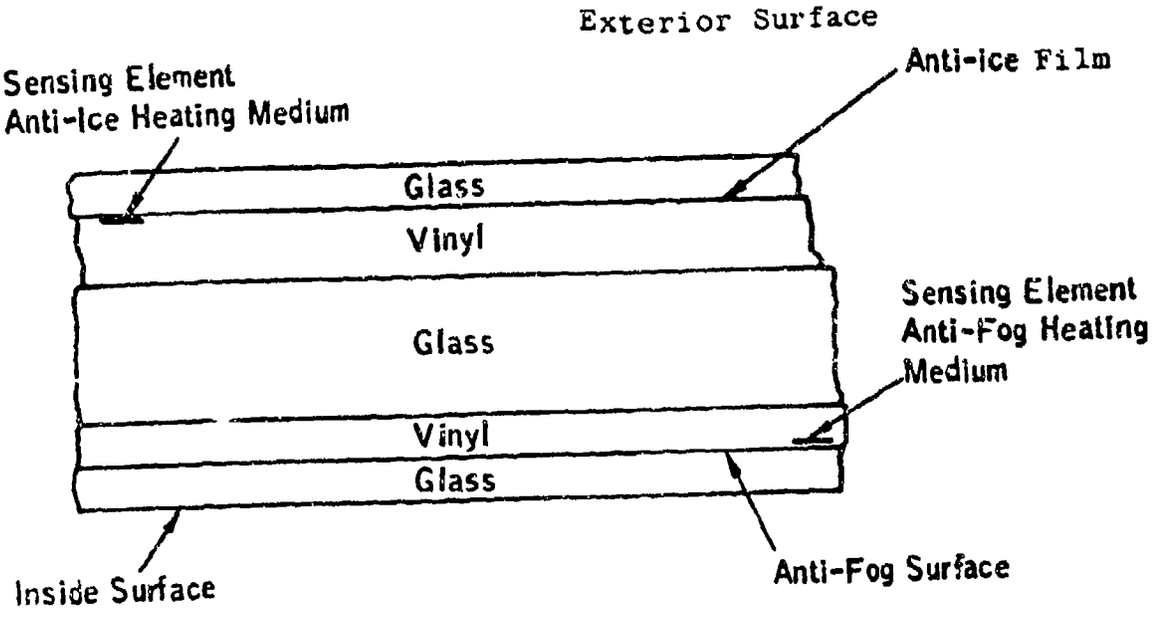

(c) Five Ply, Nearly Rectangular,
Birdproof Glass Windshield

FIGURE 2-9c. TYPICAL MAIN WINDSHIELD SHOWING CONSTRUCTION AND LOCATION OF CONDUCTIVE FILMS AND SENSING ELEMENTS

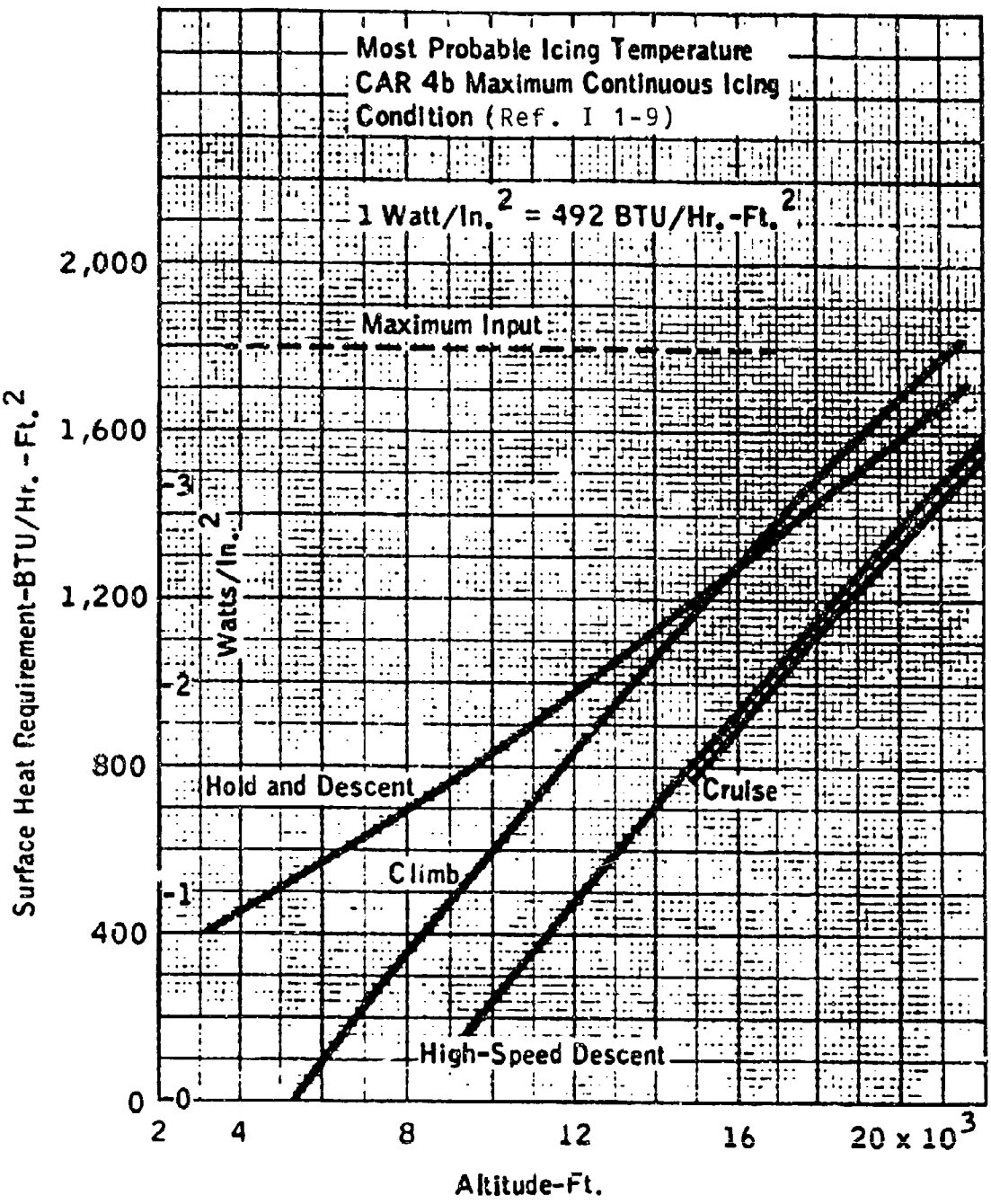

FIGURE 2-10. TYPICAL ANTI-ICING HEAT REQUIREMENTS VS. ALTITUDE FOR CENTER WINDSHIELD PANEL

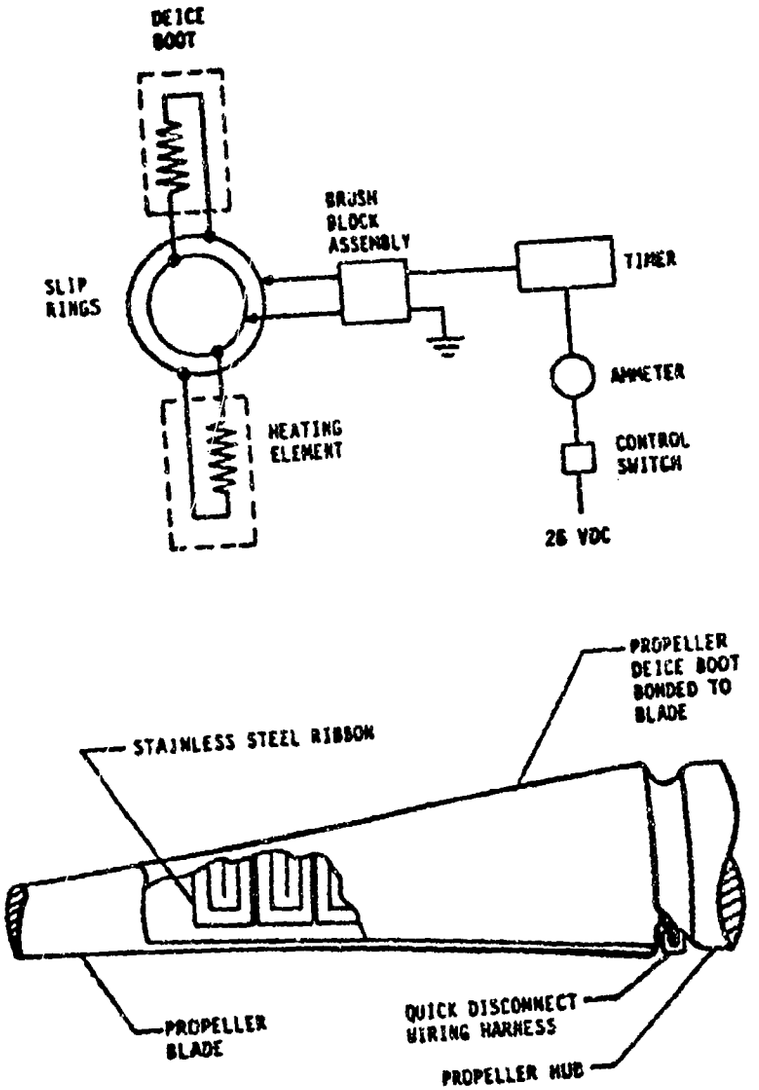

FIGURE 2-11. ELECTRO-THERMAL PROPELLER DE-ICE SYSTEM

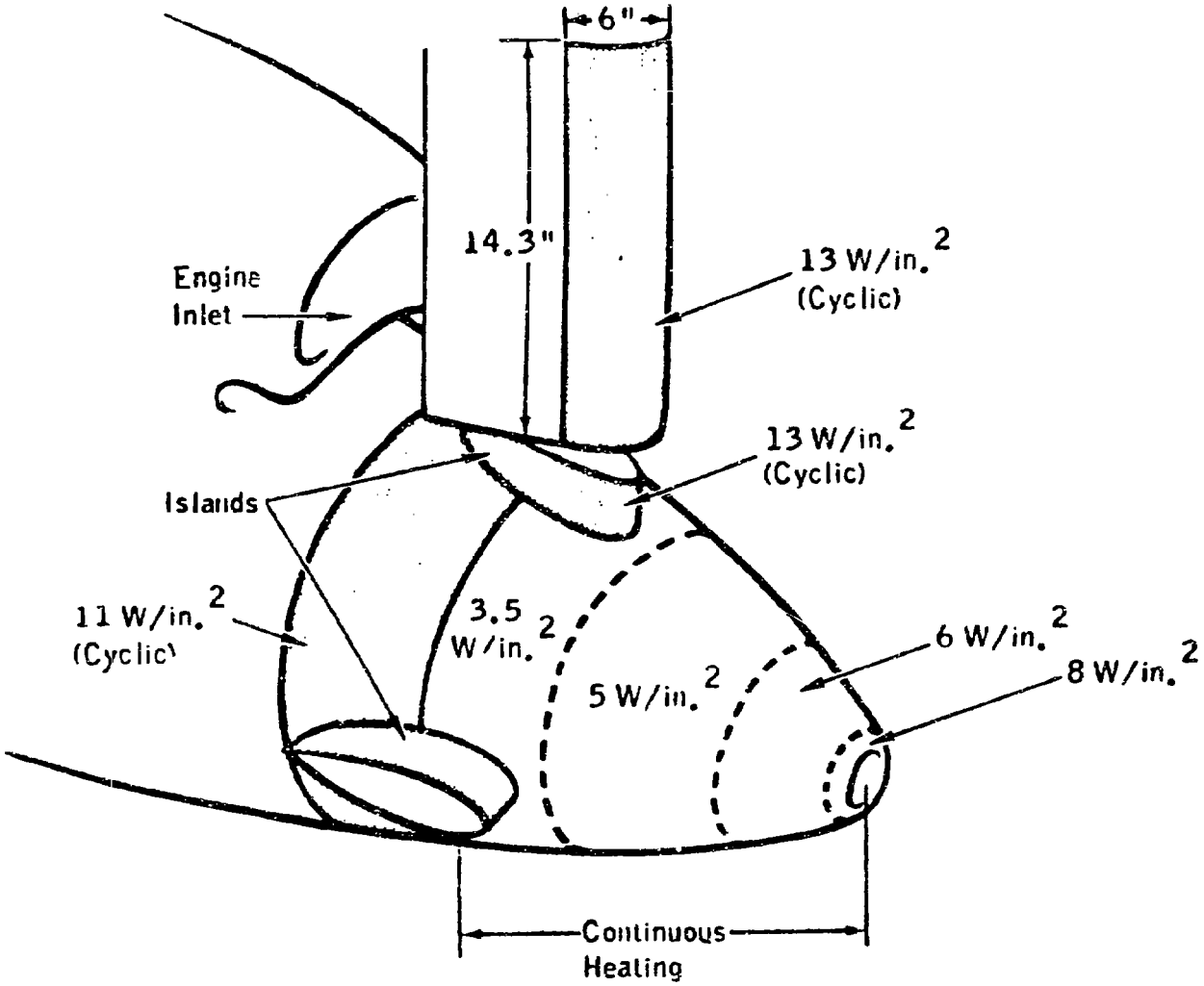

FIGURE 2-12. TYPICAL PROPELLER AND SPINNER ICE PROTECTION FOR TURBOPROP AIRCRAFT

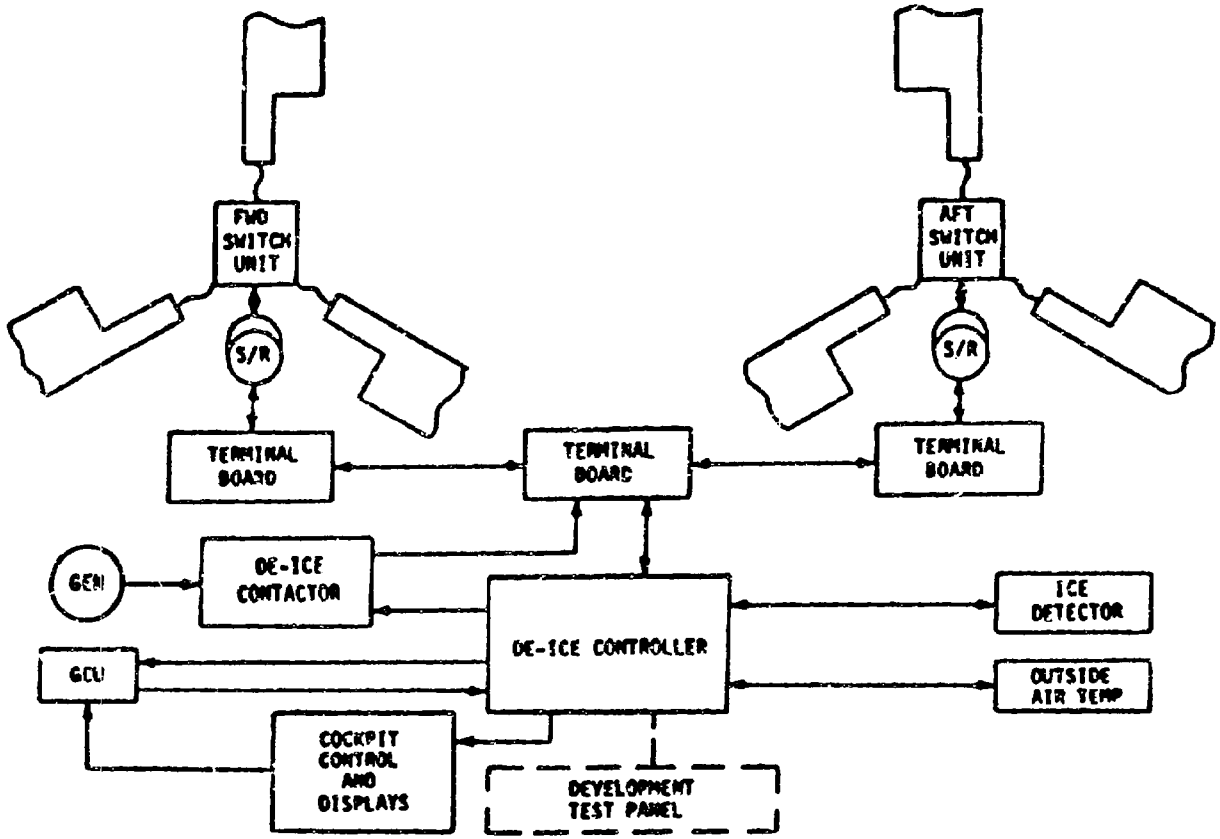

FIGURE 2-13. MAIN COMPONENTS FOR ROTOR DEICE SYSTEM

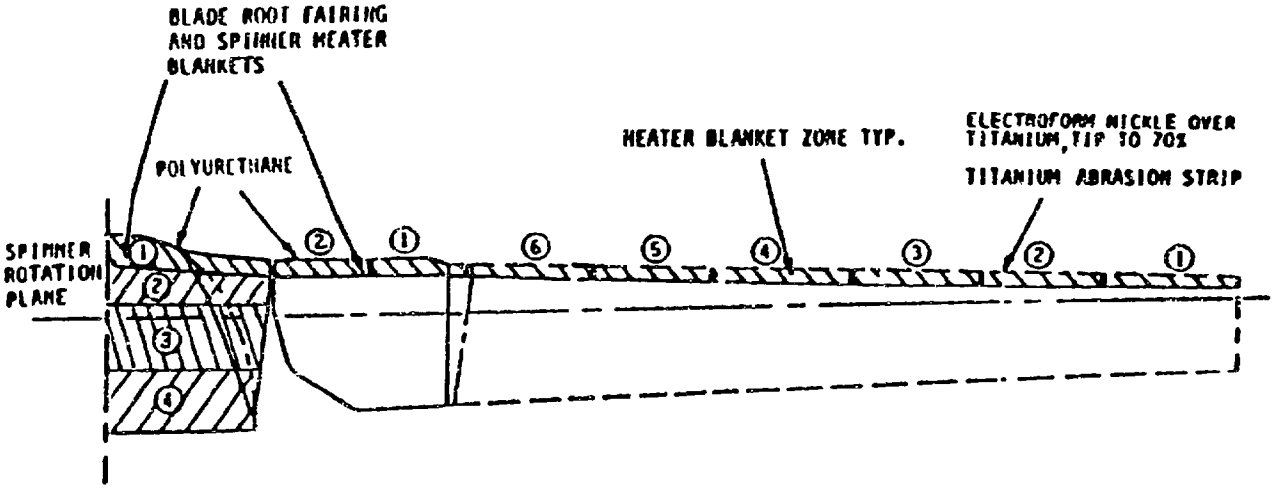

FIGURE 2-14. SPANWISE HEATER ELEMENT ARRANGEMENT

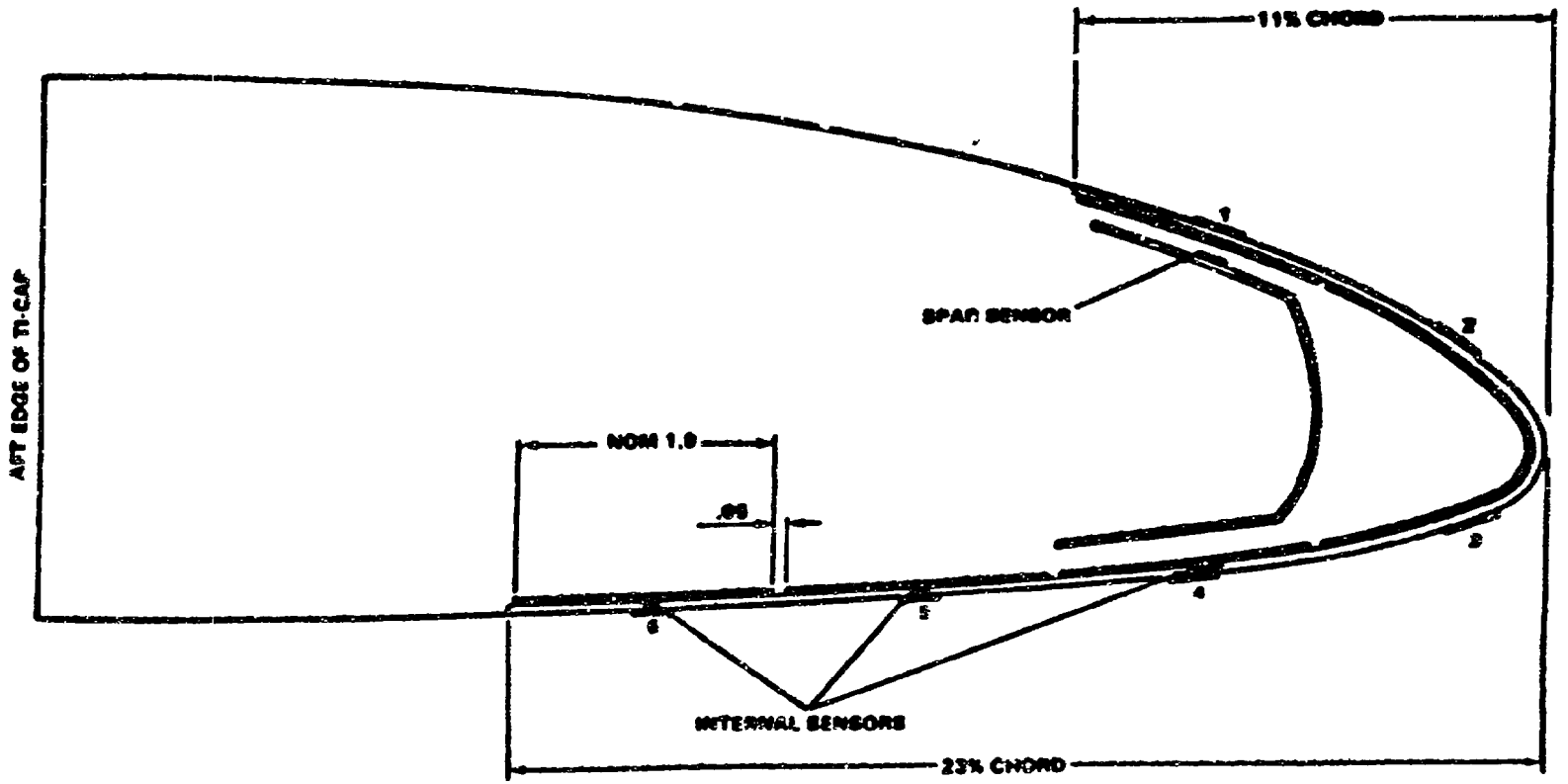

FIGURE 2-15. CHORDWISE HEATER ELEMENT ARRANGEMENT

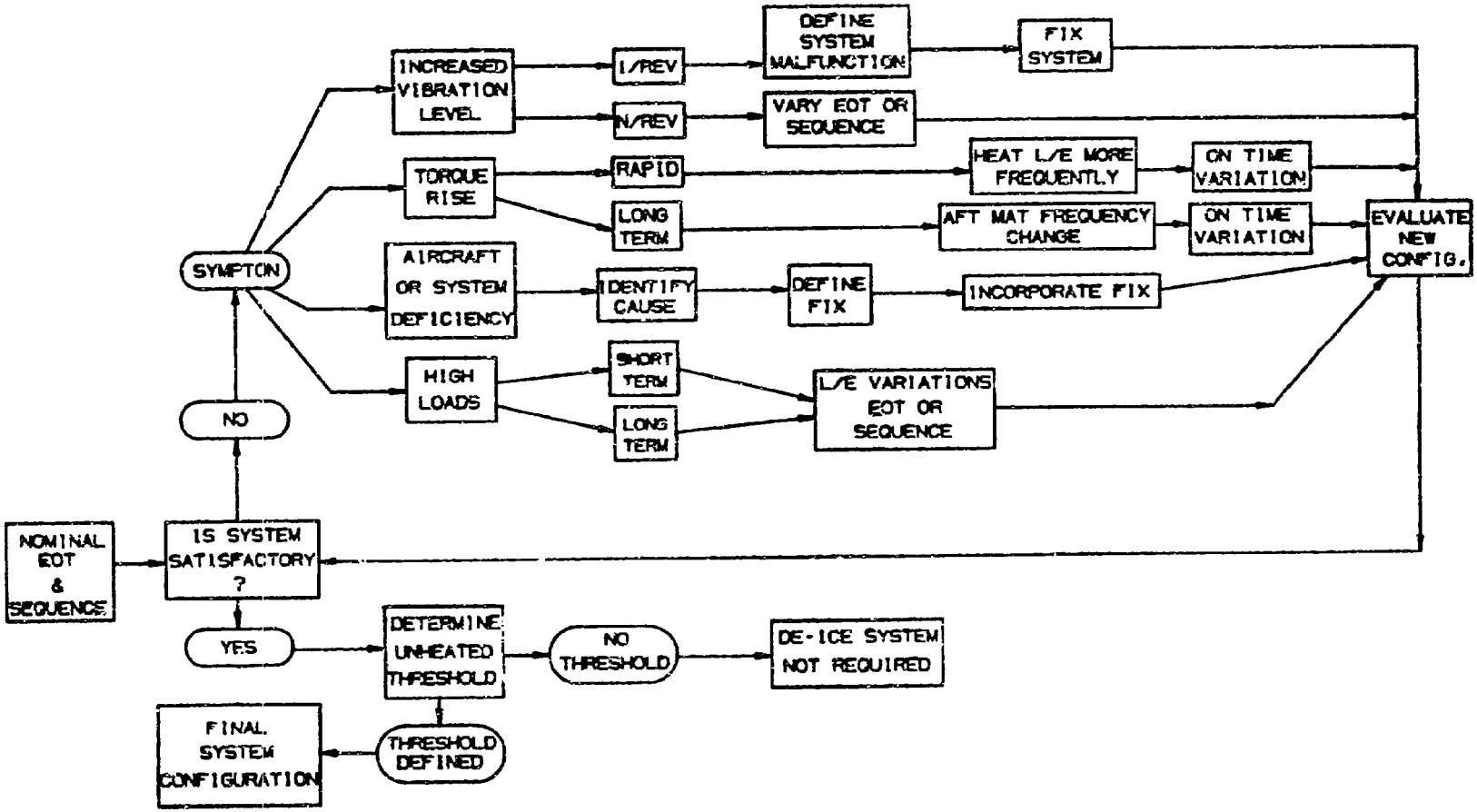

FIGURE 2-16. DE-ICING SYSTEM OPTIMIZATION

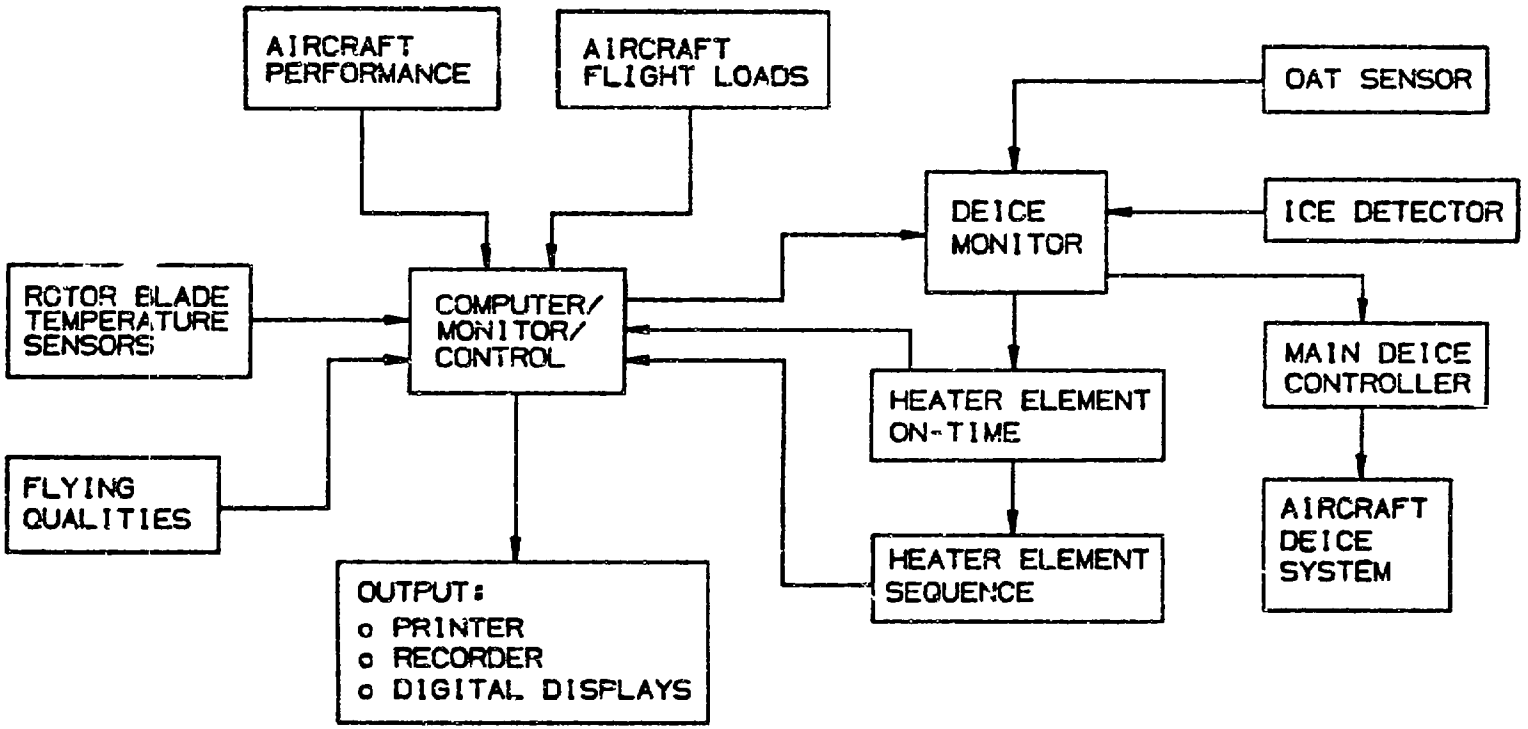

FIGURE 2-17. DATA AND CONTROL FUNCTION IN-FLIGHT MONITOR

CHAPTER III
SECTION 3.0
FLUID ICE PROTECTION SYSTEMS

CHAPTER III - ICE PROTECTION METHODS
CONTENTS
SECTION 3.0 FLUID ICE PROTECTION SYSTEMS

	Page
LIST OF TABLES	III 3-iii
LIST OF FIGURES	III 3-iv
SYMBOLS AND ABBREVIATIONS	III 3-v
GLOSSARY	III 3-vi
III.3.1 OPERATING CONCEPTS AND COMPONENTS	III 3-1
III.3.2 DESIGN GUIDANCE	III 3-2
3.2.1 Anti-Icing	III 3-2
3.2.2 Natural De-Icing	III 3-2
3.2.3 De-Icing	III 3-2
3.2.4 Fluid Selection	III 3-3
3.2.5 Fluid Supply System	III 3-4
III.3.3 USAGES AND SPECIAL REQUIREMENTS	III 3-5
3.3.1 Airfoils and Leading Edge Devices	III 3-5
3.3.2 Windshields	III 3-5
3.3.3 Engine Inlet Lips and Components	III 3-6
3.3.4 Turbofan Components	III 3-6
3.3.5 Propellers, Spinners, and Nose Cones	III 3-6
3.3.6 Helicopter Rotors and Hubs	III 3-6
3.3.7 Miscellaneous Intakes and Vents	III 3-7
III.3.4 FLUID AND WEIGHT REQUIREMENTS	III 3-7
III.3.5 ACTUATION	III 3-8
III.3.6 OPERATIONAL USE	III 3-8
III.3.7 MAINTENANCE, INSPECTION, AND RELIABILITY	III 3-9
III.3.8 PENALTIES	III 3-10
III.3.9 ADVANTAGES AND LIMITATIONS	III 3-10
III.3.10 CONCERNS	III 3-11
III.3.11 REFERENCES	III 3-12

LIST OF TABLES

		Page
3-1	Physical Properties of Monoethylene Glycol (MEG)	III 3-13
3-2	Physical Properties of TKS 80	III 3-14
3-3	Physical Properties of DTD 406B (AL-5)	III 3-15

LIST OF FIGURES

		Page
3-1	Freezing Point Plots for Aqueous Solutions of Several Freezing Point Depressant Fluids	III 3-16
3-2	FPD Freeze Point Increase Due to Dilution	III 3-17
3-3	Viscosity Characteristics of TKS 80 and DTD 406B (AL-5)	III 3-18
3-4	Construction of a Typical Porous Panel	III 3-19
3-5	Cross-Section of a Typical Porous Panel	III 3-20
3-6	Typical Panel Installation Illustrating Active Region and Stagnation Point Travel	III 3-21
3-7a	Typical Methods of Attaching Porous Panels to Aircraft Structure	III 3-22
3-7b	(Continued)	III 3-23
3-7c	(Continued)	III 3-24
3-8	Schematic of a Simple Fluid Ice Protection System	III 3-25
3-9	Schematic of Fluid Ice Protection System With Fully Redundant Equipment	III 3-26
3-10	Schematic of Helicopter Fluid Ice Protection System	III 3-27

SYMBOLS AND ABBREVIATIONS

Symbol	Description
AGARD	Advisory Group for Aerospace Research and Development
°C	Degrees Celsius
cm	Centimeter
cSt	Centi-Stokes (viscosity index)
°F	Degrees Fahrenheit
FAA	Federal Aviation Administration
FOD	Foreign Object Damage
FPD	Freezing Point Depressant
G	Gram
Hg	Chemical symbol for mercury
LWC	Liquid Water Content
m	Meter
MEG	Monoethylene Glycol
mg	Milligram
ml	Milliliter
mm	Millimeter
NASA	National Aeronautics and Space Administration
O.D.	Outside Diameter
SAE	Society of Automotive Engineers
WPAFB	Wright Patterson Air Force Base

GLOSSARY

biodegradable - The ability of a substance when exposed to a natural outdoor environment to spontaneously break down chemically into compounds which have no harmful environmental effects.

liquid water content (LWC) - The total mass of water contained in all the liquid cloud droplets within a unit volume of cloud. Units of LWC are usually grams of water per cubic meter of air (g/m^3).

micron (μm) - One millionth of a meter.

sintering - A metal hardening process such as heat tempering or adding an alloy to the base metal to produce a higher density material.

slinger ring - A torus-shaped tube with holes in the outer surface radius which serves as the distributor of anti-icing fluid for propeller and rotor blades. The ring is located at the hub of the rotor or propeller and rotates with the blades.

III.3.0 FLUID ICE PROTECTION SYSTEMS

III.3.1 OPERATING CONCEPTS AND COMPONENTS

Fluid ice protection systems operate on the principle that the surface to be protected is coated with a fluid that acts as a Freezing Point Depressant (FPD). When supercooled water droplets impinge on a surface, they combine with the FPD fluid to form a mixture with a freezing temperature below the temperature of the ambient air. The mixture then flows aft under the influence of the boundary layer and is either evaporated or shed from the trailing edge of the surface.

FPD fluid is distributed onto the surface leading edge to be protected by pumping it under pressure through porous material, by channeling the FPD fluid along leading edge grooves using centrifugal forces, or by spraying the fluid onto a surface using an external spray bar. The use of a fluid freezing point depressant can provide anti-icing or de-icing protection for almost any surface onto which the fluid can be distributed. The two primary means for accomplishing this are spray nozzles and porous skin panels.

Current systems normally use a glycol based fluid. Descriptions of various FPD fluids and factors to be considered in fluid selection are presented in Section 3.2.4.

Fluid ice protection systems for fixed wing aircraft were introduced in the mid-1930's by Kilfrost Ltd. and Dunlop Ltd. in Great Britain. Early systems used fabric wicks covered with wire gauze which was glued (or stitched, in the case of fabric covered wings) to the airfoil leading edges. The development of armored leading edges with barrage balloon cable cutters during World War II created the need for a compatible ice protection system. Neither pneumatic boots nor the fluid systems then available were suitable, because their installation impeded the free sliding of the balloon cable along the leading edge. In 1942, TKS (Aircraft De-Icing) Ltd. was formed at the instigation of the British government to meet this need. This new company was formed by bringing together three companies with suitable specialist knowledge. "T" was Tecalemit Ltd., a company specializing in the manufacture of lubrication equipment, and in particular, metering pumps. "K" was Kilfrost Ltd., a chemical company specializing in de-icing chemicals. "S" was Sheepbridge Stokes (now part of the GKN group), a company producing newly developed porous metals using powder metallurgy. TKS produced an ice protection system which used, as the fluid dispenser, tubes of 0.5 inch square (1.3 cm) cross-section which were recessed into the airfoil leading edges. The exposed face of these tubes was formed from porous powder metal through which the de-icing fluid exuded. This so called "strip" system went into service towards the end of World War II and was extensively used on British and European aircraft. In about 1950 porous panels were introduced by TKS as a more efficient means of distributing FPD fluid onto the airfoil leading edge. Initially, the outer skin of these panels was formed from stainless steel powder and later from rolled and sintered wire cloth. Porous panels constructed from sintered wire cloth proved very successful and still form a significant proportion of production. Examples of panels manufactured from this material may be seen on all versions of the

British Aerospace HS-125 aircraft including the 125-800 version.

The main features of the porous panels remain unchanged from the designs of the 1950's, but recent designs utilize adhesive bonding and tend to extend beyond the minimum working region, often forming the complete leading edge. In such cases the choice of material thicknesses and some construction features are usually influenced by structural strength requirements, bird strike and lightning strike considerations. The most recent development is the use of laser-drilled titanium for the porous leading edge. In comparison with sintered stainless steel mesh, this material offers a nearly 50% weight reduction, a greater resistance to impact damage, and a smoother surface finish. Examples of titanium panels may be found on the Cessna Citation SII (both civil and Navy versions) and the Beech Starship.

References 3-1 and 3-2 report the results of icing tunnel tests on various fluid ice protection installations that were conducted to improve the design data base for this concept.

Reference 3-3 is a FAA Technical Note on FPD methods containing many helpful insights and certification considerations.

III.3.2 DESIGN GUIDANCE

3.2.1 Anti-Icing

When sufficient fluid is present so that at the point of maximum water mass collection, the freezing point of the water-fluid mixture is below the local air temperature, no ice will form and the system functions in an anti-icing mode. This is the normal mode of operation for a fluid system in light to moderate icing conditions. It is achieved by turning the system ON prior to or immediately upon encountering icing conditions, then providing a continuous liquid supply in sufficient quantity to prevent ice formation.

3.2.. atural De-Icing

If icing conditions become too severe there may be insufficient fluid flow to totally prevent formation of ice. When this occurs, ice will begin to form at the point of maximum accretion, usually at or near the aerodynamic stagnation point. If the fluid continues to be pumped onto the surface the ice will not be able to bond firmly to the surface and the ice will grow until aerodynamic forces are sufficient to sweep it off the wet surface into the airstream. The process of periodic growth and shedding of ice, with the system in continuous operation, is referred to as the natural de-icing mode of the system.

3.2.3 De-Icing

The de-ice mode is a condition where ice is allowed to build up before the FPD fluid flow is begun, thus allowing ice to accumulate and bond to the wing surface. When the fluid ice protection

system is turned on, a flow is introduced between the ice and the surface to weaken the bond so that the ice will be shed by aerodynamic forces. However, there is evidence to suggest that, for some conditions, it may not be possible to deice a surface in this manner (reference 3-3). Fluid ice protection system testing should confirm satisfactory de-icing over the full range of operating conditions that the aircraft is likely to encounter if certification for the de-ice mode operations is desired.

Ice on windshields and ice accumulated aft of the active porous skin of a leading edge can be removed by spraying fluid, or allowing it to flow, onto the ice outer surface. With sufficient fluid, after a time interval, the surface ice will be both melted and loosened. Either of these two processes, in which the system is activated to remove established ice, is called the de-icing mode.

3.2.4 Fluid Selection

There are several chemicals which, when mixed with water, lower the water's freezing point. Glycol, alcohol, calcium chloride, nitric acid and sodium chloride are among those that exhibit this characteristic (reference 3-3). The most commonly used chemicals for in-flight or ground de-icing or anti-icing are glycol and alcohol. Glycol's freezing point is about 10°F (-12°C), but when mixed with an equal volume of water, the freezing point lowers to -10°F to -40°F (-22°C to -40°C), depending on the type of glycol. Fluid ice protection for an airfoil can be obtained by mixing glycol based fluids and cloud water droplets on the airfoil leading edge.

Most fluids in the alcohol and glycol groups have freezing point depressant qualities that would make them suitable for ice protection purposes (see figure 3-1); hence their other properties are more important in choosing an appropriate fluid for a fluid ice protection system. See Section 3.10 for consideration of toxicity

For aircraft systems using a freezing point depressant fluid, service experience has shown that the most suitable fluid is a mixture consisting of about 80 percent monoethylene glycol and the balance distilled water, with possibly a small proportion of alcohol. Alcohols have been widely used in the past for windshield and propeller ice protection but they have the following disadvantages:

a. There is a high fire risk associated with alcohol.
b. Alcohol's relatively high volatility causes it to evaporate rapidly from the surface to be protected, reducing its effectiveness. The latent heat of vaporization tends to lower the surface temperature, aggravating the icing problem.
c. The viscosity of alcohols is too low.
d. In some cases (e.g., methanol) the toxicological hazard is unacceptable.
e. Alcohol may induce stress crazing of acrylic windshields.

The principal constituent of aircraft freezing point depressant fluids is monoethylene glycol (MEG). Physical properties of MEG are presented in table 3-1 and figure 3-2. MEG has suitable viscosity characteristics, although the temperature dependency is greater than ideal. It has a low volatility and presents a negligible fire hazard.

The two most common fluids used in fluid ice protection systems today are TKS 80 and DTD 406B (also known as AL-5). Their characteristics are presented in tables 3-2 and 3-3 and in figures 3-2, 3-3. At present, AL-5 is the more readily available fluid in the United States.

The difference in viscosity between the two fluids makes it possible to extend the usable temperatures at either end of the range, depending on which fluid is chosen. There is virtually no difference in the freezing point of the two liquids in aqueous solution.

Many other fluid combinations may perform satisfactorily in a liquid ice protection system and better FPD fluids may be developed in the future. An ideal fluid will have a very low freezing temperature to minimize the flow rate required, and will have low viscosity sensitivity to temperature changes to reduce the range of operating pressures in the system.

3.2.5 Fluid Supply System

A freezing point depressant fluid is stored in a tank installed at a convenient aircraft location. The location should provide easy access for tank refilling and for strainer replacement. The storage tank must be totally corrosion free. Suitable tank materials that have been used include anodized aluminum, stainless steel, plastic, and fiberglass.

In operation the fluid passes through a strainer to a pump which meters the system total fluid flow requirements. A filter should be installed downstream of the pump to protect system components against blockage by contamination from solid particles. The strainer between storage tank and pump should he nominally 20 microns. The filter, which is nominally 0.8 microns, causes a pressure drop that necessitates its location downstream of the pump.

Nylon is normally used for plumbing to distribute the fluid to the various system components. Pipe sizes generally range from 0.1875 inch O.D. (0.5 cm) to 0.5 inch O.D. (1.27 cm) depending on the location and flow rate required. Special metal compression fittings should be used to ensure plumbing connection reliability.

The metering pump is usually driven by a direct current electric motor. This pump must produce a nearly constant flow rate nearly independent of back pressure. Two preset flow rates are normally provided. The higher flow rate can be used: 1) for a preset period (e.g., one or two minutes) when the system is initially activated to establish flow and to remove existing ice; 2) to remove significant amounts of ice that have accumulated due to failure to activate system promptly; and 3) to provide anti-icing or natural de-icing protection during abnormally severe icing conditions. The normal flow rate is designed to provide anti-icing protection during maximum continuous icing conditions. Manual flow rate selection should be available to the flight crew.

The filtered fluid is supplied to proportioning units in the surface being protected by the system. The proportioning units are essentially manifolds that contain calibrated capillary tubes, one for each outlet, which divide the total flow into the requirements of each porous panel on the leading edge surface. Each proportioning unit outlet also houses a non-return valve to prevent porous panel drainage when the system is not in use.

Porous panels are constructed typically of sintered stainless steel mesh or laser-drilled titanium for the outer skin, a stainless steel or titanium backplate to form a reservoir, and a porous plastic liner to provide uniform control of panel porosity and sufficient resistance to fluid flow to maintain adequate reservoir pressure. If the reservoir pressure is not considerably higher than the air stagnation pressure the flow rate will be attenuated at the stagnation point where the water droplet impingement is highest. A typical panel cross-section is shown in figures 3-4 and 3-5.

The stainless steel porous skin consists or two or three layers (depending on strength requirements) of wire cloth that are rolled, sintered, and then finish-rolled to thickness. The layers are oriented 90 degrees with respect to each adjacent layer.

Use of titanium instead of stainless steel provides a 50% reduction in panel weight, greater resistance to impact damage (including bird strikes), and improved surface finish. Further research is expected to produce other candidate materials and construction techniques for porous leading edge panels.

III.3.3 USAGES AND SPECIAL REQUIREMENTS

3.3.1 Airfoils and Leading Edge Devices

Panel installation on surface leading edges and other surfaces for which ice protection is required should cover the proportion of the span where ice protection is needed. The porous panel is positioned so that the stagnation point is well within the extent of an active portion of the panel over the entire range of angle of attack for which continuous protection is desired. The stagnation point travel is normally determined through wind tunnel tests or flight tests with the use of small tufts, wing pressure surveys, or by analysis. The panel active portion should extend 1 to 2 cm behind the extreme locations of the stagnation point to provide FPD fluid to mix with water impinging both above and below the stagnation region at all times, as illustrated in figure 3-6. Porous panels may be designed to be part of an integral leading edge structure (figure 3-7A-E), or may be added to an existing wing leading edge as shown in figure 3-7F.

3.3.2 Windshields

The spray nozzle distribution method is used primarily for windshield de-icing. For this application a tube is installed at the base of the windshield behind a strip of material that deflects the airflow over the tube. Small holes are drilled in the tube at intervals of a few centimeters. The

holes are located such that when fluid is pumped into the tube the holes direct a spray onto the windshield in the same manner as a conventional automobile windshield washing system. A separate pump is normally supplied for this application. The pilot actuates the system manually for a 5 to 10 second interval when it is necessary to clear the windshield. Several such bursts may be required to completely clear the window. Continuous anti-icing of a window could require excessive amounts of fluid and is not usually necessary.

3.3.3 Engine Inlet Lips and Components

Porous panels may he manufactured in almost any shape permitting liquid injection anti-icing to be used on engine inlet leading edges. As on other surfaces, the panel active portion for inlet lips must cover the entire range of stagnation point travel, with 1 to 2 cm extra, depending on the inlet size. For turbofan engines the fluid is normally swept aft on the inlet inside surface into the fan duct with no fluid entering the engine core. For pure jet engines one should make sure that internal engine components and bleed ports are compatible with the glycol based fluid, and that contamination of bleed air for cabin pressurization is avoided.

To avoid ice ingestion damage, the fluid flow rate must be sufficient to achieve anti-icing protection or ensure that any ice shed is smaller in size than that permitted for ingestion according to the engine manufacturer. This is also true for leading edge segments of a wing that may be located ahead of an engine inlet.

3.3.4 Turbofan Components

Fluid injection systems have not been used for internal turbofan engine components.

3.3.5 Propellers, Spinners, and Nose Cones

Liquid ice protection of propellers can be achieved by distributing FPD fluid onto the leading edge of the propeller blades. This is accomplished by feeding the same fluid used on wing surfaces into a propeller slinger ring. The slinger ring retains the fluid by centrifugal force, allowing it to flow through a smaller feeder tube which deposits the fluid on the leading edge at the root of each blade. A rubber boot channels the fluid out along the blade leading edge to a point where centrifugal forces are sufficient to keep the blades free of ice.

3.3.6 Helicopter Rotors and Hubs

The problem of rotorcraft ice protection is primarily related to the lifting rotor. The tail rotor can be protected using methods applied to conventional propellers while other surfaces can be protected in the same manner as a fixed wing aircraft.

An experimental investigation of a liquid ice protection system on a helicopter rotor was conducted in 1961-62 (references 3-4, 3-5 and 3-6). The system used a slinger ring to transfer the fluid from a fixed nozzle to the rotating blades. Flexible hoses were used to supply fluid from the slinger ring to the rotor blades. The main rotor blades were production blades modified to include a fluid distribution system consisting of grooves milled into the forward and aft surfaces of the blade nose block and holes drilled into the stainless steel leading edge. The anti-icing liquid was channeled down the aft grooves, then forward to the two leading edge grooves where it escaped through the holes in the leading edge and flowed over the blade surface. Tests in natural and man-made icing showed that adequate ice protection for the rotor could be achieved with such a system. Nevertheless, no further development was conducted on the system.

There are no helicopters in the U.S. that currently use a liquid ice protection system. However, a research project is now underway to develop a system using porous metal leading edges and a distribution system that minimizes the effect of centrifugal pressure gradients along the rotor span. It is believed that such a system can be feasible, effective, and practicable.

3.3.7 Miscellaneous Intakes and Vents

The fluid injection method has been used to provide anti-icing protection of a large Foreign Object Damage (FOD) deflector in front of the engine of the Westland Sea King helicopter. The FOD deflector tended to collect ice which could be ingested by the engine when shed. To prevent this, several flat porous panels were installed flush to the surface of the FOD deflector in chevron patterns. These were sufficient to provide full anti-icing of the deflector during normal flight operations.

III.3.4 FLUID AND WEIGHT REQUIREMENTS

System weight is highly dependent on the FPD fluid reserve requirements. Fluid systems are unique in comparison with most other ice protection systems in that there is a finite endurance, depending on the quantity of fluid aboard. Requiring sufficient fluid to operate the system for the maximum endurance capability has been considered an unreasonable requirement (reference 3-3). Fluid requirements should be based on the airplanes operational environment and the icing envelope extent prescribed in Appendix C of FAR 25. Different minimum values of fluid duration may apply for airframe and engine. Some of the factors to be considered in specifying fluid minimums are as follows.

Jet aircraft generally fly above the icing environment for the majority of their flights, being exposed to icing conditions only during climb, descent, holding, approach and landing operations. Since holding times at busy airports sometimes exceed 45 minutes, FAA has required jet aircraft ice protection with accretions on the unprotected surfaces to be safe for operation at 0.5 g/m^3 LWC for continuous icing for 45 minutes.

Aircraft operating at lower altitudes, such as reciprocating engine and some turbopropeller powered airplanes and helicopters, can be exposed to icing over a major portion of their flight profile. The system endurance should he consistent with this operating environment.

For gas turbine powered airplanes with maximum operating altitudes above 30,000 feet (reference 3-3) fluid requirements, with continuous maximum fluid flow, are 90 minutes or 15 percent of the maximum endurance of the airplane, whichever is greater.

For reciprocating engine and turbopropeller powered airplanes with maximum operating altitudes below 30,000 feet, continuous maximum flow of FPD fluid should be provided for 150 minutes or 20 percent of the maximum airplane endurance, whichever is greater.

In either case, a fluid quantity indicator and a low fluid level condition (for approximately 15 minutes remaining) should be installed in the cockpit visible to the crew.

Tables 6-1 through 6-10 in Section III.6.0 provide estimated weights for fluid ice protection systems for various types of aircraft in comparison to other ice protection systems.

III.3.5 ACTUATION

A fluid ice protection system can be actuated either manually or automatically. The primary control with automatic actuation is an ice detector to activate the pump whenever icing conditions are sensed. It is also possible to provide automatic timing and sequencing controllers to run the pump at high speed for an interval and then at normal speed. If an ice detector senses icing severity it could conceivably regulate the speed of the pump to provide optimum fluid flow rate.

For visual ice detection, a location or object must be selected which ices before any other part of the airplane and is easily observable by the pilot both day and night.

Other automatic features available in fluid systems include the integration of pressure sensing switches with a programmed microprocessor controller. The controller automatically senses each failure then activates pumps and solenoid valves as appropriate to maintain system operation using redundant design features.

III.3.6 OPERATIONAL USE

If icing conditions are anticipated in flight, the system should be activated during the preflight inspection to insure that fluid is being delivered to the surface of each panel, slinger ring, and/or windshield. This also serves to prime the system.

In flight, the system should be activated immediately prior to or upon entering icing conditions. This may be accomplished with the use of an ice detector as discussed earlier. Provisions should he made for the pilot to manually increase the flow rate (approximately double) to help protect against unusually severe icing conditions or to quickly remove any significant amount of ice that may have accumulated due to the failure to activate the system in a timely manner.

A gauge should be provided to monitor fluid level in the tank, perhaps combined with a low level warning light. Handbook data can be used to translate fluid level to ice protection duration for different selectable flow rates. If pressure sensing switches are installed anywhere in the system (see Section 3.7), the panel should display the status of each switch to alert the pilot to any problem or failure.

III.3.7 MAINTENANCE, INSPECTION, AND RELIABILITY

Maintenance of a fluid system is relatively simple and straightforward. All hardware components are designed to last the life of the airframe. Filters are normally replaced at regular intervals of 1000 flight hours or annually, whichever is shorter.

Porous panels are usually designed in 4 to 6 foot (1.2 to 1.8 m) lengths. Thus, if a panel becomes damaged for any reason, the replacement cost is minimized. Special attention is required in caring for the panels They may be cleaned with only water and a mild soap or detergent. Oil based deposits may be removed with alcohol or aviation fuel. Cleaning fluids or solvents can cause irreparable damage to internal panel components. Likewise any paint, wax, or polishing agents applied to the leading edge may plug up the porous panels, rendering them ineffective.

The clogging of holes in the porous leading edge by dust or insects has been a concern. However, flight tests at NASA Langley Research Center (reference 3-7) indicate that FPD systems may provide a means of removing the insect contaminant using very small fluid flow rates. The glycol based fluid softens and removes the debris when the system is activated, similar to the process of backflushing a filter.

Other maintenance requirements involve periodic checking of all components for proper operation or leaks and making appropriate replacement of any defective components. If blockage occurs due to solids in the pipeline or proportioning units, the affected portion of the system must be thoroughly flushed with clean water. To prevent the accumulation of any water, foreign material, or air in any portion of the system, some fluid should always be in the reservoir and the system should be primed at regular intervals.

Fluid systems tend to be quite reliable because the pump is the only moving component. A high quality pump is recommended to minimize the chance of failure. To assure system operation in the event of pump failure, systems may be designed with dual pumps. The two pumps may normally operate continuously with one pump at double normal speed, supplying the entire system in the event of a failure, or one pump may operate only in a standby mode.

Pressure switches can be provided at various points to monitor system operation and provide a failure indication if the operating pressures are outside normal limits. Duplication of critical items can he provided to meet various failure cases.

Figure 3-8 shows a simple basic system with no redundant components and only one pressure switch. Figure 3-9 shows a complex system with fully redundant pumps and supply lines to the proportioning units and numerous pressure switches to monitor system performance.

III.3.8 PENALTIES

The principle penalty of the fluid infection system is the fluid storage requirement. The stored fluid weight may be significant when compared to other candidate ice protection systems. Added maintenance is required to check and resupply fluid to the system. Until a large number of airplanes use this system the pilot cannot rely on the fluid being available at all airports and may be required to carry an extra supply.

III.3.9 ADVANTAGES AND LIMITATIONS

Advantages of a Liquid Ice Protection System:

a. Reliable anti-icing protection is normally provided, thus there is no aerodynamic penalty due to ice accumulation.
b. The smooth flush panels impose no aerodynamic penalty due to the installation.
c. Runback icing is prevented due to the natural runback of the fluid.
d. Low power of typically 30 to 100 watts is required. No engine power is required for ground testing and emergency operation.
e. Hardware weight is comparable to or less than other systems. (See tables in Section III.6.)
f. Components (except fluid and filters) are designed for the life of the aircraft, resulting in low maintenance requirements and cost.
g. Pilot skill and judgement required to operate the system are minimal.
h. The system can be used to prevent insect contamination on critical leading edge surfaces.

Disadvantages:

a. The system has a finite period of protection, dependent on fluid supply.
b. Initial cost is higher than for a pneumatic system.
c. Fluid weight reduces useful aircraft load.
d. Fluid sometimes drips from the wings after use in flight.

III.3.10 CONCERNS

Environmental considerations related to the use of a fluid ice protection system must be concerned with two aspects, the toxicity of the fluid to humans when they are in direct contact with the fluid or its vapors, and the longer term effects on the environment after fluid is shed into the atmosphere during flight. In this regard, only the characteristics of monoethylene glycol (MEG) are considered here.

While MEG can be toxic, it poses no danger to humans unless it is ingested in large quantities, or a saturated mist or vapor is breathed for an extended period of time. Numerous studies (references 3-8, 3-9 and 3-10) have established that the threshold limit value for MEG vapor is approximately 125 mg/m^3. This is far in excess of vapor concentrations that can be induced due to natural evaporation of MEG in an airplane or airport environment. For droplets and mists of MEG, the threshold limit value is 10 mg/m^3. The single oral dose lethal to adult humans is estimated to he approximately 100 ml (reference 3-8). The principal effect of repeated small doses is on the kidneys due to the breakdown of MEG in the body producing kidney poisons. As with other fluids used in aircraft systems, care should be exercised to ensure that MEG is not accidentally swallowed.

If cabin pressurization is provided by compressor bleed air, a test of cabin air should be included while engine inlet anti-icing by FPD is taking place.

With respect to the environment, experiments (reference 3-11) have shown that MEG is biodegradable, with the rate being a function of temperature and the concentration of micro organisms present. MEG biodegrades completely in 3 days at a temperature of 60°F (20°C). At water temperatures of less than 46 °F (8°C), biodegradation is completed in 7 to 14 days.

It should be noted that MEG is the principal constituent of the fluids used in great quantities to de-ice airplanes on the ground at major airports, with a minimal effect on the environment. The amount of fluid placed in the environment by a liquid ice protection system is quite small compared with the amount required to de-ice the same airplane on the ground. Therefore, it is claimed that the use of glycol based fluids in aircraft liquid ice protection systems will have no adverse effects on humans or the environment.

Some concern has been expressed (reference 3-3) for the possible effects of FPD fluid on other parts of the aircraft: engine accessories, electrical insulation, or gold or silver-surfaced electrical contacts. However, no evidence of deterioration has been documented in the several decades of use of FPD fluid for ground and flight ice protection.

III.3.11 REFERENCES

3-1 Kohlman, D.L., Schweikhard, W.G. and Evanich, P., "Icing Tunnel Tests of Glycol-Exuding, Porous Leading-Edge Ice Protection System." Journal of Aircraft, Vol. 19, No. 8, Aug. 1982, pp. 647-654.

3-2 Albright, A.E., "Experimental and Analytical Investigation of a Freezing Point Depressant Fluid Ice Protection System," NASA CR 174758, September 1984.

3-3 Hackler, L. and Rissmiller, R., "Fluid Ice Protection Systems." FAA Technical Note DOT/FAA/CT-TN 86/11, July 1986.

3-4 Van Wyckhouse, J., DeTore, J., and Lynn R.R., "Liquid Ice Protection System Development and Flight Test of a Liquid and Electrothermal Ice Protection System for the Rotors of the HU-1 Series Helicopter," Bell Report 518-099-001, 8 November 1960.

3-5 Van Wyckhouse, J., and Lynn, R.R., "Development and Icing Flight Tests of a Chemical Ice Protection System for the Main and Tail Rotors of the HU-1 Helicopter," Bell Report 518-099-002, June 5, 1961.

3-6 Coffman, Herb J., Jr., "Helicopter Rotor Icing Protection Methods," Presented at the Annual Meeting of the American Helicopter Society, Fort Worth, March 1985.

3-7 Croom, C.C. and Holmes, B.J., "Flight Evaluation of an Insect Contamination Protection System for Laminar Flow Wings," S.A.E. Paper 850860.

3-8 Rowe, V.K., "Industrial Hygiene and Toxicology," Interscience, NY 1962, 2nd ed., Vol. II, pp. 1497-1502.

3-9 Harris, E.S., "Inhalation Toxicity of Ethylene Glycol," Aerospace Medical Research Laboratory, WPAFB, Rept. AMRL-TR-69-130, 1969, pp. 99-104.

3-10 Felts, M.F., "Effects of Exposure to Ethylene Glycol on Chimpanzees," Aerospace Medical Research Laboratory, WPAFB, Rept. AMRL-TR-69-130, 1969, pp. 105-120.

3-11 Evans, W.H. and Uavid, E.J., "Biodegradation of Mono-, Di-, and Tri-ethylene Glycols in River Waters," Water Research, Vol. 8, pp. 97-100.

3-12 "Rotorcraft Icing - Status and Prospects," AGARD Advisory Report No. 166, August 1981.

3-13 Albright, A.E., Kohlman, D.L., "An Improved Method of Predicting Anti-icing Flow Rates for a Fluid Ice Protection System," AIAA 22nd Aerospace Science Meeting, Reno, NV, January 9-12, 1984.

3-14 Albright A., "A Summary of NASA's Research on the Fluid Ice Protection System," AIAA 23rd Aerospace Science Meeting, Reno, NV, January 14-17, 1985.

TABLE 3-1

PHYSICAL PROPERTIES OF MONOETHYLENE GLYCOL (MEG)

Formula	HOCH2CH20H
Synonyms	1,2 ethane diol
	1,2 dihydroxy ethane
	MEG
Appearance/Odor	Clear, colorless, odorless liquid
Specific Gravity	1.115-1.116
Flash Point	241°F (116°C)
Boiling Range	383-390°F (195-199°C)
Freezing Temperature	See figure 3-2
Auto-Ignition Temperature	743°F (413°C)
Explosive Limits in Air	Upper: 28% by volume
	Lower: 3.2% by volume
	V. por Pressure 0.05 mm Hg @ 20°C
Viscosity	18.8 cSt @ 20°C
Miscibility With Water	Completely miscible

TABLE 3-2

PHYSICAL PROPERTIES OF TKS 80

Composition, % Volume	80% monoethylene glycol
	20% distilled or deionized water
Appearance/Odor	Clear, colorless, odorless liquid
Specific Gravity	.099-1.103 8 68°F (20°C)
Conductivity	4 micromho/cm
Viscosity	9.3 cSt @ 68°F (20°C) See fig. 3-3
Flash Point	None
Vapor Pressure	7.87 mm Hg 8 68°F (20°C)
Boiling Point	253°F (123°C)
Freezing Point	See figure 3-2

TABLE 3-3

PHYSICAL PROPERTIES OF DTD 406B (AL-5)

Composition, % Volume	85% monoethylene glycol
	10% distilled or de-ionized water
	5% ethyl or isopropyl alcohol
Appearance/Odor	Clear, colorless, odorless liquid
Specific Gravity	1.082-1.087 @ 20°C
Conductivity	5 micromho/cm
Viscosity	12.0 cSt @ 20°C (see figure 3-3)
Flash Point	129°F (54°C)
Vapor Pressure	7.38 mm Hg (20°C)
Freezing Point	See figure 3-2

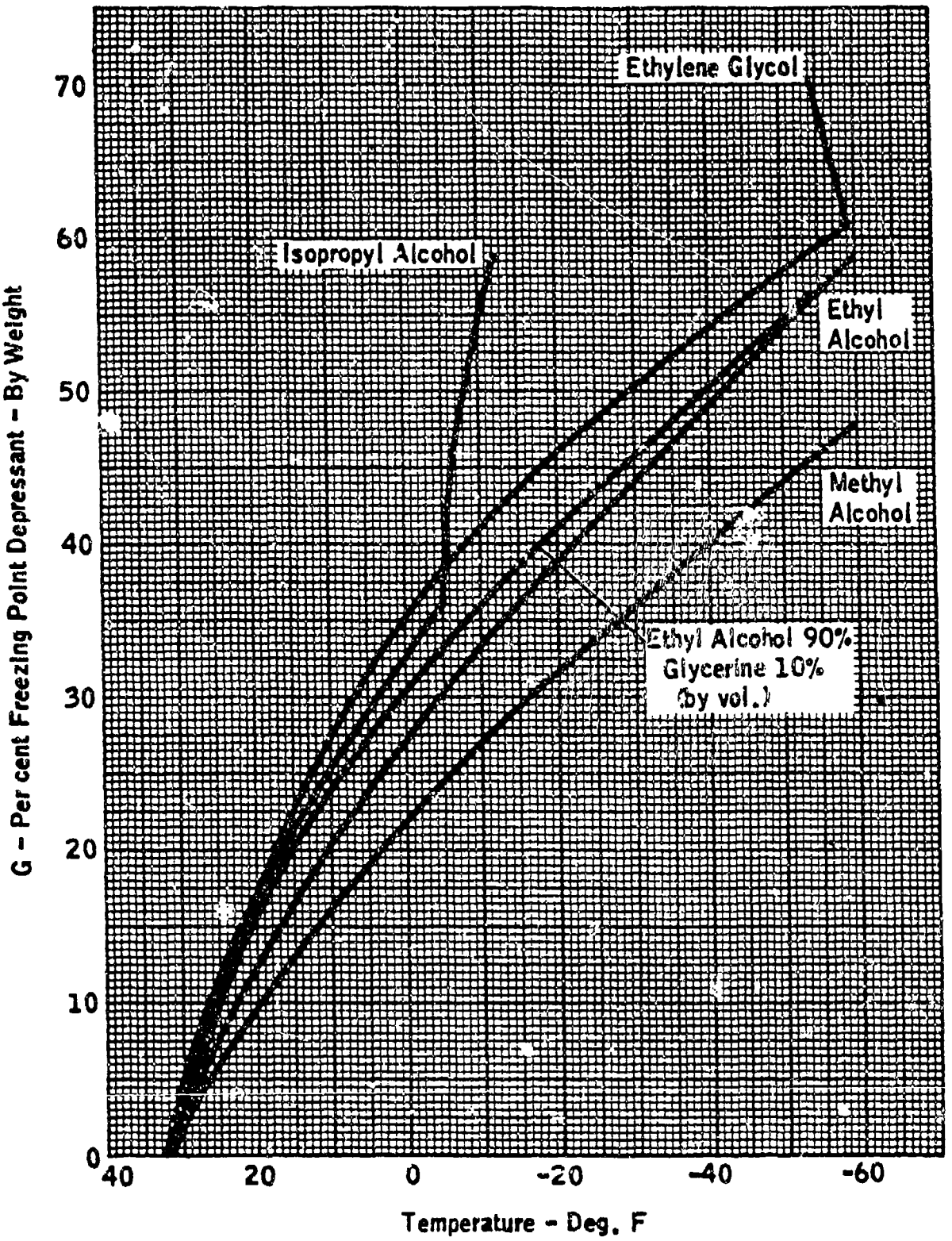

FIGURE 3-1. FREEZING POINT PLOTS FOR AQUEOUS SOLUTIONS OF SEVERAL FREEZING POINT DEPRESSANT FLUIDS

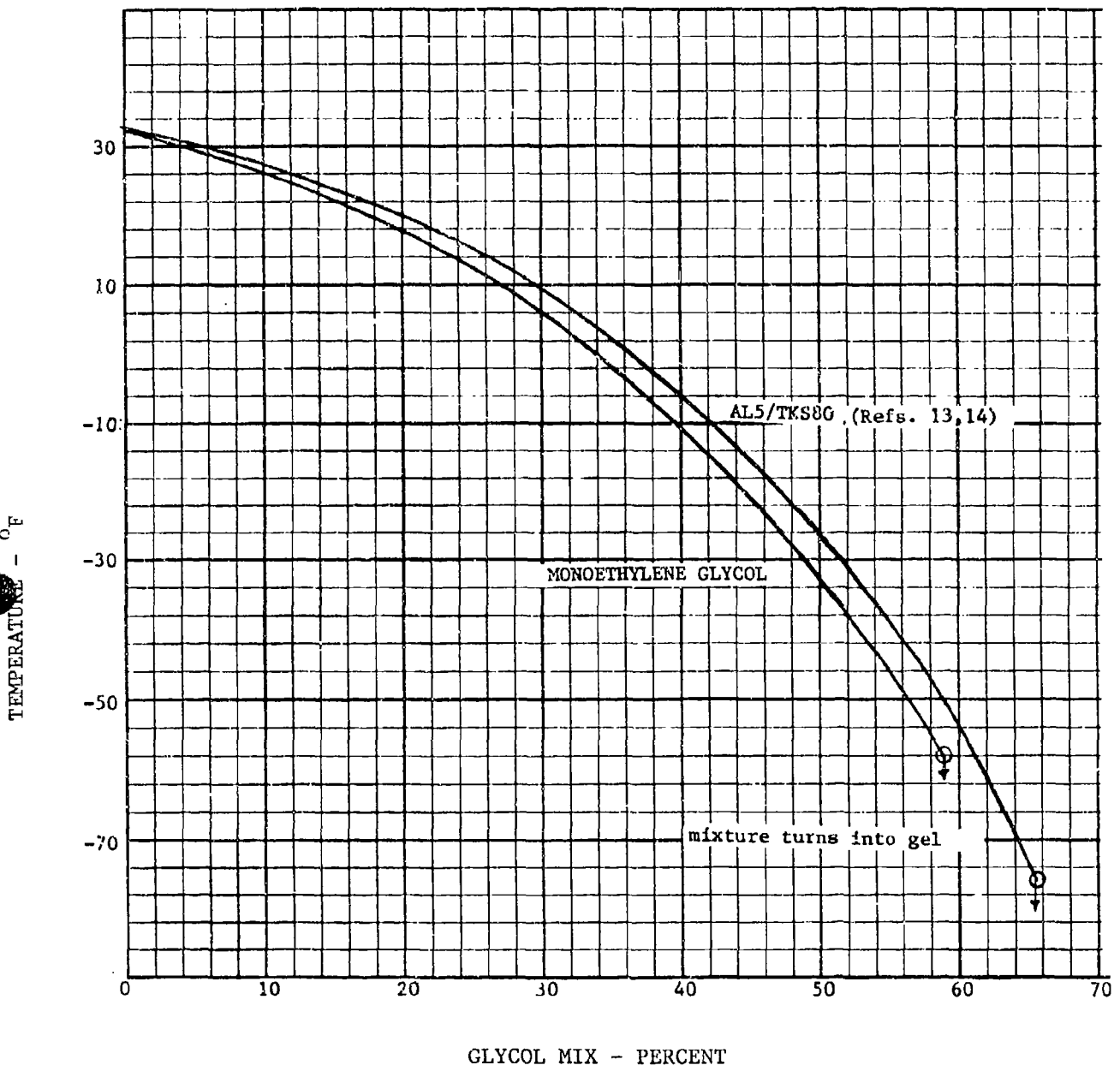

FIGURE 3-2. FPD FREEZE POINT INCREASE DUE TO DILUTION

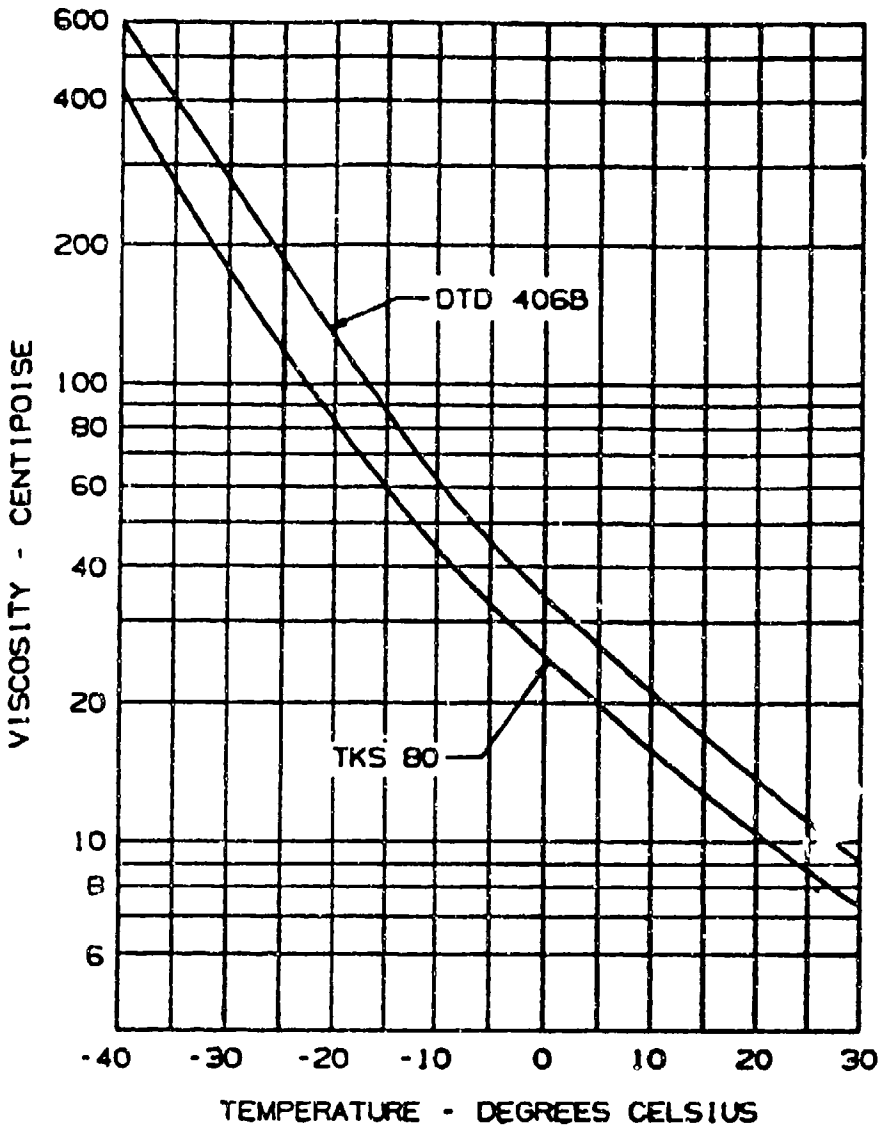

FIGURE 3-3. VISCOSITY CHARACTERISTICS OF TKS 80 AND DTD 406B (AL-5)

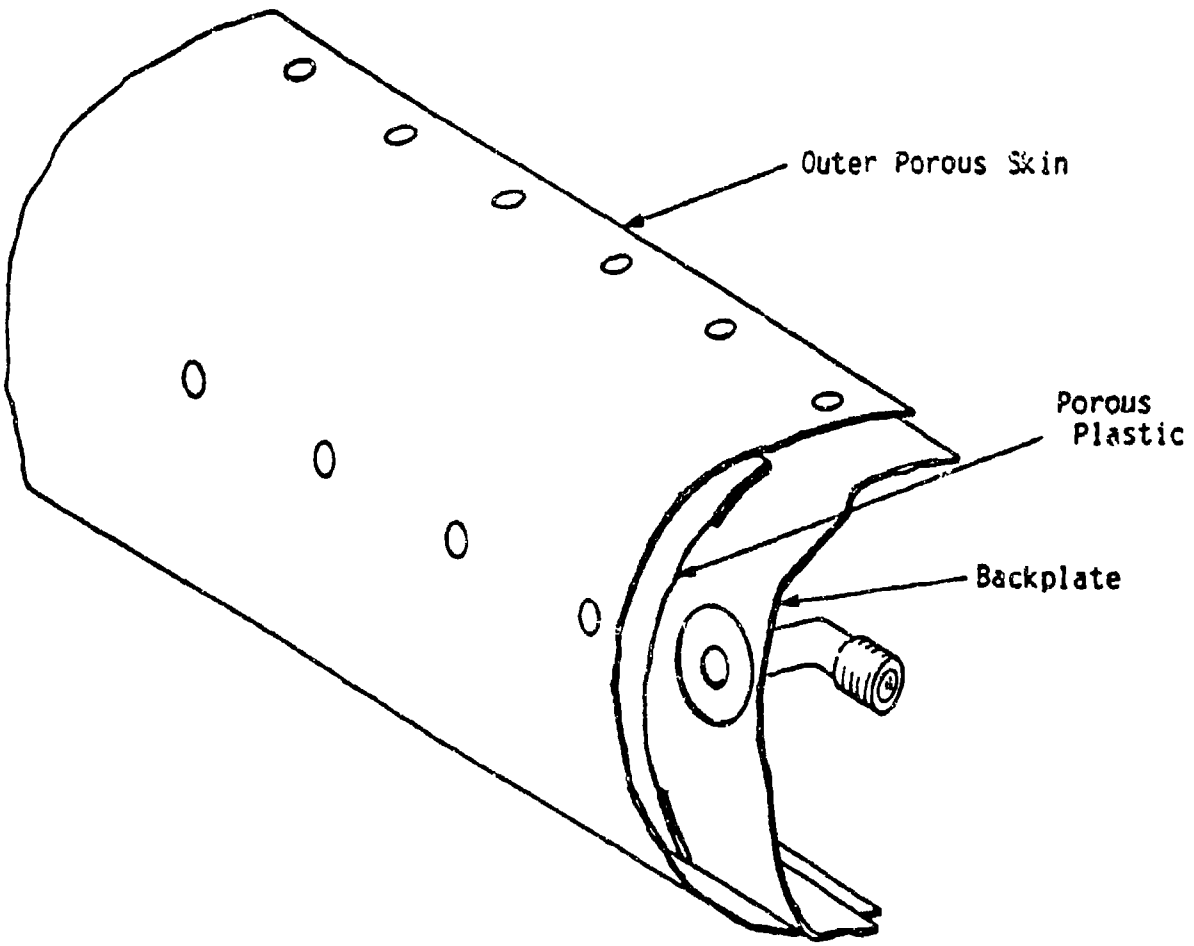

FIGURE 3-4. CONSTRUCTION OF A TYPICAL POROUS PANEL

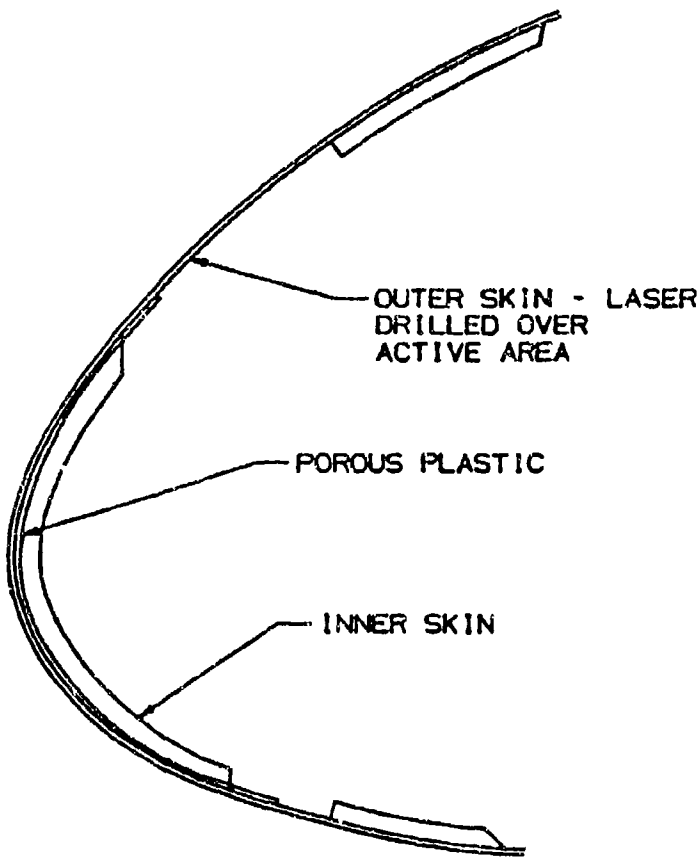

FIGURE 3-5. CROSS-SECTION OF A TYPICAL POROUS PANEL

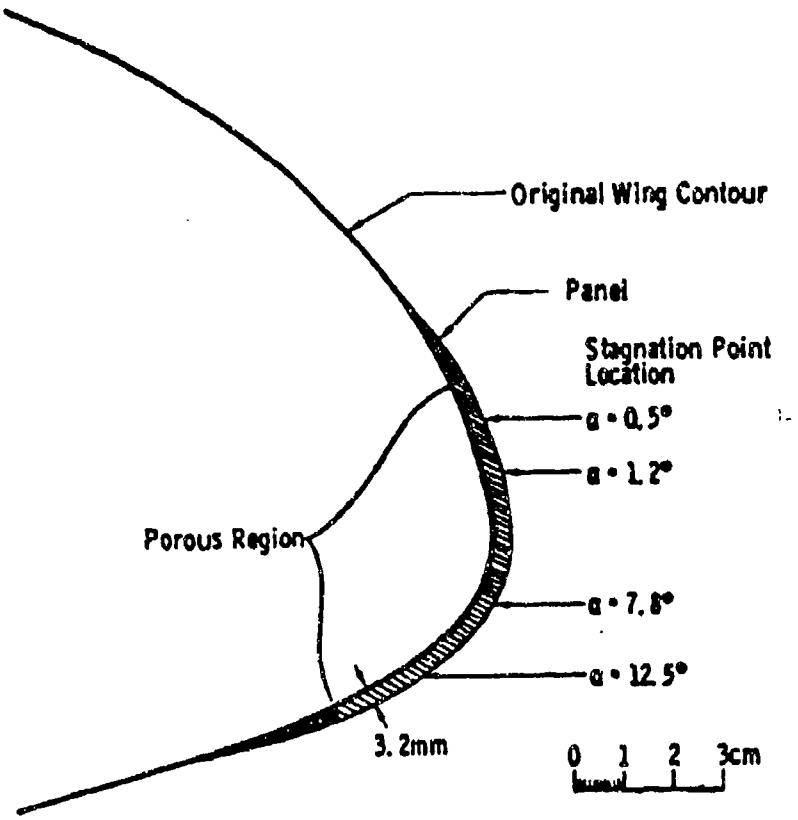

FIGURE 3-6. TYPICAL PANEL INSTALLATION ILLUSTRATING ACTIVE REGION AND STAGNATION POINT TRAVEL

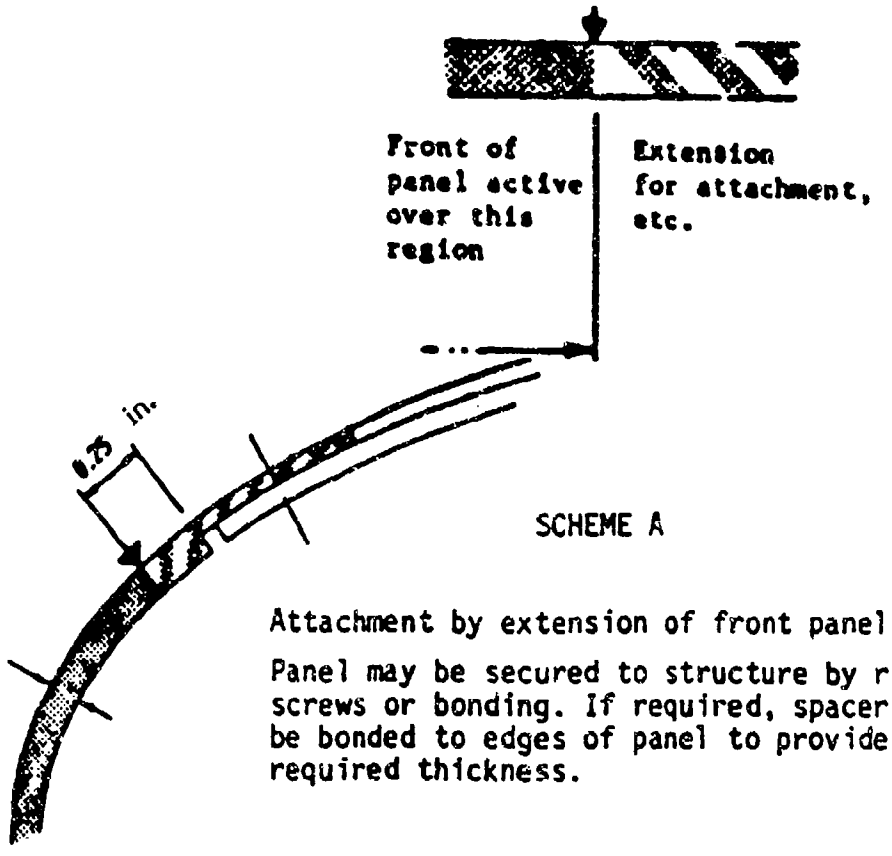

SCHEME A

Attachment by extension of front panel skin.

Panel may be secured to structure by rivets, screws or bonding. If required, spacers can be bonded to edges of panel to provide any required thickness.

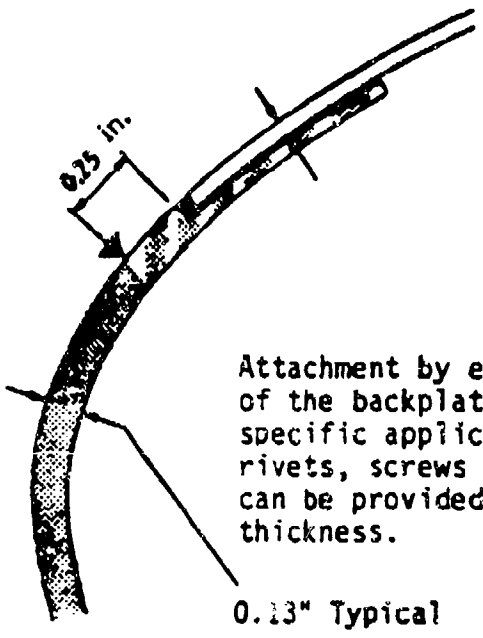

SCHEME B

Attachment by extension of backplate. The material of the backplate varies with the requirements of specific applications. The panel may be secured by rivets, screws or adhesive bonding and dimension "t" can be provided as required to match the mating skin thickness.

FIGURE 3-7. TYPICAL METHODS OF ATTACHING POROUS PANELS TO AIRCRAFT STRUCTURE

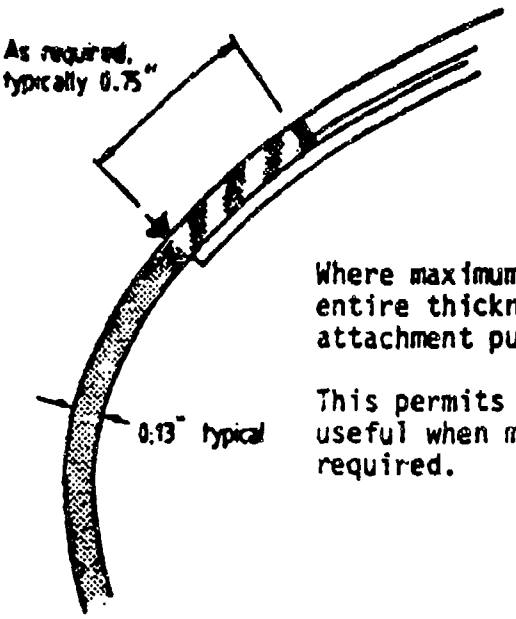

SCHEME C

Where maximum structural strength is required, the entire thickness of the panel can be extended for attachment purposes.

This permits the use of larger fasteners, and is useful when maximum resistance to bird strikes is required.

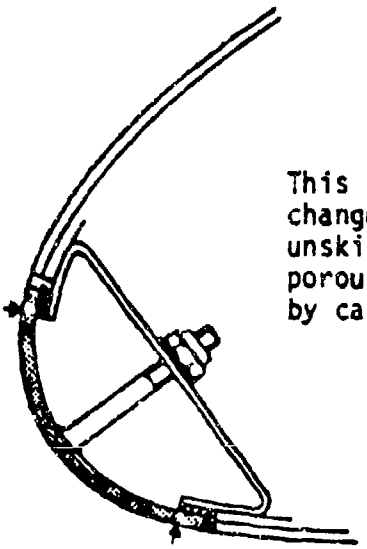

SCHEME D

This scheme is intended to provide total interchangeability with maximum ease of fitting by unskilled operators. Build tolerances of both porous panel and aircraft structure are eliminated by casting an accurate seating to all mating faces.

FIGURE 3-7. TYPICAL METHODS OF ATTACHING POROUS PANELS TO AIRCRAFT STRUCTURE (CONTINUED)

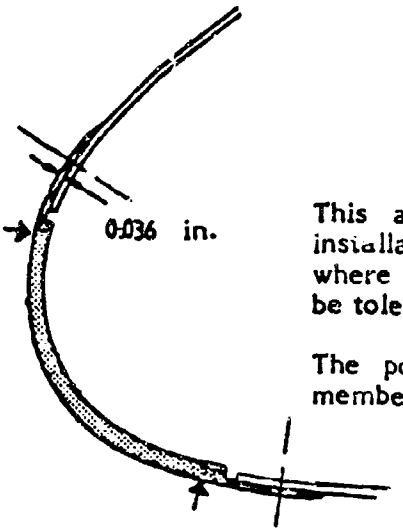

SCHEME E

This arrangement provides a cheaper form of installation than schemes A, B, C, or D, in cases where a small aerodynamic profile disturbance can be tolerated.

The potential for using the panel as structural member is retained.

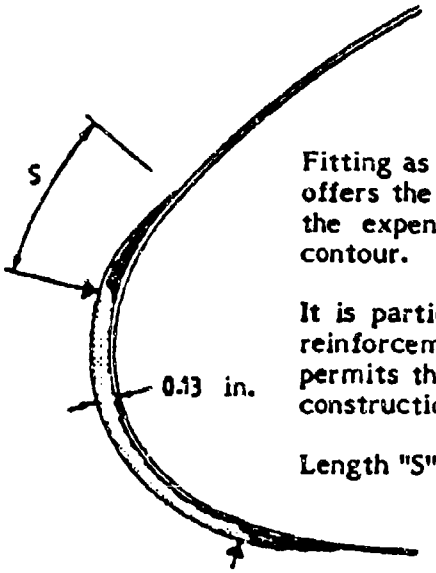

SCHEME F

Fitting as an "overshoe" avoids cutting the skin and offers the most economical method of fitting, but at the expense of deviation from true aerodynamic contour.

It is particularly suited to light aircraft since the reinforcement provided by the leading edge skin permits the use of thinner gage materials for panel construction.

Length "S" is as required for aerodynamic fairing.

FIGURE 3-7. TYPICAL METHODS OF ATTACHING POROUS PANELS TO AIRCRAFT STRUCTURE (CONCLUDED)

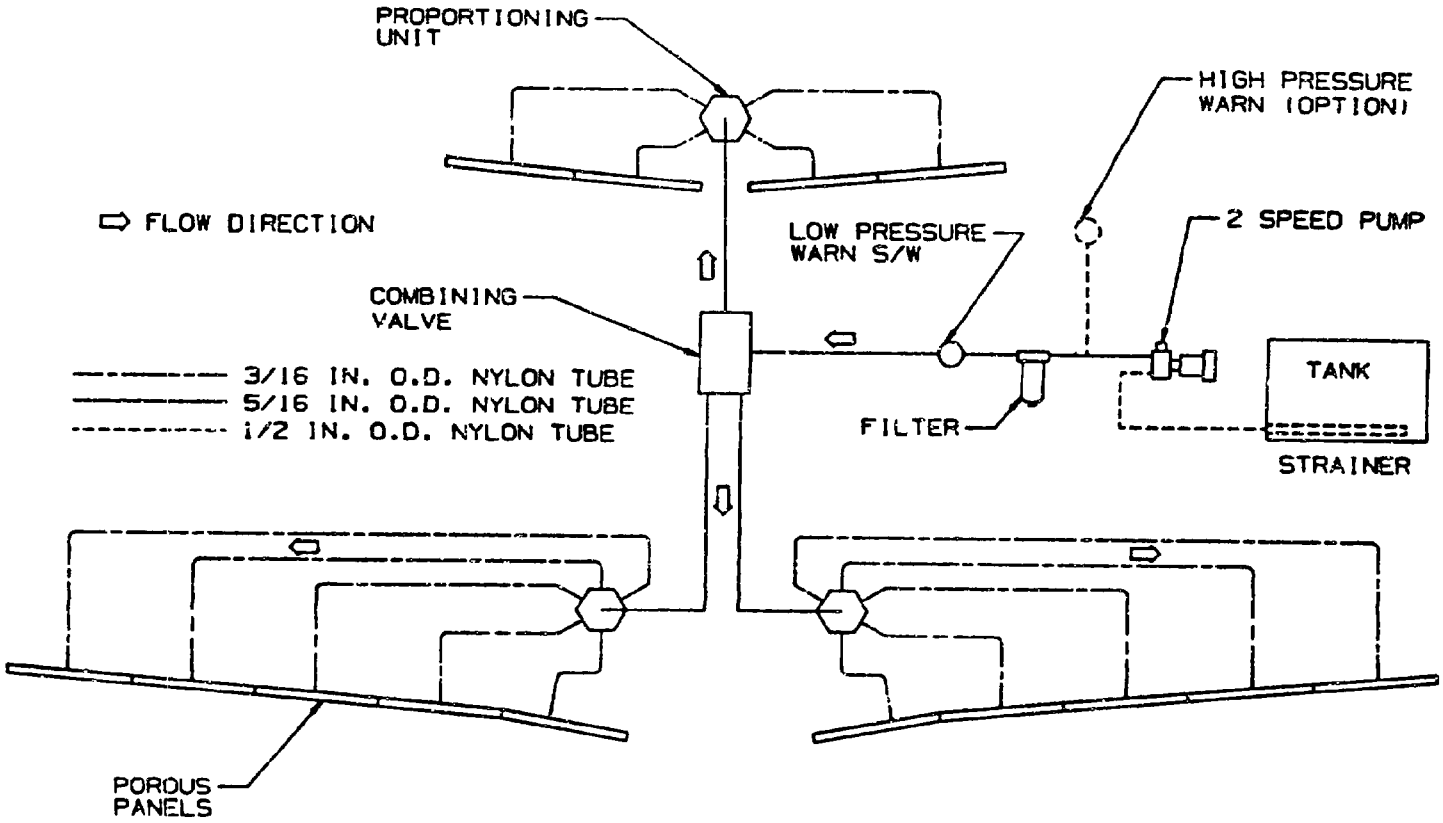

FIGURE 3-8. SCHEMATIC OF A SIMPLE FLUID ICE PROTECTION SYSTEM

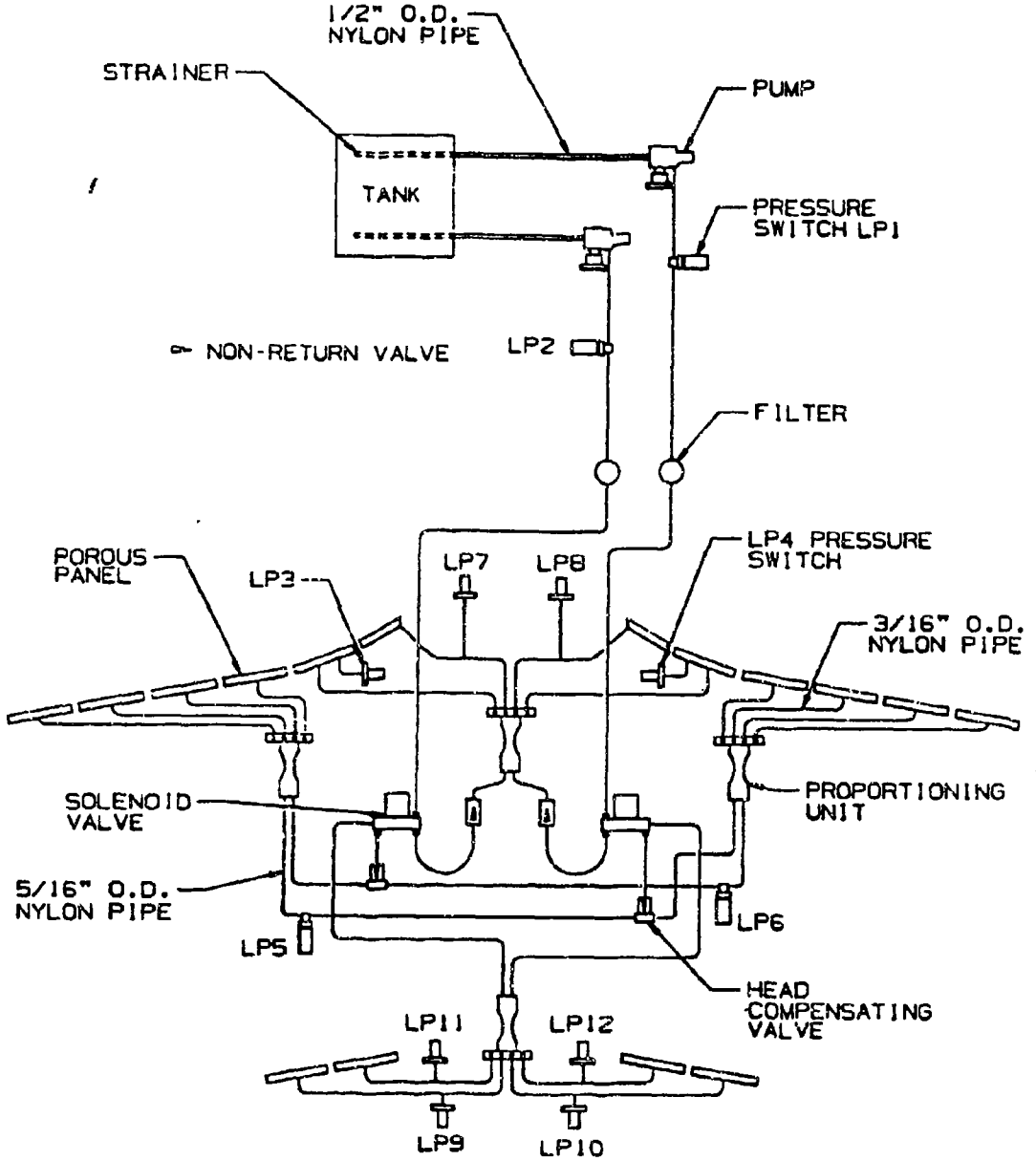

FIGURE 3-9. SCHEMATIC OF FLUID ICE PROTECTION SYSTEM WITH FULLY REDUNDANT EQUIPMENT

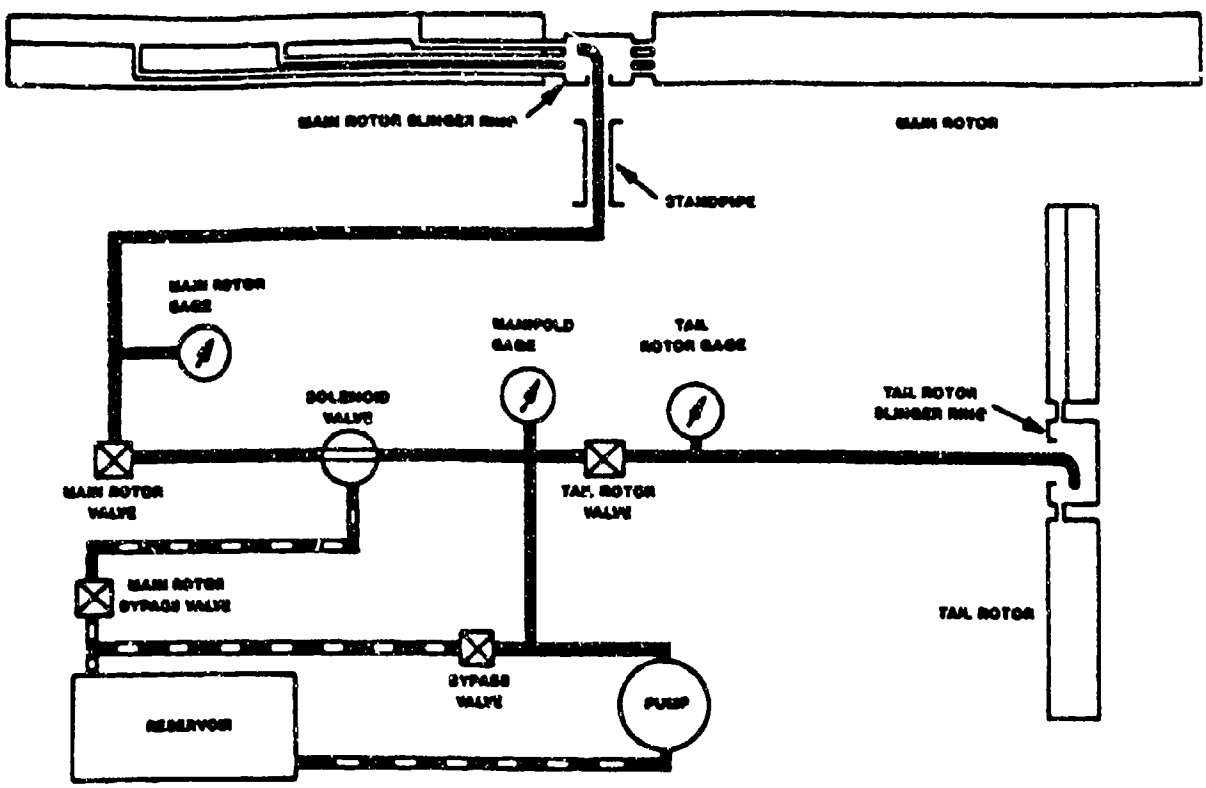

FIGURE 3-10. SCHEMATIC OF HELICOPTER FLUID ICE PROTECTION SYSTEM (REFERENCE 3-12)

CHAPTER III
SECTION 4.0
ELECTRO-IMPULSE DE-ICING SYSTEMS

CHAPTER III - ICE PROTECTION METHODS
CONTENTS
SECTION 4.0 ELECTRO-IMPULSE SYSTEMS

	Page
LIST OF FIGURES	III 4-iii
SYMBOLS AND ABBREVIATIONS	III 4-iv
GLOSSARY	III 4-v
III.4.1 OPERATING CONCEPTS AND COMPONENTS	III 4-1
III.4.2 DESIGN GUIDANCE	III 4-2
4.2.1 Pulse Width Matching	III 4-2
4.2.2 Power Supply and Sequencing	III 4-2
4.2.3 Coil Design and Installation	III 4-3
III.4.3 USAGES AND SPECIAL REQUIREMENTS	III 4-3
4.3.1 Airfoil and Leading Edges	III 4-3
4.3.2 Windshields	III 4-3
4.3.3 Engine Inlet Lips and Components	III 4-4
4.3.4 Turbofan Components	III 4-4
4.3.5 Propellers, Spinners, and Nose Cones	III 4-4
4.3.6 Helicopter Rotors and Hubs	III 4-5
4.3.7 Flight Sensors	III 4-5
4.3.8 Radomes and Antennas	III 4-5
4.3.9 Miscellaneous Intakes and Vents	III 4-5
4.3.10 Other	III 4-6
III.4.4 WEIGHT AND POWER REQUIREMENTS	III 4-6
III.4.5 ACTUATION, REGULATION, AND CONTROL	III 4-6
III.4.6 OPERATIONAL USE	III 4-6
III.4.7 MAINTENANCE, INSPECTION, AND RELIABILITY	III 4-7
III.4.8 PENALTIES	III 4-7
III.4.9 ADVANTAGES AND LIMITATIONS	III 4-7
III.4.10 CONCERNS	III 4-8
III.4.11 REFERENCES	III 4-9

LIST OF FIGURES

		Page
4-1	EIDI Impulse Coils in a Leading Edge	III 4-10
4-2	Basic EIDI Circuit	III 4-11
4-3	A Basic Electro-Impulse De-Icing System in a Wing	III 4-12
4-4	EIDI System Schematic	III 4-13
4-5	EIDI System in a Large Aircraft Wing	III 4-14
4-6	Falcon Fanjet Inlet Being Deiced by EIDI	III 4-15

SYMBOLS AND ABBREVIATIONS

Symbol	Description
AC	Alternating Current
°C	Degrees Celsius
cm	Centimeter
DC	Direct Current
EIDI	Electro-Impulse De-Icing
EMI	Electromagnetic Interference
°F	Degrees Fahrenheit
FAA	Federal Aviation Administration
ft	Feet or foot
in.	Inch
kHz	Kilohertz
kw	Kilowatt
lbf	Pounds force
lbs_m	Pounds mass
LWC	Liquid Water Content
m	Meter
mm	Millimeter
NASA	National Aeronautics and Space Administration
SCR	Silicon Controlled Rectifier
USSR	Union of Soviet Socialist Republics
v	Volts
VDC	Volts Direct Current

GLOSSARY

liquid water content (LWC) - The total mass of water contained in all the liquid cloud droplets within a unit volume of cloud. Units of LWC are usually grams of water per cubic meter of air (g/m^3).

median volumetric diameter (MVD) - The droplet diameter which divides the total water volume present in the droplet distribution in half; i.e., half the water volume will be in larger drops and half the volume in smaller drops. The value is obtained by actual drop size measurements.

thyristor - A solid state bistable device comprising three or more junctions using silicon controlled rectifiers. Used as a current limiting device or to reverse polarity. Also called pnpn-type switch.

III.4.0 ELECTRO-IMPULSE SYSTEMS

III.4.1 OPERATING CONCEPTS AND COMPONENTS

Electro-Impulse De-Icing (EIDI) is classified as a mechanical ice protection method. Ice is shattered, de-bonded, and expelled from a surface by a hammer-like blow delivered electro-dynamically. Removal of the ice shard is aided by turbulent airflow; thus, relatively low electrical energy is required.

Physically, the EIDI system consists of ribbon-wire coils rigidly supported inside the aircraft surface to be de-iced, but separated from the skin surface by a small air gap (figure 4-1). A sudden high voltage (typically 800 to 1400 v) electric current is discharged through the coil (figure 4-2). The circuit must have low resistance and inductance to permit the discharge to be very rapid, typically less than one-half millisecond in duration. A strong electromagnetic field forms and collapses, inducing Eddy currents in the aircraft skin. The Eddy current and coil current fields are mutually repulsive, resulting in a toroidal-shaped pressure on the skin opposite the coil. The peak force on the skin is typically 400-500 pounds (1780-2220 Newtons) and is delivered so sharply as to produce a sound resembling a metal-on-metal blow. Actual surface deflection is small, generally less than 0.01 inches (0.25 mm), but acceleration is rapid.

The coil may be supported from a spar, a beam between ribs, or from the skin itself. In any case, the coil's mount or direct support should be non-metallic to avoid interaction with the coil's magnetic field. At a leading edge spanwise station there may be a single coil at the nose, a pair of coils at upper and lower skin positions near the nose, or even a single coil placed eccentrically on either upper or lower surfaces.

During EIDI systems operations a coil receives 2 or 3 successive pulses from the capacitor unit with pulses separated by the time required to recharge the capacitor, typically 2 to 4 seconds. The spanwise extent of wing leading edge that each coil (or coil pair) will de-ice depends largely on the structural properties of the leading edge, but it is nominally 18 inches (0.5 meters). The capacitor is then switched to another coil station, and then to another until it cycles around the aircraft. The time to complete the de-icing cycle must be less than the time for acceptable ice accretion for the protected surfaces.

The system consists of a power-and-sequencing box, often located in the fuselage, and a number of coils in the wing, empennage, and engine inlet lip surfaces which are connected to the power box. Figure 4-3 shows the system in its simplest form. The capacitor discharge occurs when a solid-state switch is remotely triggered to close the circuit. This high voltage, rapid response switch is a Silicon-Controlled-Rectifier (SCR) or "Thyristor". Gas tube thyristors ("thyratrons") are also available but have not been used in the USA for EIDI. The circuit often includes a "clamping" diode, as shown in figure 4-2, to prevent reverse charging of the capacitors.

The first nation to use EIDI was the USSR, which had a fully equipped aircraft in 1972 and has equipped several transport-sized airplanes since (reference 4-1). Unfortunately, no operational data are available.

The EIDI system has had extensive testing in the NASA Lewis Research Center's Icing Research Tunnel (references 4-4 and 4-6) and limited flight testing in the USA by NASA and Cessna Aircraft Company (references 4-6 and 4-7). Other testing has been done by Boeing Commercial Airplane Company (including a flight test series in a B-757), Rohr Industries (icing tunnel tests of engine inlets), and Douglas Aircraft Company (laboratory and icing tunnel tests), Wichita State University (Fatigue and Electromagnetic Interference Tests, reference 4-8) and Electroimpact Inc. (Electromagnetic Testing of Modular Low Voltage EIDI Systems, reference 4-9).

III.4.2 DESIGN GUIDANCE

4.2.1 Pulse Width Matching

The EIDI system requires a careful and rather sophisticated design (references 4-2, 4-3, 4-8, 4-10 and 4-11). The current pulse width in the coil resu ting from the capacitor discharge must be properly matched to the skin electrical properties (reference 4-4) and to the leading edge structural dynamic response (reference 4-5). Failure to do this properly severely reduces the coil's ice expelling performance. When skin conductivity is too small, a higher conductivity metal disc is bonded to the inside of the skin opposite the coil. This disc is termed a "doubler" and should be slightly larger in diameter than the coil (figure 4-1). Copper or unalloyed aluminum are the common doubler materials. Doublers increase the skin stiffness locally but may distribute the impulse load more evenly. A structural dynamic analysis will provide guidance for the proper placement of the coil for maximum efficiency.

4.2.2 Power Supply and Sequencing

The power supply and sequencing may be packaged in a single box. The sequencing system can be confirmed for a single sequence around the aircraft or for continuous resequencing. Power supplies are available for common aircraft voltages and frequencies.

Installation of the power supply and control system in the aircraft should be done in a manner that minimizes the distance through which the high energy electrical pulse must travel. Ideally, the discharge capacitors should be located in close proximity to the inductor coils while the power supply, with its "trickle charge" to the capacitors, should be located near the aircraft electrical generator and away from the capacitors. Figure 4-4 shows a system schematic, and figure 4-5 shows a large airplane application. Each aircraft will require a trade-off study to determine the number of coils to be supplied by one capacitor. For large aircraft, the weight and electrical losses of the high current lines requires several capacitor sets. However devoting a capacitor to each coil pair may result in a costly, heavy system, so a compromise between those extremes is needed.

Redundancy can also be obtained by using multiple power boxes which are cross connected. This provides power tc all coils at longer intervals if one box fails. An alternate safety system, which increases cabling, is to supply alternate coils from different power sources. That is, connect odd numbered coils to one power supply and even numbered coils to another. In case of one power box failure, only limited amounts of ice will collect on the unprotected area, unless very stiff nose ribs separate the leading edge segments.

Note in figure 4-5 that the SCRs ("thyristors") are placed on the capacitor side of the coil to avoid having high voltage on coils not being fired.

4.2.3 Coil Design and Installation

Coil placement and mounting methods are critical. Coil mounts must be quite rigid to avoid energy losses due to mount flexing. Mounts are generally made of composite material. Typical coils are about 2 inches (50 mm) in diameter, 0.12 to 0.20 inches (3 to 5 mm) thick, and are contoured to match the leading edge skin inner shape. A layer of insulating enamel and a thin layer of fiberglass cloth are usually bonded over the coil. The air gap between the leading edge inner surface or doubler and the coil must be sufficient so that the vibrating skin will not strike the coil.

Special attention must be paid to the attachment methods for the doubler since very high loads will be passing through the doubler into the leading edge skin. If attachment of the doubler is done with mechanical fasteners, it should be done in a manner such that no part of the fastener will be drawn into the engine in event of fastener failure. However, adhesives are available for bonding of doublers, and so mechanical fasteners are not required for most installations.

III.4.3 USAGES AND SPECIAL REQUIREMENTS

4.3.1 Airfoil and Leading Edges

Coils are generally wired so that two spanwise positions are in series to reduce the number of cables and thyristors and to achieve better structural response. The two coil positions wired in series can be adjacent span stations or alternate positions. The thyristors (or "SCR"s") are usually located near the surface to be deiced to permit use of a common supply cable for several coils (figure 4-3).

Installation is most satisfactorily accomplished as original equipment at the factory. Retrofitting can be accomplished, but may require structural modification to the leading edge to suit coil placement and spacing. The small radius of curvature of empennage leading edges on small airplanes often precludes the use of a single nose coil, requiring two smaller opposing coils at the upper and lower sides of the leading edge.

4.3.2 Windshields

EIDI is not recommended for windshield de-icing.

4.3.3 Engine Inlet Lips and Components

Icing Wind Tunnel tests have been conducted on an EIDI system installed in a nacelle (figure 4-6) from a business jet aircraft (references 4-3 and 4-12). These tests show EIDI to be a viable method for aircraft engine inlet lip ice protection. Since EIDI expels ice particles, some of which are ingested by the engine, ice pieces were collected in a net for examination. From these observations and high speed photographic studies, the general rule was proposed that the effective diameter of particles expelled will be no larger than three times the maximum thickness of the ice layer. For these specific observations ice particle thickness was no larger than 1/8 inch and it was concluded that these particles will be able to be ingested by the engine without damage. In addition, this type engine ice ingestion must not cause an engine flameout. This requirement may call for more frequent impulses than for a wing or empennage protection system. No difficulty was experienced in de-icing due to added stiffness inherent in the inlet lip compound curvature. For inlets tested, a single coil on the inlet lip inner portion was better than either a nose coil placement or an inside-outside pair of coils. Spanwise spacing of the coils was about the same as for small airplanes, nominally about 18 inches (0.5 m). This system offers a significant reduction in the energy needed for ice protection when compared to hot air (bleed air) anti-icing systems. The potential applications for EIDI in engine inlets are numerous and encompass large-diameter, high bypass ratio turbofans, small-diameter business jet engine inlets, and circular or noncircular turboprop engine inlets. Considerations other than inlet type or shape will be the determining factor in the selection of EIDI as the best ice protection system. Initially, a determination should be made of the ice ingestion capability of the engine. EIDI can be designed to remove ice of a specified thickness, with larger thicknesses becoming progressively easier to remove. If the engine can handle short periods of cyclic ice ingestion of a specified size without undue compressor or fan blade erosion in the long term, EIDI can be safely used. The relatively small pieces of ice are a product of the removal mechanism that shatters the ice build-up. The ice will not shed in large continuous pieces if the system is properly designed and operated.

4.3.4 Turbofan Components

EIDI has not been applied to engine components such as inlet guide vanes because of their small size.

4.3.5 Propellers, Spinners, and Nose Cones

EIDI is not considered applicable to propellers because of their small blade cross section and rigid structure in the small radius portion which has the greatest tendency to accrete ice.

Spinners and nose cones can be deiced by electro-impulse. Coils can be supported on mounts fastened to nearby structure or can be skin-mounted. Nonrotating nose cones can be wired in the same manner as wing leading edge coils. Rotating cones or spinners introduce the complexity of commutator rings to transmit electrical power. It is generally poor practice to transmit the EIDI pulse

across commutator rings due to the high currents and voltages involved. This suggests placing the capacitors in the spinner, and transmitting low voltage recharge current across the commutator ring. A separate charging and firing circuit is then required for each spinner. This complexity may limit EIDI use for spinners.

4.3.6 Helicopter Rotors and Hubs

Application of EIDI to rotorcraft rotors is still in the development stage at the present time (1989). Retrofit is usually not possible because no leading edge cavity exists in which to place the coils and cable runs. Because of the critical balance and aeroelastic requirements, the EIDI equipment should he designed into the blade at the factory. An unbonded metal leading edge will be required on a rotorcraft blade. This is usually the abrasion shield which is fitted tightly over the leading edge substructure and bonded only at the downstream edges. The coils may be recessed into the leading edge composite material with a gap between the coil face and the abrasion shield. If the abrasion shield has insufficient conductivity, a doubler of higher conductivity material may be bonded to it opposite the coil location.

First plans to use EIDI in rotorcraft call for the power and sequencing boxes to be placed in the rotating hub column, with a commutator ring bringing in the low voltage current to a transformer and rectifier in the hub for continuous recharging of capacitors. Care must be taken to de-ice opposing blades symmetrically.

The damping effect of the rotor sub-structure on the metal surface makes it necessary to have coils at closer spacing intervals than for the fixed wing hollow structures. The small geometry usually dictates the use of a coil at the lower side rather than at the nose of the leading edge. Once the power and sequencing unit is provided in the rotor hub, the addition of coils to deice the hub's external surface is as easily accomplished as for a wing leading edge.

4.3.7 Flight Sensors

EIDI is not applicable to flight sensing instruments.

4.3.8 Radomes and Antennas

Aircraft radome and antenna de-icing have not been accomplished with electro-impulse. Before using EIDI coils for such de-icing, the possibility of electromagnetic interference with the transmitter/receiver should be evaluated.

4.3.9 Miscellaneous Intakes and Vents

Only components which are large compared to a minimum radius coil are possible candidates for EIDI protection. The minimum radius of impulse coils is approximately 1.25 inches (33 mm).

4.3.10 Other

EIDI coils can be varied in configuration and size for installation in structural numbers whose remote locations or complex shapes make them difficult to de-ice by thermal or pneumatic boot systems. This is particularly true of surfaces which contribute drag but do not reduce lift when iced. Struts which are aluminum extrusions used for wing braces on small airplanes are easily de-iced because of their structural dynamics (reference 4-4). Other candidates for EIDI usage are engine pylons and wheel covers.

III.4.4 WEIGHT AND POWER REQUIREMENTS

Estimates of weight and power required for EIDI are tentative at this early stage of development. The data presented below are, nevertheless, considered by the system developers to be conservative:

Aircraft	Power*	Weight**
6-place, propeller driven	400 watts	60 lbs***
150 passenger turbofan transport		
no redundancy:	2 kilowatts	250 lbs
full redundancy:	2 kilowatts	400 lbs
250 passenger transport		
no redundancy:	3 kilowatts	350 lbs
full redundancy:	3 kilowatts	500 lbs

* Based on 3 minute cycle for all surfaces.

** For wings and empennage surfaces; for engine inlets, increase by 25%.

*** Also includes wing struts for small airplanes.

III.4.5 ACTUATION, REGULATION, AND CONTROL

For surfaces not visible to the pilot, such as inboard wing areas or empennage, actuation by an ice detection or measurement instrument is advised. Additional surfaces may need to have automatic ice protection system actuation. Controls should be mounted in the cockpit with the ice detector indicator in an easily visible position.

III.4.6 OPERATIONAL USE

A simple test of small airplane systems can be performed on the ground by placing one's hand on the leading edge skin as each coil fires. Audible differences are evident for coils whose mounting has failed or whose circuit contains an electrical fault. An oscilloscope view of the current from the capacitor box may reveal changes in EIDI system physical geometry or electrical circuit faults. The more sophisticated units may have test circuitry installed in the aircraft for inflight system checkout.

III.4.7 MAINTENANCE, INSPECTION, AND RELIABILITY

Lack of sufficient operational experience at this time does not permit assessment of maintenance requirements or reliability. The power and sequencing box must be accessible for inspection. Terminals should be available in the box for attaching test leads to each coil's set of wires. For units using electrolytic capacitors, degraded performance may result if the capacitors are operated at colder temperatures (reference 4-14) and damage to the capacitors may result at temperatures below -40 degrees F (-40 degrees C). Inspection tests should evaluate capacitance after cold exposure. For many uses, the more costly metalized capacitors are required; these are not damaged by low temperature.

III.4.8 PENALTIES

See limitations below.

III.4.9 ADVANTAGES AND LIMITATIONS

Advantages of the EIDI System are:

a. Low power required. EIDI system power consumption is only about 1% of that required for hot air or electro-thermal anti-ice systems. It is claimed that power requirements for an EIDI system are about the same as for the landing lights for the same aircraft (see Section 4.4 above).

b. Reliable de-icing. Ice of all types is expelled, with only light residual ice remaining after the impulses. Ice thicknesses from 0.1 to 1.0 inch (2.5 to 25 min) have been consistently shed.

c. Non-intrusive in the airstream, hence no aerodynamic penalty.

d. Weight comparable to other deicing systems.

e. Low maintenance. Since there are no moving parts, the system should, in principle, be maintenance free.

f. No run-back re-freezing occurs.

g. Pilot skill and judgement required to operate the system are minimal.

Limitations of the EIDI system are:

a. It is new and has limited use at this writing (1989).

b. It is not an anti-icing system, so some ice will be present over most of the aircraft leading edges during flight in icing. This drawback is inherent in any de-icing method.

c. Outside the aircraft the discharges may be quite loud, resembling a light gunshot. Inside small aircraft, the impulses are audible but have been found to be almost imperceptible in a large transport category airplane.

III.4.10 CONCERNS

Concerns not resolved because of lack of operational experience are:

a. Possible fatigue of skin, coil mounts, insulation, etc. Testing indicates that coil mountings must be well designed to avoid fatigue failure. Laboratory testing has been done with small airplane leading edges, both aluminum and composite, at low temperatures and for normal de-icing electrical engines. No fatigue damage was found after impulses equaling the number expected in a twenty-year aircraft lifetime. Similar laboratory tests for a transport aircraft slat exceeding 200,000 impulses showed no fatigue damage (reference 4-8). All of these used doublers with the skins.

b. Electromagnetic interference (EMI). The discharge of 1000 volts to create transient electromagnetic fields might he expected to cause undesirable signals in communication, control, or navigation equipment. However, both laboratory and flight tests have failed to detect appreciable interference for metal air foils (references 4-6 and 4-7). The reasons suggested for this are: (1) the aluminum wing box provides a good shield (note that this might not be true for a non-metallic leading edge); (2) the frequency of the pulse is below 3 khz, which is below that of current aircraft avionics systems; and (3) the pulse is a pure wave (or half wave) without the "overtones" of a spark. In flight tests, added equipment has been carried specifically to detect EMI; these included LORAN-C, digital readout systems, and a radar pod mounted on the wing. One of these had control wiring which shared space with the EIDI cables. However, care should be taken to check for EMI, especially if non-shielded leads are physically near the EIDI power cables.

c. Possible adverse effects of lightning strikes. Since the EIDI system is electrical, there is the possibility of its being disabled by a lightning strike. Sudden overload protection of critical components may be required. If the EIDI system is installed in an aircraft whose structure is largely of composite materials, the EIDI cables could become the primary electrical paths through the structure when it is struck by lightning. Additional lightning paths through the aircraft may be required.

d. Failure modes and their consequences have yet to be clearly defined. Compliance with the failure analyses as described in FAA AC 25.1309-1A (reference 4-13) is required. The failure modes and redundancy possibilities will be quite different, however, for small and large aircraft.

III.4.11 REFERENCES

4-1 Levin, I.A., "USSR Electric Impulse De-Icing Design," Aircraft Engineering, pg. 7, July 1972.

4-2 Zumwalt, G.W. and Friedberg, R.A., "Designing in Electro-Impulse De-Icing System," AIAA 24th Aerospace Sciences Meeting, Reno, NV, January 6-9, 1986.

4-3 Zumwalt, G.W., "Electromagnetic Impulse De-Icing Applied to a Nacelle Nose Lip," AIAA/SAE/ASME 23rd Joint Propulsion Conference, Monterey, CA, July 8-10, 1985, AIAA Paper 85-1118.

4-4 Schrag, R.L. and Zumwalt, G.W., "Electro-Impulse De-Icing: Concept and Electrodynamic Studies," AIAA 22nd Aerospace Sciences Meeting, Reno, NV, January 9-12, 1984, Paper No. 84-0021.

4-5 Bernhart, W.D. and Zumwalt, G.W., "Electro-Impulse De-Icing: Structural Dynamic Studies, Icing Tunnel Tests and Applications," AIAA 22nd Aerospace Sciences Meeting, Reno, NV, January 9-12, 1984, AIAA Paper No. 84-0022.

4-6 Zumwalt, G.W. and Mueller, A.A., "Flight and Wind Tunnel Tests of an Electro-Impulse De-Icing System," AIAA/NASA General Aviation Technology Conference, Hampton, VA, July 10-12, 1984, AIAA Paper No. 84-2234.

4-7 Mueller, A.A., Ellis, D.R., and Basset, D.C., "Flight Evaluation of an Electro-Impulse De-Icing System on a Light General Aviation Airplane," AIAA/AHS/ASEE Aircraft Design Systems and Operation Meeting, San Diego, CA, October 31-November 2, 1984, AIAA Paper No. 84-2495.

4-8 Zumwalt, G. W., Friedberg, R.A., Schwartz, J.A, "Electro-Impulse De-icing Research (Fatigue and EMI Tests)," Federal Avation Administration Technical Report, DOT/FAA/CT-88/27, March 1989

4-9 Zieve, P.B., "Electromagnetic Emissions from a Modular Low Voltage Electro-Impulse De-Icing System," FAA Technical Report, DOT/FAA/CT-88/31, March 1989.

4-10 Zumwalt, G.W., Schrag, R.L., Bernhart, W.D., and Friedberg, R.A., "Analysis and Tests for Design for an Electro-Impulse De-Icing System," NASA CR 174919, May 1985.

4-11 Lewis, G.J., "The Electrodynamic Operation of Electro-Impulse De-Icing Systems," AIAA 24th Aerospace Sciences Meeting, Reno, NV, January 6-9, 1986, AIAA Paper No. 86-0547.

4-12 Nelepovitz, D. O. and Rosenthal, H. A., "Electro-Impulse De-Icing of Aircraft Engine Inlets," AIAA 24th Aerospace Sciences Meeting, Reno, NV, January 6-9, 1986, AIAA Paper No. 85-0546.

4-13 "System Design Analysis," FAA Advisory Circular 25.1309-1A (Draft, Sept. 1986).

4-14 Masters, C. O., "Electro-Impulse De-Icing Systems: Issues and Concerns for Certification," AIAA 27th Aero Space Science meeting, Reno NV, January 9-12, 1989 AIAA Paper No. 89-0761

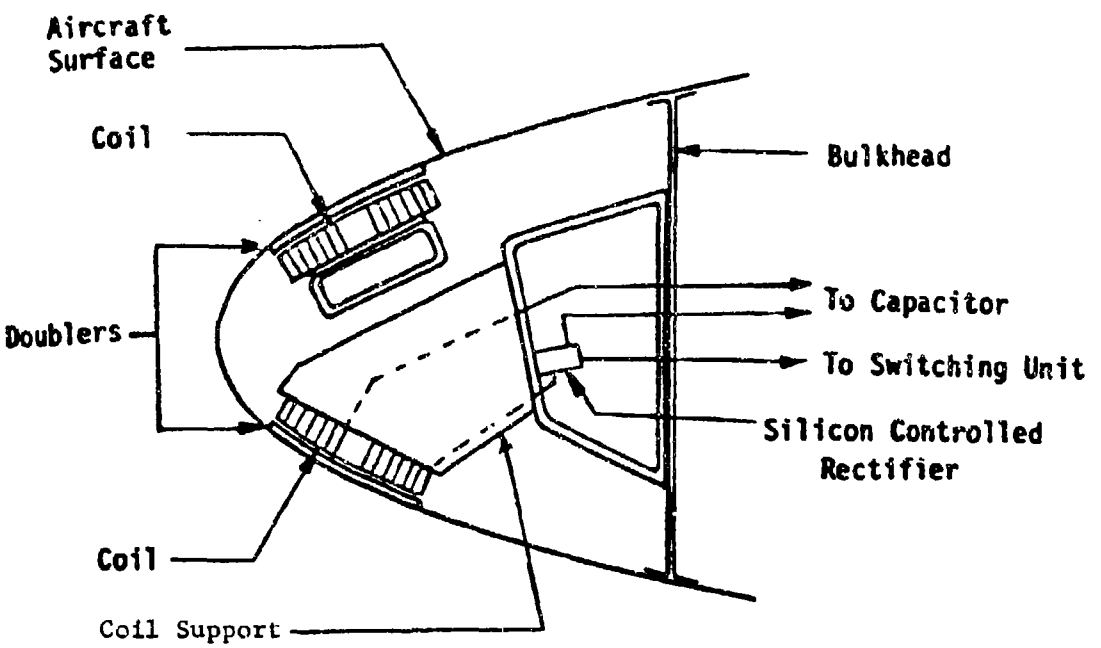

FIGURE 4-1. IMPULSE COILS IN A LEADING EDGE

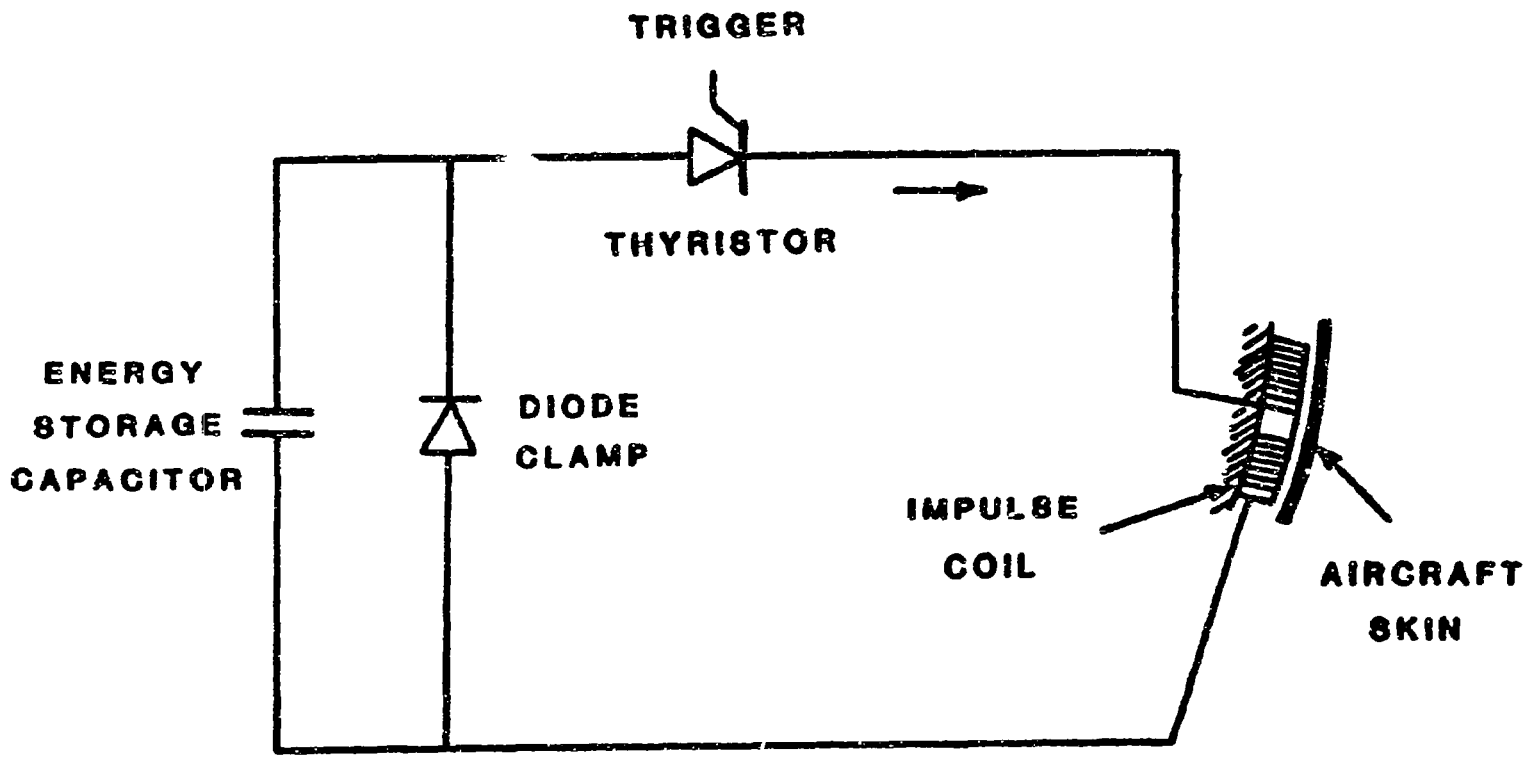

FIGURE 4-2. BASIC CIRCUIT

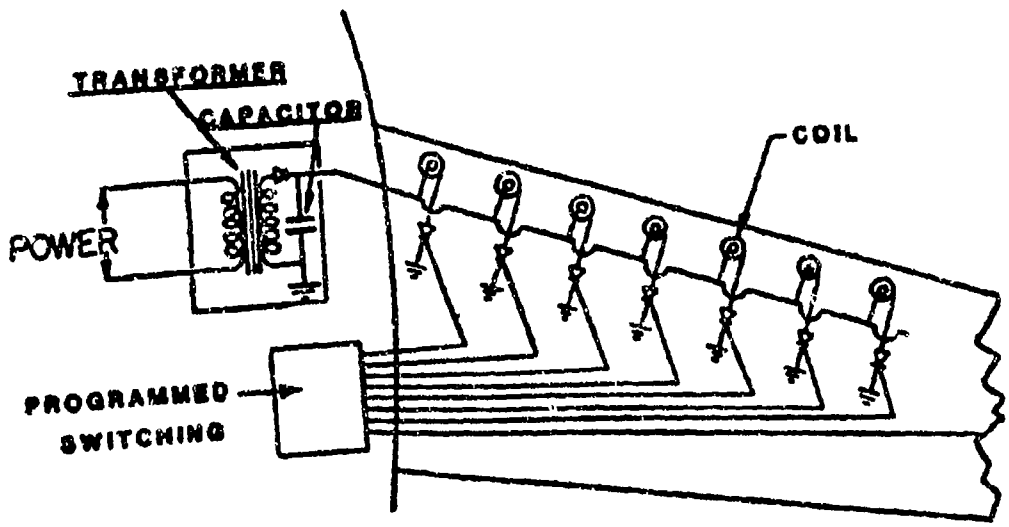

FIGURE 4-3. A BASIC ELECTRO-IMPULSE DE-ICING SYSTEM IN A WING

THE IMPULSE DE-ICING SYSTEM
FULL FEATURE SYSTEM

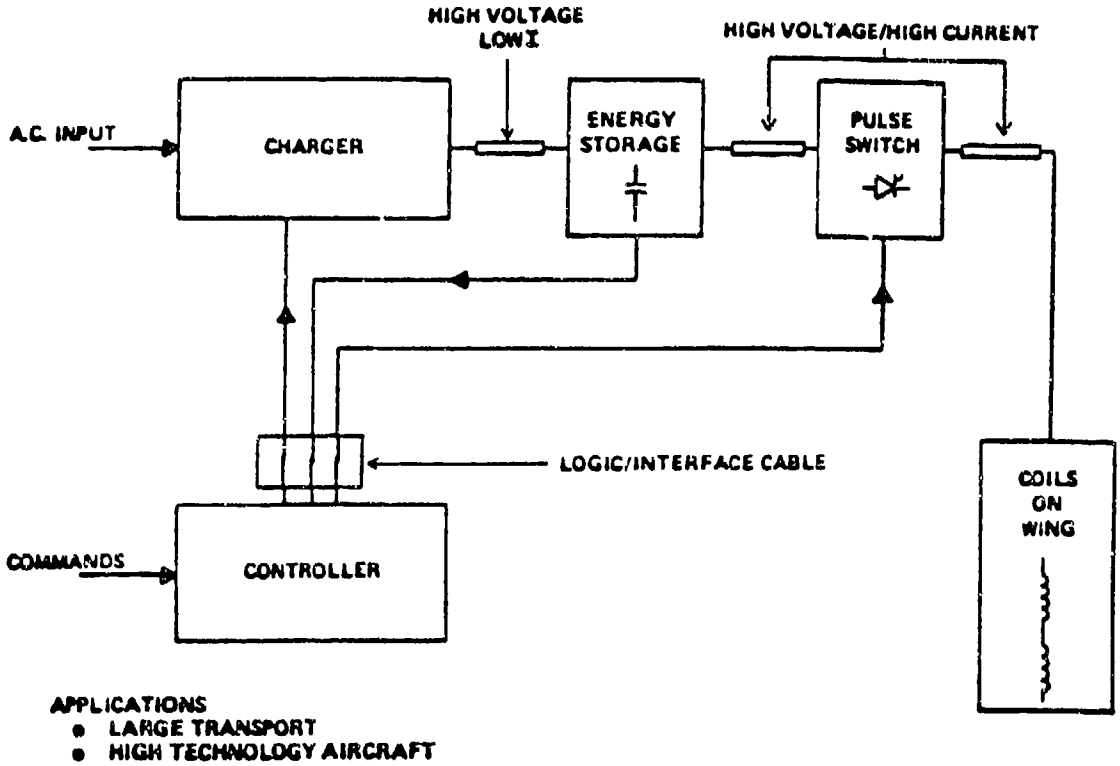

FIGURE 4-4. EIDI SYSTEM SCHEMATIC

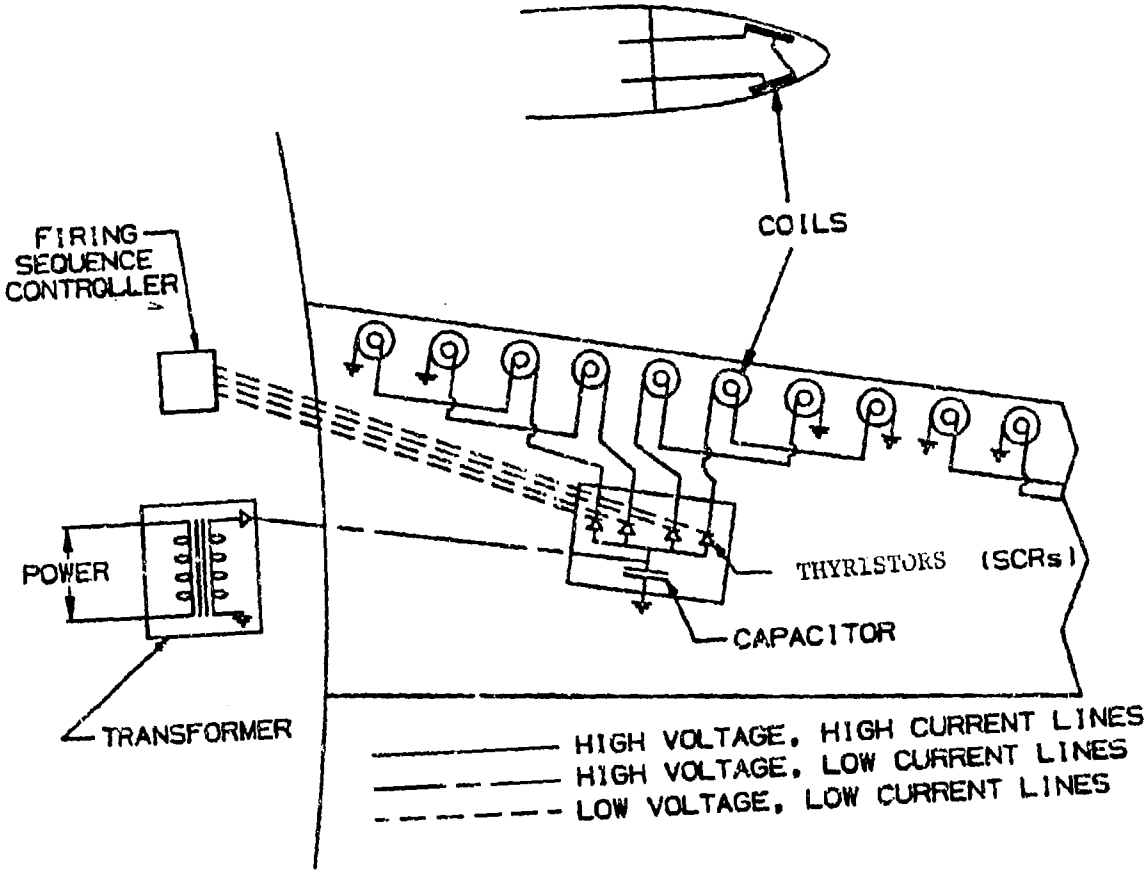

FIGURE 4-5. EIDI SYSTEM IN A LARGE AIRCRAFT WING

A. Accreted Ice on the Engine Inlet

B. Accreted Ice from the Engine Inlet Has Been Removed by EIDI

FIGURE 4-6. FALCON FANJET ENGINE INLET BEING DE-ICED BY EIDI

CHAPTER III
SECTION 5.0
HOT AIR SYSTEMS

CHAPTER III - ICE PROTECTION METHODS

CONTENTS

SECTION 5.0 HOT AIR SYSTEMS

	Page
LIST OF TABLES	III 5-iv
LIST OF FIGURES	III 5-v
SYMBOLS AND ABBREVIATIONS	III 5-viii
GLOSSARY	III 5-x
III.5.1 OPERATING CONCEPTS AND COMPONENTS	III 5-1
III.5.2 DESIGN GUIDANCE	III 5-1
5.2.1 Anti-icing	III 5-2
5.2.2 De-Icing	III 5-2
III.5.3 USAGES AND SPECIAL REQUIREMENTS	III 5-3
5.3.1 Airfoils and Leading Edge Devices	III 5-3
5.3.1.1 Wing Hot Air Anti-Icing	III 5-3
5.3.1.2 Wing Hot Air De-Icing	III 5-5
5.3.1.3 Slats and Krueger Flaps	III 5-7
5.3.1.4 Empennage Anti-Icing and De-Icing	III 5-8
5.3.1.5 Typical System Description	III 5-10
5.3.2 Windshields	III 5-11
5.3.2.1 Double-Pane Anti-Icing System	III 5-11
5.3.2.2 External Air Blast Anti-Icing	III 5-12
5.3.3 Engine Inlet Lips and Components	III 5-13
5.3.4 Turbofan Components	III 5-14
5.3.4.1 Typical System Description	III 5-14
5.3.4.2 System Design (Compressor Bleed)	III 5-15
5.3.4.3 Selection of Compressor Bleed Stage - Considerations	III 5-16
5.3.4.4 Selection of Compressor Bleed Stage - Calculations	III 5-17
5.3.5 Propellers, Spinners, and Nose Cones	III 5-18
5.3.6 Helicopter Rotors and Hubs	III 5-18
5.3.7 Flight Sensors	III 5-19
5.3.8 Radomes and Antennas	III 5-19
5.3.9 Miscellaneous Intakes and Vents	III 5-20
5.3.10 Other Usages	III 5-20
5.3.10.1 Strakes	III 5-20
III.5.4 WEIGHT AND POWER REQUIREMENTS	III 5-21
III.5.5 ACTUATION, REGULATION, AND CONTROL	III 5-22
III.5.6 OPERATIONAL USE	III 5-23

CONTENTS (CONTINUED)

	Page
III.5.7 MAINTENANCE, INSPECTION, AND RELIABILITY	III 5-23
III.5.8 PENALTIES	III 5-24
5.8.1 Advanced Turbofans	III 5-24
5.8.2 Future Advanced Engines	III 5-24
III.5.9 ADVANTAGES AND LIMITATIONS	III 5-25
III.5.10 CONCERNS	III 5-27
III.5.11 REFERENCES	III 5-28

LIST OF TABLES

		Page
5-1	Icing Tunnel Test Conditions for Figure 5-28	III 5-29
5-2	Design Point Flight and Icing Conditions	III 5-30
5-3	Strake Minimum Surface Temperature	III 5-31

LIST OF FIGURES

		Page
5-1	Areas of Airframe that May Use Hot Air Ice Protection	III 5-32
5-2	Air Flow in Typical Leading Edges of Heated Wings	III 5-33
5-3	Typical Cross-Sections of Double-Skin Gas Passages	III 5-34
5-4	Single Skin Hot Air Anti-Icing Installation	III 5-35
5-5	Arrangement for Cyclic Thermal De-Icing	III 5-36
5-6	Construction Details of Gas-Heated Airfoil for Cyclic De-Icing	III 5-37
5-7	Typical FAR 25 Jet Transport	III 5-38
5-8	Typical Hot-Air Anti-Icing System	III 5-39
5-9	Typical Hot-Air Anti-Iced Wing Leading Edge	III 5-40
5-10	Anti-Icing Heat Requirement vs. Wing Station - Hold Condition	III 5-41
5-11	Air Flow Rates for Wing Anti-Icing - Hold Condition	III 5-42
5-12	Typical Hot-Gas De-Icing System for Four-Engine Transport	III 5-43
5-13	Typical Wing Leading Edge Cross-Section for Two Types of Hot-Gas De-Icing Systems	III 5-44
5-14	De-Icing Time vs. Datum Temperature for Two Typical Hot-Gas De-Icing Systems	III 5-45
5-15	Typical Wing Leading Edge with Slat	III 5-46
5-16	Typical Wing Leading Edge with Krueger Flap	III 5-47
5-17	Ice Accretion on Unprotected Extended Leading Edge Flap for Maximum Continuous Icing Conditions	III 5-48
5-18	Tail Ice Protection System Duct Schematic	III 5-49
5-19	Wing Leading Edge Cross-Section - Double Skin Flow Passage	III 5-50
5-20	Horizontal Stabilizer Cross-Section - Direct Impingement	III 5-51
5-21	Horizontal Stabilizer De-Icing Flow Passage	III 5-52
5-22	De-Icing Thermal Network	III 5-53
5-23	De-Icing Supply Air Temperatures vs. Time	III 5-54
5-24	De-Icing Thermal Network - Double Skin Flow Passage	III 5-55

LIST OF FIGURES (CONTINUED)

		Page
5-25a	Time Temperature Response for Horizontal Stabilizer - Upper Surface	III 5-56
5-25b	Time Temperature Response for Horizontal Stabilizer - Lower Surface	III 5-57
5-26	Wing Parallel Flow Single Skin System	III 5-58
5-27	Wing Parallel Flow Double Skin System	III 5-59
5-28	Performance Comparison of Single and Double Skin Anti-Icing	III 5-60
5-29	Typical Windshield Areas to be Protected for Two Windshield Arrangements on Multi-Engine Transport	III 5-61
5-31	External Air Blast Windshield Anti-Icing and Rain Removal System	III 5-62
5-32	Windshield Anti-Icing Heat Requirements	III 5-63
5-33	Typical Anti-Icing Heat Requirements vs. Altitude for Center Windshield Panel	III 5-64
5-34	Typical Engine Inlet Lip Anti-Icing System	III 5-65
5-35	Typical Engine Inlet Lip Anti-Icing Heat Release vs. Altitude	III 5-66
5-36	Typical Engine Inlet Lip Anti-Icing Air Flow Requirements vs. Altitude	III 5-67
5-37	Typical Inlet Guide Vane for Single-Pass Internal Flow Scheme	III 5-68
5-38	Multi-Pass Anti-Icing Internal Flow Scheme for a Stator	III 5-69
5-39	Typical Routing of Anti-Icing Air	III 5-70
5-40	Nose Section of an Inlet Guide Vane	III 5-71
5-41	Bleed Stage Selection Limitations	III 5-72
5-42	Typical Hot Air Anti-Icing System for Nose Radome	III 5-73
5-43	Strake Schematic Flow Diagram System	III 5-74
5-44	Engine Specific Thrust and Airflow vs. Bypass Ratio(BPR) (Relative to a 5.5 BPR Engine)	III 5-75

LIST OF FIGURES (CONTINUED)

		Page
5-45	All Bleed System Allocation	III 5-76
5-46	The Bleed Air Problem - 150 Passenger Airplane	III 5-77

SYMBOLS AND ABBREVIATIONS

Symbol	Description
A_{flow}	Flow area in guide vane, ft^2
A_{surf}	Area of surface leading edge, ft^2
b	Height of duct in inlet guide vane, ft
BPR	Bypass ratio
BTU	British Thermal Units
°C	Degrees Celsius
C_D	Discharge coefficient
cm	Centimeter
C_p	Specific heat at constant pressure, Btu/(lb-°R)
D_h	Diameter of heat flow duct, ft
°F	Degrees Fahrenheit
ft	Feet or foot
FP_{isen}	Flow parameter at isentropic conditions, $lbm(°R)0.5(lb_f)^{-1}$
h_{AI}	Convective heat transfer coefficient, $Btu/(sec\text{-}ft^2\text{-}°R)$
HP	Horsepower
hr	Hour
K	Conduction heat transfer coefficient of air, Btu/(ft-sec-°R)
kg	Kilogram
kg/s	Kilograms per Second
kJ	Kilojoules
kN	Kilonewton
lb_f	Pounds force
lb_m/s	Pounds mass per second
m	Meter
mm	Millimeter
mph	Miles per hour
mps	Meters per second
M	Mach number
P	Pressure of airflow, lb/ft^2
Pr	Prandtl number of air
psig	Pressure in pounds per square inch gage

Symbol	Description
Q''_{reqd}	Heat required, Btu/(sec-ft^2)
°R	Degrees Rankine
Re_{Dh}	Duct Reynolds number
s or sec	Second
scfm	Specific cubic feet per minute
TSFC	Thrust Specific Fuel Consumption
w_{AI}	Weight flow rate of air, lb_m/s
W_M	Water catch rate, lb_m/hr-ft span
μ	Dynamic viscosity of air, lb_m/(ft-sec)

Subscripts

AI	Anti-icing air

GLOSSARY

glaze ice - Coating of generally clear, smooth ice deposited on surfaces exposed to a film of supercooled water.

liquid water content (LWC) - The total mass of water contained in all the liquid cloud droplets within a unit volume of cloud. Units of LWC are usually grams of water per cubic meter of air (g/m^3).

median volumetric diameter (MVD) - The droplet diameter which divides the total water volume present in the droplet distribution in half; i.e., half the water volume will be in larger drops and half the volume in smaller drops. The value is obtained by actual drop size measurements.

micron (μ)m - One millionth of a meter.

rime ice - Deposit of white or milky, opaque granular ice formed by instantaneous freezing of supercooled water droplet impingement. Rime ice usually contains tiny air pockets.

stagnation point - The point on a surface where the local velocity is zero.

datum temperature - The temperature of an unheated surface in an icing environment.

III.5.0 HOT AIR SYSTEMS

III.5.1 OPERATING CONCEPTS AND COMPONENTS

As in all thermal ice protection systems, heat is applied to an area encompassing the water droplet impingement region. The heat is used to either prevent the freezing of impinging droplets or to evaporate impinging droplets (anti-icing) or to debond the accreted ice (de-icing). In either case, a source of heated air is required. Four sources that can be considered alone or in combination are:

a. Extraction of engine compressor air (bleed air), generally used on turbojet or turboprop aircraft.
b. Compression of ram air using a dedicated electric-driven or shaft-driven compressor.
c. Recovery of exhaust gas waste heat, generally used on piston driven engines.
d. Heating of ram air using a fuel-burning combustion heater.

The hot air supply is ducted to the surface requiring ice protection. It is then distributed to the surfaces by means of special tubing or ducting such that maximum utilization of the available heat is achieved. Major components of a hot air system include:

a. Source of hot air.
b. Temperature and/or pressure control for source air.
c. Ducting (insulated or non-insulated) to route the hot air to the desired areas.
d. Distribution equipment at the surfaces to be heated (e.g., double skin ducts, piccolo tubes).
e. Temperature and/or pressure control at the heated surface.
f. Manual or automatic control unit to condition the air at either the source or at the distribution area, or both.
g. Cockpit panel mounted display to advise crew of system operation (e.g., warning lights, skin temperature indicators, pressure gages).

Safe operation dictates that the pressure and temperature of the heated air must be controlled. For ducts routed in an area that is a potential fire zone, the bleed air temperature is generally kept below 450°F which is compatible with the autogenous ignition limit of jet fuel. The pressure is also limited to less than approximately 50 lb_f/in^2 (345 kN/m^2) to minimize the possibility of a ruptured duct and to reduce weight of downstream ducting and components.

Redundant heated air sources are generally provided to ensure a high dispatch reliability into icing conditions and to ensure safe system operation.

III.5.2 DESIGN GUIDANCE

Two basic methods are used for hot air ice protection: anti-icing and de-icing. An anti-icing system prevents the formation of ice in the specified area whereas a de-icing system allows ice to build up and then removes the accreted ice.

5.2.1 Anti-icing

Hot air anti-icing systems use heated air to maintain the temperature of the surface to be protected above freezing throughout an icing encounter. Hot air anti-icing systems are classified as fully evaporative or running wet. Evaporative systems supply sufficient heat to evaporate all water droplets impinging upon the heated surface. Running wet systems provide only enough heat to prevent freezing on the heated surface. Beyond the heated surface of a running wet system, the water could freeze (generally called runback ice). For this reason, running wet systems must be carefully designed to prevent runback ice buildup in critical locations. For example, the heated surface of a running wet system for a turboprop or turbojet inlet should extend into the inlet to the compressor face so that the water runoff will combine with the intake air and not strike cold surfaces where it could re-freeze, break off, and possibly damage the engine.

For anti-icing, the heat source must remain on throughout the icing encounter. Areas of an aircraft that may be afforded hot air ice protection are shown in figure 5-1. Areas usually protected by a hot air system are engine inlets, wing leading edges, and empennage leading edges. Basically, the hot air is manifolded to the various portions of the aircraft to be protected and distributed by one of several methods, as shown in figures 5-2, 5-3, and 5-4. The hot air is generally introduced near the stagnation point of the surface to be protected and permitted to flow chordwise toward an exit point through gas passages. The exhaust is generally dumped overboard at a non-critical location.

5.2.2 De-Icing

In a de-icing system, ice accretion is permitted on the surfaces to be protected and is removed periodically. Hot air de-icing systems function by applying sufficient heat to the ice surface to melt the bonding layer of ice. Aerodynamic or centrifugal forces then remove the bulk of the ice. The areas that may be protected by a de-icing system are also shown in figure 5-1.

Large areas to be protected are usually divided into small shedding sections by continuously heated (anti-icing) chordwise and spanwise parting strips. Figure 5-5 is a schematic of such a division showing the spanwise parting strip located along the stagnation line of the airfoil and the parting strips running chordwise. Cyclic de-icing is usually reserved for the larger areas as the weight and complexity of control does not justify its use on small areas.

Sources of hot air for de-icing vary depending upon the type of powerplant. In turbojet and turboprop engines, hot air may be obtained directly from compressor bleed or from a heat exchanger located in the exhaust system. Combustion heaters may be used with either piston or turbine engines. The hot air is distributed from its source to the shedding section by ducts. For each shedding section, hot air is supplied continuously to the parting strips and intermittently to the de-icing duct. Airflow to the various de-ice sections is controlled by valves that cycle the hot air to at least two sections at a time, thereby keeping the remaining accreted ice on the airfoils as symmetric as possible. Figure 5-6 shows a NACA air heated cyclic de-icing wing section with a continuously heated parting strip

for cyclically heating the shedding sections (reference 5-1). The air is then discharged overboard at some convenient location.

On some aircraft, icing of the horizontal and/or vertical stabilizers does not impose an intolerable penalty during flight but the ice must be removed prior to landing (to avoid increasing the landing speed). For this type of application, "one-shot" empennage de-icing has been used. As the name suggests, ice protection is not used until sometime during the descent or approach phase. At that time, a single de-icing cycle is imposed which sheds the accreted ice. A parting strip near the stagnation region is sometimes heated continuously during the icing encounter to help facilitate de-icing during descent.

III.5.3 USAGES AND SPECIAL REQUIREMENTS

5.3.1 Airfoils and Leading Edge Devices

Hot air ice protection can be implemented using either an anti-icing or de-icing system. These methods will be compared in Sections 5.3.1.1 and 5.3.1.2. The methods used for a typical four-engine turbojet aircraft and its wing ice protection systems will be described.

The general characteristics of the selected aircraft are illustrated in figure 5-7. Its four engines are pod-mounted beneath the wings. Wing span is approximately 120 feet (36.6 m) with a fuselage length of 129 feet (39.3 m). Maximum gross weight is approximately 185,000 lb (83,900 kg).

Hot air ice protection for high-lift leading edge devices is discussed in Section 5.3.1.3 and "one-shot" empennage de-icing in Section 5.3.1.4. Section 5.3.1.5 presents comparative data on the single-skin (spray tube) and double-skin designs.

5.3.1.1 Wing Hot Air Anti-Icing

The wing ice protection system selected for a typical turbojet powered aircraft is hot air anti-icing. The source of the hot air is the engine compressor bleed air. This high pressure, high temperature air is ducted through regulating valves to each wing section (inboard, center, and outboard) at approximately 13 lb/in^2 (figure 5-8). Higher pressure is used for some wing anti-icing applications. In each section are piccolo tubes which discharge the air to a plenum area at approximately 2 lb/in^2 (13.8 kN/m^2). The air then flows through narrow-gap, high efficiency, chordwise gas passages which form the wing leading edge. The air then is discharged overboard through ports on the lower surface just forward of the front spar. This is illustrated in figure 5-9. The chordwise gas passages are designed to use 85 to 90 percent of the initial heat energy before it is discharged. The extent of chordwise coverage needed depends on the airfoil, angle of attack, and other flight parameters, as well as on the effects of runback icing on airfoil drag. To determine wing hot air ice protection system requirements, a performance evaluation point is first established. The performance evaluation point chosen is the holding condition at 5,000 ft (1524 m) altitude. This point was established by the following considerations: (1) Calculating the water catch rate and heat required

for complete evaporation at several wing stations for various flight conditions, and (2) using bleed air temperature schedule for these flight conditions to determine the condition requiring the maximum bleed air flow. Some illustrative values for these calculations, taken at wing station 120 (i.e., 120 inches (3.05 m) from the aircraft centerline) and at the holding design condition, are:

a. Impingement limit upper surface (S_U) = 1.32 inches (3.35 cm) (20 micron droplet size).

b. Impingement limit lower surface (S_L) = 9.91 inches (25.2 cm) (20 micron droplet size).

c. Water catch rate (W_M) = 10.1 lb/hr-ft span (15.03 kg/hr - meter span).

(Note: The impingement limits for 40 micron drops are roughly twice the 20 micron limits; however, the bulk of the ice formation lies between the 20 micron limits.)

The heat-transfer coefficient at several wing stations is determined. With these heat transfer coefficients water catch rates and performance evaluation flight conditions, the heat requirements for evaporative anti-icing are determined. A plot of these requirements versus span station for the entire wing are presented in figure 5-10.

This heat requirement must be converted into a hot-air flow requirement to determine the feasibility of using hot air. Information needed for calculating the hot-air flow requirement is the piccolo tube air temperature decay and the leading edge air passage efficiency. Piccolo tube air temperature decay and air passage efficiency may be determined by analysis or laboratory tests. The required and actual hot air flow rates versus altitude are presented in figure 5-11. As shown, the system is marginal but adequate at the evaluation point; performance is in excess of requirements for other flight conditions.

Typical weight flows for wing anti-icing protection at the design conditions are:

Inboard	0.76 lb/s (.35 kg/s)
Center	0.82 lb/s (.37 kg/s)
Outboard	0.66 lb/s (.30 kg/s)
Total	2.24 lb/s (1.02 kg/s) (semi-span)
Grand Total	4.48 lb/s (2.04 kg/s)

A system that reduces the bleed air temperature by recirculation of anti-icing discharge air also may be used for anti-icing protection. In this system, unregulated and uncooled bleed air is distributed to the wings (and empennage if hot air protected) in stainless-steel or titanium ducts. At each section, a regulator valve (usually thermostatically regulated) passes the air into piccolo tubes where the air is discharged through a large number of small ejector nozzles. The air from the ejectors mixes with plenum air, is cooled, and then passes through the leading edge double skin heat exchangers and back into the plenum. The excess air is dumped overboard. The thermostatic sensor used to control the regulating shutoff valves is located at the heat exchanger exit and controls the air to a discharge temperature of approximately 135°F (57°C). This system achieves high efficiency with

relative deep air passages (1/8 to 3/16 inch (3.2 to 4.8 mm)) as opposed to the single pass system which requires narrow passages (on order of 0.04 to 0.05 inch (1.02 to 1.27 mm).

On turbine engines having two compressors, bleed air from the low pressure compressor, with its lower energy air, will require larger volume flows. To handle these larger volume flows, the ducting and leading edge heat exchanger passages will have to be larger, but in other ways the system will be generally the same as the high pressure bleed air anti-icing protection system. Difficulty may be experienced in obtaining adequate protection at low engine rpm, as in descent and holding, but use of low pressure bleed may allow elimination of pressure and/or temperature regulation, thus simplifying the system. Installed weights may be lower because the reduced temperature and pressure will allow lighter ducting; this is offset to a large extent by the requirement for handling larger mass flows (for a given thermal requirement). A mixing system may also be used that employs low pressure bleed air augmented by high pressure bleed as required to achieve a desired temperature.

There may be occasions when an anti-icing system is used in a de-icing manner. Prior to such usage, the system should be tested for de-icing adequacy. Methods of testing are discussed in Section 5.6.

5.3.1.2 Wing Hot Air De-Icing

In a turbine engine powered aircraft, particularly one with turboprops or high bypass ratio turbofans, adequate bleed air may not be available under all flight conditions. In this case, a solution is the use of a hot air de-icing system. This system has been used on at least one military turboprop transport and one long range commercial transport. Unfortunately, the advantage of reduced bleed air requirements is offset by increased system complexity and, in some cases, increased weight. Thus, the choice of hot air de-icing versus hot air anti-icing must be made with due regard to all factors of a particular aircraft's requirements.

Actual analysis and design of a hot air de-icing system would require a major engineering effort because of the degree of complexity and the necessary transient analysis. A full description of the results of such an effort is beyond the scope of this report. Instead, a de-icing system that would suit the needs of a typical aircraft is described, with comments and suggestions on adaptations that would be required for other types of transport aircraft.

The operating principles of a hot air de-icing system are identical to those of an electro-thermal cyclic de-icing system. Only the mode of energy supply is changed. A sketch of a simple system for a swept wing transport is shown in figure 5-12. The bleed air from four engines is directed into a common spanwise manifold from which the de-icing ducts are led for the six wing sections and for the empennage. Only nine sections are shown in this arrangement, resulting in the de-icing of 18 to 20 foot span (5-6 m) sections at one time. Performance could be improved by supplying air at the center of each section rather than at each end as shown in the illustration. Further economies in air supply would be effected by using 18 ten foot (3 m) sections rather than 9 twenty foot sections, but with increased system complexity.

The system shown in figure 5-12 does not use or require spanwise parting strips because the sweep angle is greater than 30 degrees. In nonswept wings, the spanwise parting strips may be required as shown in figure 5-13. Use of parting strips almost doubles system complexity and increases air flow requirements. Where parting strips are needed, the method most likely to produce uniform spanwise width is that shown in figure 5-13. The duct is split to allow air to flow the length of the duct in one direction, reversing and flowing back in the opposite direction.

The air passages shown in figure 5-13 are the typical corrugated skin type often used for anti-icing, although the passages may be tapered to allow equal heating of the surface. (The increased heat transfer coefficient at the aft end of the gas passage compensates for the decreased gas temperature.)

Air supply ducts may or may not be used to carry air spanwise in the leading edge, depending on temperature, duct length, and strength/temperature characteristics of the aluminum alloy used for the skins and baffles. Below 450°F (223°C) gas temperature, ducts may not be required.

The de-icing cycle used for hot air systems will usually involve somewhat longer heat-on and heat-off times than for a cyclic electric system. This results from the thermal inertia of the inner and outer skins, baffles, etc., as compared to a cyclic electric heat that heats only a very thin layer of insulation and skin. For the system in figure 5-12, 30 seconds on (maximum) and 240 seconds off would be a typical cycle. At higher datum temperatures than the minimum value it is desirable to reduce heat-on time as a function of datum temperature (see figure 5-14). This minimizes refreeze at the higher temperatures. Timers are available commercially to perform this function. The heat-off time may be fixed or may be made manually variable. Flight experience with a cyclic de-icing system has indicated that heat-off times of as much as six to eight minutes may be required to allow a system with high thermal inertia to cool down and collect sufficient ice before the next application of heat is required. Heat-off time may also be made variable by use of an ice measuring instrument to indicate icing severity.

De-icing time versus datum temperature is shown in figure 5-14 for two typical de-icing systems. At 25°F (-4°C) de-icing times are about 4 to 8 seconds, whereas at -10°F (-23°C), 28 to 29 seconds are required. The de-icing air flow is 1.16 to 1.74 lb/s (.53 to .79 kg/s) based on 20 foot (6 m) sections, depending on the system used and air temperature. Details are not shown on parting strip flow requirements. In most current applications, (swept wing), parting strips are not needed. For nonswept wings, data may be found in reference 5-1.

Various combinations of anti-icing and de-icing also may be used, depending on the needs of a particular aircraft. For example, it might be desirable to anti-ice the more critical outboard wing areas and de-ice the inboard wing and empennage leading edges after leaving an icing condition. This procedure could be an acceptable compromise between available bleed air and excessive system complexity.

5.3.1.3 Slats and Krueger Flaps

The preceding descriptions of ice protection systems for the wing of a transport aircraft assumed a fixed leading edge. Wings with movable leading edge devices will have the same ice protection requirements but methods of meeting these requirements will differ and will be more complex.

Leading edge devices may consist of slats, slots, or flaps. A wing leading edge slat configuration is shown in figure 5-15. This figure represents a hot air anti-icing system as applied to the aircraft shown in figure 5-7. The slat portion of the wing leading edge incorporates a piccolo tube which gives ice protection to the leading edge, upper surface of the leading edge, and to a small portion of the lower surface. The fixed portion of the wing leading edge also has a piccolo tube which supplies ice protection to the remainder of the airfoil's lower surface and to part of the fixed leading edge within the slot. The slat piccolo tube is supplied hot air by means of a telescoping duct. The fixed wing behind the slot may or may not require protection depending on geometry, ice accretion characteristics, and time in icing. For each new aircraft a study should be made of the need for heating this area.

The anti-icing air flow must be divided between the slat and fixed leading edge in proportion to their requirements. This is accomplished by the correct sizing of the piccolo tube discharge coefficients. At the example design point (5,000 ft (1524 m) altitude holding condition) the flow requirement of 0.8 lb/s (0.4 kg/s) for the center section is divided 60 percent for the slat and 40 percent for the fixed leading edge.

Leading edge Krueger flaps may or may not be protected depending upon the effects of ice accretion on performance. Figure 5-16 illustrates an unprotected leading edge flap as might be installed on the example aircraft (figure 5-7). Ice protection requirements for the wing leading edge will remain the same but because of the flap installation, there will be a reduction in the heated area on the lower surface. Water may runback from the heated leading edge and freeze in the flap, if the leading edge anti-icing system is not fully evaporative. Also, there will be a small amount of direct impingement. Evaluation of need for heating the flaps can be made by an aerodynamic analysis.

Ice accretion may occur when the flap is extended during takeoff and approach. Figure 5-17 illustrates the amount of ice that may accumulate, based on 30 minute holding in icing. No appreciable ice is accumulated during takeoff, as flaps are retracted about 1.5 minutes after brake release. If the flap is unprotected, flight tests should be conducted to determine the effects of this ice accretion. One flight test method which may be employed is to simulate the predicted ice shapes and weight with wood or other materials and attach them to the flap. Then the airplane performance and handling characteristics may be evaluated in clear air. The ice shape used and its orientation on the leading edge should be verified by natural icing tests.

Ice protection may be provided for the flap using hot air by fabricating the flap as a double skinned heat exchanger similar to the wing leading edge. The hot gas may be transmitted to the flap either through a telescoping duct or a swivel fitting and duct.

De-icing requirements would be similar to the requirements of a fixed leading edge. Shedding characteristics will probably be different because of the airfoil shape and the aerodynamic forces the ice will encounter. An icing tunnel test program may be required due to the difficulty in predicting shedding forces and impingement.

5.3.1.4 Empennage Anti-Icing and De-Icing

Empennage hot air anti-icing may be accomplished using a system similar to the wing installation. For a typical turbojet aircraft, this would require ducting the hot air from the engines the 90 feet (27 m) to the empennage through the pressurized fuselage. Aircraft with a tail mounted engine will not encounter these problems but will encounter the same problem for ducting hot air to the wings.

The design point for determining empennage anti-icing requirements will normally be the same as for the wings. The air flow requirement calculations will have to account for the air temperature losses experienced in the 90 feet of ducting. An approximate value of the flow required to anti-ice the empennage at the design point is 2.0 lb/s (0.91 kg/s).

The design of the "one-shot" empennage de-icing concept of ice protection is described for a typical transport aircraft horizontal stabilizer using a double-skin hot air de-icing installation. Hot air for horizontal stabilizer de-icing is supplied from the pneumatic system which mixes high and low pressure bleed air to obtain a regulated pressure and temperature of 20 lb/in^2 (138 KN/m^2) and 380 to 490°F (193 to 254°C) respectively. From the main pneumatic system, the heated air is ducted through the empennage shut-off valve and flow limiting venturi and up through the vertical stabilizer supply ducting (for "T-tail" configuration). At a point near the top of the vertical stabilizer, the flow is split for the right and left horizontal stabilizer. The de-icing air is ducted outboard and is supplied to two piccolo tubes located within the "D" ducts. The most inboard piccolo tube, which is 1.25 inches (32 mm) diameter, supplies de-icing air for the inboard section. The other piccolo tube, which varies in diameter from 3 inches at the inlet to 1 inch at the tip, supplies de-icing air for the outboard section. Schematically, the system is shown in figure 5-18.

From the piccolo tube, hot air is supplied to typical double skin de-icing flow passages located chordwise along the leading edge. These passages extend from the leading edge to the aft edge of the "D" duct where the de-icing air is exhausted to the horizontal stabilizer interior. Figure 5-19 shows this configuration. Sometimes, double-skin flow passages are not used. Instead, hot air from the piccolo tube is allowed to impinge directly onto the leading edge skin (figure 5-20). Since it is not necessary to provide continuous ice protection (for some aircraft) for the horizontal stabilizer, a manually controlled "single shot" de-icing system was selected. This system, although normally used just prior to landing, may be operated at any time if it is considered necessary or desirable.

The horizontal stabilizer de-icing system is interlocked with the wing anti-icing system to prevent simultaneous operation which would exceed the bleed air supply capacity. To place the empennage system in operation, the wing anti-icing switches must be placed to the ON position and the horizontal stabilizer timer button pushed. When the horizontal stabilizer timer button is pushed, the air supply

is switched from the wing system to the empennage de-icing system. Hot air is then supplied to the empennage for a period of 150 seconds, whereupon the air supply is returned to the wing anti-icing system.

The horizontal stabilizer ice protection system was designed to remove ice accumulations which would adversely affect aircraft performance as the result of flight through continuous maximum and intermittent maximum icing conditions defined by FAR Part 25 Appendix C.

Some wind tunnel tests of the horizontal stabilizer with simulated ice accretion installed on the leading edge have indicated that it may be necessary to remove ice from the leading edge prior to landing. These tests have also shown that the leading edge ice accumulation permits acceptable airfoil performance during other flight conditions. Therefore, a low altitude holding flight condition was selected for the design point. This combination of altitude, airspeed, and ambient temperature results in the maximum ice accretion thickness.

The design analysis is conducted in two parts. The first part predicts the time-temperature response for the de-icing supply air ducting from the horizontal stabilizer shut-off valve to the double skin de-icing flow passage inlets. The second part of the analysis predicts the time-temperature response of the double skin de-iced areas at various locations.

A transient heat transfer analysis was conducted for the ducting which supplies high temperature pneumatic air to the horizontal stabilizer double skin flow passages (figure 5-21). Each side of the horizontal stabilizer is divided into 9 individual ducting segments for computer analysis. For each of these nine segments, thermal resistance and capacitance of the ducting system was calculated. A thermal network which represents the physical duct system and is suitable for establishing computer input is shown in figure 5-22. A standard thermal analyzer computer program was used to compute the transient thermal performance of the horizontal stabilizer de-icing supply for the conditions of the design point. Figure 5-23 shows how the de-icing supply air temperature at inboard and outboard locations varies with time. The duct system was initially cold soaked to -65°F (-54°C).

A transient heat transfer analysis was conducted at several leading edge locations. From this analysis, de-icing airflow required to provide effective system performance was determined. The design conditions were:

Flight Condition	Hold
Altitude	10,000 feet
Speed	200 knots
Outside Air Temperature	12°F
Bleed Air Temperature	370°F
Bleed Air Pressure	20 lb/in^2

The first step in the analysis was to set up thermal networks which would represent the leading edge sections at each of the analysis locations. These networks are combinations of resistances and capacitances which describe the physical system and are suitable for computer input. A typical example is shown in figure 5-24. Having determined the thermal networks, resistance and capacitance values were calculated and a standard thermal analyzer computer program was used to calculate the transient thermal response. The previously determined transient supply air temperature was used as an input.

Figures 5-25a and 5-25b show how the upper and lower airfoil skin surface temperatures vary with time and airflow. The plotted temperatures were determined at a point on the outside surface of the airfoil adjacent to the double skin flow passage exit. Examination of these curves shows that the upper airfoil surfaces require more airflow than the lower surfaces to reach the same temperature in the same period of time. Since both surfaces will receive equal flow from a common piccolo tube, the system airflow requirements were established using the higher values.

Based on icing tunnel test data, the accreted ice will always shed when the skin temperature adjacent to the "D" duct web is 50°F (10°C). The analysis is based on worst case conditions and includes several conservative assumptions and therefore provides a high degree of confidence in successful operation. Final confirmation of de-icing performance can be demonstrated by tests such as icing wind tunnel simulation and artificial or natural icing flight tests.

5.3.1.5 Typical System Description

Most commercial transport aircraft use one of two concepts for hot air ice protection: single skin or double skin. The single-skin concept uses the direct impingement of high velocity hot air jets to develop the internal heat transfer coefficient necessary to transmit the heat from the air to the leading edge skin. A typical design is shown in figure 5-26. The jets are created by means of a spray tube which distributes high-pressure, high-temperature air spanwise along the leading edge. A pattern of orifices in the spray tube is used to create the jets which impinge on the inner surface of the skin. The orifices are located to achieve a desired flow pattern: either unidirectional (as shown in figure 5-26), or bidirectional (symmetrically divided flow between the upper and lower surfaces) or any variation between these two extremes.

The double-skin concept uses an inner skin to form passages to permit higher effectiveness and better control of the heat transfer process. A typical design is shown in figure 5-27. The supply duct is similar to the single skin design except that the orifices are used fundamentally for flow control and only secondarily to direct the flow. The hot air is confined so that it is forced to flow through the passages formed by the inner skin. In the design shown in figure 5-27, the outer skin is chem-milled to a depth of 0.045 inches (1 mm) to form passages. The total flow area is kept small to develop high velocities and high internal heat transfer coefficients. In addition, the inner skin acts as a fin, further improving the transfer of heat. In other designs, the inner skin is preformed in "pillows" to create flow passages when the skins are riveted together (figure 5-21). Flow distribution is controlled by the

pressure drop characteristics of the channels. Chem-milling permits close control of the flow area and, hence, the flow distribution. If required, orifices can be used at the exit of the pillows for flow distribution control.

The performance of the single-skin and double-skin concepts can be compared in an icing wind tunnel in two ways. The first method involves a comparison of the minimum flow required to completely evaporate impinging water droplets. Possibly as a result of the variability of tunnel conditions and the presence of tunnel frost, a great deal of scatter may be experienced in such a measurement. An indirect method was used in which the quantity of runback ice was measured as a function of airflow for specified combinations of heated air temperature, ambient temperature, air velocity, liquid water content, mean effective droplet diameter, and angle of attack. The measured data were extrapolated to zero runback to provide an estimate of the minimum required flow for each case. The results are presented in figures 5-28 for both single and double skin designs. The legend for the test conditions is given in table 5-1. In cases where direct comparison can be made, the double-skin configuration provides equivalent performance with 5 percent to 20 percent lower air flow. The second comparison of performance involves the time required for de-icing as a function of flow for various hot air temperature. Generally, the test data confirm the results of the anti-icing tests described above.

5.3.2 Windshields

Anti-icing protection is usually provided for the forward-facing windshield panels on both military and commercial aircraft that are required to operate in all-weather conditions. The two most commonly used hot air methods are the external air blast system (that may also be used for rain removal) and a double-paned windshield with hot air circulated between the panes. Hot air flowing through a double pane windshield has been used for anti-icing in the past, but is seldom used currently because of problems of installation, noise, collection of dirt between panes, weight, cracking, and other undesirable effects. Further, a uniformly heated windshield may be necessary in order to meet the bird-impact requirements of FAR Part 25 for transport category aircraft.

Windshield arrangement of a typical multi-engine transport are shown in figure 5-29. Ice protection is needed for the forward facing windshields (main and center) but not for the sliding and aft windows which are at minimum angle to the airstream and would not collect ice. An alternate arrangement often used deletes the center windshield and increases the size of the main windshield.

5.3.2.1 Double-Pane Anti-Icing System

Although seldom used, the double pane system (figure 5-30) is possible. A source of hot air is needed (such as a combustion heater or a compressor bleed diluted or cooled to an acceptable temperature), with a control valve and appropriate ducting. Surface heat requirements are the same as for an electrical system; however, the total heat input will be two to three times as large, depending

on air gap width and resulting channel efficiency. Methods of analysis given for airfoil anti-icing may be used to determine air flow requirements.

Special attention must be given to solution of the problems of noise, duct installation, leakage, accumulation of dirt, dust, and oil, and stress problems resulting from temperature gradients in the windshield panes.

5.3.2.2 External Air Blast Anti-Icing

For many high performance aircraft, an external jet blast rain removal system employing compressor bleed air is used in place of windshield wipers. The bleed air is discharged at the base of the windshield by a wide, slotted nozzle that directs air parallel to the windshield surface (figure 5-31). Design of such systems is empirical to a large degree; however, general recommendations may be found in SAE AIR 805 (reference 5-2). Required air flow rates are usually between 2 and 7 lb/min/in (width) of cleared area.

In most cases rain removal air flow requirements will exceed windshield anti-icing requirements. Airflow rates of 4.5 to 7 lb/min/in provide the most satisfactory results for rain removal. Typical surface temperatures are discussed in Chapter V. Care must be exercised in designing such a system to avoid blowing excessively hot air across the windshield. This can cause overeating of the interlayer or cracking of the outer glass ply.

Windshield anti-icing, defrosting, and defogging requirements for military aircraft are specified in reference 5-3. Figure 5-32 is a curve of heat requirements from reference 5-3 to be met during all conditions up to normal cruising speed of the airplane with an exterior windshield surface temperature of 35°F. Reference 5-3 requires that the windshield anti-icing system shall be capable of operation during engine warm-up, taxi, takeoff and touchdown, as well as during normal flight. The specification values are based on the most severe conditions of a windshield normal to the airstream. Less heat will be needed for inclined windshields.

Methods of calculating heat requirements are shown in Chapter V. Typical results for a jet transport center windshield are shown in figure 5-33. For the flight profile studied, a maximum input of 1800 BTU/hr-ft^2 (345 kJ/hr-m^2) was found to be adequate. Inward heat losses have not been considered here as analysis shows them to be less than 5 percent. Calculations were based on buildup of the air boundary layer from the nose of the aircraft. For windshields that depart abruptly from the fuselage contour, a new boundary layer starts at the windshield's base and heat requirements will be higher (as described in Chapter V).

Military specifications state that exhaust gases from either turboprop or turbojet engines shall not come into contact with any portion of the aircraft other than the exhaust ducts; consequently, if the energy of the exhaust gases is to be used, a heat exchanger must be incorporated. This is necessary because of the toxic and corrosive nature of the exhaust gases (reference 5-4).

5.3.3 Engine Inlet Lips and Components

Ice protection is necessary for turbojet engine inlet lips or aerodynamic surfaces in front of them to prevent engine damage due to ingestion of ice. Decrease of the inlet area due to ice buildup is not a significant factor, except for extremely small engines. Because compressor bleed air is readily available from the engine and its delivery maintenance requirements are low, this air is usually preferred as the heat source. The hot air is usually drawn from the high pressure compressor through a bleed manifold. The anti-ice system ducts this air forward from the engine to the inlet and convectively heats by directing the hot air against the inner surface of the inlet lip.

There exist three basic geometric arrangements for such a convective heating system. The first is called the piccolo tube system (figure 5-34). It uses a hoop of small diameter tubing to distribute the hot bleed air circumferentially. Along the tube periphery, small exit holes are drilled in order to direct the air as jets against the inlet lip skin where it transfers heat to the super cooled water droplets impinging on the outside of the lip skin. The spent anti-icing air then flows aft into the rear chamber through holes in the front bulkhead near the inlet throat. In the rear chamber, warming of the inlet inner barrel occurs before the air is vented overboard through an exit in the outer barrel. Although it is less thermally efficient, this arrangement is particularly useful for thin leading edges (as on supersonic wings) or flush scoops. Cost of manufacturing the single skin system may be lower for many applications.

The second arrangement is called the double-walled system because of the heating channel formed between an inner skin and the exterior skin (figure 5-34). This method introduces the air into the inlet lip "D-duct" (figure 5-34) and is then forced to flow into the channel between the two walls. Here heat exchange occurs between the hot air and the external skin. In the double-walled system, high circumferential air velocities between the walls is necessary to obtain a good distribution around the D-duct. This suggests that an effective heating system can be obtained without the need of a double wall. This new concept is called the "swirl system."

The third arrangement is the swirl system. The swirl nozzle introduces the air in the tangential direction at the centroid of the lip cross-sectional area. The nozzle acts as an ejector which pumps the air in the lip around the circumferential chamber producing a swirl flow several times larger than the nozzle flow. The swirl nozzles also act as a flow restrictor as it operates choked at all flight conditions, and its exit diameter controls the flow of hot air needed for anti-icing purposes. The hot air transfers heat to the lip skin, then flows aft into the rear chamber through holes similar to the ones in the piccolo system. The hot air is then vented overboard through the outer barrel.

A hot gas anti-icing system for the engine inlet lip of a typical FAR Part 25 transport is illustrated in figure 5-34. The area of the nacelle requiring anti-icing extends aft from the leading edge along the inner and outer surface of the inlet lip; a horizontal distance of 6 inches (15 cm) is typical. However, the exact distance may depend on cowl configuration and impingement area. The anti-icing engine compressor bleed air is distributed around the lip by a modified "D" duct and passes through holes in the leading edge of the inner skin into 0.40 inch (10 mm) gas passages. The air flows

aft through these passages into a plenum chamber between the D-duct and a baffle and then is discharged tangentially into the inlet stream via several discharge ports (usually six). Heat and airflow requirements for anti-icing this engine inlet were determined at a number of different flight conditions. Since the calculations show the greatest air flow demand at the 15,000 foot (4572 m) cruise altitude, the system was designed to meet the heat requirements at this condition. The system will provide complete evaporation of the impinging water droplets in maximum continuous icing for all flight conditions except descent (due to lower bleed temperatures). The heated area will be maintained above 35°F (2°C) (running wet) for descent. In maximum intermittent icing, the heated surface will be running wet for all flight conditions. The amount of refreeze is not significant for these encounters because of the short duration of exposure. Calculated values of both actual and required heat release are shown in figure 5-35 for comparison. Figure 5-36 shows calculated values for both actual and required air flows.

The calculation of water catch, impingement limits, heat release, and air flow requirements for a turbojet engine inlet lip is described in Chapter V. Knowing the bleed air pressure available at the different flight conditions, the actual air flows can be calculated by performing a pressure drop a' lysis of the system. The heat release can then be found knowing the actual air flows.

For other aircraft with engines having a shorter distance from the inlet lip to the compressor face, it may be feasible to provide running wet protection for the entire area aft to the compressor face so that runback does not build up and shed into the engine. This would not be practical for the typical transport aircraft because the compressor face of its engines is on the order of 4 feet (1 m) or greater aft of the inlet lip.

5.3.4 Turbofan Components

5.3.4.1 Typical System Description

The typical hot air system bleeds off a portion of the relatively high temperature and high pressure air in the compressor gas path and uses that air to heat the component in question. The anti-icing heat available is dependent upon bleed location, ambient temperature and pressure, flight Mach number, and engine power level. The necessary elements of such a system are a bleed port at the proper compressor stage, piping or passages to transport the air between bleed port and the component, convective heat transfer passages within the component, and a location to expel the air once it has done the job of anti-icing (usually back into a low pressure region of the compressor gas path). A flow metering restriction should also be provided, whether it be an orifice or the anti-iced component itself. Such a system is an integral part of the powerplant.

Non-rotating parts such as inlet guide vanes and stators usually incorporate an external piping bleed system. The airfoil may be of single pass or multiple pass internal flow configuration, as shown in figures 5-37 and 5-38. Stiffening strips and vibration damping materials are fairly common within inlet guide vanes. An on-off valve is a standard feature so that when anti-icing is not needed the

bleed flow can be turned off. On engines with inlet guide vanes, generally the same air anti-ices both the vanes and the non-rotating spinner using a series flow system. The anti-icing hot air passes first through the vanes and then the spinner.

Anti-icing of a rotating spinner would require that the bleed air must get "on board" rotating parts internal to the engine. The most practical way to route bleed air is from the gas path through the shaft which drives the fan and spinner. The convective passages for the spinner may be double wall configuration with a narrow passage height. Such a system is usually "always on" because of the obvious difficulty with incorporating a valve in the rotating hardware.

Typical external and internal bleed anti-icing flow routing paths are shown in figure 5-39 reprinted from reference 5-7.

5.3.4.2 System Design (Compressor Bleed)

If the analyses described in Chapter V indicate that an anti-icing system is required or desirable for protection against a potential icing problem, the recommended design philosophy is to provide enough heating to maintain a running wet surface of 35°F (2°C) or greater, at the design point condition recommended below using the thermodynamic heat balance equations described in Chapter V. The design analysis should be based upon the FAR Part 25 intermittent maximum (cumuliform) cloud criteria, from which the following single design point is recommended as a minimum requirement.

Power Setting	Minimum Holding
Ambient Air Temperature	-4°F (-20°C)
Cloud LWC	1.7 g/m^3
Mean Volumetric Diameter	20 microns
Minimum Surface Temperature	35°F (2°C)

A guide vane or stator anti-icing system designed to this condition usually has the bleed source located at a mid-stage of the high pressure compressor and, in general, the vanes will accumulate some ice during lower power idle operation when there is insufficient heat available from the bleed air to anti-ice them. Ice that accumulates on inlet guide vanes during the relatively short duration of idle descent is not necessarily detrimental, although engine operability and tolerance to such ice accumulation must be thoroughly verified for both the short duration idle descent and for ground idle operation. Icing tests and analysis may show the need for powered-up engines during descent in severe icing conditions and for periodic power increases during longer duration ground operation as discussed in detail in references 5-6 and 5-7.

Some engine designers have found the need for a more complex anti-icing system which will provide higher pressure and temperature compressor discharge air to the anti-iced parts at lower power operation to alleviate the problem of insufficient heat from the low or mid-pressure compressor. This type of system incorporates a switching valve to go to higher pressure and temperature compressor air as required.

The general procedure for the final design of a hot-air anti-icing system involves: (1) using the design point above to estimate the bleed flow/temperature required to achieve a 35°F (2°C) or greater surface, (2) using the resultant bleed flow/temperature to select the required compressor bleed stage location, (3) sizing the pipes and bleed ports to get the required bleed flow at the selected temperature, and (4) performing the thermal design of the anti-iced part.

Preliminary calculations based upon one-dimensional heat transfer may be used to get a rough idea of the bleed flow and temperature required. The final detailed heat transfer analysis can be accomplished via a three-dimensional finite difference heat transfer computer analysis, using the one-dimensional result as a starting internal boundary condition. Fine adjustments to bleed flow can then be made, based upon this analysis.

5.3.4.3 Selection of Compressor Bleed Stage - Considerations

Details of a preliminary calculation procedure for determining the optimum compressor bleed location are given at the end of this section, using a typical inlet guide vane as an example. Prior to beginning the calculations, the designer should note several aspects of the selection process.

Fixing both the design point condition and engine geometry establishes the airfoil external heat load, hence, the anti-icing heat required. The internal (hot side) heat transfer coefficient is a function of the bleed flow and the vane passage geometry; therefore, one should have a rough knowledge of the minimum cross-sectional flow area (A_{flow}), hydraulic diameter (D_h), passage surface distance (S), and passage width (b), as indicated on figure 5-40. Since internal heat transfer coefficient depends upon flow, both the bleed air temperature needed to meet the required heating and the source pressure needed to deliver that flow quantity will change for various assumed values of bleed flow. Parametric curves similar to those of Figure 5-41 (reference 5-7) can be plotted to compare bleed temperature and pressure requirements against availability throughout the compressor stages.

It should be noted that the further forward in the compressor the bleed location is selected, the more the source air temperature will decrease, the greater will be the bleed flow required, and the greater will be the source pressure required. As the selected bleed air location continues to move forward in the compressor, a point will finally be reached where the stage pressure available is inadequate for delivering the required bleed flow. In addition to the above, other practical considerations are usually involved in selecting the bleed location. The hot air system must be configured to meet primary requirements for structural integrity, engine performance, cost, compressor aerodynamics, and airframe bleed requirements. Typically, the

anti-icing bleed system is secondary to these other factors, and therefore a primary or priority bleed location also serves as a simultaneous anti-icing source.

A hot air anti-icing system further requires that the inlet case be designed to survive the highest temperatures and pressures produced by the bleed air system, such as might occur during maximum power, hot day conditions with the anti-icing valve open. The current practice for the inlet case and the anti-icing system is to design them for low weight and cost. As such, they are usually constructed of titanium with vibration damping materials of moderate temperature capability incorporated in the guide vanes. Modern engines produce compressor discharge air temperatures in excess of 1000°F (538°C), and because this may be too severe for the inlet case structure, the anti-icing bleed is usually located at a mid-stage of the compressor.

Sizing of the bleed ports and ducting is also important to assure that the available system pressure drop delivers the needed flow. With the ever present weight concern, the ducts should be no larger than necessary. Since the stators of a compressor act as a diffuser, the static pressure of the gas path is higher downstream of the stator than it is behind the rotor of the same stage. It is because of this that the bleed is usually located aft of the stator.

To ensure structural integrity, it is recommended that a detailed heat transfer analysis be made on the anti-iced structure for maximum power, hot day and take-off conditions with the anti-icing system operating. The resulting temperature levels and gradients will be vastly different for this operating condition than for icing conditions.

5.3.4.4 Selection of Compressor Bleed Stage - Calculations

The following is a step-by-step procedure which can be used for preliminary calculations to determine the optimum compressor bleed location. A typical inlet guide vane nose section scheme is used for discussion purposes (figure 5-40).

a. Calculate the heat required (Q"reqd) for a 35°F (2°C) leading edge (stagnation point) using the recommended design point condition and one dimensional heat balance equations of Chapter V, Section 2.2.

b. Calculate the internal heat transfer coefficient using the passage geometry by assuming the required air flow w_{AI} reqd.

$$h_{AI} = 0.023 \frac{K}{D_h} (Re_{D_h})^{0.8} (Pr)^{0.4}$$

where

$$D_h = \frac{4 A_{flow}}{S + b}$$

$$Re_{D_h} = \frac{W_{AI\ reqd}\ D_h}{A_{flow}\ \mu}$$

c. The required bleed air temperature $T_{AI\ out}$ associated with the assumed flow is conservatively estimated (neglecting conduction) from

$$Q''_{reqd} = h_{AI}(T_{AI\ out} - 35°F)$$

d. Find the bleed air cool-down, and thus T_{AI} in using the assumption that the entire nose-section is at 35°F for full span.

$$\frac{T_{AI\ out} - 35}{T_{AI\ in} - 35} = \exp\left[-\frac{h_{AI}\ A_{surf\ nose}}{W_{AI\ reqd}\ C_p}\right]$$

e. Most of the system available pressure drop should be taken across the inlet guide vane (ducting losses should be small) and the required source pressure may be estimated as

$$P_{source\ reqd} = \frac{W_{AI\ reqd}(T_{AI\ in})^{.5}}{FP_{isen}\ C_D\ A_{flow}}$$

where

$$FP_{isen} = 0.92\ M\ (1 + .2M^2)^{.5}$$

f. Steps (a) through (e) can be repeated for several assumed values of w_{AI} reqd and a curve similar to figure 5-41 plotted.

g. Obtain values of air temperature and pressure available at each stage of the compressor from aerodynamic analysis or test data.

5.3.5 Propellers, Spinners, and Nose Cones

Ice protection for propellers, spinners, and nose cones on propeller or turboprop aircraft is commonly provided by the electro-thermal method. (Reference Chapter III, Section 2.0.)

5.3.6 Helicopter Rotors and Hubs

At this writing (1989), no applications of hot air ice protection for helicopter rotors or hubs are known.

5.3.7 Flight Sensors

Any large aircraft has small components that accumulate ice if not protected. Typical examples are pitot tubes, angle of attack sensors, etc. The need for ice protection of these components can be determined by answering the following questions.

a. Will ice accumulate on the object in question and in what amount?
b. Will this accumulation adversely affect the component's function?
c. If the component function is affected, will it have an effect on safe flight of the aircraft?
d. What is the effect of ice shedding on other components, such as engine inlets? Will ice shedding affect engine operation?

The current practice for small, critical components is the application of electrical heat (Chapter III, Section 2.0) applied to the critical area. In the case of engine inlet total pressure probes, engine bleed air also has been used successfully for anti-icing. In any case, where ice protection is provided in small components, effect of a single failure should be considered. In the case of pitot tubes, for example, if the pilot's pitot tube fails, the copilot's may be used.

5.3.8 Radomes and Antennas

Most transport aircraft now use radar to detect and avoid severe weather conditions. The radar commonly is housed in a nose radome made of reinforced fiberglass. Since ice formation on the radome affects radar transmission, anti-icing systems were developed to protect radomes. Although experience has suggested that loss in radar range from ice on the radome is not critical (studies show maximum degradation values of 10 percent), this section contains brief data on typical hot gas systems.

The method that has been used on several specific kinds of aircraft is an air-heated radome. Gas passages are formed by a patented process of the "lost wax" type, as shown in figure 5-42. Air is supplied from a half-circle supply manifold at the rear of the radome, through passages, and into a similar collector manifold, and then is dumped overboard. An ejector system is used to mix compressor bleed air with ambient air (or radome discharge air).

Analytical studies of such a system for a typical transport aircraft showed that with 1/2 inch (13 mm) deep gas passages an air flow rate of 0.75 lb/s (0.34 kg/s) was required. Of this 0.31 lb/s (0.14 kg/s) was bleed air and 0.44 lb/s (0.20 kg/s) was obtained from the radome discharge. Mixed air temperatures vary from 175°F to 375°F (79°C to 191°C). The system is designed for running wet protection in continuous maximum icing conditions of FAR Part 25.

The major disadvantages of the air-heated radome are:

a. Complex geometry - may be costly.
b. Gas passage size may be compromised by radar transmission requirements.
c. Adequate heat transfer at stagnation point requires a thin skin, whereas rain erosion considerations demand a thick skin plus erosion coating.
d. Radome strength may be adversely affected by heating.

At present, radome ice protection is not generally provided on commercial aircraft because the transmission losses due to icing are small and do not represent an unacceptable effect on radar range. Changes in technology, work on reduced landing minimums, etc., could result in a greater need for ice protection, in which case the foregoing information will be more useful.

Ice protection for antennas, if provided, would probably be of the electro-thermal type (Chapter III Section 2.0). However, a few installations of the hot gas thermal type have been utilized. General practice has been to not provide antenna ice protection; however, significant amounts of ice can form on large antennas and should be considered especially for aft mounted engines.

5.3.9 Miscellaneous Intakes and Vents

General practice has been to not provide protection for flush inlets and vents. Although detailed studies must be made for each new application it is usually found that the flush inlet will not close completely in icing, therefore, protection is not provided. Inlets for air conditioning system may or may not be protected depending on whether ice formed on the inlet would shed into the heat exchangers or turbocompressors and cause damage.

5.3.10 Other Usages

5.3.10.1 Strakes

Fuselage strakes, located near the forward end of the fuselage, are used to improve directional stability of the aircraft. These aerodynamic devices have been maintained ice-free by use of a hot air anti-icing system. This is to preclude ice being shed from them that could damage the wing or aft mounted engines.

The strakes are anti-iced using the same bleed air source as the wings and are anti-iced whenever the wing ice protection system is activated. Typically, bleed air at a temperature between 400°F and 450°F (204°C to 232°C) and a pressure of 20 lb/in^2 (138 kN/m^2) is routed to the strakes through insulated ducting. Each strake is divided into leading, center and trailing-edge sections as shown in figure 5-43. The air enters a plenum, flows into chem-milled passages and exits through slots in the lower surface. The design provides accurate and uniform temperature control of the entire strake surface.

To determine the critical design conditions, analytical investigations were performed using the variation in gross weights, operational altitudes, airspeeds and ambient temperatures for the aircraft throughout the FAR 25 envelope. As a result of these investigations, it became apparent that the major combination of factors to be considered in determining the system design point were low ambient temperature,low engine power settings, high air velocities across the strake external surfaces, and highest liquid water content associated with the ambient temperature.

The predominant mode of heat loss from the strake is convective and this is most strongly influenced by the temperature difference between total air temperature and strake surface temperature. Since the design intent is to provide a minimum surface temperature of 35°F (2°C), the highest heat losses will be experienced at a minimum ambient temperature, i.e., -22°F (-30°C) which exists at altitudes within the icing envelope at 22,000 feet (6700 meters). Also influencing the convective heat loss is the heat transfer coefficient, which is dependent upon temperature, velocity, and density of the air. The heat transfer coefficient is typically higher at the higher altitudes. These considerations of the convective heat losses locate the most critical altitude at 22,000 feet (6700 meters), the top of the icing envelope.

Heat loss associated with raising the water temperature from ambient temperature to strake surface temperature and then the evaporation from the 35°F (2°C) running wet surface is small relative to the convective losses. Thus, the need here is to maximize this effect at the conditions providing high convective losses. This centers attention on the smallest cloud extent for a maximum intermittent icing encounter, i.e., a cloud with a three-mile horizontal extent.

Heat available to balance the losses is a function of the heating air temperature and the airflow rate. The air temperature reaches a minimum during descent conditions. The airflow is a function of the pressure available to force the air to flow and the density of the air. Both of these parameters decrease with an increase in altitude when the engine power is the minimum. Thus, the minimum airflow will be provided at the top of the icing envelope.

From the above considerations, the conclusion is reached that the design point is a high speed descent through a three-mile cloud in an intermittent maximum icing encounter at 22,000 feet (6700 meters) with descent engine power. This operating condition is shown in table 5-2. With the strake anti-icing flow rates determined for the above conditions, performance was evaluated at the off design conditions of climb, cruise, and hold. The results of this evaluation are shown in table 5-3.

III.5.4 WEIGHT AND POWER REQUIREMENTS

The effect of an installed hot air ice protection system on the weight and performance of a light twin jet aircraft is given below. For illustration purposes, an engine inlet lip anti-icing system is used. It was determined that the energy requirement would be 43,000 BTU/min (755 kJ/s) and an air flow rate of 13.1 lb/m would be needed. For this condition, the hot air system weight would be 100 pounds (45 kg). From this information, actual performance penalties can be predicted. These numbers are representative of what would be required but a more detailed analysis would be necessary to determine them more exactly for any particular airplane (reference 5-8).

III.5.5 ACTUATION, REGULATION, AND CONTROL

Hot air anti-icing systems are normally controlled by solenoid-operated pneumatic valves or motor-operated valves. Overheat protection and/or warning can be provided by means of thermoswitches, thermistors, or wire-wound resistance sensors, plus an associated bridge circuit. In the case of engine and inlet anti-icing, it may be required (as on commercial aircraft) to have a means of indicating proper system functioning. A pressure switch is commonly used, connected to a control panel mounted warning light to warn of inadequate pressure (and thus inadequate anti-icing) to the system. A valve position indicator or the temperature of a critical anti-icing surface may also be used to indicate proper system operation. Many commercial aircraft turbine engines have used pressure switches or valve position indicators for reasons of cost and reliability.

Hot air de-icing systems normally use solenoid-actuated pneumatic valves to allow rapid opening and closing. A timer is needed to control the various valves. A fixed cycle may be used. However, a variable heat-on time (varying with total air temperature) is more common. Time between cycles can also be made variable if desired. This time is usually three to four minutes. However, longer periods may be tolerated in moderate icing conditions. One approach that has been used is to provide normal heat-on (15 to 20 seconds) and heat-off (three to four minutes) periods, with longer heating periods every fourth or fifth cycle. The additional heat period removes runback that may have accumulated during the previous cycles. An overtemperature warning or control is also desirable.

All hot air systems may or may not contain control of the basic air source. Bleed air systems usually are controlled by pressure regulating valves. In addition, maximum bleed air temperature may be limited by several methods. One is by mixing outside air or exhaust air from the gas passages using an ejector mixing system. Another is mixing low temperature air from the low pressure compressor of a dual rotor compressor with high temperature bleed air from the high pressure compressor. Ram air cooled heat exchangers may also be used, although in practice, this may be limited to integration with an air conditioning system.

Another method in use on turbine engine anti-icing systems that could be adapted to airframe use is a temperature-modulating valve that reduces air flow as bleed air temperature increases. A coiled thermostatic spring and vane assembly is used to restrict flow at high temperatures. Overheat of the inlet guide vanes and front frame is avoided by use of this type of valve. An on-off type pneumatic control valve is usually in series with the modulating valve.

The final consideration for all control systems is that any single failure should not result in unsafe operation of the aircraft.

III.5.6 OPERATIONAL USE

Operation of a hot air ice protection system requires a source of bleed air or equivalent. Operation on the ground for checkout or calibration purposes can be conducted using an ambient temperature, high pressure air source. System operation is controlled from the cockpit, usually by a simple ON/OFF control. Often when a system is turned ON, a DISAGREE light will illuminate during the transient valve travel and then will extinguish. This allows a check on the monitoring system prior to system use.

Operation of a hot air ice protection system on the ground can cause serious overheating problems. Normal bleed air sources can be at a temperature of 450°F (232°C). Without ambient airflow over the external surface, the skin temperature will approach the bleed air temperature which could anneal some aluminum alloys. This is especially true of evaporative systems that purposely operate at high heat flux levels. Caution during ground operation is also required when dispatching with any control valve fixed or locked OPEN.

Prior to delivery, each system should be tested to ensure the proper flow distribution among the many branches, for proper electrical system operation, and for leaks. Some of these tests must be repeated if parts are replaced during maintenance operations. Proper system operation may be checked on the flight line by means of the valve disagreement lights, temperature and pressure warning devices, a change in EPR or NI when the system is turned ON, and a pneumatic system switch point check (if applicable). Often, the engine pressure level at which the pneumatic system is switched from a high-stage to a mid-stage of the compressor is increased for ice protection over the normal air conditioning requirement. This may be checked by setting the engine at the minimum EPR (or NI) for operation on mid-stage bleed with ice protection OFF. When ice protection is selected ON, the pneumatic system pressure will generally increase because of the change in switch point.

III.5.7 MAINTENANCE, INSPECTION, AND RELIABILITY

Hot air ice protection systems are generally noted for high reliability and low maintenance. The major type of inspection and maintenance activities involve failures of the hot air supply regulator and/or shutoff valves, leaks, and duct failure. The telescoping duct, used to transmit hot air from the fixed wing to the moveable slat, is a unique area of concern. Failure of this unit can be detected by an increase in flow measured by excessive pressure differential across an orifice.

The hot air flow control valve also has unique problems due to its infrequent operation and its location. For wing ice protection, the control valve may be located in an area of uncontrolled temperature. Condensation in the high-pressure, low-temperature bleed air can cause corrosion or may freeze during higher altitude operation. In either case, a malfunction is often experienced unless precautions are taken when designing the component and during installation.

III.5.8 PENALTIES

Bleed air from the engine compressor for use in an anti-ice protection system can result in a significant specific fuel consumption (SFC) penalty. Detailed penalty analysis must consider bleed flow quantity, compressor stage location of the bleed, engine configuration, component efficiencies, and airplane/engine operation. Such complexity is considered beyond the scope of this discussion. Presented instead is a general level of trade penalty for an available advanced turbofan and some important considerations for addressing advanced technology applications utilizing very high bypass ratio engines of the future. Bypass ratio (BPR) is defined as

$$\text{BPR} = \frac{\text{Total Airflow - Core Airflow}}{\text{Core Airflow}}$$

where total airflow is all air that is being "moved" by the fan/prop, and core airflow is that which flows in the engine core (gas generator) eventually leading to the combustor and turbine components.

5.8.1 Advanced Turbofans

A modern representative, turbofan engine for transport aircraft application has a BPR in the range of 5 to 6. The ice protection system usually bleeds air from the middle-stage region of the high pressure compressor during the cruise through climb power range. A general level of penalty associated with such a situation is that bleeding 1 percent of core engine airflow costs approximately 1 percent in thrust specific fuel consumption (TSFC) at constant thrust setting. Typical usage for engine inlet cowl plus wing anti-icing protection on a two engine transport aircraft, for the above mentioned power range, requires about 2.5 percent to 4.5 percent of core airflow per engine. Since the trade is one-for-one, the cost is that same percentage in TSFC. During very low power holding and descent operation, the airframe service bleed location typically switches to the compressor exit stage, where the bleed flow as a percentage of core flow increases, and the fuel consumption penalty rises accordingly.

5.8.2 Future Advanced Engines

Significant performance improvement gains are being projected for future engines through utilization of geared fans (advanced ducted props) and counter-rotating unducted props which increase propulsive efficiency. Figure 5-44 shows specific thrust and engine airflow trends versus bypass ratio that result from conducting performance simulation studies. The parameters are non-dimensionalized relative to an available turbofan of 5.5 BPR. Note that for geared turbofans BPR is around 13 to 20 while for unducted props it is about three times greater. Clearly, specific thrust decreases with the higher BPR engines. This means that the fan or prop must "move" more total airflow to maintain a constant thrust requirement. Core airflow for the higher BPR engines is also projected to be only 75 to 80 percent of the base turbofan with the same constant thrust restraint, a result that has major

implications on bleed penalties if these engines are to replace the base 5.5 BPR turbofan on a given airplane.

Consider the trends in hot air anti-icing system bleed requirements when the base turbofan is replaced by the higher BPR engine configurations of the same thrust level. Incorporation of the geared turbofan, which is ducted, would require a larger inlet duct. Assuming that the duct diameter would increase proportionally with the square root of fan total airflow, a 20 BPR engine moving 2.6 times the airflow would require an inlet duct diameter 61 percent larger. Since the inlet cowl surface area requiring protection increases significantly, so would the anti-icing system absolute bleed flow. Wing protection would probably remain constant on an absolute flow basis. The resultant total ice protection system bleed with the geared fan engine would be a significantly larger percentage of core flow since cowl system absolute flow is up and engine core flow is down by more than 20 percent. Thus, the TSFC penalty would be greater.

Incorporation of the "pusher" counter-rotating prop (unducted) engine of BPR 60 would present differing ice protection considerations. Since the inlet duct passes only core airflow, which amounts to about 11 percent the total duct flow of the base 5.5 BPR turbofan, the inlet diameter would be only 33 percent as large. Cowl anti-ice flow would be less, but the smaller core engine front frame/ compressor may require active anti-icing. These "pusher" engines would probably be aft-fuselage mounted which requires greater wing area protection to preclude wing shed ice damaging the props. Additionally, the engine mount struts would require protection for the same reasoning. Total ice protection system flow as a percentage of core airflow is expected to be larger for this engine substitution scheme.

Reference 5-9 summarizes these considerations, along with potential changes in cabin environmental conditions. In addition to expanded ice protection for the airplane with incorporation of the high bypass ratio engine, it is projected that the overall service bleed problem will be compounded by the need to raise fresh air levels in the cabin via increased environmental system bleed flow. Figures 5-45 and 5-46 graphically show the anticipated service bleed trends for the ultra BPR prop-fan engine relative to the base turbo-fan. With bleed air consuming upwards of 30 percent core flow under certain low power operating conditions, there is a definite need for developing alternative ice protection methods.

III.5.9 ADVANTAGES AND LIMITATIONS

The advantages and limitations of the hot gas system will be discussed and compared with those of other candidate systems in Chapter III, Section 6.0. Hot air anti-icing systems have several advantages and disadvantages. On the positive side are: the availability of ice protection energy in the form of bleed air at a reasonable penalty to aircraft performance (for low bypass ratio turbo-fans and turbojets); the ducting used for ice protection is often used for other purposes, thereby saving weight; the systems for hot air distribution are relatively simple, trouble-free and easy to maintain; and there is no decrease in aircraft performance for anti-icing because ice accretion does not occur. A

disadvantage of some hot air anti-icing protection systems is the potential high cost of installation which results from designing and fabricating the leading edge heat exchangers. The system must be designed into the original leading edge and cannot be "added on" at a later date without major retrofit problems. For high bypass ratio turbofans, the performance penalty for extraction of sufficient bleed air may be too severe.

The performance evaluation point for determining empennage anti-ice requirements will normally be the same as for the wings. The airflow requirement calculations will have to account for the air temperature losses experienced in some 90 ft. (27 meter) of ducting, for transport aircraft with wing mounted engines. An approximate value of the flow required to anti-ice the empennage of the airplane in figure 5-7 at the evaluation point is 2.0 lb/sec (.91 Kg/sec).

A system that reduces the bleed air temperature by recirculation of anti-icing discharge air also may be used for anti-icing protection. In this system, unregulated and uncooled bleed air is distributed to the wings (and empennage if hot-air protected) in stainless steel or titanium ducts. At each protected section, a thermostatically regulated valve passes the air into piccolo tubes where the air is discharged through a large number of small ejector nozzles. The air from the ejectors mixes with plenum air, is cooled, and then passes through the leading edge double skin heat exchangers and back into the plenum. The excess air is dumped overboard. The thermostatic sensor used to control the regulating shutoff valves is located at the heat exchanger exit and controls the air to a discharge temperature of approximately 135°F (57°C). This system achieves high efficiency with relatively deep air passages (1/8 to 3/16 inch (3.2 to 4.8 mm)) as opposed to the single pass system which requires narrow passages on the order of 0.040 to 0.050 inch (1.02 to 1.27 mm).

On turbojet engines having two compressors, bleed air from the low pressure compressor may also be used for anti-ice protection. To provide anti-ice protection with this lower energy air, larger mass flows will be required. To handle these larger mass flows, the ducting and leading edge heat exchanger passages will have to be larger, but in other ways the system will be generally the same as the high pressure bleed air anti-ice protection system. Difficulty may be experienced in obtaining adequate protection at low rpm, as in descent and hold, but use of low pressure bleed may allow elimination of pressure and/or temperature regulation, thus simplifying the system. Installed weights may be lower, because the reduced temperature and pressure will allow lighter ducting; this is offset to a large extent by the requirement for handling larger mass flows (for a given thermal requirement) at lower densities. Mixing systems may also be used that employ low pressure bleed air augmented by high pressure bleed as required to achieve a desired air temperature.

III.5.10 CONCERNS

Whenever a hot air ice protection system operates in a "running wet" condition (the heat applied does not fully evaporate all of the impinging water droplets), there is a danger of freezing the water that runs back. A typical location in which this condition may occur is the wing leading edge or engine cowl. In these locations, any water not fully evaporated may run back onto an unheated surface that is below the freezing point. Several detrimental effects may result if the water freezes on these surfaces:

a. The aerodynamics of the surface may be affected. Generally, the maximum lift coefficient ($C_{L_{max}}$) is most severely affected and this could require an increase in landing speed.

b. The runback ice could damage downstream equipment. If the runback icing condition is held for a significant period of time, the mass of ice may become large. Supercooled droplets may impinge directly onto the runback ice If the flight conditions are then changed such that the skin temperature exceeds about 35°F (2°C), the runback icecap may be released, allowing aerodynamic forces to carry the ice into an engine, the tail surfaces, ailerons, flaps, etc. Serious damage could result.

c. If the runback ice forms near a movable surface, it may form an obstruction. Runback ice from an extended slat or Krueger flap could form an obstruction when the retraction of the slat or Krueger flap is attempted. The forces developed by the retraction mechanism could damage structural elements, result in partial retraction and change the aerodynamic forces on the aircraft.

The designer should ascertain the potential effects of all runback ice and eliminate those that could seriously degrade the safety of the aircraft. Final evaluation of the effects of runback ice should be part of the natural icing flight test program (Chapter V).

III.5.11 REFERENCES

5-1 Gray, V.H. and Bowden, D.T., "Comparison of Several Methods of Cyclic De-Icing of a Gas Heated Airfoil," NACA RM E53C27, June 1953.

5-2 "Jet Blast Windshield Rain Removal Systems for Aircraft," SAE Aerospace Information Report, AIR 805A, 30 July 1965.

5-3 "Transparent Areas, on Aircraft Surfaces (Windshields and Canopies), Rain Removing and Washing Systems for Defrosting, De-Icing, Defogging; General Specifications For," MIL-T-5842B, 29 March 1985.

5-4 "Anti-Icing Equipment for Aircraft, Heated Surface Type. General Specifications For," MIL-A-9482, 2 September 1954, amended 2 April 1981.

5-5 Grabe, W. and Vanslyke, G.K." "Icing Tests on the JT15D Turbofan Engine. Proceedings of the Tenth National Conference on Environmental Effects on Aircraft and Propulsion Systems," Sponsored by Naval Air Propulsion Test Center, 18-20 May 1971.

5-6 Striebel, E.E., "Ice Protection for Turbine Engines," FAA Report of Symposium on Aircraft Ice Protection, 28-30 April 1969.

5-7 Pfeifer, G.D. and Maier, G.P., "Engineering Summary of Powerplant Technical Data," Report Number FAA-RD-77-76, July 1977.

5-8 Bowden, D.T., Gensen, A.E. and Skeen, C.A., "Engineering Summary of Air-frame Icing Technical Data," FAA ADS-4, December 1963.

5-9 Cozby, D.E., "Effects of Recent Engine.Developments on Boeing Aircraft Ice Protection Requirements," Symposium on Electro-Impulse De-Icing System at NASA Lewis Research Center, 13 June 1985.

5-10 Sogin, H.H., "A Design Manual for Thermal Anti-Icing Systems," WADC Technical Report 54-313, Illinois Institute of Technology, 1 September 1954.

5-11 SAE Aerospace "Applied Thermodynamics Manual," SAE AIR 1168, 1969.

5-12 Duffy, R.J. and Shattuck, B.F., "Integral Engine Inlet Particle Separator, Volume II - Design Guide," Report Number USAAMRDL-TR-75-31B, August 1975.

TABLE 5-1
Icing Tunnel Test Conditions for Figure 5-28

Symbol	Configuration	Velocity (mph/mps)	Temperature °F/°C	LWC (g/m^3)	MVD (microns)	Angle of Attack (Degrees)
⊙	Double Skin	175/78	20/-7	1.22	20	1.5
⊙	Double Skin	175/78	20/-7	1.22	20	3.4
●	Single Skin	175/78	20/-7	1.22	20	3.4
▽	Double Skin	175/78	16/-9	0.95	16	1.5
△	Double Skin	211/94	11/-12	0.75	15	1.5
⊡	Double Skin	211/94	0/-18	0.92	17	1.5
⊡	Double Skin	211/94	0/-18	0.92	17	3.4
■	Single Skin	211/94	0/-18	0.92	17	3.4
◈	Double Skin	175/78	0/-18	0.95	16	1.5
◆	Single Skin	175/78	0/-18	0.95	16	1.5
⊙	Double Skin	175/78	0/-18	0.765	14	1.5
◆	Single Skin	211/94	-15/-26	0.75	15	1.5

TABLE 5-2

Design Point Flight and Icing Conditions

Flight Condition	High Speed Descent
Altitude	22,000 ft. (6705 m)
Aircraft Gross Weight	All
Aircraft Speed	M = 0.8 (823 FPS = 488 Kts)
Icing Condition	Intermittent Maximum
Cloud Length	3 miles
Mean Volume Diameter	20 microns
Outside Air Temperature	-22°F
Cloud Liquid Water Content (Free Stream)	1.1 Grams/Cubic Meter

TABLE 5-3

Strake Minimum Surface Temperature

Attitude	Altitude Ft.	Mach No.	Icing Cond.	LWC g/m^3	α_o Fus Degree	OAT °F	Supply** Air Temp °F	Min. Surf. Temp. °F
				DESIGN POINT				
High Speed Descent	22,000 (6705 m)	.80	Int. Max.	1.1	1.1	-22	421	35
				OFF DESIGN POINTS				
Hold	10,000 (3048 m)	.359	Cont. Max.	0.40	6.1	12	470	56
High Speed Cruise	30,000 (9144 m)	.84	Int. Max.	0.19	0.4	-40	470	39
High Speed Climb	15,000 (4572 m)	.572	Int. Max.	0.82	1.8	-26	470	42

* Int. Max. - 3 mile cloud
Cont. Max. - 20 mile cloud

** At the discharge of the ice protection pressure regulator

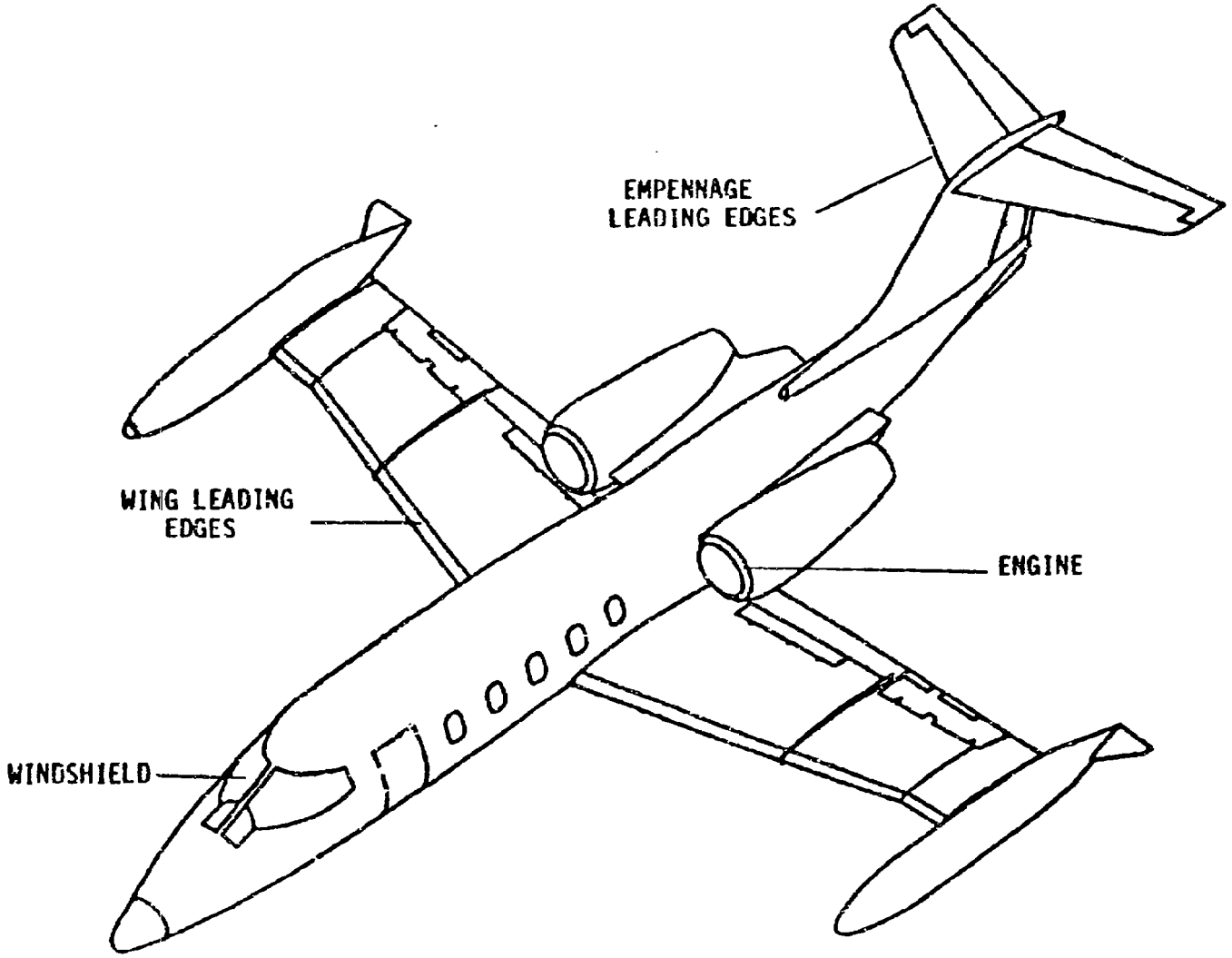

FIGURE 5-1. AREAS OF AIRFRAME THAT MAY USE HOT AIR ICE PROTECTION

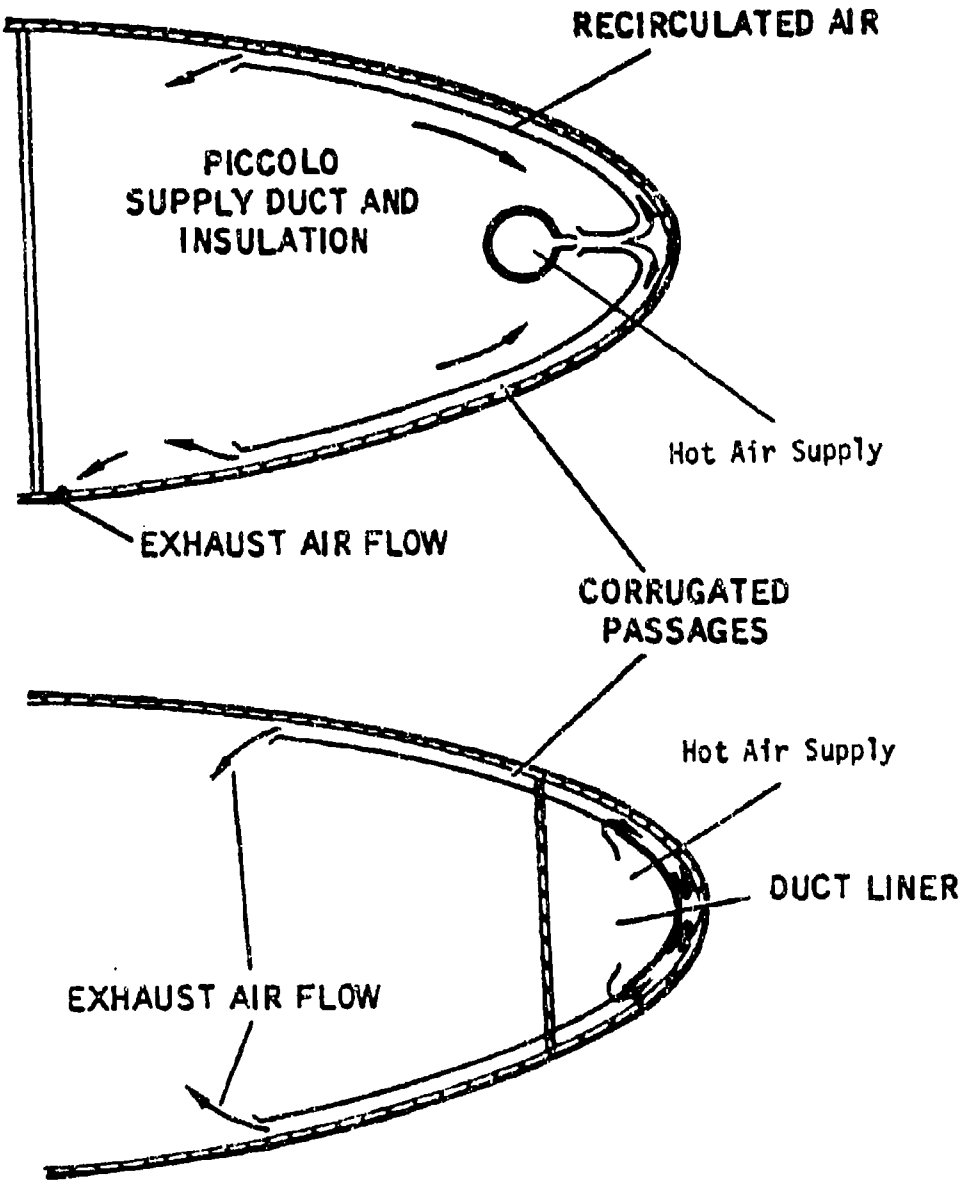

FIGURE 5-2. AIR FLOW IN TYPICAL DOUBLE-SKINNED LEADING EDGES OF HEATED WINGS (REF. 5-10)

CORRUGATED CHANNEL

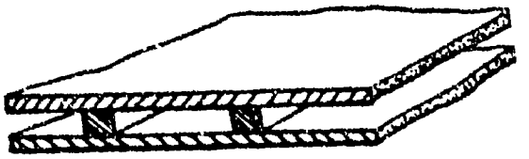

SPACER STRIPS

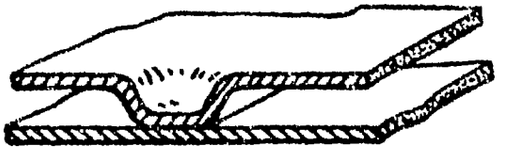

DIMPLE EMBOSS

ETCHED CHANNEL

FIGURE 5-3. TYPICAL CROSS-SECTIONS OF DOUBLE-SKIN GAS PASSAGES

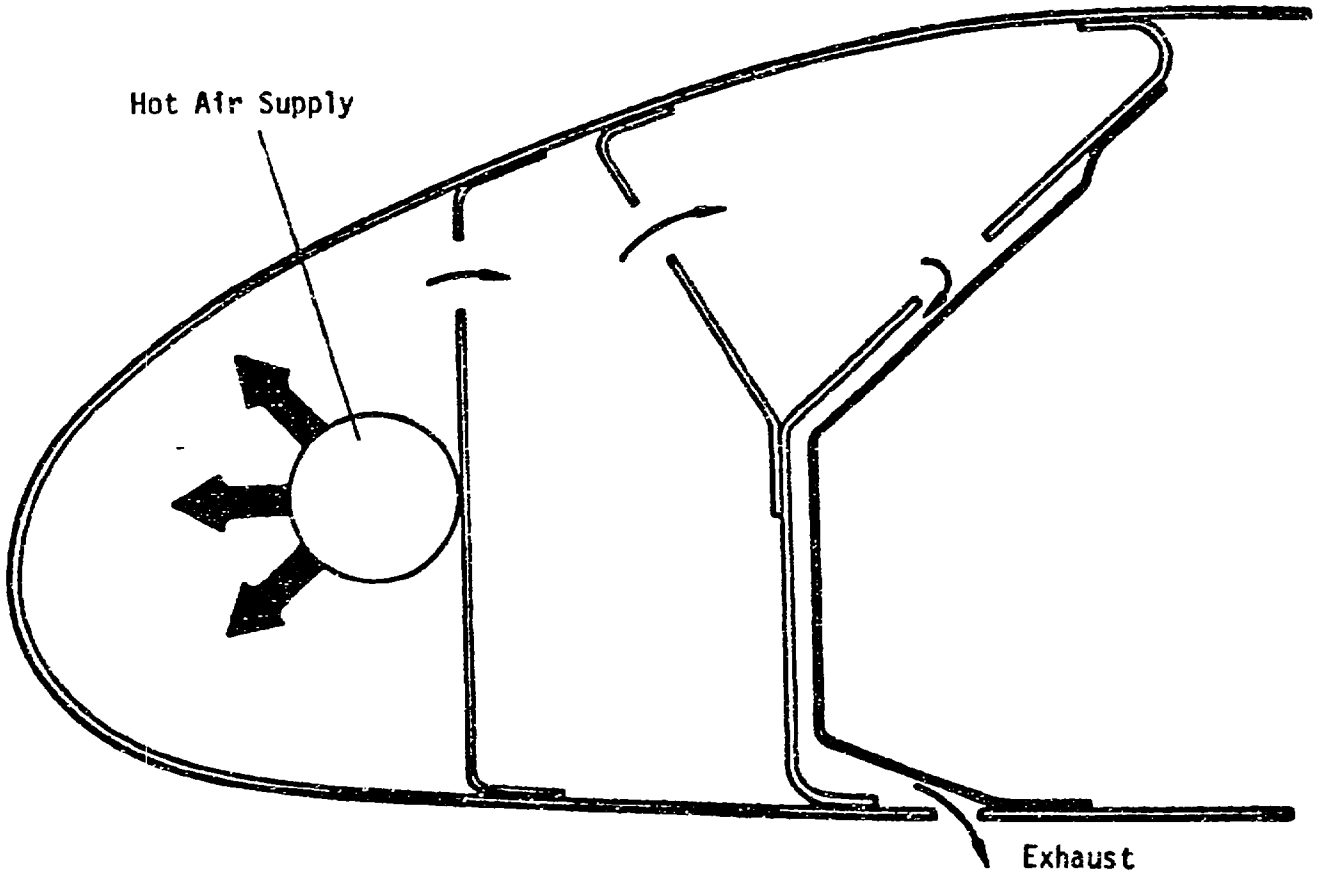

FIGURE 5-4. "SINGLE SKIN" HOT AIR INSTALLATION

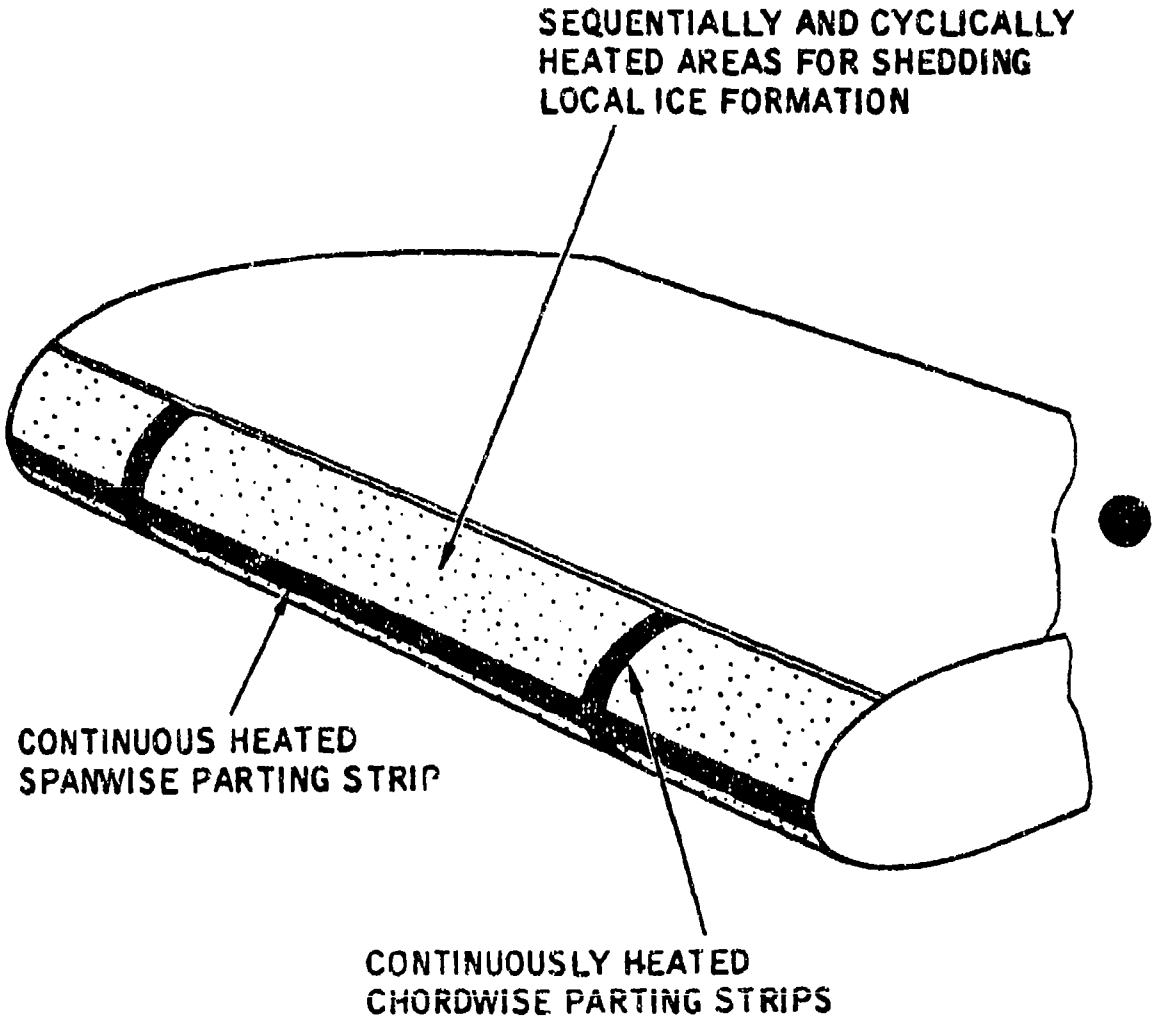

FIGURE 5-5. ARRANGEMENT FOR CYCLIC THERMAL DE-ICING

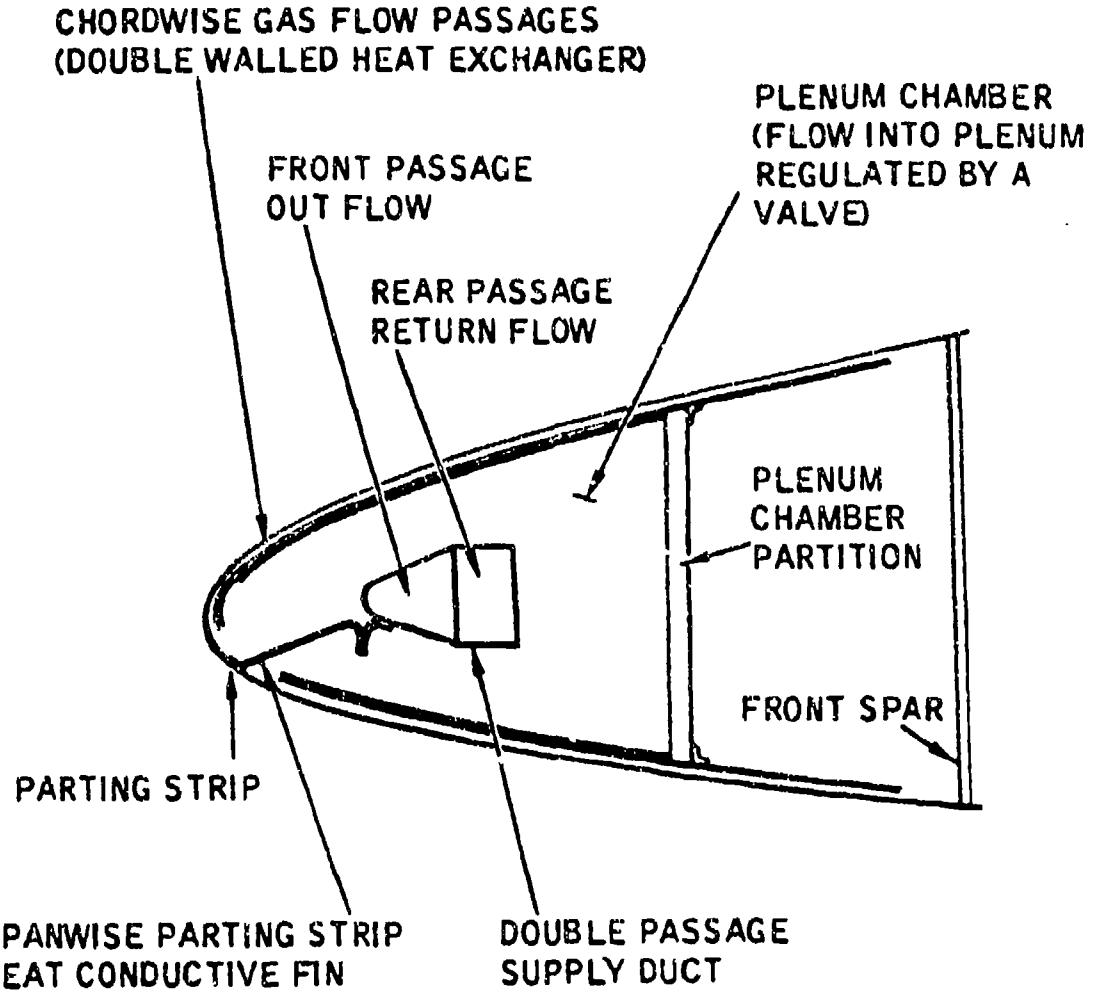

FIGURE 5-6. CONSTRUCTION DETAILS OF GAS-HEATED AIRFOIL FOR CYCLIC DE-ICING (REF. 5-1)

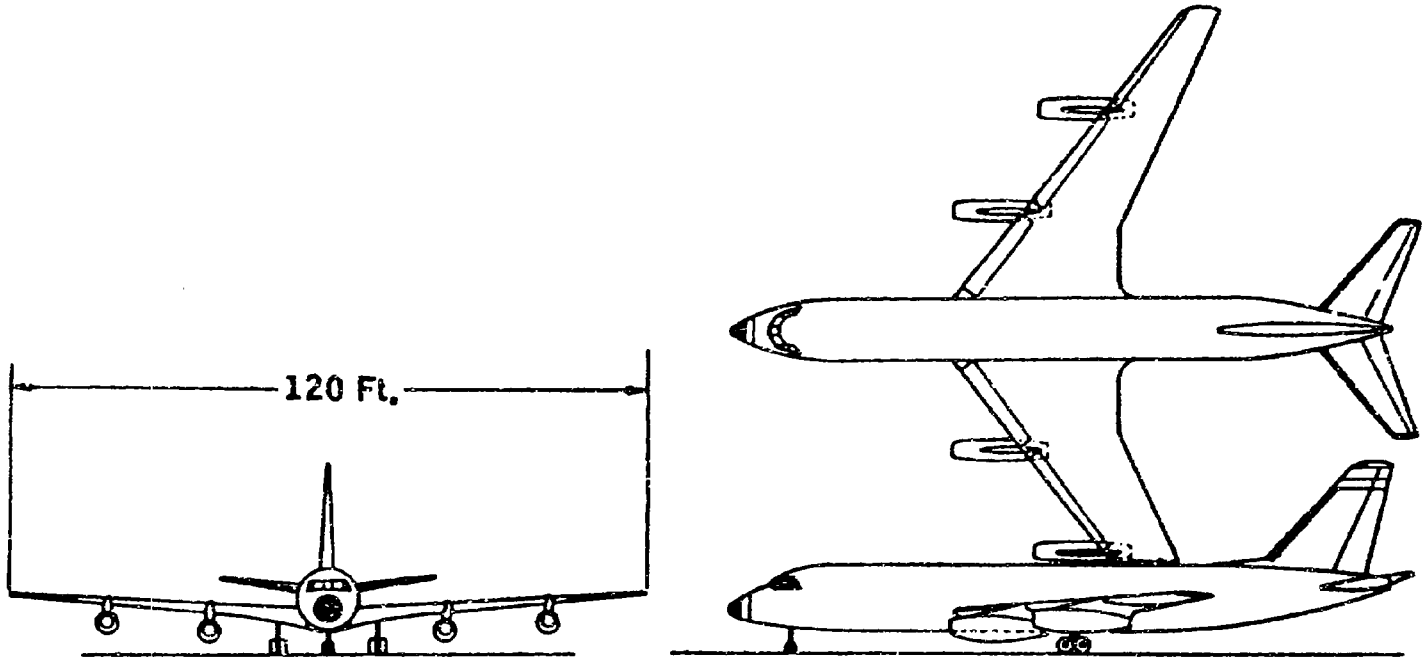

FIGURE 5-7. TYPICAL FAR 25 JET TRANSPORT

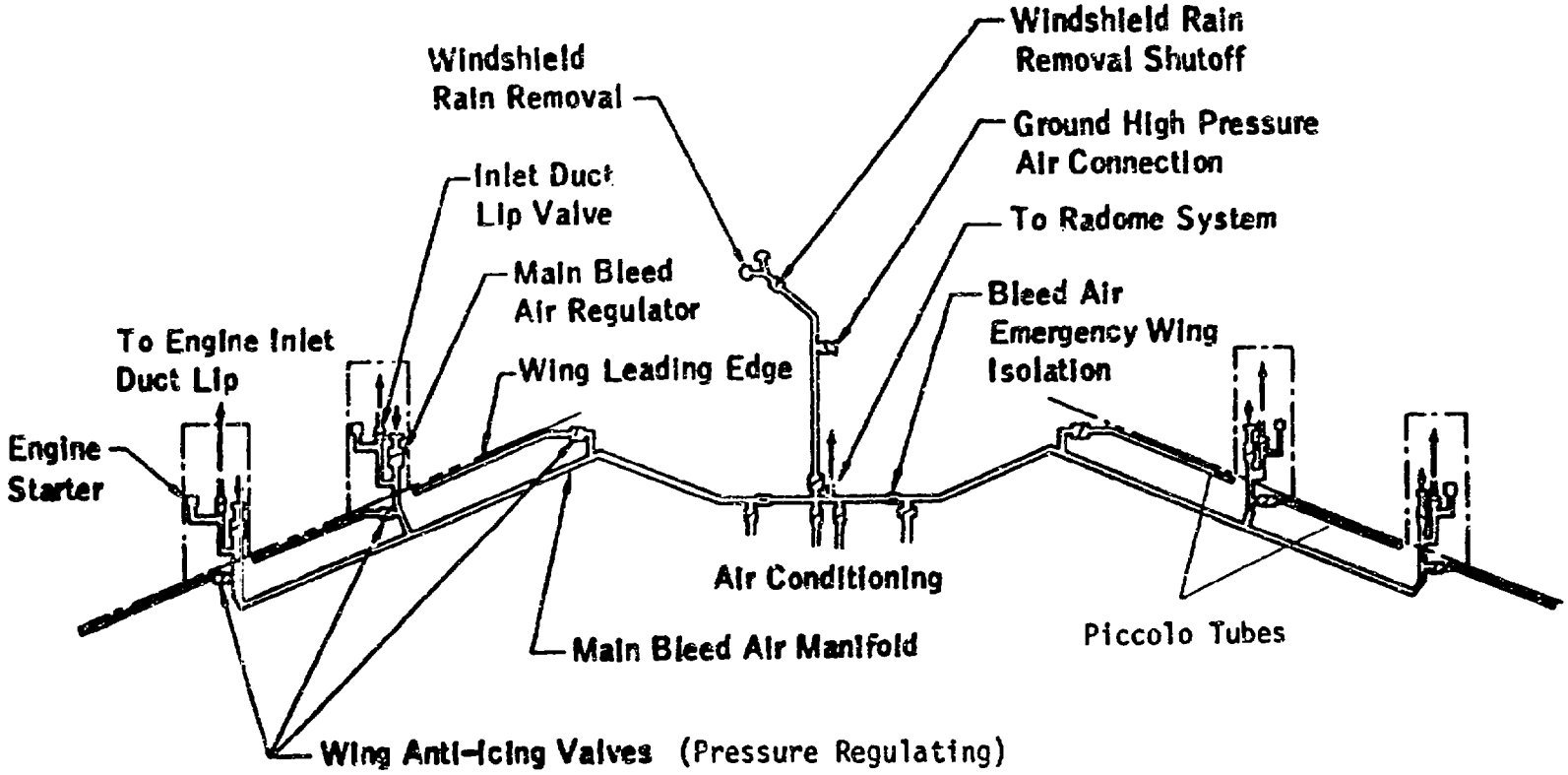

FIGURE 5-8. TYPICAL HOT-AIR ANTI-ICING SYSTEM

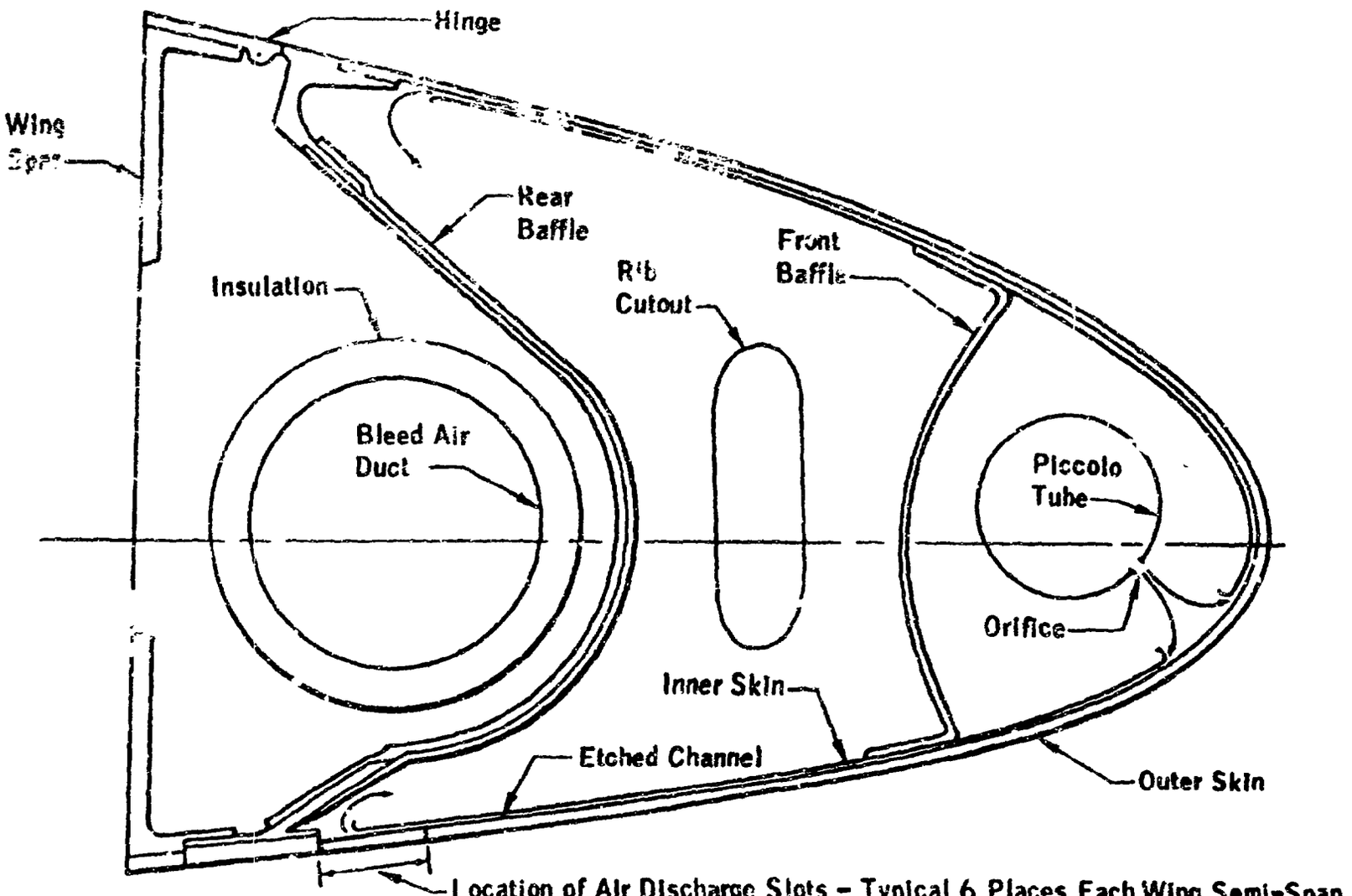

FIGURE 5-9. TYPICAL HOT-AIR ANTI-ICED WING LEADING EDGE

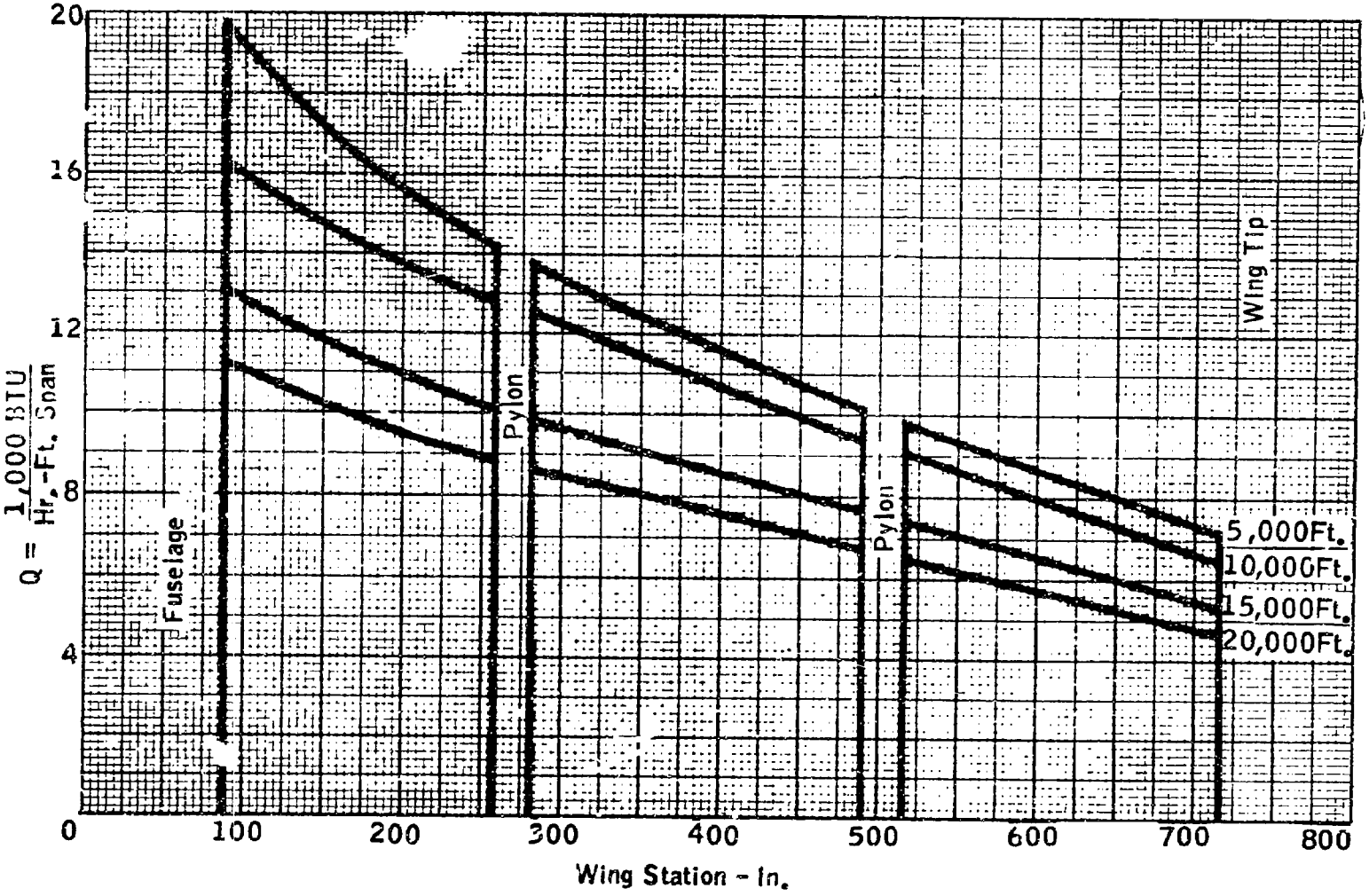

FIGURE 5-10. ANTI-ICING HEAT REQUIREMENT Vs. WING STATION, HOLD CONDITION (REF. 5-8)

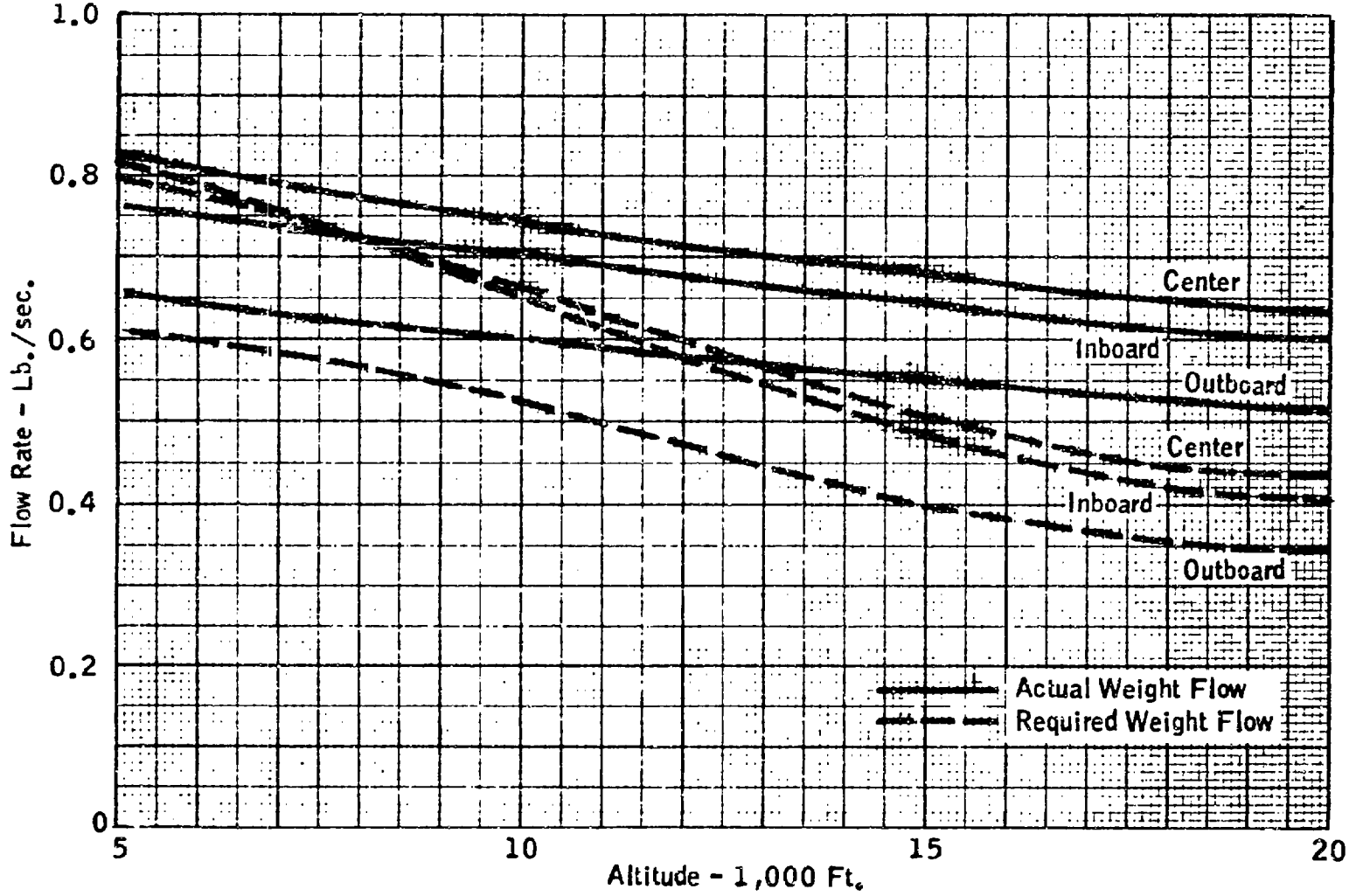

FIGURE 5-11. AIR FLOW RATES FOR WING ANTI-ICING, HOLD CONDITION (REF. 5-8)

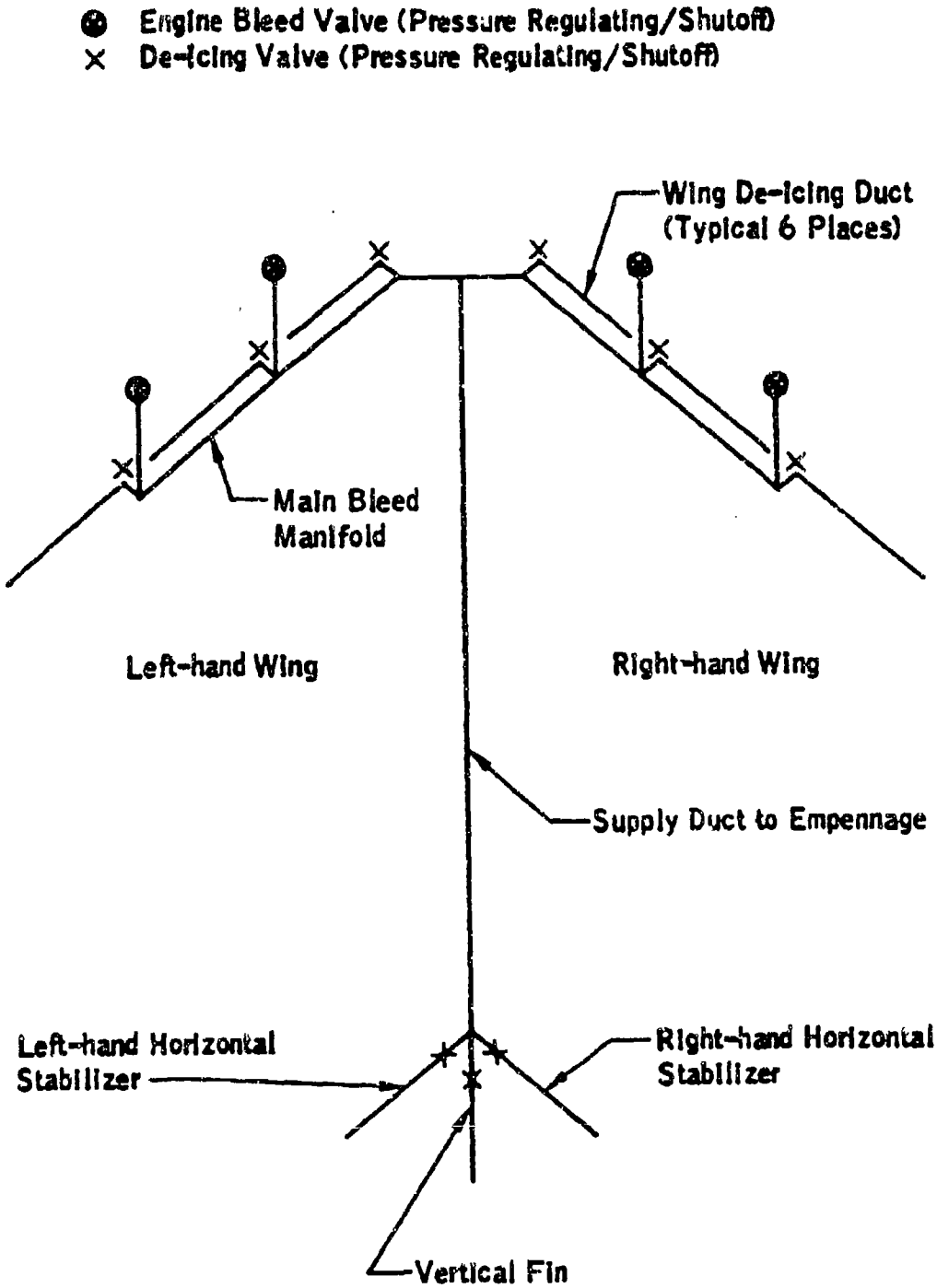

FIGURE 5-12. TYPICAL HOT-GAS DE-ICING SYSTEM FOR FOUR-ENGINE TRANSPORT

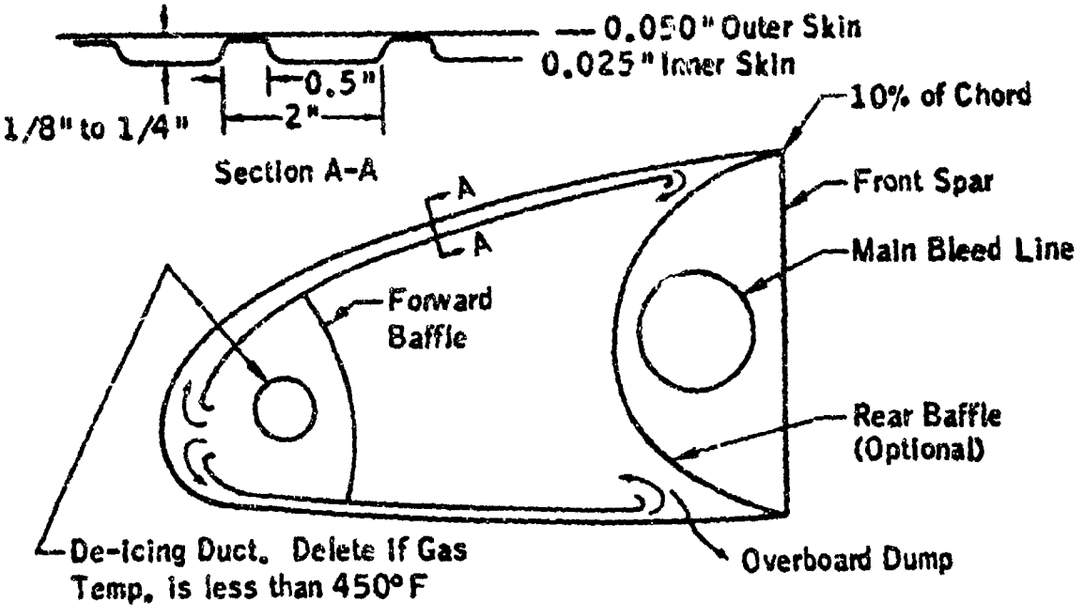

(a) Design for Swept-wing (over 30° sweep)

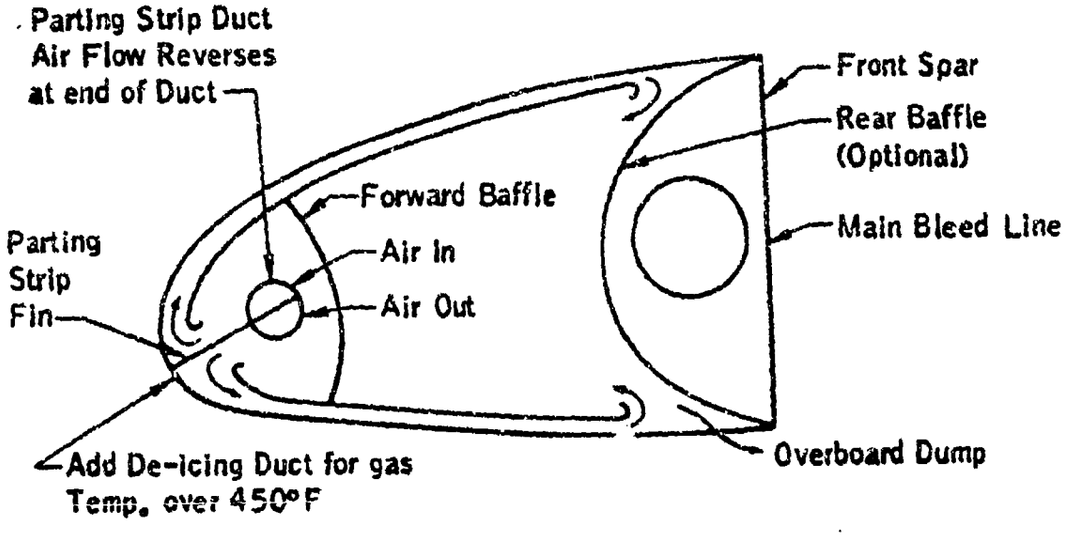

(b) Design for Non-swept Wing (less than 30° sweep)

FIGURE 5-13. TYPICAL WING LEADING EDGE CROSS SECTION FOR TWO TYPES OF HOT-GAS DE-ICING SYSTEMS

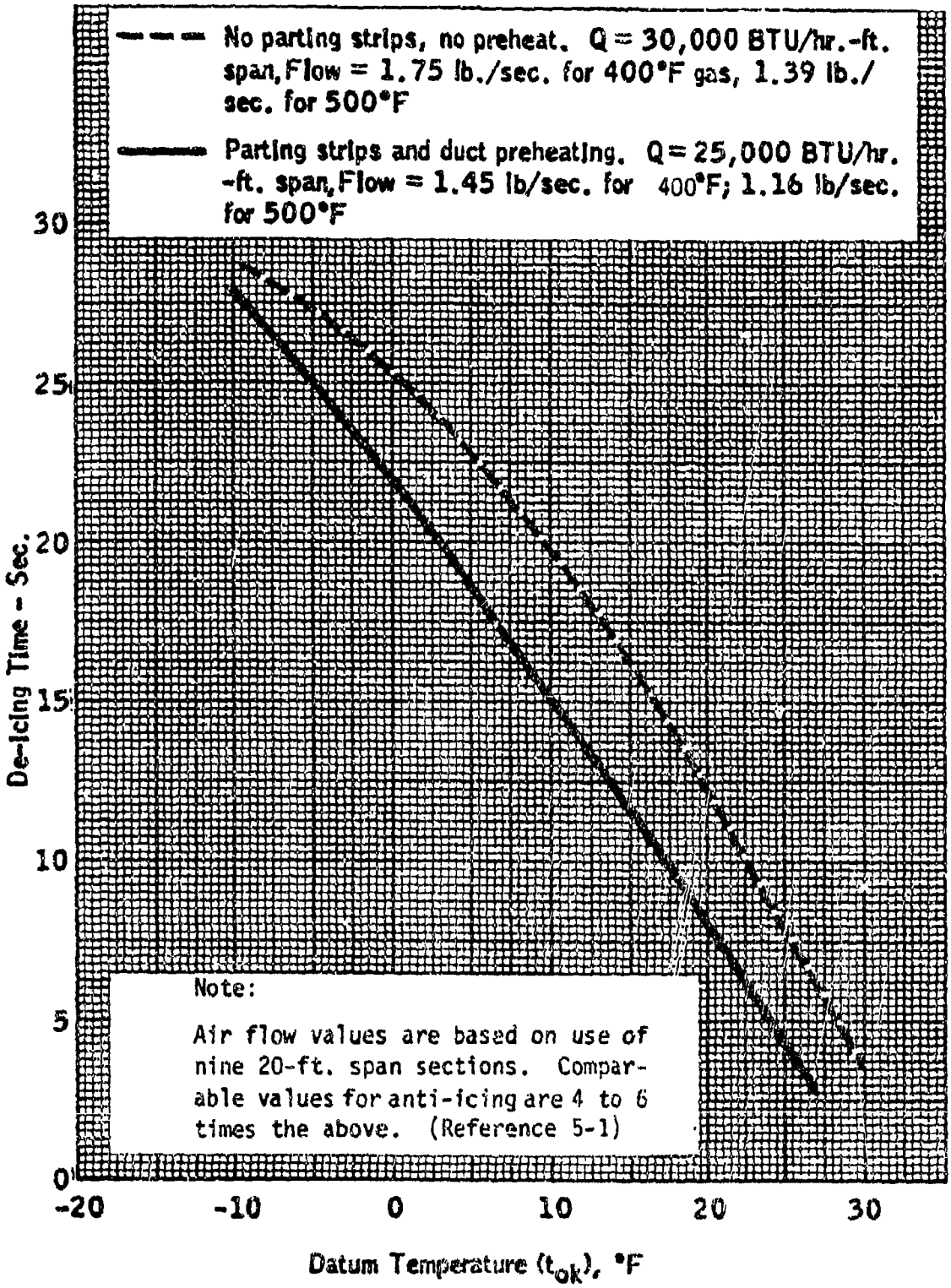

FIGURE 5-14. DE-ICING TIME VS. DATUM TEMPERATURE FOR TWO TYPICAL HOT-GAS DE-ICING SYSTEMS

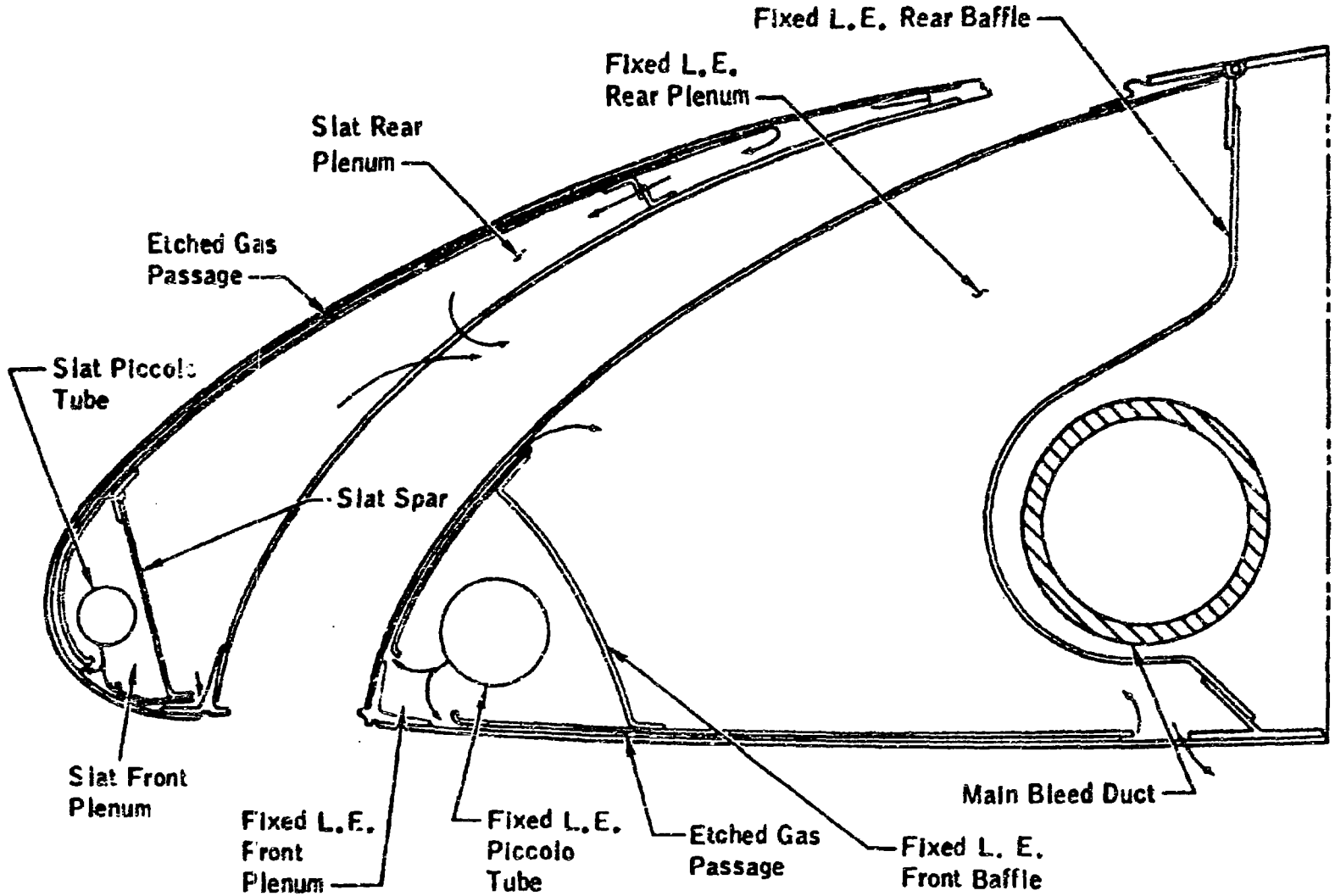

FIGURE 5-15. TYPICAL WING LEADING EDGE WITH SLAT

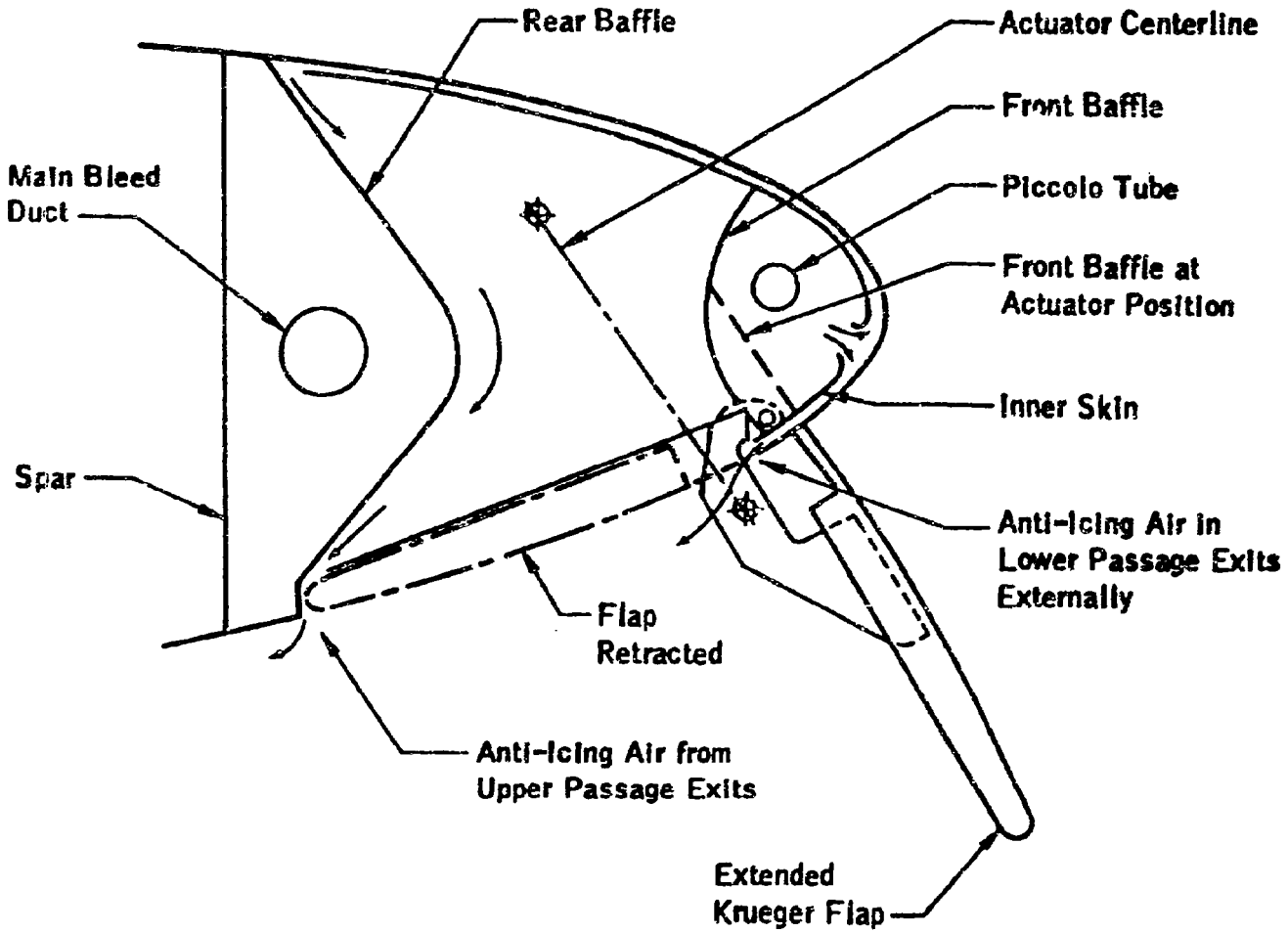

FIGURE 5-16. TYPICAL WING LEADING EDGE "KRUEGER" FLAP

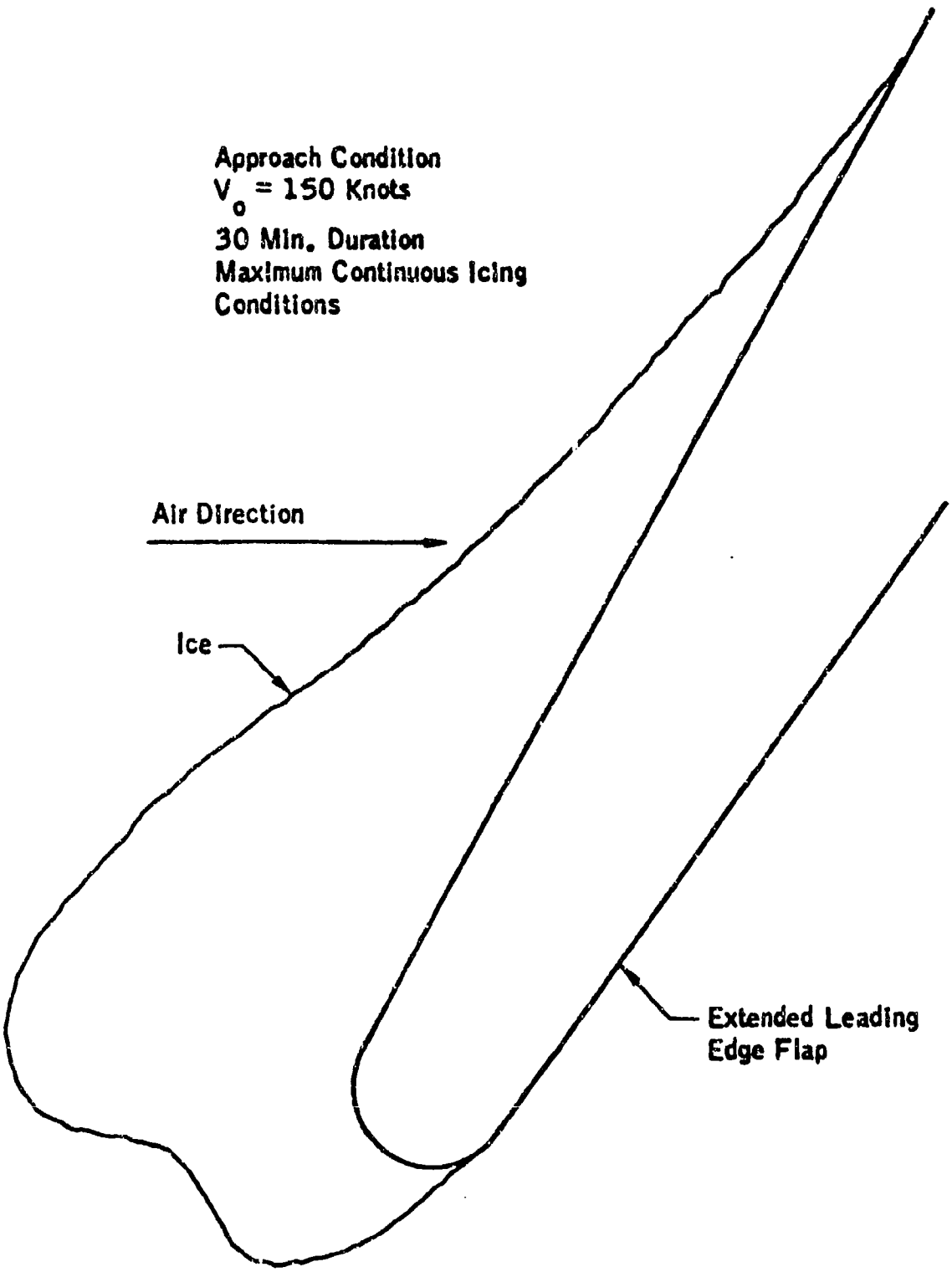

FIGURE 5-17. ICE ACCRETION ON UNPROTECTED EXTENDED LEADING EDGE FLAP FOR MAXIMUM CONTINUOUS ICING CONDITIONS

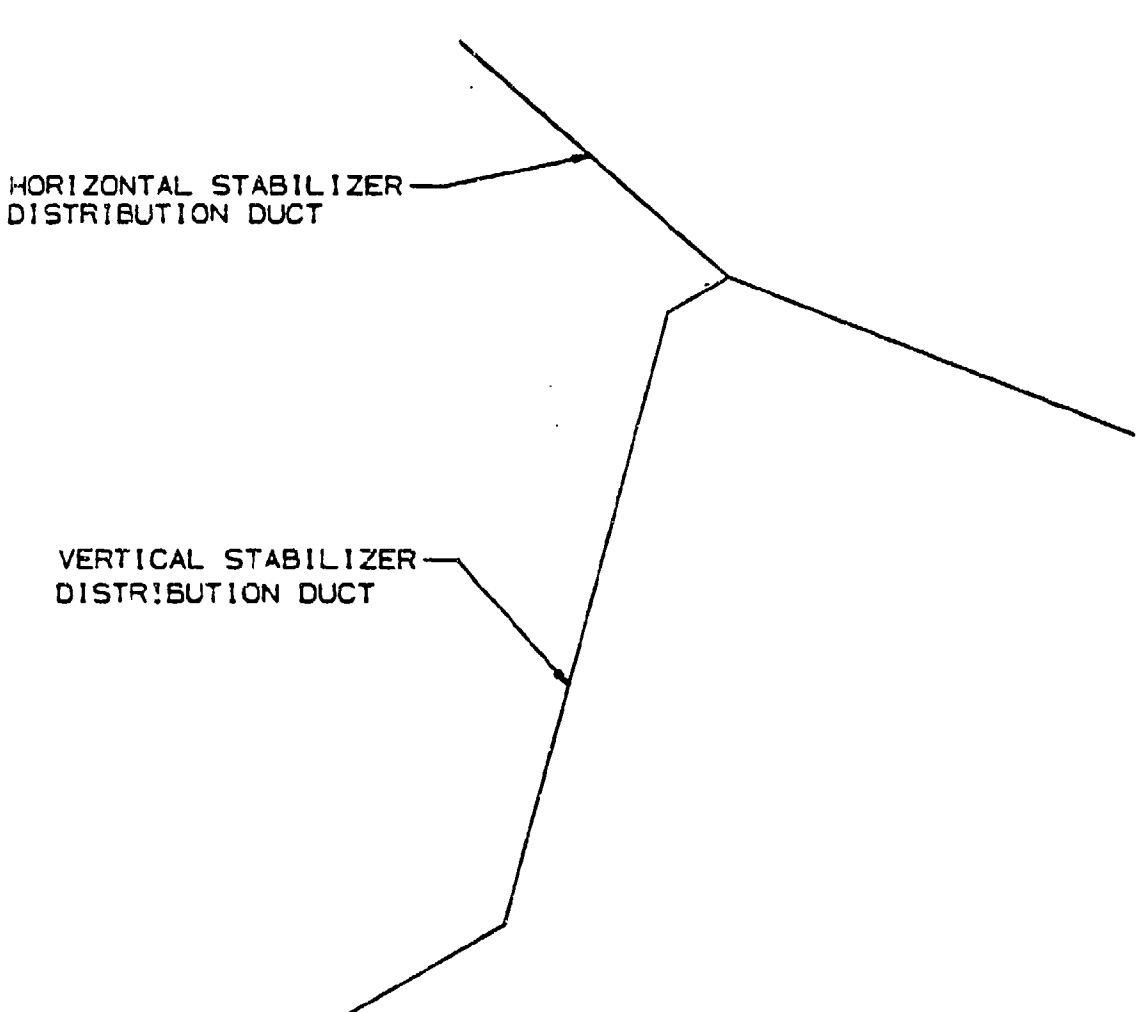

FIGURE 5-18. TAIL ICE PROTECTION SYSTEM DUCT SCHEMATIC

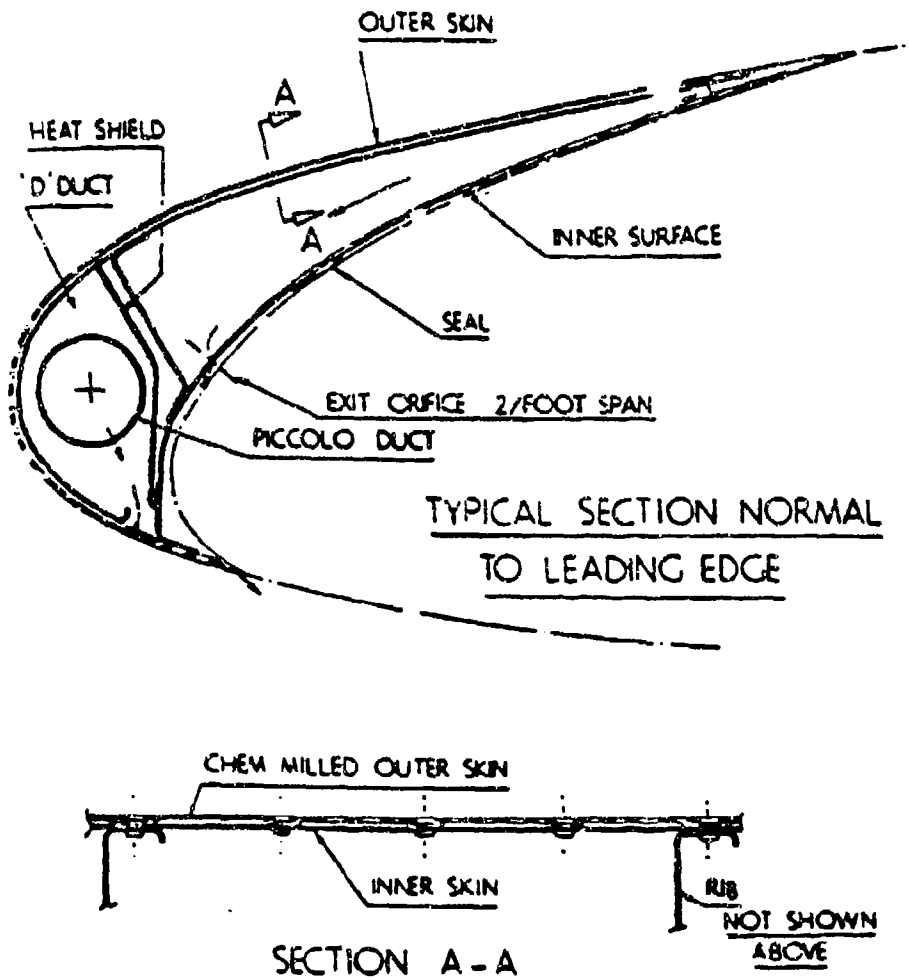

FIGURE 5-19. WING LEADING EDGE CROSS SECTION
- DOUBLE SKIN FLOW PASSAGES

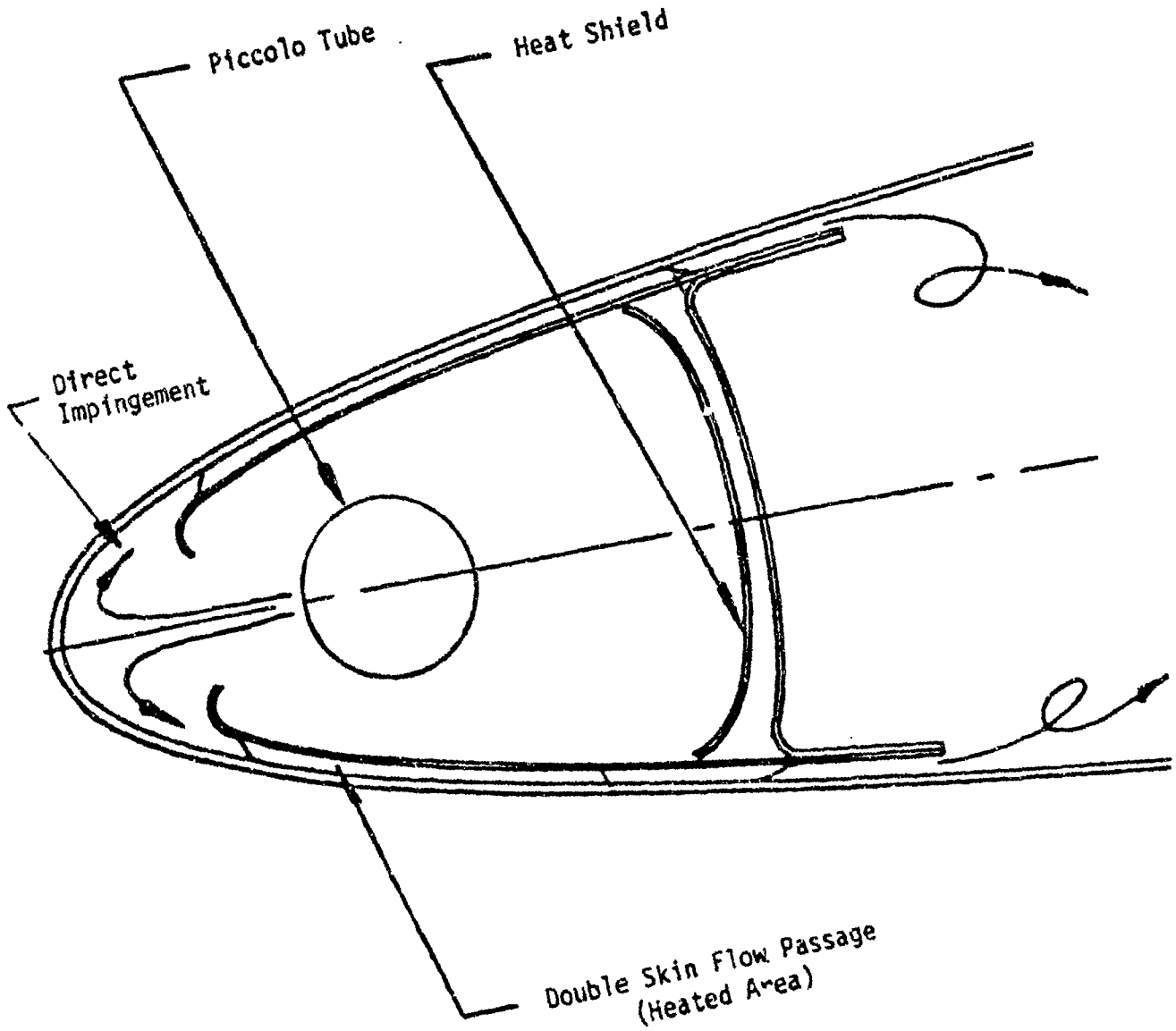

FIGURE 5-20. HORIZONTAL STABILIZER CROSS SECTION - DIRECT IMPINGEMENT

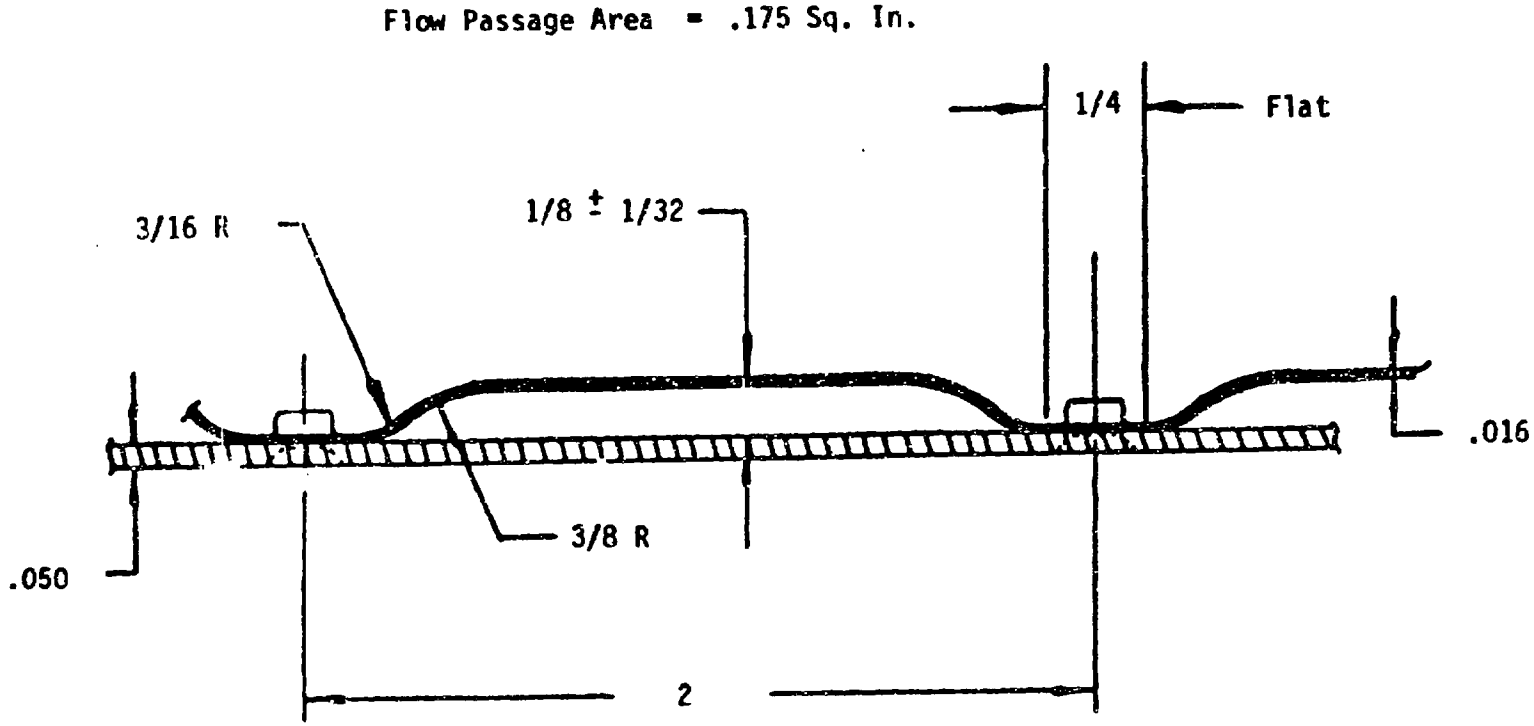

FIGURE 5-21. HORIZONTAL STABILIZER DE-ICING FLOW PASSAGE

Horizontal Stabilizer Supply Duct and Piccolo Tube

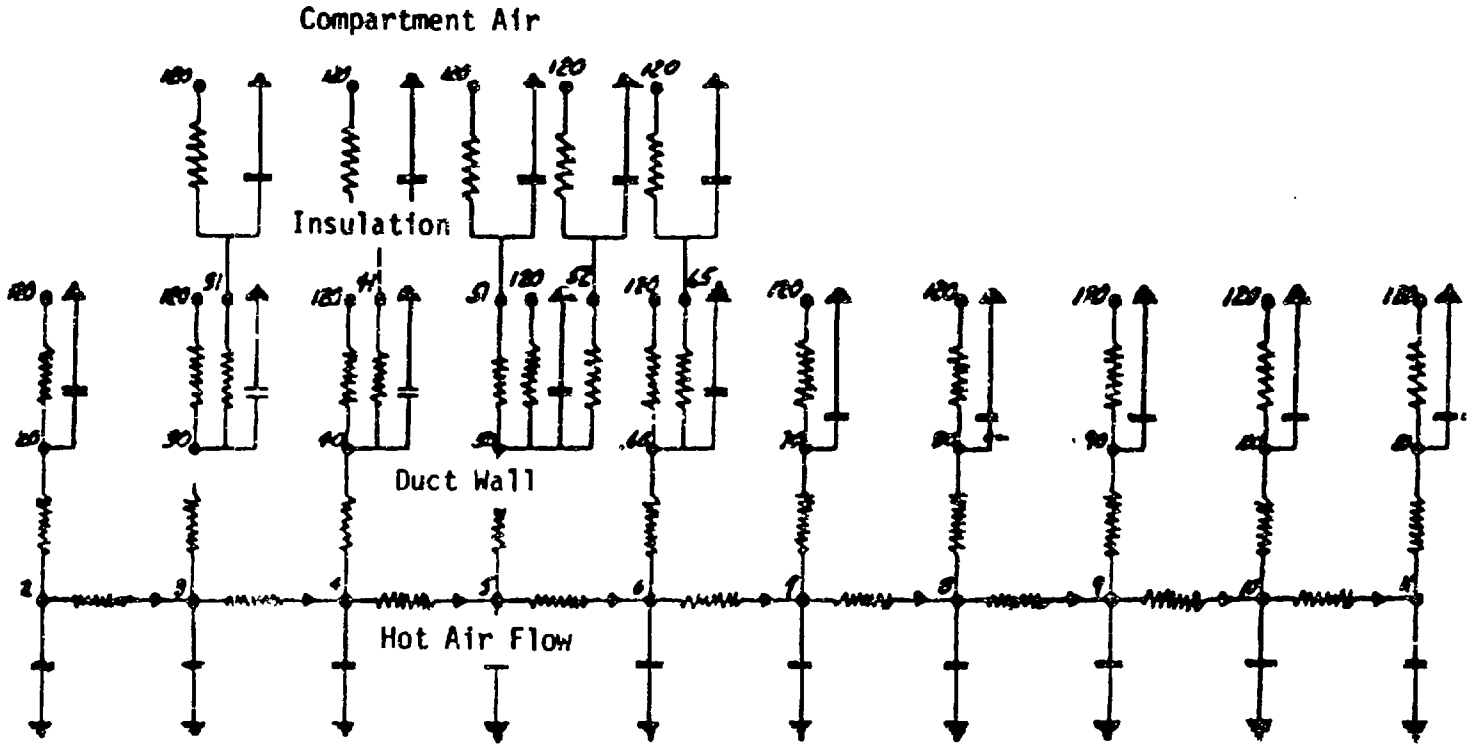

FIGURE 5-22. DE-ICING THERMAL NETWORK

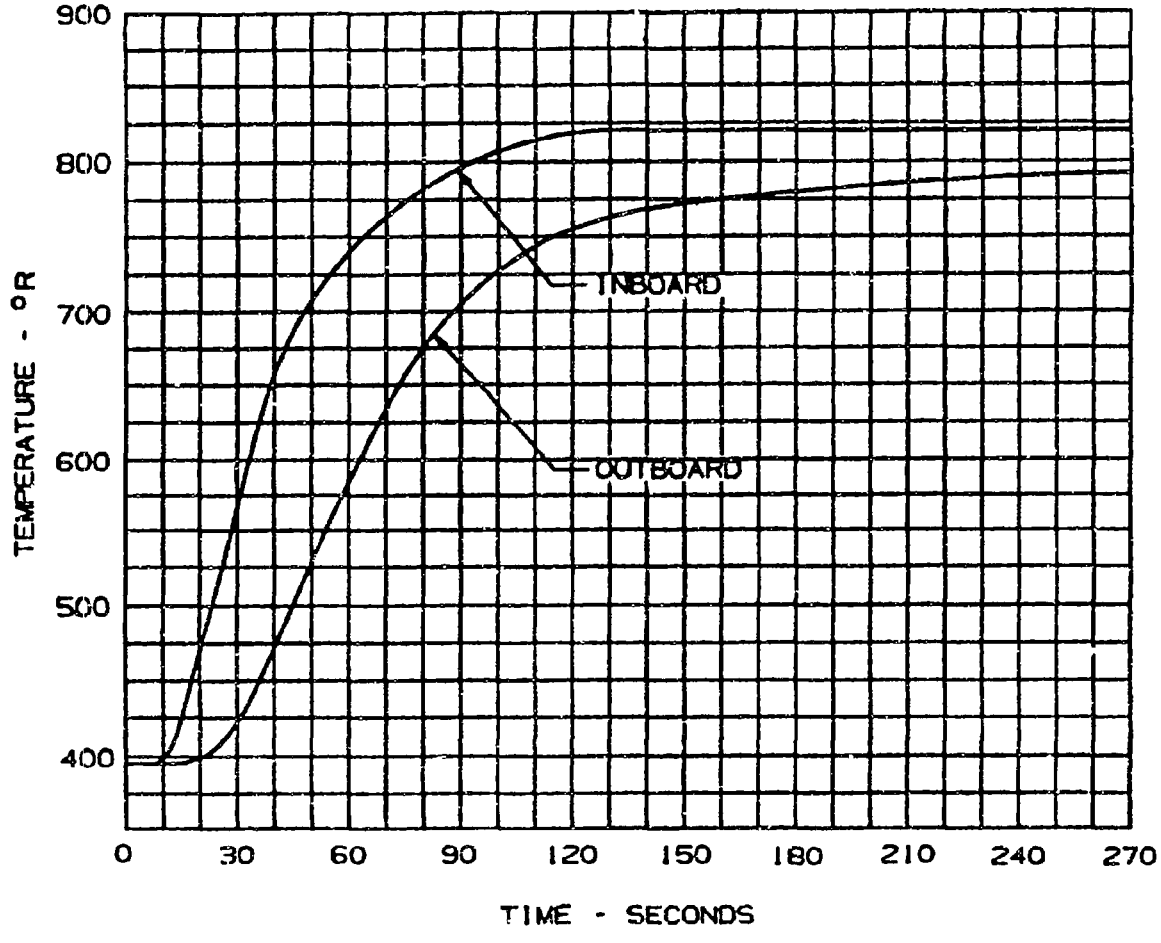

FIGURE 5-23. DE-ICING SUPPLY AIR TEMPERATURE VS. TIME

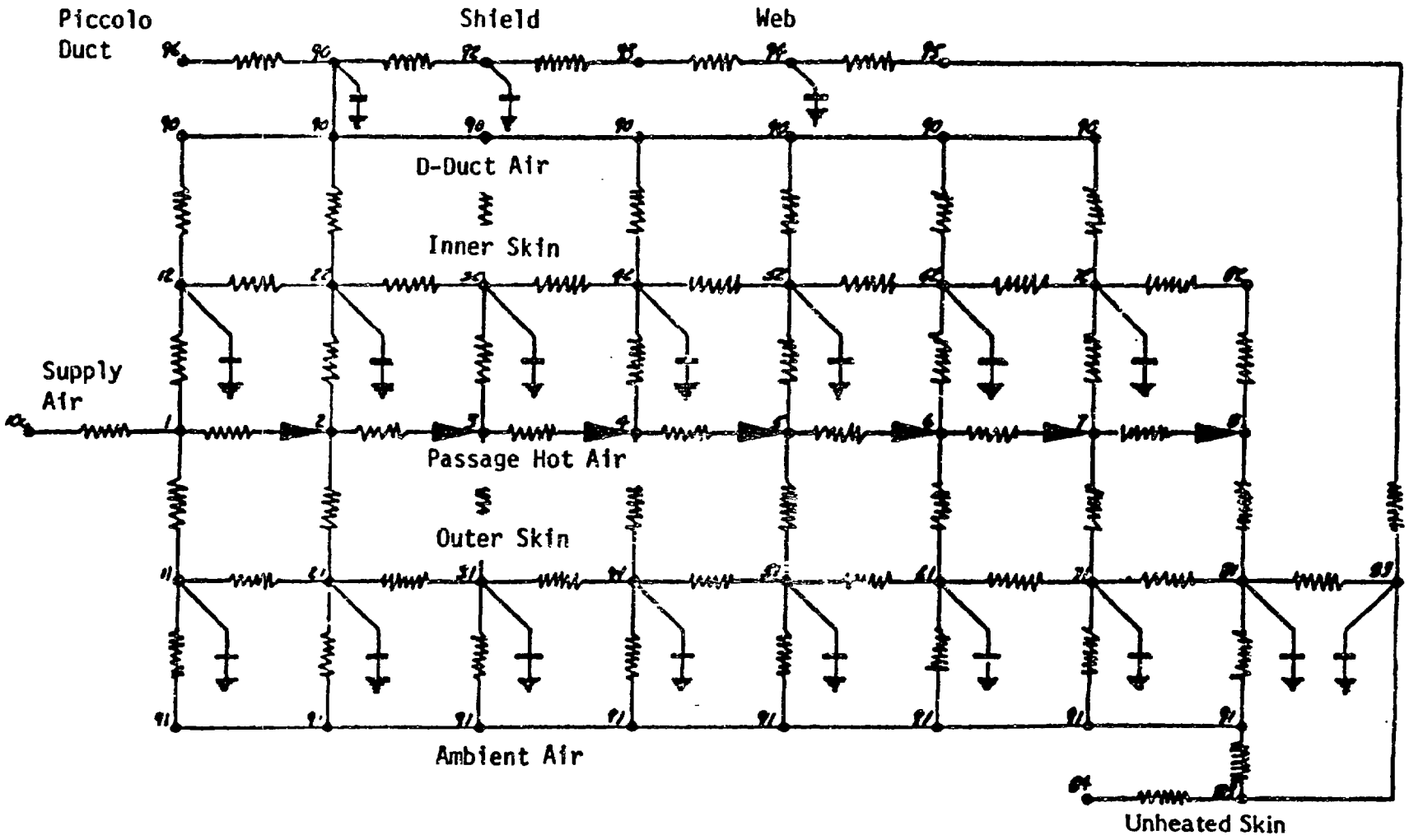

FIGURE 5-24. DE-ICING THERMAL NETWORK - DOUBLE SKIN FLOW PASSAGE

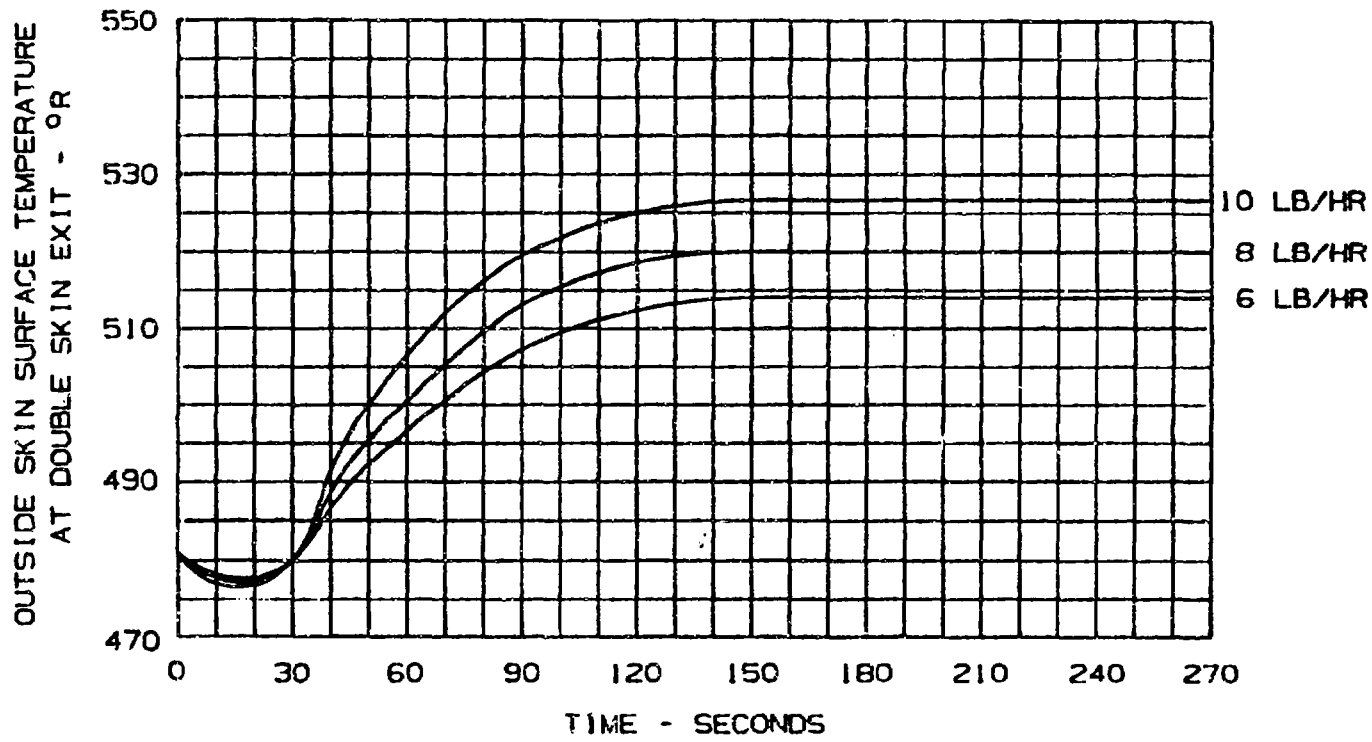

FIGURE 5-25a. TIME TEMPERATURE RESPONSE FOR HORIZONTAL STABILIZER - UPPER SURFACE

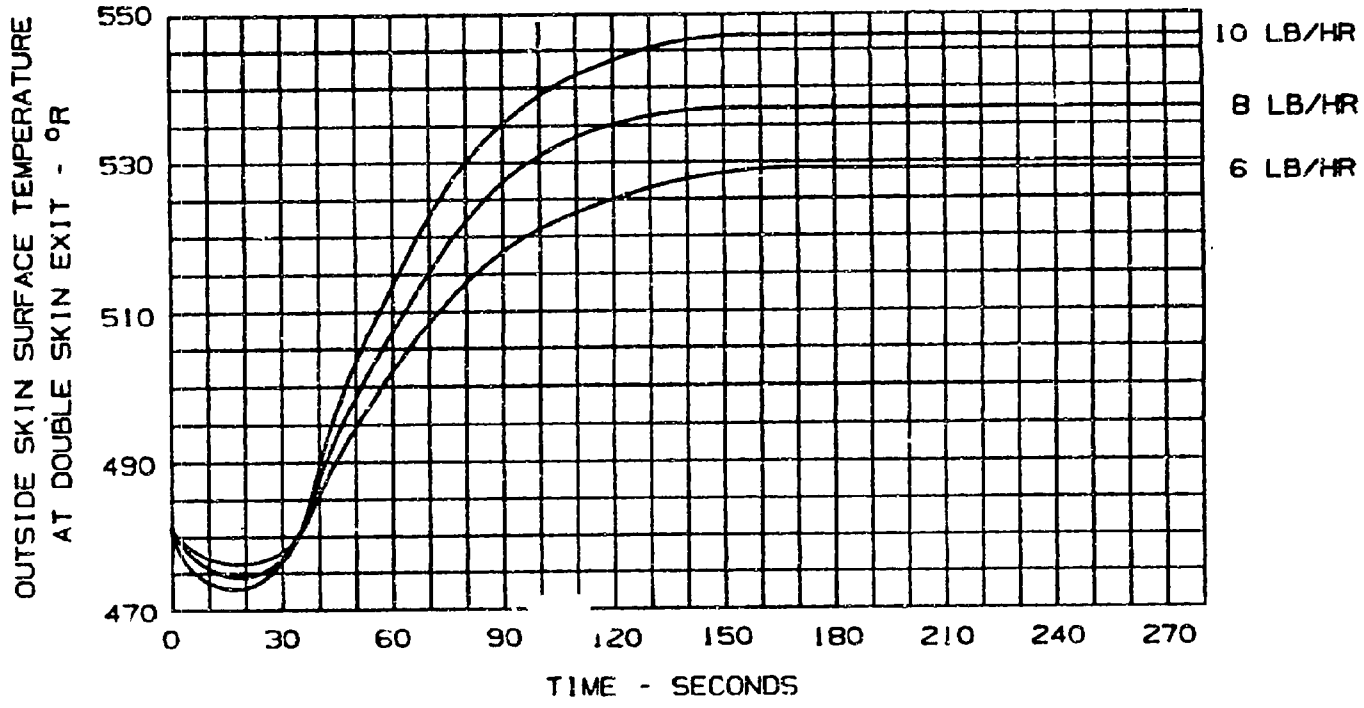

FIGURE 5-25b. TIME TEMPERATURE RESPONSE FOR HORIZONTAL STABILIZER - LOWER SURFACE

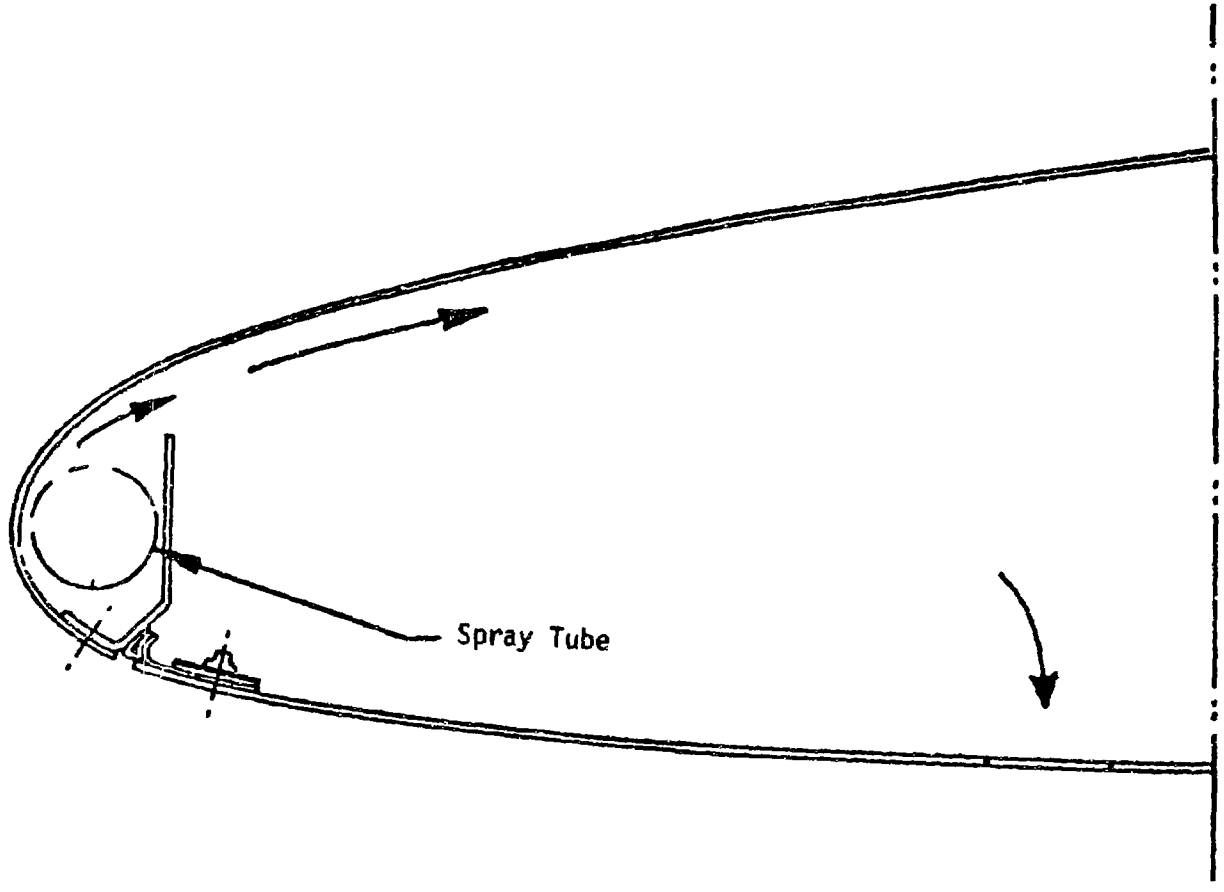

FIGURE 5-26. WING PARALLEL FLOW SINGLE SKIN SYSTEM

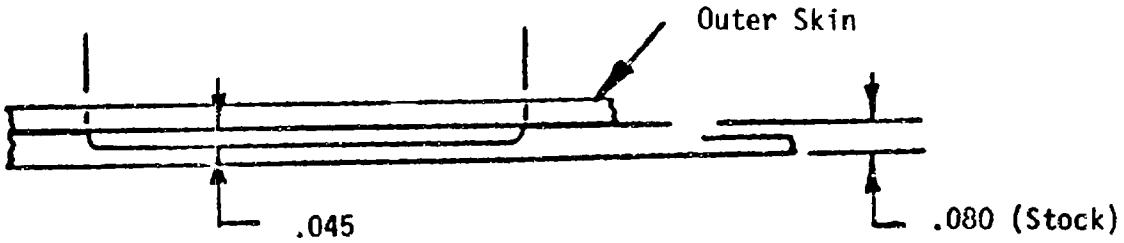

Detail - Cross Section
of Double Skin

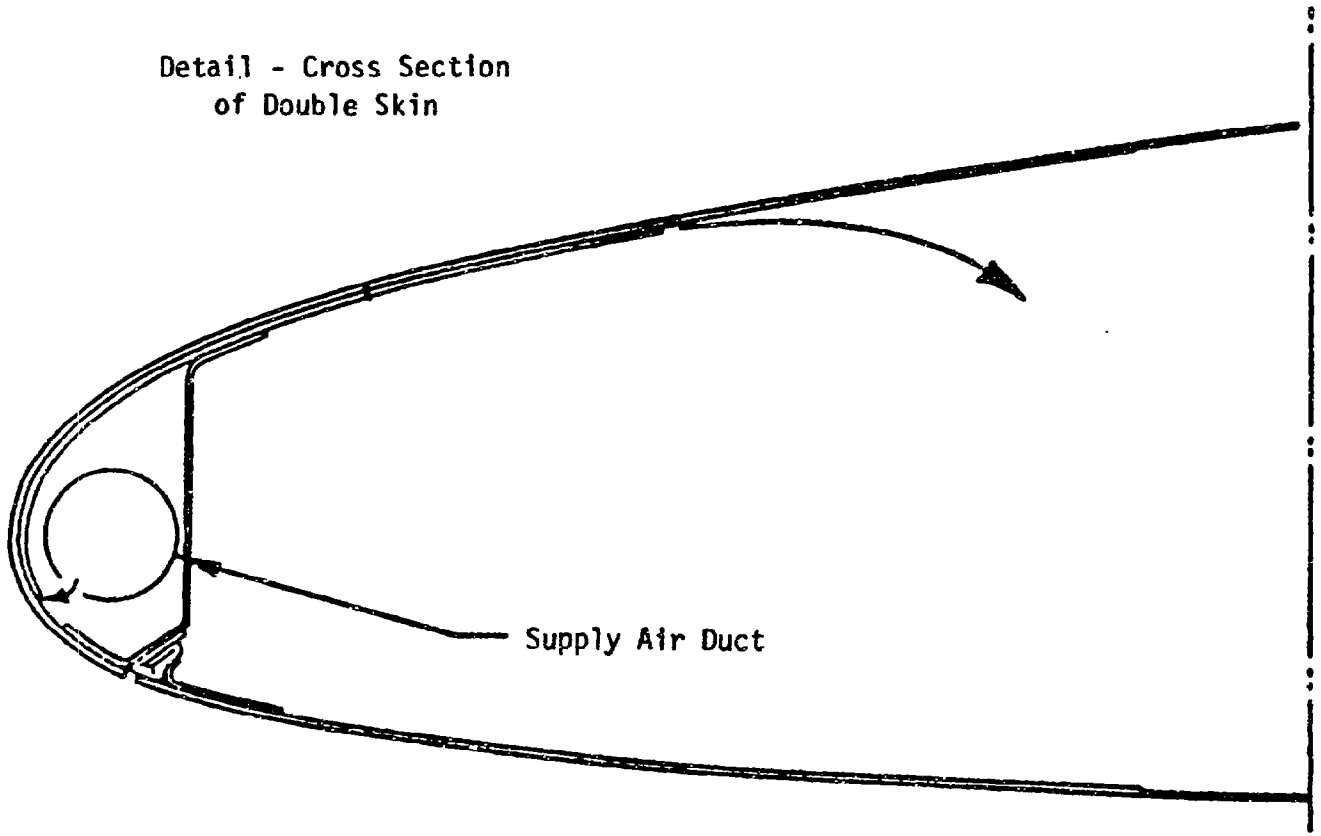

FIGURE 5-27. WING PARALLEL FLOW DOUBLE SKIN SYSTEM

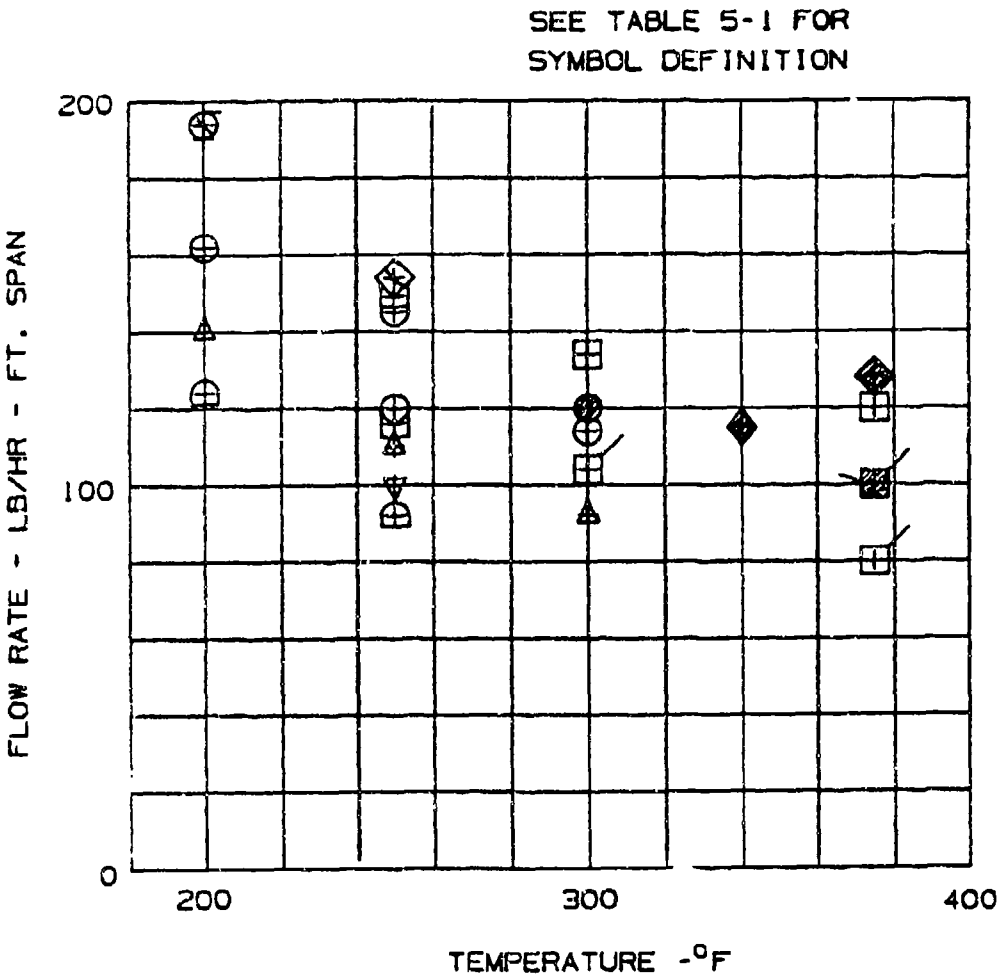

FIGURE 5-28. PERFORMANCE COMPARISON OF SINGLE AND DOUBLE SKIN ANTI-ICING

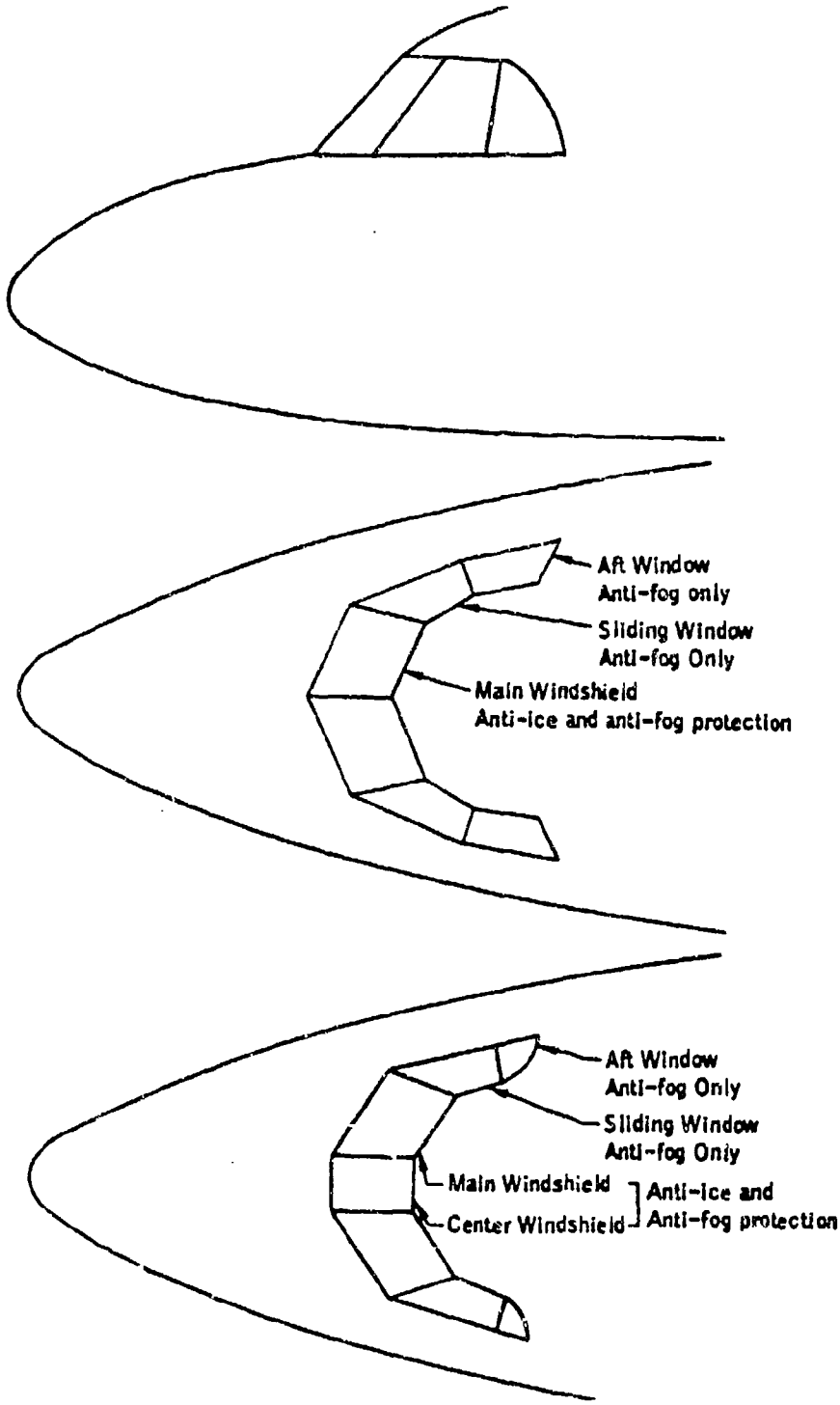

FIGURE 5-29. TYPICAL WINDSHIELD AREAS TO BE PROTECTED FOR TWO WINDSHIELD ARRANGEMENTS ON MULTI-ENGINE TRANSPORT

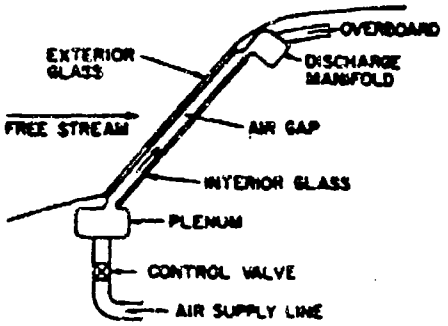

FIGURE 5-30. DOUBLE PANE HOT AIR WINDSHIELD ANTI-ICING SYSTEM

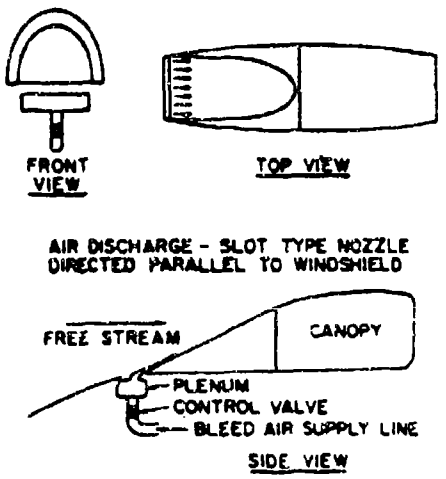

FIGURE 5-31. EXTERNAL AIR BLAST WINDSHIELD ANTI-ICING AND RAIN REMOVAL SYSTEM

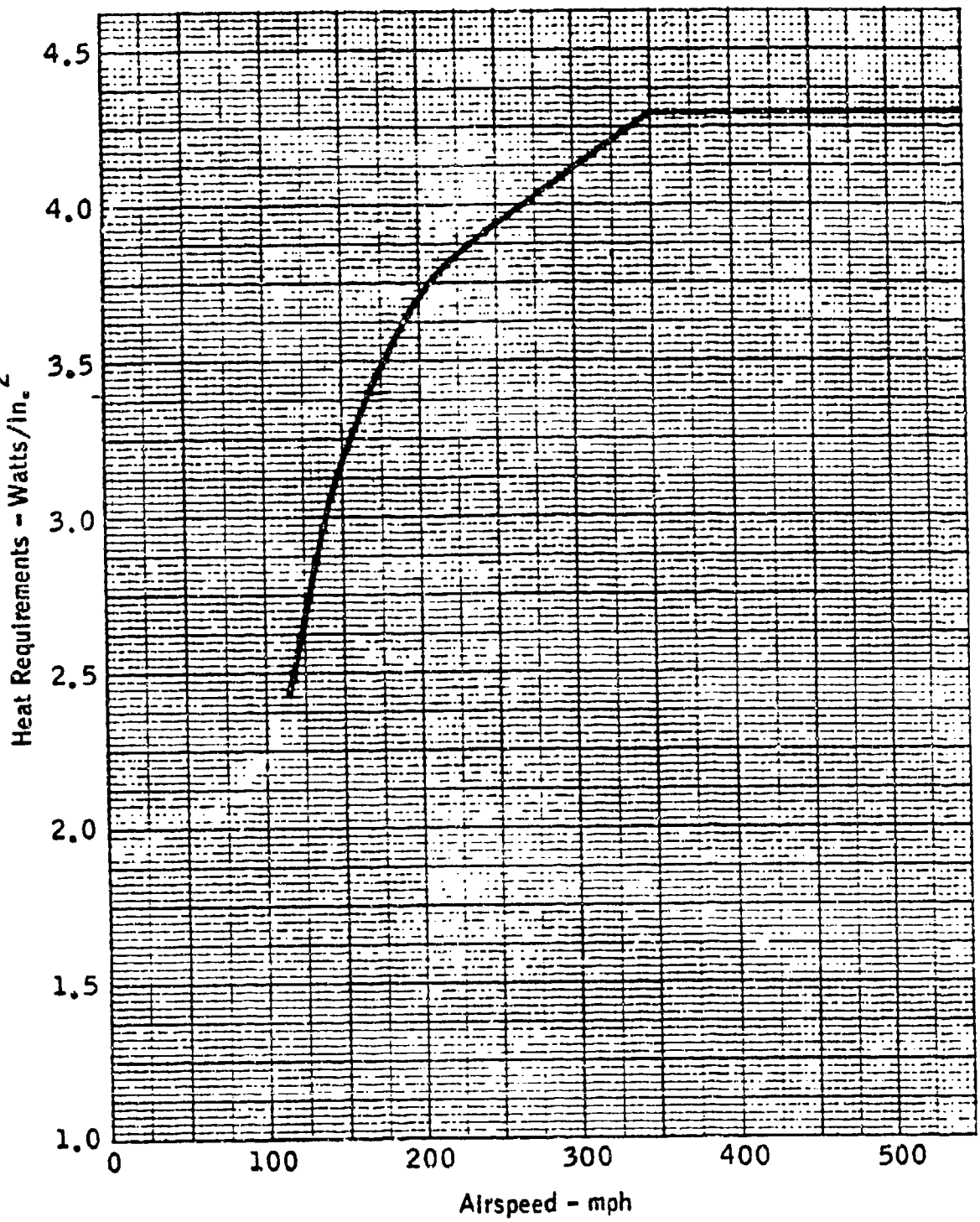

FIGURE 5-32. WINDSHIELD ANTI-ICING HEAT REQUIREMENTS (REF. 5-3)

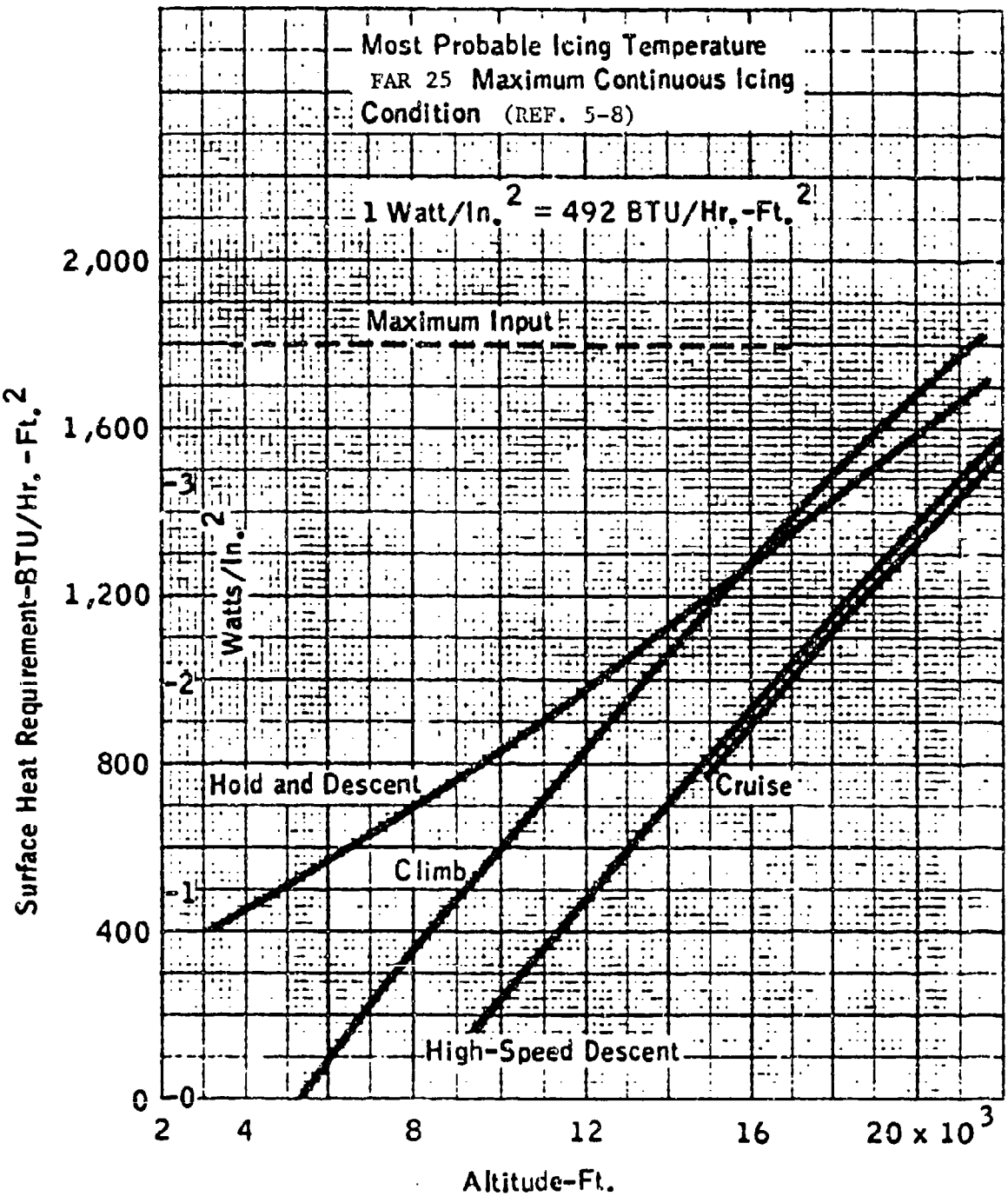

FIGURE 5-33. TYPICAL ANTI-ICING HEAT REQUIREMENTS VS. ALTITUDE FOR CENTER WINDSHIELD PANEL

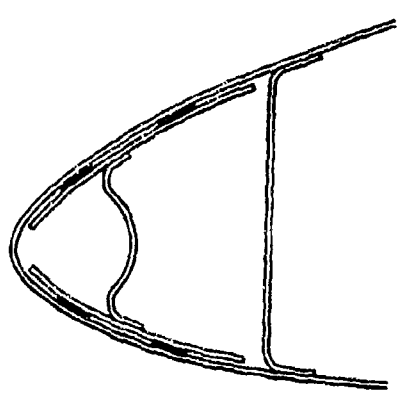

SECTION A - A
TYPICAL DOUBLE SKIN
ARRANGEMENT

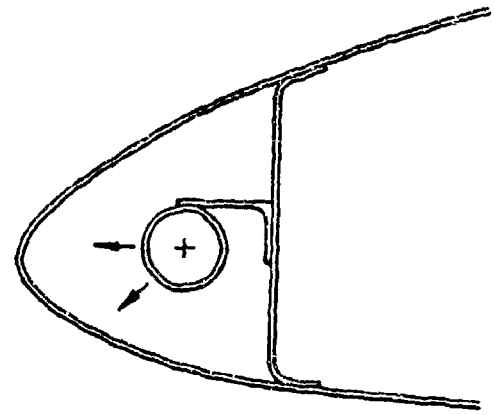

SECTION A - A
TYPICAL SINGLE SKIN
ARRANGEMENT

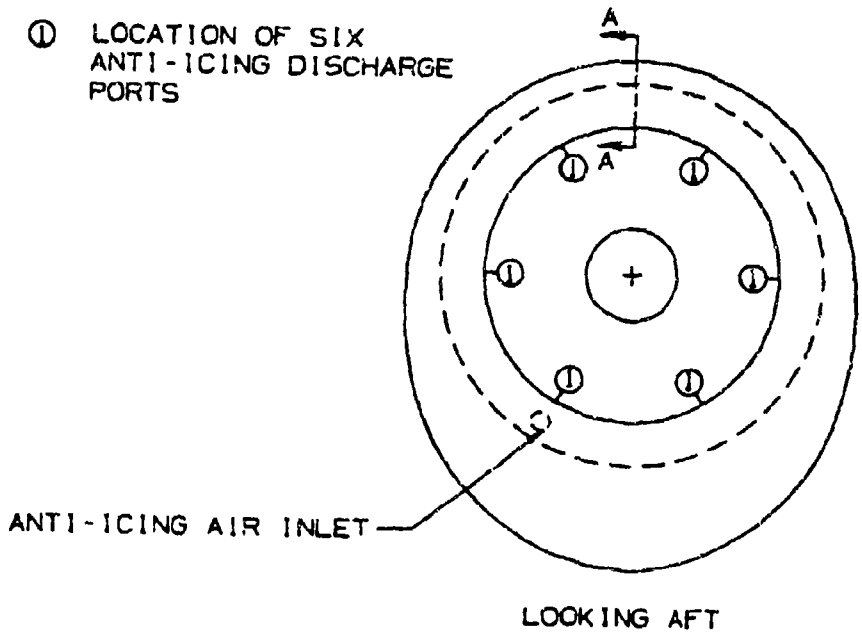

FIGURE 5-34. TYPICAL ENGINE INLET LIP
ANTI-ICING SYSTEM

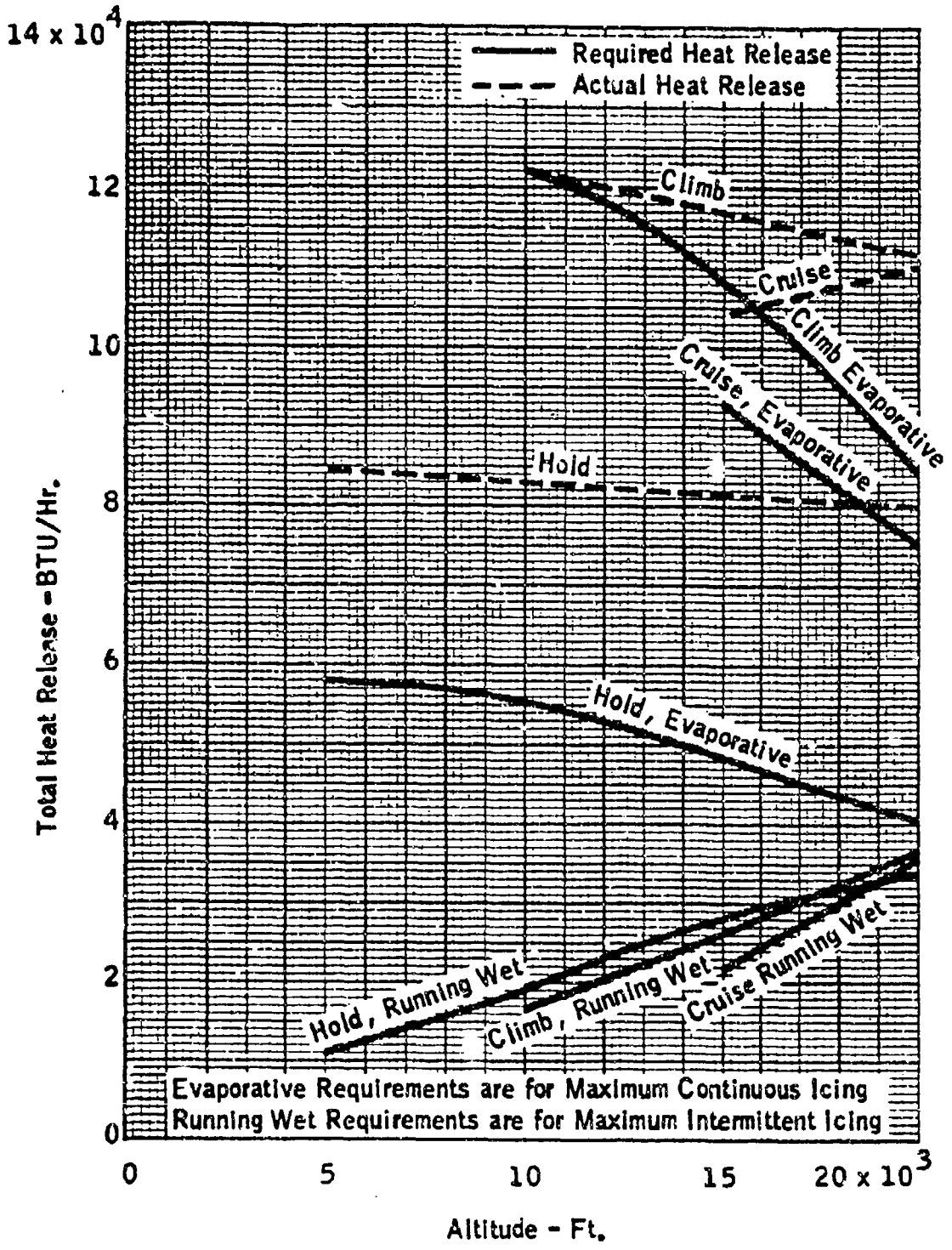

FIGURE 5-35. TYPICAL ENGINE INLET LIP ANTI-ICING HEAT RELEASE VS. ALTITUDE (REF. 5-8)

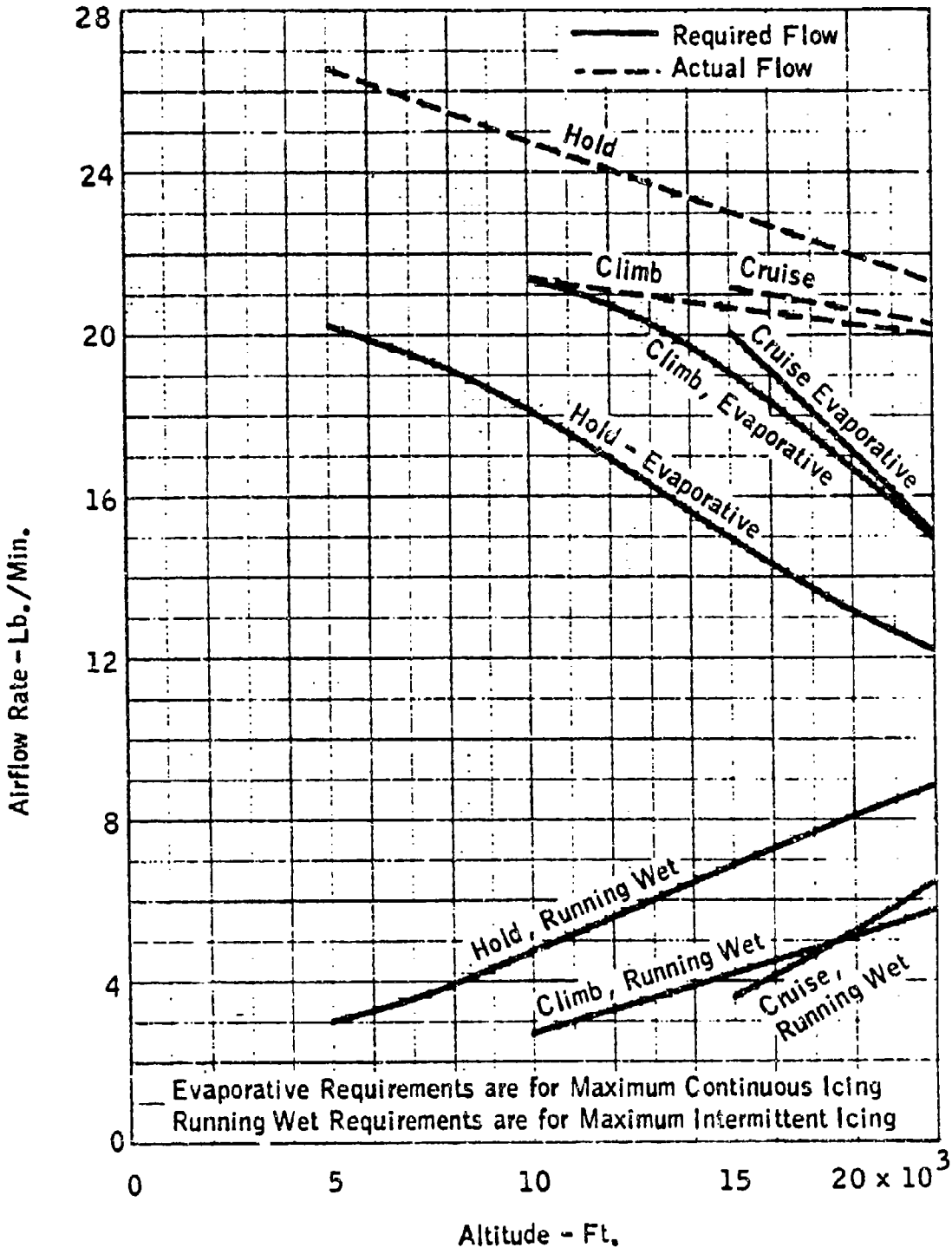

FIGURE 5-36. TYPICAL ENGINE INLET LIP ANTI-ICING AIR FLOW REQUIREMENTS VS. ALTITUDE (REF. 5-8)

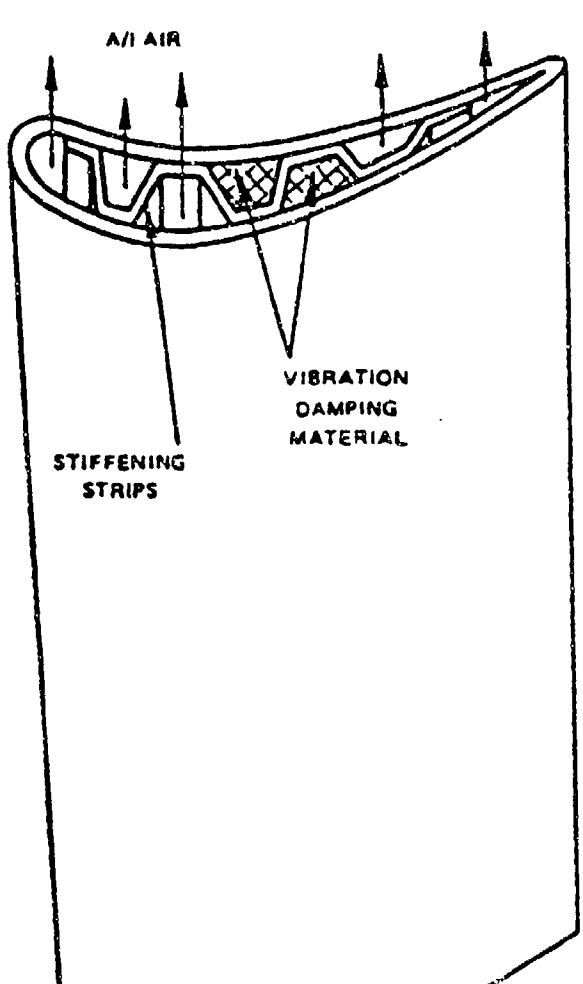

FIGURE 5-? . TYPICAL INLET GUIDE VANE FOR SINGLE-PASS INTERNAL FLOW SCHEME (REF. 5-7)

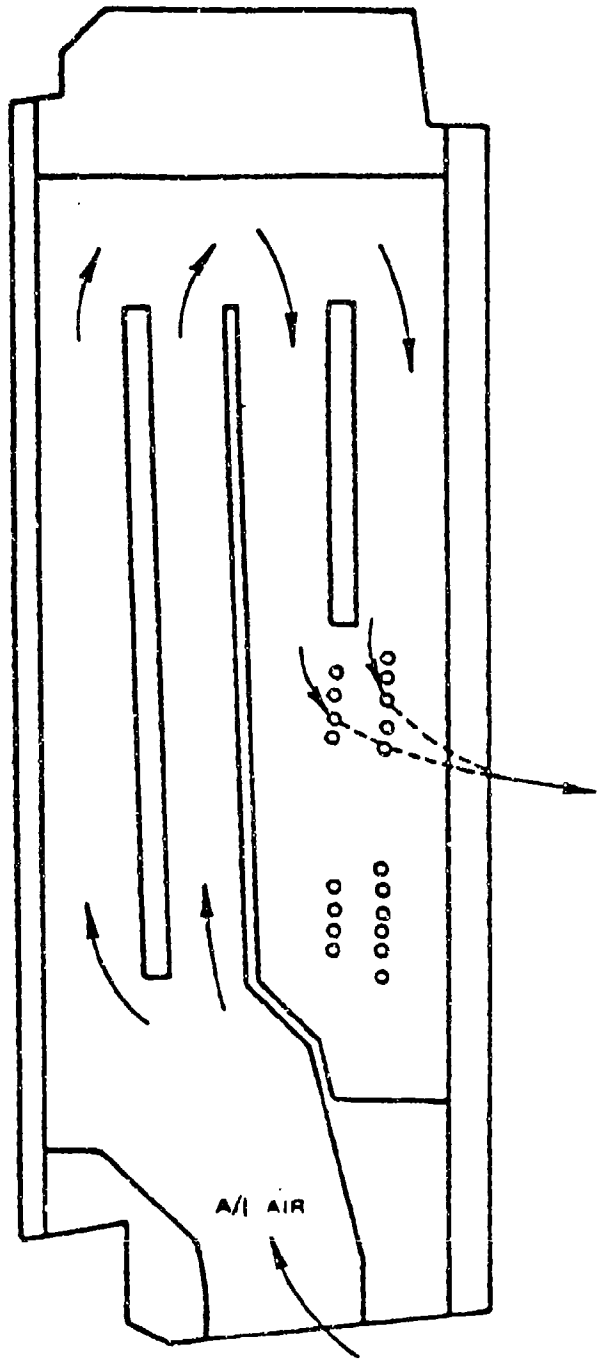

FIGURE 5-38. MULTIPASS A/I INTERNAL FLOW SCHEME FOR A STATOR (REF. 5-7)

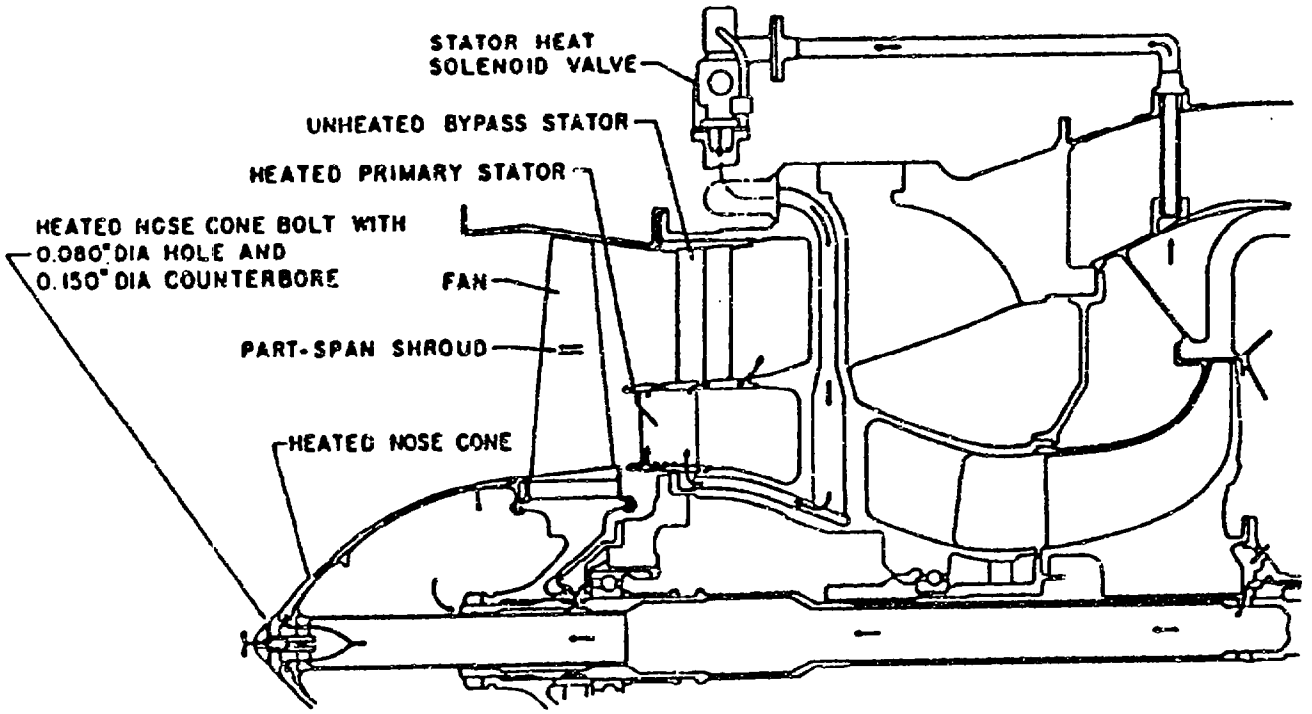

FIGURE 5-39. TYPICAL ROUTING OF ANTI-ICING AIR (Ref. 5-7)

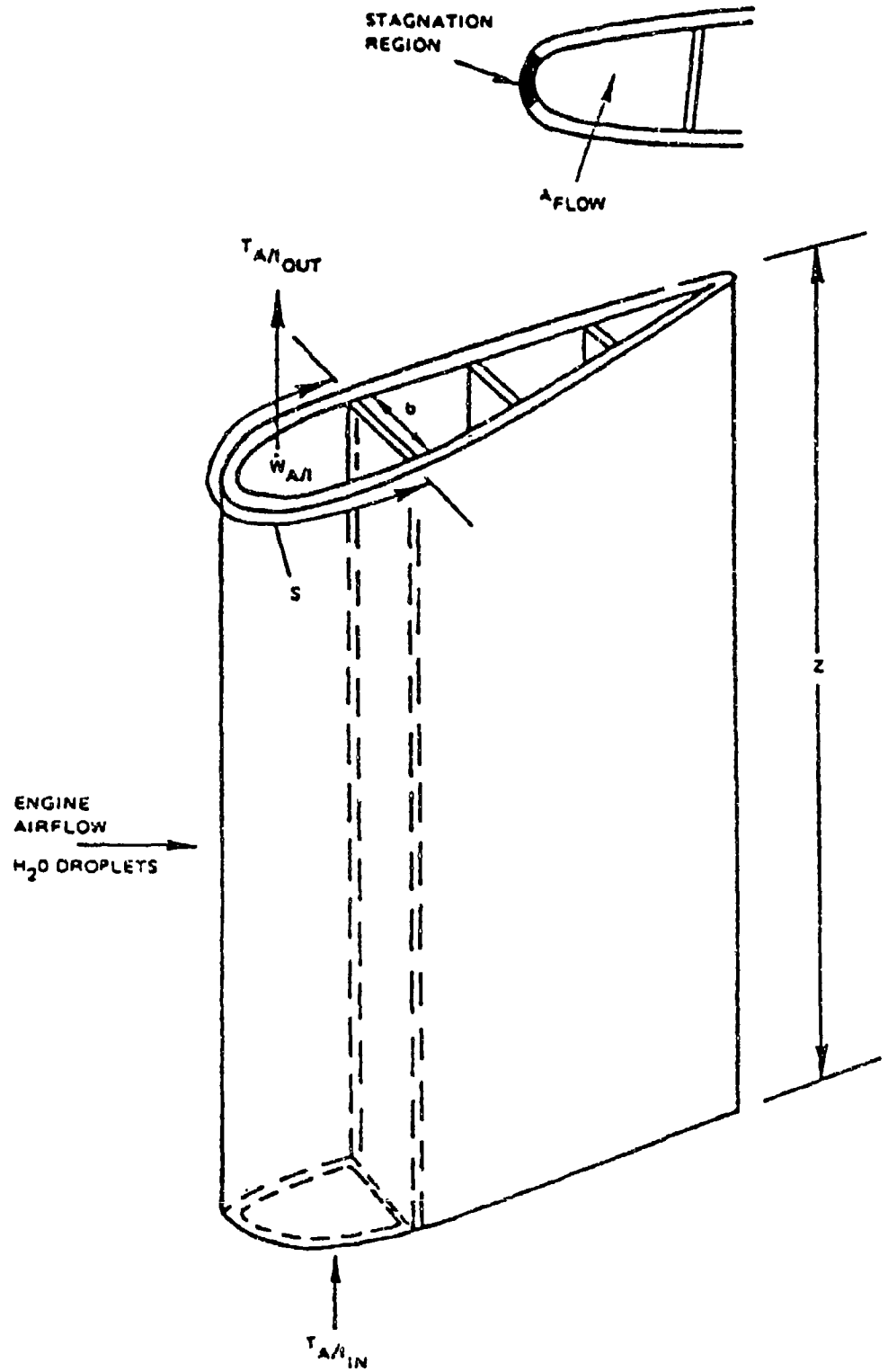

FIGURE 5-40. NOSE SECTION OF AN INLET GUIDE VANE (REF. 5-7)

FLOW REQUIRED & STAGE NO. VS. AIR TEMPERATURE

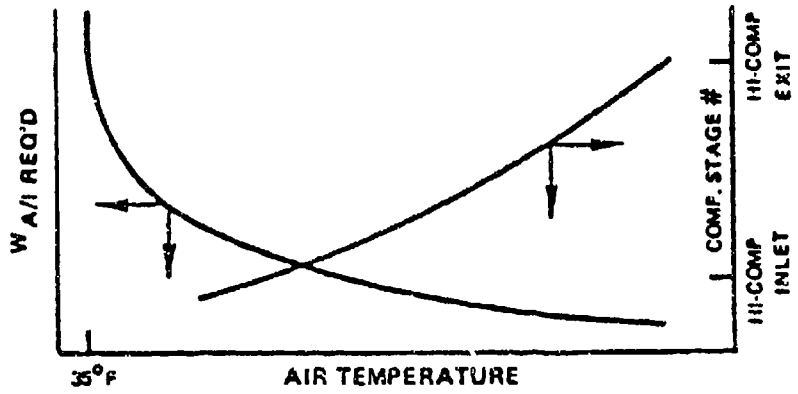

FLOW REQUIRED VERSUS STAGE NO.

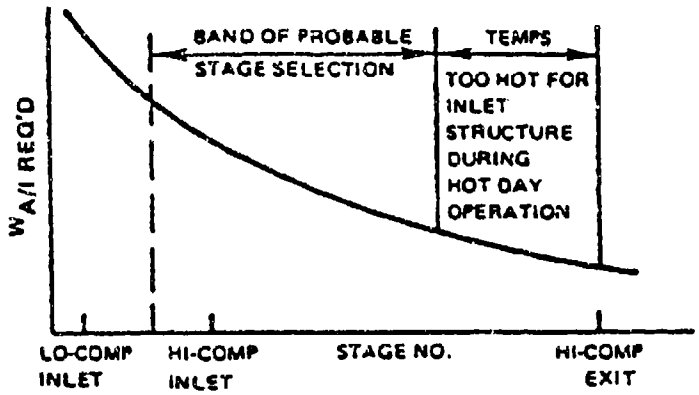

PRESS. AVAIL. & REQ'D VERSUS STAGE NO.

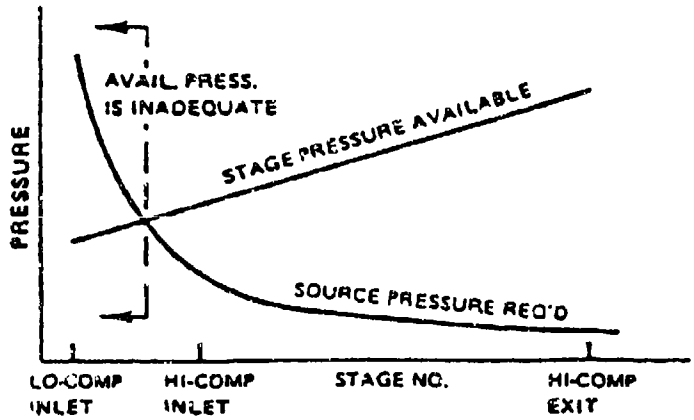

FIGURE 5-41. BLEED STAGE SELECTION LIMITATIONS (REF. 5-7)

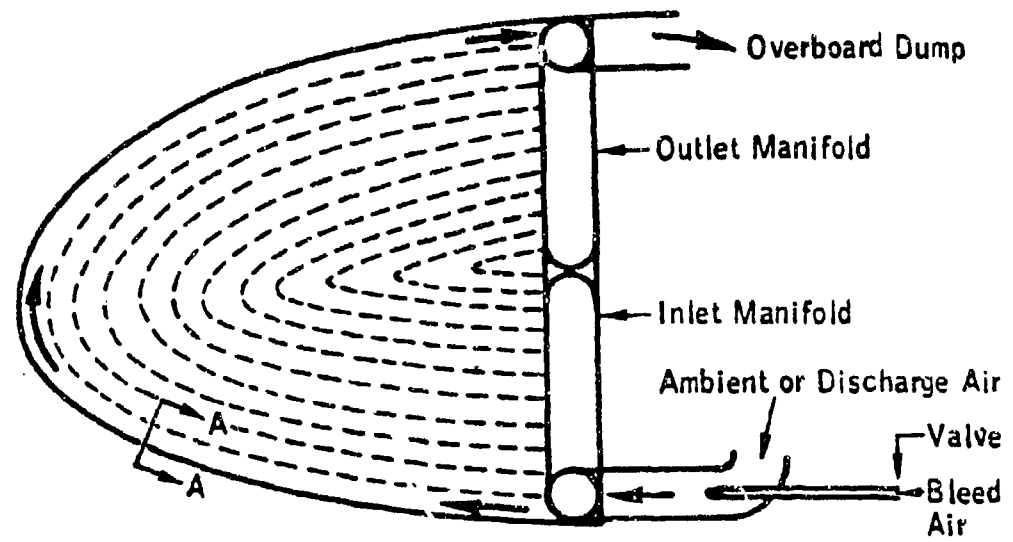

Side View

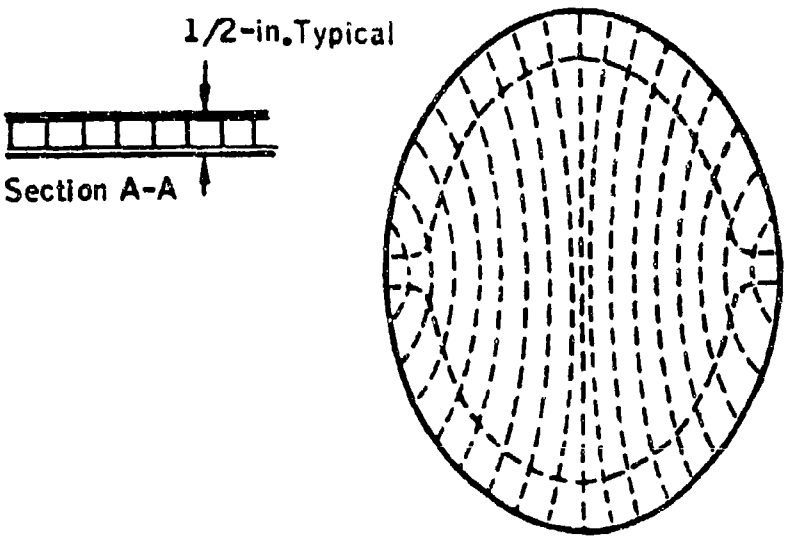

Front View

FIGURE 5-42. TYPICAL HOT-AIR ANTI-ICING SYSTEM FOR NOSE RADOME

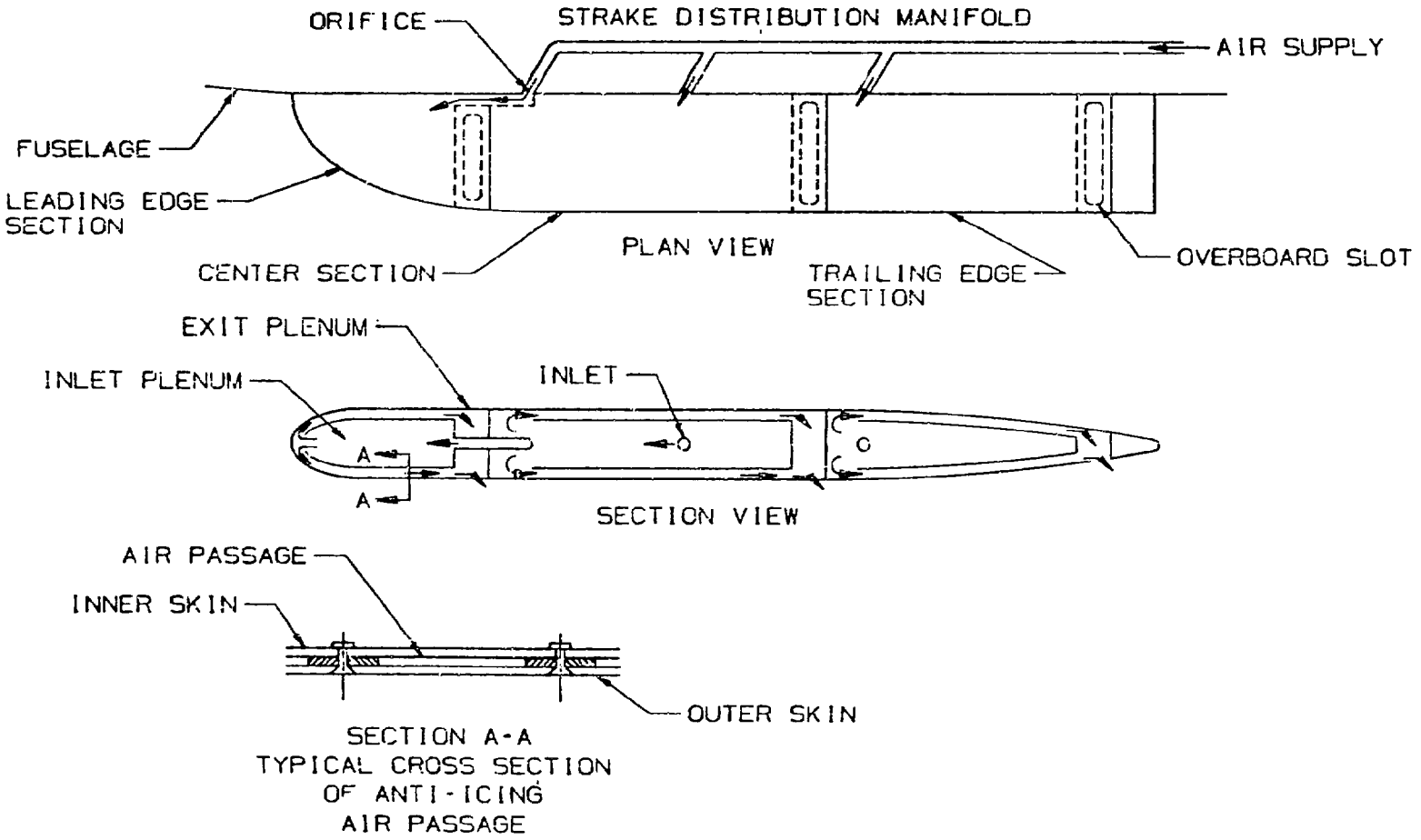

FIGURE 5-43. STRAKE SCHEMATIC FLOW DIAGRAM SYSTEM

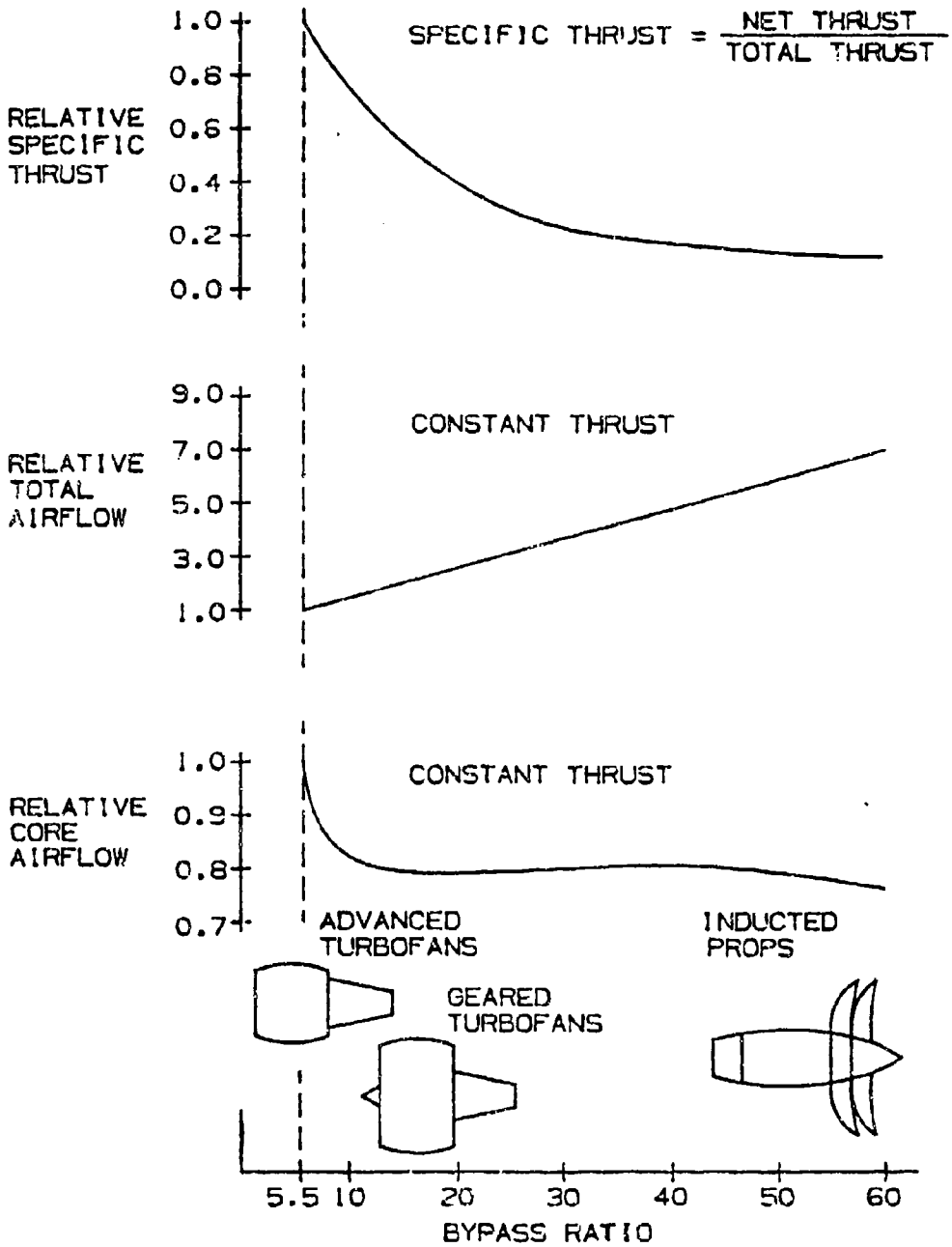

FIGURE 5-44. ENGINE SPECIFIC THRUST AND AIRFLOW VS. BYPASS RATIO (RELATIVE TO A 5.5 BPR ENGINE)

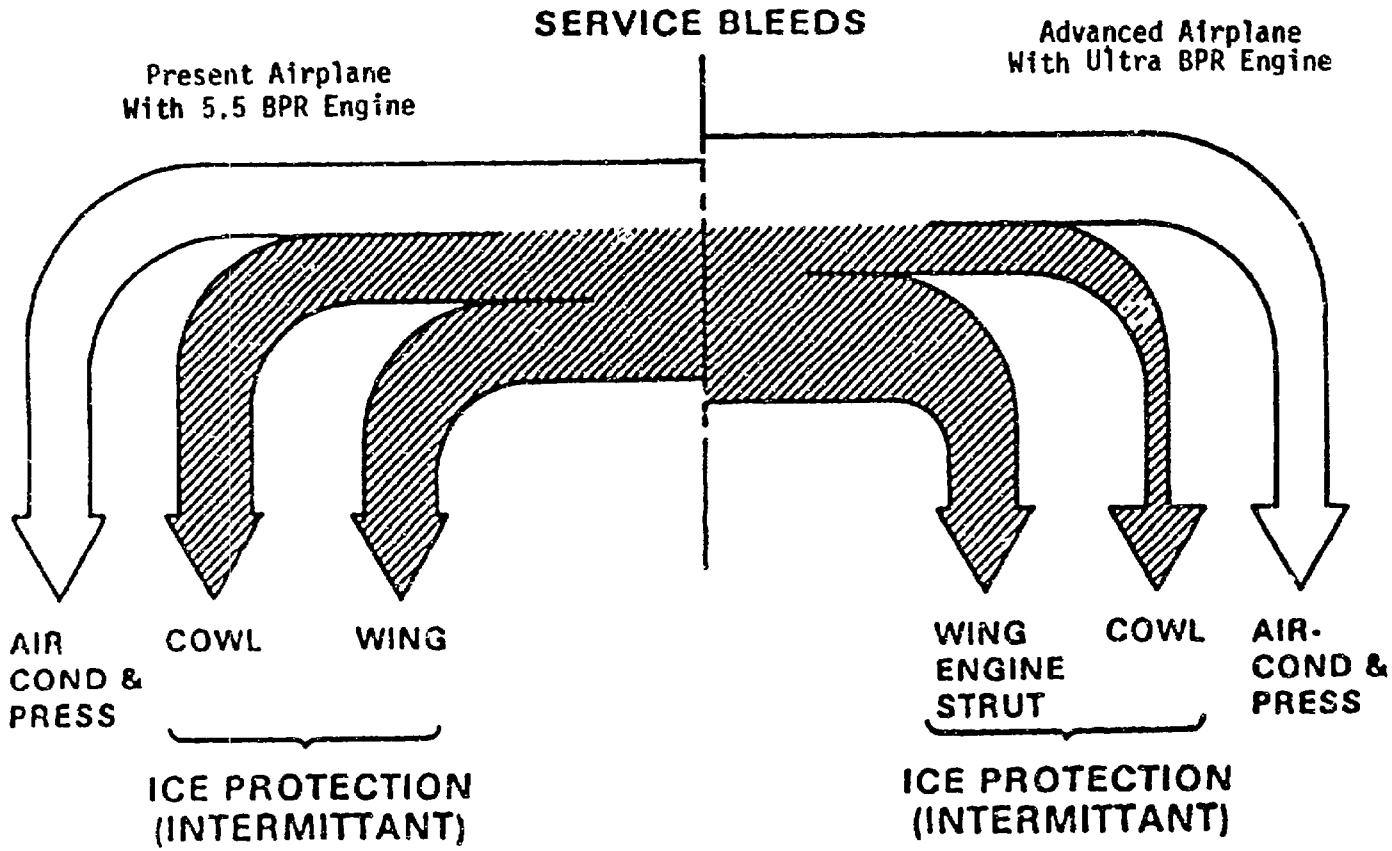

FIGURE 5-45. ALL-BLEED SYSTEM ALLOCATION (REF. 5-9)

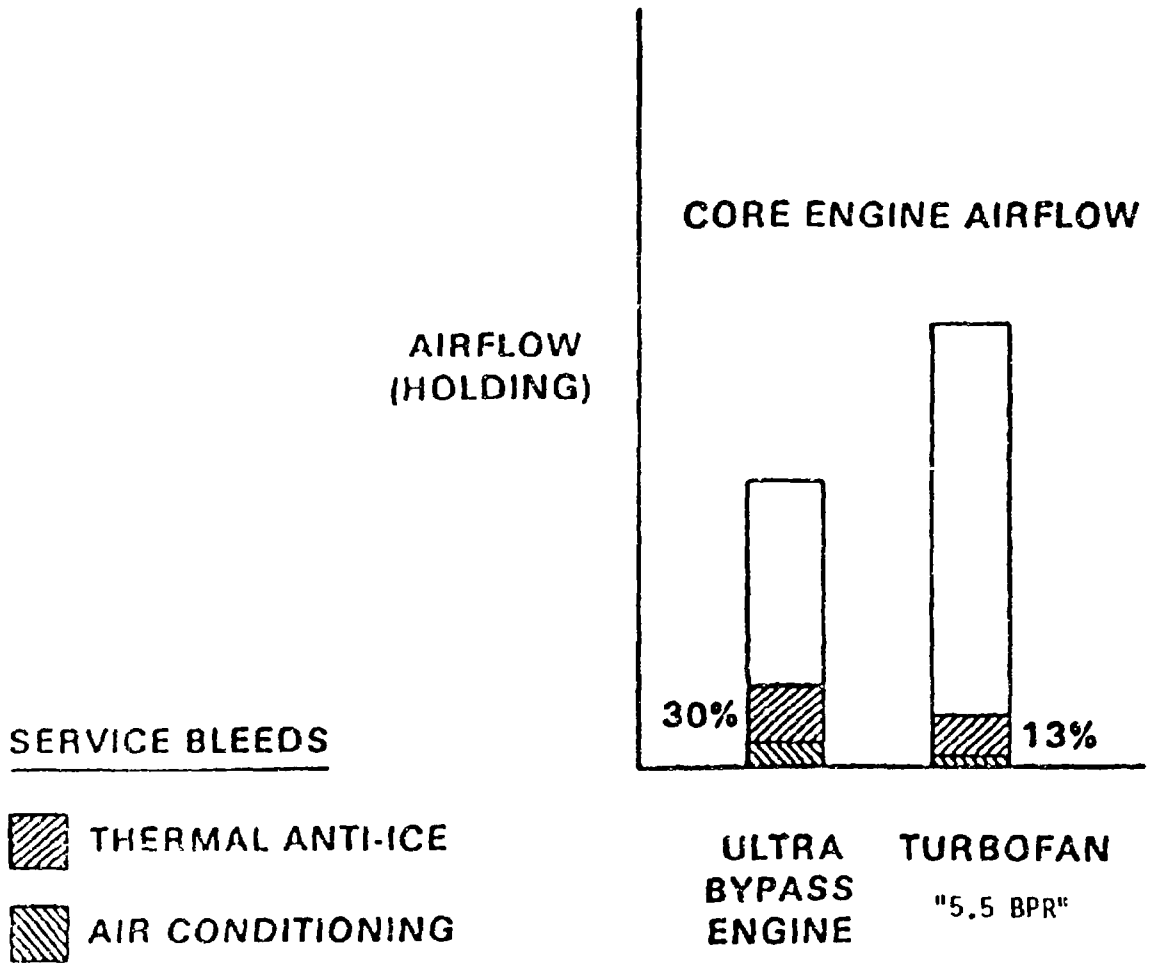

FIGURE 5-46. THE BLEED AIR PROBLEM; 150 PASSENGER AIRPLANE (REF. 5-9)

CHAPTER III
SECTION 6.0
SYSTEM SELECTION

CHAPTER III - ICE PROTECTION METHODS
CONTENTS
SECTION 6.0 SYSTEM SELECTION

	Page
LIST OF TABLES	III 6-iv
LIST OF FIGURES	III 6-v
SYMBOLS AND ABBREVIATIONS	III 6-vi
GLOSSARY	III 6-vii
III.6.1 SELECTION CRITERIA	III 6-1
III.6.2 EFFECTS OF ICE ON UNPROTECTED COMPONENTS	III 6-2
III.6.3 COMPONENT CANDIDATE SYSTEMS	III 6-3
6.3.1 Airfoils and Leading Edge Devices	III 6-3
6.3.1.1 Fixed Leading Edge	III 6-3
6.3.1.2 Leading Edge Slots, Slats, and Krueger Flaps	III 6-6
6.3.2 Control Surface Balance Horns	III 6-7
6.3.3 Windshields	III 6-7
6.3.4 Engine Inlet Lips and Components	III 6-8
6.3.5 Turbofan Components	III 6-9
6.3.5.1 Electrical Systems for Turbofans	III 6-9
6.3.5.2 Hot Air Systems for Turbofans	III 6-9
6.3.6 Propellers, Spinners, and Nose Caps	III 6-10
6.3.7 Helicopter Rotors, Hubs, and Droop Stops	III 6-10
6.3.7.1 System Selection for Rotorcraft	III 6-10
6.3.7.2 Distinctive Rotorcraft Icing Problems	III 6-11
6.3.7.3 Rotors	III 6-11
6.3.8 Flight Sensors	III 6-13
6.3.8.1 Pitot and Static Probes	III 6-13
6.3.8.2 Stall Warning Transducers	III 6-13
6.3.9 Radomes and Antennas	III 6-13
6.3.9.1 Radomes	III 6-13
6.3.9.2 Antennas	III 6-14
6.3.10 Miscellaneous Intakes and Vents	III 6-14
6.3.10.1 Air Scoops	III 6-14
6.3.10.2 Fuel Vents	III 6-14
6.3.11 Drain Masts and Pipes	III 6-14

CONTENTS (CONTINUED)

	Page
III.6.4 WEIGHT, ENERGY, AND POWER COMPARISONS	III 6-15
III.6.5 DISTINCTIVE SMALL AIRPLANE ICING PROBLEMS (FAR PART 23)	III 6-15
III.6.6 DISTINCTIVE TRANSPORT CATEGORY AIRPLANE PROBLEMS (FAR PART 25)	III 6-15
III.6.7 DISTINCTIVE ROTORCRAFT ICING PROBLEMS (FAR PART 27/29)	III 6-16
III.6.8 REFERENCES	III 6-17

LIST OF TABLES

		Page
6-1	Aircraft Ice Protection System Attributes - FAR 23 Small Single Engine Aircraft	III 6-18
6-2	Weight Summary - Wing and Tail Systems - FAR 23 Small Single Engine Aircraft	III 6-19
6-3	Aircraft Ice Protection System Attributes - FAR 23 Small Twin Engine Aircraft	III 6-20
6-4	Weight Summary - Wings and Tail Systems - FAR 23 Small Twin Engine Aircraft	III 6-21
6-5	Aircraft Ice Protection System Attributes - FAR 25 Business Jet Aircraft	III 6-22
6-6	Weight Summary - Wings and Tail Systems - FAR 25 Business Jet Aircraft	III 6-23
6-7	Aircraft Ice Protection System Attributes - FAR 25 Large Transport Category Aircraft	III 6-24
6-8	Weight Summary - Wing and Tail Systems - FAR 25 Large Transport Category Aircraft	III 6-25
6-9	Advantages and Disadvantages of Ice Protection Systems	III 6-26
6-10	Significant Engine Inlet Ice Protection Selection Considerations	III 6-27
6-11	Rotorcraft Main Rotor De-Icing System Attributes	III 6-28
6-12	Weight Summary - Main Rotor De-Icing System	III 6-29
6-13	Weight Summary - Complete Helicopter Ice Protection System Sized for the Helicopter in Figure 6-71	III 6-30

LIST OF FIGURES

		Page
6-1	System Selection Flow Diagram	III 6-31
6-2	Typical Single-Engine Aircraft	III 6-33
6-3	Typical Light Twin-Engine Aircraft	III 6-34
6-4	Typical Twin-Jet Business Aircraft	III 6-35
6-5	Typical Jet Transport	III 6-36
6-6	Typical FAR Part 29 or Military Helicopter	III 6-37

SYMBOLS AND ABBREVIATIONS

Symbol	Description
APU	Auxiliary Power Unit
BTU	British Thermal Unit
°C	Degrees Celsius
cm	Centimeter
EIDI	Electro-Impulse De-Icing
EMI	Electromagnetic Interference
°F	Degrees Fahrenheit
FPD	Freezing point depressant
ft	Feet or foot
gpm	Gallons per minute
HP	Horsepower
I/P	Ice Protection
kg	Kilogram
kN	Kilonewton
kw	Kilowatt
lbf	Pounds force
lbm	Pounds mass
lbs	Pounds
m	Meter
mm	Millimeter
psig	Pounds per square inch gauge (pressure)
°R	Degrees Rankine
scfm	Specific cubic feet per minute
VCK	Variable Camber Krueger Flap
w	Watts

GLOSSARY

bleed air - A relatively small amount of air diverted to an auxiliary use.

liquid water content (LWC) - The total mass of water contained in all the liquid cloud droplets within a unit volume of cloud. Units of LWC are usually grams of water per cubic meter of air (g/m^3).

median volumetric diameter (MVD) - The droplet diameter which divides the total water volume present in the droplet distribution in half; i.e., half the water volume will be in larger drops and half the volume in smaller drops. The value is obtained by actual drop size measurements.

micron (μm) - One millionth of a meter.

stagnation point - The point on a surface where the local free stream velocity is zero. It is also the point of maximum collection efficiency.

III.6.0 SYSTEM SELECTION

III.6.1 SELECTION CRITERIA

The available ice protection methods for various aircraft surfaces and components have been discussed in previous sections of this chapter. It should be noted that there is no one best system for use on all types of aircraft and each aircraft represents an independent design problem for ice protection. The following considerations should be made in the selection of the best ice protection system for a particular aircraft:

a. What is needed for flight in known icing conditions? For aircraft operating in the temperate zone, service experience indicates that holding in icing conditions for as long as 45 minutes is an expected operating condition. Icing probabilities and characteristics are discussed in Section I.1.0 and certification requirements are discussed in Chapters V and VI. Generally, ice protection systems should be capable of ice removal or prevention at altitudes from sea level to 22,000 feet (6700 m) with temperatures of 32°F (0°C) to -22°F (-30°C) and with LWC of 0 to 2.8 g/m^3.

b. What is the effect of icing on the aircraft's performance? Analysis and flight tests of the aircraft and components should be performed to determine ice impingement limits, worst case ice shapes, and the effect of this on aircraft performance and handling characteristics. For example, some aircraft are sensitive to empennage icing and others can tolerate unprotected empennage surfaces. Section I.2.3 discusses aerodynamic penalties of ice.

c. What power is available for ice protection systems? Compressor bleed air may be available from gas turbine engines. Hot air from exhaust gas heat exchangers may be used in piston engines. Hot exhaust gas alone is rarely used due to its corrosive nature. A separate combustion heater transferring its heat to air is another alternative. High temperature air could be provided by an Auxiliary Power Unit (APU) compressor. Surplus electrical power may be available or could be provided by a larger capacity generator or an auxiliary generator. Some light aircraft have used electro-thermal and fluid ice protection systems with good results.

d. In view of the power available and the components needing ice protection, which of the ice protection methods discussed in this chapter are candidates for the particular aircraft in question? Examination of the trade-offs between the benefits and costs of the candidate systems suitable for each aircraft component must be performed. Costs include system weight, power consumption, maintenance, and required system testing, in addition to initial and development costs.

e. Will two or more types of ice protection system be needed? Often propellers and windscreens are de-iced or anti-iced by electric resistance heaters while aerodynamic surfaces are pneumatic boot or hot gas de-iced. Many other combinations occur. This may increase inspection and maintenance complexity.

f. Other considerations which sometimes apply include:

1. Run-back icing concerns
2. Aerodynamic smoothness requirements
3. Maintenance requirements
4. Installation costs and time, if the system is being retrofitted
5. Confidence in the selected system based on previous experience in similar applications
6. Electromagnetic interference concerns
7. Environmental impact concerns
8. Certification difficulties anticipated
9. Redundancy requirements

Figure 6-1 is a flow diagram that can be used in the system selection process. Following this procedure should result in the optimum system for each component to be protected with the only constraint being adequate power available. After the totally integrated system is complete, factors such as cost, weight, reliability, and environmental impact should he considered or reconsidered. It is quite possible that any one of these may force a redesign of some of the component systems.

III.6.2 EFFECTS OF ICE ON UNPROTECTED COMPONENTS

Some components will be judged as experiencing such a small penalty due to icing that ice protection is not justified. Common examples are the vertical stabilizer, wing struts, wheel covers on small airplanes, and wing tip tanks. Some of these are very difficult to de-ice due to their placement or shape, but the decision to leave them unprotected should be made taking into account aerodynamic penalties and changes in handling qualities. The effects may be subtle, e.g., a wing strut was found to create tail buffet when iced due to its increased wake turbulence and so de-icing was necessary even though its drag was tolerable. Section I.2.3 discusses this subject more fully.

The effect of ice accretion can be estimated by calculation (Section IV.2.0), or by experimental testing of simulated ice shapes on the component (Section IV.1.0).

III.6.3 COMPONENT CANDIDATE SYSTEMS

6.3.1 Airfoils and Leading Edge Devices

The chordwise extent of the ice formation on an airfoil is basically a function of the ambient conditions and the airspeed. Some characteristics of the airfoil that will also affect the icing impingement limits and chordwise coverage area are:

a. Type and size of airfoil
b. Leading edge radius
c. Thickness ratio
d. Leading edge sweep angle
e. Angle of attack
f. Type and deflection of leading edge device

When selecting an icing protection system for an airfoil surface, all of the above items should be considered. Aerodynamic smoothness of the ice protection system in normal dry air flight conditions may be another important factor.

Some airfoils that have large leading edge radii may not shed ice well under all flight and ambient conditions.

The hot gas thermal systems are used on the wing of most transport category aircraft. The pneumatic boot de-ice system is used on the empennage of transport aircraft and the majority of light aircraft for wing and empennage surface ice protection. Some light aircraft have used the electro-thermal (on empennage) and the fluid injection systems with good results. Current rotorcraft use electro-thermal systems. Electro-impulse de-icing is too new for application experience. For compliance requirements, see Chapter V.

6.3.1.1 Fixed Leading Edge

Light Aircraft (FAR 23)

The dominant factors in the selection of an ice protection system for single engine aircraft (figure 6-2) are probably cost, weight, and power available. Ice protection is usually not provided for these aircraft. When it is, the system requirements analysis should be made in the same manner as for light twin aircraft (figure 6-3).

A summary of leading edge ice protection system attributes, weight, and power requirements for a typical single-engine aircraft are presented in tables 6-1 and 6-2. Values are shown for different types of systems considered to be the most desirable for this type of aircraft.

A summary of leading edge ice protection system attributes, weight, and power requirements for a typical light twin-engine aircraft (figure 6-3) are presented in tables 6-3 and 6-4. Values are shown for the types of systems considered to be the most desirable for this type of aircraft.

Transport Category Aircraft (FAR 25)

In the selection of ice protection for the wing leading edge of a typical light jet (figure 6-4), the requirements are found in the same manner as for the reciprocating twin-engine light plane. A summary of system attributes, weights, and power extraction for several different systems is presented in tables 6-5 and 6-6.

The most desirable systems for the reciprocating twin will not necessarily be the most desirable for the jet. More consideration may be given to hot air anti-icing systems for the wing and tail of the jet because of the availability of engine bleed air. Also, the jet aircraft may have more power available for electrical protection systems. Requirements must always be determined for ice protection of turbine engine inlets. If aft-mounted engines are used, special consideration must be given to the potential problem of ice shedding from sections of the inboard wing.

The selection process for a large multi-engine transport (figure 6-5) is much different than for the business jet because it will, in general, have sufficient power available so that several methods of ice protection become feasible. A summary of system attributes, weights, and power requirements for a typical large jet transport aircraft is shown in tables 6-7 and 6-8.

The dominant factor that affects the selection of an ice protection system for jet aircraft is probably the bleed air supply provided by the engines. Depending on the amount of bleed air available and that required for ice protection, the system selection can be divided into two categories.

a. Sufficient Supply of Bleed Air for Anti-Icing

For high performance lifting surfaces used on commercial transport aircraft, priority may be given to the hot-air anti-icing system which has been proven over the years to be a reliable and effective system. However, the projected shift to unducted fan engines and ultra-high bypass engines forces a trend toward de-icing rather than anti-icing. These types of engines, much like the turboprop engines, may not have enough compressor bleed air for anti-icing (see Section III.5.8.2).

b. Bleed Air Not Available or Insufficient for Anti-Icing

A detailed trade-off study must be conducted for the following non-bleed or low bleed alternatives:

- pneumatic boot de-icing
- fluid anti-icing or de-icing
- electro-impulse de-icing
- electro-thermal anti- or de-icing
- hot-air de-icing (bleed air)
- hot-air anti-icing or de-icing (combustion heater)

The advantages and disadvantages of each system are shown in table 6-9. Major considerations recommended for the trade-off study are provided as follows:

a. Pneumatic boot de-icing
   - aero effects due to boots (both inflated and deflated position); can be evaluated using tube profile data provided by boot manufacturer
   - aero effects due to required ice buildup between de-icing cycles
   - aero effects due to auto-inflation (failed suction system)
   - service life of boot (may be function of hangaring practice)
   - ice ingestion into tail-mounted engines and/or propellers; work together with engine and propeller manufacturers · weight of the system
   - owner's acceptance for maintenance procedures and external appearance
   - maintenance costs
   - non-recurring costs

b. Fluid anti-ice or de-icing
   - weight of anti-icing fluid required based on stagnation point travel, specific fluid requirement to provide anti-icing per unit area at design icing condition, and the amount of ice protection required.
   - if fluid requirement for anti-icing is too high, how about de-icing or cyclic de-icing?
   - aero effects due to ice buildup between cycles (de-icing mode)
   - ice ingestion by tail-mounted engines and/or propellers (de-icing mode)
   - fluid ingestion by tail-mounted engines
   - weight of the system
   - fluid costs and availability
   - maintenance costs
   - non-recurring costs
   - owner's acceptance (washing of aircraft usually needed after use)
   - benefits resulting from aerodynamically cleaner surfaces (less insects, dirt; protection of trailing edge)

c. Electro-impulse de-icing
   - aero effects due to ice buildup between cycles
   - aero effects due to residual ice
   - ice ingestion by tail-mounted engines and/or propellers
   - fatigue effects on structural components
   - weight of the system
   - weight addition due to extra electric generating capacity (if required)
   - electro-magnetic interference (if any)
   - noise level during coil discharge
   - maintenance costs

- maintenance costs
- non-recurring costs

d. Electro-thermal de-icing or anti-icing
- aero effects due to ice buildup between cycles
- ice ingestion by tail-mounted engines and/or propellers
- additional electrical generating capacity
- weight of the system
- weight addition due to extra electric generating capacity (if required)
- fuel cost for system operation
- maintenance costs
- non-recurring costs

e. Hot-air anti-icing or de-icing (bleed air)
- weight of the system
- effects on engine performance due to bleed air extraction
- fuel cost and weight penalty for system operation
- aero effects due to ice buildup between cycles (de-icing mode)
- ice ingestion by tail-mounted engines and/or propellers (de-icing mode)
- maintenance costs
- non-recurring costs

f. Hot-gas anti-icing or de-icing (combustion heaters)
- air compression ratio to determine size and weight of compressor and motor
- weight of the system
- weight addition due to extra electric generating capacity (for electric-driven motor)
- fuel cost and weight penalty for system operation
- aero effects due to ice buildup between cycles (de-icing mode)
- ice ingestion into tail-mounted engines and/or propellers (de-icing mode)
- maintenance costs
- non-recurring costs

6.3.1.2 Leading Edge Slots, Slats, and Krueger Flaps

The discussion of fixed leading edge system selection (Section III.6.3.1.1) is applicable to slot and slat configurations with the exception that slats require a means of transmitting the heated air, freezing point depressant (FPD), or electrical power from the fixed wing to the moveable slat. A telescoping duct that is capable of rotating and extending has been used for hot air systems. Swivel fitting and flexible hoses have been used for liquid FPD transmission. In all cases, the means of transmission presents an added degree of complexity and potential failure that must be considered during the trade-off studies used as a basis of system selection.

Since the Krueger flap retracts into the lower airfoil section, many applications have not required ice protection. When ice protection is required, any of the concepts discussed in Section III.6.3.1.1 may be considered. In addition, a variable camber Krueger (VCK) has been used that provides automatic de-icing. In this design, the linkage that extends the VCK also alters the camber to increase lift. During retraction after ice has accumulated, flexing the VCK debonds and shatters the ice cap allowing aerodynamic forces to remove the ice. This concept has the normal penalties of de-icing systems as discussed in Section III.6.3.1.1. In addition, the flexing may not debond the leading edge ice sufficiently to allow removal by aerodynamic forces.

6.3.2 Control Surface Balance Horns

Control surfaces having leading edges which can collect ice must be protected. Often the leading edge is in the shadow of the fixed surface and does not collect ice; e.g., ailerons and split flaps. But if the leading edge rotates out of the wing plane, it will leave the protection of the upstream airfoil and is in danger of collecting ice in such quantity as to jam the control surface in the extended position. Examples are rudder or elevator balance horns and Fowler flaps. Decreasing the gap between the fixed and moving surface helps to decrease the danger, but active ice protection for the leading edge may be required.

Ice protection system candidates for this application are limited due to the small size and hinge-type supports. An electrical method is probably best, either electro-thermal or electro-impulse.

Icing tunnel or flight tests may be necessary to determine the extent of the problem and decide whether upstream shielding or de-icing is needed.

6.3.3 Windshields

Aircraft with ice protection commonly use electrically heated laminated windshields. Typically, these systems consist of vacuum deposited metallic coatings applied to a glass surface equipped with contacts and temperature sensing devices. The coated glass plate is then laminated to other plates of glass and plastic depending on the specific windshield design (references 61 and 6-2).

Another electrical system design uses very fine wires laminated in the plates of glass and plastic. Electrical power is supplied to the wires through two bus bars at the ends of the windshield.

Both of these systems require a controller to regulate the power applied to the heating element to ensure adequate anti-icing performance and to prevent overheating of the windshield. These systems may also provide defogging of the windshield if designed so the internal windshield surface temperature is above the cockpit air dew point.

A fluid de-icing system has been used on some aircraft for windshield protection. This system uses a freezing point depressant, such as an ethylene glycol/water mixture, which is sprayed on the windshield. This produces a slush which is then blown off the windshield by aerodynamic forces.

The principal disadvantage is the residue left by the fluid and the quantity of fluid required for adequate protection.

On aircraft powered by turbine engines, with an abundant supply of bleed air, an external hot air windshield anti-ice system may be considered. This system may also be utilized for rain removal. A major design problem is maintaining the correct air flow and temperature requirements for icing without overheating the windshield. The air flow and temperature requirements for anti-icing may be less than for rain removal.

Although hot air anti-iced windshields have been used in the past, all current commercial transport aircraft use electrically heated anti-icing systems. The selection of detailed design features of each windshield is influenced by the unique features of the particular aircraft and must consider the integrated design and requirements of the entire windshield. Some of the paramount considerations in addition to normal structural and anti-icing concerns are: hail impact, bird strike, pressurization, environmental extremes including transient effects, rain removal, fogging, visibility, materials properties, lightning, static electrical charge, electrical system design, plus numerous considerations based on in-service experience. Obviously, the design of a windshield must be a closely coordinated activity of a team including structural, electrical, and environmental engineering; specialists in materials, lightning strikes, and manufacturing processes; and the specific vendor(s).

Care must be exercised in the design of the maximum heating capabilities of any windshield anti-icing (de-icing) system. Excessive temperature applied to the windshield could cause fogging of the plastic laminates, crazing, delamination and/or distorted visibility.

6.3.4 Engine Inlet Lips and Components

Icing protection for engine inlets can be hot air or electrical. On turbine engine aircraft, the inlets are usually heated with bleed air. They are frequently designed to be evaporative under continuous maximum icing conditions and running wet under intermittent maximum conditions. Electro-thermal boots may be used if adequate electrical power is available.

Extra precautions should be taken to prevent engine damage, by ice shedding into the inlet or by possible runback and refreeze that could be shed into the engine. Aerodynamic surfaces ahead of the engine inlet should be considered as extensions of the engine inlet lips and ice protection should be provided accordingly.

The concept generally selected for turbojet inlet ice protection has been hot air anti-icing. The main considerations in making this decision have been availability of bleed air, high-reliability of the installation, and the excellent anti-icing performance of bleed air. Recently, due to the high cost of fuel and the limited availability of excess bleed air from the newer high-bypass ratio engines, more consideration is being given to electro-impulse de-icing and fluid anti-icing. Electro-thermal ice protection is feasible for the smallest turboprop inlets, but is generally impractical on turbofan engine inlet lips due to the high power consumption requirements.

Both de-icing and anti-icing systems may be considered for engine inlets. The primary concern regarding ice buildup for a de-icing system is the engine limitation on ice ingestion. The effect of ice buildup on inlet flow aerodynamics is generally less critical than on wings except in the inlet throat region.

The selection of the ice protection system for an engine inlet should be based on a cost-of-ownership analysis and weighted by factors such as development risk and the general preference for anti-icing as opposed to de-icing. Some of the factors to be considered in any trade-off study are summarized in table 6-10.

For a more complete treatment of ice protection for engine components, the reader is directed to reference 6-3.

6.3.5 Turbofan Components

The design engineer who is faced with configuring an engine anti-icing system must be aware of the various types of systems from which to choose, their effectiveness, relative complexity and reliability, and other practical limitations. Typical systems for consideration for turbofan engines are electrical and compressor hot air bleed. The design engineer should also be aware of hot scavenge oil systems for stators which provide anti-icing protection in some turboshaft engines, as described in reference 6-4.

6.3.5.1 Electrical Systems for Turbofans

A typical electrical anti-icing system which embeds resistance heaters within the component to be protected obtains its energy from the airframe supplied generator. Such a system would not be an integral part of the powerplant and sizing of the generator would be affected by the engine anti-icing requirements. Electrical heating of rotating components, such as a spinner, would require the incorporation of a slip ring arrangement which would probably present a reliability problem. A particular merit of an electrical system would be the ability to embed the heat source close to the leading edge of a very thin stator where routing of hot air to achieve sufficient anti-icing effectiveness would be difficult. All aspects considered, it appears that electrical anti-icing systems for turbine engines are not generally accepted by the industry.

6.3.5.2 Hot Air Systems for Turbofans

Thermal systems may vary in the level of protection they provide, ranging from complete evaporation of all water that impinges, to allowing the body surface to run wet (with water runback) at a preselected temperature above freezing. Furthermore, a periodic de-icing system is also a feasible alternative in some cases. In general, a system that achieves a high degree of evaporation on engine components is also one that requires an uneconomically high heat input. Therefore, the accepted design philosophy is to provide a running wet surface in icing conditions. The designer should also investigate closely the hot air flow requirements for the anti-icing system, which could be a substantial

amount of the total engine air flow, with an adverse effect on engine performance. A hot air anti-icing system is the major type of system used on large transport aircraft engines of today for protecting inlet guide vanes and nose cones. Typical hot air engine anti-icing systems are described in Section III.5.2.3.

6.3.6 Propellers, Spinners, and Nose Caps

The most popular current propeller anti-icing system used today is an electro-thermal boot which is bonded to the propeller blades. The heating element usually consists of a stainless steel ribbon embedded in the boot. This heating element is designed to provide more heat at the root of the propeller blade, where the ice buildup is the heaviest and progressively less heat outboard, where centrifugal force reduces buildup problems.

Total boot coverage is approximately 15% of the chord on the suction surface and approximately 30% of the pressure surface. The power to the boots is supplied through slip rings at the propeller hub. Spanwise extent of the heated surface is usually about 30% of blade length.

The propeller thermal anti-icing requirements will vary depending upon propeller diameter, rotational speed, and aircraft forward velocity.

Another propeller anti-icing system is the fluid system, which uses an ethylene glycol/water mixture pumped to the propeller hub and dispersed to the blades through slinger rings. The system is limited by the quantity of the fluid.

De-icing by electro-thermal boots is also used, with the electric power sequenced from one blade segment to the other. Cyclic heating must be sequenced so as to avoid asymmetric shedding. For an even number of blades, opposing blades are heated simultaneously moving from large radius to small radius positions. For an odd number of blades, all blades must be deiced at the same radial sections simultaneously. Outer positions are deiced first to avoid acting as a dam for the debonded inner ice which is being pushed outward by centrifugal forces.

6.3.7 Helicopter Rotors, Hubs, and Droop Stops

6.3.7.1 System Selection for Rotorcraft

The selection of appropriate ice protection systems for rotorcraft requires a knowledge of mission requirements and constraints. Preceding sections have presented the attributes of pneumatic boot systems, electro-thermal systems, fluid injection systems, electro-impulse systems, and hot air systems. Those sections provide information that describe potential applications, many of which are common to both airplanes and rotorcraft. Sections III.6.3.1, III.6.3.3, III.6.3.4, III.6.3.8, III.6.3.9 and III.6.3.10 are directly applicable to rotorcraft and need not be discussed further in this section. The following sections deal only with the application of de-icing and anti-icing systems to problems that are unique to rotorcraft.

6.3.7.2 Distinctive Rotorcraft Icing Problems

While the rotor has many of the attributes of the propeller, the flight environment and larger diameter tend to set the required ice protection systems apart from propeller ice protection system design. Droplets from supercooled clouds generally freeze forward of 15% chord on the upper airfoil surface and 25% chord on the lower airfoil surface. An anti-icing system that melts ice only in this region will result in an ice formation aft of the heated region due to refreezing of melted ice. The resultant penalties in the lift, drag, and pitching moment are not acceptable. Thermal anti-icing of the whole blade surface may impose unacceptable increases in system cost, weight, and power. A fluid anti-icing system, which lowers the freezing temperature of the droplets below the ambient temperature, avoids the runback problem. However, at present no fluid rotor ice protection system has been certified. Rotor hubs are generally exposed on a helicopter, but experience has shown that the only components requiring ice protection are droop stops which tend to freeze in the "fly" position if the hinge pin is unheated. Stores support systems are unprotected and attention must then be given only to the prevention of ice shedding into engines and rotors. Engines must be qualified for flight not only in forward flight, but also in hover, rearward, and sideward flight. Although icing may not actually occur in these flight modes, the helicopter must be able to approach and land after flight in icing.

6.3.7.3 Rotors

The selection of a rotor ice protection system involves a thorough understanding of mission requirements and design constraints. The eventual solution may he possible to justify in terms of weight and cost, but other factors may enter into the decision-making process. The current level of maturity of a concept may be important to a designer, but other goals may require investigation of advanced systems which, as of this writing, have not been applied to modern helicopters. Advances in ice detection and accretion measurement systems may also become a part of the de-ice system selection process.

The electro-thermal system, the only de-ice system now in production, is in use on the Aerospatiale AS332 Super Puma, Sikorsky UH-60A BLACK HAWK, and SH-60B SEAHAWK. The CHSS-2 (Canadian Armed Forces Sikorsky S-61A) electro-thermal system was previously in production. Several helicopter models are also in various stages of de-ice system qualification (Boeing Vertol Model 234 and HC-MK1, Bell 214ST and 412, Bell/Boeing V-22, McDonnell Douglas AH-64A, and Sikorsky S-76B) and each of these rotorcraft uses electro-thermal rotor de-ice systems. Electro-thermal systems have been tested on Aerospatiale SA330, Bell UH-1H, MBB B0-105, Sikorsky H-34 and SH-3, and Westland Wessex 5 helicopters. While this type of system would appear to he the overwhelming choice of designers, this is essentially by default. The level of technology available in the 1970s precluded the use of fluid, vibratory, and pneumatic hoot systems and development had not started on the pneumatic-impulse de-icing system (PIDI). Work on the electro-impulse de-icing system (EIDI) prior to 1980 was conducted in the Soviet Union, but development in the United States

did not start in earnest until 1982. As described in greater detail in the preceding sections, research is continuing on alternatives to electro-thermal systems, and advances in the state-of-the-art for each system are expected. Flight tests were conducted in the early 1960s on a UH-1 equipped with a fluid anti-icing system and recent NASA airfoil tests studied fluid protection systems in both anti-icing and de-icing modes. A main rotor hot air anti-icing system was tested on a Sikorsky S-51 (H-5) helicopter. This used a 200,000 BTU/hr (70 HP) heater with sufficient hot air introduced into the blade spar to keep the leading edge free of ice. The system did keep the leading edges free of ice at less than critical conditions, but the moisture froze on the unheated blade surface. The system was deemed impractical for this and other reasons. Ice phobic tests on an AH-56 helicopter shows no benefits. Shear stresses must be as low as 1 psi to have an effective system. Tail rotor ice protection systems are derived using techniques applicable to both rotors and propellers. The following protection limits are recommended for main and tail rotors:

	Main Rotor	Tail Rotor
Chordwise Coverage - Upper Surface	0 to 15%	0 to 13%
Lower Surface	0 to 25%	0 to 13%
Spanwise Coverage -	20% to 99%	25% to 70%

The main part of the ice formation generally forms forward of 8% chord. The following material summarizes the attributes of rotor de-icing and anti-icing systems and is intended to serve as a guide for system selection. Tabular summaries are given in tables 6-11, 6-12, and 6-13 for the helicopter shown in figure 6-6.

Blade construction may dictate the type of system to be used. A typical rotor blade leading edge is solid, containing counterweights and filler material. Since fluid and EIDI systems are added to an airfoil section internally, retrofit of these systems to existing blades would be an expensive process. Therefore, these systems are currently not recommended as add-on ice protection systems. Also, at the current stage of coil development, application of EIDI to airfoils with chords less than 15 inches is not practical.

Useful life, reliability, and maintainability must be considered in the system selection. Rotor blades are designed with nickel or titanium leading edge abrasion protection to withstand the harsh environment imposed on a rotor operating in rain or near the ground. The maintainability of an erosion resistant pneumatic de-icing boot has been demonstrated during flight testing, but experiments conducted to date have not been sufficient to determine boot life during helicopter operations, or the costs associated with system maintenance. Metallic abrasion strips can be incorporated. into other designs to reduce or eliminate the impact of the ice protection system on blade erosion, but special techniques may be necessary to adapt the abrasion strip to the de-ice system requirements.

Each system involves either an electronic or mechanical union to transfer signals from the controller and power sources to the blades. Fluid systems, while mechanically simple, must be kept

free of foreign objects that could block the pores or tubes in the leading edge. Components of systems that must be imbedded in the blade must be very reliable, since repair or replacement is difficult and costly.

Fixed wing designers have employed various systems on a single aircraft, using the optimum system for each de-ice or anti-ice requirement. Rotorcraft ice protection systems have generally utilized electro-thermal techniques (there are some nacelle bleed air systems now in use). Advances in de-ice system design may allow the same flexibility of system selection available to the fixed wing designer. For example, a system could be specified to use bleed air engine inlet anti-icing, EIDI main rotor blade de-icing, electro-thermal windshield, droop stop, and pitot protection, and a pneumatic boot on inboard portions of the tail rotor.

6.3.8 Flight Sensors

6.3.8.1 Pitot and Static Probes

Pitot probes and static port assemblies are usually heated with internal electric elements which are an integral part of the assembly. The pitot and static port assemblies must be designed to operate in all icing conditions including exposure to water and slush from the landing gear during takeoff and landing.

6.3.8.2 Stall Warning Transducers

Stall warning transducers are very delicate and sensitive assemblies. The icing protection on this type of equipment must be integrated into the overall design by the manufacturer. Ice buildup on the adjacent surface may disrupt the air flow and prevent the system from accurately indicating an imminent stall. (NOTE: The stall speed will increase when ice accumulates on the surfaces of any airplane.)

The transducer assembly is usually equipped with anti-icing capability on both the mounting plate and the vane. Internal electrical heating elements provide a minimum level of heat for ground operation, and an increased level for flight operations. Electro-thermal heat is used since it is the most compact and easiest system to control.

6.3.9 Radomes and Antennas

6.3.9.1 Radomes

When radomes are protected from ice accumulations, designers ordinarily use hot air anti-icing, pneumatic boot de-icing, or fluid spray (alcohol or glycol) on the external surface. The selection of the system for radomes thus depends on the availability of sufficient bleed air and the feasability and appropriateness of pneumatic boots or fluid spray.

6.3.9.2 Antennas

Many different sizes and shapes of antennas are installed on aircraft today. Some of these antennas may not function properly with ice on their external surfaces. Ice accumulated on the antennas may also create flutter and vibration problems; however, many antennas are designed to withstand the maximum ice accretion. Dry air flight testing with simulated ice shapes may be helpful in resolving some of these problems.

Ice protection may not be required if the antenna is small and is located where accumulated ice will not shed and cause damage to other aircraft components. Each antenna installation should be evaluated carefully for icing requirements. If ice protection for the antenna mast is required, electrical heaters may be designed into the units by the manufacturers or added to the external surface by installing an electro-thermal de-ice boot. Radio interference could be a problem with an electro-thermal de-ice boot.

A pneumatic de-ice boot may also be installed if the external contour permits. Radio interference is not a problem with a pneumatic de-icer boot.

6.3.10 Miscellaneous Intakes and Vents

6.3.10.1 Air Scoops

Flush or recessed scoops may not require ice protection. External scoops can be protected with hot air, electro-thermal, or pneumatic boots. This selection will depend on the size of the scoop, the power available, system complexity, and location.

6.3.10.2 Fuel Vents

Electrical heaters may be used on fuel vents and are usually controlled manually with an "ON", "OFF" switch located on the instrument panel. Fuel systems usually have a dual vent system, one vent is recessed to prevent icing and one vent is electrically heated and used as a backup. Some fuel vent plumbing lines are protected against icing by electrically heated jackets. These heaters may be controlled automatically and turned "ON" for all flight operations.

6.3.11 Drain Masts and Pipes

Waste water drains from galley or cabin washbowls or condensate drains from the air conditioning system constitute special hazards. At low speeds or very low atmospheric temperatures, water may freeze in the outlet and block the drain. More commonly, water is blown back and freezes to form a large ice mass. Upon descent into warmer air, the aircraft then sheds the ice. Ice-falls to the ground of up to 100 lb. have been reported. (Reference 6-5, pp. 4.2-29, -30.) For these reasons, water draining in flight should be avoided if at all possible.

III.6.4 WEIGHT, ENERGY, AND POWER COMPARISONS

Weight, energy and power requirement comparisons for ice protection system on four typical aircraft (figure 6-2 through 6-5) are presented in tables 6-1 through 6-8.

III.6.5 DISTINCTIVE SMALL AIRPLANE ICING PROBLEMS (FAR PART 23)

Aircraft in this category (reference 6-5) can be single or multi-engine aircraft with a maximum takeoff weight of 12,500 pounds or less, and with either reciprocating or turbine engines. On aircraft with reciprocating engine installations, pneumatic boot, electro-thermal, fluid injection, or electro-impulse icing systems may be selected for lifting surface ice protection. On turbine engine aircraft, hot-air anti-icing systems may also be considered, due to the availability of engine bleed air as a heat source. On small aircraft, the total icing system weight and cost are major factors in selecting a satisfactory system.

Ice protection may be more critical for small airplanes than for larger aircraft. Overflying an icing cloud is often impossible due to lower service ceilings. Their limited range makes weather avoidance or using alternate landing sites more difficult. There are usually more non-protected components, such as struts, non-retracting wheels, and steps. Smaller component sizes tend to have higher collection efficiencies, thus relatively larger ice accretions occur. Engine power margins are less and excess engine power to drive accessories is limited. The single engine airplane inherently has reduced system redundancies and thus a reduced reliability. FAR23.1309 states that equipment, systems, and installations of a single engine airplane must be designed to minimize hazards to the airplane whereas those of a multiengine airplane must be designed to prevent hazards in the event of a probable malfunction or failure.

III.6.6 DISTINCTIVE TRANSPORT CATEGORY AIRPLANE PROBLEMS (FAR PART 25)

Aircraft in this category can be either small, medium or large and each would have somewhat distinctive ice protection problems. Added to this is the complication that these aircraft can be powered by piston engines, turboprop engines and propellers, or jet engines (high or low bypass ratio).

A distinctive advantage of these aircraft lies in the availability of bleed air and relatively large amounts of power for ice protection. Thus all forms of ice protection can be supported. The use of more than one type is likely because this flexibility allows the designers to install the optimum system for each component that is to be protected.

An ice protection area that is perhaps unique to this category of aircraft is wing leading edge devices. The possible need for radome ice protection is a consideration for aircraft in this category which need not be addressed for some Part 23 aircraft.

III.6.7 DISTINCTIVE ROTORCRAFT ICING PROBLEMS (FAR PART 27/29)

The protection of helicopter components presents some unique problems. Early designers thought that vibration and centrifugal forces would prevent appreciable ice accretion on helicopter rotors. This is not the case - ice does accrete and the increased drag causes an increase in the power requirements of the helicopter. On small helicopters, the increase in airfoil drag may be sufficient to force the aircraft to land, while on some large helicopters the power increments may be acceptable. When self-shedding does occur, it is usually asymmetrical, and this causes an imbalance that may result in severe vibration.

Ice accretion in relatively small quantities may create severe hazards to a helicopter. These hazards may be from excessive vibration caused by asymmetrical self-shedding of ice from the main and tail rotors, from ice impact damage when self-shedding occurs, or from the increase in airfoil drag when self-shedding does not occur.

Another area of a helicopter that may require ice protection is the rotor head mechanism. The rotor head mechanism is not likely to freeze up during flight or malfunction if the mechanism is actuated frequently. But, if icing is a hazard to the mechanism, then a simple windscreen or some de-icing system may he necessary.

Propulsion system ice protection may consist of inlet screen anti-icing and turbine engine inlet anti-icing. On one flight test program involving a light, turbine-powered helicopter, the inlet screen iced in a waffle pattern and caused approximately 15 percent air blockage. The total open area of the inlet screen was twice the engine inlet area; consequently, the ice blockage did not affect the engine performance. This area ratio may not always occur, and icing on an inlet screen may cause sufficient blockage to affect engine performance. Other inlet screens for compartment cooling, carburetor inlets, etc., may also require ice protection.

III.6.8 REFERENCES

6-1 Lawrence, James H., "Guidelines for the Design of Aircraft Windshields/ Canopy Systems," AFWAL-TR-80-3003, February 1980.

6-2 Hassard, Richard S., "Plastics for Aerospace Vehicles, Part II, Transparent Glazing Materials," MIL-HDBK-17A, Part II, January 1973.

6-3 Pfeifer, G.O. and Maier, G.P., "Engineering Summary of Powerplant Icing Technical Data," FAA Report RD-77-76, July 1977.

6-4 Duffy, R.J. and Shattuck, B.F., "Integral Engine Inlet Particle Separator, Volume II - Design Guide," Report Number USAAMRDL-TR-75-31B, August 1975.

6-5 "Aircraft Ice Protection," FAA Advisory Circular 20-73, April 1971.

6-6 Bowden, D.T., Gensemer, A.E. and Speen, C.A., "Engineering Summary of Airframe Icing Technical Data," FAA Technical Report ADS-4, March, 1964.

TABLE 6-1. AIRCRAFT ICE PROTECTION SYSTEM ATTRIBUTES FAR 23 SMALL SINGLE ENGINE AIRCRAFT

Aircraft Component	System Type	Weight lb.	Power KW	Bleed Air lb min	POTENTIAL FOR PROBLEMS? Partial Shed	Runback	Fatigue
Wing and Tail	Pneumatic De-Icing	25		Negl	Low	None	None
Windshield	Elec. Anti-Icing	8	1.4		Low	Low	None
Propeller	Elec. De-Icing	5	0.6		Some	None	None
	Generator	10					
Total		48	2.0				
Wing and Tail	Elec. Impulse Deice	50	0.3	None	Low	None	Yes
Windshield	Elec. Anti-Icing	8	1.4		Low	Low	None
Propeller	Elec. De-Icing	5	0.6		Some	None	None
	Generator	10					
Total		73	2.3				
Wing and Tail	Fluid Anti-Icing	40	Negl	None	No	Low	None
Windshield	Fluid Anti-Icing	3	Negl		Low	Low	None
Propeller	Elec. De-Icing	2	0.6		Some	None	None
	Fluid	55					
Total		100	0.6				

Notes: Electro-thermal for wings and tail exceeds power available.
Hot bleed air usually not available on this class aircraft.

TABLE 6-2. WEIGHT SUMMARY - WING AND TAIL SYSTEMS
FAR 23 SMALL SINGLE ENGINE AIRCRAFT (1)

SYSTEM	Pneumatic Boots	EIDI	Fluid Protection
SYSTEM TYPE	De-Icing	De-Icing	Anti- or De-Icing
Alternators	0	0	0
Controls	3	16	1.5
Wiring	0	12	1.0
Distributors	2	0	3.0
Coils and Mounts	0	22	0
Surface Modifications	20	0	20
Fluid	0	0	50
Pumps, Tanks, Trapped Fluid	0	0	14.5
	---	---	----
Weight Total	30	50	90

(1) All numbers are approximate in pounds.

TABLE 6-3. AIRCRAFT ICE PROTECTION SYSTEM ATTRIBUTES FAR 23 SMALL TWIN ENGINE AIRCRAFT

Aircraft Component	System Type	Weight lb.	Power KW	Bleed Air lb/min	POTENTIAL FOR PROBLEMS? Partial Shed	Runback	Fatigue
Wing and Tail	Pneumatic De-Icing	28		Negl	Low	None	None
Windshield	Elec. Anti-Icing	10	1.5		Low	Low	None
Propeller	Elec. De-Icing	10	0.8		Some	None	None
	Generator	10					
Total		58	2.3				
Wing and Tail	Elec. Impulse Deice	63	0.5	None	Low	None	Yes
Windshield	Elec. Anti-Icing	10	1.5		Low	Low	None
Propeller	Elec. De-Icing	10	0.8		Some	None	None
	Generator	12					
Total		95	2.8				
Wing and Tail	Fluid Anti-Icing	40		None	None	Low	None
Windshield	Fluid Anti-Icing	4			Low	Low	None
Propeller	Elec. Anti-Icing	10	1.2		Low	Some	None
	Fluid	65					
Total		125	1.2				

TABLE 6-4. WEIGHT SUMMARY - WING AND TAIL SYSTEMS FAR 23 SMALL TWIN ENGINE AIRCRAFT (1)

SYSTEM	Pneumatic Boots	EIDI	Fluid Protection
SYSTEM TYPE	De-Icing	De-Icing	Anti- or De-Icing
Alternators	0	0	0
Controls	4	17	3
Wiring	0	15	2
Distributors	4	0	4
Coils and Mounts	0	31	0
Surface Modifications	30	0	23
Fluid	0	0	60
Pumps, Tanks, Trapped Fluid	0	0	14
	---	---	---
Weight Total	38	6	106

(1) All numbers are approximate in pounds.

TABLE 6-5. AIRCRAFT ICE PROTECTION SYSTEM ATTRIBUTES FAR 25 BUSINESS JET AIRCRAFT

Aircraft Component	System Type	Weight lb.	Power KW	Bleed Air lb/min	POTENTIAL FOR PROBLEMS? Partial Shed	Runback	Fatigue
Wing and Tail	Hot Air Anti-Icing	80		42*	Yes	Yes	None
Windshield	Elec. Anti-Icing	10	1.5		Low	Low	None
Engine Inlet	Hot Air Anti-Icing	15		13	Yes	Yes	None
	Generator	10					
Total		115	1.5	55			
Wing and Tail	Elec. Impulse De-ice	90	0.7		Low	None	Yes
Windshield	Elec. Anti-Icing	10	1.5		Low	Low	None
Engine Inlet	Elec. Impulse De-ice	20	0.2		Low	None	Yes?
	Generator	10					
Total		130	2.4				
Wing and Tail	Fluid Anti-Icing	110	0.1		None	Low	None
Windshield	Fluid Anti-Icing	10			None	Low	None
Engine Inlet	Hot Gas Anti-Icing	15		13	Yes	Yes	None
Total		135	0.1	13			
Wing and Tail	Pneumatic De-Icing	35		Negl	Low	None	None
Windshield	Elec. Anti-Icing	10	1.5		Low	Low	None
Engine Inlet	Elec. Anti-Icing	10	8.8		Low	Low	None
	Generator	20					
Total		75	10.3				
Wing and Tail	Electrical De-Icing	20	11.7		Some	None	None
Windshield	Elec. Anti-Icing	10	1.5		Low	Low	None
Engine Inlet	Elec. Anti-Icing	10	8.8		Low	Low	None
	Generator	20					
Total		20	22.0				

Notes: All numbers are approximate. *About 2.5% of Engine Core Airflow

TABLE 6-6. WEIGHT SUMMARY - WING AND TAIL SYSTEMS FAR 25 BUSINESS JET AIRCRAFT (1)

SYSTEM	Pneumatic Boots	EIDI	Hot Air	Fluid Protection	Electro-Thermal
SYSTEM TYPE	De-Icing	De-Icing	Anti- or De-Icing	Anti- or De-Icing	De-Icing
Alternators	0	0	0	0	10
Controls	5	18	9	3	3
Wiring	0	22	1	2	2
Distributors	5	0	40	4	0
Coils and Mounts	0	50	0	0	0
Surface Modifications	25	0	30	26	15
Fluid	0	0	0	60	0
Pumps, Tanks, Trapped Fluid	0	0	0	15	0
	--	--	--	---	--
Weight Total	45	90	80	110	30

(1) All numbers are approximate in pounds.

TABLE 5-7. AIRCRAFT ICE PROTECTION SYSTEM ATTRIBUTES FAR 25 LARGE TRANSPORT CATEGORY AIRCRAFT (250 PASSENGERS)[1]

Aircraft Component	System Type	Weight lb.	Power KW	Bleed Air % Core Flow	POTENTIAL FOR PROBLEMS? Partial Shed	Runback	Fatigue
Wing and Tail	Hot Air Anti-ice[3]	190	-	2.5	Low	Yes	No
Windshield	Elec. Anti-Icing[2]	25	3.0	-	Low	Low	No
Engine Inlet	Hot Air Anti-Ice	45	-	0.7	Low	Yes	No
Total		260	3.0	3.2			
Wing and Tail	Elec. Impul. De-ice[4]	400	2.6	-	Low	No	Yes
Windshield	Elec. Anti-Icing	25	3.0	-	Low	Low	No
Engine Inlet	Elec. Impul. De-ice	90	0.6	-	Some	No	Yes
Total		515	6.2	-			
Wing and Tail	Fluid Anti-Icing	340	0.1	-	No	Low	No
Windshield	Fluid Anti-Icing	25	3.0	-	Low	Low	No
Engine Inlet	Hot Air Anti-Icing	45	-	0.7	Low	Yes	No
Total		410	3.1	0.7			
Wing and Tail	Electrical De-ice	140	60.0	-	Low	Low	No
Windshield	Elec. Anti-Icing[2]	25	3.0	-	Low	Low	No
Engine Inlet	Hot Air Anti-Ice	45	-	0.7	Low	Yes	No
Total		210	63.0	0.7			
Wing and Tail	Pneumatic De-ice	195	-	-	Low	No	No
Windshield	Elec. Anti-Icing[2]	25	3.0	-	Low	Low	No
Engine Inlet	Hot Air Anti-Ice	45	-	0.7	Low	Yes	No
Total		265	3.0	3.2			

[1]All numbers are approximate.
[2]Weight for windshield anti-icing includes extra generator capacity.
[3]Excludes weight of ducts and controls shared with other bleed air uses.
[4]Includes partial redundancy in the system.

TABLE 6-8. WEIGHT SUMMARY - WING AND TAIL SYSTEMS FAR 25 LARGE TRANSPORT CATEGORY AIRCRAFT (250 PASSENGERS) (1)

SYSTEM	EIDI(2)	Hot Air(3)	Fluid Protection	Electro-Thermal	Pneumatic Boots
SYSTEM TYPE	De-Icing	Anti- or De-Icing	Anti- or De-Icing	De-Icing	De-Icing
Alternators	0	0	0	50	0
Controls	100	15	3	40	5
Wiring	100	0	3	18	0
Distributors	0	135	20	0	15
Coils and Mounts	200	0	0	0	0
Surface Modifications	0	40	110	32	175
Fluid	0	0	150	0	0
Pumps, Tanks, Trapped Fluid	0	0	54	0	0
	---	---	---	---	---
Weight Total	400	190	340	140	195

(1) All numbers are approximate in pounds.
(2) System provides for partial redundancy.
(3) Excludes weight of ducts and controls shared with other bleed air uses.

TABLE 6-9. ADVANTAGES AND DISADVANTAGES OF ICE PROTECTION SYSTEMS

SYSTEM	ADVANTAGES	DISADVANTAGES
Hot-Air (Bleed)	conventional method good I/P performance (anti-icing) easy to maintain	reduced engine efficiency and power typical de-icing penalties* (if operated in de-icing mode)
Hot-Air (Combustion heater)	good I/P performance (anti-icing) non-bleed method	high weight penalty expensive to operate typical de-icing penalties* (if operated in de-icing mode)
Pneumatic Boot	low initial cost light weight low bleed air requirement in common use-proven long history	aero effects due to deicer itself aero effects due to residual ice typical de-icing penalties* short service life poor appearance
Fluid Protection	good I/P performance (anti-icing) relatively low maintenance non-bleed method high initial cost	typical de-icing penalties* (if operated in de-icing mode) fluid ingestion into engines
Electro-Impulse	non-bleed method low power consumption low maintenance	aero effects due to residual ice typical de-icing penalties* possible fatigue to structures unproven for transport aircraft
Electro-Thermal	non-bleed method	excessive power consumption for large area of I/P coverage typical de-icing penalties*

* Typical de-icing penalties include aerodynamic effects due to ice buildup before de-icing and possible ice ingestion into tail-mounted engines and or propellers.

TABLE 6-10. SIGNIFICANT ENGINE INLET ICE PROTECTION SELECTION CONSIDERATIONS

		Hot Air Anti-Icing	Hot Air De-Icing	Electro-Impulse De-Icing	Fluid Anti-Icing	Fluid De-Icing	Electro-Thermal Anti-Icing	Electro-Thermal De-Icing	Pneumati De-Icing
1.	Aerodynamic effects of ice cap		X	X		X		X	X
2.	Aerodynamic effects of runback ice	X					X		
3.	Ice ingestion (de-icing)		X	X		X		X	X
4.	Ice ingestion (runback)	X					X		
5.	Bleed air penalty	X	X						
6.	Weight penalty	X	X	X	X	X	X	X	X
7.	Weight for additional electrical power generation						X	X	
8.	Power penalty	X					X	X	
9.	Fluid costs				X	X			
10.	Maintenance costs	X	X		X	X	X	X	X
11.	Non-recurring costs	X	X	X	X	X	X	X	X
12.	Fluid ingestion and toxicity				X	X			
13.	EMI			?			X	X	
14.	Noise	?	?	X					
15.	Fatigue	?	?	X					
16.	Development risk			X	X	X	X	X	

TABLE 6-11. ROTORCRAFT MAIN ROTOR DE-ICING SYSTEM ATTRIBUTES
FAR 27/29 ROTORCRAFT (1)
SYSTEM SIZED FOR FOUR 24-FOOT MAIN ROTOR BLADES

SYSTEM	Pneumatic Boots	Electro-Thermal	EIDI	Fluid Protection	Vibratory	Ice Phobic
SYSTEM TYPE	De-Icing	Anti- or De-Icing	De-Icing	Anti- or De-Icing		
Weight, Pounds	54	84	110	192	110	34
Dry Air Parasite Drag, Ft^2	0.7	0.7	Negl	0	Negl	0
Dry Air Profile Power Delta, Hp	50 (2)	25 (2)	0	(4)	0	0
Electrical Extraction, HP	Negl	35 (3)	1	1	2	0
Bleed Air Power Loss, HP	Negl	0	0	0	0	0
Minimum Ice Thickness, In	.25	.15	.15	0	.30	.30
Average Power Rise Due to Ice, %	20	15	15	0	25	25
Partial Shed Potential	Low	Low	Low	None	High	High
Runback Potential	No	Yes	No	No	No	No
Fatigue Stress Increase	No	No	Yes	No	Yes	No

(1) All numbers are approximate and apply to the helicopter in Figure 6-6.
(2) Delta HP = 0 for in-contour installation.
(3) Approximately 60 horsepower is required for the CH-47 Chinook tandem rotor helicopter.
(4) Depends on airfoil porosity and roughness.

TABLE 6-12. WEIGHT SUMMARY - MAIN ROTOR DE-ICING SYSTEM SIZED FOR FOUR 24-FOOT MAIN ROTOR BLADES (1)

SYSTEM	Pneumatic Boots	Electro-Thermal	EIDI (2)	Fluid Protection	Vibratory	Ice Phobic
SYSTEM TYPE	De-Icing	Anti- or De-Icing	De-Icing	Anti- or De-Icing	De-Icing	De-Icing
Alternators (increment)	0	14	0	0	0	0
Controls	5	6	12	15	15	0
Wiring	0	11	13	0	20	0
Distributors	15	31	20	12	150	0
Blade and Hub Modifications	34	22	65	28	60	34
Fluid	0	0	0	117	0	0
Pumps, Tanks, Trapped Fluid	0	0	0	20	0	0
Weight Total, Pounds	54 (3)	84	110	192 (4)	110	34

(1) All numbers are approximate and in pounds for helicopter in Figure 6-6.
(2) Does not include protection for engine inlet lip - add approximately 25% to all terms for engine lip.
(3) Weight for the UH-1H system (two blades) is 40 pounds.
(4) This becomes 68 pounds during non-icing season with trapped and consummable fluids removed.

TABLE 6-13. WEIGHT SUMMARY - COMPLETE HELICOPTER ICE PROTECTION SYSTEM SIZED FOR HELICOPTER IN FIGURE 6-6

System	Component	Comp. Wt. (lb)	Sys. Wt. (lb)
Windshield	Film Conductor	Negl	14.4
	Wiring	8.2	
	Control Units (3)	6.2	
Pitot-Static	Conductor	Negl	1.6
	Wiring and Control	1.3	
	Temperature Sensor	0.3	
Nacelle	Bleed Air Plumbing	5.0	13.6
	Control Wiring	2.2	
	Modulating Valve	6.4	
Droop Stops	Heating Unit	3.2	3.2*
	Control Wiring	Incl. in Main Rotor	
	Control Unit	Incl. in Main Rotor	
Main Rotor	Blade Heater Mats (Foils)	10.2	67.3*
	Distributor	16.2	
	Wire Harnesses	11.3	
	Slip Ring Assembly	5.5	
	Junction Box Assembly	9.6	
	Control Unit	3.8	
	Control Panel	1.0	
	Fault Monitor	1.1	
	Misc. Seals, Tubes, Brackets	8.6	
Tail Rotor	Blade Heater Mats (Foils)	1.4	7.4
	Distributor	Incl in MR	
	Wire Harnesses	Incl in MR	
	Slip Ring Assembly	4.6	
	Control Unit and Panel	Incl in MR	
	Misc. Brackets	1.4	
Ice Detector	Detector Unit	1.2	4.0
	LWC Panel	2.8	
Temperature Sensor		0.4	0.4
Generators	30/45 vs 20/30	12.4	13.9*
	Lower Gauge Generator Wire	1.5	

Total Ice Protection System Weight			125.8

*Included in Table 6-11 for Electro-Thermal Protection of Main Rotor

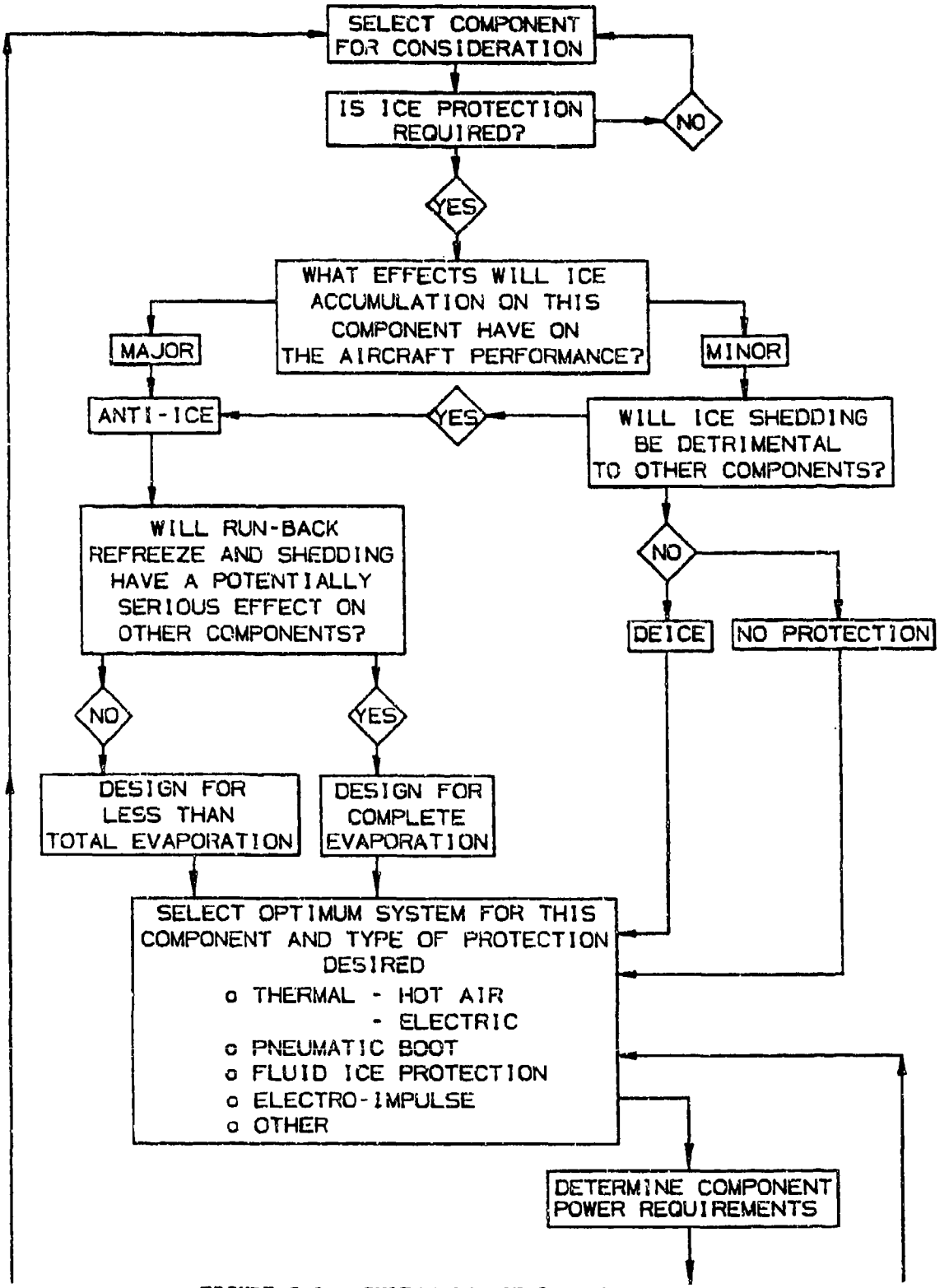

FIGURE 6-1. SYSTEM SELECTION FLOW DIAGRAM

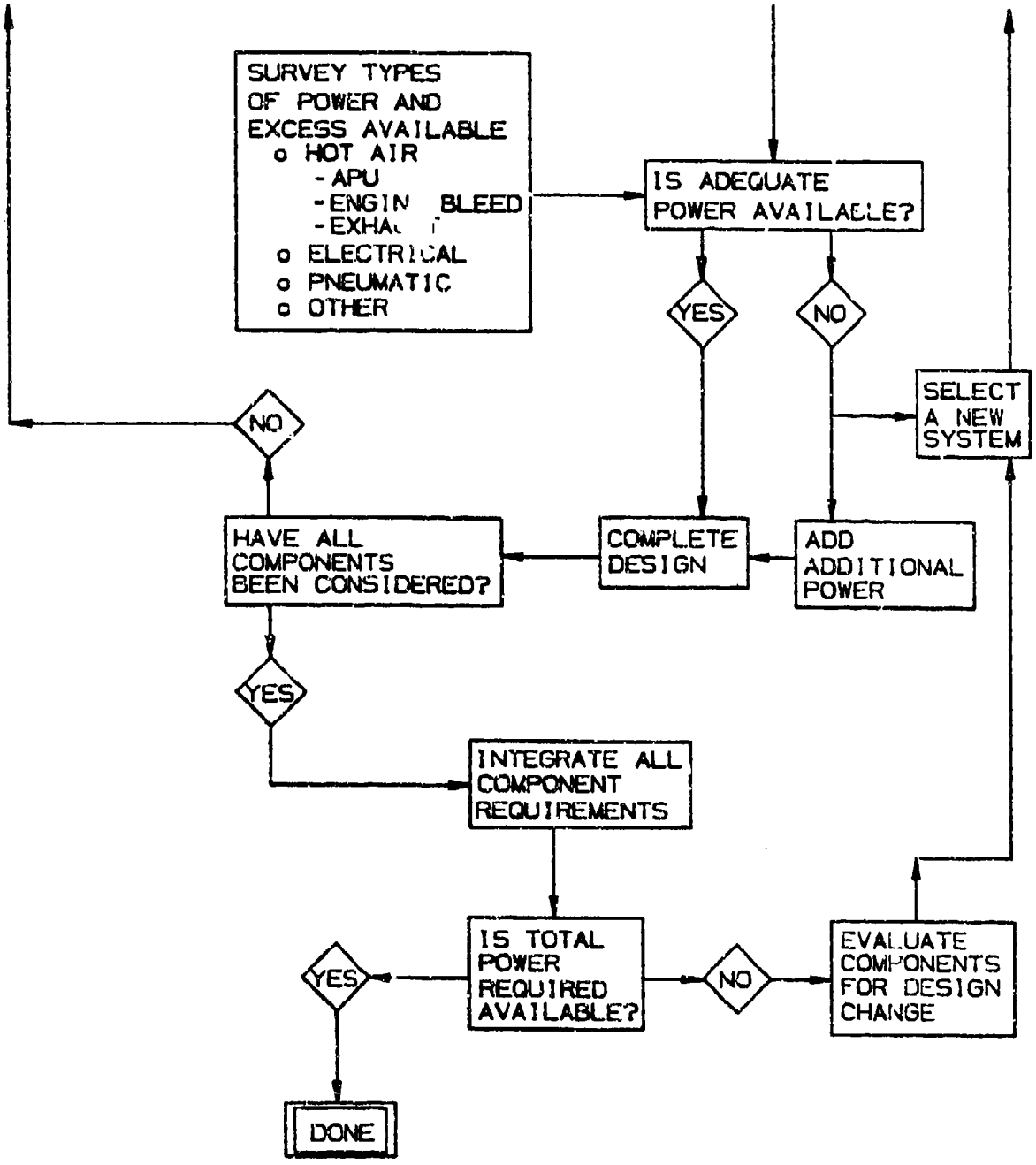

FIGURE 6-1. SYSTEM SELECTION FLOW DIAGRAM (CONTINUED)

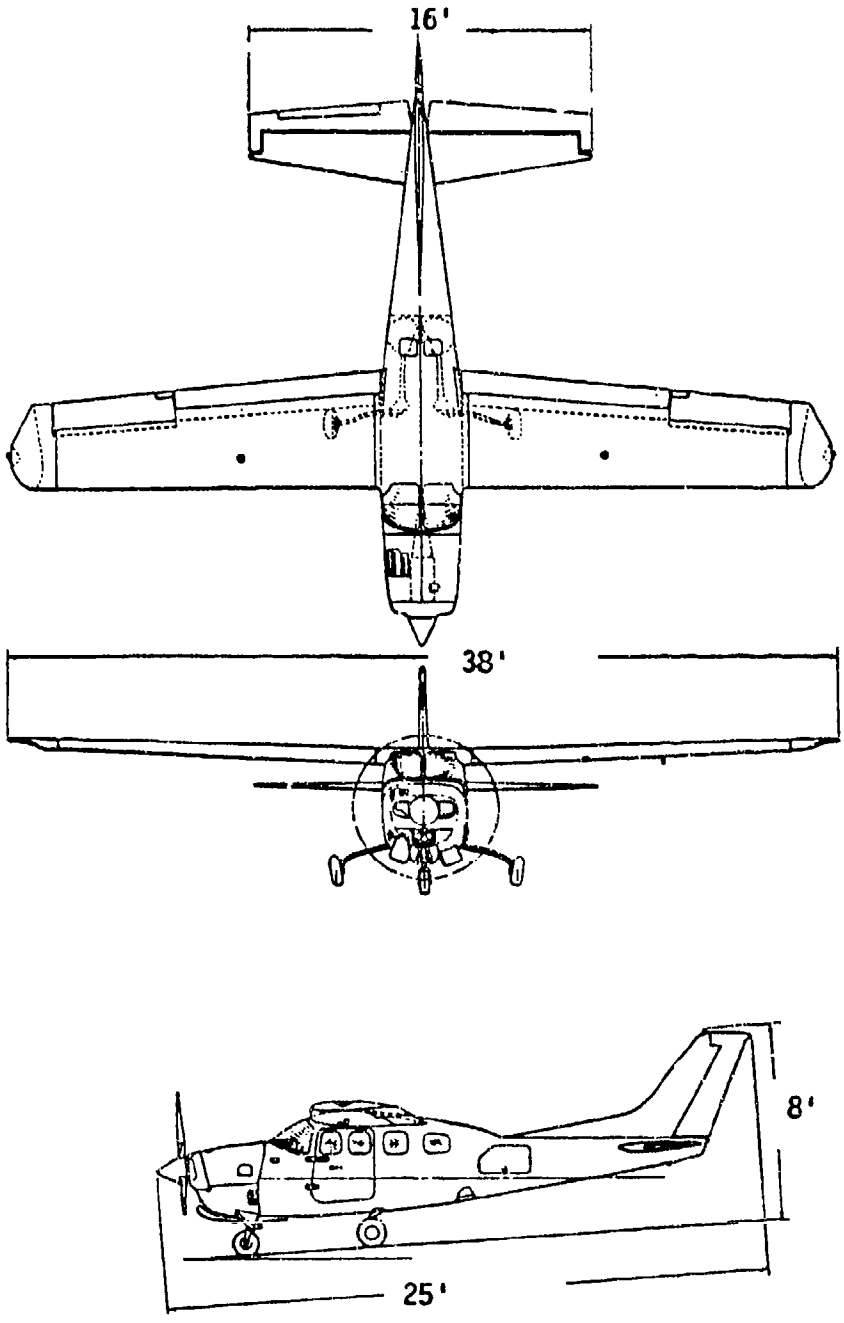

FIGURE 6-2. TYPICAL SINGLE-ENGINE AIRCRAFT

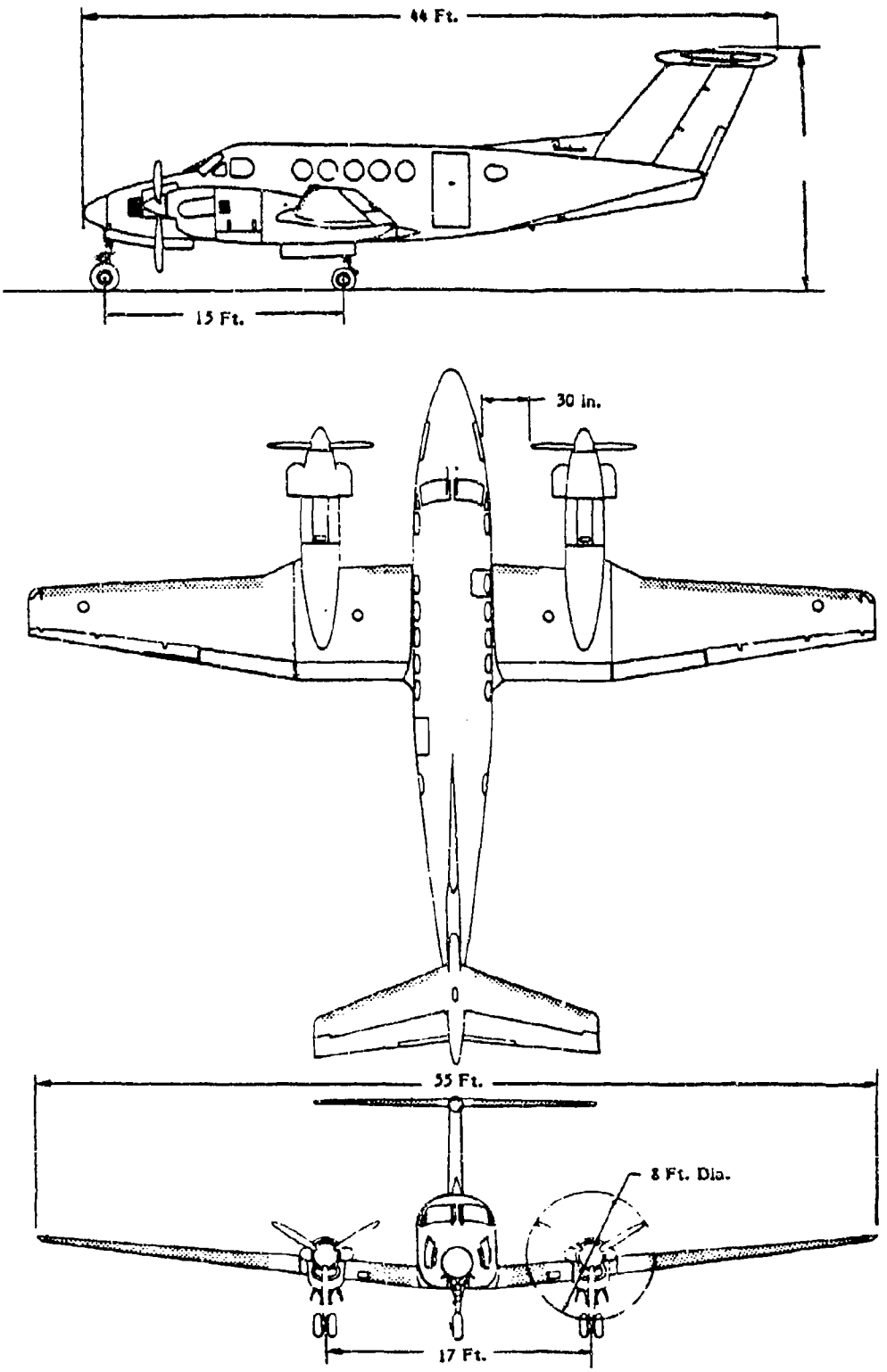

FIGURE 6-3. TYPICAL LIGHT TWIN-ENGINE AIRCRAFT

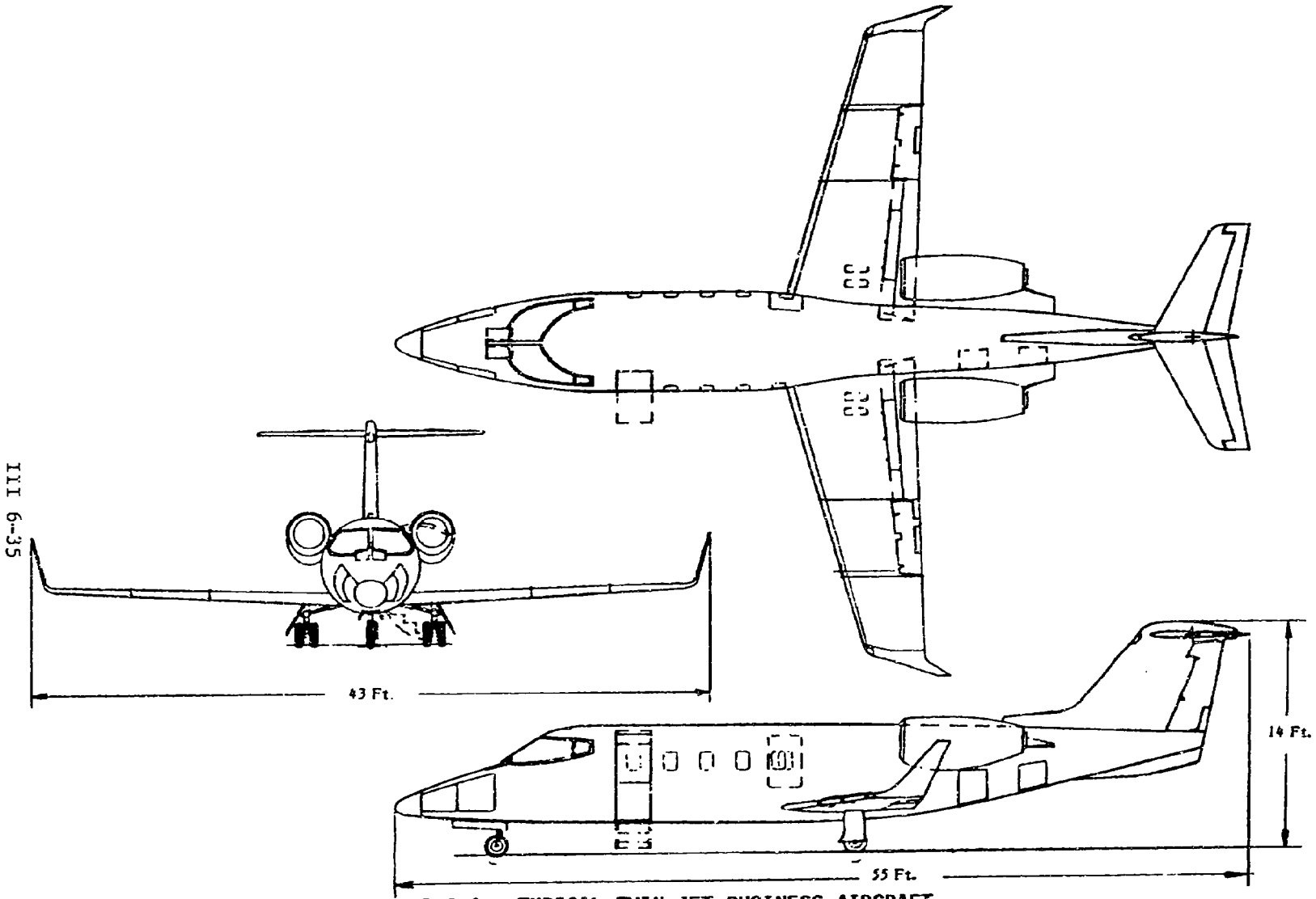

FIGURE 6-4. TYPICAL TWIN-JET BUSINESS AIRCRAFT

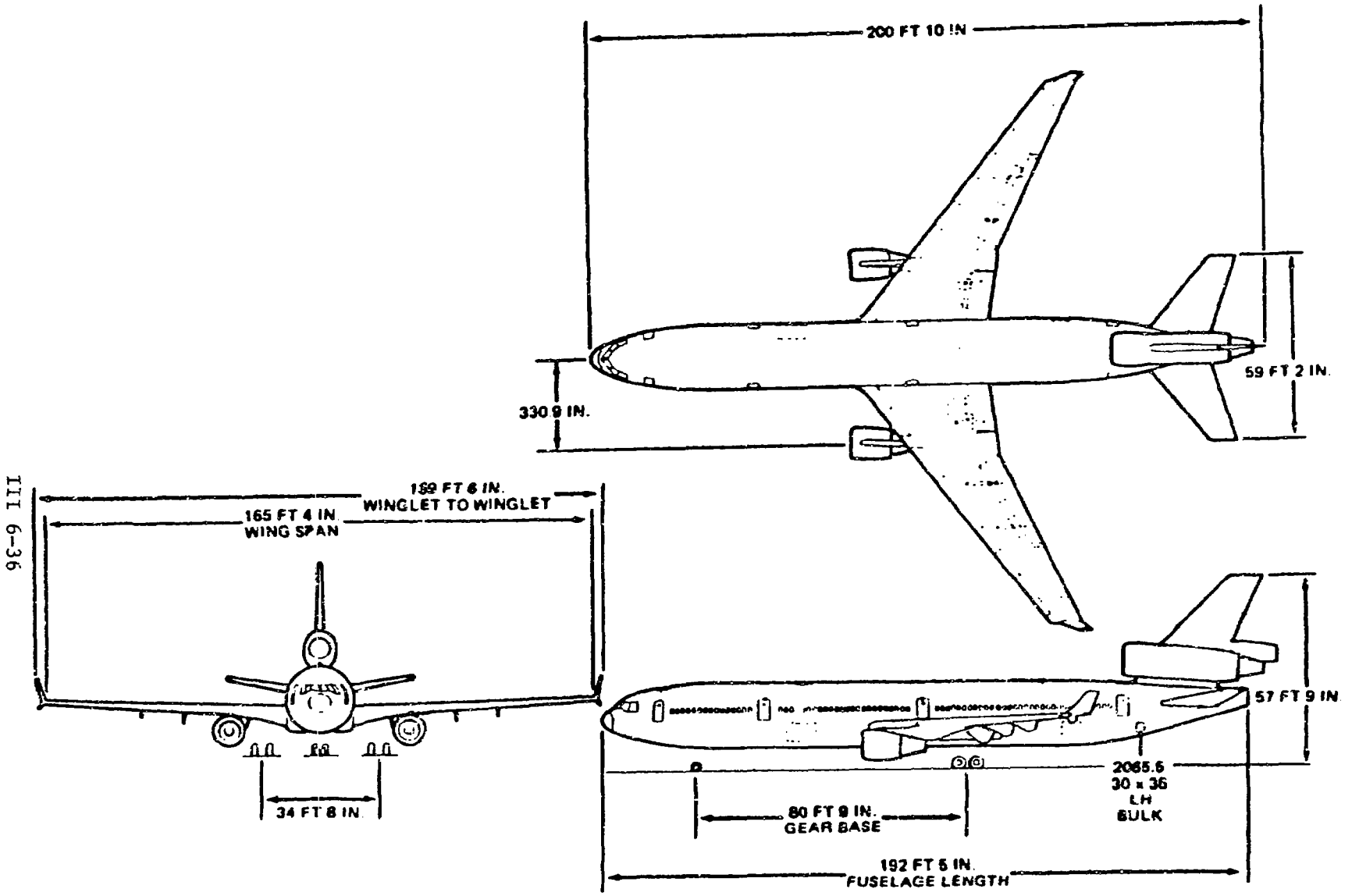

FIGURE 6-5. TYPICAL JET TRANSPORT

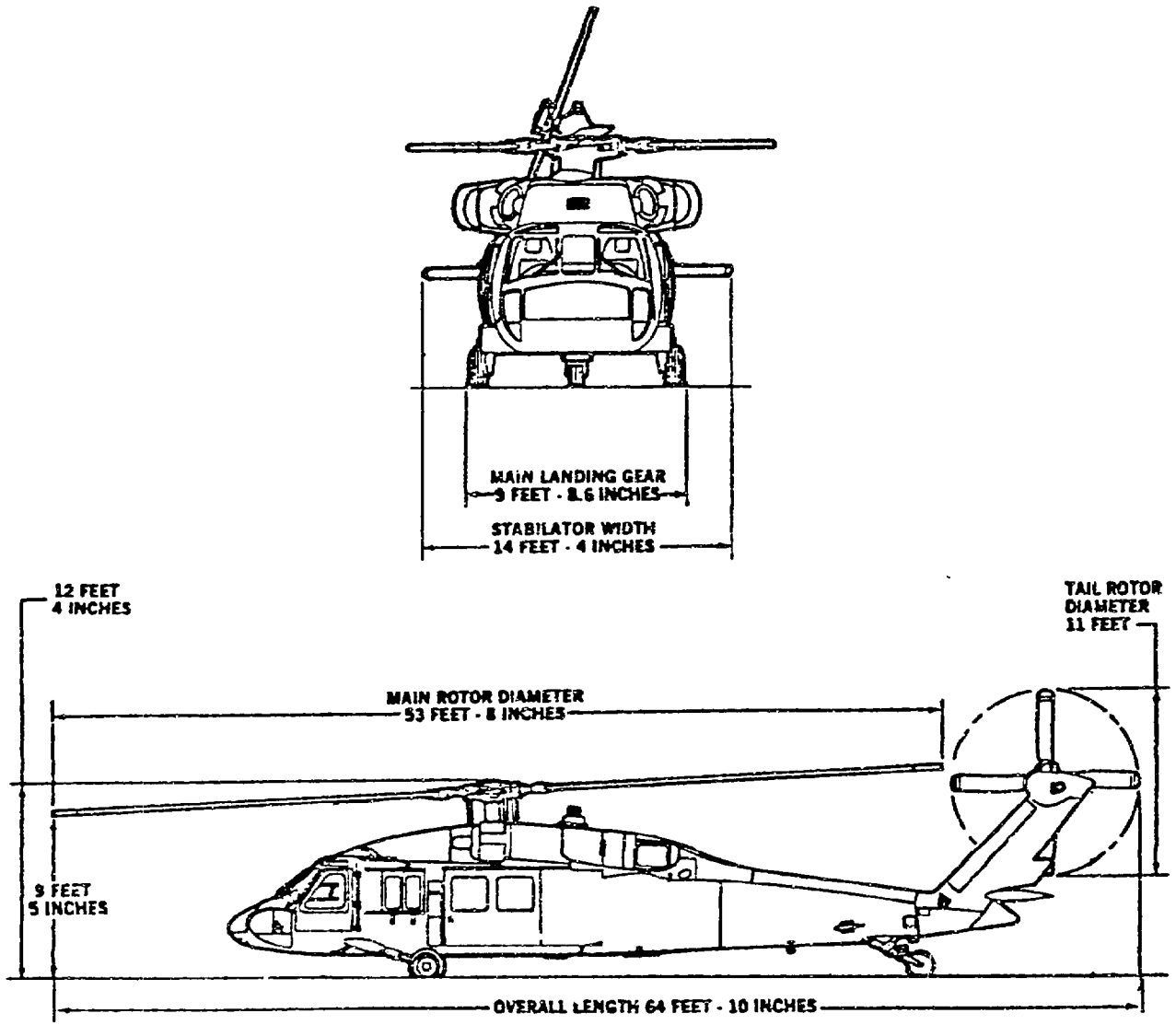

FIGURE 6-6. TYPICAL FAR PART 29 OR MILITARY HELICOPTER

CHAPTER IV
ICING SIMULATION METHODS
SECTION 1.0 - TEST METHODS AND FACILITIES
SECTION 2.0 - ANALYTICAL METHODS

CHAPTER IV
SECTION 1.0
TEST METHODS AND FACILITIES

CHAPTER IV - ICING SIMULATION METHODS
CONTENTS
SECTION 1.0 TEST METHODS AND FACILITIES

	Page
LIST OF TABLES	IV 1-iii
LIST OF FIGURES	IV 1-iv
SYMBOLS AND ABBREVIATIONS	IV 1-v
GLOSSARY	IV 1-vii
IV.1.1 SUMMARY	IV 1-1
IV.1.2 ICING WIND TUNNELS	IV 1-2
1.2.1 Introduction	IV 1-2
1.2.2 Icing Wind Tunnel	IV 1-3
1.2.2.1 NASA Lewis Research Tunnel	IV 1-3
1.2.2.2 Industrial Icing Tunnels	IV 1-6
1.2.2.3 European Icing Tunnels	IV 1-9
1.2.2.4 Test Techniques	IV 1-9
1.2.3 Engine Icing Tunnels	IV 1-10
1.2.3.1 AEDC Engine Test Facility	IV 1-10
1.2.3.2 Naval Air Propulsion Facility (NAPF)	IV 1-11
1.2.3.3 Test Techniques	IV 1-11
IV.1.3 GROUND SPRAY RIGS	IV 1-13
1.3.1 Introduction	IV 1-13
1.3.2 Helicopter Spray Rigs	IV 1-13
1.3.3 G.E. Cross Wind Engine Test Facility	IV 1-13
1.3.4 McKinley Climatic Laboratory	IV 1-14
1.3.5 Limitations of Ground Spray Rigs	IV 1-15
1.3.6 Test Techniques	IV 1-15
IV.1.4 TANKER SPRAY AIRCRAFT	IV 1-16
1.4.1 Introduction	IV 1-16
1.4.2 Available Tanker Aircraft	IV 1-17
1.4.3 Limitations	IV 1-17
1.4.4 Test Techniques	IV 1-18
1.4.4.1 Instrumentation	IV 1-18
1.4.4.2 Factors Affecting Icing Simulation	IV 1-19
IV.1.5 SIMULATED ICE SHAPES	IV 1-20
IV.1.6 REFERENCES	IV 1-21

LIST OF TABLES

		Page
1-1	Available Wind Tunnels	IV 1-23
1-2	European Icing Tunnels	IV 1-24
1-3	Available Engine Test Facilities	IV 1-25
1-4	Available Ground Spray Rigs	IV 1-27
1-5	Available Tanker Spray Aircraft	IV 1-28

Note: These tables do not reflect any changes since 1987. However, some of the information in the text, in particular the discusssion of the NASA Lewis Icing Research Tunnel, is current as of December 1990.

LIST OF FIGURES

		Page
1-1	Types of Icing Simulation Facilities	IV 1-29
1-2	Plan View of NASA Lewis Icing Research Tunnel facility	IV 1-30
1-3	Liquid Water Contour Plots for an airspeed of 145 mph for NASA Lewis IRT	IV 1-31
1-4	NASA Lewis IRT Operating Envelopes	IV 1-32
1-5	Comparison of IRT Operating Envelopes to FAR 25, Appendix C Atmospheric Icing Envelopes	IV 1-33
1-6	Fluidyne 22 x 22 Inch Transonic Icing Wind Tunnel	IV 1-34
1-7	An Isometric View of the BFGoodrich Icing Tunnel	IV 1-35
1-8	Arnold Engineering Development Center Icing Research Cell	IV 1-36
1-9	Schematic Showing Possible Streamtube Configurations for Turbofan Icing Conditions	IV 1-37
1-10	Ground and Spray Rigs	IV 1-38
1-11	C-5A Aircraft in Main Chamber at Eglin AFB McKinley Climatic Laboratory	IV 1-39
1-12	F-16 in Main Chamber at Eglin AFB McKinley Climatic Laboratory	IV 1-40
1-13	Flight Tests with Helicopter Tanker	IV 1-41
1-14	HISS Tanker Schematic	IV 1-42
1-15	Vertical Variation of Liquid Water Content Within HISS Spray Cloud	IV 1-43
1-16	Vertical Variation of Droplet Size Within HISS Spray Cloud	IV 1-44
1-17	Altitude vs. Airspeed Envelopes (HISS, KC-135, C-130)	IV 1-45

SYMBOLS AND ABBREVIATIONS

Symbol	Description
AEDC	Arnold Engineering Development Center
AGARD	Advisory Group for Aerospace Research and Development
AIAA	American Institute of Aeronautics and Astronautics
ASTF	Aeropropulsion System Test Facility
°C	Degrees Celsius
CEAT	Centre d'Essais Aeronutique de Toulouse (Icing Wind Tunnel)
CEP_r	Centre d'Essais de Propulseus (Engine Icing Tunnel)
cm	Centimeter
CRT	Cathode Ray Tube
d	Ice thickness
E	Local collection efficiency
ETF	Engine Test Facility
°F	Degrees Fahrenheit
FAA	Federal Aviation Administration
FAR	Federal Aviation Regulation
g/m^3	Grams per cubic meter
HISS	Helicopter Icing Spray System
hp	Horsepower
IRT	Icing Research Tunnel
k	Scaling factor
KIAS	Knots Indicated Air Speed
km	Kilometer
KIAS	Knots True Air Speed
kw	Kilowatt
LWC	Liquid Water Content
m	Meter
MVD	Median Volumetric Diameter
NAPF	Naval Air Propulsion Facility
n mi	Nautical mile
p	Density

SYMBOLS AND ABBREVIATIONS (CONTINUED)

Symbol	Description
PMS	Particle Measuring System
UCLA	University of California Los Angeles
μm	Microns
USAANRDL	U.S. Army Aviation National Research and Development Laboratory

GLOSSARY

glaze ice - Coating of generally clear, smooth ice deposited on surfaces exposed to a film of supercooled water. Glaze ice usually contains some air pockets.

liquid water content (LWC) - The total mass of water contained in all the liquid cloud droplets within a unit volume of cloud. Units of LWC are usually grams of water per cubic meter of air (g/m^3).

median volumetric diameter (MVD) - The droplet diameter which divides the total water volume present in the droplet distribution in half; i.e., half the water volume will be in larger drops and half the volume in smaller drops. The value is obtained by actual drop size measurements.

micron (μm) - One millionth of a meter.

rime ice - Deposit of white or milky, opaque granular ice formed by instantaneous freezing of supercooled water droplet impingement.

IV.1.0 TEST METHODS AND FACILITIES

IV.1.1 SUMMARY

Ice protection system adequacy may be examined with the use of icing simulation techniques. These techniques, both analytical and experimental, help to identify the critical icing design points for an aircraft or its components, and the experimental techniques may be used to demonstrate compliance with Federal Aviation Administration (FAA) regulations.

This chapter presents experimental and analytical methods used for icing simulation. The capabilities of these techniques are described, along with information to aid users in their application.

Four types of facilities are used to provide experimental icing simulation. These are: icing wind tunnels, engine icing test cells, ground spray rigs, and tanker spray aircraft. The differences among these facilities are in their size, aerodynamic characteristics, spray capabilities, and types of components that can be tested. All of these facilities generate an icing cloud by injection of water into a cold airstream via spray nozzles. Both water and pressurized air may be heated to preclude freezing in the spray nozzles or plumbing. Although the spray nozzles may differ from facility to facility, a calibration of water flow rate and droplet size are usually available at the facility. To cover as large a portion as possible of the FAR 25, Appendix C envelope throughout the airspeed range of the facility requires water and air spray pressure changes, or changes in the number and/or types of spray nozzles. Generally, adequate coverage with a uniform spray cannot be achieved by pressure changes alone; the spray nozzle types, numbers and/or geometries must be varied. This applies to all four types of facilities. Changing spray nozzles lengthens the testing program by causing delays during testing. Changing spray nozzles will change, sometimes drastically, the degree and spatial extent of cloud uniformity.

The droplets should reach the test model with the droplet size undiminished by evaporation, but with sufficient flow length so that the droplets have time to reach a temperature approximately equal to that of the air. This calls for location of the spray nozzles well upstream of the test object and high humidity in the air stream. It is easier to achieve these conditions in a wind tunnel than in atmospheric testing.

A review of experimental techniques and types of testing is presented in Sections IV.1.2, IV.1.3 and IV.1.4. Factors affecting icing simulation are discussed for each technique. The instrumentation requirements and the type of data obtainable from each technique are presented. A list of existing icing test facilities is provided for each facility type.

IV.1.2 ICING WIND TUNNELS

1.2.1 Introduction

Icing wind tunnels are equipped with a droplet spray system and a means for cooling the air to produce simulated supercooled clouds for icing tests. A droplet spray system, located upstream of the test section, is used to produce a simulated cloud having known droplet diameters and liquid water content (LWC). Tunnels are equipped to control airspeed and (usually) air temperatures in the test section. Some open return tunnels depend on ambient temperatures near or below freezing. These provide no air cooling or a reduced refrigerating capacity. Some icing tunnels are specifically equipped for turbine engine testing. These provide the airflow, air temperature, air pressure, exhaust gas outflow and droplet clouds necessary to test engines under simulated operating conditions. See figure 1-1 for examples of the types described herein.

Icing tunnel testing is often the least expensive and most comprehensive method for determining the performance of ice protection systems. The costs include tunnel fees, model construction and transport, instrumentation, data reduction, and crew travel and living costs. These are usually less than the cost of aircraft flight tests, especially if difficulty is experienced in finding atmospheric icing conditions. Refrigerated icing tunnel tests can be scheduled in all seasons. Both meteorological and flight variables can be controlled and maintained at steady state conditions. Measurements can be made which would be very difficult in flight, e.g., the aerodynamic forces and moments on a component or section of the aircraft. Observation of icing and de-icing phenomena is usually better than in flight, and photography is easier. Model modification and retesting can be more quickly accomplished.

Offsetting these advantages are several limitations. Test section sizes usually limit aircraft testing to scale models or full scale portions of the aircraft. Scale model testing in icing conditions requires the use of scaling techniques to interpret the test results for the full-scale aircraft. Scaling techniques are discussed in Section IV.2.

Truly uniform and low turbulence cloud simulation is very difficult to achieve by spraying water from nozzles into an airstream. Nonetheless, tunnel conditions are ordinarily more uniform both spatially and temporarily that those encountered in flight. Some argue that ice shapes may differ to an unknown extent from those in flight at nominally similar conditions. Heat transfer may be increased by tunnel turbulence (although the evidence is conflicting - see, for example, reference 1-1), in which case tunnel tests may be considered to give a conservative result for thermal ice protection.

A continuing concern is the degree of agreement in cloud measurement methods from one facility to another. One would hope that approximately equal ice accretions would occur in two different facilities if tunnel conditions were stated to be equal between the two facilities. This is not always the case, in part because different types of instruments and procedures are used in the calibration of

different facilities (references 1-2 and 1-3). A common calibration, even for the major facilities in the United States, does not yet exist.

Because of its relative simplicity, the icing blade (reference 1-3) is still used for calibration of LWC in a number of tunnels. The icing blade is a manually operated and measured device. It consists of a metal bar, 1/8 x 3/4 inch (3 x 19 mm) in cross-section and several inches long. It is tapered to form a sharp edge and then mounted in the airstream with the blunt 1/8th-inch-wide edge facing the flow. Such a thin, two-dimensional object has an ice collection efficiency of nearly 100% for a wide range of droplet sizes and airspeeds. (The actual collection efficiency can be calculated by a particle trajectory and impingement code.) The blade is mounted in a shield and is extended for exposure to the droplet flow for a short time, typically 30 seconds. The tunnel air temperature is reduced to insure rime ice collection for the test. For most icing test facilities this is an acceptable calibration procedure, since LWC is independent of air temperature. The collected rime ice is found to grow at almost constant width on the blade, indicating high collection efficiency. Its thickness is measured and LWC is calculated from known airspeed and collection efficiency.

Currently available icing wind tunnel facilities are presented and discussed in the following paragraphs. These include government, industrial, and foreign tunnels. The capabilities of these facilities, their limitations, and test techniques are also presented. Reference 1-2 provides additional description of icing tunnel facilities.

1.2.2 Icing Wind Tunnel

Data on tunnels available in North America are given in table 1-1. Data for a limited number of foreign icing tunnels are given in table 1-2. None of the tables in this section reflect changes since 1987.

1.2.2.1 NASA Lewis Research Tunnel

The largest refrigerated tunnel in the world is the Icing Research Tunnel (IRT) at the NASA Lewis Research Center in Cleveland, Ohio. The information which follows reflects the tunnel performance and capability following the major rehabilitation which it underwent in 1986 and 1987 and the subsequent recalibration (reference 1-5). However, data on the IRT listed in table 1-1 does not reflect changes due to the rehabilitation and recalibration.

The IRT, a closed-return atmospheric-type tunnel with rectangular cross sections, is equipped to support testing of low-speed models (reference 1-6). A schematic of the tunnel, shop, and control room is given in figure 1-2. The test section is 6 feet high by 9 feet wide by 20 feet long (1.83 meters by 2.7 meters by 6.1 meters). Airspeed is varied by changing the rotary speed of the fan, which is driven by a 5,000 hp (3,730 kw) motor. The fan, a fixed-pitch, 12-bladed fan fabricated from laminated Sitka spruce, has a diameter of 25.17 feet (7.67 meters) and maximum rotational speed of 460 rpm. Fan speed can be accurately controlled to within ±1/2 rpm of the desired value and

can be ramped from 50 to 460 rpm. Airspeed in the empty test section varies from 50 to 300 mph (80.5 to 483 km/hr). Maximum airspeed with a model installed depends on model blockage; for a "typical" model it is 250 mph (402.5 km/hr). The temperature range for air is controlled between -20 and 28 °F through the utilization of a heat exchanger and refrigeration plant. The tunnel is operated at atmospheric pressure. The test chamber and control room are in an air tight building which requires entry and exit through an air lock when the tunnel is operating.

The spray system, located in the plenum upstream of the test section, has eight bars and is supplied with demineralized water and filtered, compressed air. Both water and atomizing air are heated to 185 °F (85 °C) to avoid freezing in the spray nozzles or manifold and to supply supercooled, but not frozen droplets to the test section. (It is believed that some droplet freeze-out may occur at high nozzle air pressures due to the temperature decrease of compressed air as it undergoes an isentropic expansion while exiting a nozzle (references 1-7 and 1-8).) Two different nozzles, referred to as "standard" and "mod-1," are used (reference 1-7). Both are air-assist atomizers (meaning that air is used to break up the water stream) and they differ only in the diameter of their water tubes, that of the mod-1 nozzle being smaller. This results in a reduced water flow and droplet size for the mod-1 nozzle when compared to the standard nozzle at the same condition and allow operation of the tunnel at the low liquid water contents which are frequently requested. During the recalibration of the IRT water flow coefficients were determined for all standard and mod-1 nozzles and then averages were computed for the two types. All nozzles used in the spray system have flow coefficients within ±5 percent of the average coefficient for that nozzle type (standard or mod-1).

All eight spray bars configured with an array of nozzles are used to develop a uniform test section icing cloud. The configuration of standard nozzles contains 94 nozzles and that of mod-1 nozzles contains 95 nozzles. Figure 1-3 shows the cloud uniformity plots for the standard and mod-1 nozzles at an airspeed of 145 mph (233.5 km/hr). The uniform LWC area is defined as the area where the LWC is within 20 percent of the center value. Note that at 145 mph the uniform LWC area for the standard nozzles is approximately 3 feet by 4 feet (.91 meters by 1.22 meters) while that for the mod-1 nozzles is approximately 2 by 3 feet (.61 meters by .91 meters). Cloud uniformity improves as the airspeed is lowered, so that at 70 mph (112.7 km/hr) the cloud is uniform over much of the test section for the standard nozzles. On the other hand, as the airspeed is increased the uniform area shrinks and is only 1.5 feet by 2.5 feet (.46 meters by .76 meters) at 220 mph (354.2 km/hr) for the standard nozzles.

The LWC in the IRT ranges from 0.2 to 3.0 g/m^3, with values under 0.5 g/m^3 possible only with the mod-1 nozzles. However, the LWC achievable decreases with increasing tunnel airspeed as does the size of the uniform LWC area. MVD ranges from 10 to 40 μm but the mod-1 nozzles are judged to be unreliable at droplet sizes below 14 μm.

Figure 1-4 shows the LWC-MVD envelopes for tunnel airspeeds of 100 mph (161 km/hr), 150 mph (241.5 km/hr), and 250 mph (402.5 km/hr). This figure well illustrates the dependence of tunnel

operating envelopes on airspeed as well as the relationship between achievable values of LWC and MVD. Figure 1-5 shows the operating envelopes of the IRT at 100 mph and 250 mph from figure 1-4 now superimposed on the FAA atmospheric icing envelopes from FAR 25, Appendix C.

Turbulence levels have been measured by hot wire anemometry. For dry air flow, turbulence levels do not exceed approximately 0.5% in the test section. Adding the nozzle air flow (i.e., spray bar pressure on but without water flow) does not increase the turbulence for airspeeds above 150 mph (241.5 km/hr), but the turbulence rises when the airspeed is decreased below this value with the turbulence intensity reaching 3.5 percent at 34 mph (37.03 km/hr) (reference 1-6). Turbulence measurements are difficult in the presence of droplet flow and have not been reported, but the indications are that turbulence is further increased when the water spray is added. Note that an acceptable turbulence level for icing simulation has not been defined and that a level which is completely acceptable for aerodynamic force measurements may not give acceptable ice shape simulation. Tunnel turbulence originates from vibrations or pulsations from the tunnel propeller, from turning vane wakes, from wall roughness or vibration, and from spray nozzle supports and water injection (reference 1-9).

A problem with testing in the IRT, and, indeed, in icing wind tunnels in general, is the collection of a very thin frost layer on the aft parts of the airfoil. Such a frost layer does not normally form during flight in a supercooled cloud. It is argued in reference 1-10 that this frost is due to tunnel turbulence, which is about an order of magnitude greater in an icing tunnel than the comparable freestream turbulence encountered in flight. However, a series of airfoil tests in the IRT reported in reference 1-11 resulted in frost on the lower surface only (varying in extent from the first 30 percent of the airfoil to the entire lower surface). It is not clear why the frost would appear only on the lower surface if its primary cause is tunnel turbulence.

Some "before-and-after-frost-removal" measurements reported in reference 1-10 indicated that the frost layer can have a large effect on the drag coefficient when the drag rise due to the ice is small (as may be the case for rime ice), but a much lesser effect drag rise due to the ice is large (as may be the case for glaze ice). However, before and after measurements made in the later study reported in reference 1-11 indicated that the major effect of the frost was an increase in pitching moment, changes in lift and drag due to the frost being less dramatic. Thus the effect of the frost on aerodynamic coefficients is not entirely clear, and perhaps, as reference 1-10 puts it, "to be on the safe side all aerodynamic measurements" should be made "with the frost removed."

The test section has a turntable on the floor which can rotate models ±20° during tests. Models are generally mounted on the turntable with a ceiling pivot. Large models can be lowered into the tunnel by a crane through a 12 feet by 4 feet (3.66 meters by 1.22 meters) hatch in the roof of the test section. Heated windows on each side and in the roof provide good vision for photography. Video cameras and monitors are available.

The diffuser section of the IRT has been used in the past to perform a limited amount of testing. However, measurements indicated that the flow quality was highly nonuniform and NASA has

undertaken a study (references 1-12 and 1-13) of the flow characteristics of the diffuser which it is hoped may suggest methods to improve the flow quality. This would permit the wider used of the diffuser as a second, larger, but lower speed, test section.

Auxiliary services available include AC (110 and 220 volt) and DC (12 and 28 volt) electric power, heated air and a vacuum pipe with a mass flow measuring system for engine exhaust simulation. Users provide their own models, test engineers and technicians; NASA provides tunnel operators and assistance in installing models. Due to the electric power demand of the refrigeration unit, testing is normally scheduled at night. The facility is available for industry use, contingent upon scheduling and priority given to government contractors. It is advisable to contact the IRT facility manager at least 1 year in advance of desired test time in the facility to permit NASA Lewis to review the proposed model design and test envelope. Prospective users should mail correspondence to:

NASA Lewis Research Center
Attn: David W. Vincent, M.S. 6-8
IRT Facility Manager
NASA Lewis Research Center
21000 Brookpark Road
Cleveland, Ohio 44135

1.2.2.2 Industrial Icing Tunnels

Several tunnels owned by industrial firms in North America are available for icing tests. None of these are comparable in size to the NASA Lewis IRT, but they can be useful in testing instruments or small components. Also briefly discussed in this section are Arnold Engineering Center (AEDC) Icing Research Cell and the icing tunnel of the National Research Council of Canada in Ottawa.

Lockheed Tunnel

This tunnel is located near the Lockheed-California plant in Burbank, California. Although it belongs to a private company, it is available for rental. It is a closed return tunnel, with the test section vented to atmosphere. Rotatable disks in each side wall are available for model mounting and angle change. A 200 hp electric motor drives a variable pitch, four-bladed fan. The spray system is about 20 feet upstream of the test section. The refrigerated coils are about 15 feet upstream of the spray system.

For information write:

Lockheed-California Co.
Box 551
Burbank, CA
Attn: Manager, Wind Tunnels
Bldg. 281, Plant 2, Rye Canyon

Boeing Tunnel

The Boeing icing tunnel is located at the Boeing Plant 2 near Boeing Field in Seattle, Washington. It is available for leasing.

For information on the Boeing tunnel, write:

Icing Wind Tunnel, M.S. 9R-28
Boeing Technical Services
P.O. Box 3707
Seattle, WA 98124

Fluidyne Tunnel (Reference 1-14) (Figure 1-6)

Fluidyne Engineering Corporation converted a transonic induction wind tunnel to an icing tunnel in 1985. This tunnel is fairly large (22 x 22 inches (.56 x .56 meters) and high speed (M = 0.8). It was moved outside the building to take advantage of the cold weather where maximum daily temperatures fail to reach 32°F (0°C) more than 70% of the time during December, January, and February. It relies completely on natural refrigeration. The user must work outdoors where the average annual snow fall is 43 inches (1.1 meters). The permanent snow cover during the winter months presents an inconvenience and sometimes precludes operation. Strong winds cause unsteady tunnel flow but this has been largely remedied by constructing a building with louvered walls over the inlet. Relative humidity typically varies from 60 to 90 percent, often on a daily cycle, but this is mostly overcome by the expansion of the air entering the tunnel, which shifts the air toward saturation.

Despite the above difficulties, the tunnel offers a higher speed than is available in most other facilities for icing tests. The transonic flow is induced by 64 air nozzles located just downstream from the test section. These nozzles accelerate high pressure air entraining the induced tunnel flow. The vector air, about 18,000 lb. of air at 500 psi, provides run times from 12 minutes at Mach 0.8 to 54 minutes at Mach 0.2, with altitude equivalents of 12,000 and 2,000 feet, respectively. Water is introduced into the plenum chamber by 25 air-atomizing spray nozzles. A limited degree of temperature control is achieved by adding heated air upstream of the water nozzles.

The top and bottom walls of the test section are solid while the side walls are one-eighth ventilated by four 11/16-inch horizontal slots to relieve model blockage at transonic speeds. Side walls are hinged for quick access to the test section.

LWC calibration was accomplished with rotating multiple cylinders and the icing blade; the facility is re-calibrated annually. Droplet size was measured by oil slide. Droplet size distributions were approximately Langmuir B for a MVD of 15 μm and approximately Langmuir D for an MVD of 30 μm (Section I.1.1). This was checked by Knollenberg with the PMS Axial Scattering and Forward Scattering Spectrometer Probes. Glaze ice accretion tests on a NACA 0012 airfoil gave significantly less ice than for similar tests in NASA's Icing Research Tunnel. Possible explanations are higher turbulence in the IRT or wall effects in the Fluidyne tunnel.

For information, write:

Fluidyne Engineering Corp.
5900 Olson Memorial Highway
Minneapolis, MN
55422
Attn: Icing Tunnel Manager

BFGoodrich Icing Wind Tunnel

The BFGoodrich Icing Wind Tunnel was completed in 1988 at the BFGoodrich De-icing Systems facilities in Uniontown, Ohio (reference 1-15). It is a subsonic, closed loop configuration with the refrigeration system situated in the center of the loop. An isometric view of the tunnel is shown in figure 1-7. The test section is 22 inches wide by 44 inches high by 5 feet in length. Automatic temperature control is supplied by a 200 hp rotary screw compressor and a single loop microprocessor controller; temperatures as low as -25 °F can be achieved. Tunnel airspeed up to 210 mph can be achieved through the use of a 200 hp rotary motor and an 80 inch diameter fan.

The spray system is composed of 5 equally spaced spraybars and 20 nozzles. The same "standard" and "mod 1" nozzles used at the NASA Lewis IRT are used in the BFGoodrich Tunnel. A wide range of droplet sizes and liquid water contents can be achieved (reference 1-16).

AEDC Icing Research Test Cell

The Icing Research Test Cell (R-1D) at the Arnold Engineering Development Center (AEDC), a U.S. Air Force facility near Tullahoma, Tennessee, has been used for many experimental icing studies. Although small, it has the advantage of offering control of atmospheric pressure as well as a good range of LWC and MVD. The test cell consists of a flow-metering venturi, plenum chamber, water spray system, bellmouth, removable connecting ducts, and a test chanmber. Water droplets are sprayed into the primary air stream through atomizing spray nozzles located in the plenum chamber, upstream of the bellmouth. The bellmouth terminates in an 18-inch-diameter duct that directs the conditioned air into a 3-foot-diameter test section (reference 1-17). The air is exhausted to the atmosphere either directly or through the Engine Test Facility exhaust plant (reference 1-18). Figure 1-8 depicts the facility.

National Research Council (Reference 1-19)

The Low Temperature Laboratory of the National Research Council (NRC) of Canada in Ottawa, Ontario maintains an icing tunnel that can simulate altitudes from ground level to 4.35 miles (7 kilometers). The test set is 22.5 inches by 22.5 inches (.57 meters by .57 meters) in cross section and can achieve an airspeed of 200 mph (322 km/hr). The working section can be reduced in size by using an insert, giving a cross-section 12 inches by 22.5 inches (.30 meters by .57 meters) and a maximum airspeed of 390 mph (630 km/hr). At maximum airspeed, the static air temperature can be

varied from -35 °C to 40 °C and the LWC can be varied from 0.1 to 1.7 g/m^3 (0.1 to 1.0 g/m^3 with insert). The MVD can be varied from 10 to 35 μm. For information, write:

Low Temperature Laboratory
Institute for Mechanical Engineering
The National Research Council of Canada
Montreal Road
Ottawa, Ontario, Canada K1A OR6
Attn: Icing Tunnel Manager
(Phone 613-993-5339)

Other Tunnels

The other tunnels listed in table 1-1 will not be discussed individually. The Rosemont tunnels are used for instrument calibration only and are not generally available for work outside the company. The Frost tunnel is quite small and the UCLA CLoud Tunnel is both small and of slow speed.

1.2.2.3 European Icing Tunnels

A limited amount of information concerning icing tunnels in Western Europe is given in table 1-2. Additional information can be found in reference 1-2.

1.2.2.4 Test Techniques

Required instrumentation includes pressure and temperature measurement systems to ensure correct aerodynamic conditions, plus droplet size and LWC instrumentation to ensure correct meteorological conditions. In addition, support systems are needed for collecting the desired test article data. Typically, the data acquired will consist of still photographs, motion pictures, video, pressure, and temperature surveys. A data acquisition system, often with interactive graphics capabilities, is usually available to collect and reduce data for display. Because of the size of the existing icing wind tunnels, scale models of large components and full-size parts of small components are usually tested. Obtaining aerodynamic and meteorological similarity for the scale models is difficult and in some cases impossible. An analysis of the parameters affecting the simulation must be accomplished prior to testing.

As was noted in the discussion of the NASA Lewis IRT, aerodynamic coefficients of lift, drag, pitching moment, etc., measured in icing tunnels may be misleading due to the presence of frost on model surfaces downstream of the icing limit, i.e., downstream of the ice accretion. This frost does not often appear in flight but sometimes collects on models. It has been ascribed to tunnel air turbulence and wall effects, but this has been questioned, and the causes remain unclear. For maximum confidence in force and moment coefficients, the frost should be removed by a steam spray or by brushing without disturbing the leading edge ice.

1.2.3 Engine Icing Tunnels

Test verification of engine ice protection systems in icing conditions is generally accomplished in two ways:

(1) Engine test in a sea-level facility with an artificially produced cloud.

(2) Engine test in a facility capable of simulating altitude conditions with an artificially produced cloud.

Engine manufacturers demonstrate compliance with FAA regulations by use of both methods. The discussions in Section 1.2.3.3 on icing test techniques for engines, however, are aimed at (2): tests in an altitude facility. Either type may be configured as illustrated in figure 1-1. Further discussion of method (1) is presented in Section IV.1.3, Ground Spray Rigs.

A listing of the available engine test facilities and their capabilities is given in table 1-3. The nomenclature is explained in figure 1-1. The engine icing test facilities in the U.S. may be better in some respects than the aircraft icing facilities (reference 1-20).

Testing in icing tunnels may have had a greater importance for engines than for the rest of the aircraft, according to reference 1-21. FAR Part 33 permits icing certification to be accomplished without flight in natural icing. Ground icing test facilities are used almost exclusively. The engines are exposed to natural icing during aircraft certification, but at this point is rather late to implement remedial changes in the engine design. However, engines are sometimes flight tested earlier by being carried aloft by an airplane "flying test bed" which may include natural icing encounters.

1.2.3.1 AEDC Engine Test Facility

The largest engine icing test facilities in the United States are those of Arnold Engineering Development Center (see table 1-3). The largest of these is the Aeropropulsion System Test Facility (ASTF), which has a 9 foot diameter jet. None of these test cells are dedicated solely to the purpose of icing testing; in fact, icing tests are performed in them but a small percentage of the time. The types of spray nozzles, as well as their number and their locations in the spray manifold, change from test to test (reference 1-3). Thus, the spray nozzles system should be recalibrated for LWC and MVD before testing.

For information, write:

AEDC Engine Test Facility
Sverdrup Technology, Inc.
P.O. Box 844
Tullahoma, TN 37388
(Phone 615-455-2611)

1.2.3.2 Naval Air Propulsion Facility (NAPF)

Facility 2-4 in table 1-3 lists the ten engine test cells located in NAPF, Trenton, New Jersey. Test parameters can be varied over a very wide range at NAPF. The entire FAA Continuous Maximum icing condition is covered and all but the high LWC portion of the Intermittent Maximum conditions. Velocities to Mach 0.7 and MVD to 50 μM are available.

For information, contact:

Resources Manager (Phone 609-896-5655)

Naval Air Propulsion Facility

Trenton, NJ 08628

1.2.3.3 Test Techniques

Ideally, a test cell for conducting engine icing test should duplicate the flow conditions at the engine compressor face experienced by an engine in flight through an icing cloud. The proper air flow conditions at the compressor face are rarely the same as flight conditions, the air having been accelerated or diffused before entering the engine, as illustrated in figures 1-1 and 1-9. It is necessary to relate the test cell flow conditions to those at the engine compressor face, not to the free stream (flight) conditions. Selection of the correct test cell conditions to provide adequate simulation at the compressor face will, therefore, depend upon the testing technique used.

From figure 1-1B(b), the entire test cell airflow is seen by the engine compressor face when the direct connect test technique is used. Therefore, the test cell flow conditions should be set to produce the conditions existing at the engine compressor face during flight through an icing cloud; i.e., the effects of the aircraft inlet should be considered for correct simulation of LWC, droplet size, air temperature, and pressure (references 1-22 and 1-23).

The flow velocity and droplet temperatures at the engine face may not be correct for the direct connect test techniques, however. Consider the case illustrated in figure 1-9a of a descent flight mode where the flight Mach number is 0.5 and the engine inlet Mach number is 0.15. The correct Mach number to be simulated is 0.15 at the engine inlet. However, all of the test cell flow goes through the engine during direct connect testing and the duct Mach number will be less than 0.5 since the test cell connecting duct will be larger than the stream tube enclosing the airflow ingested by the engine in flight.

In addition to the Mach number simulation, it is often necessary to consider the effect of the residence time of the droplet between free stream conditions and the compressor inlet condition. As pointed out in reference 1-23, the water entering the compressor during flight will generally not be in thermodynamic equilibrium with the air. In the case of a direct connect test, however, the resident time of a droplet in the airstream is sufficient for the inlet flow to reach thermodynamic equilibrium (reference 1-22). Hence, simulation will be conducted with droplet temperatures higher than those occurring in flight.

The selection of the proper flow conditions to achieve adequate icing simulation for direct connect testing is addressed in references 1-23 and 1-24. These studies are primarily concerned with testing of anti-icing systems. The methods outlined in the references to compensate for velocity and temperature differences do not, in general, apply for power-off icing testing or de-icing studies. However, a study of icing scaling for unheated surfaces (reference 1-22) may aid in the selection of the proper flow conditions when performing de-icing studies or power-off icing tests.

The foregoing problems of velocity and droplet temperature test simulation in engine inlets are of concern only if testing is accomplished in the direct connect mode. If testing is conducted in the freejet mode, figure 1-1B(a), the velocity and droplet temperature will reach their compressor face conditions as they would during flight through an atmospheric icing cloud. Hence, the test cell condition to be set when testing in the freejet mode are the actual freestream (flight) conditions of the atmospheric icing cloud. Testing in the freejet mode is not without limitations. In general, the size and flow requirements of the facility are large. Hence, only small engine-inlet combinations could be tested in a freejet. An exception is the General Electric Facility in Peebles, Ohio, but this has very limited airspeed. Also, an accurate method for measuring thrust during freejet testing has not yet been identified. Engine performance degradation because of ice accretion would be difficult, if not impossible, to determine by freejet testing. However, the method can indeed be utilized to study the icing protection systems performance for the inlet and engine.

Additional instrumentation (over that required to support a standard engine test) is needed for an engine icing test. The additional equipment is essentially the same as for supporting wind tunnel icing tests. Pressure, temperature, and icing cloud conditions must be determined to insure proper test cell conditions are set. The photographic coverage is essential to icing engine testing since witnessing the results of an icing run, especially in the direct connect mode, is almost impossible. Documentation of engine icing test results is often in the form of video, still photographs, and motion pictures. The location and installation of the cameras in the test cell are critical to insure the desired field of view and noninterference with the icing flow field. Time correlation of photographic data with other data is essential.

A more extensive discussion of testing in engine icing tunnels is found in Chapter 6 and Appendix B of reference 1-24.

IV.1.3 GROUND SPRAY RIGS

1.3.1 Introduction

Ground spray rigs are low velocity icing simulation facilities. They can be categorized as indoor or outdoor rigs, and the spray cloud can be blown either by fan or natural wind. The large size of this type facility allows testing of the ice protection system for the entire aircraft engine-inlet. Icing tests can be conducted on large unheated surfaces such as leading edges of high lift devices to determine the probable extent of ice accumulation. Ground spray rig tests of full scale aircraft may be used in the substantiation of the critical design points, provided the spray can be calibrated to produce the design LWC and droplet diameter. The ease of access to the test article in these facilities is an obvious advantage in performing ice accumulation testing. The main disadvantages are the effects of the ground plane and the lack of high forward speeds.

1.3.2 Helicopter Spray Rigs

Figure 1-10 shows a schematic of two types of helicopter spray rigs. Table 1-4 presents the details of available ground spray rigs. At present, no indoor facility is capable of fully immersing a helicopter rotor system. Figure 1-10(b) represents the National Research Council helicopter spray rig located in an open field near Ottawa, Canada. In this case, the test helicopter hovers in the wind-blown spray. An oil slide is normally used to determine the local droplet size, and LWC is calculated from wind speed and nozzle calibration or by rotating cylinder.

Full scale rotor testing in the Ottawa spray rig has been conducted for a number of years, both for research and for ice protection system development. It has been useful as a "first look" technique for the initial proving of new de-icing systems. However, efforts to take advantage of this facility to assist in setting up electrothermal de-icing systems have produced mixed results (reference 1-25). Thus, its potential to assist in the certification process is not clear at this time.

At Mount Washington Meteorological Observatory, tests are conducted in natural icing on tied-down equipment (including helicopters in the 1950's). It has a unique electrically heated pitot-static type anemometer to monitor winds under icing conditions. Icing clouds and high winds are common from October through April. Multicylinder and impingement type instruments are used for measurement of cloud droplet size and LWC. For information contact:

Mount Washington Observatory
Gorham, N.H. 03581 Phone 603/466-3388

1.3.3 G.E. Cross Wind Engine Test Facility

The General Electric Icing Test Facility in Peebles, Ohio is basically an outdoor engine test stand located directly downstream of a large, free jet wind tunnel. The facility is unique because of its large size - the tunnel exit is approximately 30 feet (9 meters) wide - and because of its movable

thrust frame which can be rotated about its vertical centerline as necessary for crosswind and tailwind simulation testing. It has several different cloud measurement systems, including oil slides, rotating cylinders, and laser spectrometer instruments.

1.3.4 McKinley Climatic Laboratory

This facility, located at Eglin Air Force Base in Florida, has a 3.3 million cubic feet (93,000 cubic meter) Main Chamber that is the largest and most complex climatic environmental test chamber in the world. Inside dimensions are 252 ft. (76.8 m) wide, 201 ft. (61.3 m) deep, and 70 ft. (21.3 m) high in the center with an appendant floor area 60 by 85 feet (18.3 by 26 meters). In this chamber, the laboratory can produce special conditions such as rainfall to 16 inches (40 cm) per hour, winds up to 163 knots, snow, solar radiation, humidity of 10 to 95 percent, freezing rain, simulated in-flight ice accretion of different types and temperature extremes from -65°F to +165°F (-55°C to +75°C). Items varying in size from a tent to the C-5A Galaxy aircraft have been tested in this chamber.

Figure 1-11 shows the C-5A Galaxy transport aircraft undergoing testing at -40°F (-40°C) inside the main chamber. Because of the tremendous size of the chamber, more than one item can be tested at one time. On one occasion a C-5A, an F-100, and an A-7 shared the test chamber.

A distinct feature of this main chamber is an air make-up system used to cool or heat air to the test temperature and inject the air into the chamber to allow the operation of jet engines during climatic tests. Up to 650 lbs/second (295 kg/second) of air may be injected into the main chamber. Sustained engine runs at -65°F (-55°C) are possible without loss of chamber temperature.

Figure 1-12 shows a typical installation of a high performance aircraft in the main chamber. The F-16 aircraft is positioned on hydraulic jacks to afford a stable platform for tie-down. Steel cables are then secured to the aircraft. This type of tie-down allows the aircraft to be run at full afterburner thrust if necessary. Hot exhaust gases from the engine are ducted out of the chamber through a duct fitted against the tailpipe of the F-16 and extending through the wall of the chamber. Test personnel and test instrumentation are housed in the white buildings in the left portion of figure 1-12.

Icing of a number of different types of aircraft may be accomplished in the main chamber. Helicopter rotor icing can be performed by a spray frame suspended vertically in front of the helicopter, or from a frame suspended horizontally above it. Liquid water contents between 0.1 g/m^3 and 5 g/m^3 are routinely produced. Typically, a spray frame is positioned in front of the aircraft and large fans are used to blow the spray cloud toward the aircraft. Cloud velocities are normally below 60 knots. The amount of water to be injected into the flow field in order to obtain the desired LWC is determined analytically. Because of rotor wash recirculation, the icing conditions are a doubtful representation of natural icing conditions.

An icing spray frame can be seen in figure 1-12 directly in front of the F-16. The small white boxes beneath the nose of the F-16 are the transmitter and receiver of the laser spectrometer instrument that is used for in-situ measurements of droplet particle sizes and velocities.

The engine test facility is used for environmental qualification and external and internal icing of turbojet engines. The facility is supplied with refrigeration from the same system that supplies the main chamber. Permanently installed instrumentation includes equipment for recording temperatures from -70°C to +165°C, gauge lines for recording pressure at over 100 pickup points, and a vibration monitoring system.

1.3.5 Limitations of Ground Spray Rigs

Because ground spray rigs are sea level facilities, consideration of altitude pressure effects cannot be accomplished without icing scaling. Sometimes investigators vary the meteorological parameters, LWC and droplet diameter, in an attempt to compensate for altitude pressure mismatch.

Forward speed simulation is limited to the local ground-level wind velocity. Thus, helicopters can be directly tested for hover condition only. Practical limits to spray tower heights result in tests with ground effects

The outdoor ground spray rigs rely on ambient temperatures for testing. Testing must be accomplished in the "time window" in which desired temperature occurs. Since all systems - test article, instrumentation, facility - must be at the ready at all times, delays in achieving the desired temperature can increase the test costs significantly.

1.3.6 Test Techniques

The testing of a helicopter in a ground spray rig may be for the purpose of obtaining ice shapes at various positions on the rotors, verifying the engine ice protection system at hover, or determining the proper sequencing times for an electrothermal de-icing system. For the latter purpose, a common technique is to make a 30-minute run in the spray cloud while periodically cycling the de-icers at preset on-time intervals. In a typical helicopter rotor blade test (reference 1-26), this procedure resulted in 5 to 12 de-icing cycles, depending on the spray LWC. At the end of the spray period, the helicopter went through a final de-icing cycle in clear air. This is considered to be a more difficult de-icing condition because the ice temperature drops when removed from the supercooled water droplet environment, simulating emergence from a cloud under natural icing conditions. At the completion of the last de-icing cycle, the rotor was visually inspected for residual ice, runback, and general ice collection.

The required meteorological data includes LWC, droplet size, relative humidity, and cloud temperature. Measurements of these parameters are essential in assuring that the icing cloud meets the desired conditions. Documentation of the test results is often in the form of photographic coverage either from the aircraft or from remote locations. Because the icing cloud produced is large, sometimes video and motion pictures cannot cover the entire aircraft. If they are obtainable, time correlation with other data is also required.

IV.1.4 TANKER SPRAY AIRCRAFT

1.4.1 Introduction

As a part of an engine/airframe certification process, it is necessary to show that the installation is tolerant to the formation and shedding of ice. For this purpose, icing tests are conducted by flight testing in natural conditions. An alternative procedure consists of "flying" in an artificially produced supercooled droplet cloud representative of natural conditions. This procedure is sometimes used along with natural icing tests. The artificial cloud is created by numerous nozzles mounted on a spray bar manifold, which is attached to the flying boom of a tanker aircraft. This scheme was originally designed for the purpose of testing airframe de-icing systems (such as on a wing leading edge). The water pattern behind the spray bar can cover an area which adequately envelops the inlet section of most engines and major portions of other components. Sampling is done in the spray for both water content and droplet size.

The advantages of using tankers are: 1) they can be available at scheduled times in the manufacturer's locality; 2) they provide the ability to run icing tests without waiting for natural icing conditions; 3) they are less expensive than natural icing flight if time for searching is typical; and 4) increased safety of flight is achieved by the ability to easily enter and exit the icing environment. In-flight icing tests using tankers can be a useful tool in discovering any problem which may not appear in component testing and in demonstrating adequate ice protection for flight into natural icing.

A tanker spray system consists of a suitable aircraft equipped with storage tanks for water, pumps, and a spray rig with suitable nozzles to produce an airborne simulated supercooled droplet cloud. A "suitable" aircraft must match the speed and altitude of the aircraft to be tested. The nozzle must atomize the water to the desired droplet sizes and produce a cloud of acceptable uniformity. To provide icing conditions, the tanker aircraft and the test aircraft must be flown in ambient temperatures that are below freezing. Tanker aircraft have limited water storage capability so test duration is limited; see spray times in table 1-5. The cloud produced by the tanker aircraft spray system is limited in size so that usually only a portion of the test aircraft can be subjected to icing conditions at any one time.

Icing testing behind a typical helicopter tanker aircraft is depicted in figure 1-13. Such testing is not considered adequate for demonstrating full compliance with FAA regulations, but it is used for icing protection system development and for indications of critical icing design points. Ice protection systems and unprotected areas can be evaluated over a broad range of meteorological conditions at various altitudes.

1.4.2 Available Tanker Aircraft

A variety of different tanker aircraft have been developed. These include jet and propeller-powered large airplanes, large helicopters, and small general aviation airplanes. A typical tanker is equipped with a large water tank and an external spray boom. A listing of available tanker aircraft, along with their stated capabilities, is given in table 1-5.

The Helicopter Icing Spray System (HISS) carries an internally mounted 1800 gallon water tank with external spray boom, suspended 19 feet beneath the aircraft, as depicted in figure 1-14. Both the spray boom and the water supply can be jettisoned in case of emergency. The water pump delivers 125 gallons/minute at 54 lb/in^2 (pump discharge) and engine bleed air at 20 to 30 lb/in^2 (measured at the boom). Design airspeed for testing is 60 to 150 KTAS, but use of 90 KTAS is predominant; the stand-off distance is then approximately 250 feet (76 meters). The resulting cloud width is 35 to 40 feet (11-12 meters). Reference 1-27 is a useful, relatively recent report on the HISS.

The USAF C-130 is a fixed-wing tanker system with a 4 foot diameter spray ring capable of providing for in-flight helicopter or airplane testing at airspeeds above 100 KTAS (185 km/hr). The USAF KC-135 is used for test speeds above 130 KTAS (241 km/hr).

Of the described spray tankers, the HISS may provide the best natural icing cloud simulation according to reference 1-21 (p. 10).

One of the problems identified with the present stable of icing spray tankers is that the availability is more limited by organizational and jurisdictional boundaries than are the ground test facilities. For example, a well developed and proven tanker aircraft operated by one branch of the military service may not be readily available for use by other government agencies or the civil industry.

1.4.3 Limitations

With a maximum icing cloud width of 35 to 40 feet (11-12 meters), all parts of an aircraft cannot be tested simultaneously. Therefore, the icing sensors for LWC and droplet size must be located on the test aircraft near the tested components in order to measure cloud conditions during the test.

Cloud parameters and cloud consistency are difficult to maintain. The artificial cloud conditions (such as liquid water content and median droplet diameter) are dependent upon location in the cloud. Figures 1-15 and 1-16 depict the variation of LWC and drop diameter as a function of location in the cloud for a HISS tanker. Maintaining a fixed relative position behind the tanker is a challenge for the pilot. The median droplet size is generally larger in artificial clouds than natural clouds due to the difficulty of maintaining small water droplets. This is due to the rate of evaporation of droplets which changes the cloud's droplet distribution and varies with local atmospheric humidity from hour to hour. For droplets with diameters less than 25 microns, the evaporation time at 90 KIAS (167 km/hr) may be about 1.5 seconds or less, depending on the humidity. Increasing the water flow rate may produce smaller droplets but also result in an undesirable droplet distribution and excessive ice

accumulation in parts of the cloud. Small droplet evaporation makes it very difficult to simulate ice accretions of shapes and types that occur in natural icing when small droplet impingement is predominant.

Turbulence is almost always high in the spray cloud due to propeller wakes and lifting surface vortices. The turbulent water is "large" since the tanker is usually larger than the test aircraft. This results in ice limits farther downstream on an airfoil and some droplets coalescing into larger drops.

1.4.4 Test Techniques

Spray tankers are used to verify the operation of various aircraft components under artificial icing conditions. It may be useful to obtain preliminary data on the ice protection system performance and the effects of unprotected areas by tanker tests before attempting natural icing flight.

The test aircraft ice protection system is functionally checked in-flight to the test area. When the tanker is at the desired airspeed and cloud conditions, the test aircraft is moved into the cloud. For some tankers, the stand-off distance is determined from an aft facing radar altimeter on board the tanker and relayed to the crew of the test aircraft. Maintaining a constant stand-off distance is difficult if the pilot's windshield is in the cloud. The icing sensors are immersed in the cloud to measure LWC and droplet size. The desired area to be tested is then immersed for the desired length of time. The aircraft time in icing conditions is limited by the tanker's water supply or any adverse effects due to accumulated ice. A dye is sometimes added to the water to improve in-flight photography. By adjusting the bleed air pressure and water pressure, the cloud conditions can be varied (i.e., liquid water content, median droplet diameter). Ambient temperatures must, of course, be below freezing. A calibrated outside air temperature probe and a dew point hygrometer are needed to provide accurate temperature and humidity measurement.

1.4.4.1 Instrumentation

During an icing test behind a spray tanker, the following data and instruments are required:

(1) pressure altitude; altimeter
(2) airspeed; indicated airspeed indicator (usually pitot-static tubes)
(3) outside air temperature; calibrated temperature probe
(4) dew point; hygrometer
(5) liquid water content; LWC meter
(6) median volume droplet diameter (MVD); droplet sizing spectrometer (or other). This is the most difficult measurement.
(7) photographs of the critical components; still or motion picture or video cameras.

These data are required as a function of flight time in the icing cloud, so time correlation of photographic data with the other data is essential. A data acquisition system is needed to collect and reduce the data for display in near-real-time. A typical data acquisition system would include a micro-processor, a data recording system, a printer or CRT for near-real-time output, and an operator control panel.

1.4.4.2 Factors Affecting Icing Simulation

Icing testing behind a tanker aircraft is difficult to control and often requires the coordination of three aircraft. The tanker aircraft lays down an icing cloud as the lead aircraft in the formation. A chase aircraft (the second aircraft) is often used to obtain photographs, visual observations, and to aid in positioning the test aircraft vertically in the icing cloud. The third aircraft is, of course, the test aircraft, which must be held in the icing cloud at the desired position.

The location of the test aircraft in the icing cloud is vital to the success of the test. Variations in the LWC and droplet size occur both in the vertical and axial positions within the cloud. This is illustrated in figures 1-15 and 1-16. Although these two figures are for the U.S. Army's Helicopter Icing Spray System (HISS) (reference 1-28), they are representative of icing clouds produced by tanker aircraft.

The variations in LWC and droplet size make it difficult to determine if the aircraft is being tested at the desired critical condition. For example, if the test condition is selected to have an LWC of 0.9 g/m^3, figure 1-15 indicates that a difference of about 2 feet (.6 meters) in altitude from that which is desired can result in LWC varying as much as 0.8 g/m^3 from the desired value. The same type of analysis can be applied to the variation in droplet size as shown in figure 1-16.

The temperature of the icing cloud is an important meteorological parameter in setting icing conditions. Unless the tanker tests are conducted during the winter months, the desired atmospheric temperatures must be achieved by flying at altitudes that are higher than normal. Under these conditions, both the pressure altitude and humidity generally do not agree with those of a naturally occurring icing cloud. To compensate for the variations, changes should be made in the LWC and droplet size of the simulated cloud. The magnitude of the change can be calculated by the procedure of reference 1-23. However, to do so requires a prior knowledge of the pressure altitude and humidity encountered during testing. Frequently this is unknown before testing so compensation for the effects of pressure altitude and humidity are not taken into account. For this case, testing behind a tanker becomes an uncontrolled experiment, and the data acquired may not represent the critical icing design condition as originally assumed.

Altitude versus airspeed envelopes are given for several tankers in figure 1-17.

IV.I.5 SIMULATED ICE SHAPES

A method of assessing the effect of ice on the performance and handling of an aircraft is flight test in dry air with ice shapes affixed to the aircraft. These simulated shapes have been made of wood, styrofoam with fiberglass covering, and a molded plastic. The surface roughness of ice may be simulated by adding body putty or epabond to the surface (reference 1-29).

The shapes can be found from icing tunnel tests, earlier icing flight tests, or an analytical model computation. For safety, some aircraft have had the ice models attached to their wings by quick-release fasteners.

IV.1.6 REFERENCES

1-1 Poinsatte, Philip E.; Van Fossen, G. James; and DeWitt, Kenneth, J., "Convective Heat Transfer Measurements from a NACA 0012 Airfoil in Flight and in the NASA Lewis Icing Research Tunnel," NASA-TM-102448, January, 1990.

1-2 Olsen, William, "Survey of Aircraft Icing Simulation Test Facilities inNorth America," NASA-TM-81707, February 1981.

1-3 Hunt, Jay D., "Spray Nozzle Calibrations," AEDC-TR-85-65, January 1986.

1-4 Stallabrass, J.R., "An Appraisal of the Single Rotating Cylinder Method of Liquid Water Content Measurement," Report LTR-LT-92, National Research Council of Canada" 1978. (Icing Blade Method on pp. 10-18.)

1-5 Reinmann, J.J.; Shaw, R.J.; and Ranaudo, R.J., "NASA's Program on Icing Research and Technology," NASA-TM-101989, May, 1989.

1-6 Soeder, Ronald H., and Andracchio, Charles R., "NASA Lewis Icing Research Tunnel User Manual," NASA-TM-102319, June 1990.

1-7 Ide, Robert F., "Liquid Water Content and Droplet Size Calibration of the NASA Lewis Icing Research Tunnel," NASA-TM-102447, January 1990.

1-8 Marek, C. John and Bartlett, C. Scott, "Stability Relationship for Water Droplet Crystallization with the NASA Lewis Icing Spray Nozzle," AIAA-88-0209, paper presented at the 26th Aerospace Sciences Meeting, Jan. 1988.

1-9 Marek, John and Olsen, William A., Jr., "Turbulent Dispersion of the Icing Cloud from Spray Nozzles Used in Icing Tunnels," Proceedings of the Third International Workshop on Atmospheric Icing of Structures, Paper 2.8, Vancouver, B.C., May, 1986.

1-10 Olsen, W.; Shaw, R.; and Newton, J., "Ice Shapes and the Resulting Drag Increase for a NACA 0012 Airfoil," NASA TM 83556, Jan. 1984.

1-11 Potapscuk, M. G. and Berkowitz, B., "An Experimental Investigation of Multi-Element Airfoil Ice Accretion and Resulting Performance Degradation," AIAA-89-0752, paper presented at the 27th Aerospace Sciences Meeting, Jan. 1989.

1-12 Addy, H.E. and Keith, Jr., T.G., "Investigation of the Flow in the Diffuser Section of the NASA-Lewis Icing Research Tunnel," AIAA-89-0755, paper presented at the 27th Aerospace Sciences Meeting, Jan. 1989.

1-13 Addy, H.E. and Keith, Jr., T.G., "A Numerical Simulation of the Flow in the Diffuser of the NASA-Lewis Icing Research Tunnel," AIAA-90-0488, paper presented at the 28th Aerospace Sciences Meeting, Jan. 1990.

1-14 Idzorek, J.J., "Observations on the Development of a Natural Refrigeration Icing Wind Tunnel," AIAA-87-0175, paper presented at the 25th Aerospace Sciences Meeting, Jan. 1987.

1-15 Tenison, G. V., "Development of a New Subsonic Icing Wind Tunnel," AIAA-89-0773, paper presented at the 27th Aerospace Sciences Meeting, Jan. 1989.

1-16 Tenison, G. V.; Bragg, M.; and Farag, K., "A Comparison of a Droplet Impingement Code to Icing Tunnel Results," AIAA-90-0670, paper presented at the 28th Aerospace Sciences Meeting, Jan. 1990.

1-17 Riley, J. T., "Comparison Test of Droplet Sizing Instruments used in Icing Research," DOT/FAA/CT-TN90/13.

1-18 Bartlett, C. S., "An Empirical Look at Tolerances in Setting Icing Test Conditions with Particular Application to Icing Similitude," AEDC-TR-87-23, DOT/FAA/CT-87/31, August 1988.

1-19 "NRC Icing Tunnel - Technical Characteristics", unpublished notes provided by NRC.

1-20 Taylor, F.R. and Adams, R.J., "National Icing Facilities Requirements Investigation," FAA Report No. FAA-CT-81-35, June 1981.

1-21 Henschke, J.E., Peterson, A.A., Cozby, D.E., and Steele, M.A., "Rationale for Research Effort to Achieve Aircraft Icing Certification Without Natural Icing Testing," FAA Report No. FAA-CT-86/4, May 1986.

1-22 Ruff, G.A., "Analysis and Verification of the Icing Scaling Equations," AEDC-TR-85-30, Vol. 1 (Revised), March 1986.

1-23 Willbanks, C.E. and Schulz, R.J., "Analytical Study of Icing Simulation for Turbine Engines in Altitude Test Cells," AEDC-TR-73-144 (AD 770069), November 1973.

1-24 Pfeifer, G.D. and Maier, G.P., "Engineering Summary of Powerplant Icing Technical Data," Federal Aviation Administration Report No. FAA-RD-77-76, July 1977.

1-25 "Rotorcraft Icing - Progress and Prospects," AGARD Advisory Report No. 223, Sept. 1986.

1-26 Cotton, R.H., "Ottawa Spray Rig Tests of an Ice Protection System Applied to UH-1H Helicopter," Lockheed California Company, USAANRDL - TR-76-32, November 1976.

1-27 Belte, D. and Woratschek, R., "Helicopter Icing Spray System (HISS) Evaluation and Improvements," Final Report, USAAEFA Project No. 82-05-3, April 1986.

1-28 Frankenberger, C.E., "United States Army Helicopter Icing Qualifications 1980," U.S. Army Aviation Engineering Flight Activity, Edwards AFB, CA, AIAA Paper 81-0406, St. Louis, Missouri, January 1981.

1-29 Wilder, R.W., "A Theoretical and Experimental Means to Predict Ice Accretion Shapes for Evaluating Aircraft Handling and Performance Characteristics," Paper No. 5 in "Aircraft Icing," AGARD-AR-127, November 1978.

TABLE 1-1. AVAILABLE WIND TUNNELS (reference 1-2)

FA-CILITY NO.	FACILITY NAME (LOCATIONS)	TYPE OF FACILITY	SIZE (See Fig 1-1), Ft		RANGE OF PARAMETERS USED IN ICING TESTS					INSTRUMENTS USED FOR LOCAL DROP SIZE AND (LWC)	TEST SEASON
			TEST CHAMBER	UNIFORM ICING CLOUD	AIR SPEED Ft/sec (KPH)	MIN TOTAL AIR TEMP °F	ALT Ft.	LWC, g/m^3	MED VOL DROP DIA microns		
1-1	NASA - Lewis Research Center (Cleveland, OH) IRT	Wind Tunnel	H = 6 W = 9 L = 20	h = 3 w = 5	70 to 380* (80 to 420)	-30	0 to 3000	0.5 to 3.0	10 to 30+	Ext Range FSSP (Icing Blade)	All Year
1-2	Lockheed (Burbank, CA)	Wind Tunnel	H = 4 W = 2.6	h = 7.6 w = 1.0	82 to 320 (90 to 340)	-20	0	0.7 to 4.0	10 to 25	Rot. Cyls. (Rot. Cyl.)	All Year
1-3	Boeing (Seattle, WA)	Wind Tunnel	H = 1.67 W = 1.33 L = 3	h = 1.3 w = 1.0	165 to 335 (180 to 370)	-30	0	0.5 to 5.0	10 to 50 (Nozzles Changed)	Rot. Cyls., Oil Slide (Sm. Cyl.)	All Year
1-4	NRC Test Cell 4 (Remodeled 1985-86)	Wind Tunnel	H=W=1.9	h = w = 1.6	27 to 337 (30 to 370)	-40	0 to 29,500	0.2 to 2	15 to 40	Oil Slide (Rot. Cyl.)	All Year
1-5	AEDC Research Cell (Arnold AFB, TN)	Free Jet	d = 3.0	d = 1.0	137 to M=.7 (150)	-30	0 to 49,000	0.2 to 3.+	15 to 30	Various modern instruments	All Year
1-6	Rosemount (Minneapolis, MN) (a) Low Speed	Wind Tunnel	H = 0.83 W = 0.83 L = 1.0	h = 0.33 w = 0.25	80 to 335 (90 to 370)	-30	0	0.2 to 1.5	10 to 50	Oil Slide (Rot. Cyl.)	All Year
	(b) High Speed	Wind Tunnel	H = 0.83 W = 0.83 L = 2.6	h = w = .33	80 to 675 (90 to 780)	-25	0 to 10,000	0.1 to 3.0	5 to 50	Oil Slide (Rot. Cyl.)	All Year
1-7	Frost Tunnel (Univ. of Alberta, Canada)	Wind Tunnel	D = 1.6 Octogenol L = 3.0	d = 1.0	9 to 219 (10 to 240)	-20	0	0.4 to 3.0	20 to 50 (Nozzles Changed)	Oil Slide (Rot. Cyl.)	All Year
1-8	Fluidyne (Minneapolis, MN)	Induction Wind Tunnel	H = 1.83 W = 1.83	h = 1.35 w = 1.35	M = 0.25 to 0.8	Ambient	1000	0.1 to 6.0	20 to 30	Various modern instruments	Winter
1-9	UCLA Cloud Tunnel (Los Angeles, CA)	Vertical Wind Tunnel	H = 0.5 W = 0.5	h = w = .33	0 to 50 (0 to 575)	-30	0	0.1 to 3.0	2 to 50	Various modern instruments	All Year

* With Model Installed

TABLE 1-2. EUROPEAN ICING TUNNELS (reference 1-2)

FACILITY NO.	FACILITY NAME (LOCATIONS)	TYPE OF FACILITY	SIZE (Inches)		RANGE OF PARAMETERS USED IN ICING TESTS					INSTRUMENTS USED FOR LOCAL DROP SIZE AND (LWC)	TEST SEASON
			TEST CHAMBER (Inches)	UNIFORM ICING CLOUD (Inches)	AIR SPEED (knots)	MIN TOTAL AIR TEMP (°F)	ALT (feet)	LWC (g/m^3)	VOL MED DROP DIA. (m)		
E-1	Lucas Aerospace (Artington, Surrey England)	Wind Tunnel	8 x 12 to 18 x 18	80% of cross section	to 360	-40	0	0.1 to 10	12 - 90	Oil slide, other	All Year
E-2	Blower Tunnel, A&AEE (Boscomb Down, England)	Free Jet Wind Tunnel	to 96" diameter Variable	48 x 72	to 250 with small jet	about 25° below ambient	Cools air by liquid n_2 injection) 0	0 - 5	10 - 1000	Oil slide, J&W Meter	Cool, Dry Weather
E-3	Onera Tunnel S1 (Modane, France)	Induction Tunnel on Mountain	to 30 ft	80 x 80	290	Atmospheric plus water spray	3600 to 8100	0.4 to 10	10 - 30	Various	Winter
E-4	Centre d'Essais de Propulsens Saclay (ONERA) France (R-6 Cell)	Free Jet Engine Test	d = 36	d = 36	140	-40	-	0.1 - 3	15 - 30	-	All Year

TABLE 1-3. AVAILABLE ENGINE TEST FACILITIES (reference 1-2)

FACILITY NO.	FACILITY NAME (LOCATIONS)	TYPE OF FACILITY	SIZE (See Fig 1-1), m		RANGE OF PARAMETERS USED IN ICING TESTS					INSTRUMENTS USED FOR LOCAL DROP SIZE AND (LWC)	TEST SEASON
			TEST CHAMBER (Inches)	UNIFORM ICING CLOUD (Inches)	AIR SPEED km/hr	MIN TOTAL AIR TEMP °C	ALT m	LWC g/m^3	VOL MED DROP SIZE m		
2-1	ATDC (Arnold AFS, TN) (a) ETF	Direct Connect d = 1.5	D = 3.7 or 4.5 L = 11	Spray Bars Sized to Engine	0 to M = 0.7+	-30	0 to 15000	0.2 to 3. +	15 to 30	Various Modern Instruments	All Year
	(b) Free Jet	Freejet d = 1.5	D = 3.7 or 4.5	Spray Bars Sized to Engine	0 to M = 0.7+	-30 and Lower	0 to 15000	0.2 to 3. +	15 to 30	Various Modern Instruments	All Year
	(c) ASTF	Freejet d = 3.7	D = 8 L = 18	Spray Bars Sized to Engine	0 to M = 0.7+	-30 and Lower	0 to 15000	0.2 to 3. +	15 to 30	Various Modern Instruments	All Year
2-2	Detroit Diesel Allison (Indianapolis, IN) (a) Comp. Test Facility	Freejet	D = 2.3 L = 9	Spray Bars Sized to Engine	0 to M = 0.7+	-30 and Lower	0	0.2 to 3.5	15 to 40	Rotating Cylinders	All Year
		Direct Connect d = 0.5					0 to 6000				
	(b) Small Engine Facility	Direct Connect	D = 0.45 L = 1.2	Spray Bars Sized to Engine	0 to M = 0.7+	-30 and lower	0 to 6000	0.2 to 3.5	15 to 40	Rotating Cylinders	All Year
2-3	P&W Altitude Facilities (E. Hartford, CT) (a) Large	Direct Connect	D = 5.6 L = 10	Spray Bars Sized to Engine	0 to M = 0.5	-25	0 to 6700	0.2 to 9.0	15 to 40	Oil Slide	All Year
	(b) Smaller	Direct Connect	D = 3.7	Spray Bars Sized to Engine	0 to M = 0.5	-30 and Lower	0 to 6700	0.2 to 9.0	15 to 40	Oil Slide	All Year
	(c) P&W Sea Level Facility	Direct Connect	Varies With Test Cells	Spray Bars Sized to Engine	0 to M = 0.5	-20 (Ambient)	0	0.2 to 9.0	15 to 40	Oil Slide	Winter

TABLE 1-3 (Concluded). AVAILABLE ENGINE TEST FACILITIES (reference 1-2)

FA-CILITY NO.	FACILITY NAME (LOCATIONS)	TYPE OF FACILITY	SIZE (See Fig 1-1), m		RANGE OF PARAMETERS USED IN ICING TESTS					INSTRUMENTS USED FOR LOCAL DROP SIZE AND (LWC)	TEST SEASON
			TEST CHAMBER (Inches)	UNIFORM ICING CLOUD (Inches)	AIR SPEED km/hr	MIN TOTAL AIR TEMP °C	ALT m	LWC g/m^3	VOL MED DROP SIZE m		
2-4	Naval Air Propulsion Facility (Trenton, NJ) (a) Five Small Engine Cells	Freejet d = 0.6	H = W = 3 L = 6	Spray Bars Sized to Engine	0 to M = 0.7+	-30 and Lower	0 to 15000	0.1 to 2	15 to 15 (Nozzles Changed)	Knollenberg Spectrometer and OAP (Rot. Cyl.)	All Year
	(b) Two Large Sea Level Cells	Freejet d = 1.2	H = 4.5 W = 7 L = 17	Spray Bars Sized to Engine	0 to M = 0.7+	-30 and Lower	0	0.1 to 2	15 to 50 (Nozzles Changed)	Knollenberg Spectrometer and OAP (Rot. Cyl.)	All Year
	(c) Three Large Altitude Cells	Freejet d = 1.2	D = 5 L = 9	Spray Bars Sized to Engine	0 to M = 0.7+	-30 and Lower	0 to 15000	0.1 to 2	15 to 15 (Nozzles Changed)	Knollenberg Spectrometer and OAP (Rot. Cyl.)	All Year
2-5	Teledyne Altitude Cells (Toledo, OH) (a) Chamber 1	Freejet or Direct Connect d = 0.2	D = 2.7 L = 5	Spray Bars Sized to Engine	0 to M = 0.7+	-30 and Lower	0 to 15000	Up to 3	15 to 25	Oil Slide	All Year
	(b) Chamber 2		H = 2.5 W = 2.5 L = 4	Spray Bars Sized to Engine	0 to M = 0.7+	-30 and Lower	0 to 15000	Up To 3	15 to 25	Rotating Cylinders	All Year
2-6	Avco Lycoming (Stratford, CT) (a) Component Facility	Direct Connect d = 0.4	------	Spray Bars Sized to Engine	0 to 370	-30 and Lower	0	0.1 to 3	15 to 40	Oil Slide (Rot. Cyl.)	All Year
	(b) Engine Test Facility	d = 0.4	W = 3.7 H = 2.7	Spray Bars Sized to Engine	0 to 200	-30 and Lower	0	0.1 to 3	15 to 40	Oil Slide (Rot. Cyl.)	All Year
		d = 1.2	Outdoors			-20					Winter
2-7	NRC. Cell #4 (Ottawa, Canada)	Freejet or Direct Connect d = 0.76	H=W=7.5	Spray Bars Sized to Engine	0 to 650	-20 and Lower	0	0.2 to 2	15 to 40	Oil Slide (Rot. Cyl.)	Winter
		d = 2.0			0 to 93	Ambient					
2-8	Garret Icing Facilities: (Phoenix, AZ) Cell 1, Cell 2, and Cell 3	Freejet or Direct Connect d = 1.0 to .1	H = 3 W = 4 L = 10	Spray Bars Sized to Engine	M = 0.01 - 0.7	-30 and Lower	0 to 15000	0.1 to 6.0	10 to 50	Rot. Cyls. (Rot. Cyls.)	All Year

TABLE 1-4. AVAILABLE GROUND SPRAY RIGS (reference 1-2)

FACILITY NO.	FACILITY NAME (LOCATIONS)	TYPE OF FACILITY	SIZE (See Fig 1-7), m		RANGE OF PARAMETERS USED IN ICING TESTS					INSTRUMENTS USED FOR LOCAL DROP SIZE AND (LWC)	TEST SEASON
			TEST CHAMBER (Inches)	UNIFORM ICING CLOUD (Inches)	AIR SPEED km/hr	MIN TOTAL AIR TEMP °F	ALT Ft	LWC g/m^3	VOL MED DROP SIZE m		
3-1	NRC Helicopter Spray Rig (Ottawa, Canada)	Wind Blown Spray Outdoors	D =	Spray Manifold h_s = 4.5 w_s = 2.3	Ambient Wind, 20 to 45 (Gusty)	-20 (Ambient)	0	0.1 to 0.8	30 to 60	Oil Slide (Rot. Cyl.)	Winter
3-2	G.E. Cross Wind Facility (Peebles, OH)	Free Jet Outdoors	D =	d_u = 4.5	90	-20 (Ambient)	0	0.4 to 3.6	15 to 20	Knollenberg Spectrometer (Rot. Cyl.)	Winter
3-3	McKinley Climatic Lab (Eglin AFB, FL) (a) Main Chamber	Fan Blown Spray Indoors	H = 21 W = 76 L = 76	Spray Manifold h_s = 3 w_s = 9	0 to (30 to 75°) (Depending on LB)	-30 and Lower	0	0.1 to 3	12 to 60 800 to 1600 (Nozzles Changed)	Particle Interferometer (Rot. Cyl.)	All Year
	(b) Engine Test Cell	Fan Blown Spray Indoors	H = 7.5 W = 9 L = 40	Spray Manifold h_s = 3 w_s = 6	0 to (30 to 75°) (Depending on LB)	-30 and Lower	0	0.1 to 3	12 to 60 800 to 1600 (Nozzles Changed)	Particle Interferometer (Rot. Cyl.)	All Year
	(c) All Weather Room	Fan Blown Spray Indoors	H = 4.5 W = 6.5 L = 12	Spray Manifold h_s = 3 w_s = 3	0 to (30 to 75°) (Depending on LB)	-30 and Lower	0	0.1 to 3	12 to 60 800 to 1600 (Nozzles Changed)	Particle Interferometer (Rot. Cyl.)	All Year
3-4	Mt. Washington Observatory (Gorham, NH)	Natural Icing of Tied Down Equipment on Top of Mountain			0 to 180 (Gusty)	-20 and Lower	6000	Generally Severe Natural Conditions		Rotating Cylinders	Fall to Spring

TABLE 1-5. AVAILABLE TANKER SPRAY AIRCRAFT (reference 1-2)

FA-CILITY NO.	FACILITY NAME (LOCATIONS)	ICING TIME AT HIGH LWC, Min	SIZE (See Fig 1-9), m		RANGE OF PARAMETERS USED IN ICING TESTS					INSTRUMENTS USED FOR LOCAL DROP SIZE AND (LWC)	TEST SEASON
			TEST AREA	SPRAY MANIFOLD	AIR SPEED km/hr	MIN TOTAL AIR TEMP °C	ALT m	LWC, g/m^3	VOL MED DROP SIZE m		
4-1	Air Force (Edwards AFB, CA) (a) KC 135 Tanker	60	At LB = 60 d = 5	d_g = 1.2	300 to 650 (370 Nom.)	-20 (Ambient)	1200 to 8000	0.05 to 1.5 / 0.05 to 32	28 to 35	Knollenberg Spectrometer (*)	All Year
	(b) C 130 Tanker	60	At LB = 60 d = 5	d_g = 1.2	190 to 390 (280 Nom.)	-20 (Ambient)	1200 to 8000	0.05 to 1.5 / 0.05 to 32	28 to 35 Desired / 200 to 800	Knollenberg Spectrometer (*)	All Year
4-2	Army HISS Helicopter Tanker (Edwards AFB, CA)	30	At LB = 50 h = 3 w = 12	h_g = 1.6 w_g = 12	110 to 140 (120 Nom.)	-20 (Ambient)	600 to 3600	0.01 to 1.0	25 to 30 Desired	Knollenberg Spectrometer (Leigh)	Normally Winter
4-3	Cessna 404 Tanker (Wichita, KS)	60	At LB = 150 d = 6	d_g = 0.6 (V-BAR)	165 to 330 (260 Nom.)	-20 (Ambient)	300 to 8000	0.05 to 4.0	20 to 49 (Water Nozzles)	Gelatin Slide (J&W)	All Year
4-4	Piper Cheyenne Tanker (Lock Haven, PA)	14	At LB = 30 h = 3 w = 5	h_g = 1.2 w_g = 1.8	200 to 300 (240 Nom.)	-20 (Ambient)	300 to 8000	0.1 to 1.7	30 to 50	Gelatin Slide (J&W)	Not Summer
4-5	Flight Systems T-33 Tanker (Mojave, CA)	45	At LB = 60 d = 2.5	h_g = 0.3 w_g = 0.9	230 to 420 (370 Nom.)	-20 (Ambient)	300 to 8000	0.1 to 1.0	17 to 50	Knollenberg Spectrometer (*)	All Year

SCHEMATIC SKETCHES FROM SIDEVIEW

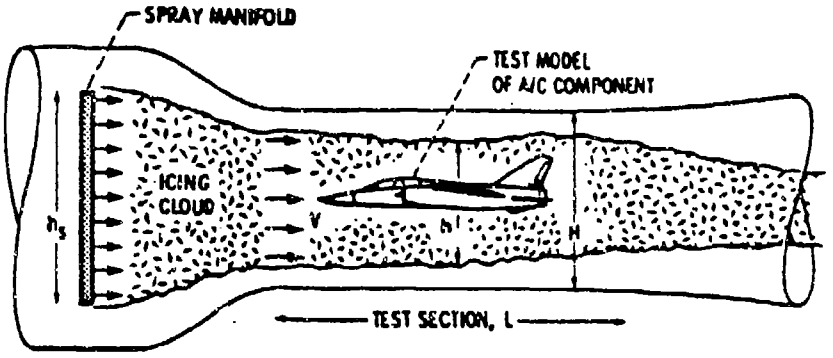

A. WIND TUNNELS

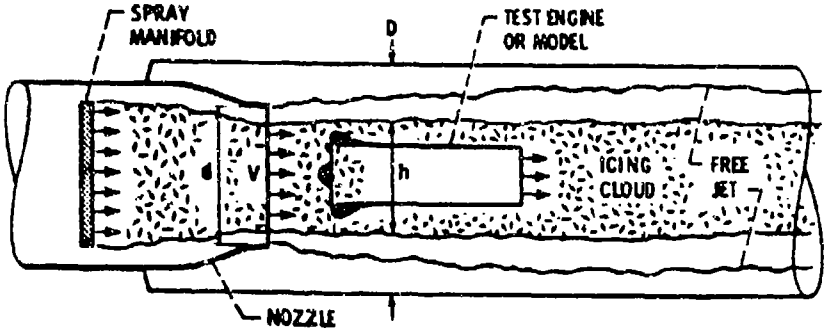

(a) FREE JET

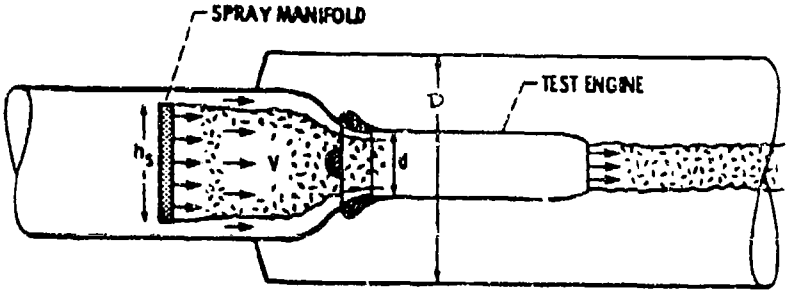

(b) DIRECT CONNECT

B. ENGINE TEST FACILITIES

FIGURE 1-1. TYPES OF ICING SIMULATION FACILITIES
[FROM NASA TM-81707] (REFERENCE 1-2)

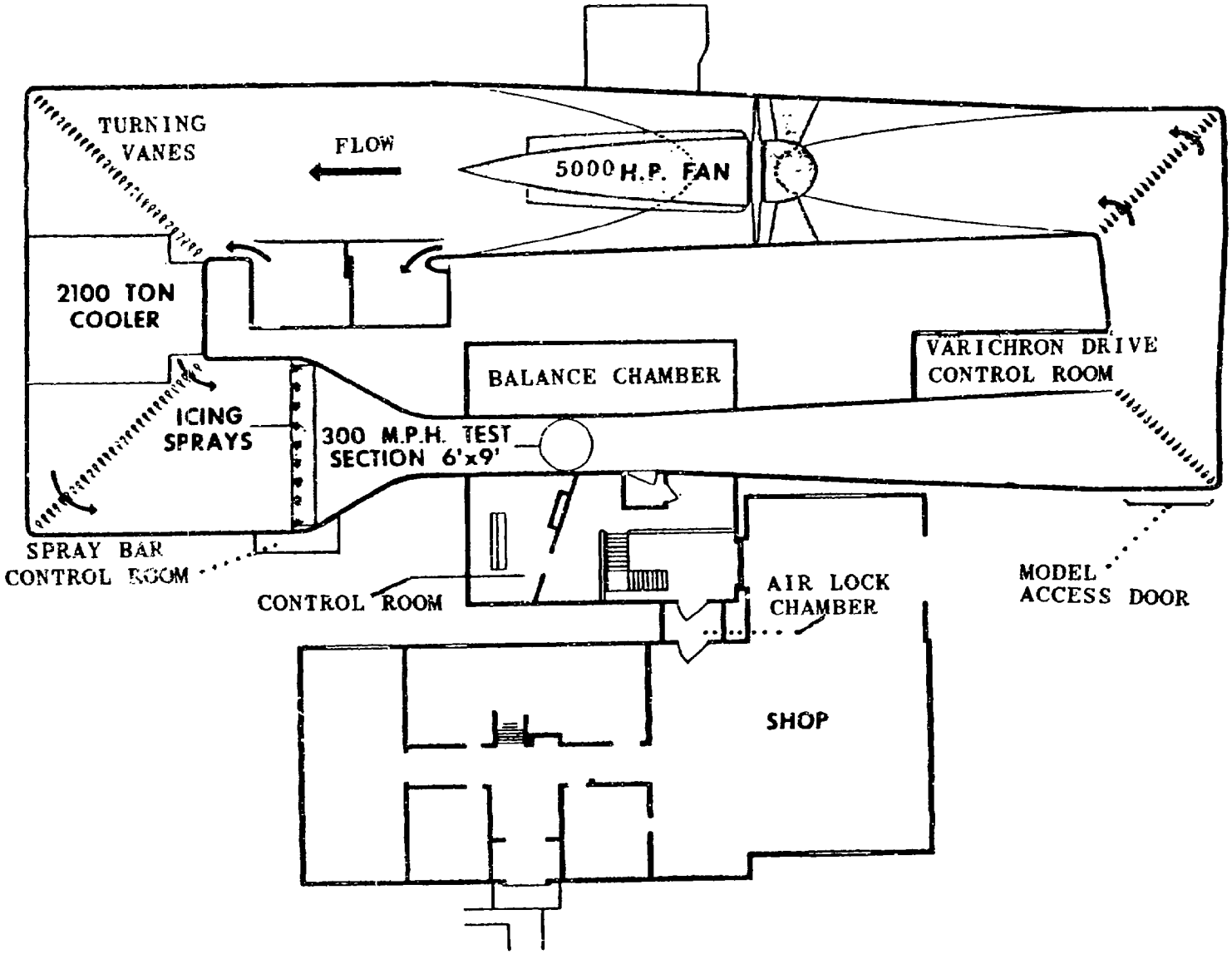

FIGURE 1-2. PLAN VIEW OF NASA LEWIS ICING RESEARCH TUNNEL FACILITY (reference 1-6)

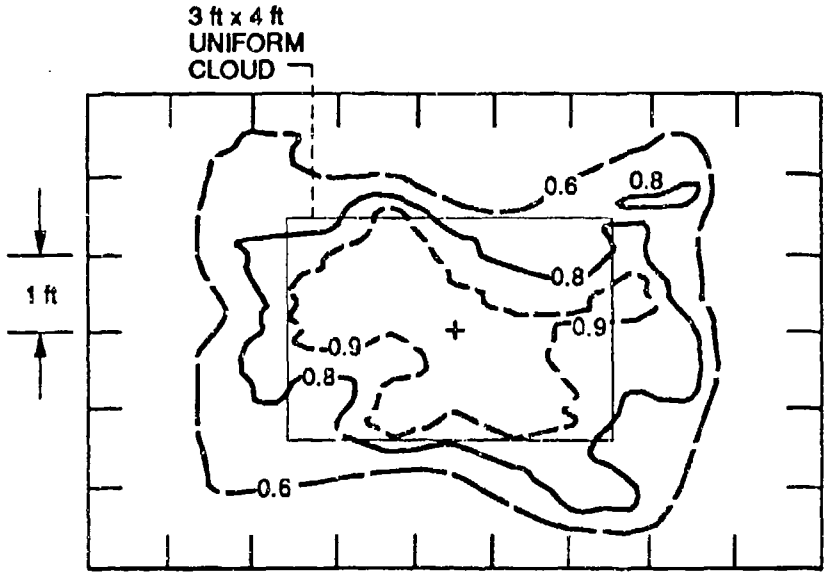

(a) Standard nozzles.

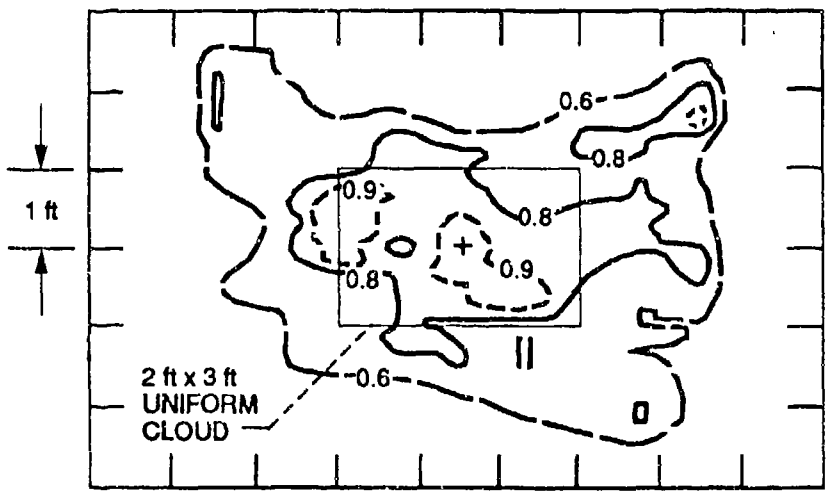

(b) Mod-1 nozzles.

FIGURE 1-3. LIQUID WATER CONTENT CONTOUR PLOTS FOR AN AIRSPEED OF 145 MPH FOR THE NASA LEWIS IRT (REFERENCE 1-7)

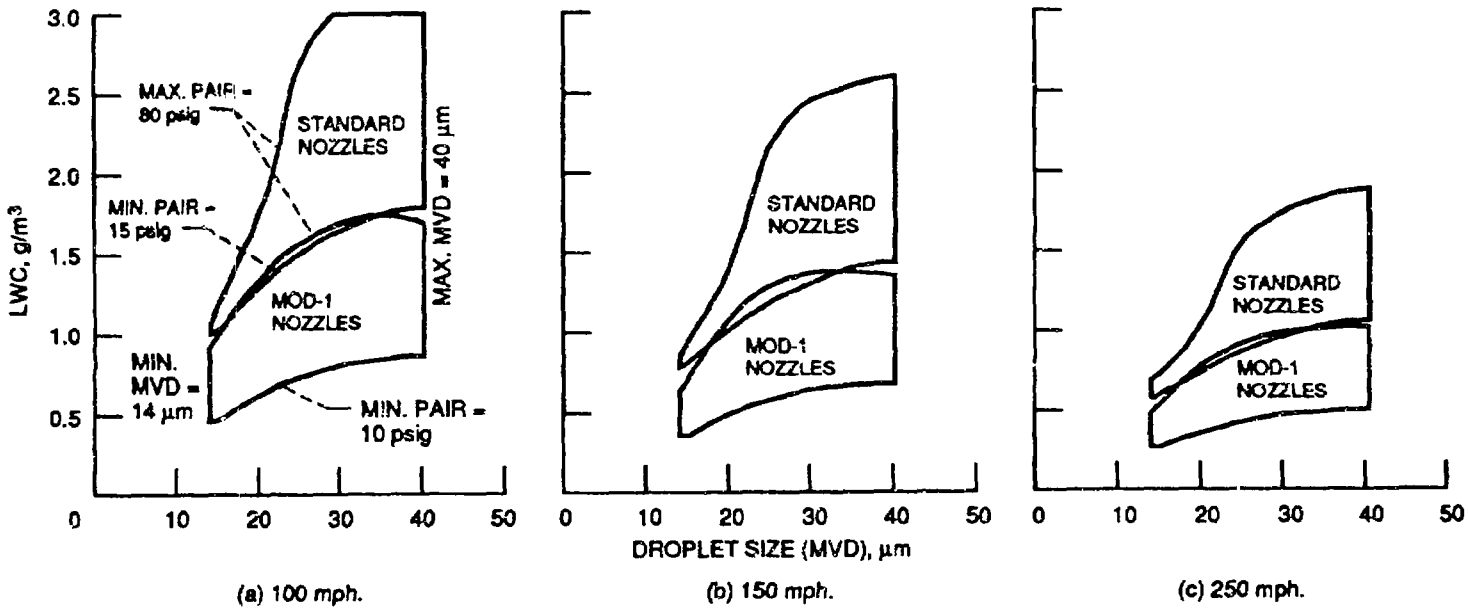

FIGURE 1-4. NASA LEWIS IRT OPERATING ENVELOPES (REFERENCE 1-7)

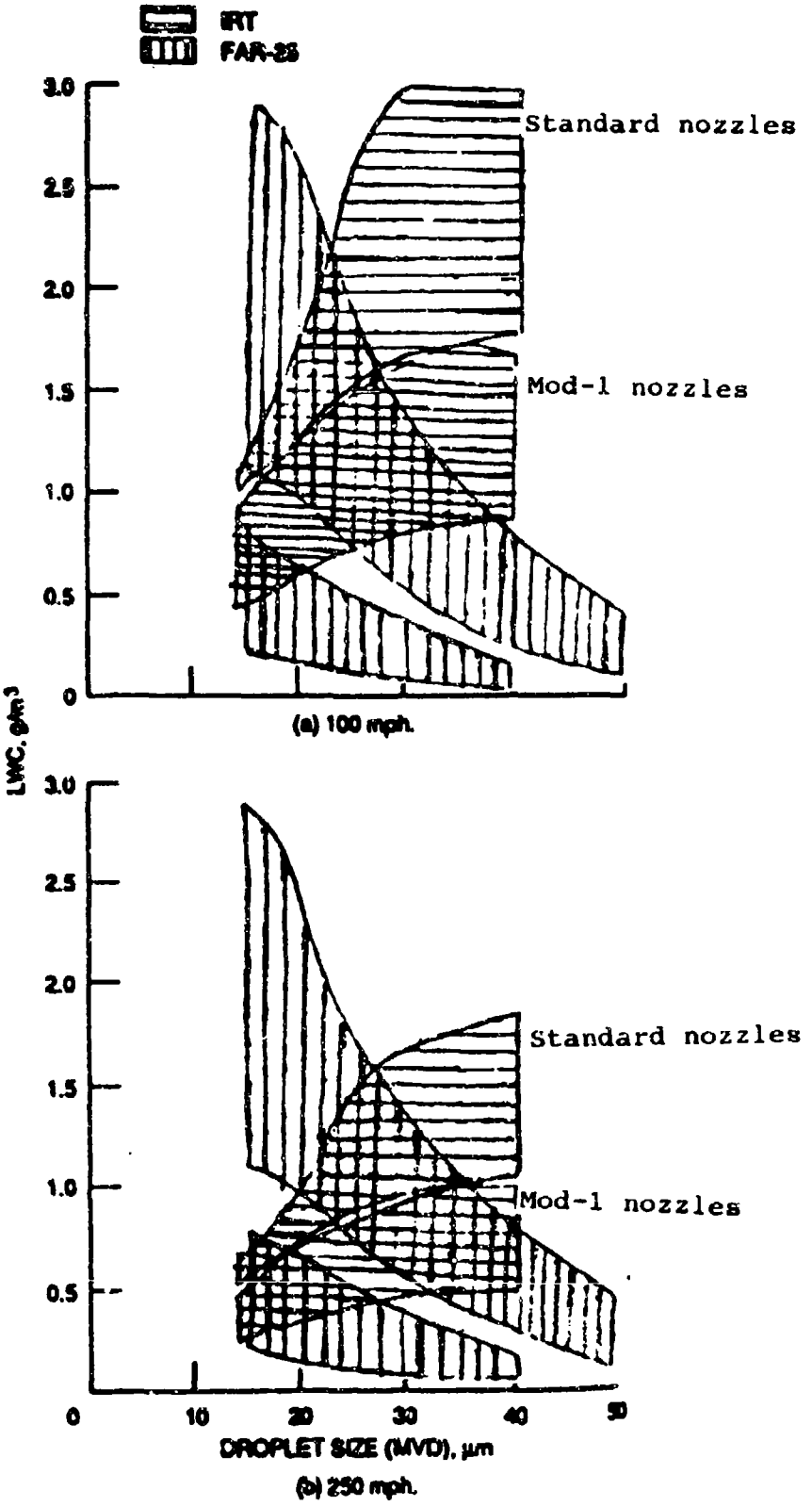

FIGURE 1-5. COMPARISON OF IRT OPERATING ENVELOPE TO FAR 25, APPENDIX C ATMOSPHERIC ICING ENVELOPES (REFERENCE 1-7)

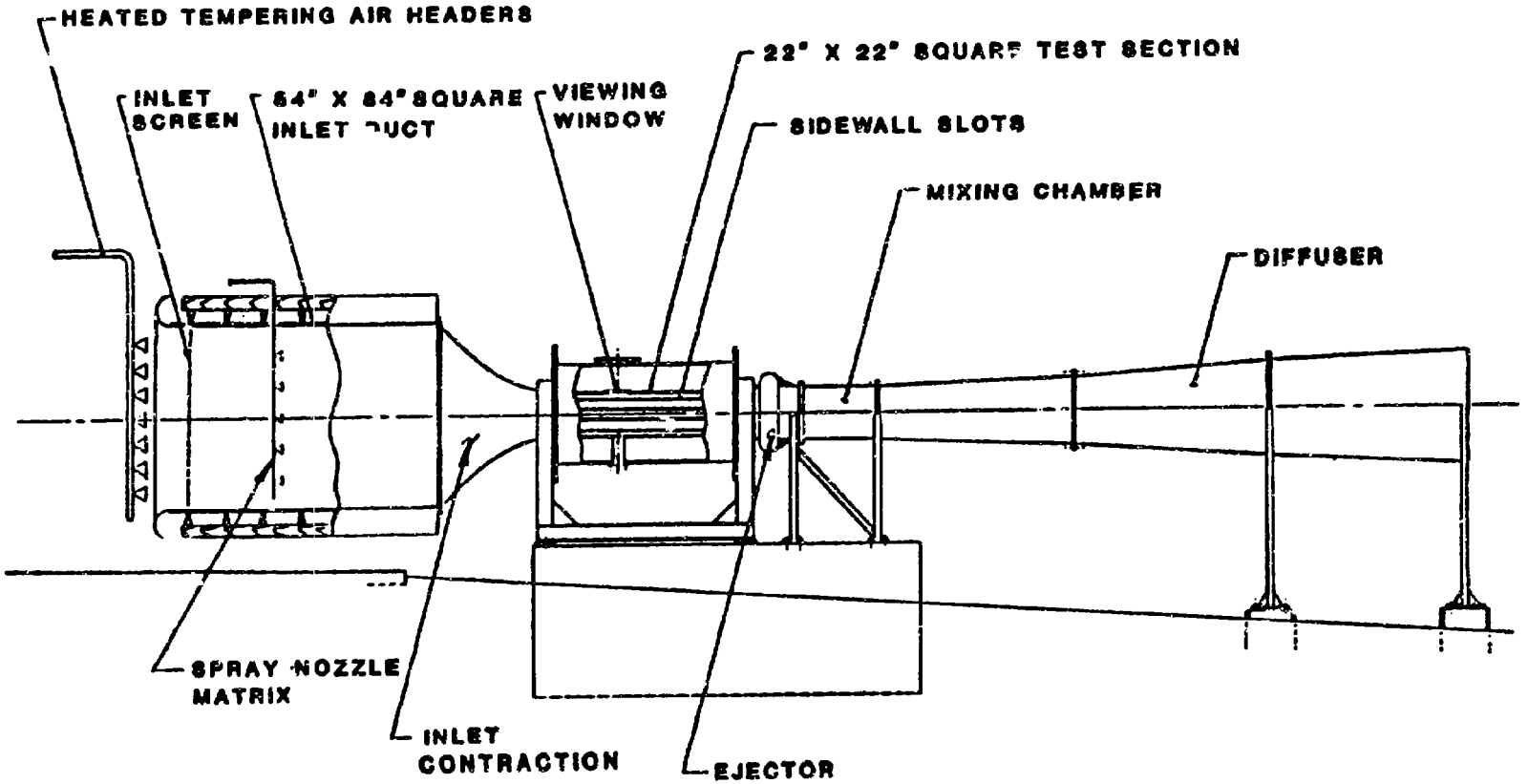

FIGURE 1-6. FLUIDYNE 22" x 22" TRANSONIC ICING WIND TUNNEL

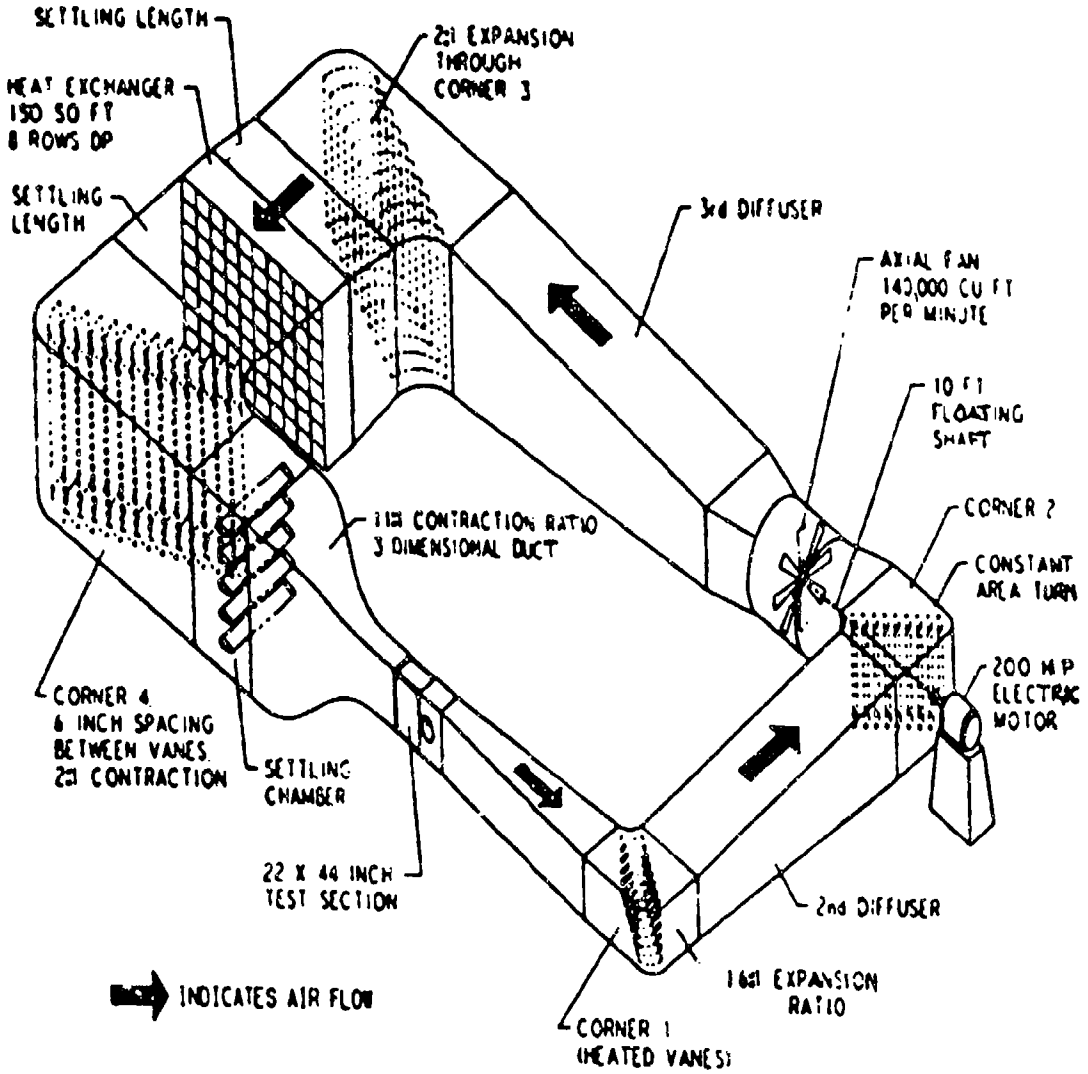

FIGURE 1-7. AN ISOMETRIC VIEW OF THE BFGOODRICH ICING TUNNEL (REFERENCE 1-15)

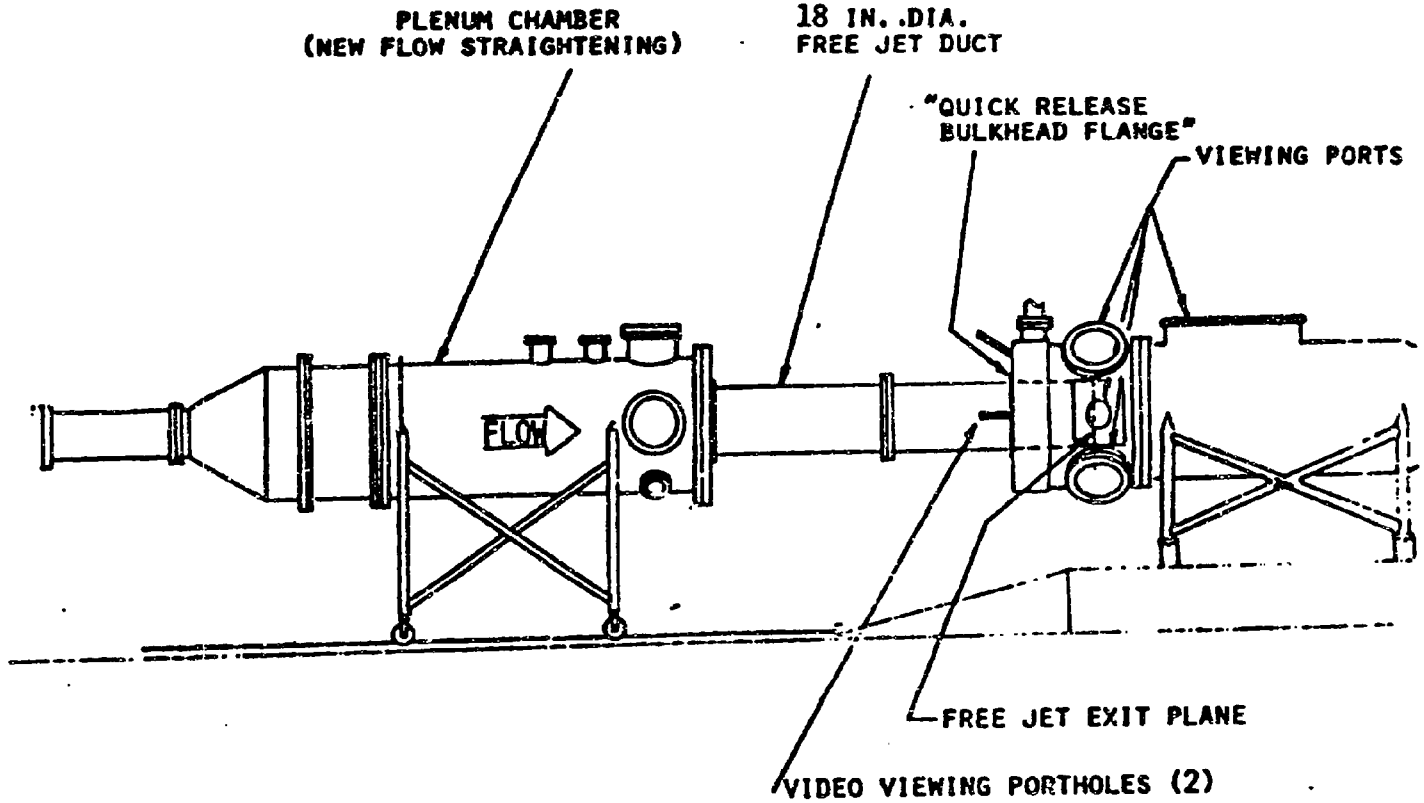

FIGURE 1-8. ARNOLD ENGINEERING DEVELOPMENT CENTER ICING RESEARCH TEST CELL (R-1D) (REFERENCE 1-17)

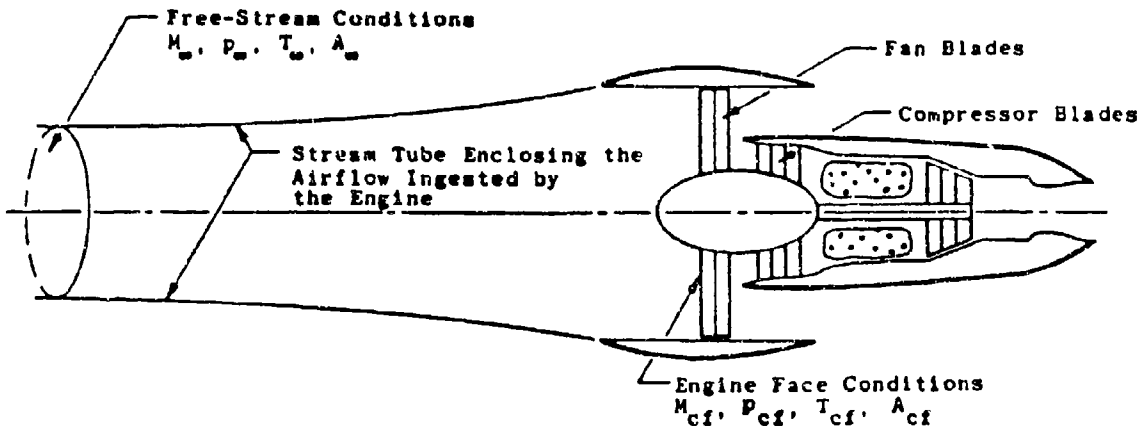

a. INLET MACH NUMBER LESS THAN FLIGHT MACH NUMBER

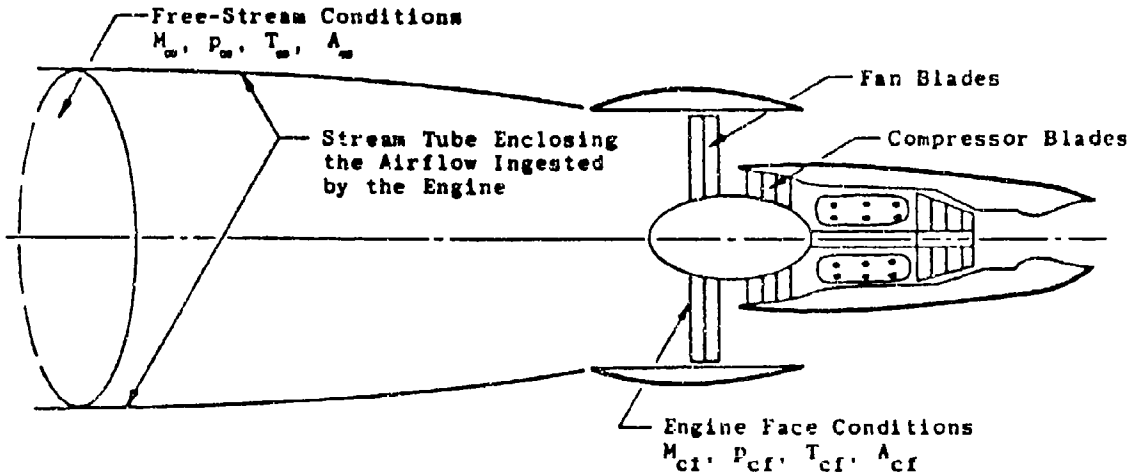

b. INLET MACH NUMBER GREATER THAN FLIGHT MACH NUMBER

FIGURE 1-9. SCHEMATIC SHOWING POSSIBLE STREAMTUBE CONFIGURATIONS FOR TURBOFAN ICING CONDITIONS
[FROM AEDC-TR-73-144] (Reference 1-23)

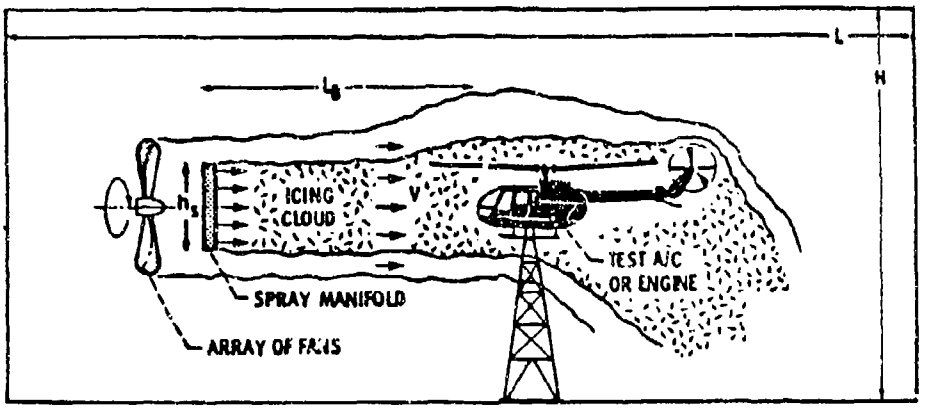

(a) FAN BLOWN SPRAY IN A LARGE ROOM OR OUTDOORS

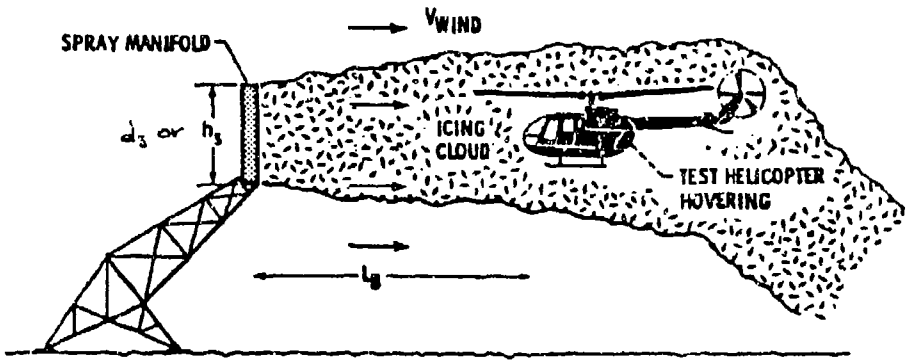

(b) WIND BLOWN SPRAY OUTDOORS

FIGURE 1-10. GROUND SPRAY RIGS

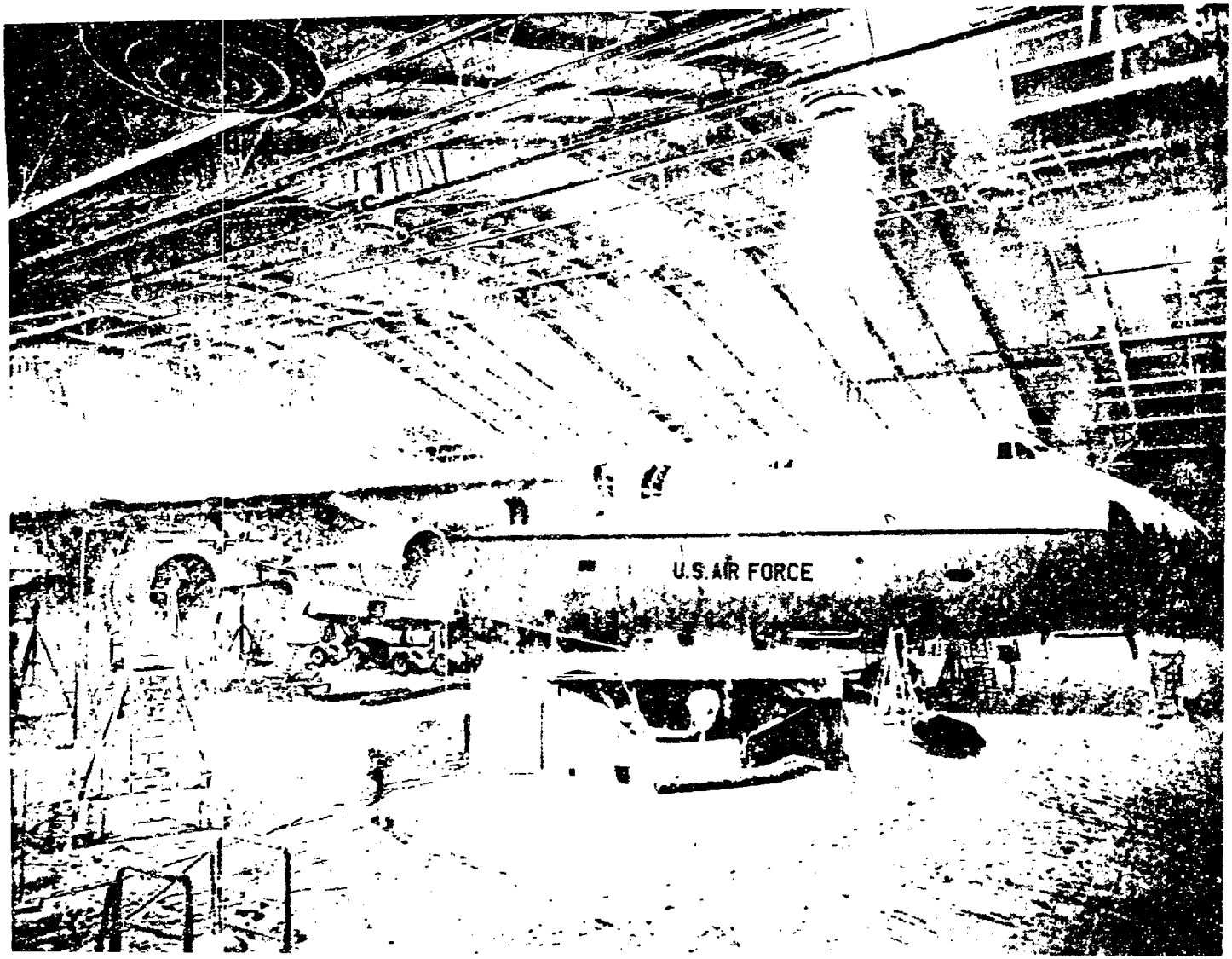

FIGURE 1-11. C-5A AIRCRAFT IN MAIN CHAMBER AT EGLIN AFB McKINLEY CLIMATIC LABORATORY

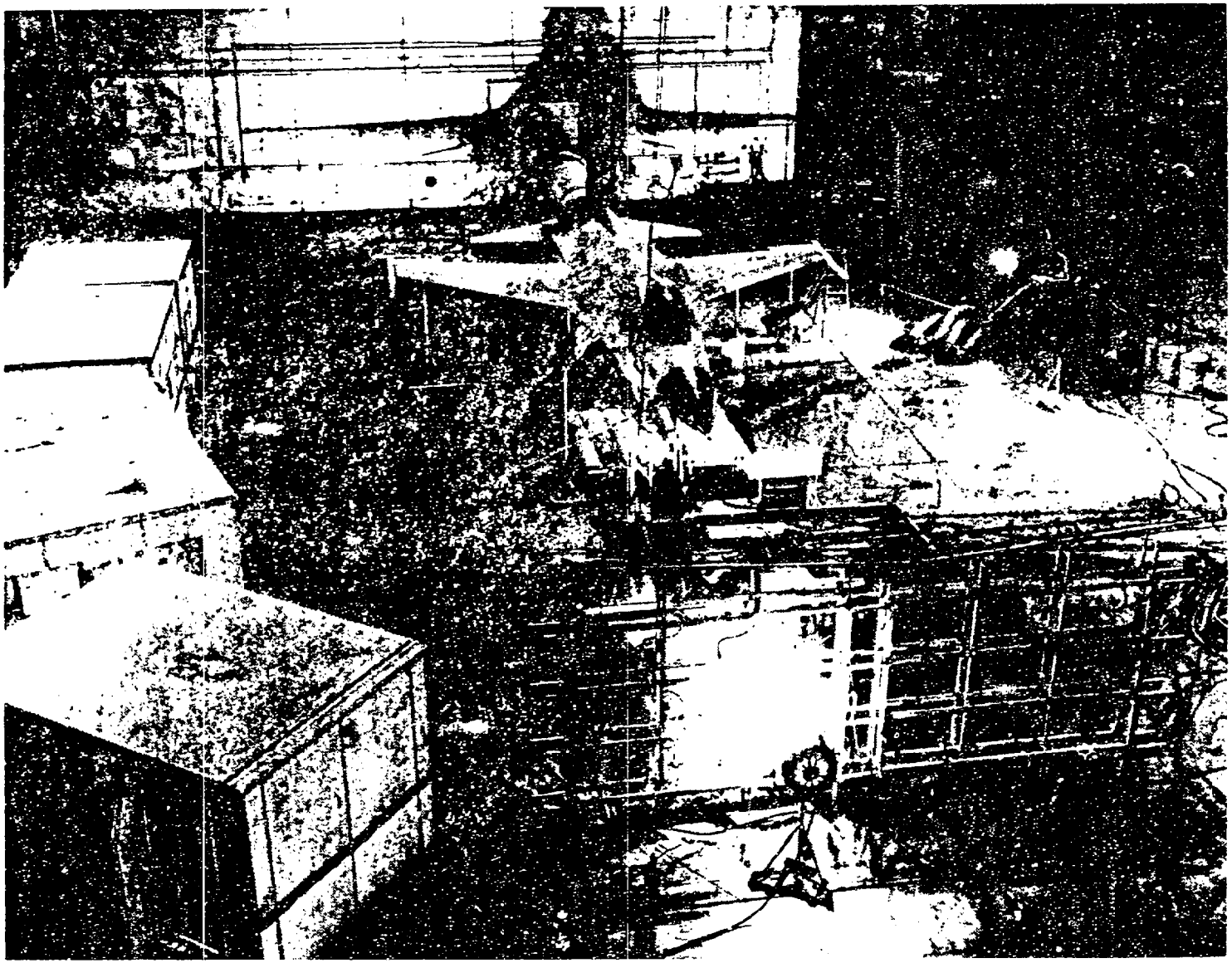

FIGURE 1-12. F-16 IN MAIN CHAMBER AT EGLIN AFB
McKINLEY CLIMATIC LABORATORY

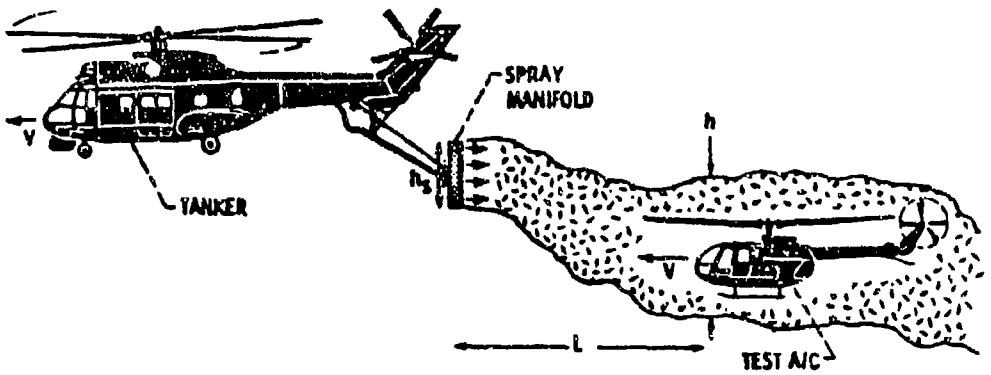

FIGURE 1-13. FLIGHT TESTS WITH HELICOPTER TANKER

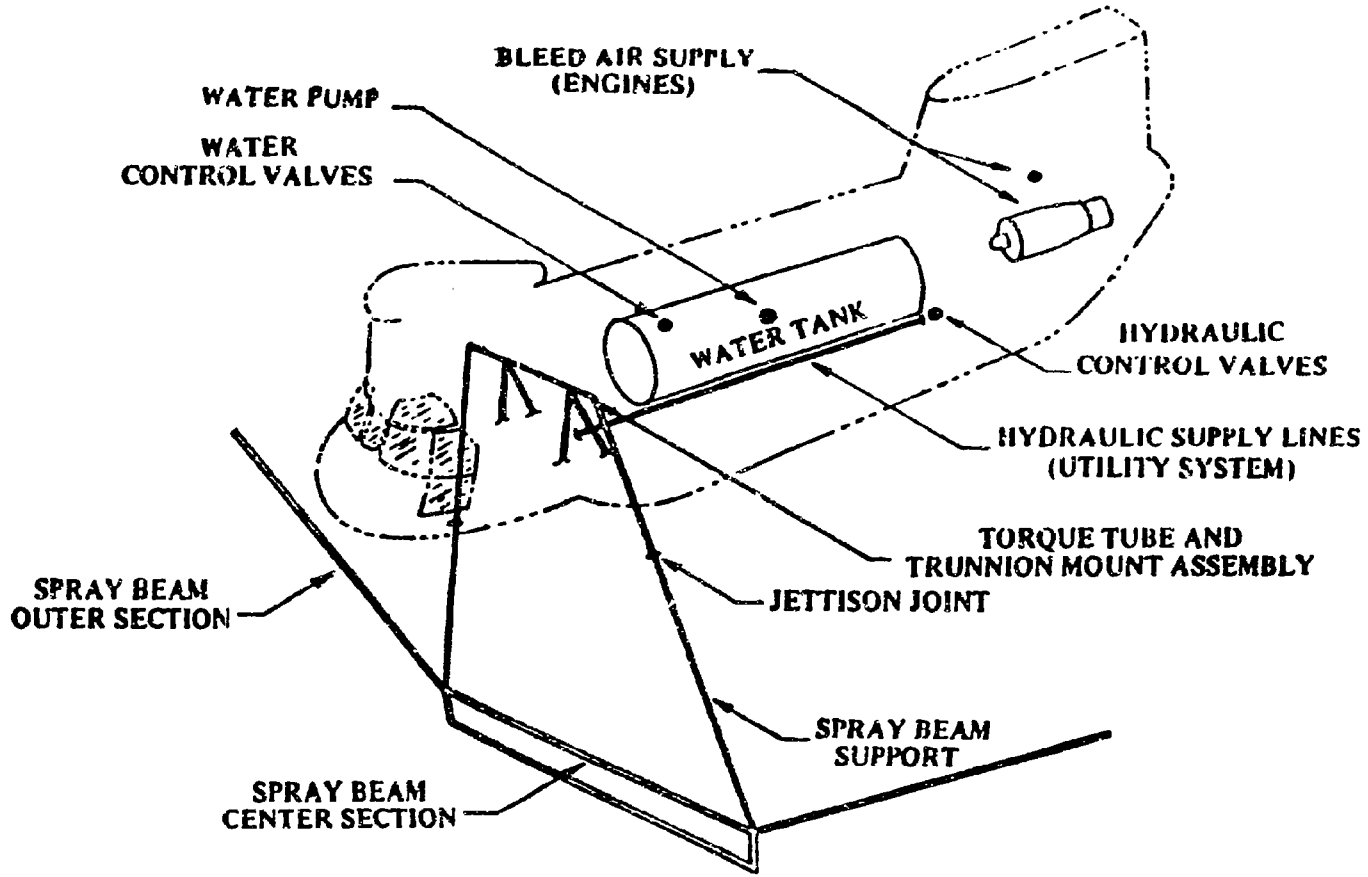

FIGURE 1-14. HISS TANKER SCHEMATIC

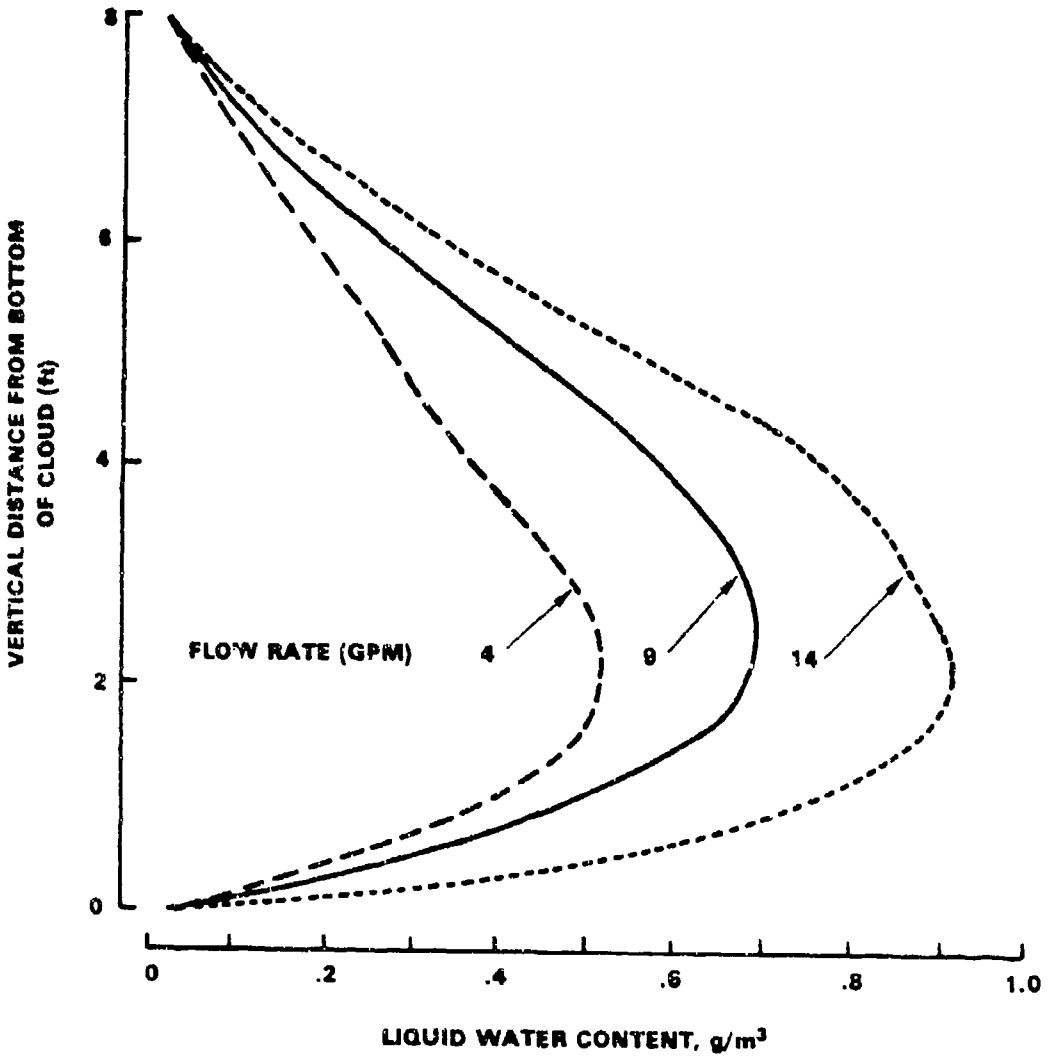

FIGURE 1-15. VERTICAL VARIATION OF LIQUID WATER CONTENT WITHIN HISS SPRAY CLOUD

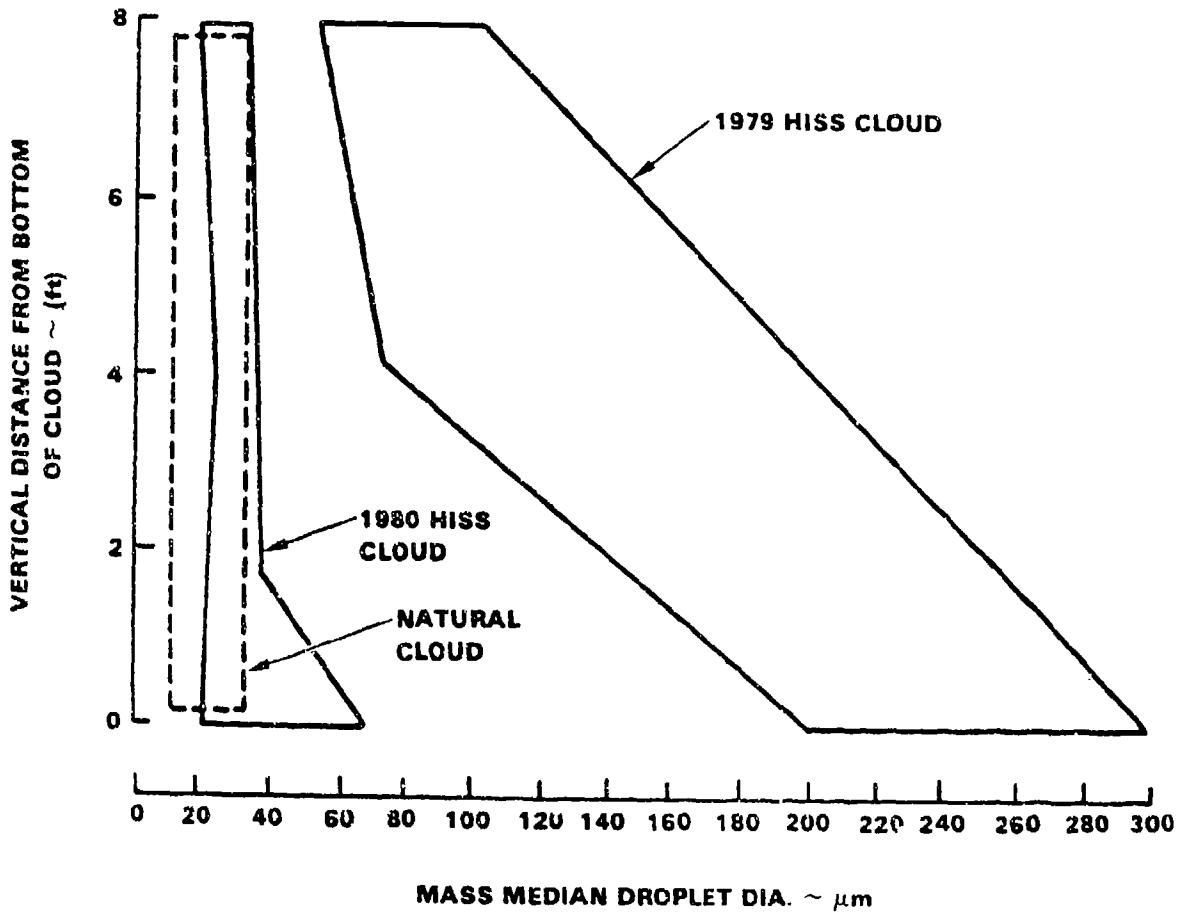

FIGURE 1-16. VERTICAL VARIATION OF DROPLET SIZE WITHIN HISS SPRAY CLOUD

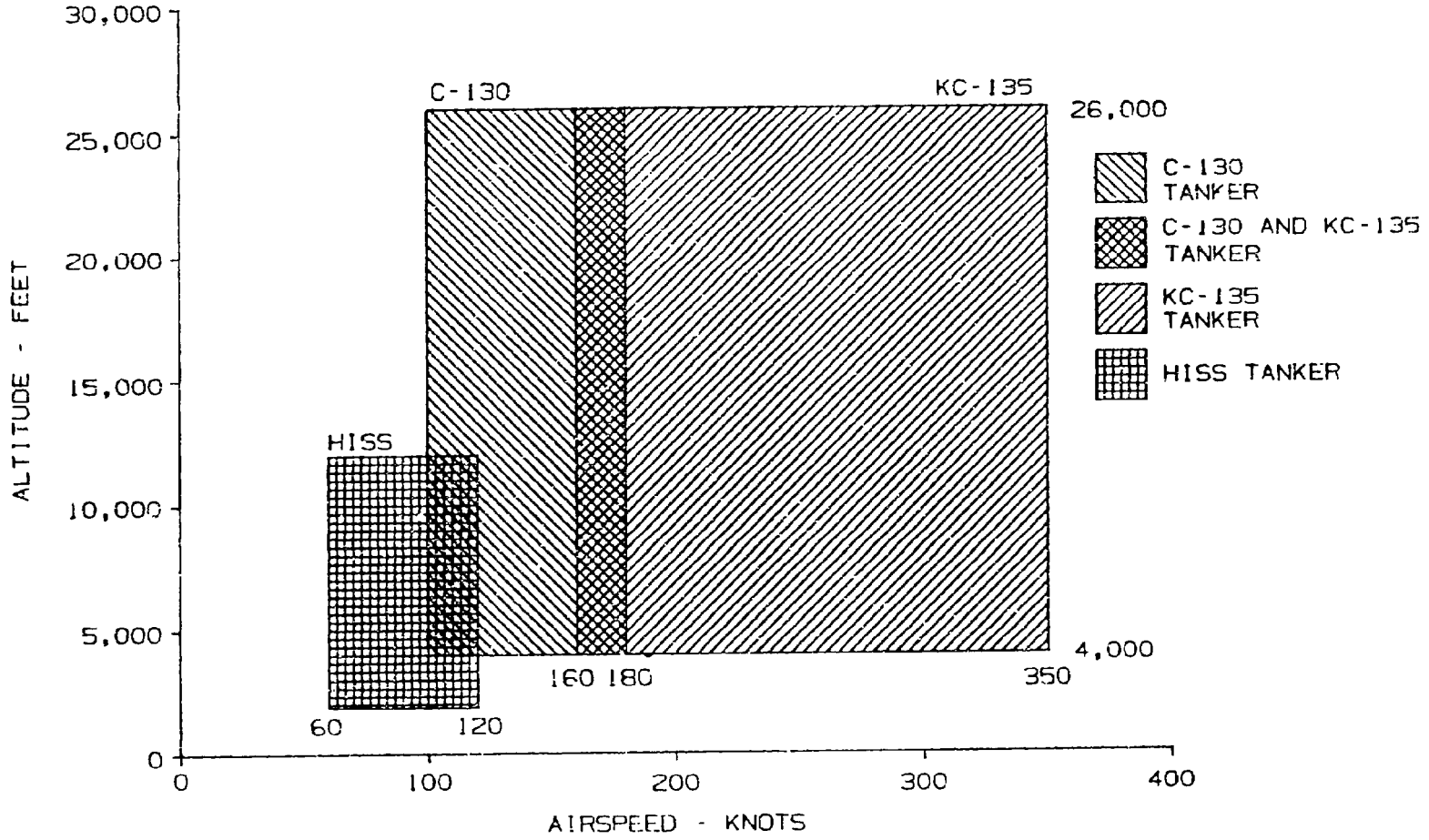

FIGURE 1-17. ALTITUDE VS AIRSPEED ENVELOPES (HISS, KC-135, C-130)

CHAPTER IV
SECTION 2.0
ANALYTICAL METHODS

CHAPTER IV - ICING SIMULATION METHODS
CONTENTS
SECTION 2.0 ANALYTICAL METHODS

	Page
LIST OF TABLES	IV 2-iii
LIST OF FIGURES	IV 2-iv
SYMBOLS AND ABBREVIATIONS	IV 2-vi
GLOSSARY	IV 2-ix
IV.2.1 INTRODUCTION	IV 2-1
IV.2.2 AIRCRAFT ICING SCALING	IV 2-2
2.2.1 Flow Field Scaling	IV 2-4
2.2.2 Droplet Trajectory Scaling	IV 2-5
2.2.3 Total Water-Catch Scaling	IV 2-7
2.2.4 Thermodynamic Scaling	IV 2-8
2.2.5 Experimental Evaluation of Icing Scaling Laws	IV 2-9
2.2.5.1 AEDC Experimental Study	IV 2-10
2.2.5.2 NASA Lewis Experimental Study	IV 2-11
2.2.6 Icing Scaling for Aircraft Engines	IV 2-12
2.2.7 Scaling of Ice Shedding	IV 2-13
IV.2.3 COMPUTER CODES	IV 2-15
2.3.1 Droplet Trajectory and Impingement Codes	IV 2-18
2.3.1.1 Airfoil Droplet Impingement Codes	IV 2-18
2.3.1.2 Axisymmetric and Three Dimensional Droplet Impingement Codes	IV 2-23
2.3.1.3 Concluding Remarks	IV 2-26
2.3.2 Ice Accretion Codes	IV 2-28
2.3.2.1 Rime Ice Codes	IV 2-29
2.3.2.2 Glaze Ice Codes	IV 2-30
2.3.2.3 Swept Wing Ice Accretion Modeling	IV 2-32
2.3.2.4 Evaluation of Codes Using Experimental Data	IV 2-33
2.3.3 Flow Codes for Predicting Aerodynamic Effects of Accreted Ice	IV 2-34
2.3.4 Computer Simulation of Aircraft Icing Protection Systems	IV 2-37
IV.2.4 ENGINE ICING ANALYSIS	IV 2-39
2.4.1 Calculations Leading to Thermodynamic Analysis of Engine Icing	IV 2-39
2.4.2 Assessing Engine Tolerance to Ice Accretion	IV 2-41
2.4.3 Engine Icing Analsysis and Icing Facility Tests	IV 2-42
IV.2.5 REFERENCES	IV 2-44

LIST OF TABLES

		Page
2-1	Scaled Variables - Example for Droplet Trajectory and Impingement	IV 2-54
2-2	Summary of Past Scaling Investigations	IV 2-55
2-3	Scaled Physical Variables and Icing Parameters	IV 2-56
2-4	Ranges of Test Parameters Investigated at the AEDC	IV 2-57
2-5	Droplet impingement on a Cylinder from Several Numerical Methods	IV 2-58
2-6	Calculated Droplet Maximum Impingement Location on an Ellipsoid of Fineness Ratio 5	IV 2-59

LIST OF FIGURES

		Page
2-1	Scaled Droplet Impingement Efficiency Curves	IV 2-60
2-2	Effect of Velocity, Static Pressure, and Model Size on the Median Droplet Diameter for a Constant Value of Modified Inertia Parameter, K_0	IV 2-61
2-3	Effect of Velocity and Model Size on the Icing Time for a Constant Value of the Accumulation Parameter, A_C	IV 2-62
2-4	Definition of Ice Shedding Analysis Terms	IV 2-63
2-5	Droplet Trajectories Perturbed by Flowfield Velocities Close to Panel Singularity Points	IV 2-64
2-6	Impingement Efficiency Curves for a NACA 63-015 Airfoil at α = 8 Degrees	IV 2-65
2-7	Impingement Efficiency Curves for a NACA 65_1-212 Airfoil at α = 0 Degrees	IV 2-66
2-8	Water Drop Flux Tube	IV 2-67
2-9	Digital Description of NASA Icing Reaserch Aircraft - Twin Otter	IV 2-68
2-10	Concentration Factor Calculations for NASA Icing Research Aircraft	IV 2-69
2-11	Digital Description of Wing-Mounted Instruments	IV 2-70
2-12	Concentration Factor vs. Water Drop Diameter for FSSP for Wing-Mounted and Isolated Instrument	IV 2-71
2-13	Local Impingement Efficiency on a Sphere - Experimental and Calculated	IV 2-72
2-14	Droplet Impingement Efficiency Comparisons for Clean and Iced Cylinders	IV 2-73
2-15a	Flow Diagram for a Single Time Step Rime Ice Accretion Code	IV 2-74
2-15b	Flow Diagram for a Multiple Time Step Rime Ice Accretion Code	IV 2-75
2-16a	Flow Diagram for a Single Time Step Glaze Ice Accretion Code	IV 2-76
2-16b	Flow Diagram for a Multiple Time Step Glaze Ice Accretion Code	IV 2-77
2-17	Comparison of Experimental and Predicted Ice Shapes for a 1" Cylinder	IV 2-78
2-18	Comparison of Experimental and Predicted Ice Shapes on an Airfoil using a Rime Ice Accretion Code	IV 2-79
2-19	Comparison of Experimental and Predicted Ice Shapes on an Airfoil using a Glaze Ice Accretion Code	IV 2-80
2-20	Heat Transfer Coefficient Data Used for Predictions in Figure 2-19	IV 2-81
2-21	Examples Comparing LEWICE Predictions to Ice Shapes Grown in the NASA Lewis Icing Research Tunnel	IV 2-82
2-22	Examples Comparing LEWICE Predictions to Ice Shapes Grown on the NASA Lewis Icing Research Aircraft	IV 2-83

LIST OF FIGURES (CONTINUED)

		Page
2-23	Aerodynamic Performance Degradation due to Icing	IV 2-84
2-24	Key Aspects of Airfoil Icing	IV 2-84
2-25	Comparison of Code Predicitons of Aerodynamic Coefficients with Experimental Measurements	IV 2-85
2-26	Profiles of Mean Velocity for "Iced" NACA 0012 Airfoil, $\alpha = 4°$	IV 2-85
2-27	Typical Inlet Configuration for a Fan Engine, Three Regions of Concern for Water Ingestion	IV 2-86
2-28	Inlet Catch Efficiency	IV 2-87
2-29	Inlet Streamline Possibilities for Splitter Duct Behind a Fan	IV 2-88
2-30	Stator Flow Capacity Dependence on Hydraulic Diameter during Icing	IV 2-89
2-31	Influence of Freezing Fraction on Stator Passage Flow Capacity Loss	IV 2-90
2-32	Water Temperature within Inlet Ducting	IV 2-91

SYMBOLS AND ABBREVIATIONS

Symbol	Description
A_C	Accumulation parameter, dimensionless, Section 2.2
A_i	Engine inlet projected area, Section 2.4
A_0	Free stream tube area, Section 2.4
A'_{0I}, A'_{0II}, A'_{0III}	Inlet stream tube areas defined in figure 2-29, Section 2.4
AGARD	Advisory Group for Aerospace Research and Development
AIAA	American Institute of Aeronautics and Astronautics
b	Relative heat factor, dimensionless, Section 2.2
c	Airfoil chord length
CFD	Computational fluid dynamics
C_t	Total concentration factor, Section 2.4
C_{te}	Water catch efficiency of core engine (i.e., inside splitter duct), Section 2.4
°C	Degrees Celsius
C_D	Drag coefficient of aircraft or arbitrary body, dimensionless
C_d	Drag coefficient of airfoil, dimensionless
C_L	Lift coefficient of airfoil or arbitrary body, dimensionless
c_l	Lift coefficient of airfoil, dimensionless
CR	Contractor Report
D_H	Hydraulic diameter, Section 2.4
E	Total collection efficiency, dimensionless, Section 2.2
°F	Degrees Fahrenheit
g/m^3	Grams per cubic meter
K	Inertia parameter, dimensionless, Section 2.2
K_0	Modified inertia parameter, dimensionless, Section 2.2
LWC	Liquid water content, g/m^3
M	Mach number, dimensionless, Section 2.2
$\dot{M}_W$	Water droplet flow rate, mass/time, Section 2.2
M_c	Critical Mach number, dimensionless, Section 2.2
m	Mass of water impingement per unit span, Section 2.2
MVD	Median volume diameter, μm
n	Freezing fraction, dimensionless

SYMBOLS AND ABBREVIATIONS (CONTINUED)

Symbol	Description
NACA	National Advisory Committee for Aeronautics
NASA	National Aeronautics and Space Administration
NRC	National Research Council (Canada)
P	Pressure
r_0	Radial coordinate for maximum impingement, Table 2-6
Re	Reynolds number, dimensionless
SAE	Society of Automotive Engineers
T	Temperature
TM	Technical Memorandum
TN	Technical Note
TR	Technical Report
V	Velocity
$\dot{W}$	Air flow rate
α	Angle of attack (degrees)
β	Local impingement efficiency
δ	Droplet diameter (μm)
Θ	Air energy transfer driving potential, Section 2.2
ρ_i	Density of ice (slugs/ft^3)
ρ_a	Density of air (slugs/ft^3)
σ	Shear stress or surface tension of water, Section 2.2
τ	Icing time, Section 2.2
ϕ	Droplet energy transfer driving potential, Section 2.2

Symbol	Description
Subscripts	
e	Denotes core engine, Section 2.4
i	Denotes the inlet plane of basic engine inlet, Section 2.4
f	Denotes fan bypass, Section 2.4
l	Denotes a local value, Section 2.4
R	Reference case, Section 2.2
S	Scaled case, Section 2.2
∞	Denotes freestream conditions
(1)	Denotes inlet plane of basic engine inlet, Section 2.4
(2)	Denotes inlet region immediately upstream of inlet guide vane or first fan blade, Section 2.4
(3)	Denotes inlet region immediately behind first fan blade, Section 2.4
0	Denotes uniform flowfield approaching any object, Section 2.4
Superscripts	
(.)	Derivative with respect to time

GLOSSARY

characteristic length - A characteristic length for a given problem is a convenient length (such as the chord of an airfoil) used to specify the geometric scale of the problem.

finite difference method - Given a partial differential equation defined in a region of space. Replace the derivatives by difference quotients and define a grid in the region of space. A solution to the resulting finite difference problem provides an approximation to the solution of the partial differential equation. The formulation of the finite difference equation, the definition of the grid, and the solution of the equation on the grid is referred to as a finite difference method.

finite element method - The finite element method is a general technique for constructing approximate solutions to boundary value problems. The method involves dividing the domain of the solution into a finite number of simple subdomains, the finite elements, and using variational concepts to construct an approximation of the solution over the collection of finite elements.

flow field - Given a region of space occupied by a fluid in motion during some time interval. A flow field is a vector function V which gives the velocity of the fluid at any point P in the region at any time t in the interval.

geometry - A geometry is a physical surface or test object, especially with reference to the mathematical description of the shape. This term is loosely synonymous with "surface," body," "object," or "shape."

impingement efficiency curve (ß-curve) - A plot of the local impingement parameter ß versus the surface distance parameter S for an airfoil or other two-dimensional object.

liquid water content (LWC) - The total mass of water contained in all the liquid cloud droplets within a unit volume of cloud. Units of LWC are usually grams of water per cubic meter of air (g/m^3).

median volumetric diameter (MVD) - The droplet diameter which divides the total water volume present in the droplet distribution in half; i.e., half the water volume will be in larger drops and half the volume in smaller drops. The value is obtained by actual drop size measurements.

micron (μm) - One millionth of a meter.

Navier-Stokes equations - The Navier-Stokes equations are the general equations which describe a viscous, compressible flow in a region of space.

Navier-Stokes solver - A Navier-Stokes solver is a computer code which implements a numerical method for the solution of the Navier-Stokes equations or a simplified version of those equations (e.g., the thin Navier-Stokes equations).

panel method - A panel method is a numerical method for calculating the incompressible, inviscid flow about a two- or three-dimensional body or configuration of arbitrary shape. The body is represented by panels (which may be line segments in two dimensions and planar regions bounded by polygons in three dimensions).

potential flow - Given a flow field specified by a vector function $\vec{V}$. If $\vec{V}$ can be written as

$$\vec{V} = \text{grad } f$$

for some scalar function ϕ, then the flow is referred to as a potential flow (and ϕ is called the potential function). Invsicid, irrotational flows are potential flows.

Reynolds number - The Reynolds number is a dimensionless parameter which is the ratio of the inertia force to viscous force for a given problem. It is calculated according to the formula

$$Re = \frac{\rho_\infty V L}{\mu},$$

where V is a characteristic velocity and L is a characteristic length for the problem and the other symbols are defined in "Symbols and Abbreviations."

stagnation point - The point on a surface where the local free stream velocity is zero. It is also the point of maximum collection efficiency for a symmetric body at zero degrees angle of attack.

Thin (or thin-layer) Navier-Stokes equations - The thin (or thin-layer) Navier-Stokes equations are an approximation to the Navier-Stokes equations in which viscous terms containing derivatives in the directions parallel to the body surface are neglected.

Weber number - The Weber number is a dimensionless parameter which is the ratio of the inertia of air to the surface tension force at the air/water interface for a given problem. (This definition can be generalized to any two fluids.) It is calculated according to the formula

$$We = \frac{\rho_a V_\infty^2 L}{\sigma},$$

where V is a characteristic velocity and L is a characteristic length for the problem and the other symbols are defined in "Symbols and Abbreviations."

ß-curve - See "impingement efficiency curve."

IV.2.0 ANALYTICAL METHODS

IV.2.1 INTRODUCTION

In this section, (1) aircraft icing scaling, (2) aircraft icing analysis using computer codes, and (3) aircraft engine icing analysis are addressed.

Aircraft icing scaling (or similitude) is discussed in Section 2.2. It is concerned with supplying answers to questions of the following sort: Suppose that a subscale model of an airfoil or engine inlet is tested in an icing facility. How are the results to be converted to reliable information on fullscale airfoils or inlets? Or, suppose that testing is required at meteorological conditions that cannot be achieved in a given facility (e.g., a specific ambient temperature is desired and testing is to be done in an outside facility where there is no control over this variable). How can conditions be determined which can be achieved in that facility and that are of equal icing severity? How can the effects observed in conditions which are achieved in that facility be used to infer effects that may occur at unachievable conditions? The use of some sort of icing scaling procedure is frequently necessary since so much testing must be done either at subscale or at meteorological conditions different from those desired. It would be very welcome it a set of icing scaling laws covering a wide range of conditions had been formulated, rigorously verified, and accepted by those concerned with problems of aircraft icing. Such a set of laws could then be presented in this handbook with guidance as to their application and illustrative examples. Unfortunately, there is at present no such set of laws. Instead, different researchers have formulated sets of laws which they have used in particular facilities to meet particular problems. It has often proved difficult to transfer such a set of laws to another facility. Section 2.2 surveys sets of laws which have been published, discusses validation efforts, and emphasizes procedures which are common to all or most of the scaling methodologies.

Computer codes used in the analysis of aircraft icing are discussed in Section 2.3. These codes include droplet trajectory and impingement codes, ice accretion codes, flow codes for predicting aerodynamic effects of accreted ice, and codes which simulate aircraft icing protection systems.

All the computer codes discussed in this section contain at least a thousand lines of code, and usually far more. All include a numerical calculation of substantial complexity, such as the use of a panel method or Navier-Stokes solver to calculate a flow field, the solution of a heat transfer problem using finite differencing over a grid, or the use of finite element methods. Icing correlation codes will not be discussed in this section.

Section 2.4 is a very brief discussion of certain aspects of engine icing analysis.

IV.2.2 AIRCRAFT ICING SCALING

Testing of aircraft components in icing facilities (Chapter IV, Section 1) is an important step in the design of ice protection systems and in the assessment of susceptibility of these components to the effects of icing. The limitations of those facilities as to size and achievable meteorological conditions make unavoidable both the use of subscale models and testing at meteorological conditions other than those desired. Thus icing scaling is essential to the interpretation of test results.

Icing scaling can be defined in a general way as a procedure used to ensure similar ice accretions on two geometrically similar (or identical) objects under differing atmospheric and flight conditions. Usually it is required that the ice be similar in shape, type, and perhaps roughness, but it may be required to be similar with respect to other properties such as resultant drag or shedding characteristics. A more formal definition of icing scaling will be useful in the discussion that follows; such a definition is stated in the next paragraph.

Given an airfoil (the reference airfoil) of chord c_R at freestream velocity $V_{\infty,R}$, ambient static temperature $T_{\infty,R}$, and ambient static pressure $P_{\infty,R}$ immersed in a cloud with liquid water content LWC_R, median volume diameter MVD_R for a duration of time τ_R and a geometrically similar second airfoil (the scaled airfoil) with chord c_S for conditions $V_{\infty,S}$, $T_{\infty,S}$, $P_{\infty,S}$, LWC_S, MVD_S, and duration τ_S. Suppose that the values of the parameters in the reference set are fixed and the value of one or more of the parameters in the scaled set is fixed at a value different from the value of the corresponding parameter in the reference set. How can the remaining parameters in the scaled set be varied so that the ice accretion formed on the scaled airfoil at the scaled conditions is "similar" to the ice accretion formed on the reference airfoil at the reference conditions?

If $c_R > c_S$, i.e., the scaled airfoil is a subscale airfoil, the term "subscale model icing scaling" is used. If $c_R = c_S$, i.e., the scaled airfoil is the same size as the reference airfoil, the term "test parameter icing scaling" is used.

The word "similar" was placed in quotes because it had not yet been defined. Different studies have used different similarity criteria. Reference 2-1 required that the type (rime, glaze, mixed) and roughness of ice formed be similar (in the subjective judgement of the experimenter) and that the dimensions of the scaled ice shapes be geometrically similar to within 10 percent of the reference ice shape. The 10 percent value was taken as representative of the limits of repeatability of the test facility where the study was conducted and of the measurement techniques that were employed to quantify the ice shapes. Reference 2-2 required that the drag coefficients of the scaled and reference cases be approximately equal. For some purposes it is desirable to require that shedding characteristics be similar. A useful discussion of possible "similitude requirements" can be found in reference 2-3.

Although this definition has been stated for airfoils, it is can be modified to apply to any geometry. For example, for icing scaling of an entire aircraft or of an engine from inlet lip to compressor face, one would require that accretions form at corresponding locations on the scaled and reference geometries and that these accretions be similar. It should also be noted that most scaling studies have been conducted for unprotected geometries.

The difficulty of achieving icing scaling varies with the complexity of the geometry and the stringency of the similarity requirements. For most of the remainder of this section, the geometry will be either an airfoil or a circular cylinder and the similarity requirements will be geometric similarity to within 10 percent plus similarity of ice type and ice roughness.

All the scaling laws to be discussed rely upon scaling parameters evaluated at the stagnation point of the clean airfoil or cylinder. They all assume either tacitly or explicitly that matching scaling parameters at this point at the beginning of the icing process will suffice to insure at least approximate similarity over the entire icing region throughout the icing process. See, for example, the discussion on pages 4 and 20 of reference 2-1.

The term "approximate similarity" was used in the previous paragraph. Reference 2-4 shows the difficulty of achieving an exact scaling methodology, even theoretically. A Buckingham Pi analysis of the icing scaling problem in this reference led to the conclusion that exact scaling required that the Reynolds number, Mach number, and Weber number be held constant for the scaled and reference cases, but it is not possible to hold all three of these parameters constant simultaneously. If surface tension were dropped from the analysis, the Weber number would also disappear along with the irresolvable conflict just mentioned. However, the remaining scaling requirements would still be extremely restrictive. It would still be necessary to hold the Reynolds number and Mach number constant, a severe constraint. Furthermore, the analysis also required that the parameters δ/c and δ/l (where δ is the droplet diameter, c is the chord size, and l is the mean distance between droplets) be held constant for the scaled and reference cases. This implies that LWC must be the same for the scaled and reference cases, another severe practical restriction. Finally, it should be noted that these results were obtained even though the analysis was simplified by omitting evaporation and sublimation. This and other work indicate that any icing scaling methodology will be approximate at best. Some conditions simply cannot be met, and others must be relaxed in order to arrive at a scheme of sufficient flexibility to be of practical use.

The formulation of an approximate icing scaling methodology has been hampered by the difficulties of formulating a satisfactory physical model of the icing process. Most efforts have been guided by the so-called "standard computational model" presented in Chapter I, Section 2. As discussed there, the very simplified treatment of the surface behavior of the liquid water has been challenged on both experimental and theoretical grounds.

Beginning about 1984, a joint program was begun by NASA Lewis Research Center and the U. S. Air Force's Arnold Engineering Development Center (AEDC) to determine the adequacy of existing scaling laws. This was done both analytically and experimentally at both facilities. Although a general approach was agreed upon, the studies were to be carried out independently. Previous work was analyzed and experiments were run to evaluate the various methods. The discussion that follows relies heavily on the two reports that came out of these studies, references 2-1 and 2-3 (although more recent work will also be addressed). Summarizing the reports provides a convenient way to survey and compare icing scaling methodologies that have been published. It will familiarize the reader with the way in which aspects of the problem have been addressed (e.g., flow field scaling) and with the various scaling parameters that have been proposed. Although it will not result in a comprehensive and general set of scaling laws, it should give the reader some guidance on scaling for particular problems, or at least show how others have scaled them. The references should prove useful for this purpose. It must be stressed that any application of a scaling methodology to a particular problem should be supported by independent experimental validation.

2.2.1 Flow Field Scaling

It has been noted (reference 2-4) that exact scaling would require that the Reynolds number and Mach number be held constant for the scaled and reference cases (which would be possible only if Weber number was neglected). None of the published icing scaling methodologies attempt to meet this severe requirement. However, some restrictions on these parameters usually are still imposed, as will now be discussed.

For surface conditions which produce similar ice accretions over two bodies, normalized pressure and temperature distributions should be similar. Since an ice accretion is approximately confined to the region of droplet impingement, the normalized pressure and temperature distributions are sometimes required to be similar only in this region.

The requirement for similar flow fields imposes airspeed limits. The velocity distributions around an airfoil will normally be preserved up to the stall by avoiding trailing edge flow separation. For this, the freestream Reynolds number based on chord length for both the scaled and reference case should exceed 2.0×10^5 (reference 2-5). Note that this corresponds to an airspeed of 31.4 ft/sec for a model airfoil section with a 1.0 ft. chord, static temperature of 0 ^{o}F and 10,000 feet pressure altitude.

An upper airspeed limit is imposed by the onset of local supersonic flow on the body at the critical Mach number M_c. Significant changes in the flow can occur above M_c, discouraging the use of results obtained at Mach numbers below but near M_c. The effects of compressibility at high subsonic Mach number (but less than M_c) on droplet impingement are discussed in Chapter I,Section 2. Greatest confidence is possible when the Mach number for both models is within the

incompressible range. This may not be possible for rotorcraft testing, where tip velocities can be very large.

Except for extreme angles of attack or complex geometries, most of the droplets strike the body in the vicinity of the stagnation point where the boundary layer is relatively thin. Thus some authors have argued that Reynolds number effects on the ice accretion may be small. However, the applicability of this assumption for complex body shapes or test conditions, including high angles of attack, should be proven experimentally or analytically prior to conducting the icing flight tests. It should also be noted that some recent icing modeling studies (references 2-6, 2-7, and 2-8) discussed in Chapter I, Section 2 suggest that a smooth-to-rough transition in the nature of the ice accreting on a cylinder may be related to boundary layer transition, which is in turn related to Reynolds number.

2.2.2 Droplet Trajectory Scaling

The droplet inertia parameter K and the freestream droplet Reynolds number Re are defined in Chapter I, Section 2.2.1.2. The discussion there implies that they can be used as approximate scaling parameters for droplet trajectories. That is, approximately similar trajectories can be ensured for a scaled and reference case by holding both K and Re constant. It is further demonstrated that K and Re can be combined into a single parameter K_0, the modified droplet inertia parameter. Approximate droplet trajectory scaling can be ensured by holding K_0 constant. The reader is referred to Chapter I, Section 2.2.1.2 for the definitions of these parameters and examples illustrating their calculation.

The advantage in using the single scaling parameter K_0 rather than both K and Re is illustrated by a simple example discussed in reference 2-9. Suppose that a fullscale reference case has chord c_R and a subscale model case has chord c_S. If both Re and K are held constant separately, this requires that

$$\delta_S = \left(\frac{c_S}{c_R}\right)\delta_R \text{ and } V_{\infty S} = \left(\frac{c_R}{c_S}\right)V_{\infty R}$$

For example, suppose that c_R = 1 m, $V_{\infty,R}$ = 100 m/s, and δ_R = 15 μm, and that c_S = .5 m. Then holding Re and K constant separately requires that δ_S = 7.5 μm, an MVD smaller than can be achieved in most icing facilities, and that V_S = 200 m/s, yielding a larger Mach number than desirable. On the other hand, suppose that it is only required that K_0 be held constant. For the fullscale conditions, K_0 = .028, and this same value can be achieved for the subscale model with δ_S = 10 μm and V_S = 97 m/s. It is interesting to note that V_S slightly decreases, whereas it previously had to greatly increased. The reason this occurs is that although Re and K are increasing with increasing V_∞, the range parameter (defined in Chapter I, Section 2) is decreasing since it is a decreasing function of Re.

It is also worthy of note that the requirement arising from the Buckingham Pi analysis of reference 2-4 that the parameters δ/c and δ/l be held constant for the scaled and reference cases is

sufficient for droplet trajectory scaling when included with the rest of that analysis. However, as noted, this would require that LWC be the same for the scaled and reference cases, a severe practical restriction and one that does not exist when K_0 is used for droplet trajectory scaling. This is a further indication of the value of this scaling parameter.

The reader is referred to references 2-9 and 2-10 for analytical explanation and justification of the use of K_0 as a droplet trajectory scaling parameter. Since it is an approximate scaling parameter, it is desirable to examine studies where MVD, c, and V_∞ have been varied while holding K_0 constant. The author is not aware of any published results on laboratory or wind tunnel experiments of this type. There also appear to be very few published results of "computer experiments" employing droplet trajectory and impingement codes for this purpose; studies of this kind are of course much easier and cheaper to do. Results of one limited study appear in table 2-1 from reference 2-10, which compares results for a reference airfoil with a one-sixth subscale model for two different values of K_0. Only the droplet diameter δ was to be varied to achieve droplet trajectory scaling. Figure 2-1 shows the calculated ß-curves for the two models for both values of K_0. (Results for Bragg's alternate parameter K (Chapter I, Section 2.2.1.2) are also shown in the figure.) Both the table and figure certainly show close agreement between the reference and scaled case. However, publication of studies of this type for a wider range of conditions which also vary V_∞ would be valuable, as would be wind tunnel experimental studies as well.

Some of the functional dependencies of K_0 are illustrated in figure 2-2 which shows lines of constant K_0 on a plot of droplet size versus velocity. This plot was constructed by calculating K_0 for the specified reference condition and then calculating the droplet size required for K_0 to be held constant at various model velocities (reference 2-1). Note that, for increasing velocities, the subscale model droplet size must be reduced to make droplet inertias similar. Also, since a subscale model will disturb the flow less than the full-scale article, the droplet diameter for the model condition likewise must be reduced. An increase in static pressure is shown to slightly increase the required subscale droplet diameter. For the range of static temperature encountered in most icing analysis, the effect of temperature on K_0 and the resulting subscale droplet diameter is negligible.

Icing clouds are composed of a distribution of droplet sizes. The use of the MVD as a representative droplet size for a cloud is discussed in Chapter I, Section 2. There it is noted that impingement calculations based on the MVD in the stagnation region give good approximations to calculations based on full droplet spectrum, but impingement limits are under-estimated since they are a function of the largest droplets present in the spectrum. All further references to droplet diameter in this section refer to the MVD unless otherwise specified.

In summary, virtually all published icing scaling methodologies include K_0, based on the median volume droplet diameter, as a droplet scaling parameter. A widely used scaling equation for droplet trajectories can, therefore, be written as follows:

$$K_0)_S = K_0)_R \tag{2-1}$$

2.2.3 Total Water-Catch Scaling

Proper droplet trajectory scaling should assure that the distribution of impinging mass on the surface of the body is similar, i.e., identical ß-curves if dimensionless surface distance (surface distance divided by chord length) is used on the horizontal axis. For ice accretions formed on two geometrically scaled objects to be similar, the total mass of impinging water per unit area should be scaled (as introduced in Chapter I, Section 2).

$$\frac{m_w}{c}\Big)_S = \frac{m_w}{c}\Big)_R \tag{2-2}$$

Here the water mass fluxes are divided by the scaled and reference airfoil chords. Other appropriate reference lengths were given in table 2-2 of Chapter I, Section 2.

The total mass of water impinging at a specific location on the surface in a time interval, τ, is given by the following equation:

$$m_w = LWC\ V\ \beta\ s \tag{2-3}$$

Substituting equation 2-3 into equation 2-2 results in scaled total masses of water per unit area impinging at each point on geometrically scaled objects:

$$\frac{LWC\ V\ \beta\ \tau}{c}\Big)_S = \frac{LWC\ V\ \beta\ \tau}{c}\Big)_R \tag{2-4}$$

Since the modified droplet inertia parameter scaling has ensured that the local collection efficiencies at corresponding locations on the two surfaces are the same, ß can be cancelled from both sides of equation 2-4 to yield an equation which is satisfied at all corresponding surface positions as specified by the dimensionless surface distance s:

$$\frac{LWC\ V\ \tau}{c}\Big)_S = \frac{LWC\ V\ \tau}{c}\Big)_R \tag{2-5}$$

Past icing analyses by various authors have related the terms of equation 2-5 to an ice thickness by dividing by the ice density. The resulting term, called the accumulation parameter, can therefore be expressed as

$$A_C = \frac{LWC\ V\ t}{\rho_i\ c} \tag{2-6}$$

Since the type of ice formed on a subscale accretion is to be the same as that formed on the fullscale, the ice densities must be identical. Equation 2-5 can then be rewritten as

$$A_C)_S = A_C)_R \tag{2-7}$$

Figure 2-3 shows relationships between the terms in the accumulation parameter. The plot shows that for a constant LWC, as the velocity is increased, the icing time must decrease so that the total mass of impinging water remains scaled. Reducing the model size at a constant velocity is also seen to reduce the icing time so that a scaled mass of water is deposited (reference 2-1).

In summary, holding A_C constant between the scaled and reference cases (i.e., scaling using equation 2-7) causes the amounts of ice accreted to be proportional to the sizes of the bodies. This assumes, of course, that the impingement properties are similar between the bodies as a consequence of holding K_0 constant.

The accumulation parameter was introduced in Chapter I, Section 2, where its calculation was illustrated and its use in the calculation of ice growth was discussed.

2.2.4 Thermodynamic Scaling

Assuming that K_0 and A_C have permitted the scaling of the total water-catch, it is necessary to introduce a parameter or parameters to scale the behavior of the liquid water on the surface. Such parameters would in some sense scale the energy balance equation presented in Chapter I, Section 2 as well as the fluid film dynamics. Most authors have concentrated on the energy balance and this has led to the use of the term "thermodynamic scaling."

The thermodynamic and heat transfer analysis of an icing surface is described in Chapter I, Section 2. Ruff (reference 2-1) derives essentially the same energy balance equation that was presented there and then extracts three proposed scaling parameters from it.

After dividing through by the heat transfer coefficient and appropriately grouping terms, he is able to isolate the freezing fraction n, the relative heat factor b (first introduced in reference 2-11), and two expressions which he terms the droplet energy transfer driving potential, ϕ, and the air energy transfer driving potential, Θ.

The freezing fraction, n, is discussed in Chapter I, Section 2. According to reference 2-1, if the stagnation-point freezing fraction n is 1, the ice accretion will be essentially rime; if n is less than approximately .3, the accretion will be essentially glaze; and finally, if n is larger than approximately .3 but less than 1, the accretion will be mixed. As the term is used here, mixed ice shows a predominantly glaze center portion surrounded by rime accretions. Furthermore, the size of the glaze center decreases as n approaches 1. This rule of thumb for interpreting n is apparently based not on theoretical work, but on observations in a particular icing facility (cell R1-D at AEDC).

The relative heat factor, b, was defined in reference 2-11 as a measure of the ratio of the sensible heat-absorbing capacity of the impinging water to the unit convective heat-dissipating capacity of the surface. It is nondimensional and since it contains the local convective heat transfer coefficient, h, and local collection efficiency, ß, it is dependent upon body geometry and position on the body. Several icing scaling studies (references 2-12, 2-13, and 2-1) recommended that the relative heat factor be held constant to produce scaled ice accretions.

ϕ and Θ have the units of temperature and contain terms relating to energy transfer caused by the droplets and the airflow, respectively.

2.2.5 Experimental Evaluation of Icing Scaling Laws

The joint NASA-AEDC program to determine the adequacy of existing scaling laws noted that existing scaling laws generally agreed as to the scaling of the droplet momentum and mass flux, including the K_0 and A_c parameters, but that there was considerable disagreement among them concerning "thermodynamic scaling."

From the preceding description of the icing process, based on reference 2-1, six "icing scaling equations" were identified.

$$K_0)_S = K_0)_R \qquad (2\text{-}8a)$$
$$A_C)_S = A_C)_R \qquad (2\text{-}8b)$$
$$n)_S = n)_R \qquad (2\text{-}8c)$$
$$b)_S = b)_R \qquad (2\text{-}8d)$$
$$\phi)_S = \phi)_R \qquad (2\text{-}8e)$$
$$\theta)_S = \theta)_R \qquad (2\text{-}8f)$$

An icing scaling law can be formulated by selecting a combination of these equations. Other equations could be used as well, of course, but the icing scaling laws to be surveyed in this section can in general be viewed as combinations of these equations. Table 2-2 lists some of the best known icing scaling laws and the combination of equations used by each. These laws are given in references 2-12 through 2-14 and 2-15 through 2-19. Of the studies listed in table 2-2, only cases 5 and 9 provided experimental support of the proposed scaling law. However, the limitations of the test facility used in the case 5 (reference 2-12) study may not have allowed adequate verification of the parameters,

especially those satisfying thermal similitude. Case 9 (reference 2-19) provided good ice shape verification, but only LWC and duration were varied. Experimental programs were conducted at NASA Lewis and AEDC, therefore, to identify what combinations of the equations were most successful in producing scaled ice accretions (references 2-1, 2-20, and 2-3). The criteria utilized to identify successful scaling were that the type and roughness of ice formed be similar, and that the dimensions of the scaled ice shapes geometrically scaled to within 10 percent of the reference accretions.

2.2.5.1 AEDC Experimental Study

The AEDC experimental program consisted of icing tunnel tests of ice shapes on the following: (a) circular cylinders of one or two inch diameter, and, (b) three model sizes (full, one-third and one-sixth) of an airfoil at zero angle of attack. No aerodynamic forces were measured. The procedure was:

1. Test the reference model at the reference conditions and measure the ice shapes.
2. Calculate the icing conditions for a scaled test according to one of the scaling law methods (cases 1-6 in table 2-2).
3. Test the scaled model for these conditions in the icing tunnel to get ice shapes repeatable to within 10% of the major linear dimensions.
4. Compare ice shapes from reference and scaled tests. Tables 2-3 and 2-4 give the test conditions used.

A proposed scaling methodology emerged from the AEDC experimental program (case 6 in table 2-2). It required that five of the scaling parameters, K_0, A_C, n, ϕ, and Θ to be held constant. These are cases 5 and 6 in table 2-2. If fewer parameters were matched, as in cases 1 through 4, Ruff found that the resulting ice shapes sometimes differ greatly. The set of "AEDC scaling equations" are thus:

$$1.\ K_0)_S = K_0)_R \tag{9a}$$
$$2.\ A_C)_S = A_C)_R \tag{9b}$$
$$3.\ n)_S = n)_R \tag{9c}$$
$$4.\ \phi)_S = \phi)_R \tag{9d}$$
$$5.\ \theta)_S = \theta)_R \tag{9e}$$

This set of equations was coded into a computer program. The icing test parameters determined from these equations are freestream velocity V_∞, ambient static pressure P_∞, ambient static temperature T_∞, with liquid water content LWC, median volume diameter MVD, and icing duration τ. Since there are six icing test parameters and only five equations, the problem is underspecified and one of the test parameters can be arbitrarily selected. In practice, this additional parameter is often selected so as to overcome a test facility limitation.

2.2.5.2 NASA Lewis Experimental Study

The experimental study at the NASA Lewis Icing Research Tunnel is reported in reference 2-3. As can be seen in table 2-2, the scaling laws tested were not identical with those tested at AEDC (reference 2-1). Apparently, cases 1 through 4, which had already been judged at AEDC to be inadequate, were not considered.

Models tested were circular cylinders of 6, 2 and 1 inch diameters, and NACA 0012 airfoils of 20 and 5 inches chords. Care was taken to get large enough ice accretions so that differences were detectable, but to avoid severe flow separation. Repeatability of ice shapes was good except for the small airfoil. The airfoil was tested at angles of attack of 0° and 4°. For the cylinders, only ice shape was measured. This was done by inserting a card with a ruled grid into a slit cut in the accreted ice. The record was then made by photographing the card from both sides, and by tracing the ice shape on the card with a pencil. For the airfoils, in addition to ice shape measurement, a wake survey probe was used to measure the momentum deficit, and the drag coefficient was calculated. (For this, the frost on the models was scraped off before making the wake survey.)

The test procedure was similar to that of the AEDC experiments.

1. A reference condition was run in the icing tunnel and ice shape and drag coefficient (for airfoils) measured.
2. A scaled condition was calculated by one of the scaling law methods.
3. The scaled case was run in the icing tunnel and ice shapes and drag measured.
4. Reference and scaled test results were compared.
5. This was repeated for a wide range of conditions and scaling law methods.

Reference 2-3 presents the results in tabular and graphical forms. The general conclusion reached was that none of the scaling laws gave consistently good results for glaze and mixed ice accretions. While agreeing with the AEDC work in reference 2-1 that cases 5 and 6 in table 2-2 gave the best results, even these sometimes (especially for mixed-type ice) gave poor ice shape agreement and greatly different drag values. There were indications that the results obtained in the AEDC and NASA facilities were functions of the test facility being used. For cases 5 and 6, ice shapes for the same reference condition at both icing tunnels agreed well, but disagreed for the corresponding scaled condition.

It was pointed out in reference 2-3 that cases 5 and 6 give considerably different results, despite their similarity in choice of scaling parameters, due to the difference in the heat transfer coefficient approximation. The h is proportional to the 0.8 power of velocity in case 5 and to the 0.5 power in case 6. The dependence of ice accretion computations on good heat transfer coefficient equations has long been appreciated. That the scaling of two experimental cases is this sensitive to the h value representation is given new emphasis here.

Another criticism of scaling law cases 5 and 6 is the difficulty in keeping Θ constant, especially at low airspeeds. Keeping Θ exactly constant can require very large airspeed differences between the scaled and reference conditions, whereas permitting only a 0.5 °C mismatch in Θ values requires no airspeed differences whatsoever. Laws 5 and 6 have also been criticized on the ground that if n is held constant, the physical basis for holding Θ and ϕ constant is unclear (reference 2-4).

Scaling law case 9 was validated by the tests, but this is the most restrictive and least general scaling law system. Case 10 is also quite restrictive, but was not validated by the tests.

NASA Lewis continues to sponsor research in this icing scaling (reference 2-21). One product of their program was reference 2-22, which proposes a new approximate scaling methodology by modifying the analysis presented in reference 2-4 which was discussed above. This methodology requires that Reynolds number, Weber number, and contact angle (but not Mach number) be held constant between the scaled and reference case. It also requires, as before, that δ/c and δ/l be held constant. Thus it is a very restrictive scheme.

A test of this methodology was conducted at the BFGoodrich Icing Tunnel in Uniontown, Ohio in the summer of 1989. The design of the test was novel in that a rotating cylinder was used and the temperature was ramped for several of the runs. Unfortunately, the results of the test were inconclusive as to the validity of the proposed scaling methodology.

2.2.6 Icing Scaling for Aircraft Engines

Several recent reports have been published that were motivated primarily by an interest in icing scaling for engines (references 2-2, 2-23, and 2-24). Some icing testing of engines and inlets is conducted in outdoor test facilities, and considerable patience may be required to achieve the approximate temperature desired. Testing at an alternate temperature that would insure equal "icing severity" would be very helpful. This is a problem in test parameter icing scaling rather that subscale scaling.

The studies employed the scaling methodology of reference 2-1, and succeeded in clarifying the use and also the limitations of this approach. Reference 2-24 gives a useful presentation of how various scaling parameters vary when meteorological or flight conditions are varied. Reference 2-2

presented experimental results that showed little effect of pressure in ice formation over a range of 6 to 14 psia. Reference 2-24 states:

> Since icing conditions change from component to component, icing scaling should be considered only for one component at a time. Conditions for scaling a particular component may change the formation of ice at other components within the engine. Thus, scaling this one component will not assure that the combined effect of icing on the full engine system will be demonstrated.

Because of this and other factors, it did not prove possible to formulate a methodology for test parameter scaling for engine icing tests.

2.2.7 Scaling of Ice Shedding

The discussion thus far has concentrated on the scaling of ice shape. However, the scaling of ice shedding is also important for some purposes. However, it appears that the shedding of ice accretions can impose limits on "velocity scaling" that are more restrictive than those for scaling ice shape.

Ice will shed from an object when the shear stress between the ice and the surface, or within the ice structure itself, reaches some critical value. This value is dependent on the conditions at which the ice was formed as well as the current conditions. If the subscale and fullscale ice accretions are formed under similar thermodynamic processes, the critical values of the shear stress should be nearly the same. The stress within the ice is a result of the aerodynamic forces on the ice accretion itself, as shown in figure 2-4. The magnitude of these forces are dependent on the size of the accretion, static pressure, and freestream velocity.

Since the forces are proportional to the dynamic pressure,

$$q = \frac{1}{2} \rho_a V^2$$

an equivalent force, F, can be defined such that the shear stress at the surface of the airfoil can be expressed as

$$\sigma = \frac{F}{A_s} = C_{D_i} \frac{1}{2} \frac{\rho_a V^2 A_{ref}}{A_s} \qquad (2\text{-}10)$$

where C_{Di} is a total drag coefficient that can be attributed to the ice accretion and is a function of the shape of the ice accretion. The areas A_{ref} and A_s are defined in figure 2-4. Since the fullscale

and subscale ice accretions have similar profiles and surface characteristics, the values of C_{Di} will be similar if the effects of the difference in Reynolds number are small.

Suppose that a full scale accretion has been formed at a velocity V_i creating drag of C_{D_i} such that the critical shear stress has just been reached, i.e., shedding is imminent. The shear stress at that time is

$$\sigma_c = C_{D_i} \frac{1}{2} \frac{\rho_a V_i^2 A_{ref}}{A_S} \qquad (2\text{-}11)$$

A subscale accretion will have the same value of C_{D_i} and the same ratio of A_{ref}/A_s, but since it has been formed at a lower velocity, the shear stress will not be near the critical value. This reasoning shows that (1) testing at lower velocities can allow ice shapes to grow larger than they would on a full scale geometry, and (2) it may be possible to scale the shedding characteristics by holding the dynamic pressure constant.

At the time the AEDC experimental study (reference 2-1) was conducted, the icing test facility could not adequately evaluate this "dynamic pressure scaling." Limited results did suggest that above M = 0.4, at a static pressure of 14.2 psia (q = 1.6 psia), shedding played a significant role in the ice accretion process and affected the final shape of the ice accretion. Therefore, without verification of the dynamic pressure scaling requirement, scaling is not recommended between fullscale and subscale when one dynamic pressure is greater than 1.6 psia and the other is less than 1.6 psia. Furthermore, accurate velocity scaling with both dynamic pressures greater than or less than 1.6 psia (but not equal to one another) may be possible only if the time-to-shed for both ice accretions has not been exceeded.

Predicting the time-to-shed is dependent on the ability to evaluate (1) the change in drag and moment coefficient as functions of time, and (2) the critical shear stresses between the ice and the surface and within the ice itself. These parameters are also functions of the aerodynamic and meteorological conditions at which the accretion was formed and are beyond the present capabilities of icing analysis. Only test results and empirical correlations can currently provide direction in defining these limits. Little if anything has been published in this area.

For ice on propellers or rotors, shedding due to centrifugal forces must be added to the aerodynamic forces.

IV.2.3 COMPUTER CODES

In this section computer codes used in aircraft icing analysis are surveyed. The discussion is restricted to those codes for which results have been published in the open literature. The purpose of this section is to provide a brief description of the methods used and the capabilities and limitations of the codes. For more information on a particular code, the reader is referred to the references.

A potential user of a computer code may ask: "Is the code validated?" Roughly speaking, he wishes to know if there is a range of conditions and geometries for which the results produced by the code are known to be reliable. Efforts to clarify this notion and also the notion of a "calibrated" code for computational fluid dynamics (CFD) will be briefly reviewed here. Many of the codes used in icing analysis are CFD codes or contain CFD modules.

The definition of "validated" and "calibrated" CFD codes has been addressed by an ad hoc committee formed by NASA's Aeronautics Advisory Committee (references 2-25 and 2-26). Reference 2-27 summarizes some of the committee findings. It was concluded that CFD validation ought to involve the detailed comparison of computed flowfields with experimental data to assure that the *numerical physics* of the code truly represent the *critical flow physics* being modeled. The following formal definitions are taken from reference 2-27.

> CFD Code Validation: Detailed surface and flowfield comparisons with experimental data to verify the code's ability to *accurately model* the *critical physics* of the flow. Validation can occur only when the accuracy and limitations of the experimental data are known and thoroughly understood and when the accuracy and limitations of the code's numerical algorithms, grid-density effects, and physical basis are equally known and understood over a *range* of specified parameters.
>
> CFD Validation Experiment: An experiment that is designed to provide detailed building block data for developing CFD codes This objective requires that the data be taken in the form and detail consistent with CFD modeling requirements and that the accuracy and limitations of the experimental data be thoroughly understood and documented.
>
> Validated CFD Code: A code whose *accuracy* and *range* of validity has been determined by detailed comparison with CFD validation experiments so that it can be applied, without calibration, directly to a geometry and flow condition of engineering interest with a high degree of confidence.

CFD Code Calibration: The comparison of CFD code results with experimental data for realistic geometries that are similar to the ones of design interest, made in order to provide a measure of the code's capability to predict specific parameters that are of importance to the design objectives without necessarily verifying that *all* of the features of the flow are correctly modeled.

Some of the icing analysis codes to be discussed below are CFD codes, so the above definitions are directly applicable. Others attempt to model other aspects of the physics of aircraft icing (sometimes including flow modeling as well). For such codes, it is straightforward to adapt the above definitions to encompass the aspects of the physics which they attempt to model. When this is done, it is clear that few if any of the codes to be discussed could be considered to be "validated" at this time. One reason for this is that validation experiments as described above are very difficult to do for some aspects of the physics of aircraft icing. Some of the codes to be discussed can be considered "calibrated," although in most cases the published documentation is not sufficient to make this judgement.

Reference 2-27 notes that the terms "validation" and "calibration" have sometimes been "loosely" used to describe any comparison with experiment. It is stressed that even favorable comparison of code results to experimental data may be insufficient to classify a code as either validated or calibrated for a well defined range of conditions and geometries. This is a common situation with icing analysis codes, at least so far as can be judged on the basis of published documentation.

Another term relevant to this discussion is "validated user" (reference 2-28). This is a user who possesses a sufficient understanding of both the experimental physics being modeled and the *numerical physics* of the code so that he is able to recognize situations when the code is giving or may be giving erroneous results. The term "validated user" is being used here in the sense of "sophisticated user," and there are of course degrees of sophistication. The most sophisticated user is ordinarily the developer of the code, and his or her understanding of the limitations of the code is built up over many trial runs. It is unusual for the code limitations listed, even for well documented codes, to encompass all the limitations the developer has encountered. Furthermore, the code will have limitations of which even the developer is unaware. Thus a new user of a code must go through a training period not simply to learn how to run a code, but to gain a good understanding of its limitations. His qualifications as a "validated user" will depend on his understanding of the physics being modeled and of the numerical techniques being used, as well as the number of runs of the code he is able to do under a broad range of conditions.

Finally, a few words are in order as to the assessment of CFD codes for use in aircraft icing analysis when those codes have already been validated or calibrated for typical aerodynamic applications and geometries. There are two primary uses of CFD codes in aircraft icing analysis. The first is the calculation of off-body flowfield velocities needed for the numerical integration of the droplet trajectory equation. Evaluation of CFD codes for non-icing applications is often done mainly

by making surface comparisons, such as the comparison of calculated surface pressure distributions to measured surface pressure distributions; evaluation of off-body velocities may be limited. Panel codes have been extensively compared to experimental data but may require modification to compute accurate off-body velocities near singularity points on a surface. Techniques employed for this purpose, when panel codes are incorporated in droplet trajectory and impingement codes, are discussed in Section 2.3.1.

The second primary use of CFD codes in aircraft icing analysis is the computation of aerodynamic coefficients for iced airfoils. The ice shapes can be very irregular and even a CFD code that has been validated for clean airfoils may fail to converge or may give incorrect results for an iced airfoil until its proper use (e.g., grid generation, turbulence modeling) for this application has been investigated.

As already noted, none of the codes to be discussed below are "validated" for icing analysis in the rigorous sense of the ad hoc committee's definition, and very few can be called "calibrated" based upon the published documentation. For such codes, it is important that the user have strong qualifications as a "validated user." If he does not, he should be very conservative in his use of the code, using it only for conditions and geometries that clearly fall within the ranges specified in the documentation. If the documentation does not state such ranges, or if he is unsure about a particular case of interest, he should consult with the code developers.

The reason for this extended discussion of validated and calibrated codes and validated users is that some discussions of aircraft icing analysis may leave the impression that once computer codes for icing analysis are developed, it is fairly routine to validate them, and therefore the day will soon be here when validated computer codes can be routinely used to greatly reduce, if not eliminate, the need for icing tunnel testing and test flights in natural icing conditions. Such expectations may tend to obscure the value of the codes. There is a strong need for icing analysis, both as a practical matter in the design and evaluation phase, and as an FAA requirement in the certification phase. Experimental results by themselves will not suffice for either design or certification; analysis is a necessity. The codes now available or under development can greatly enhance the knowledgeable engineer's ability to carry out various kinds of icing analysis; when used carefully, they are the best tools available for this task.

2.3.1 Droplet Trajectory and Impingement Codes

A number of droplet trajectory and impingement codes have been developed in recent years. Output from these codes can be used for ice protection system design and as input to an ice accretion code. These codes still rely upon the classic formulation of the problem presented by Langmuir and Blodgett (reference 2-29) in 1946, but reflect the great strides that have been made in computing power since that time. Some of the new codes can solve efficiently for the droplet trajectories about a complex body geometry. In this section, the codes used for airfoils or other two-dimensional planar bodies will be presented, followed by a discussion of the codes available for axisymmetric and three-dimensional flowfields. (Several of the planar codes can also be run in an axisymmetric mode.)

2.3.1.1 Airfoil Droplet Impingement Codes

Many airfoil droplet impingement codes exist in the U.S. Codes currently in use and having published results are discussed here. Codes of specialized capability exist for cylinders and other specific geometries. These are usually used solely as part of ice accretion codes and will not be discussed here.

The reader is referred to Chapter I, Section 2 for the definition and explanation of droplet trajectory and impingement terms used in this section.

Description of Codes

A droplet trajectory and impingement code can usually be run in two different modes. In the first mode, it computes a single trajectory of a droplet as it approaches an airfoil, determining whether or not the droplet strikes airfoil, and the location where it strikes if it does. The primary output in this mode is a graph displaying the trajectory. See figure 2-2 in Chapter I, Section 2 for such a graph. In the second mode, the code computes a large number of trajectories in order to determine the pattern of impingement on the body. The general approach often used is described in Chapter I, Section 2. The primary output in this mode is ordinarily an impingement efficiency curve or ß-curve such as shown in figure 2-8 in Chapter I, Section 2.

A trajectory is calculated by numerically integrating the droplet trajectory equation. Each step of the integration requires the calculation of the components of the flowfield velocity at the present position of the droplet. Thus a flowfield module must be part of the code, and a method must be determined for providing the flowfield velocities at the required positions for the numerical integration. If the flowfield is computed by a panel code, the so-called "direct" approach can be used. In this approach, source and vorticity strengths are stored for each panel along with panel geometry characteristics. Flowfield velocity components at any position required by the trajectory module can then be calculated by summing the contributions of each panel. In the grid generation and velocity interpolation approach, referred to as the "grid" or "indirect" approach, the user must specify a fixed grid of points surrounding the airfoil. The flow code then computes and stores the velocity at each grid point using a finite difference algorithm or some other method (even a panel code can be used

for this purpose). Flowfield components are obtained at any position required by the trajectory module by interpolation of the velocities at the "surrounding" grid points (reference 2-30).

Users of both approaches seem to be in agreement that the coding of the direct approach is very straightforward by comparison to the grid approach, while the direct approach is considerably more CPU-intensive than the grid approach, particularly when many trajectories must be calculated.

Both of these approaches may have special requirements near the airfoil surface. In the case of the direct approach using a panel code, problems can arise if the droplet trajectory passes "close" to a singularity point on a panel. The flowfield velocity components at such points can result in the calculation of very erratic trajectories. This is illustrated in figure 2-5, which is taken from reference 2-31. (The pseudo-impingement surface shown in this figure will be discussed later.) In the case of the grid approach, the user must be sure that the grid is fine enough near the airfoil surface to resolve the large local flow accelerations which may occur.

Further discussion of the relative advantages and disadvantages of the direct and indirect or "grid" method can be found in references 2-30, 2-32 (pp. 5-6), and 2-33.

An algorithm must also be chosen for the numerical integration of the droplet trajectory equation presented in Chapter I, Section 2. Predictor-corrector algorithms with adjustable time step are used. It has been argued that the trajectory equation is "stiff" for the smaller droplet sizes (reference 2-9). Reference 2-34 presents a detailed analysis of "stiffness" as a function of droplet size. Several codes use algorithms, such as Gear's algorithm (reference 2-35), which are specially designed for stiff ordinary differential equations.

The Boeing 2-D/axisymmetric droplet trajectory and impingement code is described in reference 2-36. This is a proprietary code which has been under continuous development since the early 1960s. It is capable of calculating droplet trajectories not only about airfoils but also about axisymmetric bodies. The grid generation and velocity interpolation approach is used, with the flowfield calculated using a full potential, finite difference code; thus compressibility effects can be calculated. The code is capable of handling multiple component configurations.

The FWG 2-D/axisymmetric droplet trajectory and impingement code, developed under contract to NASA-Lewis by FWG Associates, is described in reference 2-37. It utilizes the direct approach with a 2-D Hess and Smith panel code which includes a compressibility correction. Figure 2-5, which was used earlier to illustrate the erratic trajectories that can result when droplets pass close to surface singularities in the panel method, was generated using this code. Figure 2-5 also indicates the method used by the code to circumvent the problem. A "pseudo-surface" is introduced slightly in front of the surface panels in the forward region of the airfoil. The ß-curve is computed using this pseudo-surface, that is, droplet trajectories are followed only until they strike the pseudo-surface. The erratic behavior of the trajectories is eliminated because the droplets never pass "close" to the singularities; they strike the pseudo-surface first. Comparisons to computations done with a Navier-Stokes code suggest that any error introduced by this procedure is small; these comparisons will be presented later when the importance of flowfield viscosity to impingement calculations is discussed.

The FWG program can handle axisymmetric geometries as well as airfoils; wind tunnel walls may also be modeled. The code is designed to calculate the trajectory not only of spherical droplets but also of non-spherical particles such as snow flakes; however, to make use of this capability the user must supply a routine to calculate the lift, drag, and moment characteristics of the non-spherical particle. The droplet trajectory equation includes gravity as well as drag (although the user can set a flag to neglect gravity); it is solved using a predictor-corrector scheme. Results from this code were presented in reference 2-38, a study of the effect of droplet size distribution on collection efficiency.

A droplet trajectory code from which many results are available in the literature is described in reference 2-9. This code is strictly for the calculation of droplet impingement characteristics of a two-dimensional airfoil; wind tunnel walls, for example, cannot be modeled. The flowfield used is an incompressible, potential flow generated using a Theodorsen transformation method. The code includes the droplet forces of drag and gravity and calculates the trajectory of the spherical particle using Gear's algorithm for stiff differential equations. While this code is more limited in scope than the two codes just described above, it generates fast solutions for airfoils. Results from the code also may be found in reference 2-39.

Several droplet trajectory codes are in use in Canada and overseas. Lozowski and Oleskiw of the University of Alberta in Canada have published several papers on their method (references 2-40 and 2-41). This method is also limited to two-dimensional planar geometries in a potential incompressible flow. The flowfield is generated using a surface panel method. The unique feature of this code is in the formulation of the droplet trajectory equation. While most codes include only the forces of droplet drag and sometimes gravity, Lozowski and Oleskiw also include the Bassett unsteady history term. This term is discussed in Chapter I, Section 2. Reference 2-40 states that the droplet trajectories calculated with the history term are less influenced by rapid changes in the airflow just before impact and so tend to travel along straighter paths than those whose trajectories ignore the history term. Inclusion of the history term complicates the solution of the equation, which is solved by a 4th order Runge-Kutta-Fehlberg method. Inclusion of the history term yields a small increase in collection efficiency, E, and corresponding increases in β_{max}, S_U and S_L, particularly at lower K_0's. That is, the effect is similar to that of slightly increasing the particle size. The inclusion of the history term may be useful in flows where the particles experience large accelerations.

R. W. Gent of the Royal Aircraft Establishment (RAE) in England has presented results of a two-dimensional droplet impingement code for airfoils in reference 2-42. As his primary interest was in ice accretion on helicopter rotor blades, the code uses a compressible, viscous flowfield code for transonic airfoils, which is a modified version of a code by Garabedian and Korn. This is probably the most sophisticated flowfield model currently in use for 2-D droplet trajectories. Using these velocities, the droplet trajectories are calculated using a Runge-Kutta integration procedure. The only droplet force term included in this code is that due to droplet drag. This method appears to be very powerful when calculations are required on airfoils at transonic speeds. At low Mach numbers, this flowfield method, judging from a limited number of trials, appears to require much more computer

time and provide no better accuracy than one of the other methods. Several results from the code are given in reference 2-42 and were used in Chapter I, Section 2 to assess the effect of compressibility on droplet impingement parameters.

All of the computer codes discussed so far calculate a series of single droplet trajectories. A different scheme is used by McComber and Touzot in reference 2-43. Here, the problem is formulated in a Eulerian frame and the droplet velocity components are solved at all points around the body; single droplet trajectories are not calculated. McComber and Touzot use a finite element technique to solve the system of partial differential equations for the droplet velocities. This code is limited to cylindrical geometries.

Evaluation of Codes Using Experimental Data

A very direct approach to the evaluation of a droplet trajectory and impingement code would be to run the code in the mode in which it computes a single trajectory of a droplet as it approaches an airfoil. If an experiment could be designed to determine the actual trajectory under the input conditions for the same body, a comparison could be made. Systematic comparison of computed and experimental trajectories for a range of cases would provide a useful basis for evaluation of the code. Unfortunately, there is apparently no reliable technology for performing the trajectory experiment at the necessary levels of accuracy and precision at a reasonable cost. At any rate, no evaluation of a droplet trajectory and impingement codes using this approach has been published.

An alternate approach, and the one that is in fact used, is to evaluate a droplet trajectory and impingement code by computing impingement patterns for a range of conditions and geometries. The computed impingement patterns can then be compared to experimental impingement patterns measured by the dyed water and blotter paper technique described in Chapter I, Section 2.

Another way of obtaining experimental impingement information on impingement patterns is to accrete a very thin layer of rime ice in an icing tunnel. The limits of the ice ought to correspond fairly closely to the limits of impingement, and the measured variations in ice thickness ought to correspond at least roughly to variations in local collection efficiency. The use of this approach to obtain qualitative information about impingement on iced airfoils is described in reference 2-30.

Until recent years, impingement data for code evaluation were very limited. Except for sphere and cylinder data, the data most often cited were those from three NACA Technical notes from the 1950s (references 2-44, 2-45 and 2-46), which were limited to low speed, 1945 vintage airfoils. The Boeing/Wichita State experimental program (see Chapter I, Section 2) sponsored by NASA and the FAA during the late 1980s has broadened the available experimental impingement data bank substantially. References 2-47 and 2-48 are preliminary reports on the first phase of this work, which is described in detail in reference 2-49. Reference 2-50 is a preliminary report on the second phase of the work. Figure 2-6 is a sample of the data compared to a ß-curve calculated by the Boeing 2-D/axisymmetric code (reference 2-49). Contact NASA Lewis Research Center concerning the acquisition of this data in digital form. The data will be referred to here, for convenience, as the NASA impingement data bank. Several other comparisons of this data to code predictions can be found in Chapter I, Section 2.

A comparison of a droplet impingement efficiency curve calculated using the FWG 2-D/axisymmetric to NACA tunnel data (reference 2-44) is shown in figure 2-7 (reference 2-38). The monodispersed droplet distribution calculation is for a single droplet of size 16.7 μm and the multidispersed droplet distribution calculation represents a Langmuir D droplet distribution with an MVD of 16.7 μm. Both calculations compare quite well to the experimental data. Since the monodispersed case does not include the larger droplets in the distribution, it underpredicts the limits of impingement. The overall impingement efficiency E is also reduced when a monodispersed droplet distribution is assumed. Other researchers (see, for example, reference 2-9) have sometimes reported slightly better agreement for the monodispersed calculation. In general, calculated impingement efficiency curves compare better to experiment when the droplet spectrum is modeled. This is particularly true if K_0 is small.

The results that have been shown are representative of the better comparisons of calculated impingement efficiency curves to experimental impingement efficiency curves. No attempt will be made here to assess the accuracy of the various codes; instead, the reader is referred to the published documentation for each code. The most complete document for this purpose for a 2-D/axisymmetric code is probably reference 2-49, where comparisons are made of experimental results to curves calculated by the Boeing 2-D code for several different geometries. Since the impingement data used in this report is available in digital form through NASA Lewis, more detailed evaluation of other codes, including these discussed in this section, is now possible.

Limited studies have been done comparing results of several codes among themselves. Although it is no substitute for comparison to experimental data, this can be useful. Table 2-5, adapted from reference 2-42, compares the predicted catch efficiencies for a cylinder calculated by several of the codes discussed above as well as by the original method of Langmuir and Blodgett. Each of the codes uses a different flowfield module and droplet trajectory integration scheme as discussed earlier. The variable Θ_m is the angle from the stagnation point of the cylinder to the maximum limit of impingement. At the higher K_0 (K_0 = 2.851), the five codes agree closely, with the compressible

results showing a slightly smaller E, as expected. At the lower K_0 (K_0 = 0.1785), a more difficult case to calculate accurately, the codes of references 2-9, 2-40, and 2-42 (incompressible) agree well. Again, the compressible code from reference 2-42 shows slightly lower collection efficiency, while Lozowski and Oleskiw's efficiencies (reference 2-40) are slightly higher. Lozowski and Oleskiw's results shown here are without the history term; with this term included, a value of E = 0.187 is found (reference 2-40).

2.3.1.2 Axisymmetric and Three Dimensional Droplet Impingement Codes

While droplet impingement on airfoils is important, similar information is needed on other aircraft components where ice may accrete. Early work by the NACA to develop computational capabilities were limited by their ability to predict the flowfield. Methods were developed to predict the droplet impingement on ellipsoids (reference 2-51 and 2-52) and spheres (reference 2-53). The problem of dealing with wing sweep was also addressed by the NACA in reference 2-54 and by NRC in reference 2-55. Today, more complex flowfields may be calculated using sophisticated computer codes which are available. Several researchers have coupled these flowfield codes with the necessary droplet dynamics to create droplet impingement codes for axisymmetric and three-dimensional bodies.

Description of Codes

Axisymmetric codes, which can be used to analyze various components including aircraft spinners, nacelles, and axisymmetric engine inlets at 0° angle of attack, are much simpler than fully three-dimensional codes. As noted, the Boeing (reference 2-36) and FWG 2-D/axisymmetric (reference 2-37) codes have axisymmetric capabilities.

Due to the computer storage and execution times they require, truly three-dimensional droplet trajectory and computer codes have been developed only relatively recently. References 2-56 and 2-32 describe the Boeing 3-D droplet trajectory and impingement code written by Kim especially for the engine inlet problem. The flowfield is generated using Reyhner's 3-D full potential solver (reference 2-57), a three-dimensional, finite difference, compressible flow code which can use either cartesian or cylindrical coordinates. It requires a preliminary setup code to define the body geometry, computational mesh, and the mesh/surface intersection points. Reference 2-58 describes two such programs used at Boeing.

Kim (reference 2-32) emphasizes the importance of using a highly accurate surface definition of the body in order that the impingement points be located precisely. His work indicates that β can be very sensitive to the local surface geometry. He suggests that flat surface definition, as used by panel codes, may not be adequate for geometries such as engine inlets unless a high panel density is used. His work utilizes a bi-cubic parametric surface modeling technique to obtain an analytical definition of the 3-D engine inlet surface. The droplet trajectory equation is written for a spherical particle in a compressible flow. The effect on the droplet of forces due to drag, buoyancy and gravity are modelled. The trajectory module uses the indirect approach of computing and storing velocities

for various points about the body and obtaining the velocities required for integration of the droplet trajectory equation by interpolation, in this case using both linear and least-squares techniques. Droplet trajectories are calculated using variable step fourth order Runge-Kutta and Adams predictor-corrector integration schemes.

Norment has developed a 3-D code (references 2-59 and 2-60) which can calculate the flow about an entire aircraft and can calculate impingement information for any part of the aircraft. The flow is calculated by a Hess-Smith panel code and the direct approach is used to pass the necessary flowfield information to the trajectory module. Thus this code faces the problem of unrealistic velocities near surface singularities causing erratic trajectories. However, it does not use the pseudo-surface approach used by the FWG code. Instead, it reduces the influence of a panel when the distance of the droplet to the panel falls below a critical value.

Initially, Norment's method was restricted to non-lifting geometries due to the limitations in the version of the Hess-Smith flowfield code used, but this limitation was removed (reference 2-60) by coupling the droplet trajectory module with a lifting version of the Hess-Smith code. The flowfield code handles subsonic cases for which the Mach number is less than 0.5. Water droplet trajectories are calculated using an Adams type predictor-corrector scheme where the forces of drag and gravity on the droplet are included. The water droplets are not restricted to being spherical and may be as large as raindrops due to Norment's formulation of the drag term. However, expressions for the drag of nonspherical objects are required from the user.

This code computes trajectories to user-specified target points. It operates in two modes (reference 2-60):

1. Single trajectories are calculated to each target point.
2. A central trajectory is computed to the target point, and a user-specified number of trajectories, evenly spaced about a circle in the target plane, are calculated such as to define a "particle flux tube" (figure 2-8).

Mode 2 is used to calculate the concentration factor, C_F, which is the ratio of particle flux at the target point to the free-stream particle flux. (Note that this method of calculating local droplet impingement information is somewhat different than that described in Chapter I, Section 2.)

This code has been used for aircraft instrumentation studies (references 2-61 and 2-62) for the NASA Lewis Icing Research Aircraft (a DeHavilland DHC6 Twin Otter). A digital description of the aircraft (figure 2-9) with approximately 3500 panels is used. Figure 2-10 (reference 2-61) shows results for the nose region of the aircraft. The purpose of this study was to look at the effects of the flowfield on droplet trajectories and, therefore, on the measurements of LWC as measured by instruments that might be located there. The results are shown in the form of concentration factor as a function of droplet diameter. The figure indicates that an instrument in this location will "see" a higher concentration of droplets than actually exist in the "undisturbed" cloud, with this amplification

effect greatest for droplets between 75 and 100 μm in diameter. (In most supercooled clouds, there are few droplets this large.)

Reference 2-63 investigates such questions for two optical droplet sizing and counting instruments, the Forward Scattering Spectrometer Probe (FSSP) and Optical Array Probe (OAP). These instruments are discussed in Chapter II of this handbook. Figure 2-11 shows the digital representation of the instruments mounted beneath the aircraft wings. The purpose of the study was to determine the effect on concentration factor resulting from the perturbation caused by the aircraft and also by the complex shapes of the instruments themselves. Figure 2-12 shows some of the results. Note that these results are quite different from those observed at the nose location (with no instrument modeled), since in the former case the concentration factor was larger than 1 while here it is smaller than 1.

The results of an earlier investigation of the effects of instrument location were published in 1984 (reference 2-64). The earlier study used a 2-D code and was a much more limited simulation.

Laschka and Jesse (reference 2-19) have conducted a study similar to those by Norment to investigate the effect of droplet size on the mass flux at the horizontal tail location for an Airbus aircraft.

References 2-65 and 2-33 describe another 3-D droplet trajectory and impingement code developed by BFGoodrich in conjunction with Ohio State University. The flow module used is VSAERO, a panel code which has been quite widely used in the aircraft industry. The capabilities of the Ohio State code appear to be similar to those of Norment's code described above.

Evaluation of Codes Using Experimental Data

Until recent years, relatively little experimental data has been available on complex three dimensional bodies to permit evaluation of these codes. Some data were available for simpler geometries. Kim in reference 2-56 has compared the Boeing 3-D code to the experimental data of Lewis and Ruggeri (reference 2-66) for a sphere. Figure 2-13 shows the droplet impingement efficiency, ß, plotted versus non-dimensional distance from the stagnation point of the sphere. The agreement to the experimental data is improved when the Cunningham correction (reference 2-67) is used. This correction accounts for the effects of rarefaction and compressibility on the sphere drag coefficient expression.

The development of the NASA impingement data bank described above and in Chapter I, Section 2 has greatly expanded the amount of three-dimensional impingement data that can be used for code evaluation. Again the reader is referred to references 2-49 and 2-50, where comparisons are made between experimental results and curves calculated by the Boeing 3-D code for several different geometries. As noted previously, the impingement data used in these reports is available in digital form through NASA Lewis for code evaluation.

Norment in reference 2-59 compares his code to the numerical results of Dorsch (reference 2-51) for an ellipsoid of fineness ratio 5. Table 2-6, also from reference 2-59, compares the limit of impingement in terms of the radial value, r_0.

As in the discussion of the two-dimensional codes, no attempt will be made here to assess as to the accuracy of the codes discussed; the reader is again referred to the published documentation for each code.

2.3.1.3 Concluding Remarks

The basic physics that must be modeled by droplet trajectory and impingement codes is well understood. For many applications, a potential flow formulation seems to be sufficient. The droplet trajectory equation is well-established, with the only significant empirical element being the choice of drag law for the droplet. There are a number of different formulations of the drag law which have been used and which seem to be adequate. The main question regarding the droplet trajectory equation is which forces on the droplet (listed in Chapter I, Section 2) can be ignored, depending on the geometry, droplet size, and flow conditions. For airfoils at subsonic conditions it seems to be acceptable to ignore all forces on the droplet except drag.

The numerical modeling of the physical phenomena is also well established. The flowfields used by several of the codes discussed above are among the most widely used, best understood, or best documented in the aerospace industry. Appropriate methods for the numerical integration of the droplet trajectory equation have been thoroughly investigated.

The uncertainty that remains concerns use of appropriate models for particular cases. Two questions will be addressed below. First, when do viscous effects become important to trajectory calculations? Second, what problems may arise for sharp-nosed airfoil calculations high angles of attack.

For "clean" or "un-iced" airfoils and other geometries, viscous effects do not appear to have a large effect on impingement patterns. However, sometimes it is desirable to compute an impingement pattern on an airfoil or geometry on which ice has already accreted. The most common situation in which this need arises is in the use of "time-dependent" ice accretion codes, which are discussed in Section 2.3.2. These codes "build up" an ice accretion, layer by layer, and so must compute the impingement pattern for each new layer leading up to the final layer. In the case of a "horned" glaze ice accretion, viscous effects are clearly important to aerodynamic calculations because of the separation and reattachment (there may be no reattachment at high angles of attack) behind the horns; how important are viscous effects to the calculation of impingement patterns?

One way to test the importance of the viscous effects is to do the impingement calculations for a clean and an iced geometry using a trajectory module coupled to a non-viscous flow code and then to a viscous flow code. Reference 2-68 describes such a study using impingement data for a clean and iced cylinder from the NASA impingement data bank. The experimental impingement efficiency curves were compared to an impingement efficiency curve calculated by a modified version of the

FWG 2-D code discussed above and also to an impingement efficiency curve calculated using the flowfield calculated by a Navier Stokes code. Figure 2-14 shows the results.

For the clean cylinder, where viscous effects would not be expected to be of major importance, the two calculated impingement efficiency curves agree very closely, and agreement with the experimental data is reasonably good. The computed tails are narrower than the experimental data since the calculations were made using the MVD rather than the entire droplet spectrum.

For the iced cylinder, where viscous effects have a significant effect on the flowfield, neither calculated impingement efficiency curve agrees well with the experimental impingement data. Experimental measurements of the surface pressure distribution about the ice shape indicated the boundary layer separated just aft of each horn. Since potential flow codes do not account for separation, the local velocities in the vicinity of each horn are overpredicted by the panel code. It was conjectured that this might account for the overprediction of ß in the horn regions by the panel code, and this provided the impetus for undertaking the impingement calculations using the Navier-Stokes flowfield. The somewhat surprising result was that the Navier-Stokes calculation also overpredicted ß in the horn regions, but agreed closely with the panel code results. Thus this experiment was inconclusive as to the importance of viscous effects to impingement calculations and raised some question about the accuracy of the experimental impingement data for the iced cylinder. In any event, the level of agreement in collection efficiency predictions using the panel and Navier-Stokes codes for both the clean and iced cylinders increases confidence in the use of panel codes for impingement calculations and also in the pseudo-surface technique used to avoid erratic velocities near panel singularities.

In sharp-nosed airfoil calculations, problems may arise when droplet impingement results are required at $K_0 < .02$ and angle of attack $\alpha > 8°$. Under these conditions very little impingement occurs, since the droplets follow the streamlines quite closely. To calculate these trajectories accurately requires large amounts of computer time, since the adjustable numerical integration step becomes very small. The droplets hit over a small region and are very sensitive to the flowfield. Thus a very accurate flowfield is required around the leading edge which requires very smooth and very dense coordinates in this region. If the local impingement efficiency is calculated using a cubic spline or similar method, difficulty may be encountered in obtaining a smooth curve and, therefore, a good $ß_{max}$ prediction.

2.3.2 Ice Accretion Codes

An ice accretion code predicts the ice accretion on an airfoil or aircraft component exposed to a supercooled cloud. Almost all existing codes are for airfoils or two-dimensional cylinders, and this discussion will concentrate on those cases.

Ice accretion codes can be classified as to whether they are able to predict only rime ice accretions or glaze (and mixed) ice as well as rime. In this context, rime ice is defined as ice formed when impinging droplets freeze on impact over the entire surface. A rime ice code in effect assumes the freezing fraction to be equal to 1 over the entire surface. A glaze ice code calculates the freezing fraction over the entire surface; if it is calculated everywhere to be equal to 1, a rime ice accretion is predicted. Otherwise, a glaze (or mixed) accretion is predicted. There is no well-defined demarcation line between glaze and mixed ice as predicted by an ice accretion code.

Ice accretion codes can also be classified as to whether on not they attempt to model the time-dependence of the ice growth process. Existing time-dependent codes apply a time-stepping procedure to "grow" the ice, layer by layer. For the first time step, the flowfield and droplet impingement pattern are determined for the clean, or "uniced," geometry. Next, the body coordinates are adjusted to account for the first layer of ice accreted. For the second time step, the flowfield and droplet impingement pattern are recomputed for the "new geometry," i.e., the original geometry with the first layer of ice added. All the computations of the first time step are now repeated for the iced surface and then the body coordinates are adjusted once more to account for the addition of the second layer of ice. This process is continued until the end of the icing encounter has been reached. Such a code is referred to as a multiple time step ice accretion code; codes which do not have this capability are referred to as single time step codes.

Figure 2-15 illustrates a single time step and multiple time step rime ice accretion code. These codes require a flowfield module, a droplet trajectory and impingement module, and an ice shape calculation module. Figure 2-16 shows that, in addition, a glaze ice accretion code must include a thermodynamic analysis module. Note that figure 2-16 indicates that it is desirable for the multiple time step code to predict not only the shape but also the ice roughness at each time step. The reason for this is that at each time step the predicted ice shape will be strongly influenced by the heat transfer coefficient which in turn varies with the surface roughness. The surface roughness varies as the ice shape grows and also varies with position on the surface. However, the "state of the art" has not advanced to the point where such predictions of surface roughness are possible. Codes which include the surface roughness as a variable ordinarily input a single roughness value which is used over the entire surface for all time steps. This reduces the fidelity with which the code is able to simulate the physical process of icing.

"Rime feathers" may develop aft of the "main" ice accretion, be it rime or glaze or mixed. The author is not aware of any ice accretion code that is able to predict these rime feathers.

Historically, perhaps the first attempt to predict ice growth was the work of Glauert (reference 2-69) in 1940. Glauert used a scheme proposed by G. I. Taylor to calculate droplet impingement on a cylinder and an airfoil. Using the calculated impingement efficiencies, he predicted rime ice shapes.

The thermodynamic analysis used in the glaze accretion codes is based upon the work of Tribus (reference 2-11) and Messinger (reference 2-70) in the late 1940s and early 1950s. It is discussed in Chapter I, Section 2.

2.3.2.1 Rime Ice Codes

Bragg (references 2-9 and 2-71) developed a multiple time step rime ice accretion code using his droplet trajectory code discussed above. The direction of ice growth assumed in a model may affect the prediction; this code can calculate growth normal to the surface and also streamwise growth.

Lozowski and Oleskiw (reference 2-40) also used their droplet impingement code discussed above as part of a multiple time step rime ice accretion code. Because of the air that is trapped within it during growth, rime ice has a density less than the nominal figure of 917 kg/m^3 for bulk ice. This code assumes a density of 890 kg/m^3 for rime ice.

Numerical difficulties that may be encountered by a multiple time step rime ice accretion code are discussed in reference 2-71. As the time stepping proceeds, small scale surface "irregularities" may appear in the ice accretion. These may be due either to the algorithm used for calculating the ice shape or to irregularities in the impingement efficiency curve. (Although these irregularities may superficially resemble small scale ice roughness, they are purely numerical "artifacts.") Irregularities which appear are often amplified in the subsequent impingement efficiency curve calculation; the next ice shape, calculated using this impingement efficiency curve, is then more irregular than the preceding one. This may ultimately result in an ice shape prediction dominated by large jagged areas that have no physical meaning.

From a conceptual point of view, using a large number of time steps ought to improve ice shape prediction since this better models the time dependence of the icing process. However, if more than a few time steps are used, the difference in the ice shapes is usually relatively small, less than the experimental uncertainty associated with the icing process. Furthermore, using a large number of small time steps greatly increases the CPU time required and in some instances may result in a poorer ice shape prediction due to numerical difficulties of the kind described above. (However, this numerical instability is rather unpredictable in its effects and may also be significant for just a few times steps if a large amount of ice is accreted for each time step.)

In cases where a relatively small ice accretion is being predicted, it may be assumed that the accreting rime ice will closely follow the contours of the airfoil and will only slightly perturb the initial flowfield about the "clean" geometry. It follows that the impingement efficiency curve will

change only slightly from the initial impingement efficiency curve; thus a single time step calculation should give a good approximation.

Note that there is an additional uncertainty associated with the use of a rime ice code for a given set of conditions: The user must satisfy himself that the input conditions are in fact "rime conditions." To do this, he might do some sort of preliminary calculation or apply a rule of thumb. Although a number of rules of thumb have been published, the experimental evidence on which they are based is often not clear. A rime ice prediction made with a glaze ice code relieves the user of this additional burden since part of the prediction is that the ice is rime.

2.3.2.2 Glaze Ice Codes

The icing process on a circular cylinder has been modelled by several researchers. The icing of a cylinder has application for power transmission lines and is representative of some blunt objects on aircraft. The cylinder continues to serve as a test case for the development of new prediction methods.

The code developed by Ackley and Templeton (reference 2-72) is a multiple time step glaze ice accretion code for cylinders. It uses Macklin's correlation for the density of accreted ice, which gives the density as a function of temperature, velocity, and droplet size (reference 2-73). The model utilizes Messinger's thermodynamic analysis. This model differs from some other glaze ice accretion models in that it assumes that water which does not freeze sheds rather than runs back.

The code described in reference 2-74 is a single step glaze ice accretion code for cylinders. Starting at the stagnation point, this code solves the steady state energy balance equation at 5 degree intervals around the cylinder. The code calculates the local equilibrium surface temperature, the freezing fraction, and the local rate of icing. The unfrozen liquid is then allowed to run back to the next 5 degree cell on the surface.

Kirchner in reference 2-75 investigated the effect of surface roughness on cylinder ice accretion. Kirchner's ice accretion code for cylinders includes a droplet trajectory code coupled with a thermodynamics model similar to that of Lozowski (reference 2-74).

The most widely used ice accretion code in the United States is LEWICE, developed under the direction of NASA Lewis. The initial work on this code was done at the University of Dayton Research Institute (reference 2-76). The use of the code is described in detail in a user's manual (reference 2-31). It is a multiple time step glaze ice accretion code, so its structure is depicted schematically in figure 2-16b. The flowfield module is a Hess-Smith panel code and the droplet trajectory and impingement module is a modified version of the FWG 2-D code discussed above. The thermodynamics model is an extension of the work by Messinger (reference 2-70). The ice density is calculated using Macklin's correlation. An integral boundary layer procedure is used to determine the convective heat transfer h. The local value of h depends chiefly on the local velocity at the boundary layer edge and the local roughness parameter k. Although the structure of the code permits the variation of k with location and time step, the code is now run using a single value of k.

As discussed above, present understanding of ice roughness does not permit a more physically meaningful approach.

How is the value of k determined in LEWICE runs? The user's manual recommends using an empirical correlation for k that was developed by Ruff as follows (reference 2-31). First, a set of icing tunnel ice accretion shapes was chosen. Second, for each experimental shape, a sequence of LEWICE runs was done varying the value of k to determine the value which gave the best agreement between the LEWICE prediction and the experimental shape. At the end of this process, a data set had been generated which contained the icing conditions and a "best" value of k for each experimental shape. Third, this data set was used to develop a "tunnel" correlation expressing k as a function of freestream velocity, LWC, and ambient temperature. Subsequently, a study was done on a set of 12 ice shapes accreted in flight on the wing of the NASA Lewis icing research aircraft. The ice shapes were recorded using a stereo photography system (references 2-77 and 2-78). It was found that for this set of ice shapes a value of k equal to 25% of the tunnel value gave, on the average, best agreement (reference 2-79). This is referred to as the "flight" correlation.

Note that because k is essentially used as a shape correlation parameter, LEWICE is not presently a candidate for "validation" in the rigorous sense discussed above. Ruff's work with k and the extension of it in 2-79 can be viewed as an attempt to calibrate the code. How successful that attempt has been will be discussed in Section 2.3.2.4.

This discussion has been restricted to the version of LEWICE released by NASA Lewis in 1986 and described in 2-31. This version will be referred to as "standard LEWICE." There have been a number of studies in the last few years reporting on results obtained when standard LEWICE was modified in some way.

Hansman and his co-workers introduced a "smooth zone - rough zone" model into LEWICE (references 2-7 and 2-8). The physical reasoning underlying this two-zone model is briefly described in Chapter I, Section 2. Hansman's work has concentrated on cylinder icing, and in figure 2-17 (reference 2-7) he compares an experimental cylinder ice shape with an ice shape predicted by his model and an ice shape predicted by standard LEWICE. The comparison with the standard LEWICE prediction is quite unsatisfactory. This indicates that if standard LEWICE is to be used to calculate cylinder icing, a different roughness correlation (which has not been formulated) will be needed. This comparison does <u>not</u> bear on the discussion in Section 2.3.2.4 concerning the accuracy of LEWICE predictions <u>for airfoils</u> when using the Ruff correlations.

Cebeci and his associates have produced a modified version of LEWICE by replacing the panel flowfield module in standard LEWICE with an interacting boundary layer (IBL) flowfield module

(references 2-80 and 2-81). If this effort is successful, the resulting code should be very valuable since it would calculate not only an ice accretion prediction but also coefficients of lift and drag.

Reference 2-82 describes a study in which LEWICE was modified by replacing the panel flowfield module with a Navier-Stokes flowfield module. This also permits the calculation of coefficients of lift and drag, but a greater expenditure of CPU time is required.

Cansdale and Gent (reference 2-83) have developed a single time step glaze ice accretion code for airfoils and 2-D cylinders. (The developers of the code have now experimented with a multiple time step version, but the original, most fully documented version, was single step.) This code incorporates the droplet trajectory code described earlier for 2-D compressible flow in reference 2-42. Since this code has been written with the helicopter rotor icing problem in mind, special care has been taken in modelling the local kinetic heating and the evaporative cooling due to low surface air pressure. As with the other models, this one is also strongly influenced by the heat transfer coefficient. Stepping back from the stagnation point, the code assumes a smooth heat transfer coefficient until runback occurs and then switches to a rough value. The authors demonstrate how the distribution of the heat transfer coefficient on the surface can be modified to improve the comparison to experiment. It is not clear to what extent the adjustment of the transfer coefficient may actually be correcting for other effects (such as time-dependence) which are not modeled.

Guffond in reference 2-84 discusses a multiple time step glaze ice accretion code for airfoils developed in France. The heat transfer coefficient is calculated from a finite difference solution of the boundary layer equations. This formulation includes surface roughness and freestream turbulence effects. The surface roughness is based on an equivalent sand grain which must be determined for the ice shape.

2.3.2.3 Swept Wing Ice Accretion Modeling

Little has been published thus far on three-dimensional ice accretion modeling. An effort to develop a three-dimensional ice accretion modeling method has been initiated by NASA Lewis (references 2-85 and 2-86). This present method might be described as quasi-three-dimensional since it does not involve a single three-dimensional calculation. Instead, a three-dimensional flowfield is calculated using a Hess-Smith panel code, droplet trajectories are computed using an approach based on the three-dimensional code of reference 2-60, and two-dimensional ice accretions are calculated along coordinate locations corresponding to streamlines using an approach based on LEWICE. Calculations have been done with a MS-317 swept wing geometry. The work thus far is promising but more work is necessary before the applicability of the method is well established.

2.3.2.4 Evaluation of Codes Using Experimental Data

The published results for the rime ice accretion codes of Bragg and Lozowski show reasonable agreement with experiment. In figure 2-18 (reference 2-71) an ice shape prediction with and without time-stepping is compared to a shape measured in the NASA Lewis Icing Research Tunnel. In the time dependent prediction three time steps were used, which in this case improves the prediction over that obtained with a single time step

Glaze ice accretion is much more difficult to predict since it adds the uncertainties in the heat transfer coefficient. Cansdale and Gent (reference 2-83) compare an experimental ice shape to predicted ice shapes, using an original and then a modified heat transfer coefficient distribution for the predictions. This comparison is shown in figure 2-19 with the heat transfer coefficients plotted in figure 2-20. The heat transfer coefficient h was changed until the predicted ice shape closely matched the measured shape. This gives some measure of the error in h, although other errors in the model may be corrected through the h distribution.

Comparisons of LEWICE predictions to ice shapes grown in the IRT and the British RAE tunnel have been encouraging. Although a systematic study has not yet been published for tunnel comparisons, NASA studies suggest that LEWICE often provides reasonable engineering approximations. Examples of comparisons between LEWICE predictions and ice shapes grown in the IRT are shown in figure 2-21. Figure 2-21a presents a fairly challenging case because of the quantity of ice, the type of ice (glaze), and the angle of attack (4 degrees). The ice shape in figure 2-21b was grown at 0 degrees angle of attack; the LEWICE prediction achieves good agreement with the impingement limits and the cross-sectional area, the main discrepancy in shape being in the region of lower horn. These examples are "typical" of tunnel comparisons with LEWICE predictions. More "extreme" cases (large amounts of glaze ice, perhaps at high angles of attack) can result in poorer comparisons.

A systematic approach is needed for assessing the accuracy of ice accretion codes. First, a criteria of agreement between prediction and experiment should be established. Second, a data set of experimental ice shapes for a wide range of conditions should be selected. Code performance employing the chosen criteria over the entire data set can then be assessed. The criteria of agreement suggested in reference 2-79 is to consider separately three attributes: (1) limits of impingement; (2) cross-sectional area; (3) shape. The first two can be treated quantitatively by measuring the percentage difference between prediction and experiment. The third attribute, shape, does not easily lend itself to a quantitative approach. One must ask if the prediction captures the important features of the actual ice shape (without predicting any additional important features not present). This approach was applied for a data set of 12 ice shapes from icing flights of the NASA Lewis icing research aircraft. It was found that predicted impingement limits were within approximately 25 percent of the observed in ten cases out of twelve, that the predicted cross-sectional area was within approximately 25 percent of the observed in nine cases out of twelve, and that the shape prediction

was rated good in seven cases out of twelve. A good and a poor ice shape prediction from this study are shown in figure 2-22.

In comparing predicted ice shapes to experimental ice shapes, the uncertainty in the experimental conditions should be take into account, although this is rarely done explicilty. For example, for a given facility a reported MVD of 20 μm may mean that the MVD lies between 16 μm and 24 μm (a 4 μm uncertainty) and a reported LWC of 1.0 g/m^3 may mean that the LWC lies between .8 and 1.2 g/m^3. The uncertainty in the other test parameters will not be so great. Suppose two computer runs are done, one for an MVD of 16 μm and LWC of .8 g/m^3 and the other for an MVD of 24 μm and LWC of 1.2 g/m^3. If the two predictions are plotted on the same graph along with the experimental ice shape, and the latter falls between the two predicted shapes, the code must be judged to be performing satisfactorily. Daughters and Berkowitz carried out a study of LEWICE using this approach with the data from 9 of the 12 selected flights of the NASA Lewis icing research aircraft. They assumed a MVD uncertainty of $\pm$4 μm and an LWC uncertainty of $\pm$20 percent, which are probably not unreasonably large for flight data. Their finding was that LEWICE's performance was satisfactory for most of the 9 encounters; if spanwise ice shape variation was taken into account, it was satisfactory for all the encounters considered (reference 2-87). Unfortunately, for some of the encounters the uncertainty in the cross-sectional area of the ice was as more than 50 percent. Uncertainty in droplet size is an important issue not only in the experimental assessment ice accretion codes but also of droplet trajectory and impingement codes; it deserves more attention.

2.3.3 Flow Codes for Predicting Aerodynamic Effects of Accreted Ice

Thin Layer Navier-Stokes and Interactive Boundary Layer Codes

(Much of the discussion of this topic is closely based on reference 2-68.)

CFD codes are used to attempt to determine the aerodynamic effects of an ice accretion on an airfoil. These CFD codes must include viscous effects; both Navier-Stokes solvers and interacting boundary layer (IBL) codes have been used. As noted in Section IV.2.3, even a CFD code which has been validated for "clean" airfoils may fail to converge or may give incorrect results for an iced airfoil until its proper use for this application has been investigated. The main thrust of research in this area is the development of the understanding and techniques necessary to extend to iced airfoils the use of CFD codes which are already well established for "clean" airfoils.

Navier-Stokes codes have been the object of study for icing analysis for more than five years. The code that has been most intensively studied is a version of ARC2D used at NASA Lewis (references 2-88, 2-89, 2-90, and 2-91). ARC2D is a "thin-layer" Navier-Stokes solver developed at NASA Ames (reference 2-92). NASA Lewis has also supported the investigation of Cebeci's 2-D interacting boundary layer (IBL) code for icing analysis (references 2-93, 2-94). An IBL code has the advantage of requiring much less CPU time than a Navier-Stokes code.

Figure 2-23 (reference 2-68) shows in schematic form the degradation in aerodynamic performance that can occur due to leading edge ice accretion on an airfoil. There is an increase in wing section drag even at low angles of attack. There is a shift in the C_l vs α line due to the decambering effect of a thickened upper surface boundary layer. There is a reduction in $C_{l_{max}}$ and premature stall due to early separation of the airfoil upper surface boundary layer.

The key aspects that must be adequately modeled for a glaze horn ice accretion are shown in figure 2-24 (2-68). An airfoil ice accretion is typically small relative to airfoil size, typically only a few percent of chord in maximum dimension. The size and distribution of the roughness elements are much different than the classical sand grain elements used in wind tunnel test programs over the years. The developing boundary layers on both the suction and pressure sides tend to separate in the vicinity of the ice accretion. At lower angles of attack, boundary layer reattachment from either or both surfaces will usually occur aft of the ice accretion, but the reattached viscous layer or layers will be thickened and distorted. As the angle-of-attack is increased, the suction surface zone will grow in size until no reattachment occurs and the airfoil stalls, often several degrees below the stall angle observed for clean airfoils. The increase in drag occurring at the lower angles-of-attack is due to thickened, distorted boundary layers which develop over the airfoil aft of the leading edge ice accretion.

Because of the complexity of this problem, NASA Lewis has recognized the need for development of a comprehensive experimental data base for evaluation of the Navier-Stokes and IBL codes (references 2-95, 2-96, 2-97, 2-98, 2-99, 2-100, and 2-101). A NACA 0012 airfoil model was modified to have an idealized ice shape on its leading edge. The shape has the gross cross-sectional features of an experimental ice shape but not the surface irregularities, since a relatively smooth surface definition is needed for input to the codes. The experimental data collected includes surface pressure distributions, wake survey probe measurements, boundary layer velocity profiles on both the suction and pressure surfaces, and flow visualization data. This experimental program is in the spirit of "validation experiments" described above.

Figure 2-25 compares the lift and drag coefficient predictions of the ARC2D and IBL codes to the experimentally determined lift and drag coefficients for the iced NACA 0012 model at angles of attack from 0° to 10°. The agreement of both codes with the data is good at the lower angles of attack. At the higher angles of attack, the ARC2D code predicted that an unsteady flowfield existed (no steady solution was reached when the code was run in the "time accurate mode"). Thus the ARC2D results for the higher angles of attack were determined by averaging the surface pressure distributions over one cycle and then calculating the resultant C_l and C_d. The IBL code also had some difficulty achieving a converged solution at these conditions but no averaging procedure was possible due to the formulation of the code.

Although these "global" comparisons are very favorable at the lower angles of attack, not enough other comparisons have been done to call them "typical." Indeed, examination of the boundary layer velocity profiles shown in figure 2-26 show significant differences between experiment and the code predictions. This might result in unacceptable global predictions for other cases.

Three possible sources of the discrepancies have been identified and investigated by NASA Lewis. The first investigation addressed ice shape description and grid generation. The goal of this work, which is continuing, is to determine how detailed the digitized input ice shape must be to yield accurate results from the aerodynamic analysis. The second study concerned transition specification. The third study concerned turbulence modeling. ARC2D uses a Baldwin-Lomax turbulence model. A Johnson-King model and a k-ϵ model were tried with little change in the results. This led to the conclusion that use of a more sophisticated, CPU-intensive turbulence model was not presently warranted.

Another limitation of these codes is the difficulty of formulating an adequate treatment of the extreme levels of surface roughness characteristic of ice shapes, particularly glaze ice shapes. The roughness modeling presently used is based on "classical" sand grain roughness elements; how appropriate this is for ice roughness is open to question.

Use of an Unstructured Mesh with Navier-Stokes Equations

As noted above, one sometimes troublesome aspect of the use of Navier-Stokes codes is grid generation. Recently, research has begun on the use of an unstructured mesh methodology for iced airfoils, a procedure that is well-suited to complex or irregular geometries. The first phase of this work is reported in reference 2-102.

Use of Full Navier-Stokes Solvers for Roughness and Heat Transfer Studies

As noted above, there is a strong need for an improved treatment of ice roughness in performance calculations and of ice roughness and heat transfer in ice accretion calculations. Studies undertaken at the University of Dayton Research Institute have made calculations using the full Navier-Stokes equations with the goal of improving understanding in this area (references 2-103, 2-104, and 2-105). This work made use of a Fourier analysis of ice roughness (reference 2-106) and an associated experimental study of local heat transfer from an iced surface (reference 2-107) carried out at the University of Kentucky.

Three-Dimensional Analysis of Flow over Iced Wings

In recent years, work has begun under the leadership of NASA Lewis on the use of three-dimensional computer codes to analyze flows over iced wings. The approach is similar to the two-dimensional effort described above in that an effort is underway to obtain a comprehensive database

for evaluation of the codes (references 2-108 and 2-109). Analytical work thus far is discussed in references 2-110 and 2-111.

2.3.4 Computer Simulation of Aircraft Icing Protection Systems

Electro-thermal De-icing Codes

A series of computer codes (references 2-112, 2-113, 2-114, 2-115, 2-116) which simulate transient heat conduction and phase change occurring with an electro-thermal de-icer pad have been developed at the University of Toledo under the sponsorship of NASA Lewis Research Center. The codes differ as to dimensionality (one-dimensional, two-dimensional rectangular, two-dimensional body-fitted), modeling of the phase change of the melting ice, numerical methods employed, and CPU requirements. For example, the one dimensional codes can be run on a PC while the two-dimensional body-fitted code is best run on a supercomputer (reference 2-61). Reference 2-117 is a useful guide to the various codes that can aid the potential user in the choice of the code best suited to a particular application. Predictions from some of the codes have been compared to experimental data for a UH-1H rotor blade (reference 2-118). Some of the less CPU-intensive codes have been used as design tools by private industry.

Very recently results were published (reference 2-119) on a three-dimensional code in this same series. The authors describe situations where a three-dimensional simulation is needed. They note that spanwise temperature gradients are particularly noticeable in systems in which cyclical heating of the de-icer zones occur and that these effects are especially evident along the edges and at corner regions between zones.

Ice shedding is a key aspect of electro-thermal de-icer performance. The one-dimensional model of reference 2-113 stipulates that shedding occurs when the thickness of melted ice reaches a value specified by the user. A more sophisticated approach to this problem is described in reference 2-120, which discusses the coupling of the electro-thermal de-icing code of reference 2-115 with the ice accretion code LEWICE discussed earlier in this section.

Electro-impulse De-icing (EIDI) Codes

Structural dynamic modeling of EIDI systems using finite element analysis is discussed in references 2-121, 2-122, and 2-123.

Anti-icing Codes

A series of models of water runback for thermal anti-icing systems have been developed at the University of Toledo with support from NASA Lewis. These models allow a multilayer representation of the solid wall with heating of the surface by means of electrical heating elements embedded within the layers or by means of compressor bleed air.

The first model (reference 2-124) uses a one-dimensional heat transfer model for the runback water. In the second model (reference 2-125) the effects of surface tension are included in order to better represent surface water behavior. The third model (reference 2-126) includes rivulets in the analysis of runback water. A two-dimensional heat transfer approach is used to calculate the temperature distributions in the runback water and the solid wall.

Shed Ice Chunk Trajectory Codes

Since many ice protection systems result in the shedding of ice chunks, this topic will be addressed here.

Ice chunks can be shed from an engine's spinner and ingested into the engine or shed from a wing or other forward surfaces and ingested into a tail-mounted engine. Shed ice is a special problem for helicopters because of the high velocity of the main rotor or tail rotor. AGARD Advisory Report No. 223 (reference 2-127) states: "So far as is known, the only attempt to analyze the trajectories of shed ice has been by France as an aid to the Puma certification." This computation was not checked by experiment. For helicopters, the computation of ice chunk trajectories is complicated by the complex flow through the rotors and around the fuselage.

Modeling ice pieces of random shapes is a statistical problem. Extreme cases of weight and aerodynamic coefficients (C_L and C_D) should be used. If the ice chunk rotates about its own center of mass, the C_L and C_D values will vary. Again, the conclusion of reference 2-127 is that, because of the assumptions and simplifications made, ice shedding trajectory computations should be used cautiously and substantiated by in-flight tests. "However, it is felt that despite these restrictions, the (computations) can be used as a flight test, development, and certification aid."

Any particle trajectory code can be adapted to this use with appropriate changes and within code limitations. Ice shed from a surface, either naturally or by de-icing system (pneumatic boot, electro-impulse, freezing point depressant, or electro-thermal), will have various sizes and shapes. The ice particles may peel off the surface with rotation and be swept into a vortical flow, thus adding randomness.

Generally, the safe estimate method for trajectories is to follow small and large particles from the iced area at various aircraft flight attitudes. Initial positions chosen should be at least as far from the surface of the iced area as the maximum expected dimension of the ice piece. Particle weight cannot be ignored for the larger pieces.

IV.2.4 ENGINE ICING ANALYSIS

This section very briefly discusses certain analytical aspects of evaluating the thermodynamics of the icing/anti-icing process as it relates to engines, and then assessing the tolerance of a particular engine to an ice accretion. Ice calculation procedures presented herein, leading up to and including the thermodynamics, are taken directly from reference 2-128. The reader is referred to that work for a much fuller discussion of these and other matters concerning engine icing.

2.4.1 Calculations Leading to Thermodynamic Analysis of Engine Icing

Liquid water-to-air concentrations within the engine inlet/compression system and droplet impingement rates on the various engine components must be determined prior to performing a thermodynamic icing calculation. Three key regions of interest for determining local LWC concentrations are shown in figure 2-27.

The inlet duct concentration factor C_t, figure 2-28, defined as the ratio of water ingested by the inlet plane area A_i to the water contained in a hypothetically extended stream tube of A_i cross-section well ahead of the inlet, or

$$C_t = \frac{\dot{M}_W \text{ in } A_i \text{ at inlet}}{\dot{M}_W \text{ in } A_i \text{ stream tube at } -\infty} \qquad (2\text{-}12)$$

It is a function of the ratio of engine inlet airflow velocity to airplane flight velocity and of droplet diameter.

The water ingested by the inlet is

$$\dot{M}_{W_{(1)}} = LWC_0 \; V_0 \; A_i \; C_t \qquad (2\text{-}13)$$

and the LWC within the inlet duct may be determined by

$$LWC_{(1)} = \frac{\dot{M}_{W_{(1)}}}{\frac{\dot{W}_i}{\rho_i}} = LWC_0 \; \frac{V_0}{V_i} \; C_t \qquad (2\text{-}14)$$

Spinner or nose cone impingement is generally only about 1% of the water ingested by the inlet. Therefore, the water flow rate at location 2 of figure 2-28 can be assumed to be the same as at location 1.

The LWC inside the core engine splitter duct, location 3, can be determined by applying the concentration characteristics of figure 2-28 to the possible streamlines approaching the splitter duct (illustrated in figure 2-29) as established by the core and fan bypass airflow splits.

Total inlet flow W_i is the sum of core engine flow W_e and fan bypass flow W_f, i.e.,

$$\dot{W}_i = \dot{W}_e + \dot{W}_f \tag{2-15}$$

The splitter duct concentration factor Cte is defined as

$$C_{te} = \frac{\text{water flow ingested by splitter duct } A_e}{\text{water flow at location 1 within streamline } A_{0II}} \tag{2-16}$$

where A'_{0II} is a forward projection of the Ae stream tube (figure 2-29). Splitter duct water ingestion rate is

$$\dot{M}_{W_{(3)}} = \dot{M}_{W_{(1)}} \frac{A_e}{A_i} C_{te} \tag{2-17}$$

where C_{te} is read from figure 2-28 at an abscissa velocity ratio equal to

$$\frac{A'_{0x}}{A_e} = \frac{A_1}{A_e} \frac{\dot{W}_e}{\dot{W}_i} \tag{2-18}$$

It follows that, at location 3, LWC is given by

$$LWC_{(3)} = \frac{\dot{M}_{W_{(3)}}}{\frac{\dot{W}_e}{\rho_{(3)}}} \tag{2-19}$$

Droplet impingement rates on the various engine components are needed next. Impingement parameters for bodies of revolution from Chapter I, Section 2 and other sources may be used on spinners and nose cones. Overall impingement rates for the leading edge of inlet guide vanes/stators are typically 90% or higher according to computations which use impingement characteristics of a cylinder to simulate the actual object, the diameter of the cylinder being taken equal to the maximum airfoil thickness. Stagnation region local impingement rate are sometimes approximated using the impingement characteristics for a cylinder of radius equal to that of the airfoil leading edge radius. These methods are discussed in reference 2-128, which also concludes using 100 percent catch efficiency for stator leading edges yields a slightly conservate analysis.

The freezing fraction n, whose significance and calculation is discussed in Chapter I, Section 2, is used in correlating engine response to icing. In the present context it would be calculated for a surface, or perhaps several small elemental surfaces on the engine component of interest. To review

the theoretical significance of the freezing fraction concept, if n lies between 0 and 1, the surface temperature is maintained exactly at the freezing level by the freezing process and only a portion of the impinging water freezes on impact. The closer n is to 0, the more "non-aerodynamic" the shape of the ice formation on the component is expected to be. If n equals 0, none of the impinging water freezes, and the surface temperature is above the freezing level. If n equals 1, the surface temperature is below the freezing level and the impinging water freezes at the point of impact. Although these "properties" of n are a valuable guide to the engineer, he must take into account the uncertainty in the calculation of this parameter.

2.4.2 Assessing Engine Tolerance to Ice Accretion

Utilization of conservative assumptions (e.g., 100% catch efficiency for stators, neglecting ice shedding and including water-to-air concentration amplification at inlets and at bypass splitters) for the thermodymamic evaluation of ice accretion can aid the designer in assessing icing tolerance of a particular gas turbine engine. The emphasis here is on the consequences of ice accretion on gas turbine engine operation.

It is of particular interest to evaluate the effects of ice accretion on fixed stators located downstream of the fan rotor in turbofan engines. Stators in the bypass duct are generally not a concern since flow blockage is seldom a problem and ice shedding is of little consequence to downstream components. The core stream is more critical, particularly in large-bypass-ratio turbofans with relatively low temperature rise for the rotor root section at reduced engine power. Excessive blockage of such a stator by ice accretion can lead to abnormal reductions in engine airflow and power. The key is to determine what level of blockage is considered excessive.

Quantification of blockage via the thermodynamic analysis comes from the conservative ice thickness calculations mentioned earlier. Ice thickness accumulation may be compared to a representative dimension describing the stator passage flow area. This dimension is the hydraulic diameter:

$$D_H = 4 \frac{\text{flow area}}{\text{wetted perimeter}}$$

The analysis shown in figure 2-30 shows that ice thickness/hydraulic diameter ratio is proportional to the fraction of flow passage blockage by ice, and is independent of stator passage aspect ratio. Consequently, a machine with a larger stator hydraulic diameter is more tolerant of ice accretion and has greater potential for satisfactory operation without an active anti-icing system (i.e., uses only fan root air temperature rise to limit ice accumulation). Good experience in commercial service with non-anti-iced stators has been realized in such an application for hydraulic diameters in excess of 2 inches (5 cm).

An engine with a hydraulic diameter of this magnitude may have good tolerance for rime ice accretion and a relatively small sensitivity to glaze ice accumulation. Glaze ice formations, particularly

at very low values of the freezing fraction, can have significant flow blockage as compared to rime ice. Although an exact prediction of glaze ice shape and blockage is difficult, it is possible to correlate the influence of freezing fraction as shown in figure 2-31. This figure shows the relative flow capacity loss for a given level of stator ice accumulation. At freezing fractions of 0.1 or less, there is a base level of flow capacity loss. Increasing the freezing fraction beyond 0.1 shows a marked drop in the influence of ice accretion. This important result significantly narrows the icing regime having detrimental ice blockage effects and highlights the importance of utilizing thermodynamic ice accretion analyses to evaluate and understand icing test results.

In summary, conservative ice accretion analyses, when coupled with consideration for stator hydraulic diameter and the relative influence of freezing fraction, can be useful in an analytical assessment of turbofan engine icing tolerance.

2.4.3 Engine Icing Analsysis and Icing Facility Tests

Testing engines in a facility that simulates icing conditions at altitude can be useful in evaluating icing tolerance. This is particularly true if one utilizes an analysis (reference 2-128) to correlate simulated conditions with the actual in-flight icing conditions. The analysis can be used to assure that characteristics observed in the facility can be viewed in the proper context of relative ice accretion severity. For example, water-to-air concentration effects at a flight inlet will be absent in a facility simulation with a direct duct connection between water spray apparatus and the engine. The analysis provides the basis for increasing lab water concentrations at the source to compensate for this effect.

One detail of facility testing is worth additional consideration. This concerns the temperature of the water at the engine inlet plane. This temperature can be adequately controlled in the facility enviroment but is subject to some uncertainty in flight operation. The temperature of water entering an engine has an obvious influence on the thermodynamics of ice accretion on engine components. Within an engine inlet section, the static air temperature is subject to rapid changes due to local velocity changes. The water temperature requires sufficient time to adjust to static temperature (via heat transfer). The required time is assured in a simulated flight icing test by providing a long entry duct ahead of the engine. In such a situation, the ice accretion analysis based upon water temperature equal to inlet duct static air temperature is expected to be quite valid. A schematic showing how water temperature adjusts within the inlet ducting is shown in figure 2-32.

This figure also depicts commercial flight inlets which are typically too short to reach thermal equilibrium between air and water. Flight conditions of greatest interest, however, involve reduced engine power at relatively high flight speeds with accompanying inlet spillage and high resultant water concentrations. Under these conditions, flow velocity drops from aircraft flight speed levels to lower inlet duct velocity levels, causing a rise in static air temperature. Assuming that water temperature reaches the engine plane at ambient levels (effectively a zero length inlet) is only approximate, but is conservative. That is, the analysis would predict excessive ice accretion relative to true engine entrance conditions. This amount of conservatism is acceptable for design purposes and for comparing various flight conditions for icing potential relative to icing tunnel testing.

IV.2.5 REFERENCES

2-1 Ruff, G.A., "Analysis and Verification of the Icing Scaling Equations," AEDC-TR-85-30, Vol. 1, November 1985.

2-2 Bartlett, C. S., "An Empirical Look at Tolerances in Setting Icing Test Conditions with Particular Application to Icing Similitude," AEDC-TR-87-23, DOT/FAA/CT-87-31, August 1988.

2-3 Olsen, W. and Newton, J., "Experimental and Analytical Evaluation of Icing Scaling Laws; A Progress Report," NASA TM 88973, 1987.

2-4 Bilanin, A.J., "Proposed Modifications to Ice Accretion/Icing Scaling Theory," AIAA-88-0203, paper presented at the 26th Aerospace Sciences Meeting, Jan. 1988.

2-5 Pope, A., "Wind Tunnel Testing," John Wiley and Sons, Inc., New York, 1947.

2-6 Hansman, R.J.; Yamaguchi, K.; Berkowitz, B.; and Potapczuk, M., "Modeling of Surface Roughness Effects on Glaze Ice Accretion," AIAA-89-0734, paper presented at the 27th Aerospace Sciences Meeting, Jan. 1989.

2-7 Yamaguchi, K. and Hansman, R.J., "Heat Transfer on Accreting Ice Surfaces," AIAA-90-0200, paper presented at the 28th Aerospace Sciences Meeting, Jan. 1990.

2-8 Yamaguchi, K. and Hansman, R.J., "Deterministic Multi-Zone Ice Accretion Modeling," AIAA-91-0265, paper presented at the 29th Aerospace Sciences Meeting, Jan. 1991.

2-9 Bragg, M. B., "Rime Ice Accretion and Its Effect on Airfoil Performance," Ph.D. dissertation, The Ohio State University, 1981, and NASA CR 165599, March 1982.

2-10 Bragg, M. B., "A Similarity Analysis of the Droplet Trajectory Equation," AIAA Journal, Vol. 20, No. 12, December 1982, pp. 1681-1686.

2-11 Tribus, M.V., et. al., "Analysis of Heat Transfer over a Small Cylinder in Icing Conditions on Mount Washington," American Society of Mechanical Engineers Transactions, Vol. 70, 1949, pp. 871-876.

2-12 Armand, C., et al, "Techniques and Facilities Used at the Onera Modane Centre for Icing Tests," North Atlantic Treaty Organization Advisory Group for Aerospace Research and Development, AGARD AF-127, November 1978.

2-13 Sibley, P.J. and Smith, R.E., Jr., "Model Testing in an Icing Wind Tunnel," Lockheed Aircraft Corporation, Report No. LR10981, 1955.

2-14 Jackson, E.T., "Development Study: The Use of Scale Models in an Icing Tunnel to Determine the Ice Catch on a Prototype Aircraft with Particular Reference to Concorde," British Aircraft Corporation (Operating) Ltd., Filton division, SST/B75T/RMMcK/242, July 1967.

2-15 Hauger, H. H. and Englar, K. G., "Analysis of Model Testing in an Icing Wind Tunnel," Douglas Aircraft Company, Inc., Report No. SM14933, 1954.

2-16 Dodson, E. O., "Scale Model Analogy for Icing Tunnel Testing," Boeing Airplane Company, Transport Division, Document No. D66-7976, March 1962.

2-17 Charpin, F. and Fasso, G., "Icing Testing in the Large Modane Wind Tunnel on Full Scale and Reduced Scale Models," L'Aeronautique et L'Astronautique, 1972, English Translation, NASA TN-75373.

2-18 Sundberg, M., Trunov, O., and Ivaniko, A., "Methods for Prediction of the Influence of Ice on Aircraft Flying Characteristics," Report JR-1, Board of Civil Aviation, Sweden, 1977.

2-19 Laschka, B. and Jesse, R.E., "Ice Accretion and Its Effects on Aerodynamics of Unprotected Aircraft Components," AGARD-AR-127, February 1979, pp. 4-1 to 4-22.

2-20 Ruff, G.A., "Verification and Application of the Icing Scaling Equations," AIAA Paper No. 86-0481, presented at the 24th Aerospace Sciences Meeting, Reno, Nevada, January 1986.

2-21 Reinmann, J. J.; Shaw, R. J.; and Ranaudo, R. J., "NASA's Program on Icing Research and Technology," NASA TM 101989, May 1989.

2-22 Bilanin, A.J., "Problems in Understanding Aicraft Icing Dynamics," AIAA-89-0735, paper presented at the 27th Aerospace Sciences Meeting, Jan. 1989.

2-23 Bartlett, C. S., "An Analytical Study of Icing Similitude for Aircraft Engine Testing," AEDC-TR-86-26 (AD-A173713), DOT/FAA/CT-86-35, October 1986.

2-24 Bartlett, C. S., "Icing Scaling Considerations for Aircraft Engine Testing," AIAA-88-0202, paper presented at the 26th Aerospace Sciences Meeting, Jan. 1988.

2-25 Bradley, R. G., "CFD Validation Philosophy," AGARD Symposium on Validation of Computational Fluid Dynamics, Lisbon, Portugal, May 1988.

2-26 NASA CFD Validation Workshop, NASA Ames Research Center, Moffet Field, CA.

2-27 Bradley, R. G., "Future Directions for Applied Computational Fluid Dynamics" in Applied Computational Aerodynamics, P. A. Henne, editor, AIAA, Washington, D.C., 1990.

2-28 Ruppert, P., Unpublished talk, presented at the 26th Aerospace Sciences Meeting, Jan. 1988.

2-29 Langmuir, I. and Blodgett, K., "A Mathematical Investigation of Water Droplet Trajectories," AAFTR 5418, February 1946.

2-30 Shaw, Robert J., "Progress Toward the Development of an Aircraft Icing Analysis Capability," NASA TM 83562, Jan. 1984.

2-31 Ruff, G. A. and Berkowitz, B. M., "Users Manual for the NASA Lewis Ice Accretion Prediction Code (LEWICE)," NASA CR 185129.

2-32 Kim, J. J., "Particle Trajectory Computation on a 3-Dimensional Engine Inlet," NASA CR 175023 (DOT-FAA-CT-86-1), January 1986.

2-33 Tenison, G., "A Comparison of a Droplet Impingement Code to Icing Tunnel Results," AIAA-90-0670, paper presented at the 28th Aerospace Sciences Meeting, Jan. 1990.

2-34 Kim, J. J. and Elangovan, R., "An Efficient Numerical Computation Scheme for Stiff Equations of Droplet Trajectories," AIAA-86-0407, paper presented at the 24th Aerospace Sciences Meeting, Jan. 1986.

2-35 Gear, C. W., "Numerical Integration of Ordinary Differential Equations," Mathematics of Computation, 21 (98), 1967, pp. 145-156.

2-36 Breer, M.D. and Seibel,W., "Particle Trajectory Computer Program-User's Manual," Boeing Document D3-9655-1, Rev. B, December 1974.

2-37 Frost, W.; Chang, H. P.; and Kimble, K. R., "Particle Trajectory Computer Program for Icing Analysis," Final Report for NASA Lewis Research Center under Contract NAS3-22448 by FWD Associates, Inc., April 1982.

2-38 Chang, H-P; Frost, W; Shaw, R. J.; and Kimble, K. R., "Influence of Multidrop Size Distribution on Icing Collection Efficiency," AIAA-83-0100, paper presented at the 21st Aerospace Sciences Meeting, Jan. 1983.

2-39 Bragg, M. B., "An Incompressible Droplet Impingement Analysis of Thirty Low and Medium Speed Airfoils," NASA Contractor's Report, to be published.

2-40 Lozowski, E. P. and Oleskiw, M. M., "Computer Modeling of Time-Dependent Rime Icing in the Atmosphere," CRREL 83-2, Jan. 1983.

2-41 Lozowski, E. P. and Oleskiw, M. M., "Computer Simulation of Aerofoil Icing Without Runback," AIAA-81-0402, paper presented at the 19th Aerospace Sciences Meeting, Jan. 1981.

2-42 Gent, R. W., "Calculation of Water Droplet Trajectories About An Aerofoil in Steady, Two-Dimensional, Compressible Flow," RAE TR 84060, June 1984.

2-43 McComber, P. and Touzot, G., "Calculation of the Impingement of Cloud Droplets on a Cylinder by the Finite Element Method," Journal of the Atmospheric Sciences, Vol. 38, May 1981, pp. 1027-1036.

2-44 Gelder, T. F.; Smyers, Jr., W. H.; and Von Glahn, U. H., "Experimental Droplet Impingement on Several Two-Dimensional Airfoils with Thickness Ratios of 6 to 16 Percent," NACA TN 3839, Dec. 1956.

2-45 Von Glahn, U.; Gelder, T. F.; and Singers, W.H., "A Dye-Tracer Technique for Experimentally Obtaining Impingement Characteristics of Arbitrary Bodies and a Method for Determining Droplet Size Distribution," NACA TN 3338, 1955.

2-46 Brun, R. J. and Vogt D. E., "Impingement of Cloud Droplets on 36.5 Percent-Thick Joukowski Airfoil at Zero Angle of Attack and Discussion of Use as Cloud Measuring Instrument in Dye-Tracing Technique," NASA TN-4035, 1957.

2-47 Papadakis, M. and Zumwalt, G. W., "An Experimental Method for Measuring Droplet Impingement Efficiency on Two- and Three-Dimensional Bodies," AIAA-86-0406, 1986.

2-48 Papadakis, M.; Elangovan, R.; Freund, G. A.; and Breer, M. D., "Experimental Water Droplet Impinge nent Data on Two-Dimensional Airfoils, Axi-symmetric Inlet and Boeing 737-300 Engine Inlets," AIAA Paper No. 87-0097, 1987.

2-49 Papadakis, M.; Elangovan, R.; Freund, Jr., G. A.; Breer, M.; Zumwalt, G. W.; and Whitmer, L., "An Experimental Method for Measuring Water Droplet Impingement Efficiency on Two- and Three-Dimensional Bodies," NASA CR 4257, DOT/FAA/CT-87/22, November 1989.

2-50 Papadakis, M.; G. A.; Breer, M.; Craig, N.; and Bidwell, C., "Experimental Water Droplet Impingement Data on Modern Aircraft Surfaces," AIAA-91-0445, paper presented at the 29th Aerospace Sciences Meeting, Jan. 1991.

2-51 Dorsch, R. G.; Brun, R. J.; and Gregg, J. L., "Impingement of Water Droplets on an Ellipsoid with Fineness Ratio 5 in Axisymmetric Flow," NACA TN 3099, March 1954.

2-52 Brun, R. J. and Dorsch, R.G., "Impingement of Water Droplets on an Ellipsoid with Fineness Ratio 10 in Axisymmetric Flow," NACA TN 3147, May 1954.

2-53 Dorsch, R. G.; Saper, P. G.; and Kadow, C. F., "Impingement of Water Droplets on a Sphere," NACA TN 3587, November 1955.

2-54 Dorsch, R.G. and Brun, R.J., "A Method for Determining Cloud-Droplet Impingement on Swept Wings," NACA TN 2931, 1953.

2-55 Rush, C.K., "Ice Shedding Tests on a 10-foot Sharp-Edged Delta Wing at Low Angles of Attack," NRC Report LR-364, December 1962.

2-56 Kim, J. J., "Computational Particle Trajectory Analysis on a 3-Dimensional Engine Inlet," AIAA-85-0411, AIAA 23rd Aerospace Sciences Meeting, Reno, Nevada, January 14-17, 1985.

2-57 Reyhner, T.A., "Three-Dimensional Transonic Potential Flow About Complex Three-Dimensional Configurations," NASA CR 3814, 1984.

2-58 Kim, J. J.; Breer, M. D.; Cass, J.; and Kneeling, D., "Sand Separator Efficiency Calculation for the JVX Tilt Rotor Aircraft Inlet," Presented at the 42nd Annual Forum of the American Helicopter Society, Washington, D.C., June 1986.

2-59 Norment, H G., "Calculation of Water Drop Trajectories to and About Arbitrary Three-Dimensional Bodies in Potential Airflow," NASA CR 3291, 1980.

2-60 Norment, H.G., "Calculation of Water Drop Trajectories to and About Arbitrary Three-Dimensional Lifting and Nonlifting Bodies in Potential Airflow," NASA CR 3935, October 1985.

2-61 Shaw, Robert J., "NASA's Aircraft Icing Analysis Program," NASA TM 88791, Sept. 1986.

2-62 Norment, H. G., "Three-Dimensional Airflow and Hydrometeor Trajectory Calculation with Applications," AIAA-85-0412, paper presented at the 23rd Aerospace Sciences Meeting, Jan. 1985.

2-63 Norment, H. G., "Three-Dimensional Trajectory Analyses of Two Drop Sizing Instruments: PMS OAP and PMS FSSP," NASA CR 4113 (DOT/FAA/CT-87130), Feb. 1988.

2-64 Drummond, A. M., "Aircraft Flow Effects on Cloud Droplet Images and Concentrations," NAE-AN-21, NRC No. 23508, June 1984.

2-65 Mohler, S. R., "A Three Dimensional Droplet Impingement Program for Aircraft Icing Analysis," M. S. Thesis, The Ohio State University, 1990.

2-66 Lewis, J.P. and Ruggeri, R.S., "Experimental Droplet Impingement on Four Bodies of Revolution," NACA TN 4092, December 1957.

2-67 Carlson, D.J. and Haglund, R.F., "Particle Drag and Heat Transfer in Rocket Nozzles," AIAA Journal, Vol. 2, No. 11, pp. 1980-1984, November 1964.

2-68 Shaw, R. J.; Potapczuk, M. G.; and Bidwell, C. S., "Predictions of Airfoil Aerodynamic Performance Degradation Due to Icing," NASA TM 101434, Jan. 1989.

2-69 Glauert, M., "A Method of constructing the Path of Raindrops of Different Diameters Moving in the Neighborhood of (1) a Circular Cylinder; (2) an Aerofoil, Placed in a Uniform Stream of Air; and a Determination of the Rate of Deposit of the Drops on the Surface and the Percentage of Drops Caught," British A.R.C., R and No. 2025, November 1940.

2-70 Messinger, B. L., "Equilibrium Temperature of an Unheated Surface as a Function of Airspeed," Journal of Aeronautical Sciences, Vol. 20, No. 1, January 1953.

2-71 Bragg, M.B., "Predicting Rime Ice Accretion on Airfoils," AIAA Journal, Vol. 23, No. 3, March 1985, pp. 381-386.

2-72 Ackley, S.F. and Templeton, M.K., "Computer Modeling of Atmospheric Ice Accretion," CRREL 79-4, March 1979.

2-73 Macklin, W. C., "The density and structure of ice formed by accretion," Quarterly Journal of the Royal Meterological Society, vol. 88, pp. 30-50.

2-74 Lozowski, E. P.; Stallabrass, J. R.; and Hearty, P. F., "The Icing of an Unheated Non-Rotating Cylinder in Liquid Water Droplet Ice Crystal Clouds," National Research Council of Canada, LTR-LT-96, February 1979.

2-75 Kirchner, R.D., "Aircraft Icing Roughness Features and Its Effect on the Icing Process," AIAA-83-0111, paper presented at the 21st Aerospace Sciences Meeting, Reno, Nevada, January 10-13, 1983.

2-76 MacArthur, C.D., "Numerical Simulation of Airfoil Ice Accretion," AIAA Paper 83-0012, January 1983.

2-77 Mikkelsen, K.L.; McKnight, R.C.; Ranaudo, R.J.; and Perkins, P.J., Jr., "Icing Flight Research: Aerodynamic Effects of Ice and Ice Shape Documentation with Stereo Photography," NASA TM 86906, 1985.

2-78 McKnight, R.C.; Palko, R.L.; and Humes, R.L., "In-Flight Photogrammetric Measurement of Wing Ice Accretions," AIAA Paper 86-0483, Jan. 1986.

2-79 Berkowitz, B. M. and Riley, J. T., "Analytical Ice Shape Predictions for Flight in Natural Icing Conditions," NASA CR 182234 (DOT/FAA/CT-88/19), Dec. 1988.

2-80 Cebeci, T.; Chen, H. H.; and Alemdaroglu, N., "Fortified LEWICE with Viscous Effects," AIAA-90-0754, paper presented at the 28th Aerospace Sciences Meeting, Jan. 1990.

2-81 Shin, J.; Berkowitz, B.; Chen, H. H.; and Cebeci, T., "Prediction of Ice Shapes and Their Effect on Airfoil Performance," AIAA-91-0264, paper presented at the 29th Aerospace Sciences Meeting, Jan. 1991.

2-82 Holcomb, J. E. and Namdar, B., "Coupled LEWICE/Navier-Stokes Code Development," AIAA-91-0804, paper presented at the 29th Aerospace Sciences Meeting, Jan. 1991.

2-83 Cansdale, I. T. and Gent, R. W., "Ice Accretion on Aerofoils in Two-dimensional Compressible Flow: A Theoretical Model," RAE TR-82128, January 1983.

2-84 Guffond, D., Cossaing, J., and Brunet, L., "Overview on Icing Research at ONERA," AIAA 85-0335, paper presented at the 23rd Aerospace Sciences Meeting, Reno, Nevada, January 14-17, 1985.

2-85 Potapczuk, M. and Bidwell, C., "Swept Wing Ice Accretion Modeling," NASA TM 102453, Jan. 1990.

2-86 Potapczuk, M. and Bidwell, C., "Numberical Simulation of Ice Growth on a MS-317 Swept Wing Geometry," AIAA-91-0203, paper presented at the 29th Aerospace Sciences Meeting, Jan. 1991.

2-87 Daughters, C. and Berkowitz, B., "Validation Efforts with the LEWICE Icing Analysis Code Using a Natural Icing Data Base," unpublished, 1989.

2-88 Potapczuk, M. G., "Progress in Development of a Navier-Stokes Solver for Evaluation of Iced Airfoil Performance," AIAA-85-0410, paper presented at the 23rd Aerospace Sciences Meeting, Jan. 1985.

2-89 Potapczuk, M. G., "Numerical Analysis of a NACA 0012 Airfoil with Leading Edge Ice Accretions," AIAA-87-0101, paper presented at the 25th Aerospace Sciences Meeting, Jan. 1987.

2-90 Zaman, K. B. M. Q. and Potapczuk, M. G., "The Low Frequency Oscillation in the Flow over a NACA 0012 Airfoil With an "Iced" Leading Edge," NASA TM 102018, June 1989.

2-91 Potapczuk, M. G. and Berkowitz, B. M., "An Experimental Investigation of Multi-Element Airfoil Ice Accretion and Resulting Performance Degradation," AIAA-89-0752, paper presented at the 27th Aerospace Sciences Meeting, Jan. 1989.

2-92 Steger, J. L., "Implicit Finite-Difference Simulation of Flow about Arbitrary Two-Dimensional Geometries," AIAA Journal, Vol. 16, No. 7, July 1978, pp. 679-686.

2-93 Cebeci, T., "Effects of Environmentally Imposed Roughness on Airfoil Performance," NASA CR 179639, 1987.

2-94 Cebeci, T., "Calculation of Flow over Iced Airfoils," AIAA Journal, Vol. 27, No. 7, July 1989, pp. 853-861.

2-95 Bragg, M. B. and Coirer, W. J., "Detailed Measurements of the Flowfield in the Vicinity of an Airfoil with Glaze Ice," AIAA-85-0409, paper presented at the 23rd Aerospace Sciences Meeting, Jan. 1985.

2-96 Bragg, M. B. and Coirer, W. J., "Aerodynamic Measurements of an Airfoil with Simulated Glaze Ice," AIAA-86-0484, paper presented at the 24th Aerospace Sciences Meeting, Jan. 1986.

2-97 Bragg, M. B., "An Experimental Study of the Aerodynamics of a NACA 0012 Airfoil with a Simulated Glaze Ice Accretion," NASA CR 197571, Jan. 1987.

2-98 Bragg, M. B. and Spring, S A., "An Experimental Study of the Flow Field about an Airfoil with Glaze Ice," AIAA-87-0100, paper presented at the 25th Aerospace Sciences Meeting, Jan. 1987.

2-99 Bragg, M. B. and Khodadoust, A., "Experimental Measurements in a Large Separation Bubble due to a Simulated Glaze Ice Accretion," AIAA-88-0116, paper presented at the 26th Aerospace Sciences Meeting, Jan. 1988.

2-100 Spring, S. A., "An Experimental Mapping of the Flow Field behind a Glaze Ice Shape on a NACA 0012 Airfoil," NASA CR 180847, Jan. 1988.

2-101 Khodadoust, A., "A Flow Visualization Study of the Leading Edge Separation Bubble on a NACA 0012 Airfoil with Simulated Glaze Ice," NASA CR 180846, Jan. 1988.

2-102 Caruso, S. C., "Development of an Unstructured Mesh/Navier-Stokes Method for Aerodynamics of Aircraft with Ice Accretions," AIAA-90-0758, paper presented at the 28th Aerospace Sciences Meeting, Jan. 1990.

2-103 Scott, J. N.; Hankey, W. L.; Geisler, F. J.; and Gielda, T. P., "Navier-Stokes Solution to the Flowfield over Ice Accretion Shapes," Journal of Aircraft, Vol. 25, No. 8, pp. 710-716.

2-104 Scott, J. N.; Gielda, T. P.; and Hankey, W. L., "Navier-Stokes Solutions of Flowfield Characteristics Produced by Ice Accretion," AIAA-88-0290, paper presented at the 26th Aerospace Sciences Meeting, Jan. 1988.

2-105 Scott, J. N. and Hankey, W. L., "A Numerical Investigation of the Influence of Surface Roughness on Heat Transfer in Ice Accretion," AIAA-89-0737, paper presented at the 26th Aerospace Sciences Meeting, Jan. 1989.

2-106 Pais, M. R. and Singh, S. N., "A Fourier Analysis Approach for Surface Definition and the Effect of Roughness on the Local Convective Heat-Transfer Coefficient as Related to Ice Accretion," AIAA-88-0117, paper presented at the 26th Aerospace Sciences Meeting, Jan. 1988.

2-107 Pais, M. R.; Singh, S. N.; and Zou, L., "Determination of the Local Heat-Transfer Characteristics on Simulated Smooth Glaze Ice Accretions on a NACA 0012 Airfoil," AIAA-88-0292, paper presented at the 26th Aerospace Sciences Meeting, Jan. 1988.

2-108 Bragg, M. B. and Khodadoust, A., "Effect of Simulated Glaze Ice on a Rectangular Wing," AIAA-89-0750, paper presented at the 27th Aerospace Sciences Meeting, Jan. 1989.

2-109 Bragg, M. B. and Khodadoust, A., "Effect of a Simulated Ice Accretion on the Aerodynamics of a Swept Wing," AIAA-91-0442, paper presented at the 29th Aerospace Sciences Meeting, Jan. 1991.

2-110 Kwon, O. J. and Sankar, L. N., "Numerical Study of the Effects of Icing on Finite Wing Aerodynamics," AIAA-90-0757, paper presented at the 28th Aerospace Sciences Meeting, Jan. 1990.

2-111 Kwon, O. J. and Sankar, L. N., "Numerical Study of the Effects of Icing on the Hover Performance of Rotorcraft," AIAA-91-0662, paper presented at the 29th Aerospace Sciences Meeting, Jan. 1991.

2-112 DeWitt, K.J. and Baliga, G., "Numerical Simulation of One-Dimensional Heat Transfer in Composite Bodies with Phase Change," NASA CR 165607, 1982.

2-113 Marano, J.J., "Numerical Simulation of an Electrothermal De-icer Pad," NASA CR 168097, 1983.

2-114 Chao, D. F. K., "Numerical Simulation of Two-Dimensional Heat Transfer in Composite Bodies with Application to De-Icing of Aircraft Components," NASA CR 168283, 1983.

2-115 Wright, W. B., "A Comparison of Numerical Methods for the Prediction of Two-Dimensional Heat Transfer in an Eelectrothermal Deicer Pad," NASA CR 4202, 1988.

2-116 Masiulaniec, K. C., "A Numerical Simulation of the Full Two-Dimensional Electrothermal De-Icer Pad," NASA CR 4194, 1988.

2-117 Keith, T. G.; DeWitt, K.J.; Wright, W. B.; and Masiulaniec, K. C., "Overview of Numerical Codes Developed for Predicted Electrothermal De-Icing of Aircraft Blades," AIAA-88-0288, paper presented at the 26th Aerospace Sciences Meeting, Jan. 1988.

2-118 Leffel, K. L., "A Numerical and Experimental Investigation of Electrothermal Aircraft De-icing," NASA CR 175024, 1986.

2-119 Yaslik, A. D.; De Witt, K.J.; Keith, T. G.; and Boronow, W., "Three-Dimensional Numerical Simulation of Electrothermal Deicing Systems," AIAA-91-0267, paper presented at the 29th Aerospace Sciences Meeting, Jan. 1991.

2-120 Wright, W. B.; Keith, T. G.; De Witt, K.J., "Numerical Simulation of Icing, Deicing, and Shedding," AIAA-91-0665, paper presented at the 29th Aerospace Sciences Meeting, Jan. 1991.

2-121 Bernhart, W. D. and Gien, P. H., "A Structural Dynamics Investigation Related to EIDI Applications," AIAA-86-0550, paper presented at the 24th Aerospace Sciences Meeting, Jan. 1986.

2-122 Khatkhate, A. A.; Scavuzzo, R. J.; and Chu, M. L., "A Finite Element Study of the EIDI System," AIAA-88-0022, paper presented at the 26th Aerospace Sciences Meeting, Jan. 1988.

2-123 Scavuzzo, R. J.; Woods, E. J.; Chu, M. L.; and Khatkhate, A. A., "Finite Element Studies of the EIDI System using Force Inputs," AIAA-89-0868, paper presented at the 27th Aerospace Sciences Meeting, Jan. 1989.

2-124 Al-Khalil, K. M.,; Keith, T. G.; De Witt, K.J.,"Thermal Analysis of Engine Inlet Anti-Icing Systems," AIAA-89-0759, paper presented at the 27th Aerospace Sciences Meeting, Jan. 1989.

2-125 Al-Khalil, K. M.,; Keith, T. G.; De Witt, K.J.,"Development of an Anti-Icing Runback Model," AIAA-90-0759, paper presented at the 28th Aerospace Sciences Meeting, Jan. 1990.

2-126 Al-Khalil, K. M.,; Keith, T. G.; De Witt, K.J., "Further Development of an Anti-Icing Runback Model," AIAA-91-0266, paper presented at the 29th Aerospace Sciences Meeting, Jan. 1991.

2-127 "Rotorcraft Icing - Progress and Potential," AGARD Advisory Report No. 223, Sept. 1986.

2-128 Pfeifer, G. D. and Maier, G. P., "Engineering Summary of Powerplant Icing Technical Data," FAA-RD-77-76, July 1977.

TABLE 2-1. SCALED VARIABLES

EXAMPLE FOR DROPLET TRAJECTORY AND IMPINGEMENT

	Full Scale with K_0 = 0.132	One-Sixth Scale with K_0 = 0.132
MVD, μm	15.0	5.05
Re	115.6	38.9
K	0.0393	0.0267
E	0.0555	0.0508
Max Local Efficiency, β_{max}	0.332	0.323

	Full Scale with K_0 = 0.039	One-Sixth Scale with K_0 = 0.039
MVD, μm	30.0	9.60
Re	231.2	73.98
K	0.1572	0.0966
E	0.173	0.166
Max Local Efficiency, β_{max}	0.568	0.563

TABLE 2-2. SUMMARY OF PAST SCALING INVESTIGATIONS
EVALUATED BY THE AEDC STUDY (REFERENCE 2-1) AND BY NASA TESTS (REFERENCE 2-3)

SCALING ANALYSIS	SCALING PARAMETERS						
	K_0	A_c	n	b	θ	ϕ	Other Matchings
AEDC Evaluations							
1. Douglas Aircraft Co. 1954 (Reference 2-15)	X	X					h, T_s ($h \sim V^{.8}$)
2. Lockheed Aircraft Corp. 1955 (Reference 2-13)	X	X	X	X			($h \sim V^{.5}$)
3. Boeing Airplane Co. 1962 (Reference 2-16)	X	X					
4. British Aircraft Corp. 1967 (Reference 2-14)	X	X	X	X			
5. ONERA Modane Centre France, 1977 (Reference 2-12) and 1972 (Reference 2-17)	X	X	X	X	X	X	($h \sim V^{.8}$)
6. AEDC, 1985 (Reference 2-1)	X	X	X	X	X	X	($h \sim V^{.5}$)
NASA Test Evaluations							
5 and 6 above	X	X	X	X	X	X	($h \sim V^{.5}$ or $V^{.8}$)
7. Russian/Swedish 1977 (Reference 2-18)	X	X					LWC and T_s
8. Same Freezing Fraction	X	X	X				($h \sim V^{.5}$)
9. AGARD, 1977 (Reference 2-19) Flight Tests with Different LWCs	All physical variables match except LWC and time (energy not balanced)						LWC·t = constant
10. Flight Tests with Different LWC and T_s Controllable by Altitude Change	Size and velocity match or matched by adjusting T_s						LWC·t = constant

TABLE 2-3. SCALED PHYSICAL VARIABLES AND ICING PARAMETERS

Variable	Full-Scale	One-Third Scale
c (in)	10.907	3.636
V (ft/sec)	200	200
LWC (g/m^3)	0.6	1.0
T_s (°F)	3.53	4.43
P_s (psia)	14.0	12.2
MVDC (μm)	30	15
t (min)	20	3.75
Scaling Parameters		
K_o	0.20	0.20
A_c	0.13	0.12
n	1.0	1.0
b	0.19	0.18
ϕ (°F)	27.7	26.8
θ (°F)	21.3	20.4

TABLE 2-4. RANGES OF TEST PARAMETERS INVESTIGATED AT THE AEDC

PARAMETER	LOW	HIGH
Velocity, fps	100	400
Static Pressure, psia	4.4	14.2
Static Temperature, °F	-5	32
LWC, g/m^3	0.26	1.54
Droplet Diameter, μm	10	45
Icing Time, min	1.5	31.0
MODEL SCALE FACTOR	0.17	6.0

TABLE 2-5. DROPLET IMPINGEMENT ON A CYLINDER FROM SEVERAL NUMERICAL METHODS

R_e	K	K_0	E_m	β_{max}	θ_m	Data Source
100	0.5	0.1785	.120	.318	29.3	RAE Compressible (M=.352) (Reference 2-42)
			.156	.348	34.2	Langmuir and Blodgett (Reference 2-29)
			.154	.358	34.1	RAE Incompressible (Reference 2-42)
			.170	.376	35.2	Lozowski and Oleskiw (Reference 2-40)
			.155	.363	34.4	Bragg (Reference 2-9)
600	18.0	2.851	.793	.889	77.3	RAE Compressible (M=.352) (Reference 2-42)
			.819	.885	79.8	Langmuir and Blodgett (Reference 2-29)
			.808	.888	79.5	RAE Incompressible (Reference 2-42)
			.814	.898	79.5	Lozowski and Oleskiw (Reference 2-40)
			.812	.900	79.1	Bragg (Reference 2-9)

TABLE 2-6. CALCULATED DROPLET MAXIMUM IMPINGEMENT LOCATION ON AN ELLIPSOID OF FINENESS RATIO 5

Freestream Speed (mph)	r_o	
	Dorsch (Reference 2-51)	Normert (Reference 2-59)
100	0.024	0.019
200	0.041	0.037
300	0.054	0.045

Altitude: 5000 ft.

Temperature: 20°F

Droplet Diameter: 20μm

Ellipsoid semi-major axis length: 5 ft.

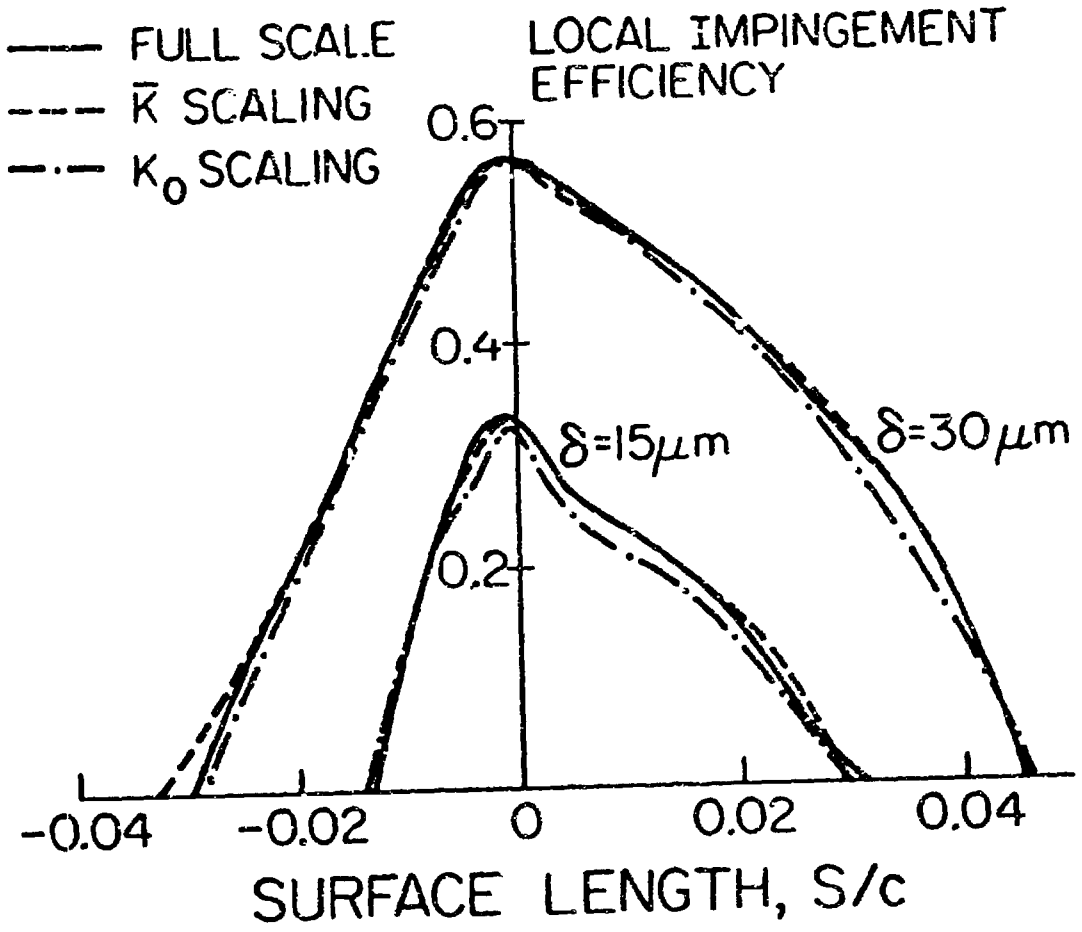

FIGURE 2-1. SCALED DROPLET IMPINGEMENT DISTRIBUTION

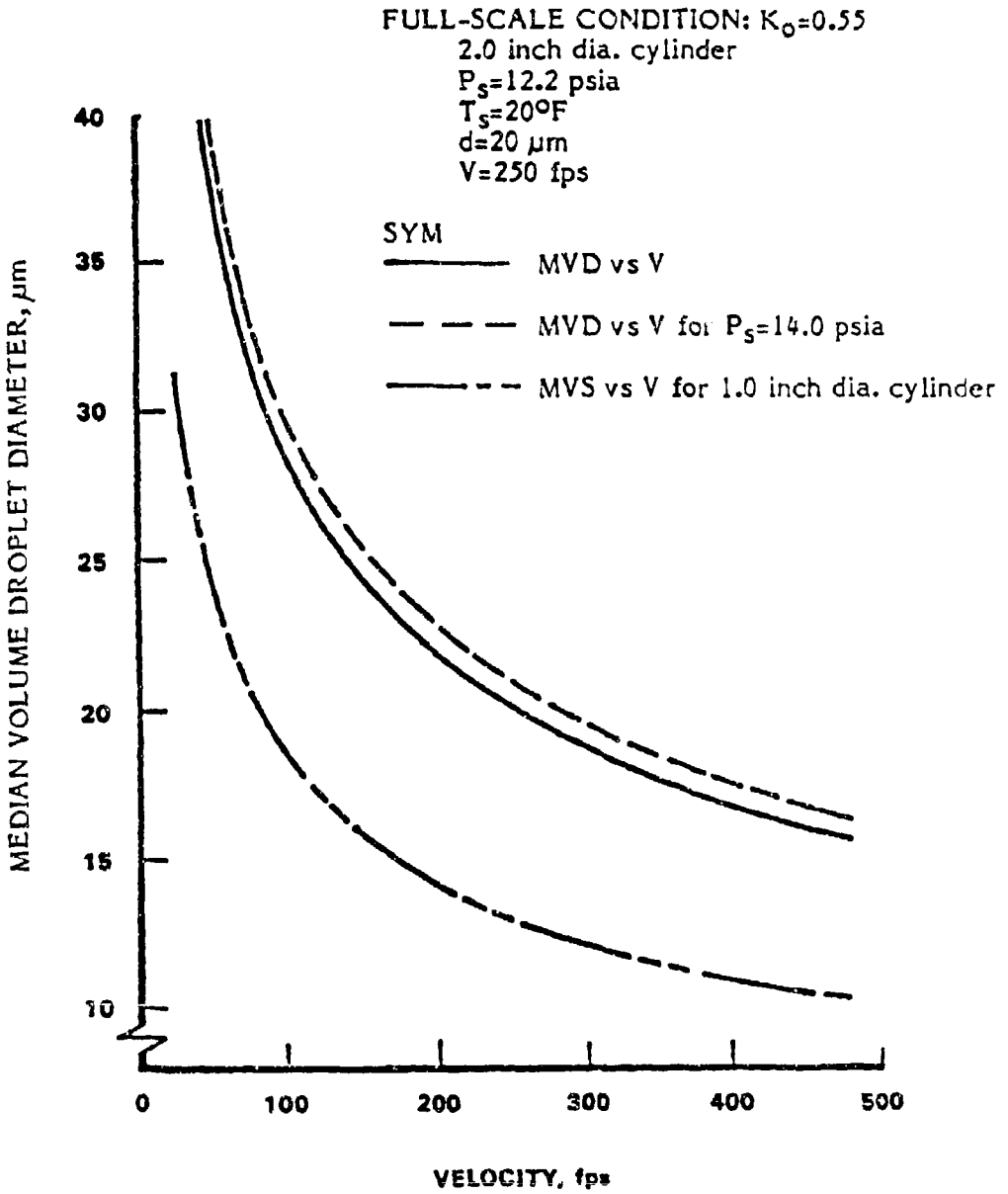

FIGURE 2-2. EFFECT OF VELOCITY, STATIC PRESSURE, AND MODEL SIZE ON THE MEDIAN DROPLET DIAMETER FOR A CONSTANT VALUE OF MODIFIED INERTIA PARAMETER, K_o (REFERENCE 2-1)

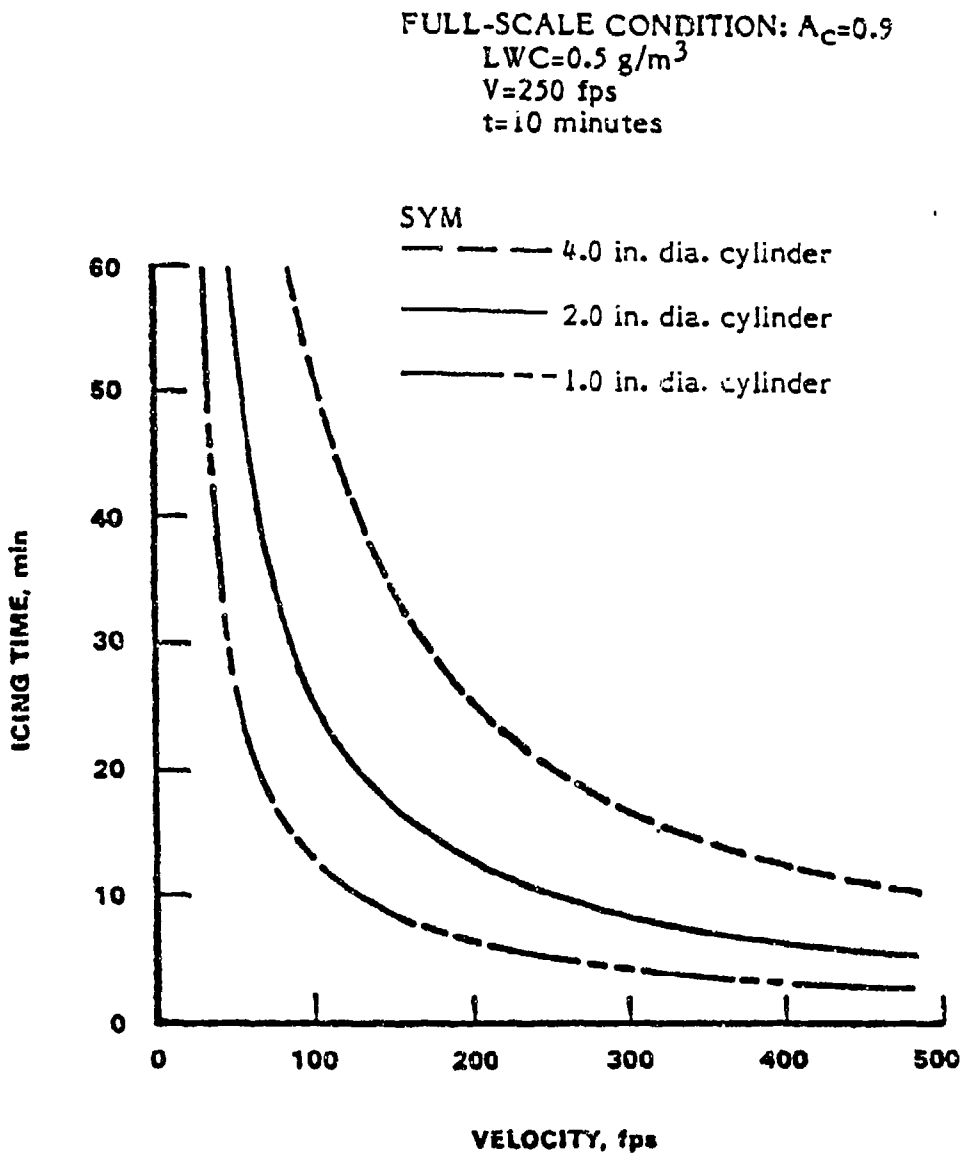

FIGURE 2-3. EFFECT OF VELOCITY AND MODEL SIZE ON THE ICING TIME FOR A CONSTANT VALUE OF ACCUMULATION PARAMETER, A_c (REFERENCE 2-1)

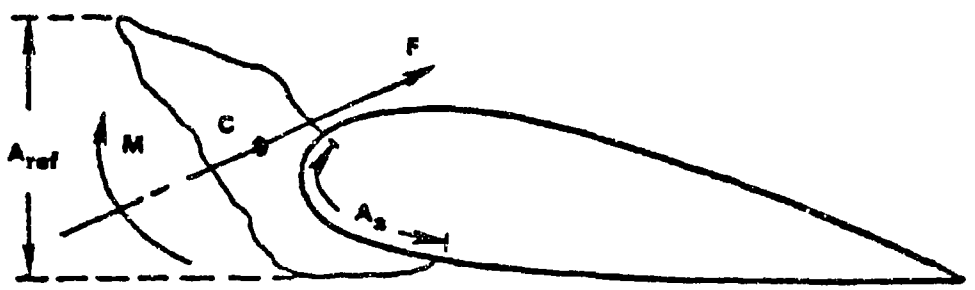

C = CENTROID OF THE ICE ACCRETION CROSS-SECTIONAL AREA
A_{ref} = REFERENCE DIMENSION FOR THE DRAG COEFFICIENT, C_{D_I}
A_a = AREA OF ATTACHMENT
F = AERODYNAMIC FORCE ACTING THROUGH THE CENTROID
M = MOMENT OF THE ICE ACCRETION ABOUT THE CENTROID

FIGURE 2-4. DEFINITION OF ICE SHEDDING ANALYSIS TERMS (REFERENCE 2-1)

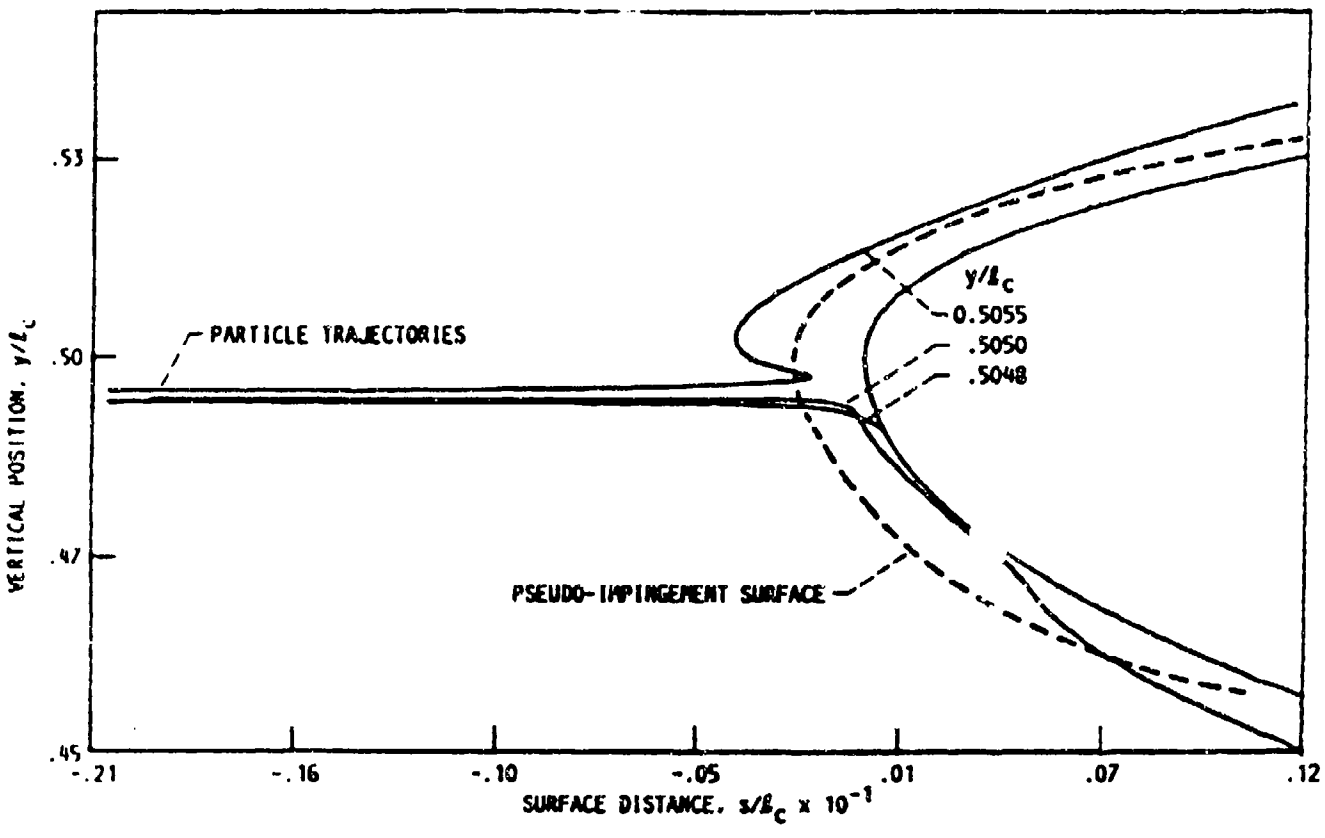

FIGURE 2-5. DROPLET TRAJECTORIES PERTURBED BY FLOWFIELD VELOCITIES CLOSE TO PANEL SINGULARITY POINTS (Reference 2-31)

Chord Length = 13.0 in. (33.0 cm)
Angle of Attack = 8.0°
True Tunnel Speed = 182.5 MPH (81.6 m/s)
Tunnel Total Temp. = 40°F (4.4°C)

▲ Test Data
_____ Theory

Langmuir "D" Distribution
About MVD = 15 Microns

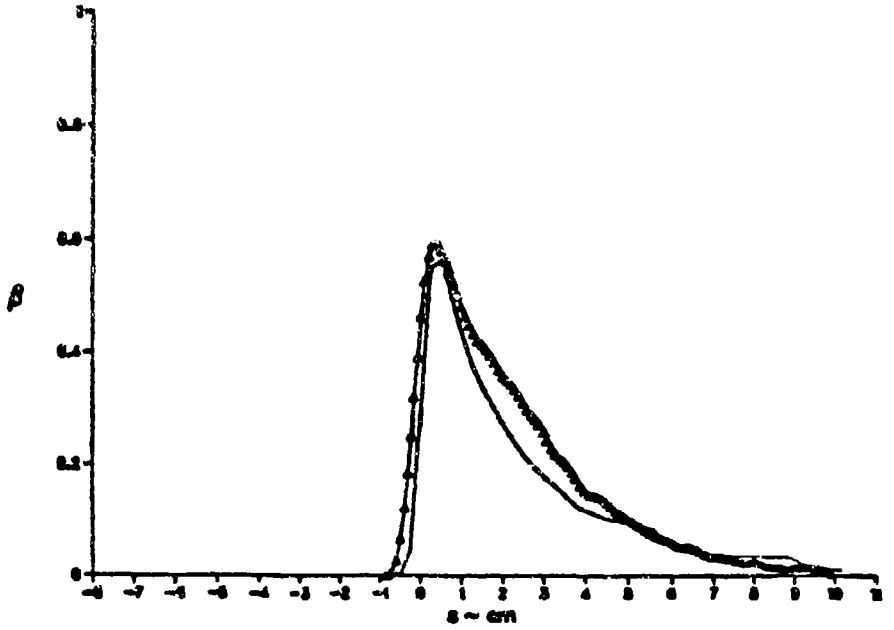

FIGURE 2-6. IMPINGEMENT EFFICIENCY CURVES FOR A NACA 65-015 AIRFOIL AT α = 8 DEGREES (Reference 2-47)

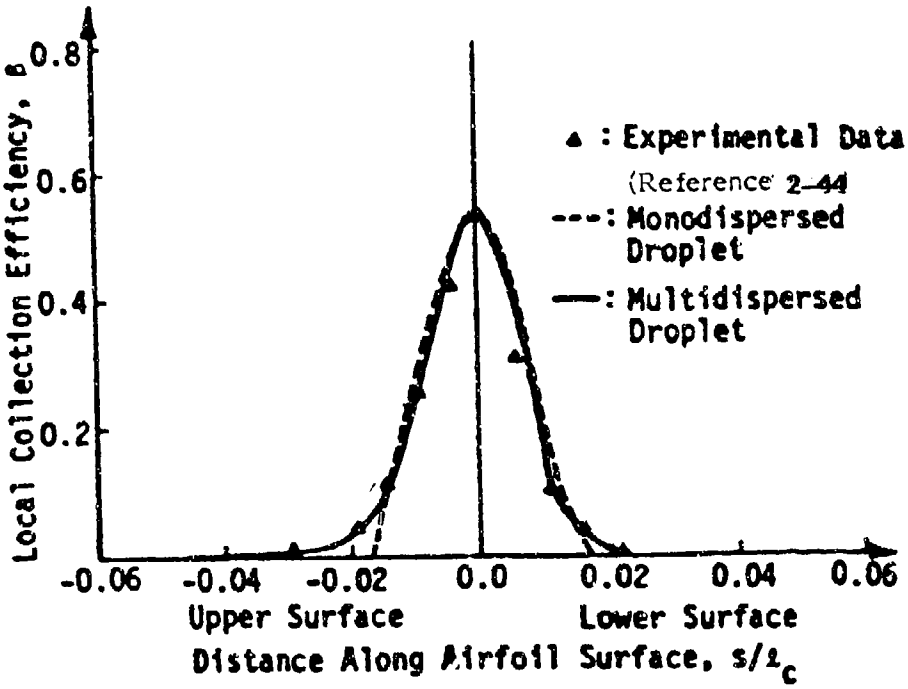

FIGURE 2-7. IMPINGEMENT EFFICIENCY CURVES FOR A NACA 65_1-212 AIRFOIL AT α = 0 DEGREES (REFERENCE 2-38)

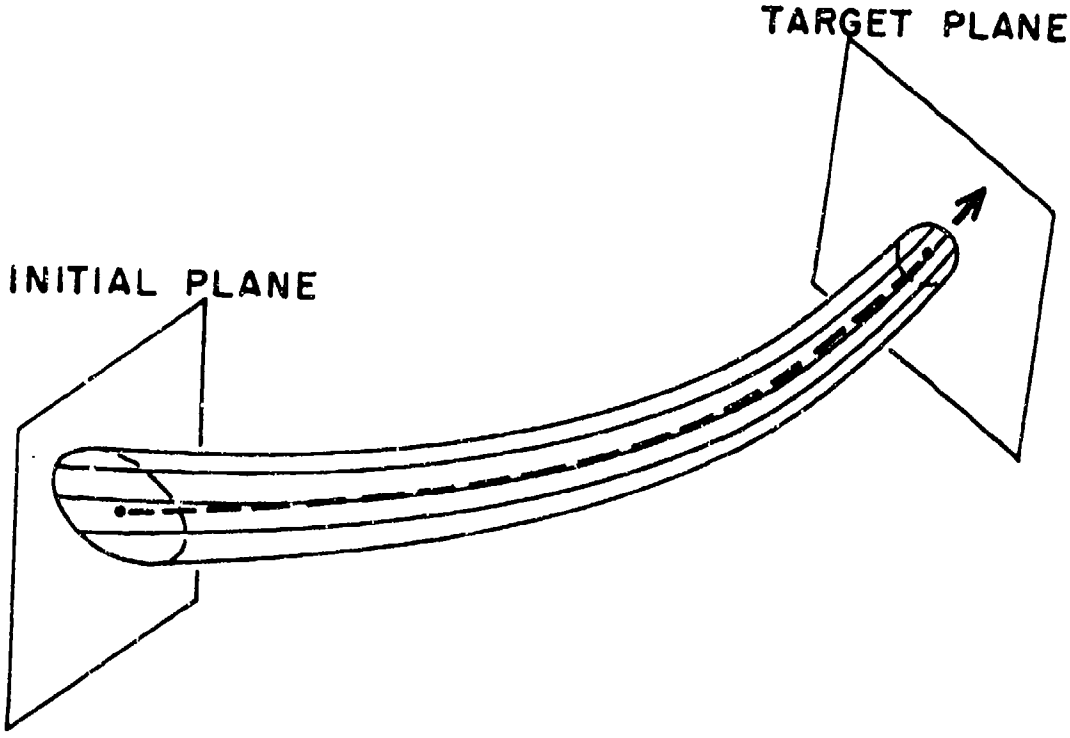

FIGURE 2-8. WATER DROP FLUX TUBE (Reference 2-63)

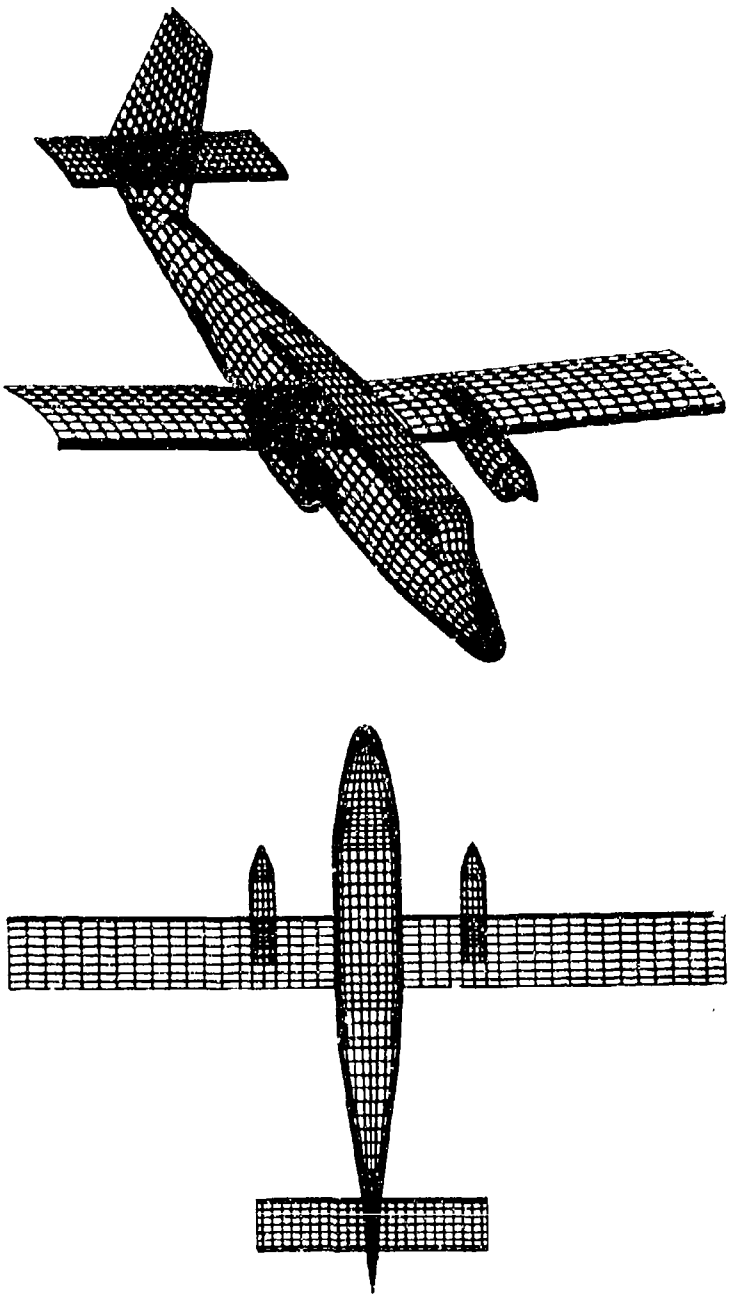

FIGURE 2-9. DIGITAL DESCRIPTION OF NASA ICING RESEARCH AIRCRAFT - TWIN OTTER

(Reference 2-30)

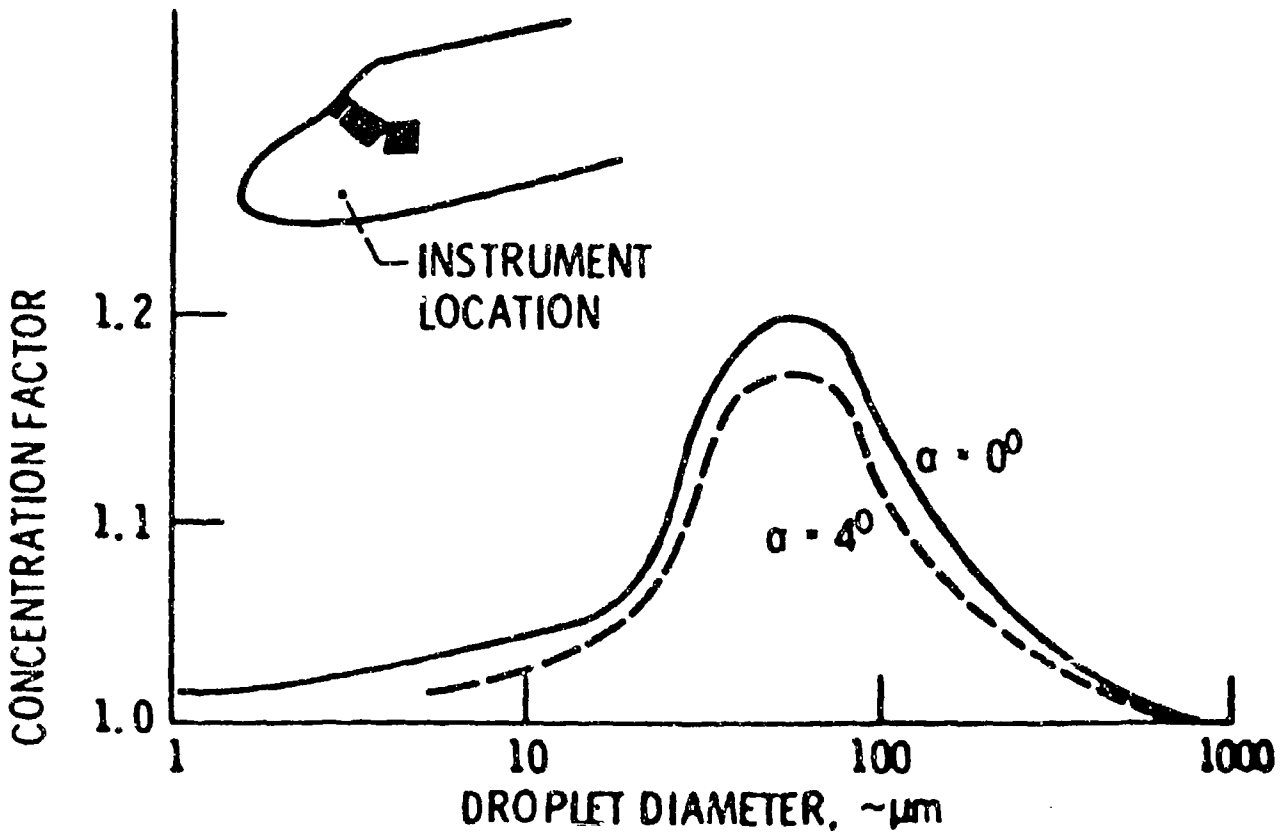

FIGURE 2-10. CONCENTRATION FACTOR CALCULATIONS FOR NASA ICING RESEARCH AIRCRAFT.

V_∞ = 67 m/sec. (Reference 2-61)

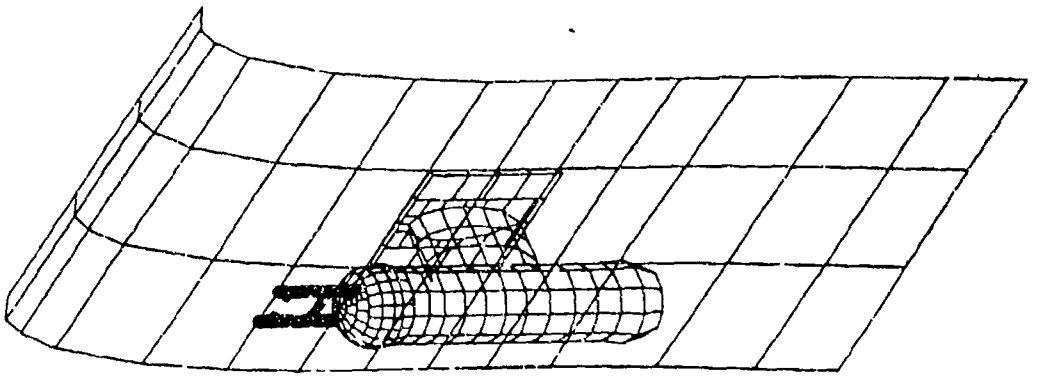

a. PMS OAP

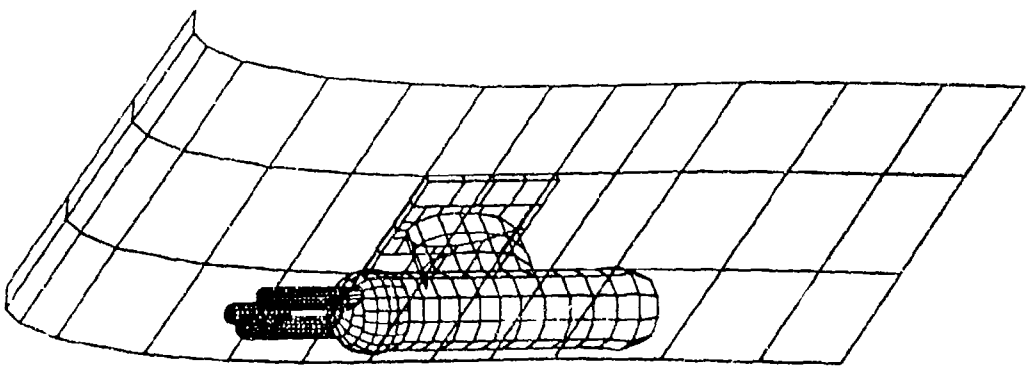

b. PMS FSSP

FIGURE 2-11. DIGITAL DESCRIPTION OF WING-MOUNTED INSTRUMENTS (Reference 2-63)

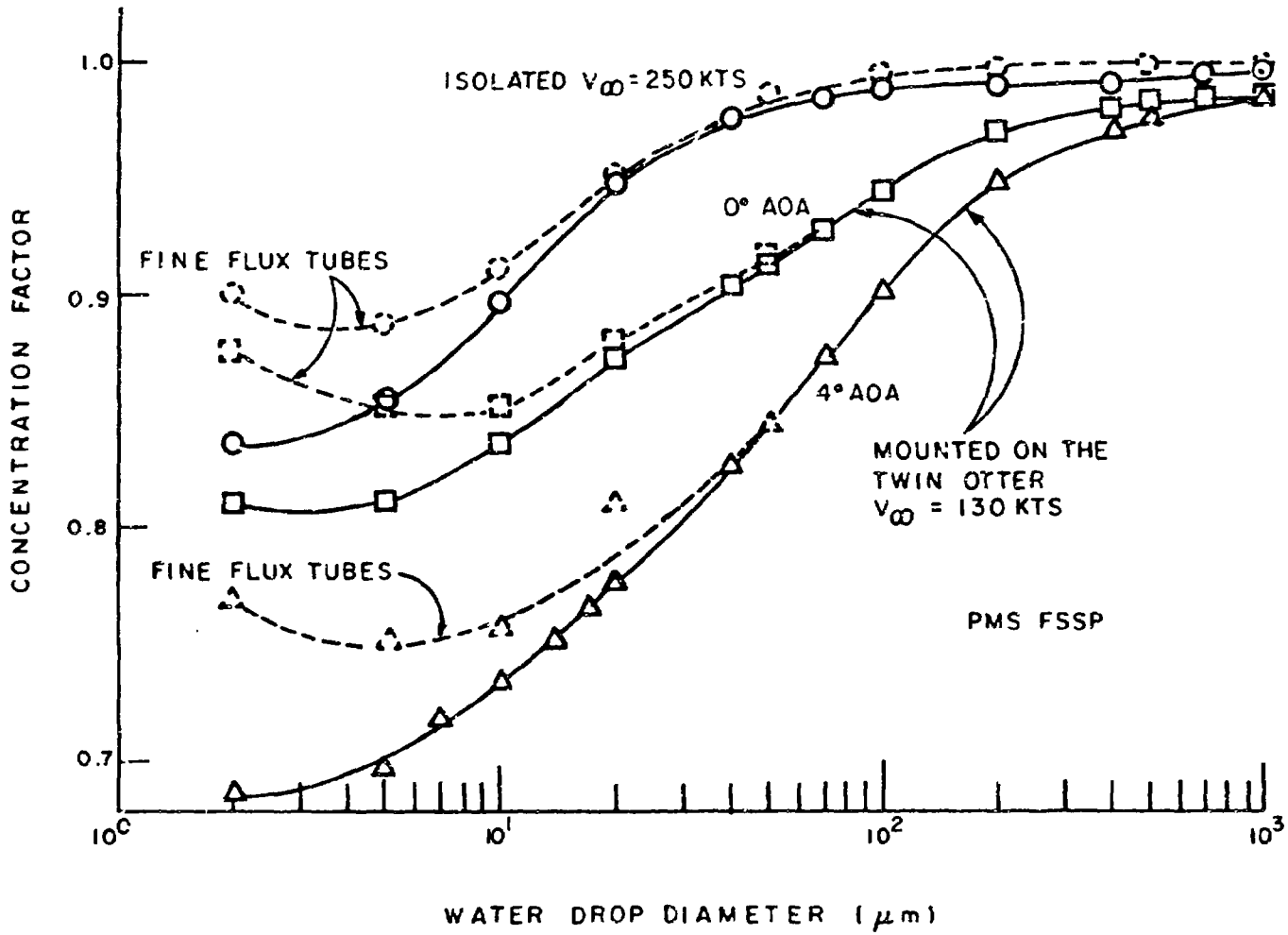

FIGURE 2-12. CONCENTRATION FACTOR VS. WATER DROP DIAMETER FOR THE FSSP WITH V_∞ = 130 AND 250 KTS RESPECTIVELY FOR THE WING-MOUNTED AND ISOLATED INSTRUMENT. (Reference 2-63)

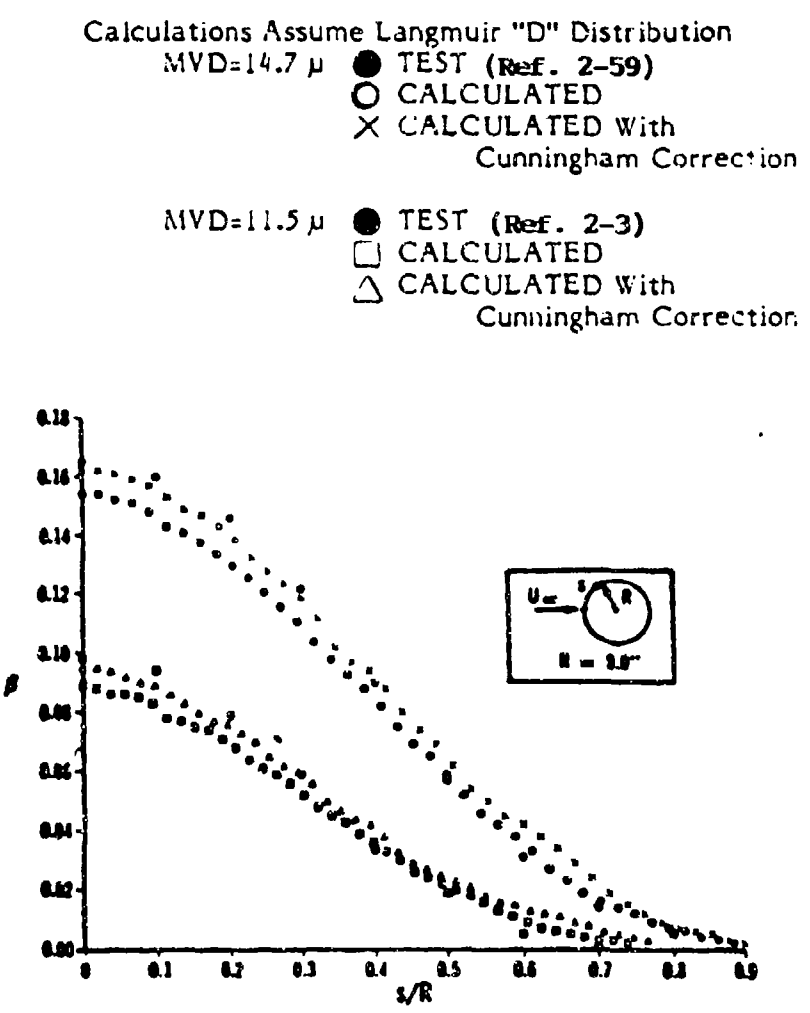

FIGURE 2-13. LOCAL IMPINGEMENT EFFICIENCY ON A SPHERE - EXPERIMENTAL AND CALCULATED

(Reference 2-56)

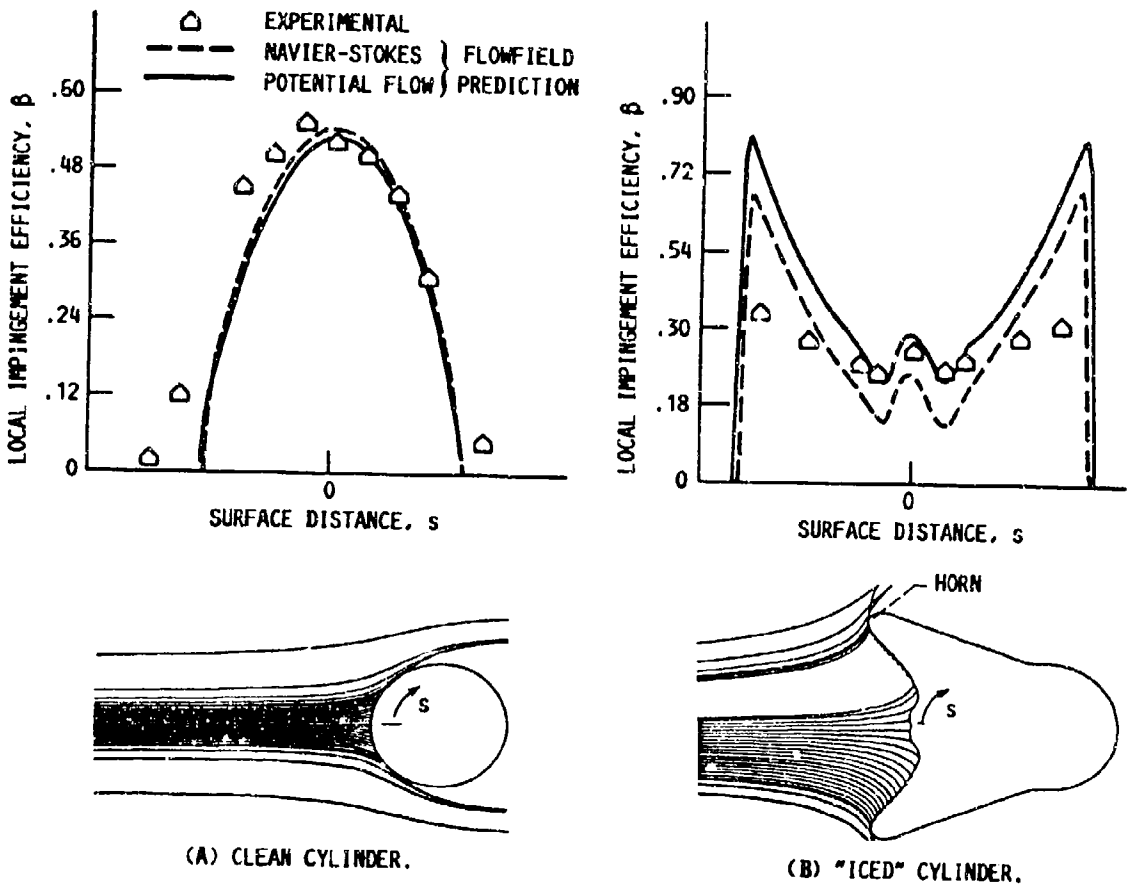

FIGURE 2-14. DROPLET COLLECTION EFFICIENCY COMPARISONS FOR CLEAN AND ICED CYLINDERS

(Reference 2-68)

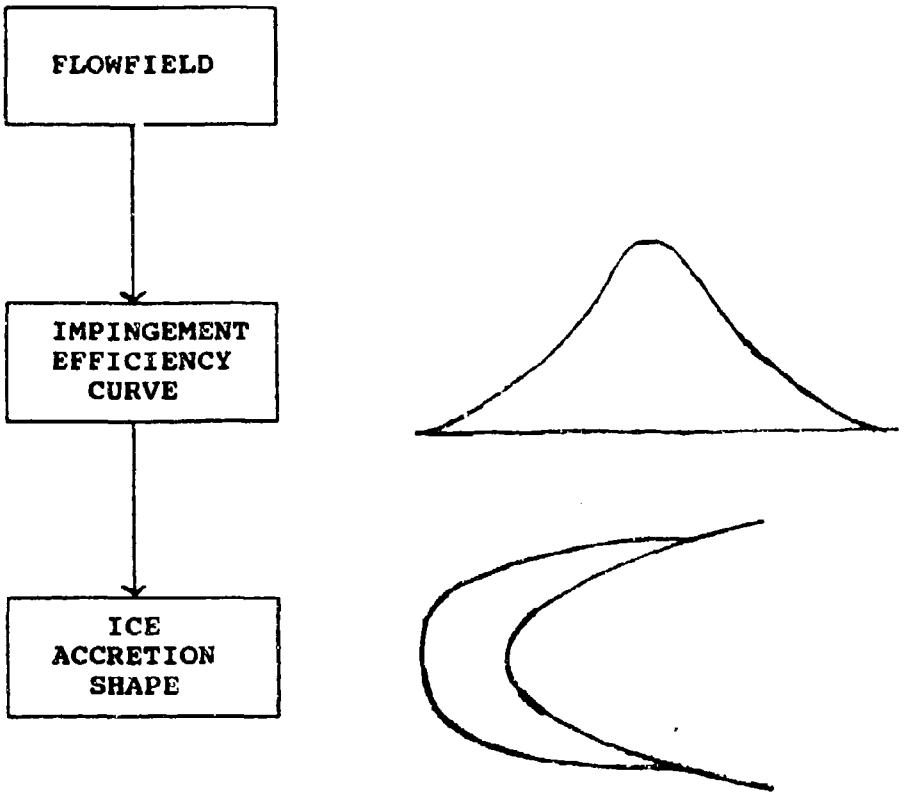

FIGURE 2-15a. FLOW DIAGRAM FOR A SINGLE TIME STEP RIME ICE ACCRETION CODE

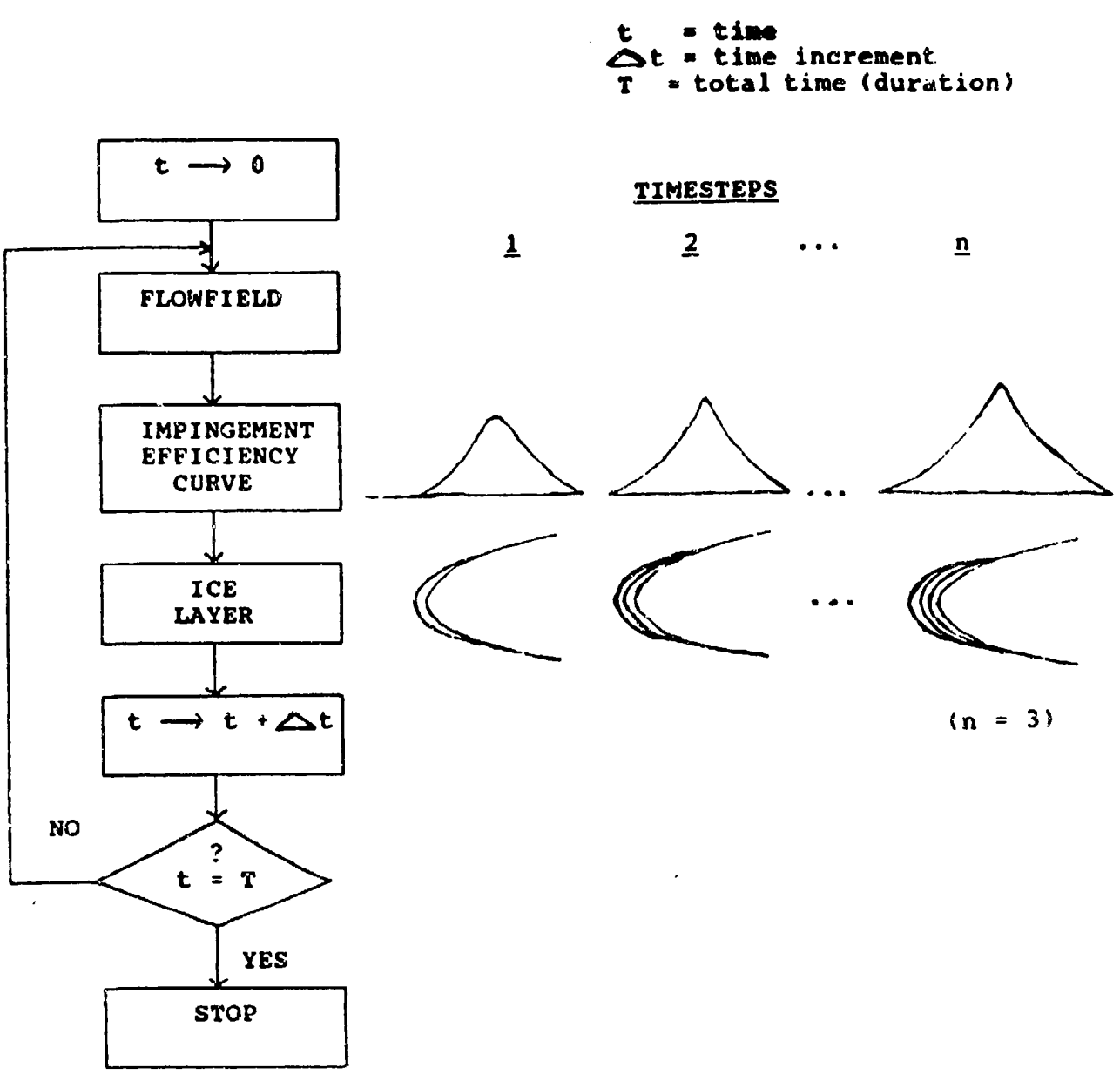

FIGURE 2-15b. FLOW DIAGRAM FOR A MULTIPLE TIME STEP RIME ICE ACC ETION CODE

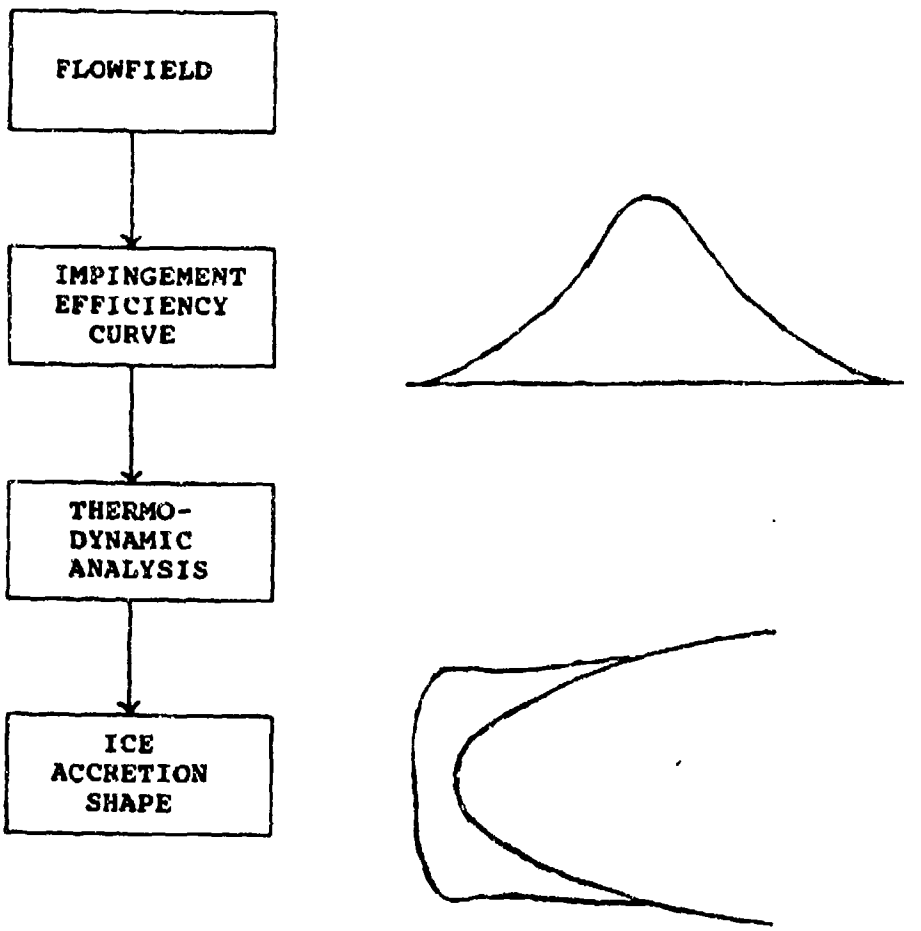

FIGURE 2-16a. FLOW DIAGRAM FOR A SINGLE TIME STEP GLAZE ICE ACCRETION CODE

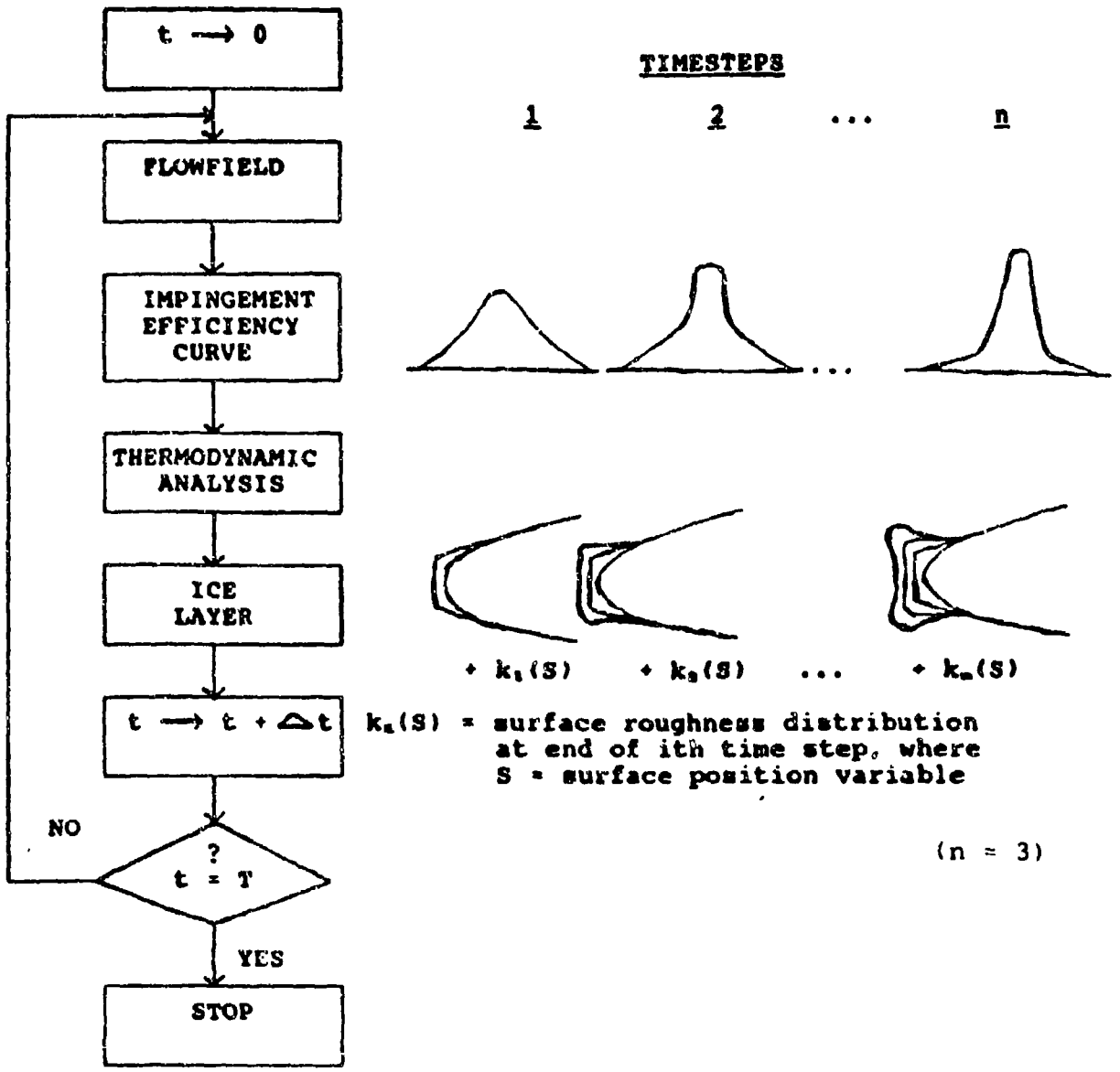

FIGURE 2-16b. FLOW DIAGRAM FOR A MULTIPLE TIME STEP GLAZE ICE ACCRETION CODE

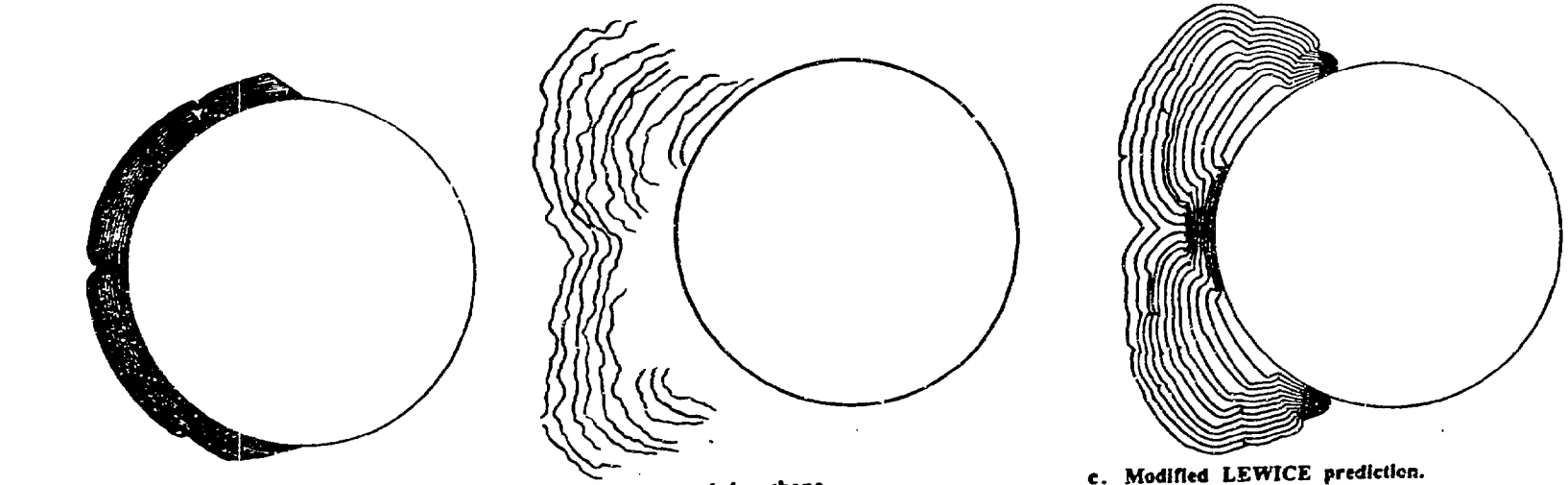

a. Original LEWICE prediction.

b. Experimental ice shape.

c. Modified LEWICE prediction.

$T = -7^{o}$ LWC = $0.8 g/m^3$ V = 125kts MVD = 12 microns

FIGURE 2-17. COMPARISON OF EXPERIMENTAL AND PREDICTED ICE SHAPES FOR A 1" CYLINDER (Reference 2-7)

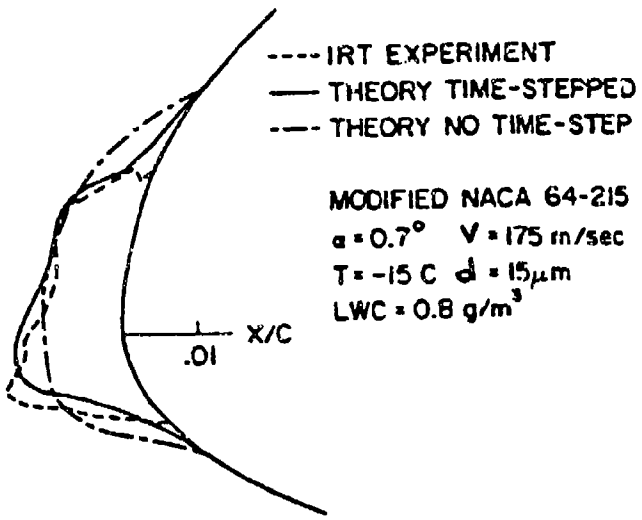

FIGURE 2-18. COMPARISON OF EXPERIMENTAL AND PREDICTED ICE SHAPES ON AN AIRFOIL USING A RIME ICE ACCRETION CODE. (Reference 2-71)

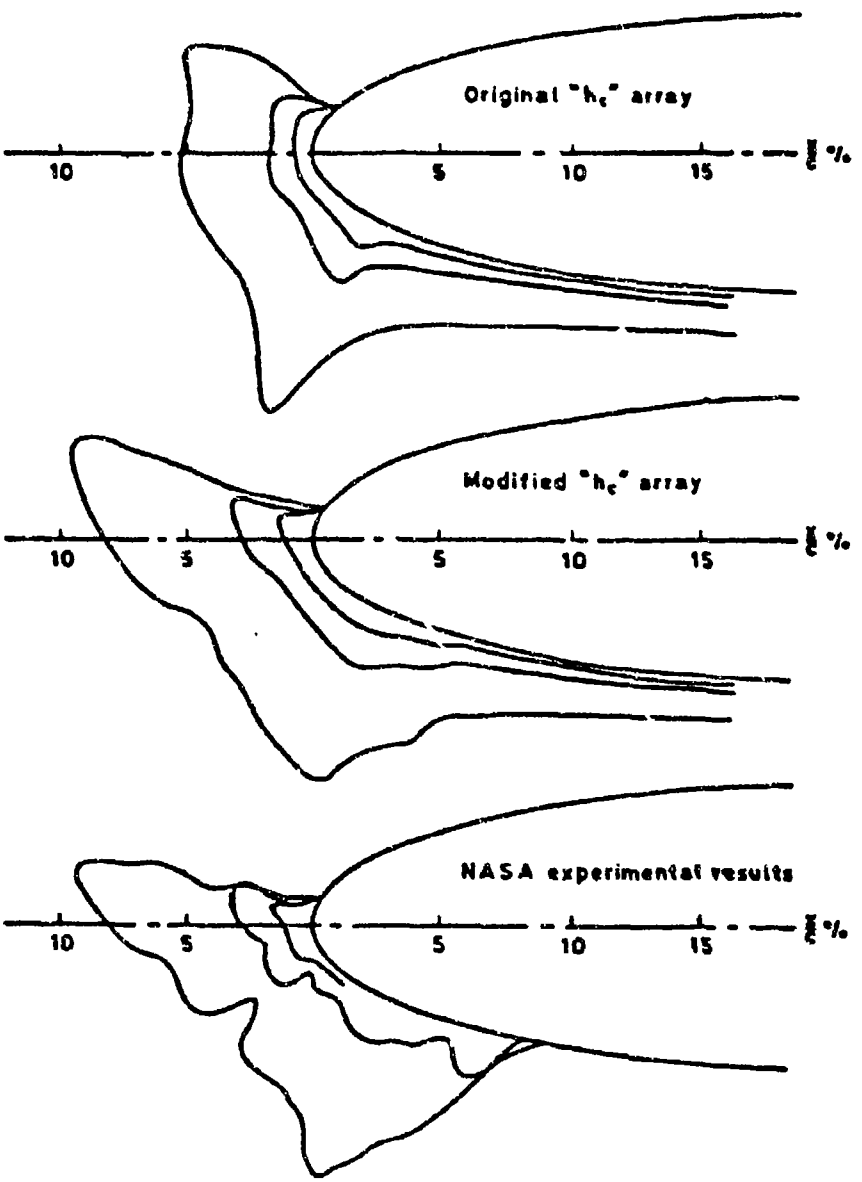

FIGURE 2-19. COMPARISON OF EXPERIMENTAL AND PREDICTED ICE SHAPES ON AN AIRFOIL USING A GLAZE ICE ACCRETION CODE WHERE: C=0.53m, M=0.175, T=9.5°C, LWC=2.1 g/m^3, AND α=8 DEGREES

(Reference 2-83)

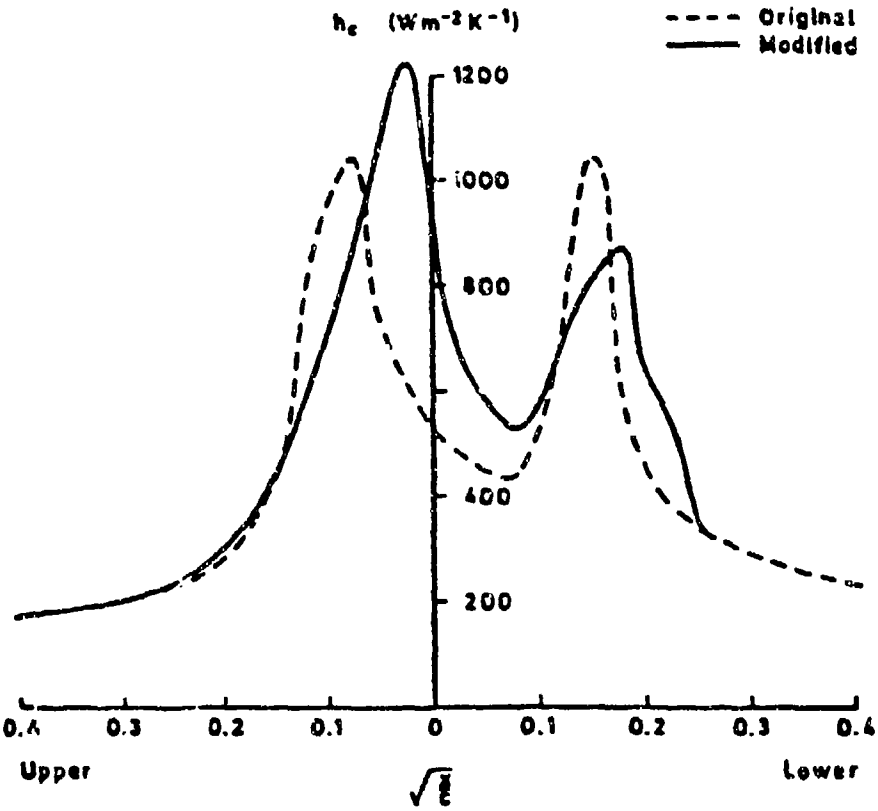

FIGURE 2-20. HEAT TRANSFER COEFFICIENT DATA USED FOR PREDICTION IN FIGURE 2-19 (Reference 2-83)

VELOCITY (M/S)	58.11
TEMPERATURE (C)	-7.78
PRESSURE (KPA)	95.76
HUMIDITY (%)	100.00
LWC (G/M**3)	2.10
DROP DIAM (MICRONS)	20.00
TIME (SEC)	300.00

Experimental

LEWICE

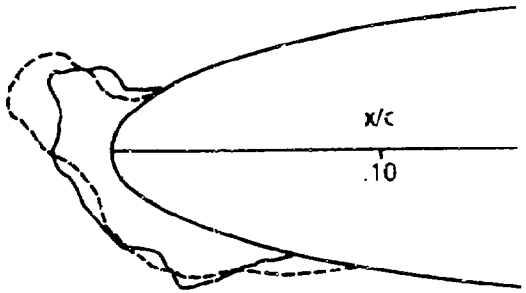

VELOCITY (M/S)	58.00
TEMPERATURE (C)	-7.78
PRESSURE (KPA)	99.12
HUMIDITY (%)	100.00
LWC (G/M**3)	2.10
DROP DIAM (MICRONS)	20.00
TIME (SEC)	150.00

Experimental

LEWICE

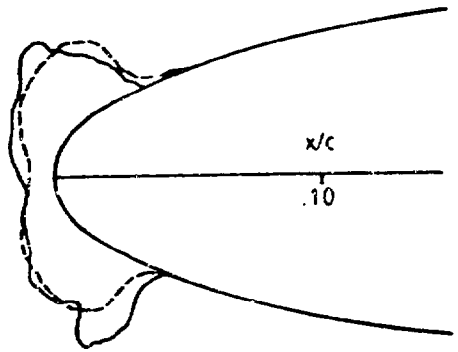

FIGURE 2-21. EXAMPLES COMPARING LEWICE PREDICTIONS TO ICE SHAPES GROWN IN THE NASA LEWIS ICING RESEARCH TUNNEL (Reference 2-79)

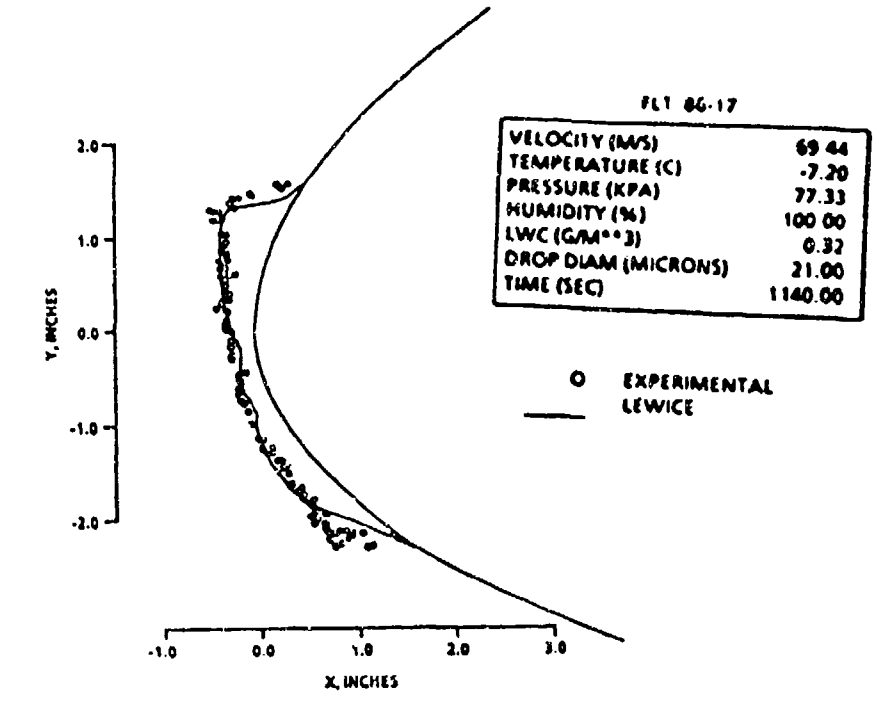

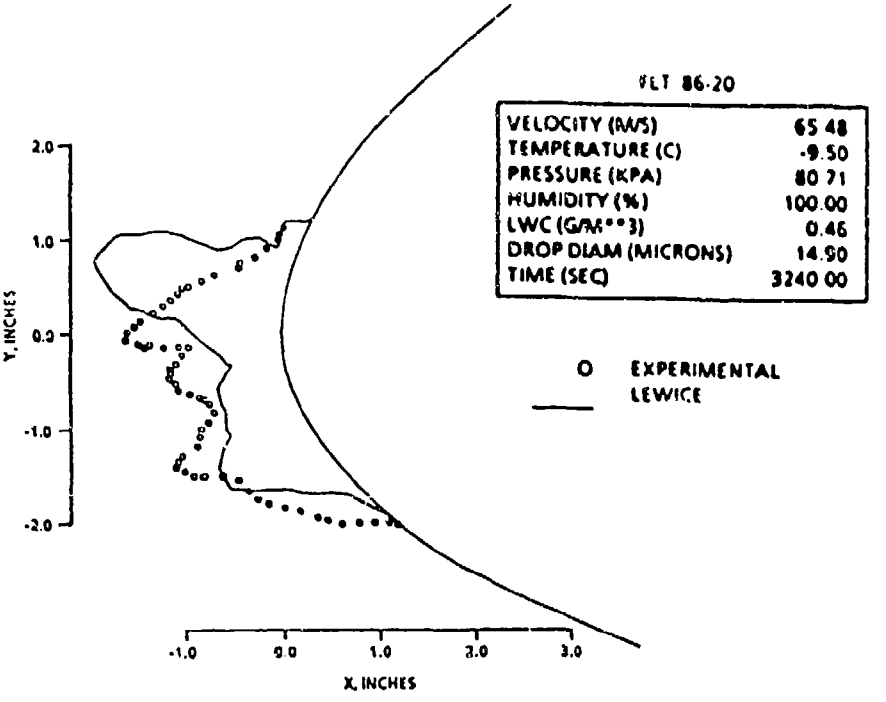

FIGURE 2-22. EXAMPLES COMPARING LEWICE PREDICTIONS TO ICE SHAPES GROWN ON THE NASA LEWIS ICING RESEARCH AIRCRAFT (Reference 2-79)

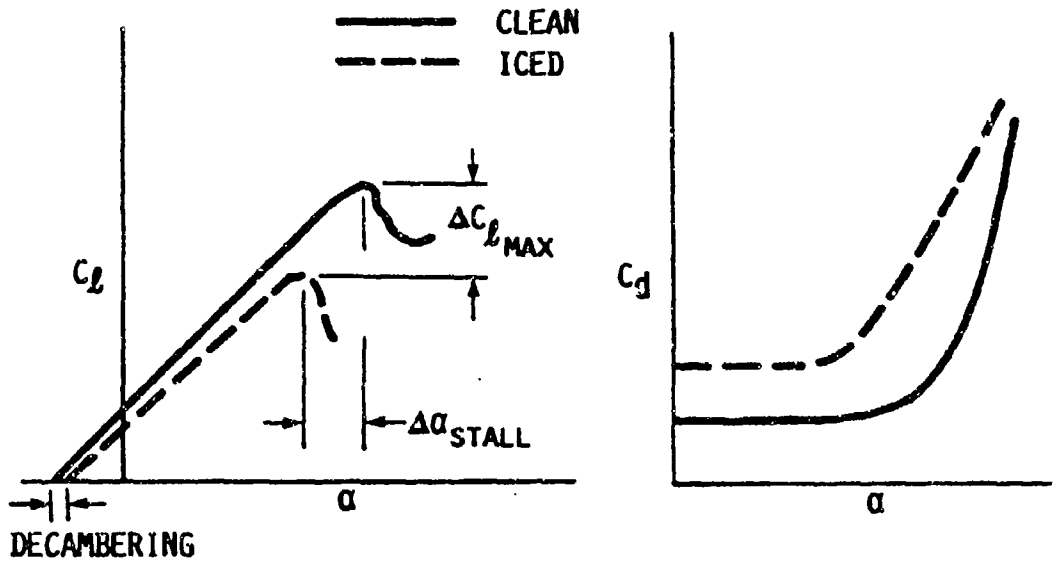

FIGURE 2-23. AERODYNAMIC PERFORMANCE DEGRADATION DUE TO ICING (Reference 2-68)

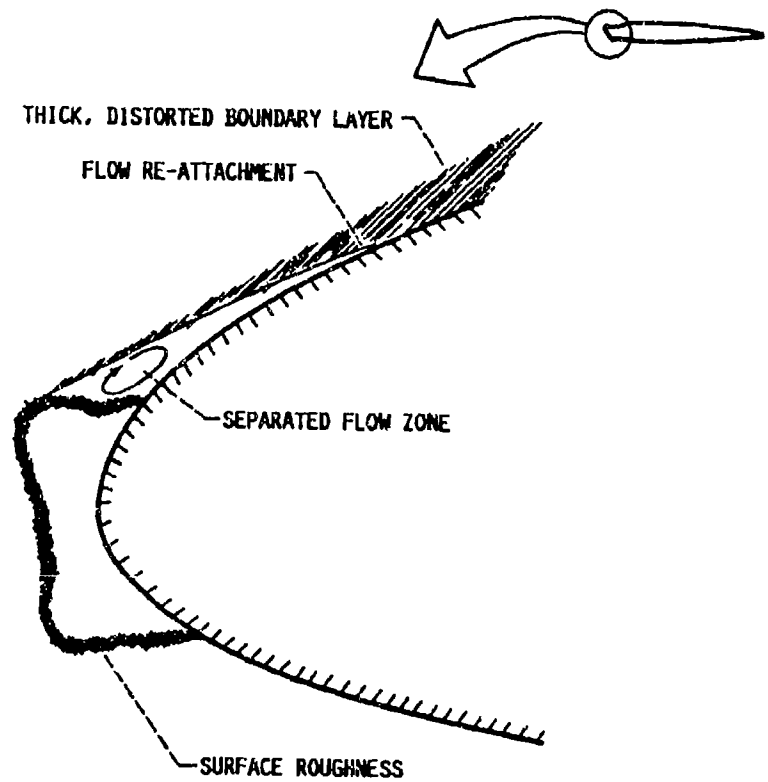

FIGURE 2-24. KEY ASPECTS OF AIRFOIL ICING (Reference 2-68)

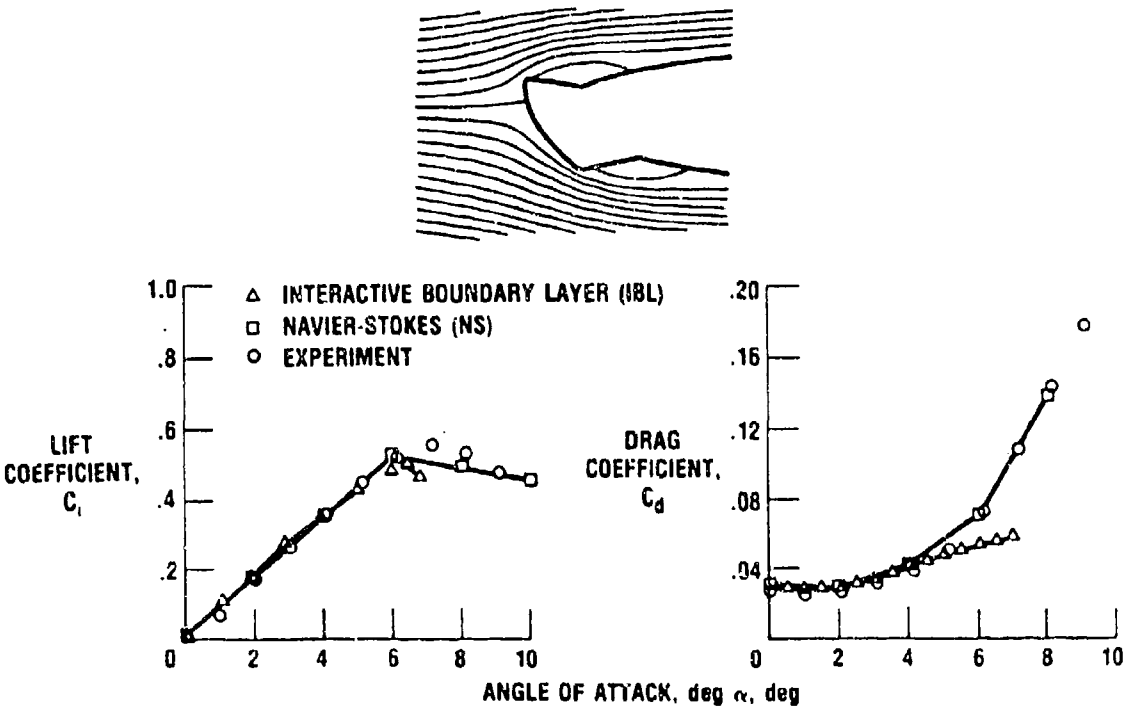

FIGURE 2-25. COMPARISON OF CODE PREDICTIONS OF AERODYNAMIC COEFFICIENTS WITH EXPERIMENTAL MEASUREMENTS. (Reference 2-68)

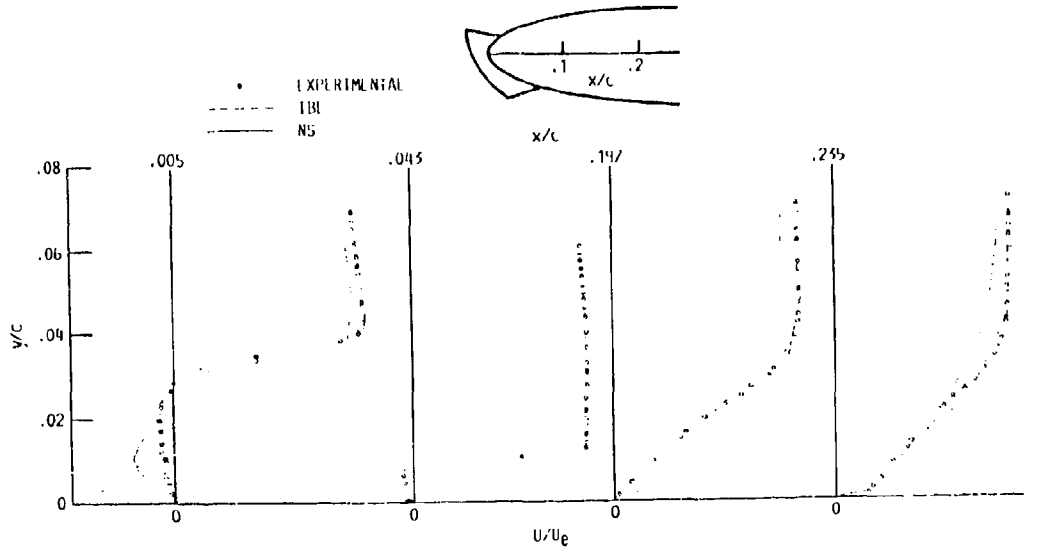

FIGURE 2-26. PROFILES OF MEANS VELOCITY FOR "ICED" NACA 0012 AIRFOIL, α = 4°

(Reference 2-68)

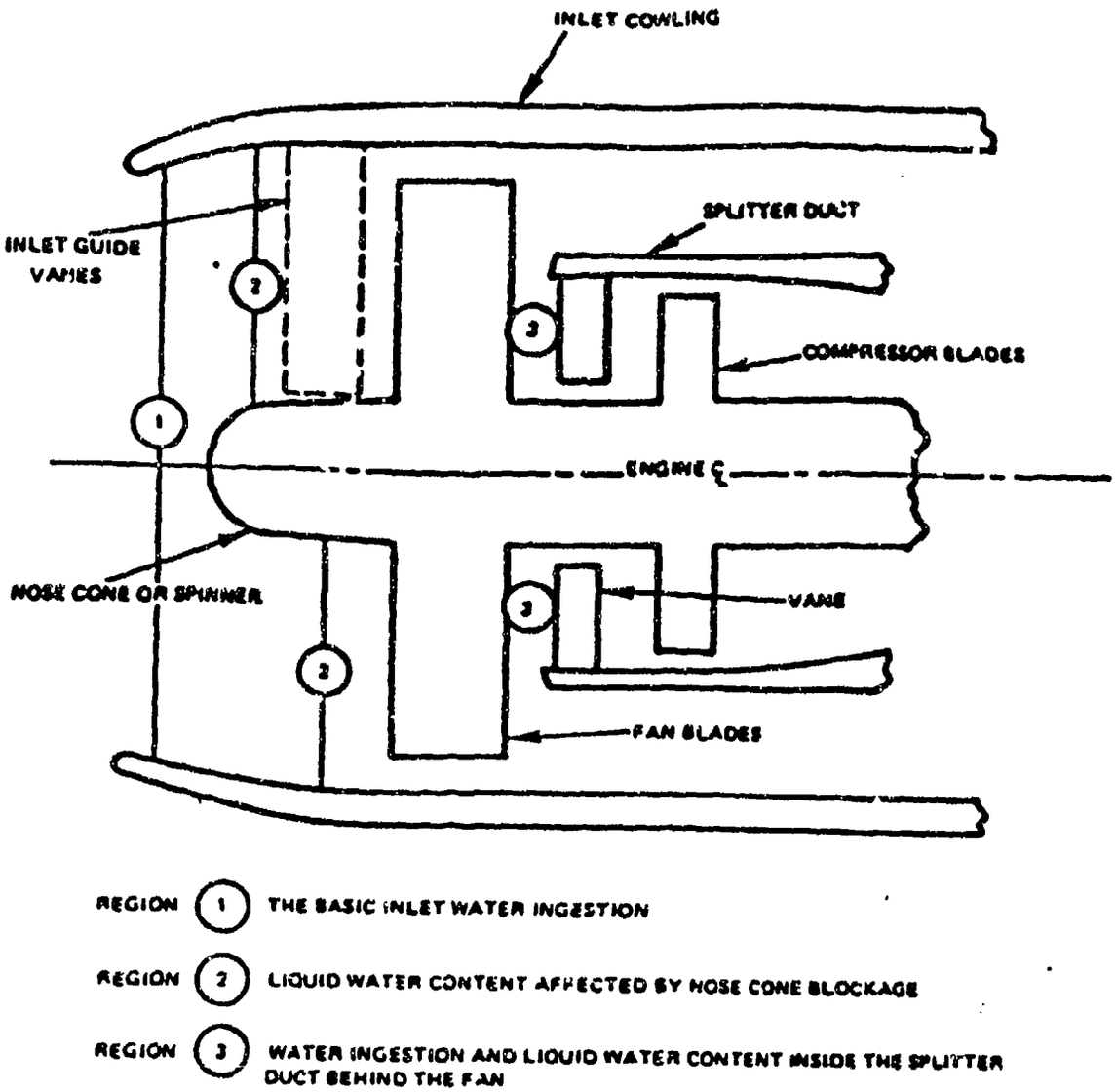

FIGURE 2-27. TYPICAL INLET CONFIGURATION FOR A FAN ENGINE, THREE REGIONS OF CONCERN FOR WATER INGESTION (Reference 2-128)

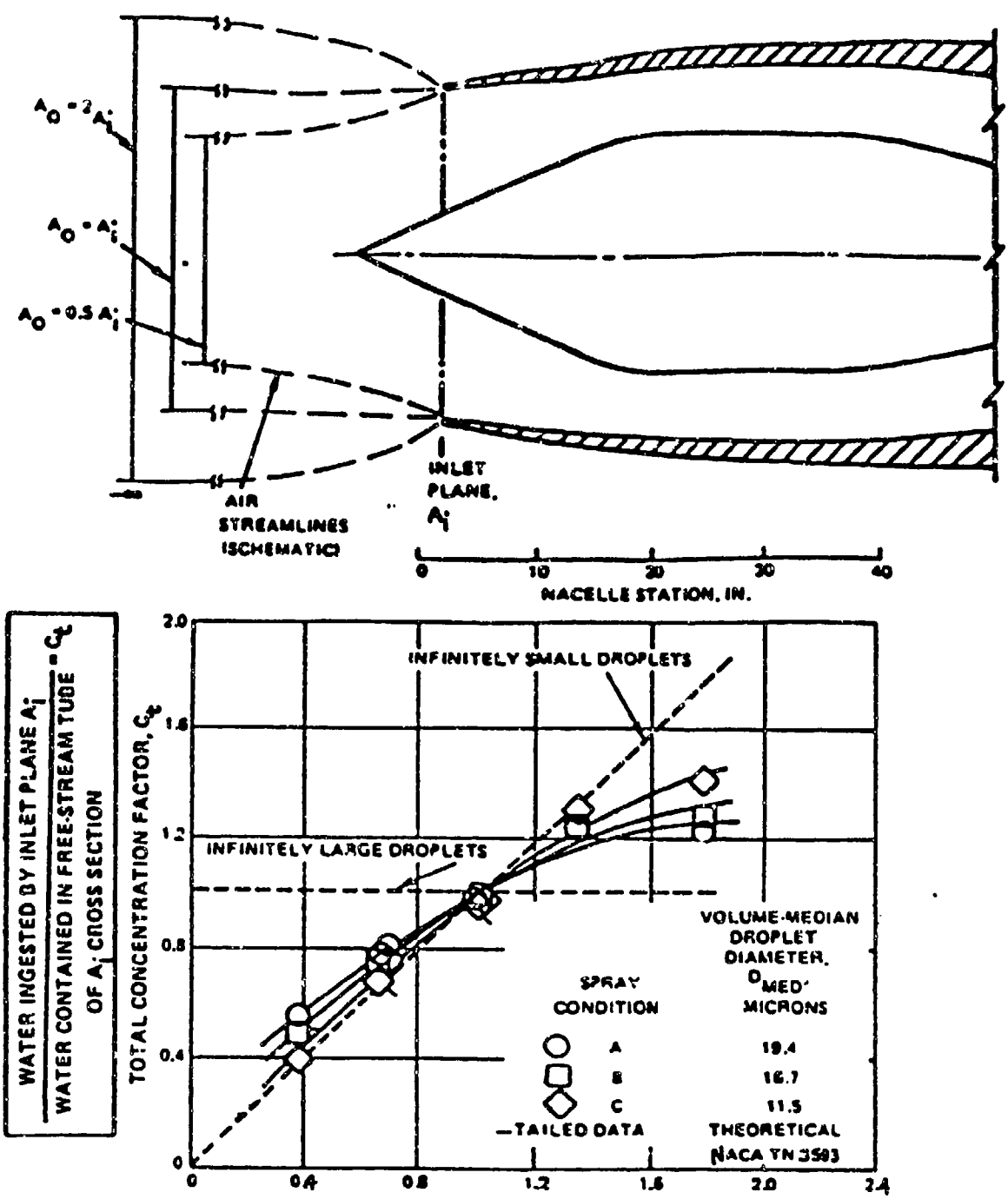

FIGURE 2-28. INLET CATCH EFFICIENCY (Reference 2-128)

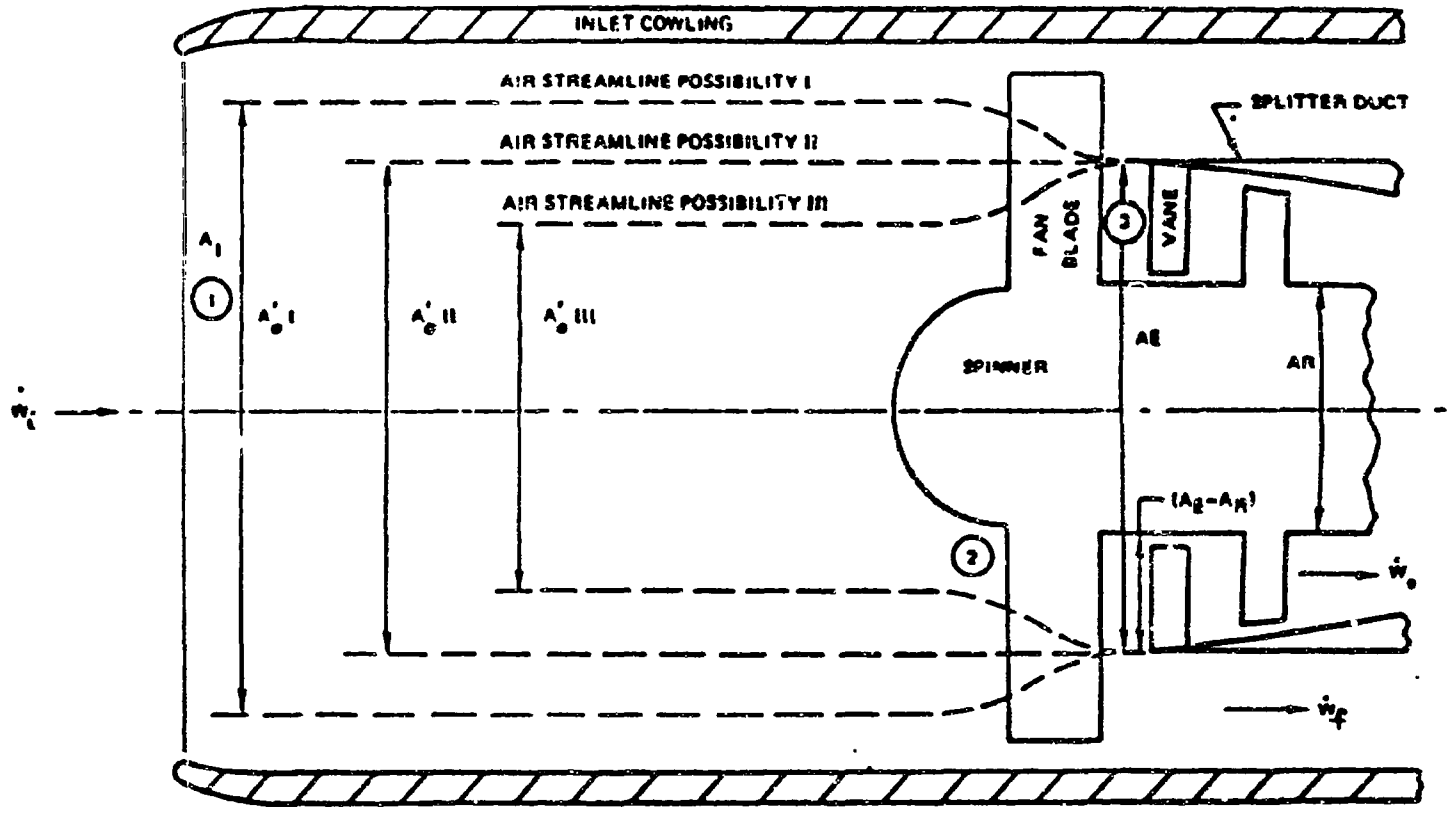

FIGURE 2-29. INLET STREAMLINE POSSIBILITIES FOR SPLINTER DUCT BEHIND A FAN (Reference 2-128)

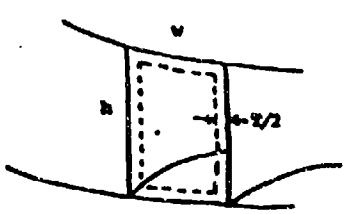

h = passage height

w = passage width

A = hw

$D_H = 4 \cdot hw/2(h + w) = \frac{2hw}{h + w}$

X = fraction of area blocked by ice

τ = ice thickness on surface of stator

$(1 - X)\,hw = (h - \tau)(w - \tau) = hw - h\tau - w\tau + \tau^2$

$(1 - X) = 1 - \frac{h + w}{hw}\tau + \frac{\tau^2}{hw}$

$X = \frac{h + w}{hw}\tau - \frac{1}{hw}\tau^2$

$X = \frac{2}{D_H}\tau - \frac{1}{hw}\tau^2$ This relation will now be used to evaluate allowable ice thickness for X equal to some allowable ice blockage (X).

$\tau^2 - \frac{2hw}{D_H}\tau + Xhw = 0$

$$\tau_{allowable} = \frac{\frac{2hw}{D_H} \pm \sqrt{\left(\frac{2hw}{D_H}\right)^2 - 4Xhw}}{2}$$

$$\frac{\tau_{allowable}}{D_H} = \frac{hw}{D_H^2} \pm \sqrt{\left(\frac{hw}{D_H^2}\right)^2 - X\frac{hw}{D_H^2}}$$

Note that hw/D_H^2 is dependant on the flow passage aspect ratio (h/w). One can solve this equation to find sensitivity to this geometric variable. The solutions of interest involve $\tau_{allow}/D_H < 1$. A plot of τ_{allow}/D_H for different assumed levels of allowable ice blockage (X) [illegible] it to be very insensitive to passage aspect ratio (hw/D_H^2).

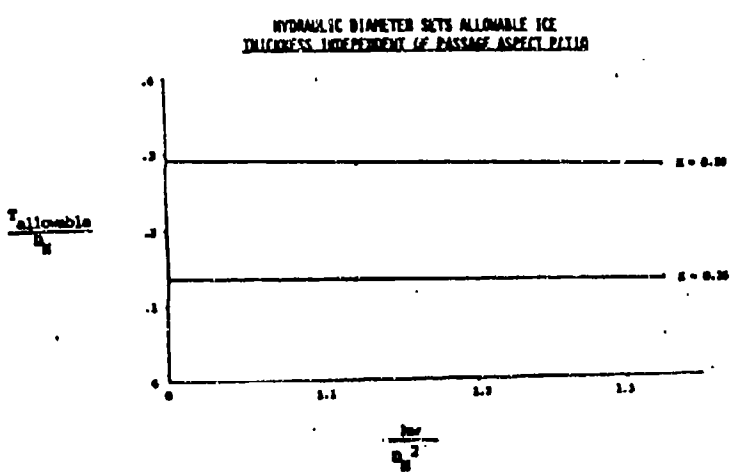

FIGURE 2-30. STATOR FLOW CAPACITY DEPENDENCE ON HYDRAULIC DIAMETER DURING ICING

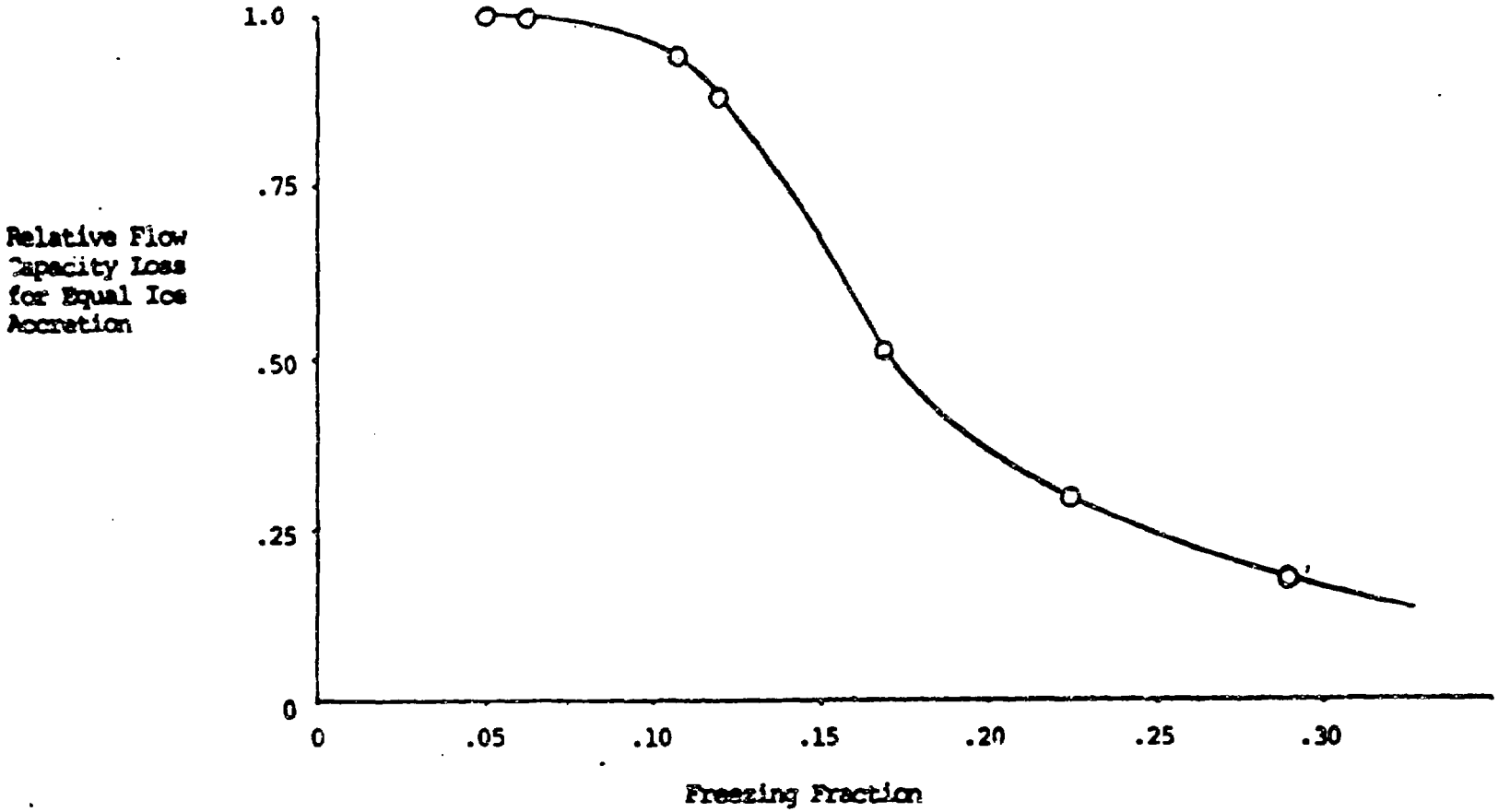

FIGURE 2-31. INFLUENCE OF FREEZING FRACTION ON STATOR PASSAGE FLOW CAPACITY LOSS.

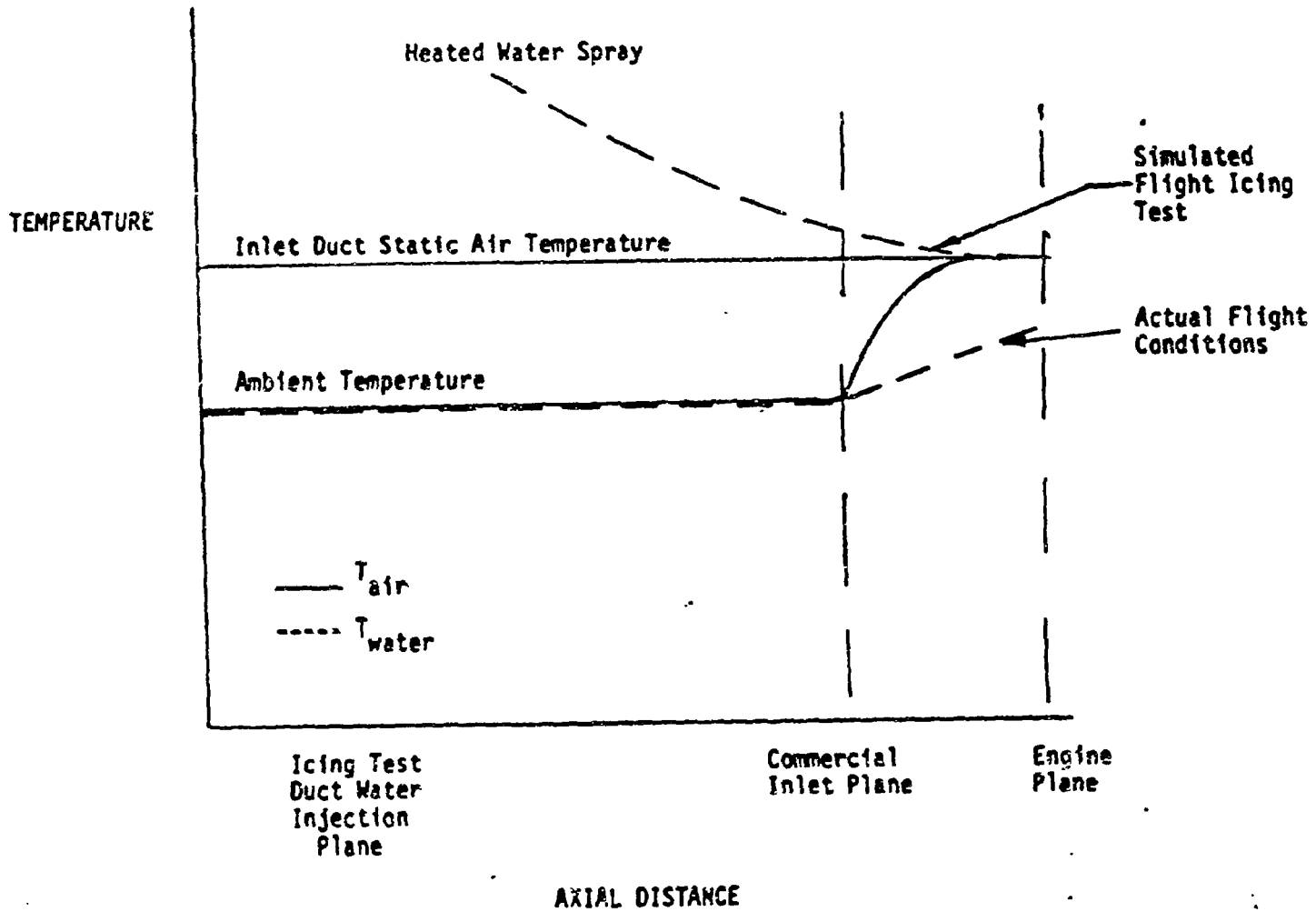

FIGURE 2-32. WATER TEMPERATURE WITHIN INLET DUCTING.

CHAPTER V
DEMONSTRATING ADEQUACY OF DESIGN

SECTION 1.0 - INTRODUCTION
SECTION 2.0 - SYSTEMS DESIGN ANALYSES AND CERTIFICATION PLANNING
SECTION 3.0 - EVALUATIONS TO DEMONSTRATE ADEQUACY
SECTION 4.0 - TESTING TO DEMONSTRATE COMPLIANCE

CHAPTER V
SECTION 1.0
INTRODUCTION

CHAPTER V - DEMONSTRATING ADEQUACY OF DESIGN

CONTENTS

SECTION 1.0 INTRODUCTION

	Page
V.1.1 PHILOSOPHY	1
1.1.1 The Design Development Process	1
1.1.2 Design Criteria	2
1.1.3 Performance-Critical System Design Points	3
1.1.4 Evaluation Criteria	3
1.1.5 Chapter Organization	4
V.1.2 ADMINISTRATION	5
1.2.1 Airworthiness and Type Certifications	5
1.2.2 Type Certification Compliance Requirements	5
1.2.3 Organizations	6
1.2.4 Certification Planning	7
V.1.3 FAA REGULATIONS, ADVISORY CIRCULARS AND SPECIAL GUIDANCE	9
1.3.1 Federal Aviation Regulations	9
1.3.2 Advisory Circulars	9
1.3.3 FAA Orders, Forms, and Special Guidance	10

V.1.0 INTRODUCTION

V.1.1 PHILOSOPHY

1.1.1 The Design Development Process

The decision to build a new aircraft moves through a succession of development stages beginning with a general concept concerning aircraft size, performance, and market potential and progressing to the ultimate decision to start production. The need to provide protection systems for operation in icing conditions may be recognized in the beginning as a part of the general concept; however, ice protection systems for the aircraft may not be a factor in the early program decisions. This is especially true when the new design mainly involves application of conventional technology and operating concepts. The assumption can often be made in these circumstances that ice protection systems similar to those used on previous aircraft will be used in the new design to provide the needed protection. Design factors based upon previous experience may be used for the airplane program decision in these circumstances and airplane specific designs can be determined at a later time in the decision process.

At some point in the process, a decision is made to produce detailed drawings and functional descriptions of the various aircraft components, structures, and systems. Systems to provide the protection needed in icing conditions affect the design of basic structures, such as a wing leading edge, an engine, the stabilizers, etc.; and analyses are prepared as soon as practical to define these systems. The scope and timing of these analyses depends upon the manufacturer's need for information. The studies may be very extensive if the design concept involves new technology, a new operating concept, or if preliminary considerations suggest that performance in one or more operating circumstances might be marginal. In other circumstances the manufacturer may decide that ice protection system design data from a previous program is sufficiently accurate for design purposes.

The type of system to be used to provide protection in icing conditions may never be an issue for some components. Alternative ice protection system designs tend to become the subject of detailed analyses when energy to operate the systems presents a problem in terms of the quantity or availability of energy at the location of the component. Alternative designs for ice protection systems would also become the subject of detailed studies if the manufacturer perceives a potential aircraft performance or economic advantage as a decision factor.

The methods of analyses used to develop aircraft and aircraft component ice protection system design data are the same methods that are used to develop information for certification purposes. Differences result because the purpose of the design studies is to select and define an optimum design, while the purpose of the information used for certification purposes is to provide proof that the selected design of the particular aircraft that is to be produced actually meets Federal Aviation Administration (FAA) design requirements. However, the various analyses and tests produced to determine the design of the ice protection systems provide a basis for the information that must be prepared for FAA certification purposes and may be prepared to serve both purposes.

The information needed to demonstrate the adequacy of ice protection systems for the aircraft to be produced tends to be accumulated at various times throughout the entire airplane program decision process up to and including FAA Type Certification of the proposed design.

Proof of the adequacy of ice protection system designs might be demonstrated by flying the aircraft in design meteorological conditions to obtain the information needed to demonstrate that the systems selected for protecting the various components are satisfactory with respect to FAA requirements. However, the family of natural icing conditions representing design meteorological requirements would be difficult to find, and the time required to complete such a program would create costly program delays. Also, over-design might be required to avoid the threat of the additional delays that would be needed to permit redesign of any unsatisfactory system.

An analytical approach represents an alternative to the flight test approach, and the demonstrations that ice protection systems on a new aircraft design are satisfactory with respect to FAA design requirements could be entirely analytical if theory were sufficiently accurate and comprehensive. However, such is not the case, and demonstrations must also include documented test data from flights in natural icing conditions to prove adequate performance.

A combination of flight and laboratory testing with analyses has been the most assurable and reliable way to demonstrate the adequacy of ice protection systems. With this approach, data obtained from tests in natural icing conditions can be used to evaluate the accuracy of analytical predictions and provide confidence that extrapolations to untested conditions are acceptable.

1.1.2 Design Criteria

Design criteria have been established to provide the information needed by those who design, develop, test, and certify aircraft for operation in icing conditions. The criteria and primary statements of policy are defined in the Federal Air Regulations (FAR). The primary statement of meteorological design criteria is defined in Appendix C of FARs Part 25 and Part 29. For rotorcraft however, reduced criteria are offered to applicants who elect to certify to a 10,000 foot pressure altitude limit. A different set of regulations exists for the various aircraft types: FAR Part 23 applies to normal category aircraft, Part 25 to transport category aircraft, Part 27 to normal category rotorcraft, Part 29 to transport category rotorcraft, and Part 33 to aircraft engines. Additional FARs are used to define regulatory requirements for other problem areas such as aircraft operation.

Advisory Circulars and Orders are used by the FAA to expand regulatory statements of policy and procedure. The numbering system for advisory circulars is related to the numbers used for the regulations. Pertinent regulations, advisory circulars, and orders are listed at the end of Section 1 of this chapter in numerical order to facilitate identification, acquisition, and determination of current status. Technical report references are listed in each section in the usual maner. Detailed information concerning Atmospheric Design Criteria and corresponding regulations is contained in Volume I, Chapter I, Sections 1 and 3.

1.1.3 Performance-Critical System Design Points

Design criteria for demonstrating adequacy of aircraft ice protection systems represent a family of icing conditions. The criteria involves the sizes, numbers of supercooled water droplets, air temperature, and altitude. Criteria also involve consideration of the intermittent maximum conditions associated with flight in cumuliform clouds; and continuous maximum conditions associated with flight in stratiform clouds. Ice protection system design must consider the entire meteorological family of design icing conditions. Technical analyses, laboratory tests, and experience indicate that specific combinations of median droplet size, droplet size distribution, liquid water content, air temperature, altitude, and aircraft operating circumstances will represent the most difficult tests of the adequacy of any particular protection system. If the system performs satisfactorily in these circumstances, it can be assumed to perform satisfactorily in all other circumstances, and the demonstration effort by flight testing can be substantially reduced. The sets of parameters that describe these conditions are referred to as performance-critical design points although the word "performance" is seldom used. There may be more than one performance-critical design point for the same component and there is always more than one performance-critical design point for an entire aircraft.

1.1.4 Evaluation Criteria

Adequacy of design is certified with respect to the envelope or family of meteorological and operational conditions in which the system is expected to be operated. Such criteria are based upon an exceedance probability of 0.001. This recognizes the fact that conditions exceeding the design conditions of FAR Part 25, Appendix C, have a chance of being exceeded one time out of 1000 encounters. Icing associated with freezing rain and icing in very high supercooled liquid water content portions of cumulonimbus clouds are examples; however, systems that perform satisfactorily in the design conditions are expected to provide the performance needed to enable safe flight while the aircraft is flown out of the conditions. The definition of a severe icing condition illustrates this point. Table 14.1 section 14, page 14.1 of Advisory Circular AC 00-45C, indicates that, "Icing/anti-icing systems fail to reduce or control the hazard, and immediate diversion is necessary in severe icing conditions."

Ice protection requirements for components having substantial adverse impact on airworthiness stipulate a greater degree of protection than those for components that merely degrade performance. For example, aircraft are often operated in performance-critical design or near design conditions for test purposes with wing, tail, and propeller ice protection systems turned off. Performance can be severely degraded in these circumstances without producing an immediate unacceptable effect on airworthiness, but loss of airspeed indication or an engine power failure could not be accepted even for test purposes. Also, unacceptable effects on airworthiness would occur if ice formations on wing or empennage surfaces were to produce a loss of stability control. Demonstrations of the adequacy of ice protection systems involve airworthiness consequences as well as performance degradation.

Degradation of performance is mostly a matter of efficient operation and may be acceptable if it is understood and controllable, but degradation of airworthiness is not acceptable. Airworthiness can be assumed when the aircraft is shown to be:

(1) in compliance with regulatory requirements.

(2) in conformity with approved specification data and flight results test data.

(3) without unsafe design features.

The FAA does not and cannot set forth a concise set of rules that, if followed by rote, will lead to automatic approval of an aircraft for flight in known icing conditions. The regulations are objective in nature; however, many methods and combinations of methods have been used by manufacturers to demonstrate compliance. Applicants are encouraged by the FAA to use their technical ingenuity and resourcefulness to develop more efficient and less costly methods of achieving the objectives of the regulations. As airframe and ice protection equipment designs vary from conventional configurations, and as advanced concepts are developed, the FAA may find it necessary to deviate from previous certification methods and procedures, however useful they may have been in the past for specific applications. Any alternate means of compliance proposed by the applicant will be given due consideration by the FAA.

The information in Advisory Circulars and Orders is neither mandatory nor regulatory in nature and is subject to periodic updating. It may be necessary to deviate from previously identified acceptable means of compliance as defined in Advisory Circulars and Orders but never from the intent of regulations.

In the early design stages, after consideration of the aircraft and component structures, the manufacturer should determine which areas of the aircraft require icing protection and how that protection can best be provided. The applicant should notify the respective FAA certification office as early in the program as possible. This will enable the FAA to schedule its participation, or to provide for alternate measures, in the review of the applicant's test, analyses, and determinations relative to demonstration of compliance.

1.1.5 Chapter Organization

The four sections in this chapter provide the instructions needed to develop, plan, conduct, and complete programs to demonstrate the adequacy of ice protection systems. Section 1.0 discusses key aspects of FAA philosophy concerning these matters and introduces the reader to administrative matters pertaining to the activity. Section 2.0 discusses key aspects of analyses prepared in connection with the selection and design of component ice protection systems for a light twin engine aircraft, including the selection of performance-critical meteorological and flight operating conditions for system design evaluation. Section 3.0 discusses key aspects of evaluations to prove the accuracy of design analyses and to demonstrate the adequacy of ice protection systems. Section 4 presents information concerning testing to demonstrate compliance.

V.1.2 ADMINISTRATION

1.2.1 Applications for Type Certification

Before an individual aircraft is allowed to operate in the United States, the aircraft must have an Airworthiness Certificate. The prerequisite for the Airworthiness Certificate is a Type Certificate (TC). The aircraft manufacturer is responsible for obtaining the TC. Modified aircraft must have a supplemental Type Certificate (STC) or an amended Type Certificate. This entails obtaining FAA approval of the engineering and manufacturing design. The manufacturer must obtain the TC or STC from the FAA. To do this, he must first submit an application for approval. The applications are submitted to the FAA Office serving the local area within which the aircraft will be manufactured. These FAA offices are designated Aircraft Certification Offices (ACO) and are located strategically throughout the United States and Europe. The ACO's report to the geographic regional headquarters which has responsibility for the certification of the various aircraft types. These are referred to as Certification Directorates.

Once applications for type certification have been received, the FAA will provide necessary assistance to the applicant to assure that the requirements for certification are understood, that the certification basis has been properly defined, and that the methodology for assuring compliance with the applicable regulations is mapped out. Although these activities are considered the responsibility of the applicant, the FAA commonly assists the applicant in this process; but the FAA does not assist the applicant in demonstrating compliance.

1.2.2 Type Certification Compliance Requirements

The requirements deemed necessary to insure safe and efficient operation of air transportation systems in the United States are defined in a set of Federal Air Regulations called FAR's. The requirements are developed by government and industry under the supervision of the FAA, and the FAA is responsible to government, industry, and to the public for their implementation. Information concerning these regulations is the subject of Chapter VI of this handbook, but the administrative aspects of certain basic regulations as they pertain to demonstrations of the adequacy of ice protection systems need to be understood at this time.

Type Certification is the administrative instrument used by the FAA to indicate its determination that a given aircraft and its systems are satisfactory with respect to regulatory requirements applicable to the particular aircraft type. The certification applies to all similar aircraft and represents approval of the design for use as planned. An aircraft need not be certified for flight in icing conditions, but the decision not to install ice protection equipment would limit aircraft operations. For example, FAR 91.209(b) states:

"...no pilot may fly—(1) under IFR into known or forecast moderate icing conditions; or (2) under VFR into known light or moderate icing conditions; unless the aircraft has functioning de-icing or anti-icing equipment protecting each propeller, windshield, wing, stabilizing or control surface, and each airspeed, altimeter, rate of climb, or flight attitude instrument system."

1.2.3 Organizations

FAA order 8100.5, dated 10/1/82, established the general procedures, practices, and organization in use today to assure effective, efficient, and expeditious communication and coordination between the four Aircraft Certification Directorates and FAA Washington headquarters, and a common understanding of the responsibilities and relationships required in their management of aircraft certification programs. The four Aircraft Certification Directorates perform the technical policy management and project management for aircraft certification programs.

Each of the directorates is responsible for certifications with respect to an area of Federal Regulations as follows:

Regulation	Certification Directorate	Location
FAR Part 23	Small Airplanes	Central Region
FAR Part 25	Transport Airplanes	Northwest Mountain Region
FAR Part 27 & 29		Rotorcraft Southwest Region
FAR Part 33 & 35		Engines and Propellers New England Region

The directorates are organizational elements in the designated regions.

Aircraft Certification Directorates have the final authority and responsibility for type certification programs and standardization of technical policy for the particular regulatory FAR Part as assigned. An Aircraft Certification Office (ACO) is an operational sub-element which administers and secures compliance with FAA regulations, programs, standards, and procedures governing the type design of aircraft, aircraft engines, or propellers; and provides certification expertise in the investigation and reporting of aircraft accidents, incidents, and service difficulties. The project manager is an individual in an ACO. The Certification Directorates and the locations of their subordinate ACO's are as follows:

Small Airplane Ceritfication Directorate - Kansas City, MO

ACO's: Atlanta, GA; Wichita, KS; Chicago, IL

Transport Airplanes Certification Directorate - Seattle, WA

ACO's: Seattle, WA; Long Beach, CA

Field Offices: Denver, CO; Anchorage, AK

Rotorcraft Certification Directorate - Fort Worth, TX

ACO's: Fort Worth, TX

Engines and Propellers Certification Directorate - Bulington, MA

ACO's: Burlington, MA; Valley Stream, NY

Aircraft Certification - Europe, Africa, and Middle East

Brussels, Belgium

1.2.4 Certification Planning

Official FAA participation in the design/development activity begins when the FAA receives an Application for Type Certification. Applications for Type Certification are submitted when design studies have progressed sufficiently to enable a fairly precise and complete description of the proposed design, including its ice protection systems. The design is not quite frozen at this time, as changes will be made as a result of subsequent analyses and testing. The FAA assigns a project manager and begins the series of actions necessary to enable Type Certification when the applications are received; however, applicants for Type Certification are encouraged to submit their applications as soon as possible to expedite FAA planning. Pre-application contacts are encouraged to minimize possible misunderstandings concerning pertinent requirements, procedures, and policy. Also, applications should be submitted as early as practicable to enable the FAA to initiate its planning actions for the proposed certification.

Actions taken to demonstrate the adequacy of aircraft ice protection systems are comparable to a final examination with the applicant writing his own test. The applicant passes the test if the FAA can certify that the design is satisfactory with respect to applicable standards; and that the test results, as well as the choices made by the applicant in the design process, are acceptable. Also, the FAA provides advice to the applicant regarding test requirements and the actions needed to resolve any issues or difficult test problems.

The requirements for demonstrating compliance of ice protection systems are governed by FAR Parts 23, 25, 27, 29, and 33. The specific method of compliance used will be influenced by the aircraft operating characteristics and the type of ice protection system installed. The certification plan submitted by the applicant should describe all of the applicant's efforts intended to lead to certification. This plan should identify, by the item to be certified, the compliance methods that the applicant intends to use. Use of a certification checklist is encouraged and it should clearly identify analyses and tests, or references to similarity of designs, which the applicant intends to use for certification of the systems. These methods of demonstrating compliance should be agreed upon between the applicant and the FAA early in the certification program. It is imperative that the applicant obtain FAA concurrence prior to conducting certification tests.

Certification plans should include the following basic information:

1. Aircraft and systems description
2. Ice protection systems description
   A. This description should address the areas to be protected, the type of protection provided, and give a functional description of each subsystem or component of the icing protection system. Any normally protected surfaces or component, such as leading edges of airfoils, which the applicant does not intend to protect, should be identified.
3. Certification Checklist (optional)

4. Description of analyses performed to date and analyses planned to demonstrate compliance.
   A. Ice shapes
   B. Similarity
   C. Math models
5. Description of tests performed to date and tests planned to demonstrate compliance.
   A. Dry air
   B. Simulated icing
      (1) Icing tunnel
      (2) Tanker
      (3) Ice Shapes
   C. Natural icing
   D. Methods of control of variables
   E. Data acquisition methods and required instrumentation
   F. Data reduction procedures
6. Projected schedules of designs, analyses, testing and reporting efforts.
   A. The plan should also include a determination of performance critical design conditions associated with the operation of the proposed aircraft in meteorological conditions of Appendix C of FAR 25 or FAR 29 and an evaluation of the expected consequences of resulting accumulations of ice, and/or the effectiveness of systems for providing protection.
   B. The plan should also show how the applicant intends to demonstrate by analyses, tests, similarity of design, or a combination of these, that the aircraft and engine are capable of operating safely throughout the icing envelope of the appropriate regulation (Part 25 or 29, Appendix C) or throughout that portion of the envelope within which the aircraft and engine is certificated for operation.

V.1.3 FAA REGULATIONS, ADVISORY CIRCULARS, AND SPECIAL GUIDANCE

1.3.1 Federal Aviation Regulations, US Department of Transportation Aviation Administration, Washington, D.C., 1986:

1. FAR Part 23, "Airworthiness Standards: Normal, Utility, Acrobatic, and Commuter Category Airplanes."
2. FAR Part 25, "Airworthiness Standards: Transport Category Airplanes."
3. FAR Part 27, "Airworthiness Standards: Normal Category Rotorcraft."
4. FAR Part 29, "Airworthiness Standards: Transport Category Rotorcraft."
5. FAR Part 33, "Airworthiness Standards: Aircraft Engines."
6. FAR Part 35, "Airworthiness Standards: Propellers."
7. CAR Part 23, "Normal, Utility, and Acrobatic Categories."
8. SFAR Number 23, "Small Aircraft Capable of Being Certified to Carry More Than 10 Occupants and for use in Operations Under FAR Part 135."
9. SFAR Number 29-4, "Limited IFR Operations of Rotorcraft," 1983.
10. SFAR Number 41, "Small Aircraft Capable of Being Certified with a Passenger Seating Configuration of 10 to not More Than 19 Seats and a Takeoff Weight of 12,500 Pounds or Less."
11. FAR Part 91, "General Operating and Flight Rules."
12. FAR Part 121, "Certification and Operations: Domestic, Flag, and Supplemental Air Carriers and Commercial Operators of Large Aircraft."
13. FAR Part 135, "Air Taxi and Commercial Operators."

1.3.2 Advisory Circulars, US Department of Transportation, Federal Aviation Administration, Washington, D.C., 1986:

14. AC 00-2.2, "Advisory Circular Checklist (and Status of Other FAA Publications)," 15 October 1988.
15. AC 00-6A, "Aviation Weather," 1975.
16. AC 00-45C, "Aviation Weather Services," 1985.
17. AC 20-29B, "Use of Aircraft Fuel Anti-Icing Additives," 18 January 1972.
18. AC 20-73, "Aircraft Ice Protection," 21 April 1971.
19. AC 20-93, "Flutter Due to Ice or Foreign Substance On or In Aircraft Control Surfaces," 29 January 1976.
20. AC 20-113, "Pilot Precautions and Procedures to be Taken in Preventing Aircraft Reciprocating Engine Induction System and Fuel System Icing Problems," 22 October 1981.
21. AC 20-117, "Hazards Following Ground Deicing and Ground Operations in Conditions Conducive to Aircraft Icing," 17 December 1982.
22. AC 20-117, "Change 1," 15 April 1983.
23. AC 21-12A, "Application for U.S. Airworthiness Certificate, FAA Form 8130-6 (OMB 2120-0018)," 26 April 1987.

24. AC 21-23, "Airworthiness Certification of Civil Aircraft Engine, Propellers, and Related Products," 7 July 1987.
25. AC 23-8A, "Flight Test Guide for Certification of Normal, Utility, and Acrobatic Category Airplanes," 9 February 1989, (Supt. Docs. SN 050-007-00773-6).
26. AC 23.629-1A, "Means of Compliance with Section 23.629, Flutter," 23 October 1985.
27. AC 23.1309-1, "Equipment and Installations in Part 23 Airplanes," 19 September 1989.
28. AC 23.1419-1, "Certification of Small Airplanes for Flight in Icing Conditions," 2 Sept. 1986.
29. AC 25-7, "Flight Test Guide for Certification of Transport Category Airplanes," 8 April 1986, (Supt. Docs. SN 050-007-00739-6).
30. AC 25.629-1 "Flutter Substantiation of Transport Category Airplanes," 4 January 1985.
31. AC 27-1, "Certification of Normal Category Rotorcraft," 29 August 1985 (Supt. Docs. SN 050-007-00708-6).
32. AC 27-1, "Change 1," 16 September 1987, (Supt. Docs. SN 050-007-00776-3).
33. AC 29-2A, "Certification of Transport Category Rotorcraft," 16 September 1987. (Supt, Docs. SN 050-007-00767-1).
34. AC 33-2A, "Aircraft Engine Type Certification Handbook," 5 June 1972.
35. AC 33-3, "Turbine and Compressor Rotor Type Certification Substantiation Procedures," 9 September 1968.

1.3.3 FAA Orders, Forms and Handbooks.

36. Order 8100.5, "Aircraft Certification Directorate Procedures."
37. Order 8110.8, "Engineering Flight Test Guide for Transport Category Airplanes."
38. Order 8130.2B, "Airworthiness Certification of Aircraft and Related Approvals."
39. FAA Form 8110-12, "Application for Type Certificate, Production Certificate, or Supplemental Type Certificate."
40. FAA Form 8130-6, "Application for Airworthiness Certificate."

CHAPTER V
SECTION 2.0
SYSTEMS DESIGN ANALYSES AND CERTIFICATION PLANNING

CHAPTER V - DEMONSTRATING ADEQUACY OF DESIGN

CONTENTS

SECTION 2.0 SYSTEMS DESIGN ANALYSES AND CERTIFICATION PLANNING

		Page
LIST OF TABLES		V 2-iv
LIST OF FIGURES		V 2-v
SYMBOLS AND ABBREVIATIONS		V 2-vi
V.2.1	AIRCRAFT DESIGN CONCEPT	V 2-1
	2.1.1 Physical Characteristics	V 2-1
	2.1.2 Operational Characteristics	V 2-4
	2.1.3 Certification Basis	V 2-6
V.2.2	ANALYSES CONSIDERATIONS FOR ICE PROTECTION SYSTEM DESIGN	V 2-7
	2.2.1 General Considerations	V 2-7
	2.2.2 The Analyses Requirement	V 2-8
	2.2.3 The Meteorological Design Envelope	V 2-10
V.2.3	THE AIRFRAME ICING PROBLEM FOR CRUISE	V 2-12
	2.3.1 Interpreting the Requirement	V 2-12
	2.3.2 Airfoil Characteristics	V 2-12
	2.3.3 Cruise Operating Problems	V 2-13
	2.3.4 Impingement Calculations	V 2-14
	2.3.5 Estimates of Water Impingement	V 2-18
	2.3.6 Estimates of Ice Formation	V 2-20
V.2.4	THE 45 MINUTE HOLDING PROBLEM	V 2-21
	2.4.1 Primary Requirements	V 2-21
	2.4.2 Operating Problems	V 2-22
	2.4.3 Impingement Calculations	V 2-22
	2.4.4 Estimates of Ice Accretion	V 2-24
V.2.5	THE ICING PROBLEM FOR CLIMB SITUATIONS	V 2-26
	2.5.1 Primary Requirements	V 2-26
	2.5.2 Operating Problems	V 2-27
	2.5.3 Impingement Calculations	V 2-27
	2.5.4 Estimates of Ice Accretion	V 2-28

CONTENTS (cont'd.)

		Page
V.2.6	WINDSHIELD ICE PROTECTION	V 2-29
	2.6.1 Primary Requirements	V 2-29
	2.6.2 Operating Problems	V 2-30
	2.6.3 Impingement Calculations	V 2-30
	2.6.4 Fluid Anti-Icing Calculations	V 2-31
	2.6.5 Electric Anti-Icing Calculations	V 2-32
V.2.7	PROPELLER ICE PROTECTION	V 2-33
	2.7.1 Primary Requirements	V 2-33
	2.7.2 Operating Problems	V 2-35
	2.7.3 Impingement Calculations	V 2-35
	2.7.4 Thermal Analyses	V 2-40
V.2.8	ENGINE INDUCTION SYSTEM	V 2-40
	2.8.1 Primary Requirements	V 2-40
	2.8.2 Operating Problems	V 2-42
	2.8.3 Analyses/Certification Demonstration	V 2-42
V.2.9	PITOT-STATIC AND STALL WARNING SYSTEM PROTECTION	V 2-42
	2.9.1 Primary Requirements	V 2-42
	2.9.2 Operating Problems	V 2-43
	2.9.3 Impingement Calculations	V 2-43
	2.9.4 Thermal Analyses	V 2-43
V.2.10	RADOME ICE PROTECTION	V 2-45
	2.10.1 Primary Requirement	V 2-45
	2.10.2 Operating Problem	V 2-45
	2.10.3 Impingement Calculations	V 2-46
	2.10.4 Estimates of Ice Accretion	V 2-46
V.2.11	MISCELLANEOUS ANALYSES	V 2-46
	2.11.1 Ice Shedding	V 2-46
	2.11.2 Flutter	V 2-47
V.2.12	THE STABILITY AND CONTROL PROBLEM	V 2-47
V.2.13	SYSTEM RELIABILITY	V 2-48
	2.13.1 Requirement	V 2-48
V.2.14	REFERENCES	V 2-51

LIST OF TABLES

		Page
2-1	FAA Form 8110-12, "Application for Type Certificate, Production Certificate, or Supplemental Type Certificate"	V 2-52
2-2	Predicted Performance of Generic Model A Aircraft	V 2-53
2-3	Comparison of Basic Transport and Normal Category Icing Requirements	V 2-54
2-4a	Langmuir and Blodgett Droplet Size Distributions	V 2-55
2-4b	"D" Distribution Droplet Sizes for Three MVD's	V 2-55
2-5	Design Meteorological Environments	V 2-56
2-6	Performance-Critical Flight Operating Situations	V 2-57
2-7	Impingement Estimates for Design Continuous Maximum Icing Conditions for Generic Model A at 7000 feet in Cruise	V 2-58
2-8	Impingement Estimates for Design Intermittent Maximum Icing Conditions for Generic Model A at 7,000 feet in Cruise	V 2-58
2-9	Generic Model A Aircraft Climb-Cruise-Climb Performance Without Ice	V 2-59
2-10	Impingement Calculations for Climb to 7,000 Feet	V 2-60
2-11	Impingement Calculations for Level Off and Cruise at 7,000 Feet	V 2-61
2-12	Radome Impingement Calculations for Cruise at 7,000 Feet	V 2-62

LIST OF FIGURES

		Page
2-1	Three View Drawing of Generic Airplane A	V 2-63
2-2	Speed-Power Data as a Function of Equivalent Airspeed	V 2-64
2-3	Lift-Drag Polars	V 2-65
2-4	USA 35-B Airfoil Lift Curve Showing Effect of Ice	V 2-66
2-5	Droplet Range Ratio as a Function of Droplet Reynolds Number	V 2-67
2-6	Collection Efficiency Versus K_0 for Airfoils - Theoretical Data at 2° Angle of Attack	V 2-68
2-7	Impingement Limit on the Upper Surface of Several Airfoils	V 2-69
2-8	Impingement Limit on the Lower Surface of Several Airfoils	V 2-70
2-9	LWC Factor, F, for Cloud Horizontal Extent in Continuous Maximum Icing Conditions	V 2-71
2-10	Ice Shape Types as a Function of Speed and Ambient Temperature for a Liquid Water Content of 0.5 g/m^3	V 2-72
2-11	Collection Efficiency Versus K_0 for Airfoils - Theoretical Data at 4° Angle of Attack	V 2-73
2-12	Angle of Attack VS. Airfoil Performance Parameters for NACA 0012 Airfoil	V 2-74
2-13	Percent Freezing Point Depressant as a Function of Temperature for Several Aqueous Solutions	V 2-75
2-14	Graphical Solutions of Anti-Icing Heat and Mass Transfer from a Surface Subject to Impingement and Heated Above Freezing	V 2-76
2-15	Power Requirements for Electrical Protection of Windshield	V 2-77
2-16	Collection Efficiency Versus K_0 for Geometric Bodies - Theoretical Data for 0° Angle of Attack	V 2-78
2-17	Impingement Limits on Several Geometric Shapes at 0° Angle of Attack - Theoretical Data	V 2-79

SYMBOLS AND ABBREVIATIONS

Symbol	Description
A	Area (ft^2)
AC	Advisory Circular
ACO	Aircraft Certification Office
A_c	Accumulation Parameter,
A_i	Cross Sectional Area of Ice Formation (Square Inches)
BTU	British Thermal Unit
C	Airfoil Chord Length (ft)
CAR	Civil Air Regulations
CG	Aircraft Center of Gravity
CAS	Calibrated Airspeed
CG	Aircraft Center of Gravity
C_d	Coefficient of Drag
C_L	Aircraft Lift Coefficient
C_{Lp}	Propeller Lift Coefficient
C_m	Airfoil Moment Coefficient
D	Aircraft Drag (Pounds)
D_d	Droplet Diameter (Microns)
E_M	Total Collection Efficiency
°F	Degrees Fahrenheit
F	Design Standard Liquid Water Content Factor
FAA	Federal Aviation Administration
FAR	Federal Aviation Regulations
G	Percent Freezing Point Depressant
HP	Horsepower (ft-lb/sec)
HP_r	Horsepower Required (ft-lb/sec)
HP_a	Horsepower Available (ft-lb/sec)
K	Inertia Parameter
K_o	Modified Inertia Parameter
KIAS	Knots Indicated Airspeed
LWC	Liquid Water Content
MVD	Droplet Median Volume Diameter (Microns)
M_w	Weight Rate of Water Impingement ($lb/hr\text{-}ft^2$)
NACA	National Advisory Committee for Aeronautics
P	Pressure Altitude ($Pounds/ft^2$)
Q	Heat (BTU/ft^2)
R_e	Droplet Reynolds Number

SYMBOLS AND ABBREVIATIONS (cont'd.)

Symbol	Description
RPM	Revolutions Per Minute
RPS	Revolutions Per Second
S	Airfoil Surface Area (ft^2)
SAE	Society of Automotive Engineers
SFAR	Special Federal Aviation Regulation
STC	Supplemental Type Certificate
S_U	Impingement Limit - Upper Surface
S_L	Impingement Limit - Lower Surface
T	Temperature
T_c	Temperature for the onset of Ice (°F)
TC	Type Certificate
T_R	Temperature (Degrees Rankin)
U_o	True Airspeed (MPH)
V_e	Equivalent Airspeed (MPH)
V_r	Propeller Rotational Speed, (True Velocity, ft/sec)
V_t	True Airspeed (ft/sec)
W	Aircraft Weight (Pounds)
W_F	Weight Rate of Anti-Icing Fluid ($lb/hr\text{-}ft^2$)
W_{Flb}	Weight of Water Catch (lb/hr)
W_M	Weight Rate of Water Catch (lb/hr-ft-span)
g	Acceleration of Gravity (ft/sec^2)
g/m^3	Grams per Cubic Meter
h	Projected Airfoil Height (ft)
h_c	Coefficient of Convective Heat Transfer ($BTU/hr\text{-}ft^2\text{-}°F$)
kw	Kilowatts
n	Freezing Fraction
n_p	Propeller Rotational Speed (PRS)
q	Dynamic Pressure ($Pounds/ft^2$)
q_p	Dynamic Pressure for Propeller Rotation ($Pounds/ft^2$)
r	Propeller Radius (feet)
t	Time
t_f	Boundary Layer Temperature (°F)
α	Angle of Attack (Degrees)
β	Local Impingement Efficiency
δ_i	Ice Thickness (Inches)
μ	Air Viscosity (Slugs/ft-sec)
τ	Heat Transfer Temperature Parameters (°F)

SYMBOLS AND ABBREVIATIONS (cont'd.)

Symbol	Description
ρ	Air Density (Slugs/ft^3)
λ/λ_s	Droplet Range Ratio
L	Airfoil Lift Force (Pounds), or Lower Surface
U	Upper Surface
W	Water
i or ice	Pertaining to ice
lb	Pounds
o	Free Stream
p	Propeller

V.2.0 SYSTEMS DESIGN ANALYSES AND CERTIFICATION PLANNING

V.2.1 AIRCRAFT DESIGN CONCEPT

2.1.1 Physical Characteristics

2.1.1.1 Aircraft

The information presented in this section is intended to illustrate the rationale for the use of technical analyses to support the critical decisions involved in aircraft design development activities and in Type Certification evaluations. The illustrations are not a complete set of instructions and the technical calculations for one problem do not always relate to those performed for other problems. Also, calculations necessary to illustrate various analytical problems will be performed manually to facilitate discussion of significant considerations. Applicants will normally use computer programs to produce information pertinent to the various technical problems encountered in connection with their efforts to demonstrate the adequacy of ice protection system designs.

Table 2-1 is a copy of FAA Form 8110-12 (dated 3-80), "Application for Type Certificate, Production Certificate, or Supplemental Type Certificate". Block 2 would be checked for Type and Production Certificates, and all three items in block 3 would be checked when approval of a new design is requested. A three view drawing of the aircraft for which certification is requested is part of the block 4 requirement and is illustrated in figure 2-1. Information prepared to demonstrate the adequacy of ice protection systems is one of the many analyses and part of the extensive documentation required to support applications for aircraft type certification.

The characteristics of a twin engine aircraft will be used to illustrate the use of information to support the technical analyses requirements for type certification. Proprietary concerns preclude the use of specific information from actual FAA Type Certification programs as examples. Therefore, a design called "Generic Model A" is used in this Chapter to illustrate the design certification process for ice protection systems. The design is an extension of the one used in reference 1, FAA report ADS-4, "Engineering Summary of Airframe Icing Technical DATA." The extension involves the use of equations to define the lift and drag relations used in the report plus additional calculations to provide a more complete set of power-required data.

Detailed information concerning icing related physical and operational characteristics of an aircraft to be certified is needed to support analyses for type certification. The major characteristics of the Generic Model A aircraft that relate to aircraft icing system analyses are as follows:

1.	Number of Engines	2
2.	Number of Seats	6 (including the pilot)
3.	Weight	4800 pounds (for test problem)
4.	Wing Span	30.2 feet
5.	Wing Area	207 sq. ft.
6.	Mean Aerodynamic Chord	67 Inches
7.	Brake Horsepower	250 each, at 2575 RPM at mean sea level in a standard atmosphere

2.1.1.2 Equipment

The Generic Model A aircraft is equipped as follows for potential FAA approval for operating in icing conditions under FAR Part 23, "Airworthiness Standards for Normal, Utility, Acrobatic, and Commuter Category Airplanes"; and FAR Part 135, "Regulations for Air Taxi and Commercial Operators":

1. Pneumatic Surface Deicers for Wings and Stabilizers
2. Electrothermal Prop Deicers
3. Hot Air Windshield Deicing
4. Optional Electro-thermal Windshield Anti-icing
5. Pilots Storm Window
6. Stall Warning and Fuel Vent Electrothermal Heaters
7. Antennas with the Strength Needed to Withstand Maximum Icing Conditions
8. Alternate Power Plant Air Intake

2.1.1.3 Surface De-Icing

Surface boots are installed to protect the wings and horizontal stabilizers. The boot de-icing system is controlled by a deice valve, two-stage regulating valves, and a control-timer. The control switch is placarded "Single Cycle Off" and "Manual Off." When the switch is pulled to "Single Cycle" the deice valve solenoid is energized, blocking air flow to the suction venturi and allowing air passage to the boots. Simultaneously, the regulator in each nacelle is energized, raising the pressure in the deice system. The inflation cycle is terminated in 6 seconds by the control timer which de-activates the control and regulator valves. The boots dump pressure and the control valve shuttles to vacuum when the pressure lowers to approximately 1.0 psi, thereby leaving the boots flat under aerodynamic pressure.

There is an indicator to inform the pilot concerning boot operation. Aiso, measurements of boot operating pressures will be obtained during tests conducted in dry air. Capability to remove ice formations will be demonstrated during icing simulation tests conducted behind a tanker aircraft. The capability will also be demonstrated on an opportunity basis after and during flights in natural icing conditions.

The "Manual Off" position allows discontinuation of a cycle prematurely if desired or in case of control malfunction.

The vertical fin is not protected based on the results of flight tests. The performance-critical condition for an unprotected vertical fin occurs in the condition that produces the greatest amount of ice and involves the formation shape and flight operating conditions that most adversely affect airplane lateral control. The "continuous maximum" icing condition was used to determine simulated ice formation shapes for these tests which included a full range of flight operating conditions. The tests demonstrated that there were no unacceptable adverse effects on aircraft attitude control characteristics. The results of this test will be reported as an addendum to this analysis.

2.1.1.4 Propeller De-icing

The propeller deicers are of standard design, having two heated sections per propeller blade. The sections are heated alternately, providing 30 seconds of current-on time for each section. Similar sections on all blades on a propeller are heated simultaneously, i.e., the inboard sections, then the outboard sections on one propeller; then the process is repeated on the second propeller. A complete cycle is accomplished in two minutes. The heat-off time is 90 seconds for each panel section during a complete two minute cycle. The boots protect to beyond the critical point of centripetal acceleration for holding airspeeds and propeller RPM.

2.1.1.5 Windshield De-icing

A 35,000 BTU heater is installed in the nose section to furnish a source of hot air for cabin heating and windshield anti-icing. Operation of the heater is controlled by a three position switch marked FAN, OFF, and HEAT. The main air valve actuator opens to the full open position when the aircraft is on the ground and the windshield anti-ice system is energized. The blower turns on to half capacity when the valve is nearly open, and to full blower capacity when the valve is completely open. This two stage system for increasing pressure from the blower minimizes the pressure "bump" effect - a temporary pressure increase that would result if the valve is not fully open when the blower system reached full capacity.

During ground operation, the heater output temperature is controlled by a temperature and flow regulating system called a duct-stat. During each duct-stat cycle, the heater bypass air valve is closed during the duct-stat "On" cycle and open during the duct-stat "Off" cycle.

A two-position electrical control called a squat switch is attached to the landing gear to change system operation when the aircraft is on the ground with weight on the landing gear. When the squat switch is in the flight position, the windshield anti-ice system is "On" and the pressurization system is "Off." The system operates the same as during the "Ground" mode except that for ambient temperatures below 40°F, the duct-stat heater control is bypassed and control given to the heater cycling switch. The duct-stat continues to operate the air bypass valve to maintain comfortable cabin temperatures during high windshield air temperature conditions.

In addition to the above flight conditions, the main air valve closes to the point which produces an air pressure differential of 14" H_2O. The valve actuator responds to the closed loop servo sensor and maintains the pressure regardless of cabin pressure level.

The test aircraft uses all the functional parameters of the automatic system described above; however, the controls are manual.

The hot air windshield de-icing system is expected to provide a clear area of approximately 80 square inches in the "continuous maximum" icing conditions and approximately 20 square inches in the -22°F condition.

2.1.1.6 Stall Warning

An electrothermally heated stall warning vane is installed. It will provide ice-free protection throughout the full icing temperature envelope. The signal generated by the instrument provides the warning signal when aircraft angle of attack approaches the normal angle for stall. There is no adjustment for warning when ice formations cause stall at reduced angles of attack and airspeeds. This aspect of stall warning system operation will be investigated during the flight test program when the effects of artificial ice formation shapes on stability and control are evaluated. Appropriate information will be included in the pilot's Handbook of Flight Operating Instructions.

2.1.1.7 Antennas

Antennas and antenna mounts are chosen with strength and resonance characteristics to withstand the maximum ice accretion without anti-icing or de-icing protection. The installation is similar to designs in use on other aircraft having similar operating characteristics. Evidence of similarity will be made available for review.

2.1.2 Operational Characteristics

The predicted performance characteristics for Generic Model A aircraft operation in a standard atmosphere are shown in table 2-2 and figure 2-2. The table shows maximum and cruise operating speeds in a standard atmosphere at flight altitudes up to 16,000 feet, plus single and two engine rates of climb. Climb speeds for two engine climb and brake horsepower for normal cruise are also shown. An equivalent airspeed of 105 MPH provides the best rate of climb and is used for climb analyses. Holding operations are conducted at an equivalent airspeed of 125 MPH.

Equivalent airspeed is the speed at sea level in a standard atmosphere that produces the same lift and drag forces that are observed at higher altitudes while maintaining the same angle of attack. It is approximately equal to indicated airspeed corrected for calibration errors. Figure 2-2 presents performance in terms of the calculated speed-power polars for the twin engine aircraft. The figure shows thrust horsepower required and thrust horsepower available as a function of equivalent airspeed. This form of presentation was selected for this report to display altitude effects on power required and power available in the various operating conditions. The curves for the higher altitudes are shown

for the most probable icing condition temperatures. This form of presentation shows how the power required increases for the same equivalent airspeed as altitude is increased. It also shows how the power available decreases with increasing altitude due to the lack of superchargers on the aircraft.

The power available data was determined by three points. One point was determined by maximum power for two 250 Horsepower engines. The second point was determined by the power required at climb speed, plus available excess power as indicated by the rate of climb. The third point was determined by the 205 MPH true air speed and power requirements used in ADS-4, reference 1, for cruise at the 7,000 foot altitude. Data for the lower speeds is arbitrary and is based upon the characteristics of similar aircraft.

Aircraft speed as it affects trip duration, and fuel consumption as it affects flight range and economy are primary aircraft performance factors affecting the pilot's choice of flight altitudes. There is very little difference in these factors for the Generic Model A design for altitudes between 4,000 and 11,000 feet although the 7,000 foot altitude provides slightly better performance. Therefore, weather factors and air traffic circumstances will be the primary consideration in flight altitude selection.

Aircraft icing effects on aircraft stability and control during landing operations must be evaluated for aircraft certification. The speeds for lowering the landing gear and flaps and aircraft stalling speeds are important in this respect. The landing gear on Generic Model A aircraft can be lowered at speeds under 150 MPH during approach. The flaps can be lowered to 1/2 at speeds below 140 MPH and to full down when speeds drop below 125 MPH. Stall speeds at 4800 pounds are 71 MPH CAS with gear and flaps retracted and 65 MPH CAS with gear extended and flaps at 50°.

Plots of the coefficient of drag as a function of the coefficient of lift are widely used for engineering purposes and are called lift drag polars. The symbol for the coefficient of drag is C_D and the symbol for the coefficient of lift is C_L. It is convenient to have a simple analytical equation to express the relation between the two coefficients. Such an expression expedites performance calculations and the reduction of flight or wind tunnel data and is useful for considering icing effects on lift and drag. An equation of the form $y = a + bx^2$ has been found to provide a reasonably accurate representation of the relation between lift and drag for many airfoils (reference 2). The coefficient of drag in the equation is y, the coefficient of lift is x, and a and b are constants. Drag polar plots are constructed with C_D as a function of C_L and also with C_D as a function of C_L^2. Plots of C_D as a function of C_L^2 are widely used for engineering analyses because of the straight line that often results for speeds greater than the climb speed (reference 3), "FAA Flight Test Guide for Certification of Normal, Utility, and Acrobatic Category Airplanes." However, wide divergence from the straight line relation often occurs for values of lift coefficients greater than 1.0 and for some airfoils (reference 2).

Figure 2-3 presents lift and drag polars for the aircraft. The following empirical equation was found to represent the relation between lift and drag coefficients for Generic Model A aircraft when speeds are greater than 110 MPH:

$$C_D = 0.046(c_L)^2 + 0.03 \qquad (2\text{-}1)$$

where C_D and C_L are defined in terms of total aircraft drag and weight, respectively for level flight.

The coefficient of drag in figure 2-3 is shown to be greater than the values predicted by the equation for the slower speeds. Calculation of the coefficients of drag for the slower speeds is more complex and was determined from power required data for the aircraft.

2.1.3 Certification Basis

The regulations applicable to the proposed design represent the certification basis. Advisory Circular AC 23.1419-1, "Certification of Small Airplanes for Flight in Icing Conditions," provides guidance concerning approval of ice protection systems for small aircraft. The guidance is applicable to actions with respect to new Type Certifications, Supplemental Type Certifications, and to amendments to existing Type Certificates that were issued under Part 3 of the CAR and Part 23 through amendment 23-13. Actions with respect to Generic Aircraft A will be taken in accordance with regulations applicable to requests for a new Type Certificate.

The regulations establish requirements specifically applicable to Generic Model A Aircraft:

FAR 23.773	through Amendment 23-14 - Pilot Compartment View
23.775	through Amendment 23-7 - Windshield and Window
23.929	through Amendment 24-14 - Engine Installation
23.1309	through Amendment 23-17 - Equipment, System, and Installation
23.1419	through Amendment 23-14 - Ice Protection
23.1325	through Amendment 23-1 - Static Pressure System
23.1327	through Amendment 23-20 - Magnetic Direction Indicator
23.1547(e)	through Amendment 23-20 - Magnetic Direction Indicator
23.1351	through Amendment 23-20 - Electrical System
23.1357	through Amendment 23-20 - Circuit Protection Devices
23.1416	through Amendment 23-23 - Pneumatic Deice Boot
23.1419	through Amendment 23-14 - Ice Protection
23.1559	through Amendment 23-23 - Operating Limitation Placard
23.1583(h)	through Amendment 23-23 - Operating Limitation

FAR 23.1419 was amended and 23.1309 was added to insure reliability of such systems and equipment. FAR 23.929 was also added to ensure operational protection against propeller and engine component icing. For multi-engine airplanes, FAR 23.1309 requires that the equipment, systems,

and installation must be designed to prevent hazards to the airplane in the event of a probable malfunction or failure. Finding of compliance with FAR 23.1309 must include consideration of the consequence of a single failure in combination with latent or undetected failures. If the consequence of the failure dictates that the only path of survival is to exit the icing conditions, the applicant must demonstrate by flight tests under the icing conditions of Appendix C of FAR Part 25 that the airplane has that ability. Also, adequate instructions and information pertaining to the exiting of the icing conditions will be included in the appropriate sections of the flight manual.

V.2.2 ANALYSES CONSIDERATIONS FOR ICE PROTECTION SYSTEM DESIGN

2.2.1 General Considerations

The technical and policy aspects of problems concerning the design of acceptable ice protection systems are the subject of previous chapters in this handbook. Having mastered the information contained in those chapters, the reader is now prepared to apply the knowledge. Characteristics representative of a twin engine propeller driven airplane called "Generic Model A" are used in this chapter to develop information illustrating the use of system design analysis to demonstrate the adequacy of ice protection systems and to relate the resulting information to the overall certification process. However, for some technical problems, it will be necessary to consider some aspects of problems related to the design certification of a jet transport and a rotorcraft.

The analysis steps taken for the design-development activity and the steps taken for the certification activity for ice protection systems are essentially the same. The major difference is the objective. The objective in the design development activity is to finalize the exact design of the ice protection systems. The objective in the certification activity is to demonstrate that the selected design actually meets FAR requirements. The input data for both instances is the aircraft design concept including the physical and operational characteristics, aeronautical and performance information, and the certification basis. With this input data, the following analysis steps are performed for the various components to achieve the analysis objectives:

1. Determine applicable FAR requirements
2. Determine icing exposure
    a. Calculate droplet impingement
    b. Calculate water and ice accretion rates, amounts and ice shape
3. Determine ice protection system specifications
    a. Define performance-critical operating problems
    b. Determine system performance requirements; heat required, etc.
    c. Define and/or select system specifications
4. Evaluate aircraft and component ice protection system performance
    a. Demonstration by analyses
    b. Demonstration by similarity
    c. Demonstration by test data

The steps taken for the various category aircraft are essentially the same. The most significant differences result from operational factors and the availability of system design choices. For example, the availability of heated air from jet engines has been a major factor in design choices concerning the use of hot air to protect the wings of large jet aircraft, while the lack of hot air, as well as costs, has resulted in the use of pneumatic boot systems on small propeller driven aircraft.

The basic ice protection requirements for transport and normal category aircraft are defined in paragraphs FAR Part 25.1419 and FAR Part 23.1419 respectively. The requirements are compared in table 2.3. Both parts are shown to require an analysis to establish, on the basis of the airplanes operational needs, the adequacy of the ice protection systems for the various components of the airplane. Both parts require flight tests to show or to demonstrate that the airplane is capable of operating in continuous maximum and intermittent maximum icing conditions as described in appendix C of FAR Part 25. However, the requirement for Part 25 category aircraft is to show the effectiveness of protection systems, and the requirement for Part 23 category aircraft is to demonstrate operating safety. The end result is essentially the same in either case.

Other differences between the statements of basic requirements for FAR Part 25 and 23 category aircraft are also of interest. Part 25 requires flight tests in measured natural icing conditions and provides more information concerning the test requirements. The Part 23 statement in paragraph 23.1419 does not specify measured natural icing conditions, but it would be difficult to demonstrate acceptable performance without an acceptable indication of flight test conditions. Paragraph (d) in Part 25 directs attention to requirements for turbine engines. The Part 23 requirement for Flight Manual material is covered elsewhere in FAR Part 25.

The basic requirements are the same with respect to objectives; if certification with ice protection provisions is desired, the applicant must prove that the aircraft is able to operate safely in the continuous maximum and intermittent maximum icing conditions determined under Appendix C of Part 25 according to the airplane's operational needs. Additional statements of icing related requirements in the regulations provide information pertinent to considerations involving specific components but do not alter the basic requirement.

2.2.2 Analyses Requirements

The applicant normally prepares the analyses needed to substantiate decisions involving application of selected ice protection equipment to areas and components and also to substantiate decisions which leave normally protected areas and components unprotected. Such analyses should clearly state the basic protection required, the assumptions made, and delineate the methods of analysis used. All analyses should be validated, either by tests or by reference to previous substantiation, using methods documented in accepted icing literature.

The substantiations should include a discussion of the assumptions made in the analyses and the design provisions included to compensate for these assumptions.

To some degree, who performs the analysis will depend on the type of ice protection devices being used. In any case, the airframe manufacturer is responsible for the analysis. An airframe manufacturer would likely perform all of the system design and most of the fabrication in-house for a hot gas anti-icing system. The analytical method used in design would be tested against flight data and its accuracy determined. An aircraft maker is less likely to fabricate the boots for a pneumatic boot system and much reliance would be placed on the analytical or empirical performance predictions supplied by the boot manufacturer. Electro-impulse de-icing and fluid freezing point depressant systems may also involve outside suppliers of either components or system design. These suppliers will be major participants in the application of analytical methods to predict system performance in untested conditions.

The credibility of results obtained through use of the various methods of analyses is improved when the results of flight and ground tests with the same aircraft are used to evaluate analyses. Care must be taken in extrapolating data to insure that the analytical methods consider qualitative changes in flow regimes such as flow separation.

The term "analysis" includes the use of standard engineering equations for computations as well as computer code simulation and scaling laws. These methods are presented in Chapters I and IV. Analyses should consider the effects of flying in ice on the whole aircraft, the protected as well as the unprotected surfaces. Dangers from ice shedding and engine probe icing should be considered. Special consideration should be given to residual and/or runback ice and its effect on aerodynamic lift, drag, stability, and control of aircraft attitude during the critical landing approach.

Where analysis is planned, the methods of analysis and the basic assumption should be clearly identified. Methods such as those described in Chapters I thru IV may be used to predict ice accretion and system performance. Advisory Circular, AC 20-73, provides more detailed guidance regarding methods of analyses and the influences of meteorological and operational factors. These methods may be used to define the critical ice shapes that would accumulate on unprotected surfaces in icing conditions described in Appendix C of FAR 25. Special emphasis should be directed toward consideration of the following items:

(1) Areas and Components to be Protected - The applicant's analysis should address the protection, if any, to be provided for the following areas and components:
   (a) Leading edges of wings, winglets, horizontal and vertical stabilizers, and canards.
   (b) Control surface balance area leading edges if not shielded.
   (c) Wing Struts.
   (d) Windshield.
   (e) Engine.
   (f) Helicopter rotor.
   (g) Propeller.
   (h) Engine induction system.
   (i) Accessory cooling air inlets and air scoops.

(j) Pitot tube, static ports, and stall warning transducer.
(k) Antennas.
(l) Fuel Tank vents.
(m) Radomes and nose caps.
(n) External hinges, tracks, and door handles.
(o) Fixed landing gear.

(2) Airfoil Leading Edge Protection - Data should include a droplet trajectory and impingement analysis of the wing, horizontal and vertical stabilizers, propellers, and any other protected areas. This analysis should consider all critical points within the icing envelope, including the minimum icing operation airspeed. This analysis establishes the aft limits of ice formation. The guidelines established in Chapters I and IV of this handbook are a means of determining protective coverage and the design and construction thereof.

2.2.3 The Meteorological Design Envelope

The analyses conducted by the manufacturer to select the performance-critical design environments for the various components on an aircraft are an important initial step in design process, and the physical characteristics of ice protection systems are defined as a result of these analyses. Type Certification of the proposed design involves demonstration that the design choices made as a consequence of these analyses produced an aircraft that meets all applicable Type Certification Requirements.

The performance-critical operating environments are defined in terms of the technical parameters that define the intensity of icing conditions that will be encountered by the proposed aircraft. Icing conditions result when cloud water droplets are super-cooled. Technical parameters are used in design studies to describe the meteorological intensity of icing conditions. One parameter is the air temperature of the icing cloud. A second parameter, the amount of water in an icing cloud, is defined in terms of the amount of water in a cubic meter of the cloud. The unit of measurement is grams per cubic meter.

The additional technical parameters used to describe the meteorological intensity of an icing condition use statistical techniques to describe the distributions of droplets in the cloud. The unit of droplet measurement is microns, and the characteristic dimension is droplet diameter although the radius is used in some instances. Droplets in the distributions are divided into class intervals according to droplet size, and each class interval contributes an amount of water according to the number of droplets in the class interval.

The amount of water in an icing cloud that is associated with droplets that are larger and smaller than the median volume diameter, MVD, is an important consideration in many analyses problems. The Langmuir-Blodgett statistical distribution system, reference 4, has been found to provide a reasonably accurate representation of the variations of droplet size in clouds with respect to the MVD.

With this system, the various distributions are represented by letters, A, B, C, etc., as shown in table 2-4a. The D type distribution is used for many ice protection system design problems and is shown in table 2-4b with droplet diameters associated with 15, 20, and 22 micron mean volume diameters.

Table 2-5 defines the various values of cloud liquid water content that are associated with the given mean volume droplet diameters and ambient air temperatures in FAR Part 25, Appendix C. The values were read or interpolated from graphs presented in the regulation. Liquid water contents for air temperature values not shown on the graphs were determined by interpolation. The continuous maximum condition is applicable from sea level to 22,000 feet. Its maximum vertical extent is 6,500 feet and its maximum horizontal extent is 17.4 nautical miles. The intermittent maximum design condition is applicable for altitudes from 4,000 to 22,000 feet, and the maximum horizontal distance is reduced to 2.6 nautical miles.

The most probable icing condition temperatures at the altitudes to be flown by the Model A aircraft were obtained from figure 1-36 in Volume I, Chapter I, Section 1 of this handbook and are listed as follows:

2,000 Feet	23.5°F	11,000 Feet	10.6°F
4,000 Feet	21°F	12,000 Feet	8.0°F
7,000 Feet	17°F	14,000 Feet	3.8°F
10,000 Feet	12°F	16,000 Feet	-1.0°F

The most probable icing condition temperature is not necessarily a performance-critical condition for demonstrating the adequacy of ice protection systems although it is a condition to be considered. Maximum droplet size is always a performance-critical consideration, and the consequence of formations resulting from the larger droplets that impinge aft of protected areas must be evaluated; but the performance-critical combinations of liquid water content, mean droplet diameter, and air temperature for protected areas are more complex.

Table 2-5 shows the significant increases in liquid water content that occur as droplet sizes become smaller or as temperatures become warmer. The rate of ice formation and the amount of ice accumulating on components increases with increasing liquid water contents and decreases as droplet sizes become smaller; and the amount of liquid water that freezes is affected by air temperature and aircraft airspeed. Although droplet size is of little consequence for problems involving the smaller components, droplet size becomes increasingly important as component size increases.

V.2.3 THE AIRFRAME ICING PROBLEM FOR CRUISE

2.3.1 Interpreting the Analysis Requirement

Ice formations on airframe structures produce performance penalties involving power requirements and aircraft stability. Most aircraft can tolerate some amount of ice on structures. The power available in excess of the amount required for level flight is relatively small on most small aircraft and is quickly lost when the formations develop.

The analysis requirement of FAR Part 23.1419 is to establish, on the basis of the airplane's operational needs, the adequacy of the ice protection systems for the various components. The amount of analysis work is reduced by selecting performance-critical situations and by showing that the selections are valid choices. State-of-the-art experience and theory have progressed to the point where very little effort is actually required to demonstrate the adequacy of a boot deicing system on an aircraft of conventional design.

2.3.2 Airfoil Characteristics

The airfoil for the Generic Model A aircraft is a modified USA 35B design. Wing area is 207 square feet and span of 30.2 feet. The chord length is constant at 67 inches. Maximum airfoil thickness is 15% of the chord length, and the airfoil angle of incidence is constant at the various span locations. (airfoil angle of incidence is normally 2 to 4 degrees less at outboard wing locations.) This is not precisely the same airfoil that was used in FAA Report ADS-4, reference 1, which used a thickness of 12.5% for some calculations and 15% for others. The use of two thicknesses was unacceptable for this work, and the characteristics of a 15% airfoil were used for impingement calculations. Also, impingement data was not available for the USA 35B airfoil, and the calculations in reference 1 and in this chapter were related to a Joukowski airfoil having a 15% chord length thickness. This substitution was made as a matter of convenience for these illustrations and would not be acceptable for an FAA Type Certification without supporting evidence showing that airflows were similar for given angles of attack.

Selection of the proper equations and curves for impingement calculations is a special problem that is beyond the scope of this chapter. Guidance on this problem is contained in Chapter I.

Figure 2-4 presents the coefficient of lift as a function of airfoil angle of attack for the USA 35B airfoil. Positive lift is shown to occur for angles as low as -5°. The lift curve can be represented by the following empirical equation for angles of attack less than 17.5°:

$$C_L = 0.0713\alpha + 0.387 \qquad (2\text{-}2)$$

where α is the wing angle of attack, and the numerical values 0.0713 and 0.387 were determined empirically to fit the straight line portion of the lift curve. The wing stalls at an angle of about 19°, but continues to produce lift as shown by figure 2-4. The indicated effect of ice on the curve is arbitrary and is only one of many possible effects.

The horizontal stabilizer is an NACA 0012 airfoil with a 12.5 foot span. It has an area of 37 square feet and a mean aerodynamic chord of 37 inches. The vertical fin has an area of 25 square feet and a span of 56 inches.

2.3.3 Cruise Operating Problems

Table 2-6 presents performance data used for impingement calculations for performance-critical flight operating situations for the Generic Model A aircraft. The equations used to calculate air density and viscosity are also shown on the table.

From experience as well as analysis, we know that the performance-critical operating problems on small aircraft are associated with the heavier operating weights. The maximum take-off and landing weight of Generic Airplane A is 4,900 pounds and a weight of 4,800 pounds will be used for the analysis problems.

Pilots operating Generic Airplane A will normally climb out to an initial cruise altitude between 4,000 and 14,000 feet. If performance were the only consideration, the pilots would select an altitude of about 7,000 feet. Icing conditions can be encountered during climb and also in cruise. For the design analysis, a worst case performance-critical cruise operating situation will be defined as one that occurs when design icing conditions are encountered after level-off at a planned cruising altitude of 7,000 feet. The pilot requests permission to climb but a higher altitude is not available and the aircraft is unable to leave the icing condition. An altitude of 7,000 feet will be used for the initial analysis and other altitudes will be examined if necessary.

There is an altitude effect on boot performance but the effect pertains to the availability of sufficient pressure to inflate the boots and break ice formations. Adequate pressure is provided by the inflation system for the Generic Model A aircraft, and necessary information will be displayed to enable the pilot to monitor boot system operation. Also, pressures will be measured at the higher cruise altitudes to demonstrate that the pressures are adequate.

Air temperature and liquid water content effects on ice formation shape and texture are known to be significant. Most formations are easily removed if boot inflation pressures are adequate. The exception is the formation of mixed rime and clear ice that develops rapidly and does not fracture properly due to its structural characteristics. These layers of the ice may not break cleanly, and a bridge of ice can form over the boots. This is a general problem with boot deicing systems, and the usual solution is to allow more ice to form before the boot system is cycled. Tests will be performed to demonstrate that system inflation pressures can break formations that are 1 to 2 inches thick. The pilot's operating instructions will include instructions to allow an inch of ice to form before cycling the boots in severe icing conditions. The effects of ice formation removal on airplane pitch control and center of gravity limits will be investigated during flight tests, and the Pilot's Flight Operating Handbook will include instructions to turn off the pitch control on the auto-pilot before the boot system is cycled if tests show that there is a problem.

2.3.4 Impingement Calculations

Droplet impingement calculations were the subject of instruction in Chapter I, Section 2 of this Handbook. The calculations are performed initially by the aircraft designer to determine where ice will form on the aircraft, the rates of accumulation, and the total amounts that might form in a design situation. Based upon these analyses, the aircraft manufacturer develops system design specifications. The rationale that guides application of this methodology and the choices made by the designers are the important consideration in the analyses required in connection with design certification.

The flight operating circumstances to be considered with respect to performance critical design questions are listed in table 2-6. The angle of attack must be determined for these circumstances as an initial step in determining water droplet impingement. This step involves two calculations which are illustrated for the wing problem as follows:

Coefficient of Lift $$C_L + \frac{L}{q\,A} \qquad (2\text{-}3)$$

Cruise 11,000 $$C_L = \frac{4800}{(70.80)(207)} = 0.3275$$

Cruise 7,000 $$C_L = \frac{4800}{(90.24)(207)} = 0.2570$$

Holding 7,000 $$C_L = \frac{4800}{(39.98)(207)} = 0.5800$$

Wing Angle of Attack $$\alpha = \frac{C_L - 0.387}{0.0713} \qquad (2\text{-}4)$$

Cruise 11,000 $$\alpha = \frac{0.3275 - 0.387}{0.0713} = -0.83^\circ$$

Cruise 7,000 $$\alpha = \frac{0.2570 - 0.387}{0.0713} = -1.80^\circ$$

Holding 7,000 $$\alpha = \frac{0.5800 - 0.387}{0.0713} = 2.71^\circ$$

Where

C_L	= Coefficient of Lift	Dimensionless
L	= Lift = Aircraft Weight	Pounds
q	= Dynamic Pressure	Pounds/ft^2
A	= Wing Area	Square Feet
α	= Wing Angle of Attack	Degrees

Air density and viscosity at flight altitudes must be used to make impingement calculations. The following equations are used to determine air density and viscosity:

Air Density $$\rho = \frac{P}{(32.2)(53.3)\ T_R} \qquad (2\text{-}5)$$

$$= \frac{P}{1716}\ (459.7 + {}^\circ F)$$

Air Viscosity $$\mu = 7.1358 \times 10^{-10}\ (459.7 + {}^\circ F) \qquad (2\text{-}6)$$

Where

P	= Pressure altitude	Pounds/ft^2
T_R	= Air temperature	(459.7 + °F)

The following additional illustrative impingement calculations can now be made for cruise at 7000 feet with 20 micron droplets and 17°F temperatures:

Droplet Free Stream Reynolds Number

$$R_e = \frac{(4.81\times10^{-6})(D_d)(\rho)(U_o)}{\mu_a} \qquad (2\text{-}7)$$

$$= \frac{(4.81\times10^{-6})(20\ \text{microns})(.001996)(205)}{.3402\times10^{-6}}$$

$$= 115.7$$

Droplet Inertia Parameter

$$K = \frac{1.705\times10^{-12}\ D_d^{\,2}\ U_o}{\mu_a\ C} \qquad (2\text{-}8)$$

$$= \frac{1.705\times10^{-12}(20^2)(205)}{.3402\times10^{-6})(5.583)}$$

$$= 0.0736$$

The numbers in the equations are constants for the units used in the equations and

D_d	= Droplet Diameter	Microns
ρ	= Air Density	Slugs /Cubic Foot
U_o	= True Air Speed	Miles Per Hour
μ	= Air Viscosity	Slugs/ft-sec
C	= Characteristic Length	Feet (Chord length for the wing)

The Modified Droplet Inertia Parameter is the basic number used to determine collection efficiencies and the limits of impingement on upper and lower surfaces of the airfoil. It is also called the Impingement Parameter. Graphs are available as discussed in Chapter I, Section 2, to show how collection efficiency and impingement vary as a function of the modified droplet inertia parameter for various airfoils. The symbol for the parameter is K_0. K_0 may be calculated directly for most values of Reynolds Number, but it may also be determined from graphs or tables showing the droplet range ratio as a function of Reynolds Number.

The droplet range ratio was determined from figure 2-5 for the calculated Reynolds numbers. It is 0.335 for a Reynolds Number of 115.7 and therefore,

$$K_0 = \text{Droplet Range Ratio} \times K \qquad \text{Dimensionless} \qquad (2\text{-}9)$$

$$= (0.335)(0.0736) = 0.02466$$

It is frequently desirable to compare the effects of different icing conditions or flight operating situations involving use of the equations for droplet Reynolds Number, R_e, and the droplet Inertia Factors, K and K_0. An appreciation of the relative magnitude of the effects is helpful. Air density and viscosity are factors in Reynolds Number calculations, and viscosity is a factor in calculation of K. Table 2-6 shows a density of .001996 at 7,000 feet and 17°F, and a density of .001730 at 11,000 feet and 12°F. For the same airspeed, droplet diameter, and viscosity, the density effects would reduce the Reynolds Number at 7,000 feet from 115.7 to 100.3 at 11,000 feet according to the following calculations:

$$R_{e,11} = \frac{.001773}{.001996} (115.7) = 100.3$$

The lower Reynolds Number would increase the Droplet Range Ratio from 0.335 at 7,000 feet to 0.355 at 11,000 feet. The Inertia Parameter, K, would remain unchanged but K_0 would be changed as a result of the different droplet range ratio from .02466 at 7,000 feet to .0261 at 11,000 feet as illustrated by the following calculations:

$$K_{o,11} = \frac{0.355}{0.335} (0.02466) = 0.0261$$

Air viscosity decreases with colder temperatures and is 0.3402×10^{-6} at 7,000 feet and 0.3366×10^{-6} at 11,000 feet. If the viscosity effect is also included in the two altitude comparisons, the Reynolds number would be reduced from 115.7 to 101.4 instead of 100.3, and the change in droplet ratio would be reduced slightly.

True airspeed and droplet diameter are factors in both equations; however, the diameter is raised to the second power for the inertia parameter, and a small change in diameter can produce large

changes in R_e, K, and K_0. Droplet diameter is subject to a large range of values such as 10, 20, or 40 microns and true airspeeds for the Generic Model A airplane vary from 100 MPH to 200 MPH or more depending upon the problem. Variations of droplet diameter and true airspeed produce relatively large changes in R_e, K, and K_0 and are the primary source of variations in droplet impingement results.

The wing angle of attack was determined to be -1.8° and this value was assumed to be equivalent to a 2° angle of attack on the Joukowski airfoil. Figure 2-6 presents the overall collection efficiency parameter, E_M, as a function of the impingement parameter for several airfoils including the 0015 Joukowski for a two degree angle of attack. The value on the graph for .02466 is approximately 0.15.

The projected height of several airfoils, including the Joukowski 0015, is presented in figure 2-16, page I 2-81 in Section 2.0 of Chapter I and is not reproduced for this section. The information is presented in terms of the ratio h/C as a function of airfoil angle of attack, where h is the projected height and C is the airfoil wing chord which is 5.583 feet on the Generic Model A airplane. The ratio, h/C, is approximately 15.3% for an angle of 2°.

The rate of water catch on the wing can now be determined from the equation:

$$W_M = [0.329\ (U_o)\ \frac{h}{C}\ C](E_M)(LWC) \qquad (2\text{-}10)$$

$$= [(0.329)(205)(0.153)(5.583)]\ (E_M)\ (LWC)$$

$$= [57.61]\ \ E_M\ \ LWC\ \ \text{in pounds per foot span per hour}$$

The term within the brackets, [57.61], separates the aeronautical factors in the equation from the meteorological factors, E_M and LWC. This separation facilitates consideration of effects of droplet size and liquid water content on rates of impingement.

Table 2-5 indicates that LWC for 17°F is 0.46 grams per cubic meter in the continuous maximum icing condition and 2.30 grams per cubic meter in the intermittent maximum condition for the 20 micron droplet environment. Therefore:

$W_M = 57.61 \times .15 \times 0.46$ for the Continuous Maximum

$= 3.97$ lb/hr-ft span

$W_M = 57.61 \times .15 \times 2.30$ for the Intermittent Maximum

$= 19.87$ lb/hr-ft span

The limits of impingement were obtained from figures 2-7 and 2-8. For these estimates, data were also used for a 15% Joukowski airfoil operating at a 2° angle of attack. (Justification for this choice would be necessary for Type Certification.) A value of .02 is read from the graph for the upper surface for K_o = .02466 and .04 for the lower surface. The product of these values times the chord length, C in inches, produces the estimate of the limits of impingement on the upper and lower surfaces.

For the upper surface, $S_U = 67 \times .02 = 1.34$ inches

For the lower surface, $S_L = 67 \times .04 = 2.68$ inches

The foregoing estimates were made for 20 micron icing conditions encountered at 7,000 feet when air temperatures were 17°F; but droplet sizes in an icing condition are not all the same and every condition is different in at least some respect. For some problems, it is prudent to calculate droplet impingement results by considering the amount of water contained in the various class intervals. The Langmuir "D" type droplet size distribution is used for impingement analyses when the effects of the larger droplets are a matter of interest. This distribution is defined in table 2-4. The table also shows the droplet sizes associated with the various class intervals when the MVD is 20 microns. For the "D" distributions and a 20 micron MVD, the table indicates that 5% of the liquid water content in the cloud is associated with 44.4 micron droplet diameters which are 2.22 x the MVD. Droplet size distributions are often an important consideration when flight test data are being evaluated and when impingement analyses pertain to droplet effects on the larger components.

2.3.5 Estimates of Water Impingement

Table 2-7 presents estimates of the rate of water impingement, W_M, on the wings of Generic Model A aircraft for various combinations of design meteorological icing conditions shown in table 2-6. The data represent conditions at 7,000 feet, a true airspeed of 205 MPH, and an A type distribution for each of the droplet size calculations. The maximum rates are shown to occur in connection with 20 micron droplets for the complete range of temperatures. Although water contents were greater for 15 micron size droplets, other factors combined to produce the reduced impingement rates. Impingement rates are also shown to decrease as temperatures become colder. This effect is due to the reduction in cloud water content that occurs as temperatures become colder.

The surface area affected by droplet impingement is increased as droplet sizes increase. Table 2-7 shows variation on the upper surface from 1.0 inches for 10 micron droplets to 3.1 inches for 40 micron droplets. Impingement on the lower surface is shown to vary from 1.3 inches for 10 micron droplets to 6.7 inches when droplet diameters are 40 microns.

Estimates of the rates of water impingement in the Intermittent Maximum icing condition are presented in table 2-8. These estimates are also for 205 MPH at the 7,000 foot altitude. The maximum rates of impingement are also shown to occur in connection with 20 micron droplets for this aircraft design and operating condition. The surface areas affected by droplet impingement are the same for the Intermittent Maximum condition as for the Continuous Maximum condition. The possibility that

water droplet impingement at one location will run back to another position is not considered in these calculations.

The rates of impingement shown in tables 2-7 and 2-8 are in pounds per hour per foot span. The design criterion for the Continuous Maximum condition extends for a distance of 17.4 nautical miles (20 statute miles). At 205 miles per hour, the duration of the encounter would be 20 ÷ 205 = 0.09756 hours or 5.85 minutes. The amount of water impinging on the wing in cruise at 7000 feet in the Continuous Maximum icing condition would be 9.756% of the amounts indicated in table 2-7. For example, the amount of water that would impinge on the wings of the Generic Model A airplane in 20 micron icing conditions when air temperatures are -17°F and liquid water contents are 0.46 grams per cubic meter would be 3.97 x .09756 = 0.387 pounds of water per foot span. This impingement would cover an area that is one foot wide from the wing leading edge back 1.3 inches on the upper surface and 2.7 inches on the lower surface.

The Intermittent Maximum design icing condition extends 2.6 nautical miles (3.0 statute miles). At 205 MPH, the duration of exposure in this situation would be 3.0 ÷ 205 = .01463 hours or .88 minutes. The amount of water impinging on the wings of Generic Model A airplane would be 1.463% of the rates indicated in table 2-8. For example, the 19.87 pounds of water per foot span per hour that impinge on the wing would deposit only 0.29 pounds of water on the wings during the 3.0 mile encounter. Maximum Intermittent icing conditions are mainly important because of the rate of water droplet impingement.

A liquid water content adjustment for distance is included in the design criteria as defined in FAR Part 25, Appendix C. The liquid water contents for the continuous and intermittent conditions were calculated for the design criteria in terms of standard distances. The distance was 17.4 nautical miles (20 statute miles) for the Continuous Maximum condition and 2.6 nautical miles (3 statute miles) for the Intermittent Maximum condition. The adjustment is called "The Liquid Water Content Factor," F. It is dimensionless and is shown in figure 2-9 for the Continuous Maximum condition. The water contents for design analyses are increased if the distance is less than the standard distance and decreased if the distances are greater than the standard distance. For example, the factor is 0.32 for a distance of 200 miles and 1.20 for a distance of 10 miles. The average liquid water content is less when the distance in the design condition is greater but the duration of exposure is greater. The total accumulation on unprotected components is also greater when the duration of exposure is longer.

The Liquid Water Content Factor, F, adds another dimension to the concept of design liquid water content and to the determination of performance-critical conditions. For example, the total accumulation of ice is a matter of concern with respect to unprotected components. W_M was determined to be 3.97 pounds of water per hour for the Generic Model A aircraft. Calculations for a 200 mile encounter provide the following results for LWC Factor of 0.32:

$$W_{lb} = \frac{3.97\ F\ 200}{MPH} = \frac{(3.97)(0.32)(200)}{205} \qquad (2\text{-}11)$$

= 1.24 pounds of water per foot span.

The Liquid Water Content Factor reduced the 3.97 lb/ft-span per hour to 1.24 lb/ft-span for an encounter that would last almost an hour. This can be compared to the 0.387 pounds per foot span that would be collected during the standard distance encounter. The accumulation resulting from a 200 mile flight in the Continuous Maximum icing condition is used as a performance-critical condition for determining icing effects on unprotected components of the Generic Model A aircraft and for considering the effects of icing encounters with wing protection system inoperative.

A different curve for the Liquid Water Content Factor is used for the Intermittent Maximum icing condition. The factor varies from 1.35 for a 0.26 nautical mile encounter to 0.85 for a 5.21 nautical mile encounter. The longer distance often produces the most critical effect. The Intermittent Maximum condition is a matter of particular concern for systems such as engines and airspeed sensors that are performance-critical with respect to rates of impingement.

Similar calculations should be made for the various potentially performance-critical flight operating situations, and temperature effects must be considered with respect to freezing fractions and water runback.

2.3.6 Estimates of Ice Formations

The density of ice varies considerably depending upon the type of ice. Clear ice weighs about 57 pounds per cubic foot but rime ice may weigh much less. Figure 2-10 presents calculated predictions of ice formation shape as a function of true air speed and ambient air temperature for icing conditions at 5,000 feet and a liquid water content of 0.5 grams per cubic meter, references 5 and 6. The calculations are for a two inch diameter cylinder and for 15 micron droplet diameters. The diameter of the leading edge circle for the modified USA 35-B airfoil is a little larger, 2 5/8 inches, while the circle for the horizontal stabilizer is smaller. The data are reasonably representative of conditions associated with the cruise icing problem. The speeds and temperatures associated with the Generic Model A cruise icing problem fall within the area representing double ridge glaze ice formations, and specific calculations are not necessary. The specific density of ice in these conditions is approximately 0.85 (A value of 1.0 was used in reference 1). The double ridge type ice weighs about 53 pounds per cubic foot.

The cross-sectional area of the resulting ice formations can now be estimated and is equal to the thickness (depth) of the formation multiplied by the sum of the inches of ice on the upper and lower surfaces. Ice formation depth is estimated by determining the volume of water, and then dividing the volume by the area over which droplets impinge and by dividing the resulting number

by the density of the ice. For example, 3.97 pounds of water per foot span per hour represent the impingement rate determined for the design problem for cruise. The resulting accumulation of water was 0.387 pounds of water per foot span for the 20 mile standard distance in continuous maximum icing conditions and 1.24 pounds of water in the 200 mile distance. The impingement area covered 1.3 inches on the upper surface and 2.7 inches on the lower surface. The total wing surface area covered by ice was 4.0 x 12 = 48 square inches. Water at 62.5 lb/ft^3 weighs 0.03617 lb/in^3. Therefore, the average depth of the resulting ice formations can be determined as follows for the 20 micron design condition:

Standard Distance Calculation for ice formation thickness

$$\delta_i = \frac{\frac{\text{Pounds Water}}{.03617}}{(\text{Area})(\text{Density of ice})} \qquad (2\text{-}12)$$

$$= \frac{\text{Volume of Water}}{(\text{Surface Area})(\text{Density of Ice})}$$

$$= \frac{\frac{0.387}{.03617}}{(48.0)(.85)} = 0.26 \text{ Inches}$$

Cross-Sectional area of ice

$$A_i = \text{Thickness } (S_U + S_L) \qquad (2\text{-}13)$$

$$= 0.26\ (2.7 + 1.3) = 1.04 \text{ square inches}$$

The ice formation thickness for the 200 Mile Distance

$$d_i = \frac{\frac{1.24}{.03617}}{(48.0)(.85)} = 0.84 \text{ Inches}$$

$$A_i = 0.84\ (2.7 + 1.3) = 3.36 \text{ square inches}$$

V.2.4 THE 45 MINUTE HOLDING OPERATION

2.4.1 Primary Requirements

The criterion to consider the effects of a 45 minute hold in continuous icing conditions is discussed in AC 23.1419-1 and in AC 20-73. One objective of the analysis is to provide information for use in developing critical ice shapes for evaluating the overall effects of a holding operation on airplane operational characteristics. The requirement states that a median droplet diameter of 22 microns and a liquid water content of 0.5 grams per cubic meter are normally used for the analysis. A more severe liquid water content may be used. An ambient air temperature and an altitude are not

specified for the holding analysis and must be determined as part of the performance-critical operating condition determination.

The airplane is assumed to be in the cloud continuously during the 45 minute holding period and to be following a rectangular course. If the analysis shows that the airplane is not capable of withstanding the 45-minute hold operating condition, a reasonable period may be established for the airplane, but a limitation must be placed in the Airplane Flight Manual. The ice shapes derived from the analysis are to be compared with shapes derived from other analyses to establish the critical ice shapes for the airplane.

2.4.2 Operating Problems

Flight altitudes of 2,000 and 7,000 feet were selected for evaluation for the purpose of this analysis. The most probable temperatures of 24°F and 17°F for the lower and higher altitudes, respectively, were also selected for the evaluation. The following information is used for impingement calculations for the two holding situations:

FLIGHT ALTITUDE, FEET	2,000	7,000
Pressure Altitude lb/ft^2	1967	1633
Equivalent Airspeed, MPH	125	125
True air speed, MPH	125	136
Ambient Air Temperature, °F	24	17
Air Density, $slugs/ft^3$	.002370	.001996
Dynamic Pressure, lb/ft^2	39.98	39.98
Air Viscosity, slugs/ft-sec	$.3452 \times 10^{-6}$	3402×10^{-6}
Aircraft Weight, pounds	4800*	4800*

* A lighter weight could be justified since a requirement to hold for 45 minutes immediately after take-off is remote. However the heavier weight represents the more severe test and would be accepted for the analysis.

2.4.3 Impingement Calculations

The wing and horizontal stabilizer will be operating at higher angles of attack when the aircraft is in a holding situation. This difference must be considered in calculating droplet impingement on the surfaces. The angles of attack can be determined from the lift curve for the wing and will be the same at 2,000 feet and at 7,000 feet when equivalent airspeeds are the same. Calculations for the wing were based upon data for the Joukowski 0015 wing as presented in figure 2-11 for the wing at a 4 degree angle of attack. This angle was selected after determining that the USA 35B airfoil was operating at an angle of 2.71 degrees as indicated by the following calculations:

Coefficient of Lift

$$C_L = \frac{W}{q\,A} = \frac{4800}{(39.98)(207)} = 0.580 \qquad (2\text{-}3)$$

Angle of Attack

$$\alpha = \frac{(C_L - .387)}{.0713} = 2.71^\circ \qquad (2\text{-}4)$$

The angle of incidence of the horizontal stabilizer is fixed on the Generic Model A Aircraft with respect to the aircraft and the wing. The angle is two degrees more than the angle of the wing, but the angle of airflow over the stabilizer is also affected by wing down-wash. As a result of these considerations, the angle of attack for the stabilizer was determined to be 4° for the holding operation. Calculations to support this choice are not presented in this analysis but would be required for FAA Certification purposes.

Data were available for the NACA 0012 airfoil used for the horizontal and vertical stabilizers. Calculations for the horizontal stabilizer and vertical fin were based upon the collection efficiency of an NACA 0012 airfoil as presented in Volume 1 of this handbook. Zero angle of attack was used for the vertical fin. Performance data for the airfoil are shown in figure 2-12.

The projected airfoil thickness, h/C, was determined to be 0.13 for the stabilizer, 0.16 for the wing, and .12 for the vertical fin. The following calculations are made with respect to droplet impingement at the 2,000 foot altitude:

PARAMETER*	WING	HORIZ. STAB.	VERT. FIN
Droplet Reynolds Number, R_e	90.8	90.8	90.08
Droplet Range Ratio	.370	.370	.370
Average Chord Length, feet	5.583	3.08	4.37
" " " , inches	67	37	52.4
Inertia Parameter, K	.0537	.0973	.0686
Modified Inertia Parameter, K_o	.0199	.0360	.0254
Collection Efficiency, E_M	0.12	0.18	0.14
Maximum Efficiency, β	0.60	0.53	
Impingement Limits			
Upper Surface, h/C	0.01	0.01	0.025
Upper surface, inches	0.67	0.37	1.31
Lower Surface, h/C	0.04	0.10	0.025
Lower Surface, inches	2.68	3.70	1.31

Similar calculations for the 7,000 foot holding altitude produced the following estimates of impingement:

PARAMETER	WING STAB.	HORIZ. FIN.	VERT.
Modified Inertia Parameter, K_o	.0207	.0375	.0264
Collection Efficiency, E_M	0.12	0.19	0.14
Maximum Efficiency, β		0.61	0.56
Impingement Limits			
upper Surface, h/C	0.01	0.01	0.028
Upper Surface, h/c	.04	0.10	0.028
Lower Surface, inches	2.68	3.70	1.47

2.4.4 Estimates of Ice Accretion

Figure 2-10 presents calculations of ice formation shape as a function of true air speed and ambient air temperature for icing conditions at 5,000 feet and a liquid water content of 0.5 grams per cubic meter. The speeds and temperatures associated with the holding operation for Generic Model A airplane fall within the area representing the double ridge glaze ice formations, and specific calculations are not necessary. In these conditions, the formations occurring on smaller components are known to grow in width as the formations develop.

The water catch on the wings, horizontal stabilizer, and vertical fin can now be determined for the holding situation:

For 2,000 feet -

Wing

$$W_{lb} = 0.329(U_o)(LWC)\frac{h}{c}x\ C\ E_M\ \frac{45}{60}$$

$$= (0.329)(125)(0.5)(0.16)(5.583)(0.12)(.75)$$

$$= (2.204)(.75) = 1.653 \text{ lb/ft span}$$

Horizontal Stabilizer

$$W_{lb} = (0.329)(125)(0.5)(0.13)(3.08)(0.18)(.75)$$

$$= (1.482)(.75) = 1.111 \text{ lb/ft- span}$$

Vertical Fin

$$W_{lb} = (0.329)(125)(0.5)(0.12)(4.37)(0.14)(.75)$$

$$= (1.510)(.75) = 1.325 \text{ lb/ft-span}$$

For 7,000 feet -

Wing $W_{lb} = (0.329)(136)(0.5)(0.16)(5.583)(0.12)(.75)$

$= 1.80$ lb/ft-span

Horizontal Stabilizer $W_{lb} = (0.329)(136)(0.5)(0.13)(3.08)(0.19)(.75)$

$= 1.28$ lb/ft-span

Vertical Fin $W_{lb} = (0.329)(136)(0.5)(0.12)(4.37)(0.14)(.75)$

$= 1.23$ lb/ft-span

The significant difference between the 2,000 and 7,000 foot holding situations is the higher true airspeed at the higher altitude. The higher speed results in a longer flight distance in the cloud and a proportionally greater accumulation of water impingement. The performance-critical holding situation for the Generic Model A aircraft is associated with the 7,000 foot altitude. Holding at even higher altitudes at the same equivalent airspeed would produce proportionally greater accumulations, and the possibility that holding at higher altitudes might be limited to less than 45 minutes will be considered in the analysis and in the test program.

The cross-sectional area and the average depth of the resulting accumulations can now be determined for 7,000 ft. (water at 62.5 lb/ft^3 = 0.03617 lb/in^3) The average depth of water is equal to its volume divided by its area.

Component	Area, Square Inches	Pounds H_2O	Cubic Inches	Depth-inches* H_2O	Depth-inches* Ice	Cross* Section
Wing	0.67+2.68 x 12 = 40.2	1.80	49.8	1.24	1.46	4.89
Hor. Stab.	0.37+3.70 x 12 = 48.84	1.28	35.4	0.72	0.88	3.58
Fin	1.47+1.47 x 12 = 35.28	1.23	34.0	0.96	1.23	3.62

*The density of ice depends upon formation type and is 0.85 for these calculations. The cross section is the chordwise length of the surface covered by ice times the average thickness in inches, $(S_U + S_L) \times \delta_i$.

Estimates based upon the mean volume droplet diameter are satisfactory for many problems but can be misleading when the location of droplet impingement is a consideration. The location of droplet impingement is a consideration with respect to determinations concerning the areas to be covered by boot deicing systems for the Generic Model A airplane. Table 2-4 presents the distribution of water content associated with the given droplet sizes for the "D" distribution. This distribution is widely used for problems associated with the larger droplet diameters. Calculation of the new Reynolds Numbers, Droplet Range Ratios, and Inertia Parameters can be simplified by observing that R_e and K for each holding altitude are different entirely because of droplet diameter. The product of the droplet diameter ratio times R_e, and the square of the ratio times K produces the new numbers.

The following calculations show the droplet distribution effect for the wing as a result of the holding problem:

						Volume Water		Area		Depth Ice
D_d	K_o	E_M	S_U	S_L	S_U+S_L	lbs	Cubic In.	Inches^2	δ_i	Total
6.8	.0031	x	x	x	x					
11.4	.0065	.0035	x	.670	.67	.178	4.9	8.04	.717	2.037
15.6	.0111	.0070	x	1.34	1.34	.356	9.8	16.08	.717	1.320
22.0	.0199	.0120	.67	2.68	3.35	.534	14.8	40.02	.433	0.603
30.1	.0333	.0165	.87	4.49	5.36	.356	9.8	64.32	.152	0.170
38.3	.0471	.2100	1.47	5.56	7.03	.178	4.9	84.40	.013	0.018
48.8	.0715	.3000	2.14	7.03	9.17	.089	2.5	110.00	.005	0.005
						Σ1.691	46.7			Σ2.037

x - Indicates value approximately equal to zero. Exact value is not available in data source for this value of K_o.

The calculated average depth was 1.46 inches of ice on the wing when the mean volume diameter was used for the estimates. Also, the formation covered only 0.67 inches on the upper surface and 2.68 inches on the lower surface. Use of the droplet size distribution for additional calculations reveals a different perspective. The smaller droplets impinge upon surface areas nearer the leading edge of the wing, and the total depth of ice at the leading edge would be 2.037 inches. Also, actual depths are greater than the average near the stagnation area for every droplet size and less as the limits of impingement are approached. The larger droplets distribute the ice over a larger area and the depths are small, even for the 45 minute holding period. Droplet diameters exceeding 38.3 microns produce ice formations that are less than .018 inches thick at locations aft of 1.47 inches on the upper surface and 5.56 inches along the lower surface. The impingement area for the larger 48.8 micron droplets extends aft as far as 2.14 inches on the upper surface and 7.03 inches on the lower surface.

Similar calculations should be made for the horizontal stabilizer, vertical fin, and for other leading edge surfaces.

V.2.5 THE ICING PROBLEM FOR CLIMB SITUATIONS

2.5.1 Primary Requirements

Advisory Circular AC 23.1419-1 includes guidance in paragraphs 10.d.(1) and 10.d.(1)(i) that is specifically applicable to the climb problem. Paragraph 10.d concerns performance and handling qualities under the subject of Flight Tests. The paragraph indicates that airplane performance and handling qualities are degraded in various ways depending upon the type, shape, size, and location of ice accumulations and that it is difficult to establish a standard method for demonstrating adequate performance and handling qualities; however, certain minimum tests are suggested to demonstrate that the airplane does not have any unsafe features or characteristics to prevent it from operating safely in the FAR Part 25, appendix C, icing envelope.

Performance losses are normally demonstrated in icing conditions only for the all-engine operating condition, and climb performance losses are established either by flight tests or by a conservative analysis acceptable to the FAA certifying office. The artificial icing shapes used for the tests are the performance-critical shapes found under the operating conditions under which such performance is expected. The Advisory Circular guidance also indicates that climb performance losses for the FAR Part 23.65 configuration for takeoff are not normally appropriate since the airplane should not be departing with residual ice on the airplane; however, climb performance with anti-ice/de-ice systems operating must be determined since that equipment could be utilized for takeoff into an icing environment.

2.5.2 Operating Problem

Table 2-9 presents flight operating data for the performance critical climb-cruise-climb operating problem for the Generic Model A aircraft. For this problem, it was assumed that the aircraft would encounter FAR 25 Continuous Maximum Icing Conditions at 2,500 feet during climb to a planned 7,000 foot cruising altitude and that icing would continue after level-off. A second climb would begin after about 3 minutes when permission to climb to 11,000 feet would have been obtained from Air Traffic Control. The top of the icing layer was assumed to be at 9,000 feet.

The thickness of the icing layer for the calculations is 6,500 feet. The air temperatures selected for the problem are approximately those associated with the most probable icing condition temperature for the various altitudes. This choice is arbitrary since a temperature profile for such a problem has not been established for design purposes. The climb operation would be performed at an equivalent airspeed of 105 MPH. Rates of climb in clear air for this problem are shown to vary from 1450 feet per minute at 2,500 feet to 1,100 feet per minute at 7,000 feet in the first climb segment. The pilot would be expected to maintain the same airspeeds during climb after icing is encountered, but rates of climb would be reduced due to the effects of ice formations. A distance of 6.56 miles would normally be traveled during the climb. This distance would increase as a result of ice formations and any reduced rates of climb.

The true airspeed is normally increased after level-off at 7,000 feet to 205 MPH and the aircraft would travel an additional distance of 10.01 miles in the 2.93 minutes that elapse before a decision is made and approved to continue the climb. An additional distance of 3.78 miles would normally be traveled during the 1.94 minutes required to climb to the 9,000 foot level at rates of climb that vary from 1100 feet per minute at 7,000 feet to 960 feet per minute at 9,000 feet and to 830 feet per minute at 11,000 feet.

2.5.3 Impingement Calculations

Impingement calculations for the first segment climb are shown in table 2-10. The calculations are based upon an average temperature of 19°F, 0.5 gr/m^3, and an average altitude of 5,000 feet. The angle of attack during the climb is 6.1° and is associated with data for a Joukowski airfoil at 8°. This

substitution is arbitrary and would require justification if it were to be used in an FAA certification problem.

The "D" type distribution of droplets is assumed for the climb to 7,000 feet, and calculations are made separately for each of the seven class intervals used for the distribution. The impingement area for the smaller 6.2 micron droplet is shown to be limited to 0.67 inches of the lower surface near the leading edge. The impingement area for the 20 micron droplets extends aft along 0.67 inches of the upper surface and 3.68 inches of the lower surface. The impingement area for the larger 44.4 micron droplets includes 1.0 inches of the upper surface and 8.04 inches of the lower surface.

2.5.4 Estimates of Ice Accretion

The total accumulation of ice during the first segment climb operation is shown to be 0.0626 inches at the wing leading edge. This value may be compared to 0.24 inches of ice that would have been measured by an icing rate meter; however, the water droplets would not freeze on impact at the leading edge in these conditions, and a double ridge type formation of mixed rime and clear ice would be developing. The shape, location, and dimensions of the resulting double ridge ice formation are empirical determinations based upon engineering judgment with supporting photographs of formations on similar components in similar conditions. The FAA provides assistance with respect to this matter, and the determination must be acceptable to the FAA. The formation assumed to be developing on the Generic Model A Airplane at the end of the first climb segment has the upper ridge located about one half inch aft of the leading edge on the upper surface with a second ridge located about one inch aft of the leading edge the lower surface. The maximum thickness of the two ridges is assumed to be about 0.1 inches.

The amount of ice on the wings as a result of the climb to 7,000 feet in design icing conditions would not alarm experienced pilots, and the developing ridges might not be noticeable. The amount of water contained in the formations would be the amount shown in the table in pounds per hour per foot span, times the climb time, divided by 60, and is shown to be 0.1151 pounds per foot span.

Impingement calculations for the accumulation of ice during the 2.93 minutes of cruise at 7,000 feet after level-off are shown in table 2-11. The calculations indicate that an additional 0.2264 pounds of ice per foot span would accumulate during this period to bring the total accumulation to 0.3415 pounds. The additional depth of ice if the water had frozen on impact at the wing leading edge is shown to be 0.1253 inches bringing the total to 0.1879 inches. The double ridge formation would be apparent to the pilot by this time and is estimated to be no more than 0.4 inches thick on the lower surface and 0.3 inches on the upper surface. For comparison purposes, an icing rate meter would have measured about 0.62 inches of ice in the 16.57 miles traveled before the second climb segment is started.

The frontal area of ice formations on small components, such as an antenna mount or a wing strut, tend to increase as the formations grow forward into the airstream when the double ridge formation occurs on wing surfaces. This condition produces the greatest increases in drag and is

assumed for the climb-cruise-climb problem. The dimensions of the resulting ice formation may be determined empirically from experience and from photographs of formations on similar surfaces. The formation on the antenna mount would be a concave structure facing into the wind and is assumed to have a frontal area that is twice the frontal area of the antenna.

The ice formations that occur on the leading edge of circular components, such as an aircraft nose or radome when the double ridge formation occurs on the wings, are a ridge that encircles the component. The location and dimensions of the ridge are also determined empirically and are based upon photographs and experience with respect to similar components in similar conditions. The formation on the nose of the Generic Model A aircraft for the climb-cruise-climb operating problems is assumed to be located about 2 inches aft of the leading edge and to be about 0.4 inches thick at that location.

V.2.6 WINDSHIELD ICE PROTECTION

2.6.1 Primary Requirements

FAR 23.775, subparagraphs (b) (3), and (d), define the principle icing related regulatory requirements pertaining to the windshields and windows on the Generic Model A airplane. The first of these requirements indicates that the design of windshields, windows, and canopies in pressurized airplanes must be based on factors peculiar to high altitude operations, including the effects of temperatures and temperature gradients. The second, as stated in subparagraph (d), indicates that the windshield and side windows must have a luminous transmittance value of not less than 70%.

Appendix 1 of AC 23.1419-1 includes a check list of the various items that should be examined for their effect on safety when operating in icing conditions. Paragraph A indicates that the light transmittance should be measured perpendicular to the surface with the windshield cleared of ice. The appendix also indicates that the capability of the cabin defogging system to clear side windows for observation of boot ice protection system operation and ice accumulations should be evaluated.

Advisory Circular AC 20-73, paragraph 21 d, indicates that the surfaces should be protected to provide visibility during the most severe icing conditions and that although these surfaces are generally protected by electrical resistance systems because of the small areas involved, there is a need to require duplication to maintain ice-free operation in all icing conditions.

FAR 25.773 contains additional statements of requirements for windshields. Conformity with this FAR means that the airplane must have a means to maintain a clear portion of the windshield sufficient for both pilots to have a sufficiently extensive view along the flight path in normal flight attitudes, and also that the system must be designed to function, without continuous attention of the crew. Chapter III, Section 2.0, paragraph 2.3.2 of this handbook includes a discussion of windshield anti-icing systems.

Military specifications for windshield ice protection systems may also be of interest for some design considerations and are discussed in Section 2.0, Chapter VI, Volume III of this handbook. The

military specifications also define requirements for windshield spray equipment and windshield areas to be protected.

2.6.2 Operating Problems

Visibility is reduced to a matter of feet in severe icing conditions, except for freezing rain and drizzle, and the wing tips become almost invisible when large numbers of the smaller droplets are present; nevertheless, experience proves that visibility is needed at all times and that it becomes vital during landing.

The performance-critical operational situation for hot air anti-icing systems for windshields occurs at the colder temperatures in combination with the larger droplet sizes. More heat is required in the colder conditions, and the larger droplets are associated with the greater amounts of water catch.

The performance-critical operational situation for the Generic Model A aircraft was determined to be at 7,000 feet during cruise at 205 MPH. The meteorological conditions selected for this analysis involve 0°F ambient air temperatures, 20 micron median volume droplet diameters, and a liquid water contents of 0.25 g/m^3. These are the conditions used in reference 1 where they were referred to as a conventional design point. An equally acceptable design condition would be -4°F, 20 microns, and 0.2 g/m^3. Both conditions represent exposures in continuous maximum icing conditions.

Running wet systems allow impinging water to run back where it may freeze around the edges of the windshield. The result can be a high drag ridge type formation of ice around the windshield. Drag computations of ice formation effects should consider this effect.

2.6.3 Impingement Calculations

The following calculations illustrate the method of determining water catch for the windshield. Water catch can be found by treating the windshield as a rectangular half-body and using the method of NACA TN 3658, reference 7. Parameters:

Altitude	7,000 ft.
True Airspeed	205 MPH., V = 300 ft/sec
Ambient Air Temperature	0°F
Liquid Water Content	0.25 g/m^3
Air Density	0.002070 $slugs/ft^3$
Air Viscosity	0.328×10^{-6}
Windshield Area	7.5 ft^2
Windshield Height	0.875 ft
Projected Windshield Area	3.5 ft^2
Windshield Width	8.57 ft

The Droplet Reynolds Number

$$R_e = \frac{(\text{Diameter})(\text{Air Density})(\text{True Speed})}{\text{Viscosity}} \qquad (2\text{-}7)$$

$$= \frac{(20)(4.81 \times 10^{-6})(0.00207)(205)}{0.328 \times 10^{-6}}$$

$$= 124$$

The Droplet Range Ratio for this Reynolds Number is 0.33

The Inertia Parameter

$$K = \frac{(\text{Coefficient})(\text{Droplet Diameter}^2)(\text{True Speed})}{(\text{Viscosity})(\text{Projected Height})} \qquad (2\text{-}8)$$

$$K = \frac{(1.705 \times 10^{-12})(20^2)(205 \frac{\text{ft}}{\text{sec}})}{(0.328 \times 10^{-6} \frac{\text{slugs}}{\text{ft-sec}})(0.875)}$$

$$K = 0.487$$

$$K_o = 0.487 \times .033 = 0.16 \qquad (2\text{-}9)$$

A collection efficiency of $E_M = 0.07$ can be found from the curve for a semi-infinite rectangle on figure 2-21 of Chapter I of this handbook.

The weight rate of water interception, lb/hr-ft-span

$$W_M = (0.329)(E_M)(h)(LWC)(U_o) \qquad (2\text{-}10)$$

$$= (0.329)(0.07)(0.875)(0.25)(205) = 1.033 \frac{\text{lb}}{\text{hr-ft-span}}$$

$$W_{lb} = 1.033 \times 8.57 = 8.85 = \frac{\text{lb}}{\text{hr}} \quad \text{total impingement}$$

The weight rate of water interception, lb/hr-ft^2 (Divide total catch by area)

$$M_W = \frac{8.85 \frac{\text{lb}}{\text{hr}}}{7.5 \text{ ft}_2} = 1.18 \frac{\text{lb}}{\text{hr-ft}^2}$$

2.6.4 Fluid Anti-Icing Calculations

The mixture of impinging water and 50 per cent ethylene glycol anti-icing fluid that will depress the freezing point to 0°F can be determined from figure 2-13, which was obtained from reference 1. The figure shows a value of 35% for the 0°F temperature condition.

The flow rate of anti-icing fluid necessary to prevent icing can be found from the following equation:

$$W_F = \frac{G\ M_W}{100 - G} \quad \frac{lb}{hr\text{-}ft^2} \qquad (2\text{-}14)$$

$$= \frac{(35)(1.18)}{100 - 35} = 0.6354 \quad \frac{lb}{hr\text{-}ft^2} \quad \text{of anti-icing fluid}$$

Where G is the percent freezing point depressant by weight (0 to 100).

The actual amount of fluid needed to accomplish the desired anti-icing objective is greater than the amounts indicated because of distribution efficiency. The actual amounts will be 1.2 to 1.5 times greater than the calculated amounts for even the well designed system, and the amounts may be 2 times greater for typical systems. The amount will be doubled for this problem.

For two 18 inch square sections of windshield, the total fluid required is then determined to be

$$\Sigma W_{Flb} = 2(0.6354)(2)\left\{\frac{18}{12}\right\}^2 = 5.72 \text{ pounds per hour}$$

2.6.5 Electric Anti-Icing Calculations

The convective heat transfer coefficient must be determined to complete calculations for windshield electric anti-icing system requirements. The coefficient can be found by assuming a flat plate surface and by using the following equation from SAE 24, reference 8.

$$h_c = 0.51 \frac{t_f^{0.8}\ (1.467\ U\ 32.2\ \rho)^{0.8}}{S_U^{0.2}} \qquad (2\text{-}15)$$

$$= 0.51 \frac{(465)^{0.8}\ (1.467\ (7.05)\ 32.2\ .00207))^{0.8}}{(8.0)^{0.2}}$$

$$= 23.15 \frac{BTU}{hr\text{-}ft^2\text{-}F}$$

where t_f is the boundary layer temperature in degrees Rankin, and where S_U in this case is the distance in feet from the airplane nose for an inclined windshield. (This distance is measured from the base of the windshield when the windshields are nearly vertical).

reference 9 is an NACA report that presents a graphical method for solving the heat transfer problem for the windshield in terms of stream conditions.
The method reduces the problem to the following equation:

$$Q = h_c (r_1 - r_2 + r_3 - r_4 + r_5) \text{ (BTU/hr.-sq. ft.)} \qquad (2\text{-}16)$$

where the terms within the brackets represent temperatures in a series of heat transfer equations.

Figure 2-14 is a reduced copy of the figure used in the NACA report, reference 9, to enable problem solution. A temperature of 35°F is selected as a surface temperature that would prevent freezing on the heated portions of the windshield surface. With this assumption and the preceding determinations of the heat transfer coefficient, the five temperatures for use in the equation are determined to be as follows:

$$Q = h_c \times (T_1 - T_2 + T_3 - T_4 + T_5) \qquad (2\text{-}16)$$

$$Q = 23.15\ (36.3 - 7 + 24.5 - 4.5 + 0)$$

$$= 1141\ \frac{BTU}{hr\text{-}ft^2} = 0.6678\ \frac{BTU}{hr\text{-}sq.in.}$$

$$= 3.413\ (0.6678) = 2.098\ \frac{watts}{sq\text{-}in}$$

where the energy required for the heated area of 648 square inches would be

$$\Sigma Q = 2.098 \times \text{heated area} = 2.098 \times 648 = 1.359\ kw$$

For comparison purposes, figure 2-15 shows a range of power density in watts per square inch as a function of ambient temperature for vertical and nearly vertical windshields for the 205 MPH cruise problem at 7,000 feet. The power density variation with temperature is shown to increase substantially for the colder temperatures.

V.2.7 PROPELLER ICE PROTECTION SYSTEM

2.7.1 Primary Requirements

The propellers on the Generic Model A aircraft are constant speed, full feathering units. Each propeller has two blades. Propeller diameter is 74 inches and the blade chord is 6 inches. The spinner has a 6 inch radius leaving a 31 inch length of blade to provide the thrust. The blade shape is an NACA 0012 (maximum thickness is 12% of the chord length) type airfoil. Propeller RPM is 2575 for the 250 rated horsepower operating condition at sea level. RPM varies from 2200 to 2400 for most flight operating problems.

The basic requirement for propeller ice protection is defined in FAR 23.929. The FAR indicates that propellers and other components of complete engine installations, except for wooden propellers, must be protected against the accumulation of ice as necessary to enable satisfactory functioning without appreciable loss of power when operated in the icing conditions for which certification is requested.

Advisory Circular AC 20-73, paragraph 33.b., indicates that the engine should be capable of operating acceptably in conditions of ground fog in addition to the meteorological conditions of

Appendix C of FAR Part 25, and over the entire engine operating envelope. The paragraph also indicates that the following data points for testing have been considered a successful means of showing compliance if used in conjunction with perfor ance-critical conditions:

Icing Condition	1	2	3
Liquid Water Content (g/m^3)	2.0	1.0	2.0
Atmospheric Temperature, (°F)	23.0	-4.0	29.0
Mean Effective Droplet Diameter, (microns)	25.0	15.0	40.0

Advisory Circular AC 20-73, paragraph 14.c., indicates that the various engine operational modes have an effect on the collection of ice on propeller surfaces and that the greatest quantity normally collects on the spinner and inner radius of the propeller. The paragraph also indicates that propeller areas on which ice may accumulate and be ingested into an engine compressor area should be anti-iced, rather than de-iced, to reduce the probability of ice being shed into the engine.

Ice formations on propellers do not necessarily produce an immediately serious hazard to continued flight as does an engine failure, and propeller protection systems that do not meet the meteorological standards of AC 20-73, paragraph 33.b., for engines may be acceptable. Paragraphs 22.a and 22.b of the Advisory Circular provide the needed additional interpretation of the requirements by indicating that the engine ice protection systems should be designed to cope with the most severe meteorological conditions occurring simultaneously with the most severe engine and/or propeller operational conditions. Also, it is stated that propeller operation would be considered unsafe if an accumulation of ice caused a serious loss of thrust horsepower, caused an unsafe engine condition to develop, caused damage to adjacent structure when detached by centrifugal force, caused vibrations which could result in engine or structural failure, or caused any other erratic engine, propeller, or airplane operation. The meteorological requirements for propeller ice protection system design depend to some extent upon the consequences of any resulting propeller ice formations and upon successful demonstration that the consequences are acceptable.

Propeller blade speed at the tip has been a limiting factor on propeller RPM and the longer propellers tend to rotate at slower speeds. Many of the design differences between propellers of the same approximate length are of little practical significance with respect to ice protection system performance, and design similarity may provide an acceptable basis for certification of a propeller ice protection system. Significant differences in blade length or shape preclude use of similarity for certification in other circumstances. Certification of a propeller ice protection system by similarity would include a detailed evaluation of the consequences of any ice formations that break loose from the propeller. A system that is acceptable for one aircraft might not be acceptable for another.

2.7.2 Operating Problem

Ice formations on propellers cause a loss of propeller efficiency. Large pieces of ice breaking loose from the propeller may cause fuselage skin damage or be ingested by the engine on turboprop aircraft, and unsymmetrical shedding of ice may result in propeller inbalance that could become hazardous.

Pilots usually increase engine RPM when icing conditions are encountered. The higher RPM increases the forces needed to break the ice formations loose from the blades and the formations that do break loose are smaller. Also, there is a speed-temperature effect that tends to protect the outer portions of the propeller blades that have the highest rotational speed. Increasing propeller RPM increases the speed-temperature protection effect by a small amount. It also reduces blade angle of attack for the same power setting and causes a favorable effect on droplet impingement.

The propeller icing aerodynamic problem involves the progressive loss of effective power that occurs as ice formations reduce thrust effectiveness and increase propeller rotational drag forces. These losses are particularly important with respect to the performance of aircraft that have little excess power. For this reason, the performance-critical operating conditions for the wings of the Generic Model A aircraft must be included in the evaluation of performance-critical conditions for propeller operation. This is in addition to the requirement to consider propeller ice protection system performance in the engine operating envelop as stated in AC 20-73, paragraph 53.b.

2.7.3 Impingement Calculations

The primary differences between impingement calculations for a wing and a propeller involve component size and speed. For calculation purposes, the propeller is a small airfoil, and its lifting forces act to produce the thrust needed to propel the aircraft through the air. Propeller drag forces resist rotation and require additional engine power. Aircraft forward speed and propeller rotation combine in a way that affect blade angle of attack with respect to air flow as well as airspeed. The resulting velocity, V_r, increases with radial distance along the propeller.

The equation for determining V_r is defined as follows:

$$V_r = [V_t^2 + (2\pi r n_p)^2]^{1/2} \qquad (2\text{-}17)$$

where

V_r = Helical Speed (ft/sec)
V_t = True Aircraft Speed (ft/sec)
r = Propeller Radial distance (ft)
n_p = Propeller Rotational Speed (RPS)

The speed-temperature effect resulting from propeller RPM can be evaluated by calculating the speed for which no ice would form on the propeller. This speed is often referred to as the icing limit. Equations 2-28 and 2-29 in Chapter I of this handbook and computer programs enable easy calculation of the of the critical speed for the occurrence of propeller icing in given operating conditions;

however, graphs are also available for this purpose in reference 10, an Air Weather Service publication on Aircraft Icing, and in reference 1. (The various equations and graphs provide slightly different answers depending upon the assumptions involved in the problem solutions, but the differences have not been considered to be operationally significant.)

Altitude effects on icing limit calculations are substantial, and selection of data from the graphs in reference 1, ADS-4, involves a difficult interpolation involving altitude. The graphs in reference 10 show the critical temperature for the occurrence of aircraft icing on wing leading edges for a complete range of altitudes and air temperatures. Data are presented for given true airspeeds in knots and also according to Mach Number. The values used for this publication were obtained from the AWS publication.

The following calculations illustrate the speed-temperature effect on a propeller rotating at 2400 RPM on an aircraft flying at a true airspeed of 205 MPH (300 ft/sec at 7,000 feet):

Temperature	Speed	Icing Limit Radius		Ice Free
°F	V_r,ft/sec	r, ft	r, in	37-r
24	456	1.36	16.3	20.7
17	608	2.10	25.2	11.8
14	659	2.33	28.0	9.0
8	760	2.78	33.4	3.6
-4	861	3.21	38.5	None

where

1. V_r is the minimum true speed for the speed effect prevention of ice according to reference 10 for the given temperatures.

2. r is the location along the propeller radius where the rotational speed is the icing limit velocity.

3. (37-r) is the ice free area of the blade measured from the propeller tip.

These calculations indicate that ice would form on the propeller spinner and on the propeller out to a radial distance of 25.2 inches in the 17°F icing conditions at 7,000 feet during cruise. The outer 11.8 inches of the blade would be ice free due to the speed effect. Also, ice would form on all of the blade in the -4°F icing conditions, and 20.7 inches of the propeller blade leading edge surface would be free of ice when ambient air temperatures are 24°F.

The speed-temperature effect becomes less significant as altitude increases; also, there is a liquid water content effect on the critical speed-temperature condition for leading edge ice as well as on ice formation shape and runback ice. These effects are mainly of consequence for components that are not heated and will not be considered in this analysis.

Some analysts have based their estimates upon calculations for the midpoint or the point along the blade radius that is the icing limit for the temperature conditions being considered Significant

errors can result from that approach because of the variation of tangential speed along the blade.

For this example it is convenient to divide the propeller into several arbitrary segments to illustrate the effects on rotational speed on the icing limit and on lift and drag forces. The following diagram illustrates the location along the blade of the previously calculated icing limits for given temperatures and the blade segments used for the illustrations:

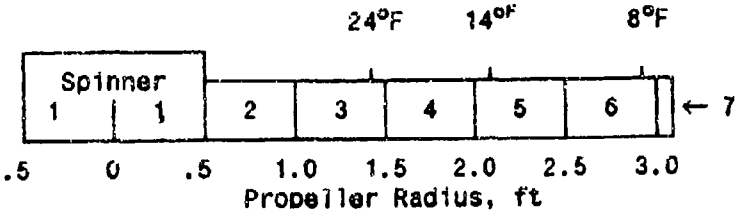

Each blade segment is six inches long and six inches wide, and section 1 is the propeller spinner. Each blade section for this example has an area of 0.25 ft^2 except for the 1 inch tip section which has an area of 0.042 ft^2.

Propeller angle of attack must be known for droplet impingement calculations. It is affected by rotational speed as well as aircraft forward speed and is measured with respect to the helical speed vector which is the vector combination of the forward and rotational velocities. Angle of attack is assumed to be constant with respect to location along the blade radius for this analysis.

Propeller blade angle of attack can be estimated through use of the lift, drag, and thrust equations for the aircraft and propeller. Aircraft thrust is equal to aircraft drag, and the thrust is a result of lift type forces generated by blade angle of attack and by the rotational speed of the propeller blade.

The radial speed at the mid point of each section along the blade is used to obtain the following estimates of the lifting forces (forward thrust) developed by each blade section:

Calculations for One Blade 2

Section	r	V_r	A	q	qA
1	Spinner				
2	0.75	354	.25	125	31.2
3	1.25	434	.25	188	47.0
4	1.75	532	.25	282	70.5
5	2.25	640	.25	409	102.2
6	2.75	743	.25	551	137.7
7	3.08	831	.04	689	27.6
			1.29		ΣA_p = 416.2 x 4=1664.8 lbs

For Generic Model A aircraft at 205 MPH at 7,000 feet and 17°F

$$C_L = \frac{W}{qS} = \frac{4800}{(90.24)(207)} = .2570$$

$$D = C_D(qS) = [.046C_L^2 + .03]\ qS = 617 \text{ pounds} = L_p \qquad (2\text{-}17)$$

And for the propeller

$$C_{Lp} = \frac{L_p}{\Sigma q_p A_p} = \frac{D}{\Sigma q_p A_p} = \frac{617}{1664.8} = .3706$$

The lift curve for an NACA 0012 airfoil, figure 2-12, shows an angle of attack of approximately 5° for a 0.37 coefficient of lift. At this angle of attack the propeller is shown to be operating at its maximum L/D ratio of about 23.

Droplet Reynolds numbers for the propeller are different from those for the wing because of the velocity factor. Chord length as well as velocity are different for the droplet Inertia Parameter calculations. A 20 micron MVD will be used to illustrate a manual method for evaluating the droplet impingement characteristics of the propeller and the variation of droplet impingement along the propeller blade.

IMPINGEMENT CALCULATIONS FOR 20 MICRON, 17°F, 7,000 FT. AND 2400 RPM

Sect.	V_r	R_e	K	λ/λ_s	K_o	E_M	β	S_U %C	S_U in	S_L %C	S_L in	$W_p/2$
2	354	136	0.9701	.315	.3056	.64	.90	.052	.31	.28	1.68	.82
3	434	167	1.1893	.290	.3449	.69	.90	.054	.32	.30	1.80	1.08
4	532	205	1.4579	.270	.3936	.72	.91	.059	.35	.32	1.90	1.38
5	640	247	1.7538	.250	.4384	.74	.91	.064	.38	.34	2.00	1.70
6	743	287	2.0361	.235	.4785	.75	.92	.070	.42	.36	2.10	2.02
7	831	320	2.2773	.230	.5238	.76	.92	.076	.46	.37	2.20	0.38
												7.38
Wing	300	115.7	.0736	.335	.02466	.15			1.34		2.68	3.97

Where W_p is the rate of water impingement per unit section in pounds per hour.

$$W_p = 0.329(V_r/1.467)\left(\frac{h}{C}\right)C(LWC)(E_M) \quad \frac{lb}{ft\text{-}span\text{-}hr}$$

$\frac{W_p}{2}$ = Pounds per half foot section per hour

$\frac{h}{C}$ = 0.14 (From Volume I, figure 2-4)

C = 6 inches = 0.5 ft

$LWC = 0.46 \frac{g}{m^3}$

The collection efficiency parameter, E_M, is substantially greater for the propeller than for the wing due to its small size and relatively greater speed. E_M was 15% for the wing as compared to 64% to 76% for the propeller.

The droplet impingement area is shown to include 0.31 to 0.37 inches on the upper (forward) surface and 1.68 to 2.20 inches on the lower surface. Water impingement is shown to be 7.38 pounds per hour on each blade; however, at 17°F most of blade section 5 and all of blade section 6 would be ice free.

Similar calculations should be made for the conditions specified in Advisory Circular AC 20-73. The following calculations are made for the midpoint of section 4, where the propeller radius is 1.75 feet and the rotational speed is 532 ft/sec or 363 MPH. The calculations define the results of exposure in the three conditions specified in AC 20-73 and are compared with the exposure to the same panel in the performance-critical condition for the wing protection system.

PROPELLER PANEL SECTION 4 AT r = 1.75 ft

								S_U		S_L		
Temp.	D_d	R_e	K	λ/λ_s	K_o	E_M	β	%C	in	%C	in	W_p
17°F	20	205	1.4579	.270	.3936	.72	.91	.059	.35	.32	1.90	1,38
23°F	25	250	2.2600	.25	.5650	.75	.93	.088	.53	.39	2.30	6.26
-4°F	15	88	0.8564	.37	.3169	.64	.87	.058	.35	.29	1.74	2.67
29°F	40	390	5.6799	.201	.1360	.92	.95	.105	.63	.43	2.58	7.68

The impingement area increased from 0.35 inches to 0.63 inches on the upper (forward) blade surface for the 40 micron droplet diameter condition and from 1.90 inches to 2.58 inches on the lower (back) surface. The total wrap-around impingement area for the 40 micron condition is 0.63 + 2.58 + 3.21 inches for the 40 micron droplet size condition. The higher liquid water contents associated with the warmer temperatures, 23°F and 29°F, would not produce ice formations on blade segment 4 due to the propeller speed-temperature effect on the icing limit

2.7.4 Thermal Analyses

Electric cyclic deicing is the typical choice for protecting propellers, and an exact thermal analyses is extremely complex due to transient conditions. Experience has been a significant factor in system design determinations. Each propeller blade on the Generic Model A aircraft has two 15 inch panels. The heat on time for each panel is 30 seconds. (Cycle times are affected by the need to maintain a constant electrical power load, and some system designs use 20 seconds.) Similar panels on each blade are cycled simultaneously; ie, the inboard panels then the outboard panels. The heat off time for each panel is 90 seconds, and a complete cycle takes two minutes. Power density is 6 watts per square inch.

The impingement calculations for the 20 micron droplet condition indicated that ice would form on an unheated blade on about 0.38 inches of the upper (forward) surface of the blade and about 2.0 inches on the lower surface. Calculations for the larger droplet diameter conditions indicated that a four inch wrap-around heater with one inch on the upper surface and three inches on the lower surface would provide protection for the areas subject to droplet impingement in the various design conditions. The total heated area for each heater panel is 4 x 15 = 60 square inches. With a power density of 6 watts per square inch, each panel would use 360 watts. Two panels on each propeller are operated simultaneously for a total of 720 watts per propeller or 1.44 kilowatts for the two propellers.

Shorter propeller deicers are used on some aircraft, and the wrap-around dimension has been reduced to about 2.5 inches in some instances; also, progressive heating elements have been used which provide more heat at the root of the prop blade and progressively less heat at the outboard locations. Another alternative involves the use of different wrap-around lengths for the various panels while keeping the same total area for each panel.

More than one performance-critical operating condition can exist for propeller ice protection systems. There are four such conditions for the Generic Model A aircraft. These are the three conditions specified in AC 20-73 plus the condition determined for aircraft structure for which power requirements become so critical.

Flight and/or wind tunnel testing would be required to demonstrate the adequacy of the protection system.

V.2.8 ENGINE INDUCTION SYSTEM

2.8.1 Primary Requirements

Primary regulatory requirements for the induction of air and fuel into the engines of Part 23 aircraft are defined in the following FAR references:

FAR Part 23.1091 Air induction.

FAR Part 23.1103 Induction system ducts.

FAR Part 23.1093 Induction system icing protection.

FAR Part 23.1105 Induction system screens.

FAR Part 33.68 Induction system icing.

The following additional requirements are applicable to aircraft using carburetors: (Generic Model A aircraft uses fuel injection systems.)

FAR 23.1095 Carburetor deicing fluid flow rate.

FAR 23.1097 Carburetor deicing fluid system capacity.

FAR 23.1099 Carburetor deicing fluid system detail design.

FAR 23.1101 Carburetor air preheater design.

Significant requirements are also defined in AC 20-73, paragraphs 14, 21, 22, and 33, where it is stated that the prime factors to be evaluated are the quantity and temperature of available air for the engine, and the airflow through the engine during the most critical operational mode. The temperature and quantity of airflow available from the engines to the various systems must also be evaluated. It is stated that the engine operational factors to be considered in determining the most severe conditions are directly related to aircraft operational procedures because changes in airplane speed and attitude are usually accompanied by changes in engine power.

Engine inlets, inlet air screens, and inlet lips are considered to be more critical with respect to accumulations of ice on surfaces exposed to engine airflow than other surfaces such as a wing leading edge. The possibility that ice may form on components within the inlet and at locations enroute to the engine in some operational modes must also be evaluated. These evaluations should include consideration of the reductions of inlet static pressure and temperature that occur in some operating modes and the possibility that the reduction in temperature might be enough to cause ice to form in the inlet.

The interaction between the various controls affecting engine operation should be analyzed to insure that control system response to icing conditions does not produce an unsafe condition. This is particularly important with respect to controls pertaining to the quantity of fuel and air provided to the engine. For example, a control system that adds fuel to increase power when airflow is reduced as a consequence of ice formations would be unacceptable.

The air induction system is required to supply the air required by the engine under the operating conditions for which certification is requested, and each reciprocating engine installation must have at least two separate air intake sources. Primary air intakes may be located within the cowling, but alternate air intakes must be located in a sheltered position and may not result in an excessive loss of power.

The regulatory requirements are quite specific and extensive and are not repeated in this discussion. In addition to the FAR Part 25, Appendix C design icing envelops, FAR Part 23 aircraft engines are required to be able to idle for 30 minutes on the ground without adverse effect, with air bleed available for the engine icing protection system operating in its critical condition when air temperatures are between 15°F and 30°F, liquid water content is not less than 0.3 g/m^3, and mean effective droplet diameters are not less than 20 microns.

2.8.2 Operating Problems

The primary source of air for engines on the Generic Model A aircraft is the ram air that enters the engine through an airscoop located under the engine cowling and behind the propeller. The ram air passes through a duct and through a filter before being inducted into the engine. The airscoop is not equipped with an ice protection system, and resulting ice formations will reduce air flow through the scoop into the duct. A heated source of alternate air is provided to insure an adequate supply of air to the engines in case the normal flow of air is restricted. The door to the supply of alternate air is spring loaded and remains closed during normal operation. The door opens automatically when the flow of ram air is restricted; also, a manual push-pull control located on the pilot's control pedestal opens the door when the control is placed in the full on position. Operating instructions direct the pilot to place the control in the full on position prior to entering known or expected icing conditions.

An air flow sensor in the throttle body uses a venturi system to measure air entering the engine and to regulate fuel flow. The fuel control system includes an inlet fuel screen, a rotary idle valve, and a rotary mixture control valve.

2.8.3 Analyses/Certification Demonstration

Wind tunnel and flight test programs will be used to demonstrate the adequacy of Generic Model A engine operation in icing conditions. The engine is not vulnerable to hazardous damage as a consequence of ice formations breaking loose form the propeller and the propeller spinner, and the source of heated alternate air insures availability of air needed for engine operation. The tests will demonstrate that the door to the supply of alternate air operates properly in all circumstances and also that its operation is not restricted by ice formations if the door is not opened prior to an icing encounter.

Analyses for certification purposes will provide the information needed to demonstrate that the tests cover the full range of meteorological and operational circumstances required for certification. Similarity will be used to demonstrate the adequacy of some components in the engine and engine control systems.

V.2.9 PITOT-STATIC AND STALL WARNING SYSTEM PROTECTION

2.9.1 Primary requirement

Ice would form on the airspeed and stall warning sensors if these devices are not protected, and the resulting loss of airspeed and stall warning indication would produce unacceptable consequences. Ice protection systems for these flight instrument sensors are required. The sensors normally selected for this protection problem are electro-thermal anti-icing systems. A surface temperature evaluation may be used to verify thermal analyses for these systems, and use of similarity analyses for demonstrating adequacy may be possible. Sensor location should be evaluated for the possibility that ice formations on nearby components could indicating accuracy.

Static pressure ports for measurement of pressure altitude, typically located on the fuselage, have not needed protection in most circumstances when the ports are located suitably and are not too near to the nose of the aircraft, as is the case for the Generic Model A aircraft.

2.9.2 Operating problems

The collection efficiency of small components, such as the pitot and stall warning sensors, is very high for small droplets as well as for the large droplets. Nearly all of the water droplets in the path of the sensors will impinge upon the sensors. Therefore, the performance-critical operating situations for these components occur in the conditions that require the greatest amount of heat to provide the needed protection. These conditions occur in the colder icing environments with the higher liquid water contents. Liquid water content in the continuous maximum icing condition at -4°F is 0.21 with 20 micron droplet diameters and 0.30 g/m^3 for the 15 micron droplet diameter condition. The smaller droplet size condition, 15 microns and 0.30 g/m^3 represents the more severe, performance-critical, condition. Liquid water content is 1.95 g/m^3 for the 15 micron droplet condition in the intermittent maximum icing condition for -4°F temperatures.

2.9.3 Impingement Calculations

Water impingement and heat transfer calculations for small components are based upon the weight rate per hour per square foot instead of the actual dimensions of the component when the calculations are used for anti-icing purposes. Equation 10 is used for the calculations and is reduced to the following expression by letting (h/C) x C = 1:

$$M_w = .329\ U_c\ LWC\ E_M \quad (lb/ft^2\text{-}hr)$$

The rate of impingement on the pitot and stall warning sensors may be calculated on the basis of collection efficiencies determined by the usual methods for such components. However, the efficiencies are so high that the E_M values can be assumed to be 100% without causing an unacceptable degree of overprotection. Therefore,

$M_w = .329\ (205)(0.30)(100\%) = 20.2\ lb/ft^2\text{-}hr$ (Continuous Maximum)

and $= .329\ (205)(1.95)(100\%) = 131.5\ lb/ft^2\text{-}hr$ (Intermittent Maximum)

2.9.4 Thermal Analyses

The graphical solutions to the heat transfer problem for the pitot tube can be obtained by the method of reference 9. This method breaks the calculations into the product of the heat transfer coefficient and the sum of five temperatures that are determined graphically from figure 2-14, where

$$Q = h_c \times [r_1 - r_2 + K(r_3 - r_4) + r_5] \qquad (2\text{-}18)$$

and where

Q = Heat transfer (BTU/ft^2-hr)

K = Surface wetness factor assumed to be = 1.0 (Dimensionless)

h_c = Convective heat transfer coefficient (BTU/ft^2-hr-°F)

τ_1 =	Intersection of		M_w/hc	and	$T_s - T_o$	(°F)
τ_2 =	"	"	M_w/h_c	and	V_o	(°F)
τ_3 =	"	"	P_L	and	T_s	(°F)
τ_4 =	"	"	P_o	and	T_o	(°F)
τ_5 =	"	"	P_L	and	P_o	(°F)

and where for the Generic Model A problem

T_s = Surface Temperature = 35°F = 459.7 + 35°F = 494.7°R

T_o = Ambient Temperature = -4°F = 459.7 - 4°F = 455.7°R

P_o = Absolute Static Pressure = 1633/70.73 = 23.09 Inches Hg

P_L = Local Pressure $P_o + q/g$ = 23.09 + 90.24/32.2 = 25.89 Inches

The heat transfer equation for a small cylinder is used for h_c determination

$$h_c = 0.194\ (T_o)^{.49}\ \frac{[g\rho\ V_o]^{.5}}{D^{0.5}}\ \frac{BTU}{ft^2\text{-hr-°F}} \qquad (2\text{-}18)$$

$$= .194(455.7)^{.49}\left[\frac{(.0672)(300)(12)}{0.28}\right]^{.5}$$

$$= 114.5\ \frac{BTU}{ft^2\text{-hr-°F}}$$

$$\frac{M_W}{h_c} = \frac{20.2}{114.5} = 0.176 \text{ for the continuous maximum}$$

and $$= \frac{131.5}{114.5} = 1.148 \text{ for the intermittent maximum}$$

The five temperatures in the heat transfer equation can now be read from figure 14 and the heat transfer can be calculated from equation 2-18 where

$$Q = 0.176\ [46 - 7 + 23 - 24 - 2] = 4129.2\ BTU/ft^2\text{-hr}$$

The heat transfer can be expressed in watts per square inch with the appropriate conversion factors as follows:

$$Q = \frac{4129.2}{\left[\frac{.2932}{144}\right]} = 8.4 \text{ watts per square inch}$$

The area of the pitot tube to be heated includes the probe and the mounting strut back to the points of maximum thickness. The area to be heated on the pitot probe is 10 square inches with 3 square inches on the mount for a total of 13 square inches for the sensor.

The total energy required to anti-ice the pitot tube would be 13 x 8.4 =109.2 watts for the continuous maximum icing condition.

The heat transfer for the intermittent maximum condition is increased because of the effects of the term M_w on the temperature parameters, τ_1 and τ_2. Q is determined to be 7099 BTU/ft^2-hr for the intermittent maximum condition.

and

$$Q = \frac{7099}{\left[\frac{.2931}{144}\right]} = 14.45 \text{ watts per square inch.}$$

The total heat required for the probe in the intermittent maximum condition would be 187.8 watts.

The calculations were based upon the heat transfer coefficient for the tip of the probe, and less heat is required for locations aft of the tip. Analytical consideration of this effect can be accomplished by assuming a flat plate with turbulent flow and by using an appropriate equation; however, the system selected for the Generic Model A aircraft uses approximately 175 watts and is a design used on a previous aircraft. Its performance for certification purposes can be based upon operational experience plus testing, and the primary problem for certification involves the possible effects of the unique location on this particular aircraft.

V.2.10 RADOME ICE PROTECTION

2.10.1 Primary Requirement

The icing certification problem for radomes is primarily a matter of ice formation effects on aircraft drag and the possibility that ice formations may break loose and cause damage to components located aft of the radome. Ice formations can affect forward radar range in some instances, and protection systems for radomes are used when radar system performance in all operating conditions is desired.

2.10.2 Operating Problem

The performance-critical situation for unprotected radomes occurs in connection with the extended encounters that produce the largest formations of ice on the radome. The formations developed in connection with the holding operation and those associated with the extended cruise problem are examples. The performance-critical problem for cruise will be used for this analysis.

Angle of attack does have an effect on the location of ice formations on radomes, but the resulting changes in drag are not nearly as great as those associated with airfoils.

2.10.3 Impingement Calculations

Impingement calculations for radomes and other bodies of revolution are essentially the same as for aircraft wings. The same equations are used for the free stream droplet Reynolds Number and the droplet Range Ratio. The equation for the Inertia Parameter is a little different. The first task is to compare the component with spherical, conical and elliptical shapes and to determine the best match. Component shape is compared in the area of expected droplet impingement and the preferred characteristic length for the inertia parameter is the radius of the semi-minor axis of the shape that makes the best fit. The radius is usually larger than the maximum radius of the component for which the calculations are to be made. Some analysts have used the length of the major axis for these problems, and errors can result in the use of reference information if the axes used for calculation and/or comparison purposes are different.

The radome and forward portion of the aircraft nose for the Generic Model A aircraft are represented for impingement calculation purposes by an ellipse with a semi-major axis radius of 2.0 feet and a fineness ratio of 3. The fineness ratio is determined by dividing the length of major axis, 6.0ft, by the length of the minor axis, 2.0ft. Figures 2-16 and 2-17 present the information needed to estimate droplet impingement and collection efficiency for several bodies of revolution. The curves for an ellipsoid with an A/B ration of 3 were used for the calculations.

2.10.4 Estimates of Ice Accretion

Impingement calculations for the radome are illustrated in table 2-12 for cruise at 7,000 feet in an icing condition with a D distribution, an MVD of 20 microns, a liquid water content of 0.46 g/m^3, and an ambient air temperature of 17°. The calculations are for a one hour period and for a flight distance of 205 miles at a speed of 205 MPH true airspeed. The total catch of water is shown to be equal to 2.908 pounds per square foot for a zero angle of attack. The ice formations vary from 0.36 inches for the 6.2 micron droplets to 11.52 inches for the 44.4 micron droplets. The maximum rate of catch is shown to occur in connection with the 27.4 micron droplets that accounted for 0.931 pounds of the total catch.

The impingement would run back a few inches before it freezes to form a ridge in the shape of a ring around the radome. This distance would need to be determined for an FAA certification analysis. Also, it should be noted that the impingement values were determined on a per square foot basis and that the actual catch should be determined before the calculations could be completed.

V.2.11 MISCELLANEOUS ANALYSES

2.11.1 Ice Shedding

Ice shed from airplane structures located forward of the powerplant may damage or erode engine components and/or the propeller. Fans, compressor blades, inlet screens and ducts, as well as propellers, are examples of powerplant components subject to damage from ice impingement.

Trajectory and impingement analyses cannot adequately predict such damage. Unpredicted ice damage caused by shedding from surfaces not considered in the analyses and ice buildup prior to activation of anti-icing systems have been found to negate the results of such analyses. Flight tests should be conducted for this reason.

2.11.2 Flutter Analysis

A limited flutter investigation as required by paragraph 629 in FARs 23, 25, 27, and 29, and Advisory Circulars 23.629-1A and 25.629-1 should be made to show that flutter characteristics are not adversely affected, taking into account the effects of mass items, i.e., ice accumulations. Surfaces such as ailerons, rudders, elevators, stabilizers, and wings are prime candidates for these investigations. The investigation relates to unprotected and to protected surfaces where residual accumulations are allowed throughout the normal airspeed-altitude envelope. However, the effect of ice shapes on aerodynamic properties need not be considered for flutter analysis.

V.2.12 THE STABILITY AND CONTROL PROBLEM

The icing problems associated with the horizontal tail are much more complex than those associated with the wing because of stability and control considerations and pilot actions to control airplane attitude. The pilot moves the elevators to a different position to change the angle of attack on the wing. This action shifts the lift curve for the stabilizer up or down depending upon the angle of the elevator. Large changes in elevator angle may also be required to compensate for the changes in pitching moments that occur when the pilot drops the flaps for landing.

The stick forces perceived by the pilot are adjusted in various ways by mechanical and electrical control systems to produce an acceptable range of stick forces as a function of stick position. When the aircraft center of gravity, the CG, is substantially ahead of the center of lift, the aircraft is nose heavy and the elevator must be deflected upwards to produce negative lift at the tail. The elevator is deflected down to produce positive lift at the tail when the aircraft is tail heavy, because the center of gravity is behind the aircraft center of lift. The pilot must use force to hold the elevators in the new position until the angle of the trim tabs has been adjusted for the new combination of speed, weight, distribution of weight, altitude, and pitching moments. In the trimmed position, the forces generated by the trim tabs hold the elevators at an angle that produces the amount of lift necessary to control pitch.

There are other complications. The effects of forces producing pitching moments on an aircraft are affected by force location relative to the center of gravity. For example, the forces are increased or decreased according to the way the same amount of weight is distributed in the airplane. The wing must provide the same amount of lift, but elevator angle must change to compensate for the change in location of the weight.

Icing effects on the stability and control problem can be illustrated by considering the typical pilot experience when large accumulations of ice have formed on the aircraft. Pilots report that the

aircraft feels heavy and that aircraft attitude control becomes sluggish. They also describe control movement and aircraft responsiveness as mushy. The aircraft feels heavy because of aerodynamic effects rather than actual increases in weight. The controls are mushy and response to stick movement is slow because flow over the control surfaces is adversely affected by the ice formations. Normal stall and stability and control warnings do not exist in these situations, and the loss of stability and control can be sudden and final.

Ice formations on the vertical stabilizer can adversely affect rudder control. This is particularly important when rudder control is marginal as it is for some light twin engine aircraft. Decisions to omit ice protection systems for the vertical stabilizer should include the analyses and tests necessary to demonstrate that adequate rudder control would be available in the event of an engine failure in icing conditions.

The envelope of flyable CG positions is affected by the limits of elevator ability to control pitching moments, and the elevator can stall in the same way that the wing can stall; however, elevator stalls represent an unplanned event with potentially catastrophic consequences. The effects of ice formations on stability and control as well as the effects on aircraft lift and drag represent problems requiring major consideration. Unfortunately, the most serious effects are associated with flight operating situations that are difficult as well as hazardous to evaluate in flight test programs. These situations occur at the edges of the CG envelope; therefore, technical analyses for aircraft type certification, as well as tests, must give serious consideration to these aspects of ice formation effects on stability.

The flight test program for the Generic Model A aircraft will be based upon technical analyses giving consideration to ice formation effects upon stability and control. The te[illegible] will include flight evaluations with simulated ice formations on wings and tail. The stability and control analyses reported in other portions of the Type Certification analyses will be used, along with technical data and experience, to define representative ice formations and flight conditions for the tests.

V.2.13 SYSTEM RELIABILITY

2.13.1 Requirement

The entire system. including both operating and monitoring functions, must meet FAR 23.1309, 25.1309, 27,1309, or 29.1309, as appropriate. These regulations require the probability of a failure condition to remain within limits which are related to the consequence of a failure condition. A first step in determining compliance with the above regulations should be to determine the effect on the airplane of each possible functional failure of the system.

For FAR 25 and FAR 29 certification, a quantitative safety analysis may be necessary for each failure condition identified by the preliminary hazard analysis as a failure that would prevent the continued safe flight and landing of the airplane. Early agreement between the applicant and the FAA should be reached on the identification of critical functions, methods of analysis to be used, and

assumptions to be used in the acceptance of the proposed analysis. More detailed guidance is provided in AC 20-73, AC 23.1309-1, AC 23.1419-1, and AC 25.1309-1, respectively. Additional information is presented in reference 11, a paper by E.E., Striebel of Pratt and Whitney Aircraft, at a 1969 FAA Symposium on Aircraft Ice Protection.

The applicant should show that he has considered the power sources in his ice protection system design. Electrical and pneumatic sources are normally used. A load analysis or test should be conducted on each power source to assure that it is able to adequately supply the ice protection system and all other essential loads under conditions requiring operation of the ice protection system. The effect of ice protection system component failure on power availability to other essential loads should be evaluated, and any resultant hazard should be prevented on single engine designs and minimized on multi-engine designs. The applicant should show that there is no hazard to the airplane in the event of electrical or pneumatic source failure during flight in icing conditions. Applicants who show that their airplane has two separate power sources would comply. These systems must be installed so that failure of one source does not affect the ability of the remaining source to provide system power. If a single source system is considered, additional reliability evaluation of the power source under airplane loading and environmental conditions may be required.

A study should be made of the overall aircraft ice protection system to establish that the system is adequate for the durations established by the design goals of the ice protection system. This study should consider the reliability of the ice protection system for each flight or between regularly scheduled maintenance activities. Many systems can be considered to be reliable for a given flight if they have a good service history or if they have inherent structural or operational reliability. Confidence inspections consisting of functional checks only, such as those normally performed during preflight, may be considered to contribute towards reliability improvements. A required pilot action following a system failure is often defined as "Depart the icing condition." This must be acceptable in the extreme because no system is fail proof; also, there may be a substantial delay before the aircraft can leave the icing condition.

Dual components with isolation protection have been used in the past to provide the required reliability; however, there are some ice protection system components on both single-engine and multi-engine airplanes that cannot be dualized, such as wing boots and their plumbing, and still other components whose failure would create a hazard to the airplane even if they were dualized. A Failure Mode and Effects Analysis (FMEA) may be necessary when such single or dualized components are used. This FMEA should show that a malfunction is unlikely, or that there are provisions or alternatives included in the design or operation relative to continued function of the system after the single component failure.

The FMEA should include each identifiable mode of failure within the system and its effect on the system's ability to prevent or limit ice buildup. Any failure which results in ice buildup beyond those levels established as allowable (by design and flight test) should be considered to have caused a hazard. Such failures shall be considered probable unless service history or environmental test data

exists which shows otherwise. The system design (including the pilot and maintenance instructions) should include provisions for eliminating or minimizing the resultant hazard.

The applicant may determine that sound engineering judgment requires a more structured analysis procedure than an FMEA. Accordingly, The applicant, at his option, may apply quantitative reliability analysis procedures to support his design. Although such procedures were not considered when the reliability requirements of the FARs were established, they have been accepted to substantiate the reliability of airplane systems and equipment certified under other parts of the FAR. In cases where a quantitative assessment is applied, failure of the ice protection equipment should be improbable; however, quantitative assessments should not be applied when inappropriate (as discussed in AC 23.1309-1) or where operational experience or engineering judgment dictates otherwise. Such quantitative assessment of the reliability levels should be consistent with the following definitions:

1. Probable - Probable events may be expected to occur several times during the operational life of each airplane and are those with a probability on the order of 1×10^{-5} or greater.

2. Improbable - Improbable events are not expected to occur during the total operational life of a random single airplane of a particular type, but may occur during the total operational life of all airplanes of a particular type and are those with a probability on the order of 1×10^{-5} or less.

REFERENCES

1. Bowden, D. T., Gensemer, A. E. and Skeen, C. A., "Engineering Summary of Airframe Icing Technical Data," FAA ADS-4, March 1964.

2. Dommash, Sherby and Connolly, "Airplane Aerodynamics," Pittman Publishing Corp, 1951.

3. FAA Advisory Circular AC 23-8, Appendix 2, "Flight Test Guide for Certification of Normal, Utility, and Acrobatic Category Airplanes," 20 October 1987.

4. Langmuir, I., et al., "A Mathematical Investigation of Water Droplet Trajectories," AAFTR 5418, February 1969.

5. Messinger, B. L., "Equilibrium Temperature of an Unheated Surface as a Function of Airspeed," Journal of Aeronautical Sciences, Vol. 20, No. 1, January 1953.

6. Dickey, T. A., "An Analysis of the Effects of Certain Variables in Determining the Form of an Ice Accretion," Presented at the Mt. Washington Spring Planning Conference, April 1952, Aeronautical Engineering Laboratory, Naval Air Experimental Station.

7. Lewis, W., Brun, R. J., "Impingement of Water Drops on a Rectangular Half Body in a Two-Dimensional Incompressible Flow Field," NACA TN 3658, February 1956.

8. "Airplane Air Condition Engineering Data - Heat Transfer," SAE Report 24, February 1, 1952.

9. Gray, Vernon H., "Simple Graphical Solution of Heat Transfer and Evaporation from Surface Heated to Prevent Icing," NACA TN 2799, October 1952.

10. Callaghan, Edmund E., and Serafini, John S., "A Method for Rapid Determination of the Icing Limit of a Body in Terms of the Stream Conditions," NACA TN-2914, March 1953.

11. Striebel, E. E., of Pratt and Whitney Aircraft, "Ice Protection for Turbojet Engines," FAA Symposium on Aircraft Ice Protection, 28 April 1969.

TABLE V 2-1

FAA FORM 8110-12, "APPLICATION FOR TYPE CERTIFICATE, PRODUCTION CERTIFICATE, OR SUPPLEMENTAL TYPE CERTIFICATE"

U.S. DEPARTMENT OF TRANSPORTATION
FEDERAL AVIATION ADMINISTRATION

APPLICATION FOR TYPE CERTIFICATE, PRODUCTION CERTIFICATE, OR SUPPLEMENTAL TYPE CERTIFICATE

FORM APPROVED
O.M.B. No. 04-R007/8

1. Name and address of applicant	2. Application made for –	3. Product involved
	☐ Type Certificate ☐ Production Certificate ☐ Supplemental Type Certificate	☐ Aircraft ☐ Engine ☐ Propeller

4. TYPE CERTIFICATE *(Complete item 4a below)*

a. Model designation(s) *(All models listed are to be completely described in the required technical data, including drawings representing the design, material, specifications, construction, and performance of the aircraft, aircraft engine, propeller which is the subject of this application.)*

5. PRODUCTION CERTIFICATE *(Complete items 5a–c below. Submit with this form, in manual form, one copy of quality control data or changes thereto covering new products, as required by applicable FAR.)*

a. Factory address *(If different from 1 above)*	b. Application is for –	P.C. No.
	☐ New Production Certificate ☐ Additions to Production Certificate *(Give P.C. No.)*	

c. Applicant is holder of or a licensee under a Type Certificate or a Supplemental Type Certificate *(Attach evidence of licensing agreement and give certificate number)* →	T.C./S.T.C. No.

6. SUPPLEMENTAL TYPE CERTIFICATE *(Complete items 6a–d below)*

a. Make and model designation of product to be modified

b. Description of modification

c. Will data be available for sale or release to other persons?	d. Will parts be manufactured for sale? *(Ref. FAR 21.303)*
☐ YES ☐ NO	☐ YES ☐ NO

7. CERTIFICATION – I certify that the above statements are true.

Signature of certifying official	Title	Date

FAA Form 8110-12 (3-80) SUPERSEDES PREVIOUS EDITION

TABLE V 2-2

PREDICTED PERFORMANCE OF GENERIC MODEL A AIRCRAFT

	AIR SPEEDS, MPH			CLIMB PERFORMANCE				BRAKE HORSEPOWER	
Flight Altitude	True Max	True Cruise	IAS Hold	2 Eng Climb ft/min	IAS	1 Eng Climb ft/min	IAS	Required for Normal Cruise	
16,000	186	180	125	480	105	*	*	111	44%
14,000	193	187	125	610	105	*	*	124	50%
10,000	205	200	125	900	105	*	*	159	64%
7,000	210	205	125	1100	105	70	94	191	76%
4,000	213	210	125	1350	105	180	95	210	84%
2,000	215	204	125	1480	105	310	96	213	85%
MSL	216	198	125	1684	105	350	97	198	79%

*The aircraft is unable to climb with one engine out at these altitudes.

TABLE V 2-3

COMPARISON OF BASIC TRANSPORT AND NORMAL CATEGORY ICING REQUIREMENTS

FAR Part 25.1419	FAR Part 23.1419
(a) If certification with ice protection equipment is desired, compliance with this section must be shown.	If certification with ice protection provisions is desired, compliance with the following requirements must be shown.
(b) The airplane must be able to operate safely in the continuous maximum and intermittent maximum conditions determined under Appendix C. An analysis must be performed to establish, on the basis of the airplane's operational needs, the adequacy of the protection systems for the various components of the airplane.	(a) The recommended procedures for the use of ice protection equipment must be set forth in the Airplane Flight Manual material.
(c) In addition to the analysis and physical evaluation described in paragraph (b) of this section, the effectiveness of the ice protection system and its components must be shown by flight tests of the airplane or its components in measured natural atmospheric icing conditions and by one or more of the following tests as found necessary to determine the adequacy of ice protection systems: (1) Laboratory dry air or simulated icing tests, or a combination of both, of the components or models of the components. (2) Flight dry air tests of the ice protection system as a whole, or of its individual components. (3) Flight tests of the airplane or its components in measured simulated icing conditions.	(b) An analysis must be performed to establish, on the basis of the airplane's operational needs, the adequacy of the ice protection system for the various components of the airplane. In addition, tests of the ice protection system for the various components of the airplane must be conducted to demonstrate that the airplane is capable of operating safely in continuous maximum and intermittent maximum icing conditions as described in Appendix C of Part 25.
(d) For turbine engine powered airplanes, the ice protection provisions of this section are considered to be applicable primarily to the airframe. For the powerplant installation, certain additional provisions of Subpart E of this part may be found applicable.	(c) Compliance with all portions of this section may be accomplished by reference, where applicable because of the similarity of designs, to analysis and tests performed for the type certification of a type certificated aircraft. (d) When monitoring of the external surfaces of the airplane by the flight crew is required for proper operation of the ice protection equipment, external lighting must be provided which is adequate to enable the monitoring to be done at night.

TABLE V 2-4a

LANGMUIR AND BLODGETT DROPLET SIZE DISTRIBUTIONS

LWC,%	A	B	C	D	E
5	1.00	0.56	0.42	0.31	0.23
10	1.00	0.72	0.61	0.52	0.44
20	1.00	0.84	0.77	0.71	0.65
30	1.00	1.00	1.00	1.00	1.00
20	1.00	1.17	1.26	1.37	1.48
10	1.00	1.32	1.51	1.74	2.00
5	1.00	1.49	1.81	2.22	2.71

TABLE V 2-4b

"D" DISTRIBUTION DROPLET SIZES FOR THREE MVD"S				
Liquid Water Content-Percent	Diameter Ratio	Diameter Microns		
5	0.31	4.6	6.2	6.8
10	0.52	7.8	10.4	11.4
20	0.71	10.6	14.2	15.6
Mean Volume 30	1.00	15.0	20.0	22.0
20	1.37	20.6	27.4	30.1
10	1.74	26.1	34.8	38.3
5	2.22	33.3	44.4	46.9

TABLE V 2-5

DESIGN METEOROLOGICAL ICING ENVIRONMENTS

DESIGN CONDITION		LWC FOR GIVEN AIR TEMPERATURES AND DROPLET DIAMETERS							
	D_d	32°F 0°C	24°F -4.4°C	17°F -8.3°C	14°F -10°C	8°F -13.3°C	-4°F -20°C	-22°F -30°C	-40°F -40°F
Continuous	15	0.80	0.72	0.65	0.63	0.48	0.30	0.20	--
Maximum,	20	0.63	0.55	**0.46**	0.42	0.32	0.21	0.15	--
MSL to	30	0.375	0.31	0.24	0.22	0.18	0.11	0.07	--
22,00 ft	40	0.15	0.13	0.11	0.10	0.09	0.06	0.04	--
Intermittent	15	2.95	E2.70*	E2.60*	2.50	2.30	1.95	1.10	.25
Maximum,	20	2.50	E2.40*	**E2.30***	2.20	2.00	1.70	1.00	.20
4,000 to	30	1.30	1.20	1.10	1.00	0.90	0.80	0.50	.10
22,000 Feet	40	0.75	0.70	0.60	0.50	0.45	0.35	0.25	.07
	50	0.40	0.37	0.32	0.30	0.25	0.20	0.10	.05

D_d Mean Volume Droplet Diameter, Microns
E* Estimated from graph

TABLE V 2-6

DATA FOR PERFORMANCE-CRITICAL FLIGHT OPERATING SITUATIONS

The following altitudes, airspeeds, temperatures, density, viscosity and pressures are associated with the flight operating problems selected for analysis:

Problem	Feet	P	MPH*	Ft/sec*	V_e	q	°F	Density	Viscosity
Cruise	11,000	1400	195	286.1	166	70.80	12	.001730	.3366 x 10^{-6}
Cruise	7,000	1633	205	300.7	188	90.24	17	.001996	.3402 "
Hold	7,000	1633	136	200.2	125	39.98	17	.001996	.3402 "
Hold	2,000	1967	125	183.4	125	39.98	24	.002370	.3452 "
Climb	11,000	1400	123	180.6	105	28.21	12	.001730	.3366 "
Climb	9,000	1513	119	174.6	105	28.21	15	.001855	.3387
Climb	7,000	1633	115	168.7	105	28.21	17	.001996	.3402 "
Climb	2,500	1932	106	155.6	105	28.21	23	.002330	.3446 "

Where:

P	=	Pressure Altitude	lb/ft^2
V_e	=	Equivalent Airspeed	MPH
q	=	Dynamic Pressure	lb/ft^3
μ_a	=	Air Viscosity	Slugs/ft-sec
	=	7.136×10^{-6} (459.7 + °F)	
ρ	=	Air Density	$Slugs/ft^3$
	=	P ÷ [1716 x (459.7 + °F)]	
W	=	Aircraft Weight	4800 Pounds

* True Airspeeds

TABLE V 2-7*

$W_{H,}$ IMPINGEMENT ESTIMATES FOR DESIGN CONTINUOUS MAXIMUM CONDITIONS

Parameters			Pounds of Water per Foot Span per Hour						Limits	
D_d	E_M	W_M/LWC	32°F	24°F	17°F	14°F	8°F	-4°F	S_U	S_L
10	.03	1.73	*	*	*	*	*	*	1.0	1.3
15	.09	5.18	4.14	3.73	3.37	3.26	2.49	1.55	1.2"	1.7"
20	.15	8.64	5.44	4.75	3.97	3.63	2.76	1.81	1.3"	2.7"
30	.24	13.83	5.19	4.29	3.32	3.04	2.49	1.52	2.2"	4.8"
40	.33	19.01	2.85	2.47	2.09	1.90	1.71	1.14	3.1"	6.7"

* Liquid Water Contents are not specified in the design standard

Estimates are for 205 MPH at 7,000 feet for Generic Model A Wing

TABLE V 2-8*

W_M IMPINGEMENT ESTIMATES FOR DESIGN MAXIMUM INTERMITTENT CONDITIONS

Parameters			Pounds of Water per Foot Span per Hour						Limits	
D_d	E_M	W_M/LWC	32°F	24°F	17°F	14°F	8°F	-4°F	S_U	S_L
15	.09	5.18	15.28	13.99	13.47	12.95	11.91	10.10	1.2	1.7"
20	.15	8.64	21.60	20.74	19.87	19.01	17.28	14.69	1.3"	2.7"
30	.24	13.83	17.98	16.60	15.21	13.83	12.44	11.06	2.2"	4.8"
40	.33	19.01	14.26	13.31	11.41	9.50	8.55	6.65	3.1"	6.7"
50	.41	23.62	9.45	8.74	7.56	7.09	5.90	4.72	4.0"	8.4"

Estimates are for 205 MPH at 7,000 feet for Generic Model A Wing

TABLE 2-9

GENERIC MODEL A AIRCRAFT CLIMB-CRUISE-CLIMB PERFORMANCE WITHOUT ICE

	Altitude Feet	Temp. °F	Speed-MPH True	V_e	Climb FPM	Time* δt	Distance* Miles	Wing C_L	α
Climb	2,500	23	106	105	1450	0.00	0.00	.82228	6.10
Climb	3,000	22	107	105	1400	+0.35	0.62	.82228	6.10
Climb	5,000	19	111	105	1250	+1.51	2.74	.82228	6.10
Climb	7,000	17	115	105	1100	+1.70	3.20	.82228	6.10
						Σ3.56	**Σ6.56**		
Cruise	7,000	17	205	188		**+2.93**	**+10.01**	.2570	-1.80
						Σ6.49	**Σ16.57**		
Climb	7,000	17	115	105	1100	+0.00	+0.00	.82228	6.10
Climb	9,000	15	119	105	960	**+1.94**	**+3.78**	.82228	6.10
Climb	11,000	12	123	105	830	*	*	.82228	6.10
Cruise	11,000	12	195	166		*	*	.35275	-0.83
	11,000	12	179	153		*	*	.38874	-0.01
						Σ8.43	**Σ20.35**		

Total time for normal climb at the icing problem altitudes is 8.43 minutes
Total distance for normal climb at the icing problem altitudes is 20.35 miles

TABLE V 2-10

IMPINGEMENT CALCULATIONS FOR CLIMB TO 7,000 FEET[a]

(D distribution, MVD=20 Microns, LWC = 0.5 gr/m^3, 19°F, 5,000 ft Avg. Alt)

D_d	LWC	R_e	K_o	E_M	S_U in.	S_L in.	Area in^2	W_{M_M}[b] lb/hr-ft	Vol[c] in^3	Depthc δ	Σ
6.2	.025	20.7	.0022	.005	.00	.67	8.04	.00484	.0093	.0012	.0626
10.4	.050	37.8	.0052	.020	.27	1.34	19.32	.03871	.0747	.0039	.0614
14.2	.100	47.5	.0090	.050	.54	2.68	38.64	.19355	.3736	.0097	.0575
20.0	.150	66.9	.0163	.095	.67	3.68	52.20	.55162	1.0646	.0204	.0478
27.4	.100	91.7	.0287	.130	.80	5.02	69.84	.50323	.9712	.0139	.0274
34.8	.050	116.4	.0401	.200	.94	6.03	83.64	.38710	.7471	.0089	.0135
44.4	.025	148.5	.0587	.270	1.00	8.04	108.50	.26129	.5042	.0046	.0046
								Σ1.94034		Σ.0626	

Pounds of ice from climb = (3.56/60) x 1.9404 = 0.1151

Notes :

a. Calculations are based upon an average altitude of 5,000 feet
b. $W_M = 0.329 \times U_o \times LWC \times (h/C) \times C \times E_M = 38.71 \times LWC \times E_M$, (lb/hr-ft-span
c. Volume and depth of ice are based upon specific density of 0.85
d. Volume of ice = W_M x (Climb time/60) x (1728/62.5) ÷ .85 = 1.93 x W_M
   Climb time in ice = 3.56 minutes
e. Depth of ice = Volume ÷ Surface area covered by the ice
f. Total cross section of ice = $\Sigma(S_U + S_L)$ x Depth, for each unit volume
   = .31115 square inches

TABLE V 2-11

IMPINGEMENT CALCULATIONS FOR LEVEL OFF AND CRUISE AT 7000 FEET

(D distribution, MVD = 20 Microns, 17°F, and LWC = 0.46 gr/m_3)

D_d	LWC	R_e	K_o	E_M	S_U in	S_L in	Area in^2	W_M lb/hr-ft	Vol* in^3	Depth* in	Σin
6.2	.023	35.9	.00355	.020	.94	1.13	24.84	.0294	.0467	.0019	.1253
10.4	.046	60.2	.00836	.055	1.07	1.47	30.48	.1620	.2574	.0084	.1234
14.2	.092	82.1	.01410	.095	1.21	1.67	34.56	.5594	.8889	.0257	.1150
20.0	.138	115.7	.02466	.150	1.34	2.68	48.24	1.3250	2.105	.0436	.0893
27.4	.092	158.5	.04143	.210	2.01	4.22	74.76	1.2370	1.966	.0263	.0457
34.8	.046	201.3	.06016	.280	2.68	5.70	100.56	.8240	1.309	.0130	.0194
44.4	.023	256.9	.08342	.340	3.35	7.03	124.56	.5000	.794	.0064	.0064
	Σ.460							Σ4.6368		Σ.1253	

Pounds of ice from cruise (2.93/60) x 4.6368 =0.2264

Plus ice accumulated during climb =0.1151 = 0.3415 pounds

Notes:

1. Volume and depth of ice are based upon a specific density of ice = 0.85
2. W_M = 0.329 x 205 x (h/C)C x LWC x E_M = 64.01 x LWC X E_M
3. Vol = (Cruise time ÷ 60) x (1728/32.5) ÷ 0.85 x W_M = 1.589 x W_M,
4. Ice cross section area = .6116 square inches

TABLE V 2-12

RADOME IMPINGEMENT CALCULATIONS FOR CRUISE AT 7000 FEET

(D distribution, MVD = 20 Microns, 17°F, and LWC = 0.46 gr/m_3)

D_d	LWC	R_o	Range	K	K_o	E_M	S_L %	S_L in	W_M
6.2	.023	35.9	.50	.0197	.00985	.005	.015	.36	.008
10.4	.046	60.2	.42	.0556	.02335	.010	.095	2.28	.031
14.2	.092	82.1	.38	.1036	.03937	.020	.165	3.96	.124
20.0	.138	115.7	.335	.2055	.06884	.070	.250	6.00	.651
27.4	.092	158.5	.30	.3857	.11571	.150	.345	8.28	.931
34.8	.046	201.3	.27	.6221	.16797	.225	.415	9.96	.698
44.4	.023	256.9	.24	1.0127	.24305	.300	.480	11.52	.465
									Σ 2.908 lb/ft^2-hr

Notes:

1. Volume and depth of ice are based upon a specific density of ice = 0.85
2. $W_M = 0.329 \times 205 \times LWC \times E_M = 67.44 \times LWC \times E_M$ lb/ft^2-hr
3. $K = 513.7 \times 10^{-6} \times D_d^2$ and is based upon a radius of 2 ft.
4. Ice cross section area, volume, and depth, calculations are not complete.

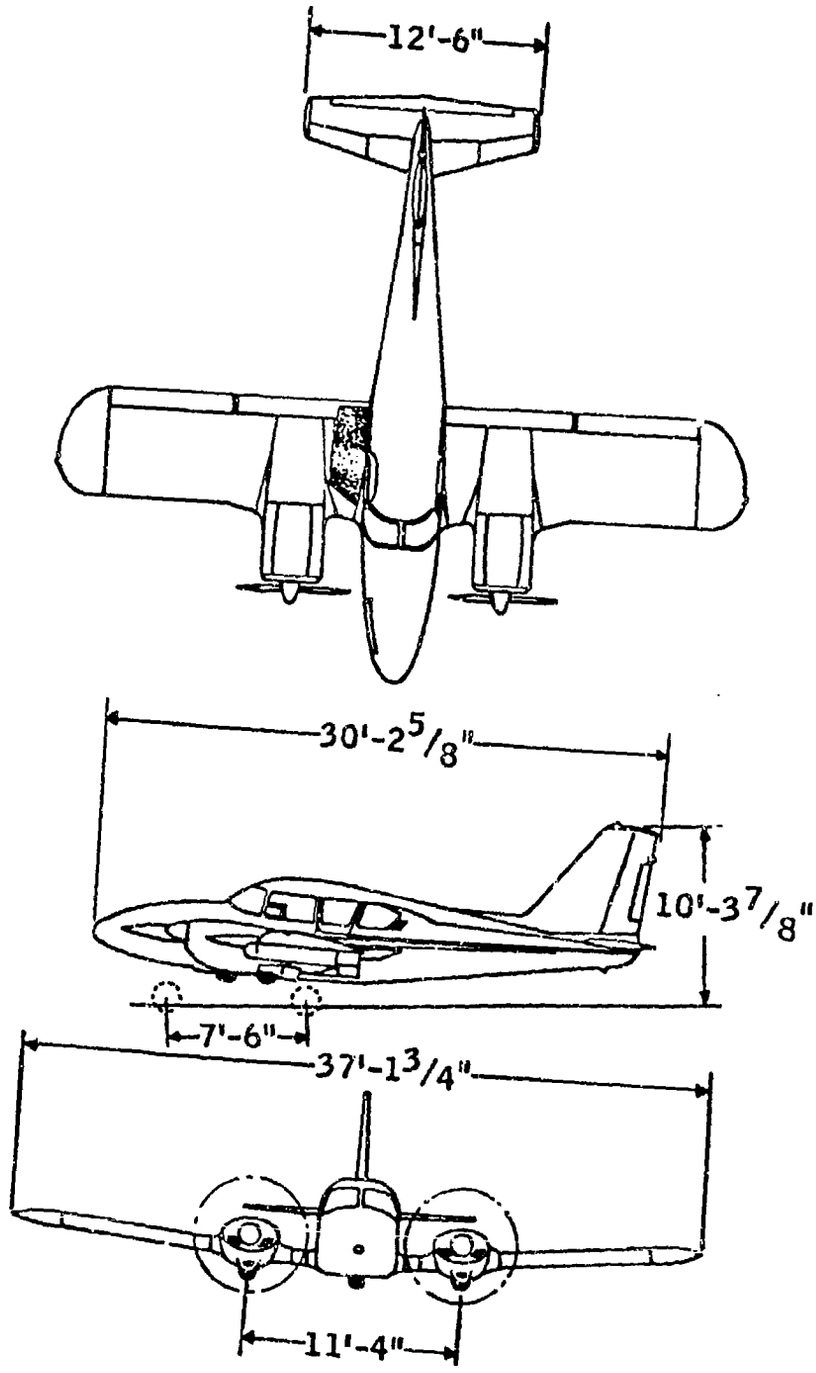

FIGURE V 2-1. THREE VIEW DRAWING OF GENERIC MODEL A AIRPLANE

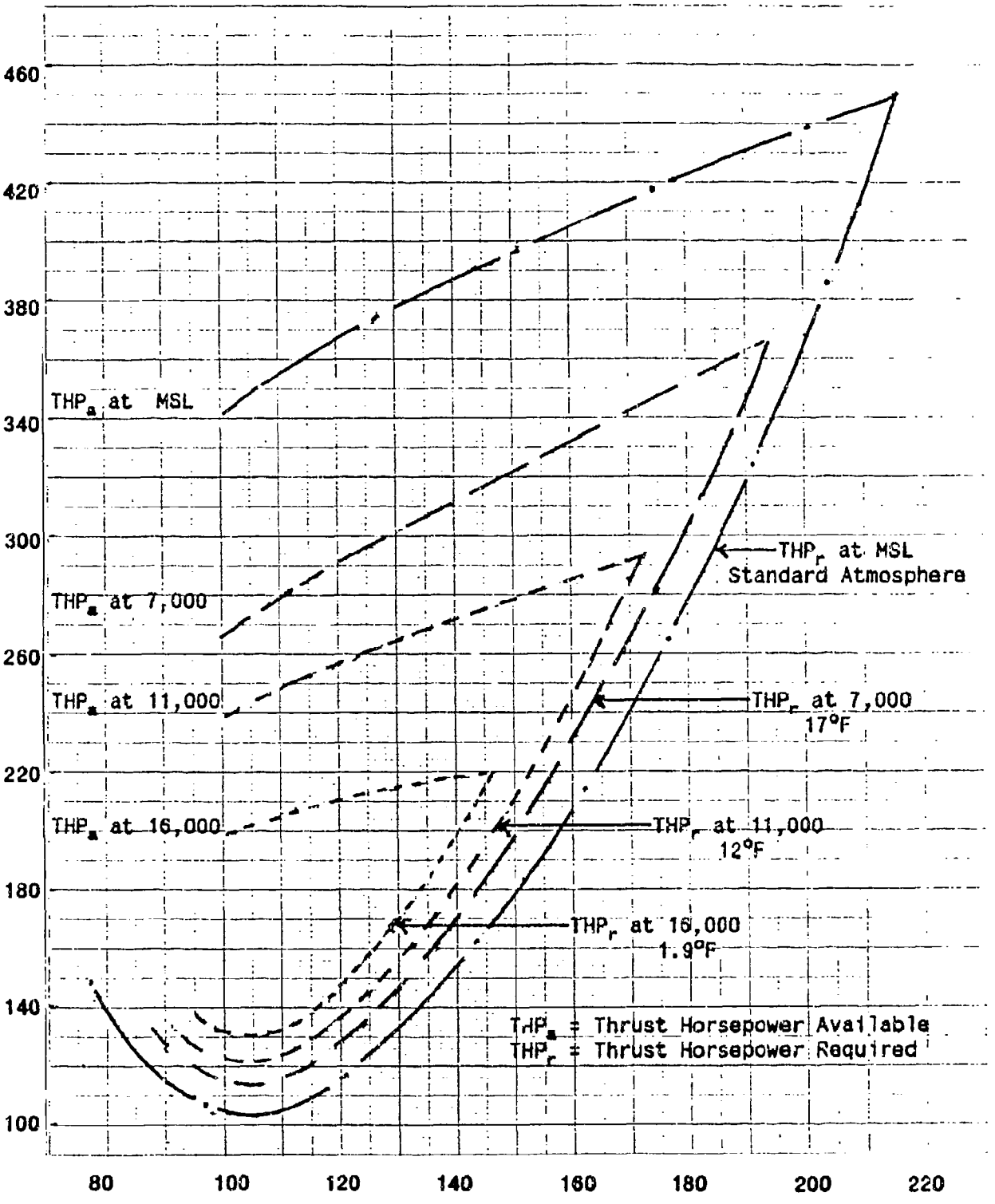

FIGURE V-2-2. SPEED-POWER DATA FOR THE GENERIC MODEL A AIRPLANE

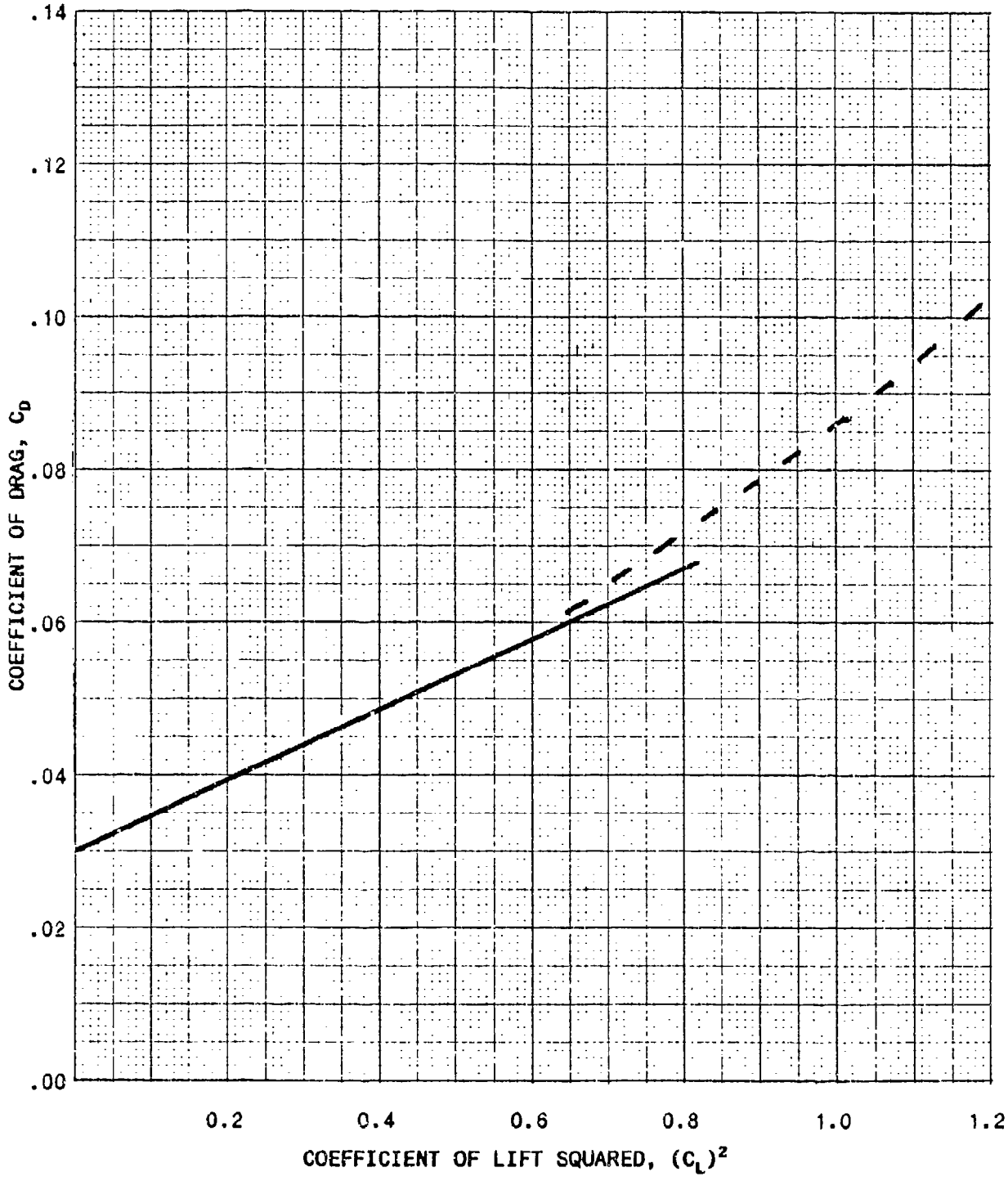

FIGURE V 2-3. LIFT-DRAG POLARS

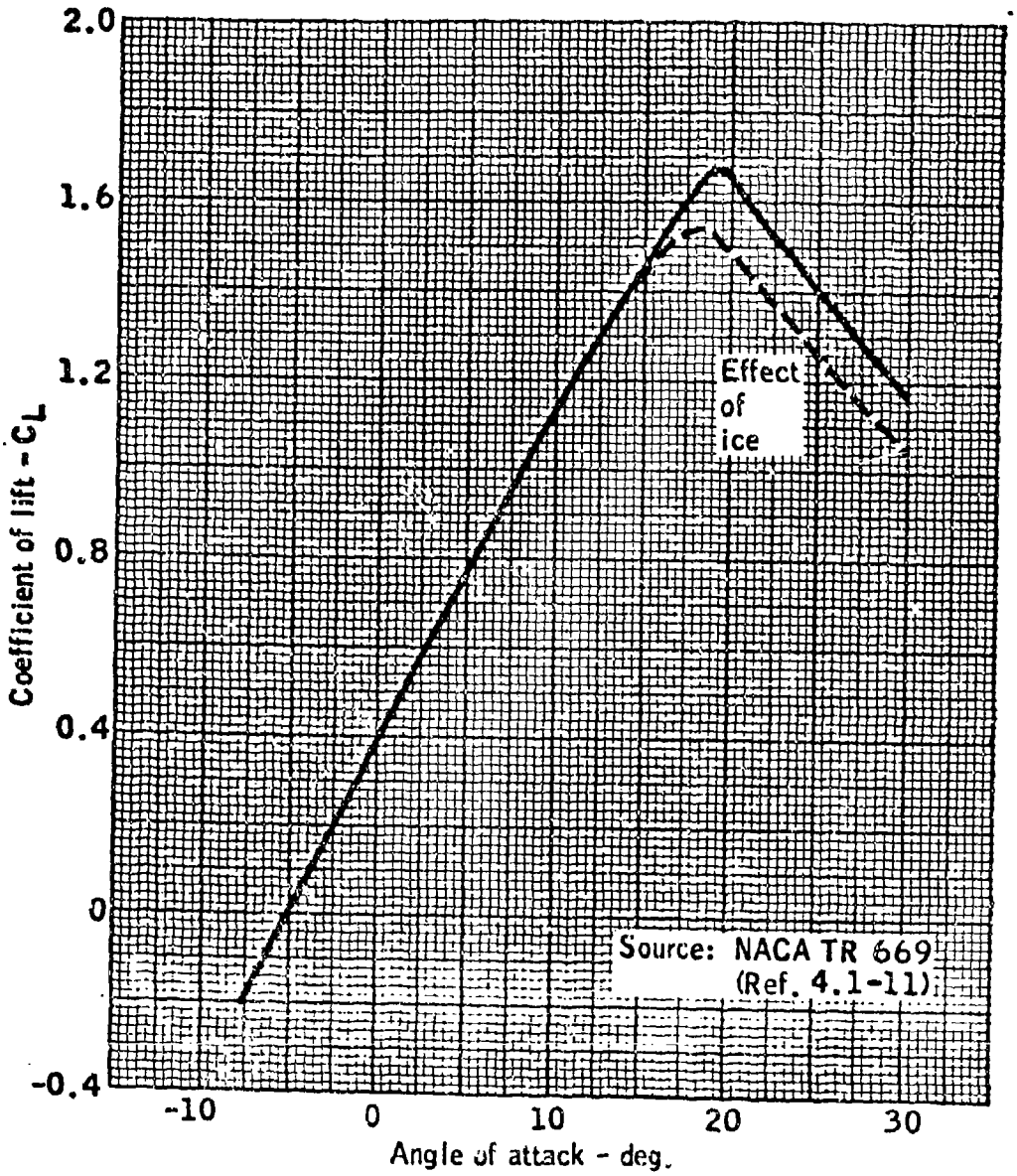

FIGURE V 2-4. USA 35-B AIRFOIL LIFT CURVE SHOWING EFFECT OF ICE

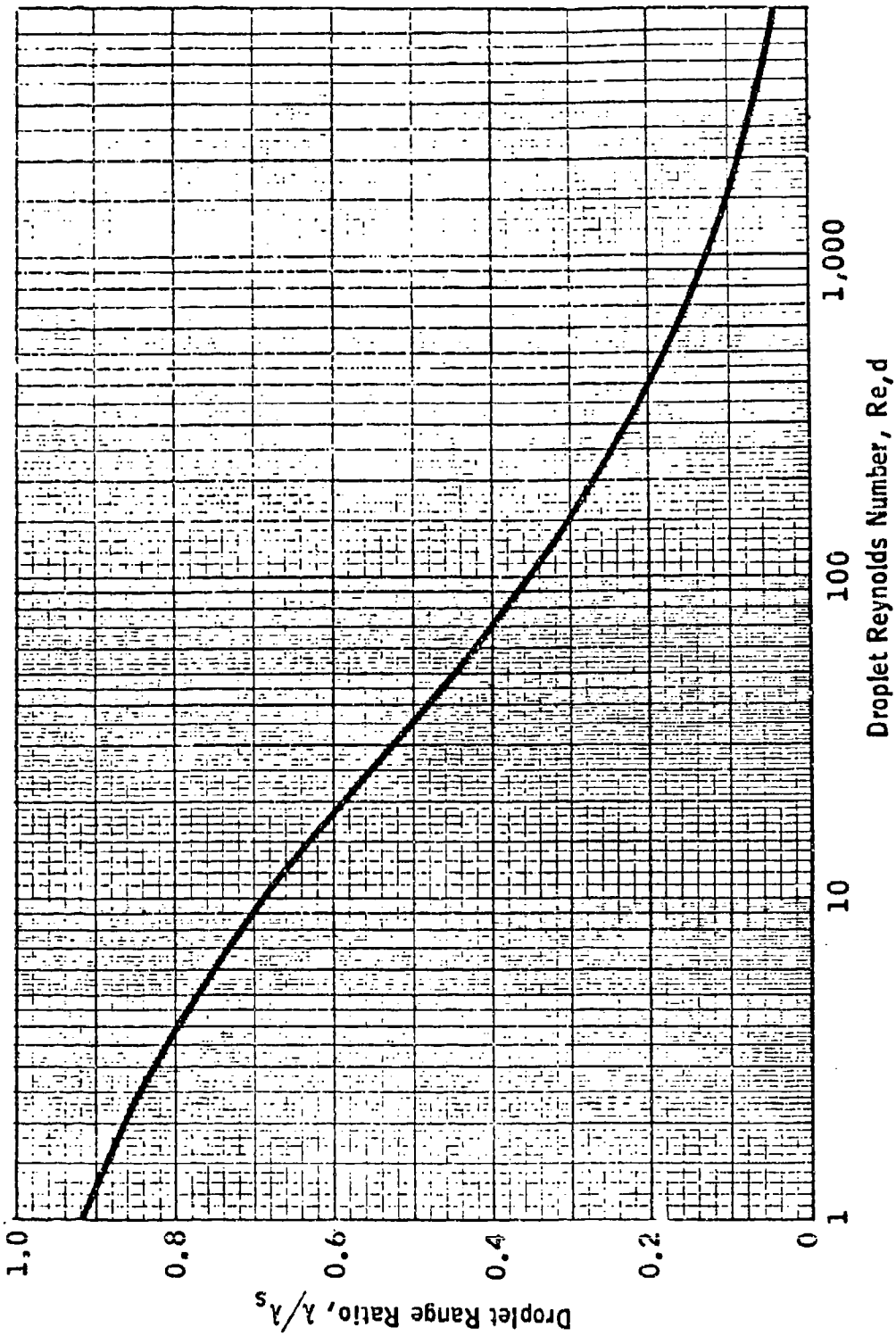

FIGURE V 2-5. DROPLET RANGE RATIO AS A FUNCTION OF REYNOLDS NUMBER

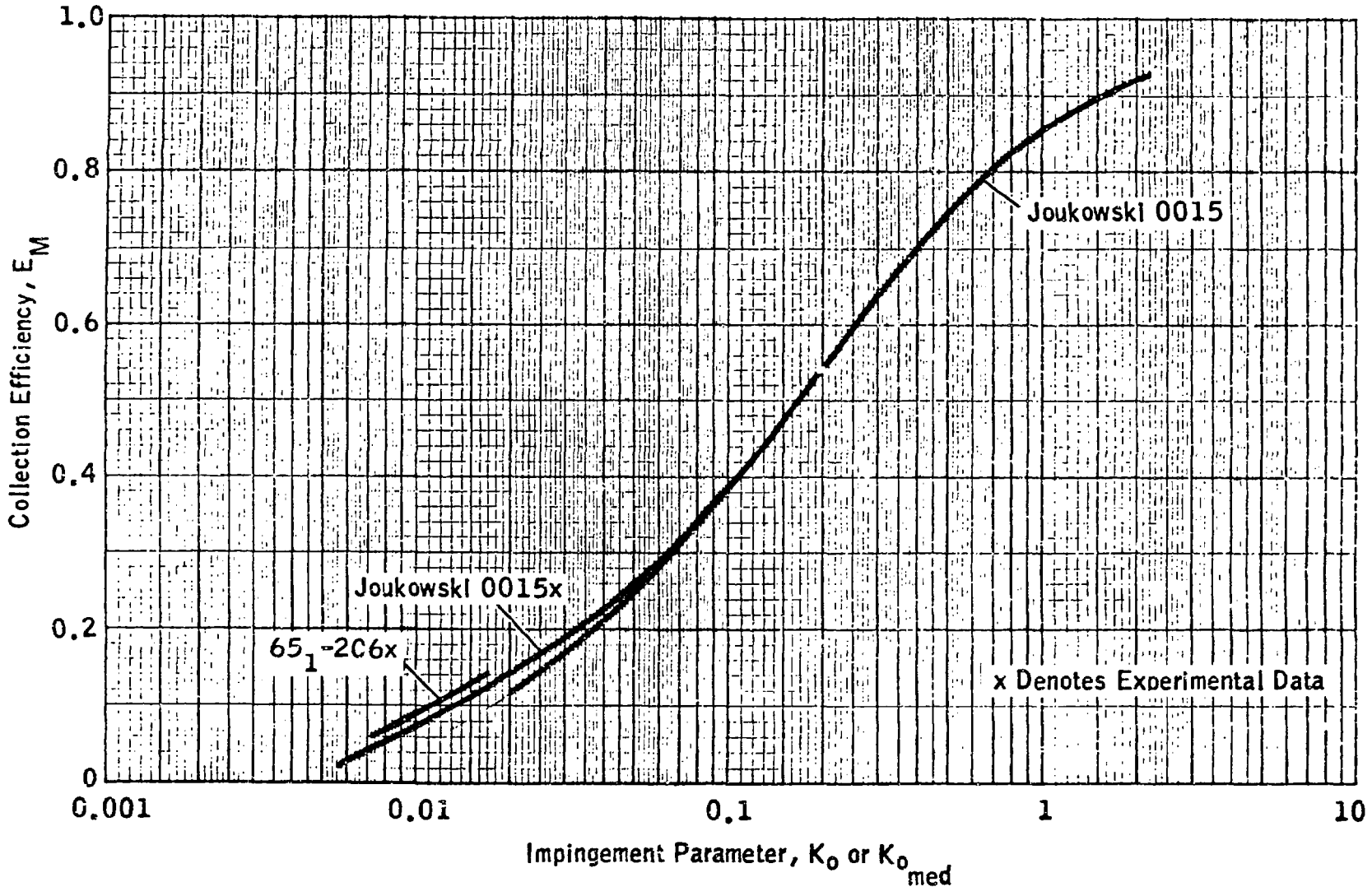

FIGURE V 2-6 Collection Efficiency Versus K_o for Airfoils — Theoretical and Experimental Data for 2° Angle of Attack.

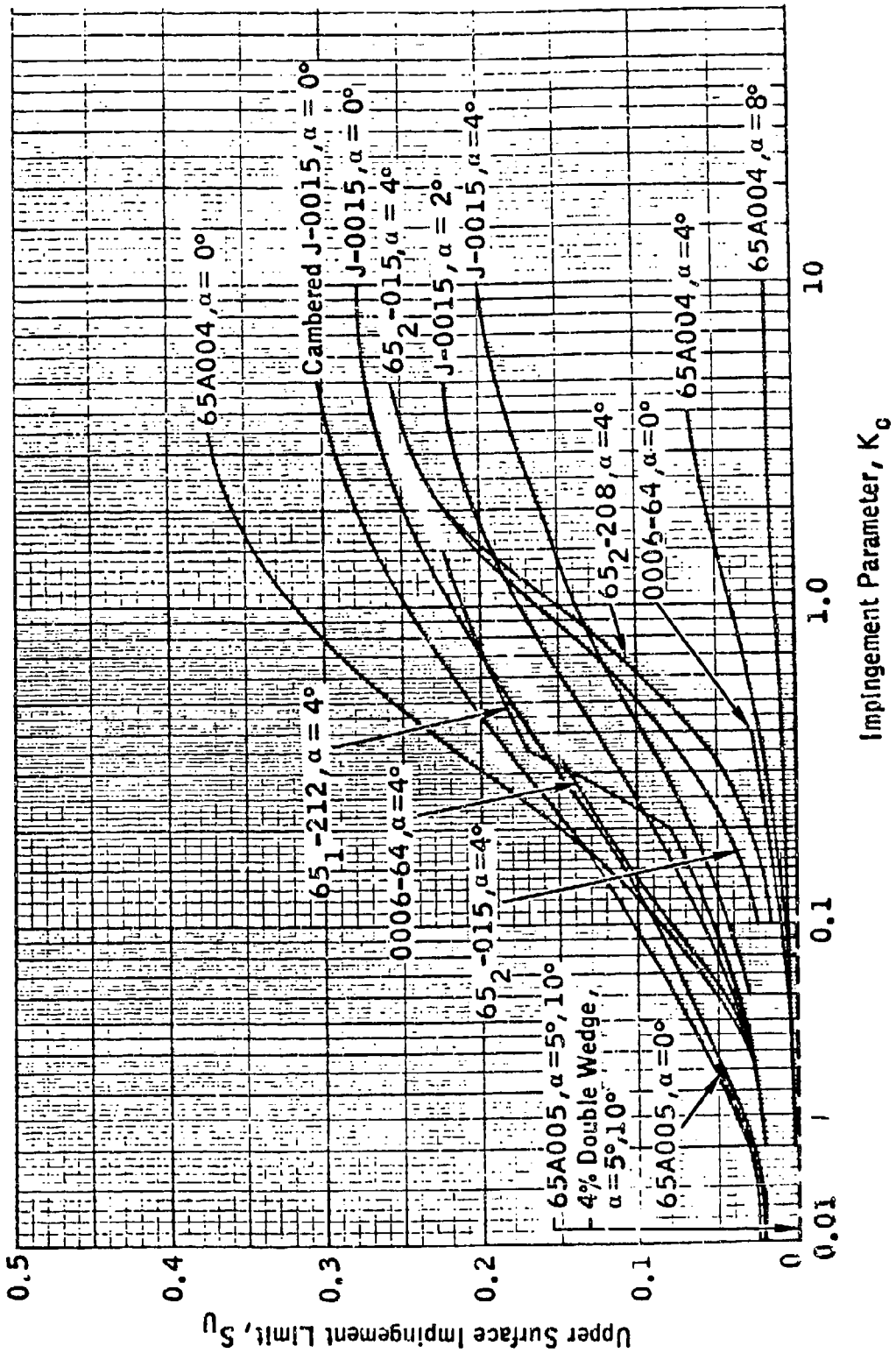

FIGURE V 2-7. IMPINGEMENT LIMIT ON THE UPPER SURFACE OF SEVERAL AIRFOILS VERSUS K_o FOR 0, 2, 4, 5, 8, and 10° ANGLES OF ATTACK

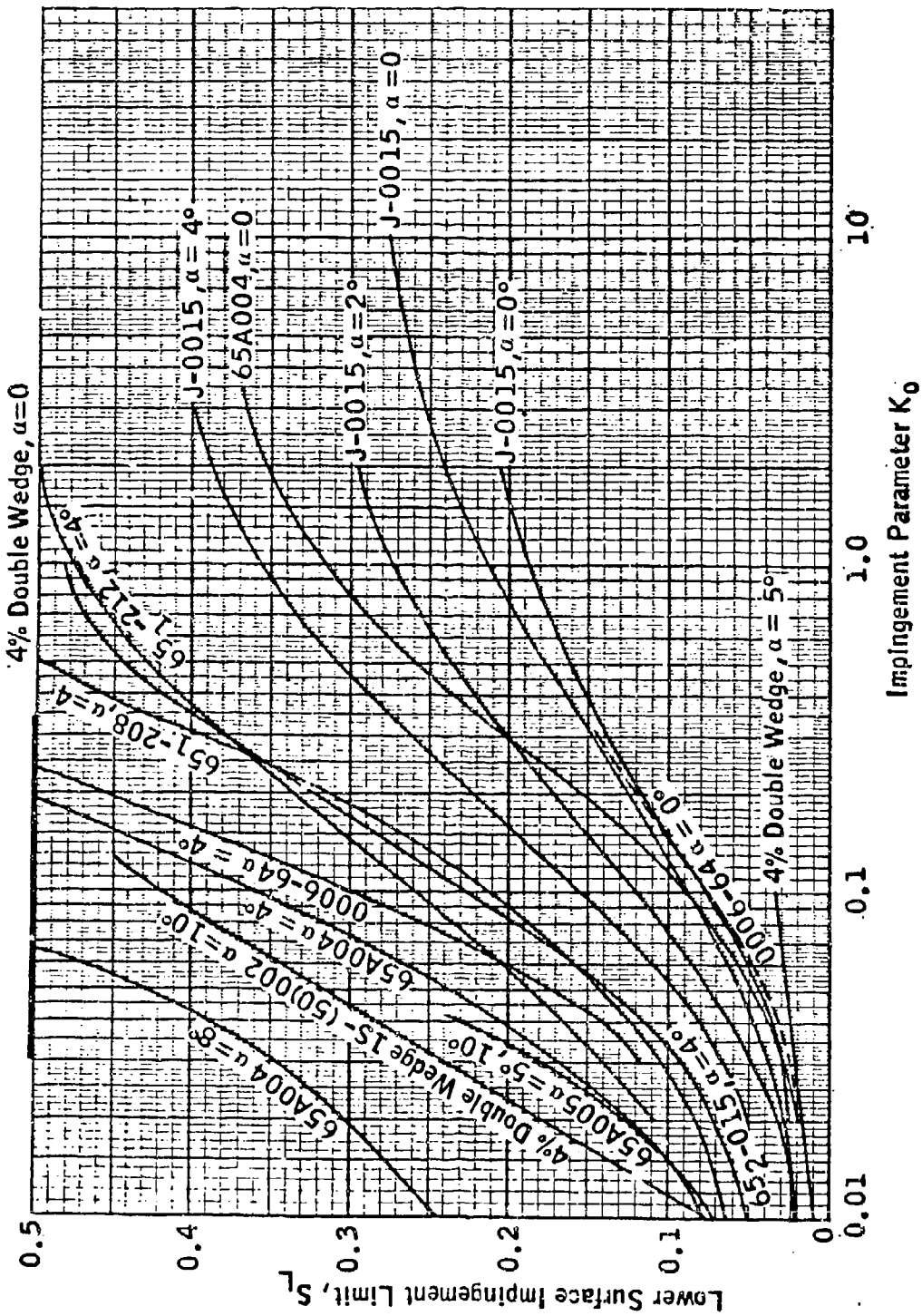

FIGURE V 2-8. IMPINGEMENT LIMIT ON THE LOWER SURFACE OF SEVERAL AIRFOILS VERSUS K_o FOR 0, 2, 4, 5, 8, AND 10° ANGLES OF ATTACK

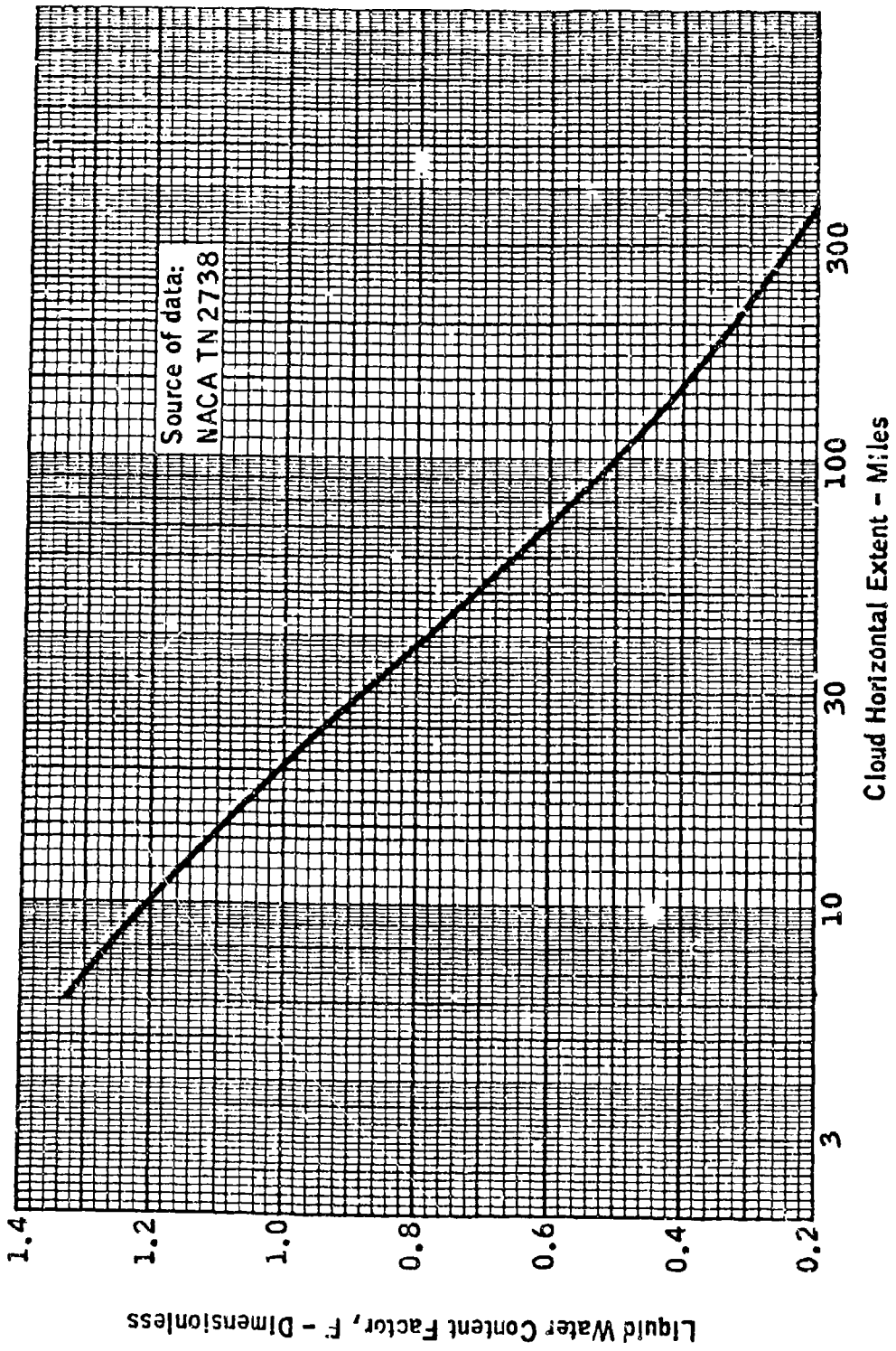

FIGURE V 2-9. LWC FACTOR, F, FOR CLOUD HORIZONTAL EXTENT IN CONTINUOUS MAXIMUM ICING CONDITIONS

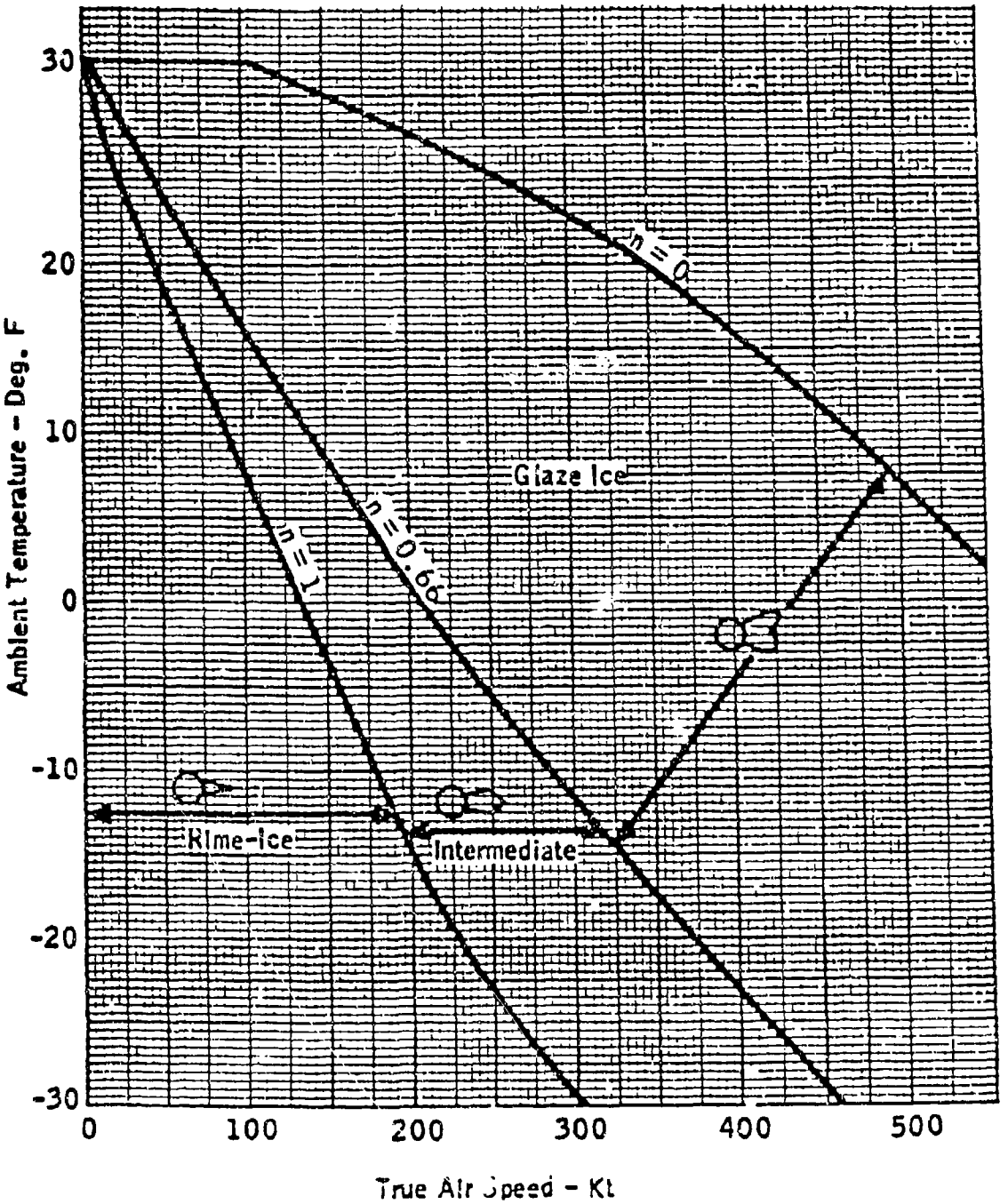

FIGURE V 2-10 ICE SHAPE TYPES AS A FUNCTION OF SPEED AND AMBIENT TEMPERATURE FOR A LIQUID WATER CONTENT OF 0.5 gr/M^3

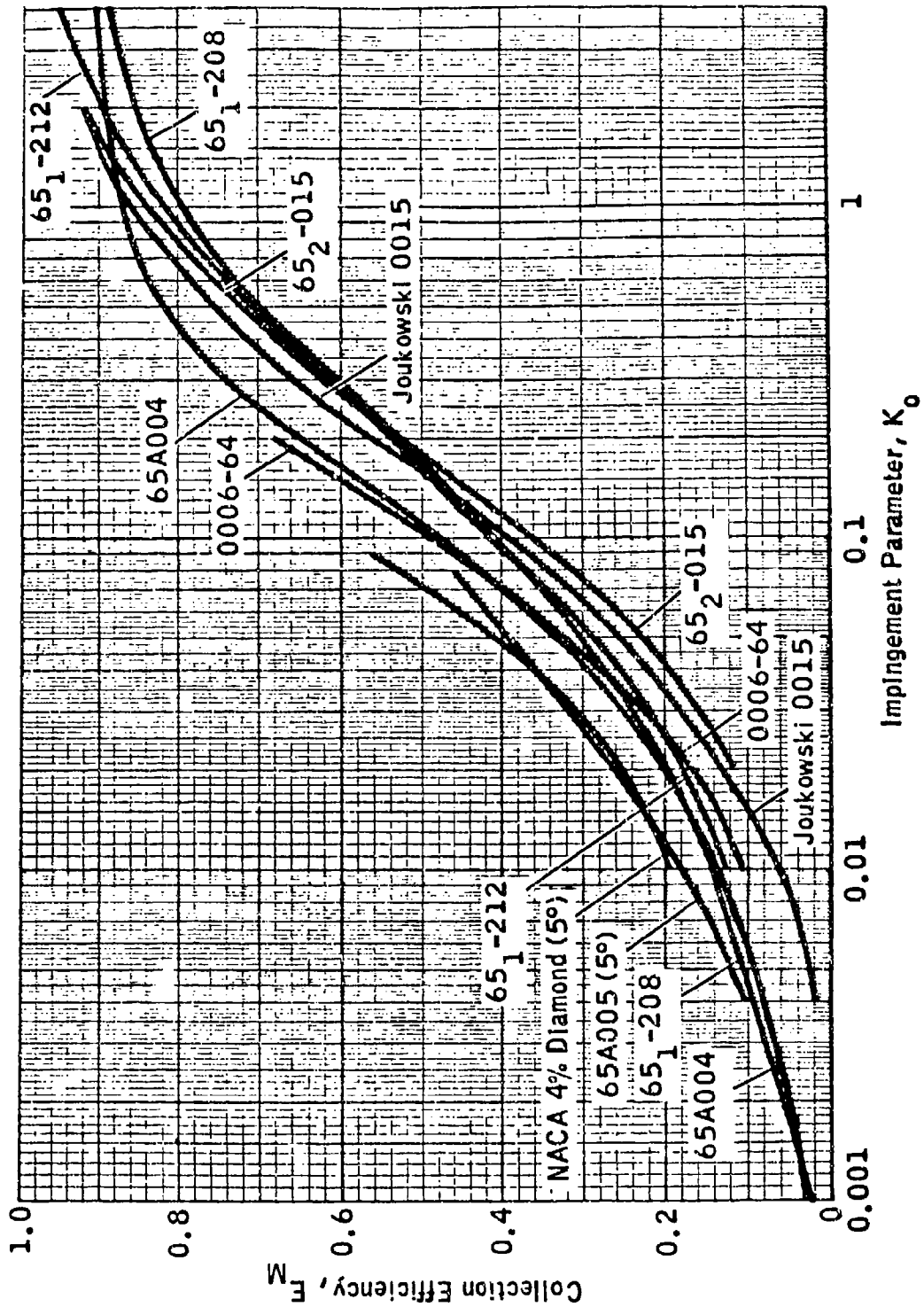

FIGURE V 2-11 COLLECTION EFFICIENCY VERSUS K_o FOR AIRFOILS - THEORETICAL DATA AT 4° ANGLE OF ATTACK

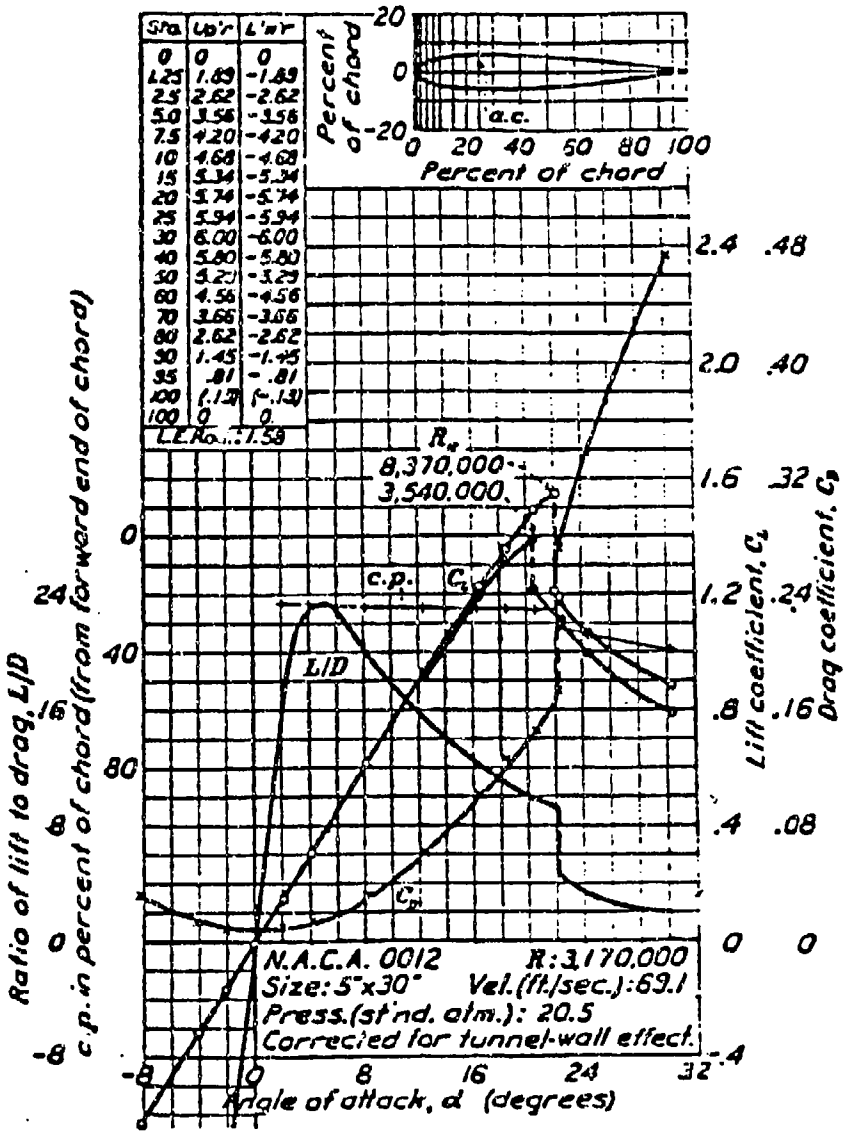

FIGURE V 2-12 ANGLE OF ATTACK VS. AIRFOIL (NACA 0012) PERFORMANCE PARAMETERS

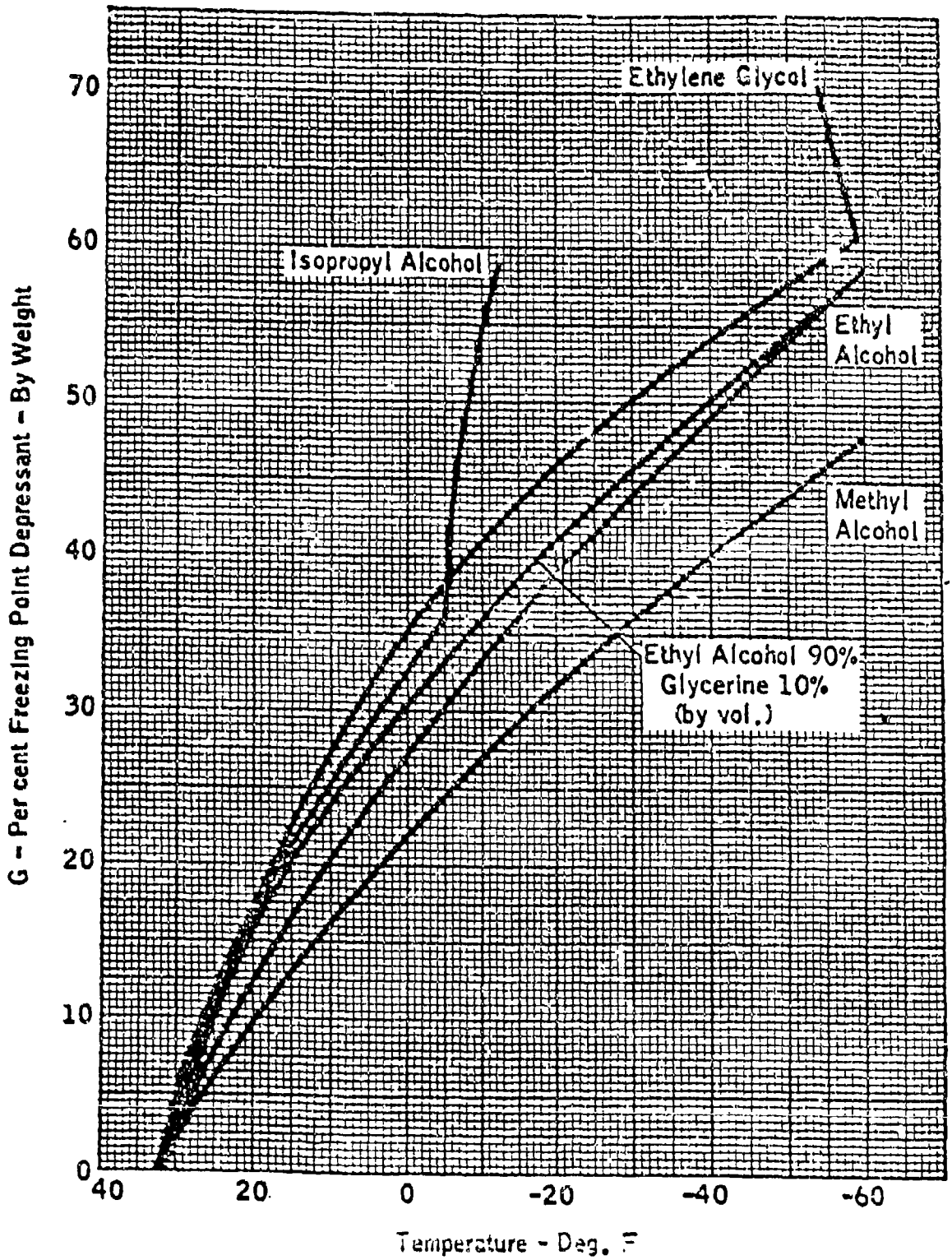

FIGURE V 2-13. FREEZING POINT PLOTS FOR AQUEOUS SOLUTIONS OF SEVERAL FREEZING POINT DEPRESSANT FLUIDS (REFERENCE 3-20)

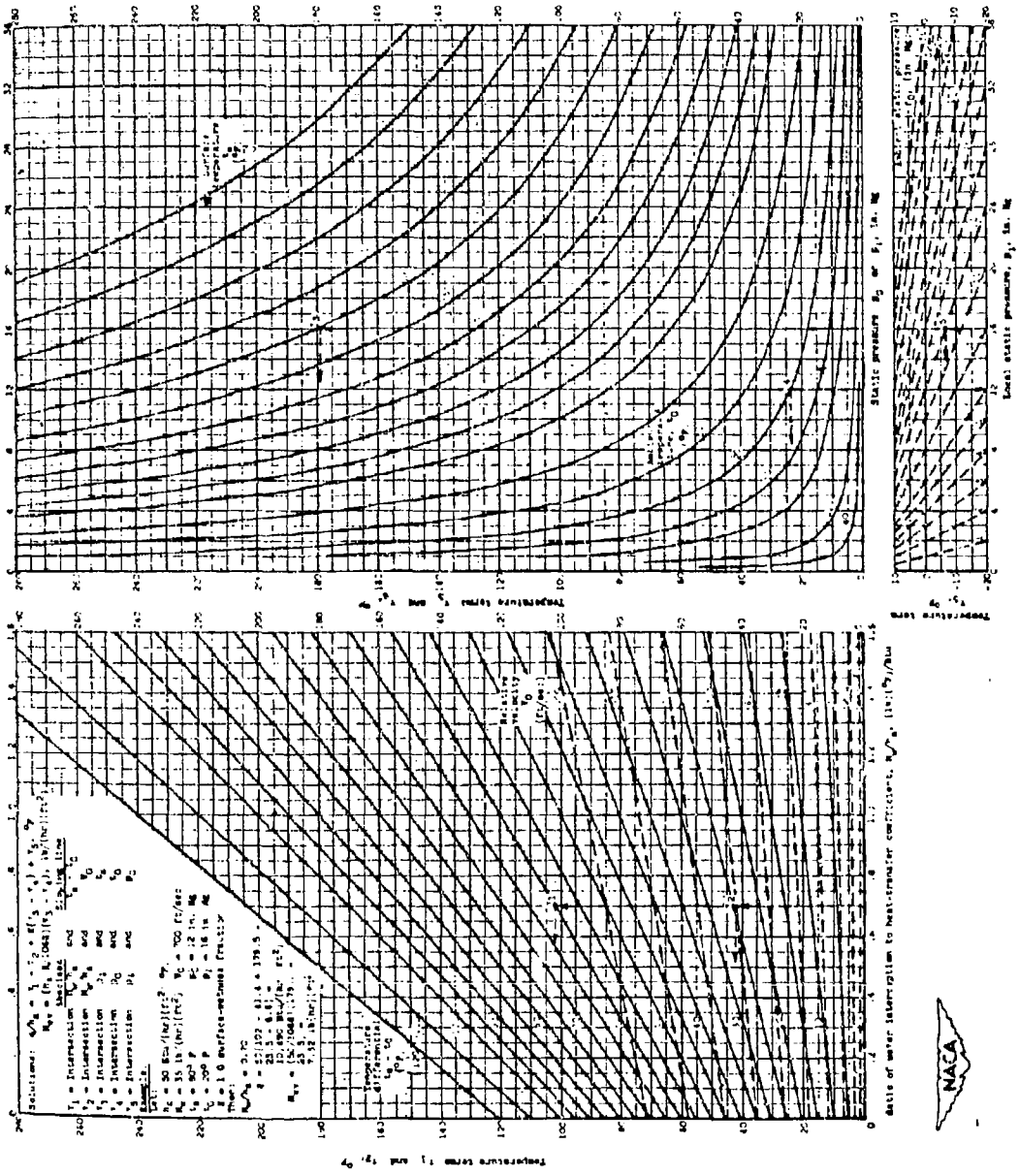

Figure 1. - Graphical solution of anti-icing heat and mass transfer from surface subject to impingement and heated above freezing. (A 17 $\frac{1}{2}$×22 inch print of this figure is attached.)

FIGURE V 2-14 . GRAPHICAL SOLUTION OF ANTI-ICING HEAT AND MASS TRANSFER FROM SURFACE SUBJECT TO IMPINGEMENT AND HEATED ABOVE FREEZING

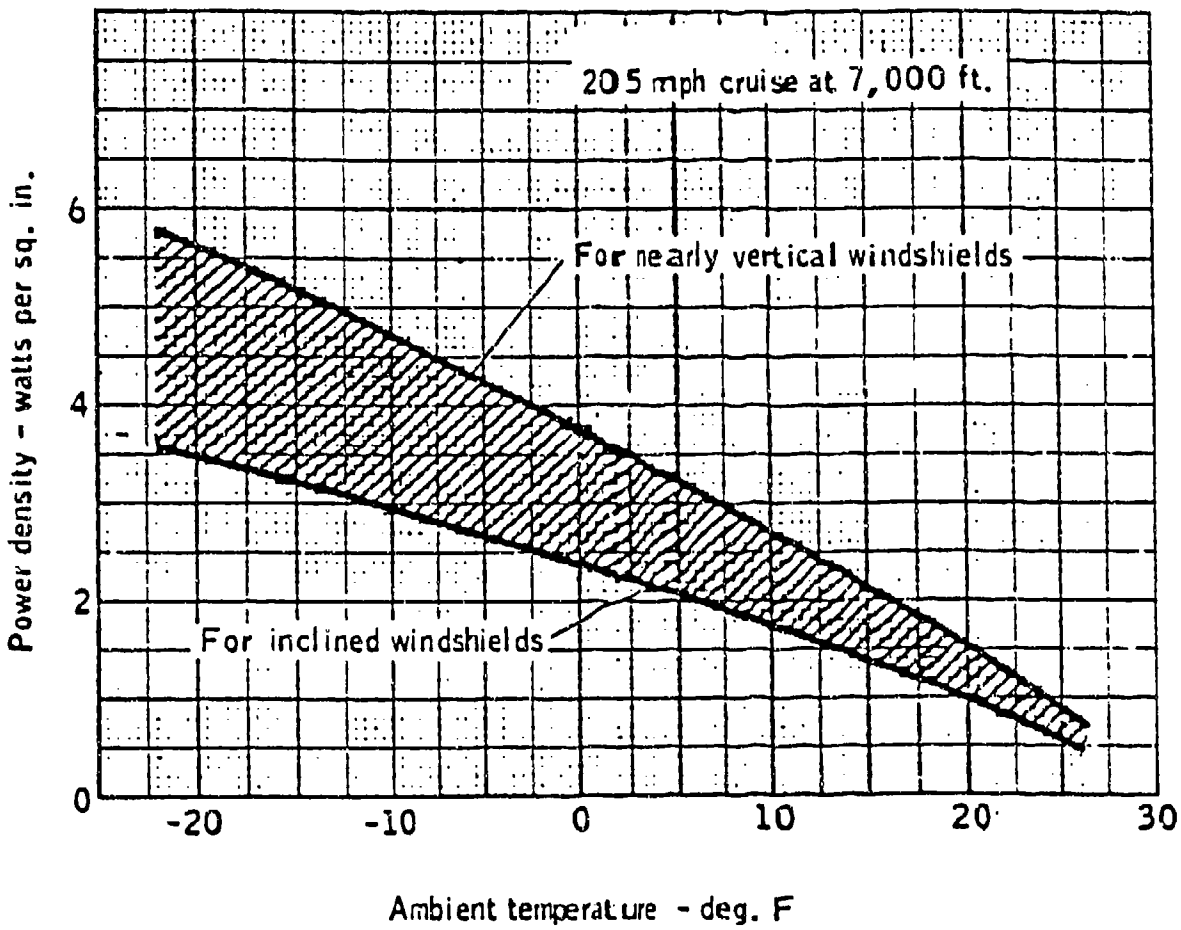

FIGURE V 2-15 POWER REQUIREMENTS FOR ELECTRICAL PROTECTION OF WINDSHIELD (REFERENCE 3-20)

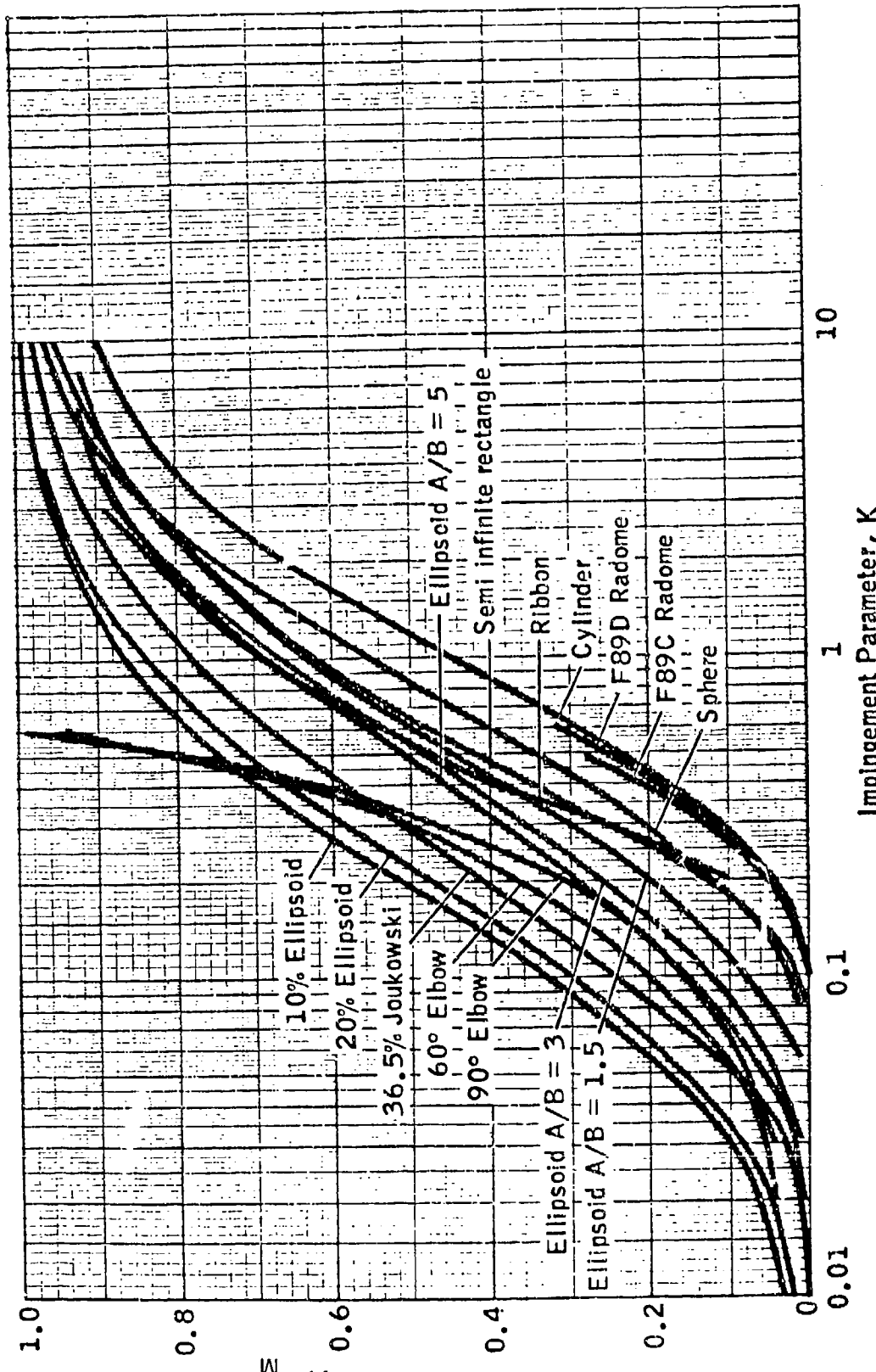

FIGURE V 2-16. COLLECTION EFFICIENCY VERSUS K_o FOR GEOMETRIC BODIES - THEORETICAL DATA FOR 0° ANGLE OF ATTACK.

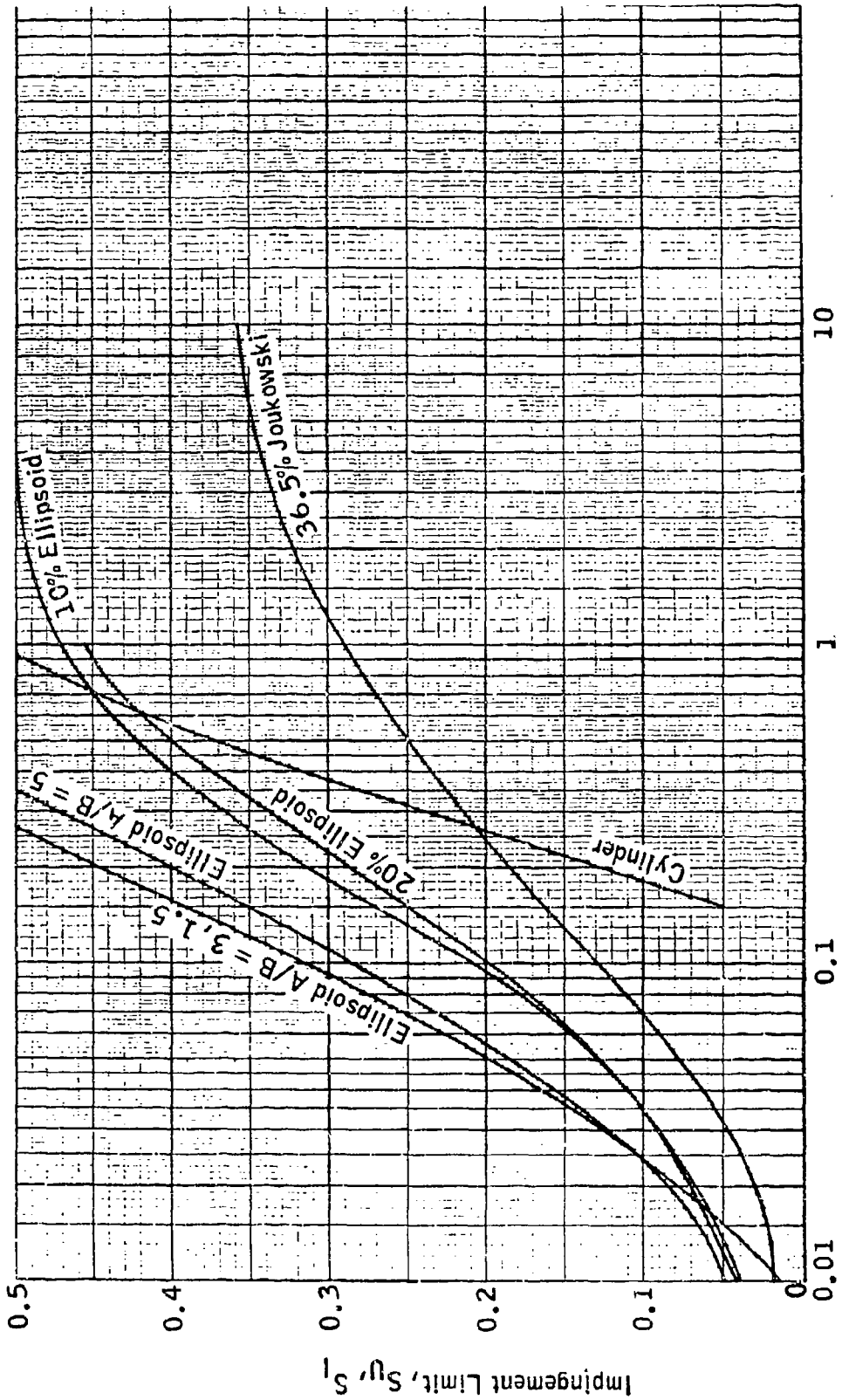

FIGURE V 2-17. IMPINGEMENT LIMITS ON SEVERAL GEOMETRIC SHAPES AT 0° ANGLE OF ATTACK - THEORETICAL DATA

CHAPTER V
SECTION 3.0
EVALUATIONS TO DEMONSTRATE ADEQUACY

CHAPTER V

CONTENTS

SECTION 3.0 EVALUATIONS TO DEMONSTRATE ADEQUACY

	Page
LIST OF TABLES	V 3-ii
LIST OF FIGURES	V 3-iii
SYMBOLS AND ABBREVIATIONS	V 3-iv
V.3.1 EVALUATIONS OF COMPONENT PERFORMANCE PREDICTIONS	V 3-1
3.1.1 Demonstrating Adequacy with Theoretical Analysis	V 3-1
3.1.2 Demonstration Adequacy with Similarity Comparisons	V 3-1
3.1.3 Demonstrating Adequacy with Test Data	V 3-2
V.3.2 AIRCRAFT OPERATION AS AN INTEGRATED SYSTEM	V 3-4
3.2.1 Flight Testing the Aircraft	V 3-4
3.2.2 Flight Test Illustrations	V 3-4
3.2.3 Stability and Control	V 3-5
3.2.4 Performance Calculations	V 3-5
3.2.5 Estimating Ice Formation Effects on Drag Forces	V 3-7
V.3.3 ICE FORMATION EFFECTS ON GENERIC MODEL A PERFORMANCE	V 3-9
3.3.1 The Performance-Critical Holding Problem	V 3-9
3.3.2 The Climb-Cruise-Climb Problem	V 3-12
3.3.3 Evaluation Criteria	V 3-14
V.3.4 FLIGHT HANDBOOK	V 3-15
3.4.1 Requirements	V 3-15
3.4.2 Operating Instructions	V 3-15
V.3.5 REFERENCES	V 3-16

LIST OF TABLES

		Page
3-1	Procedure for Calculating Drag Increase Based Upon the Weight of Ice Formations	V 3-17
3-2	Generic Model A Aircraft Climb-Cruise-Climb Performance Without Ice	V 3-18
3-3	Wing Icing Accumulations for Climb-Cruise-Climb Problem	V 3-19
3-4	Airfoil Drag Increase Calculations for Climb-Cruise-Climb Problem	V 3-19
3-5	Estimated Icing Effects on Performance for Climb Problem	V 3-20

LIST OF FIGURES

		Page
3-1	Typical Engine Inlet Lip Anti-Icing Heat Release VS. Altitude	V 3-21
3-2	Correlation Between Flight Test and Estimated Icing Cruise Performance Decrements for Super Skymaster	V 3-22
3-3	Ai: foil Section Drag Increase Versus Angle of Attack for Rime Ice and Ridge-Type Glaze Ice	V 3-23

SYMBOLS AND ABBREVIATIONS

Symbols	Abbreviations
BHP	Brake Horse Power (ft-lb/sec)
C_D	Coefficient of Drag (Dimensionless)
C_L	Coefficient of Lift (Dimensionless)
D	Drag (pounds)
D_d	Droplet Diameter (Microns)
FPM	Feet Per Minute (ft/min)
MAC	Mean Aerodynamic Chord (Feet)
MVD	Median Volume Droplet Diameter (Microns)
LWC	Liquid Water Content (g/m^3)
RC	Rate of Climb (ft/min)
S	Airfoil Surface Area (ft^2)
T	Thrust (Pounds)
THP	Thrust Horsepower (ft-lb/sec)
V	True Airspeed (ft/sec)
W	Aircraft Weight (Pounds)
W_{lb}	Weight of Water Impingement (lb/ft-span)

Symbols	Description
g	Weight (Grams)
m	Length (Meter)
n	Propeller Efficiency (Dimensionless)
q	Dynamic Pressure (lb/ft^2)

Symbols	Descriptions
α	Angle of Attack (Degrees)
δ	Incremental Change (Dimensionless)

Subscripts	Description
a	Available
r	Required
i	Icing Related
h	Horizontal Stabilizer
t	Vertical Tail

V.3.0 EVALUATIONS TO DEMONSTRATE ADEQUACY OF ICE PROTECTION SYSTEMS

V.3.1 EVALUATIONS OF COMPONENT PERFORMANCE PREDICTIONS

3.1.1 Demonstrating Adequacy with Theoretical Analyses

The basic theory for predicting the performance of aircraft ice protection systems has been in use for more than a quarter of a century, and the ability to apply the theory has been substantially improved as new and more efficient programs have been made possible by today's computer technology. The theory in one form or another has been used for the design, development, and certification of the entire fleet of all-weather aircraft in operation throughout the world today. There is no evidence that an unsatisfactory ice protection system has resulted from proper application of appropriate theory, although some aircraft designs have experienced icing problems; nevertheless, a completely theoretical approach to ice protection system design and design certification activities is not acceptable as a sufficient basis for demonstrating system adequacy because of the lack of data to substantiate the theoretical steps involved.

3.1.2 Demonstrating Adequacy with Similarity Comparisons

Design similarity can be the basis for demonstrating the adequacy of ice protection system designs when it can be shown that a new certification application involves a design that is essentially the same as a previously certified design. This option typically occurs in connection with the development of an improved model of an existing aircraft. It can also involve installation of a previously approved component on a different aircraft. In either instance, it is necessary to make physical, technical, and operational comparisons and to show that information from the previous demonstrations is valid for the new application. For example, assume that the Generic Model A aircraft has been certified for flight into known icing conditions and that certification is desired for the same aircraft with a more powerful engine. The additional horsepower is to be obtained by increasing the crankshaft stroke. The external shape and size of the two engines and engine cowlings are the same, and it can be shown that the alternator, air compressor, and engine accessories are mounted in the same locations and that the air induction and alternate air by-pass systems are identical. No adverse consequence with respect to operation in icing conditions could be expected as a result of the change. Demonstration by similarity would be a reasonable basis for certification of the new model for flight in known icing conditions providing that all of the non-icing certification requirements can be met. A letter to the FAA could be prepared to request certification on the basis of similarity and should include the documentation necessary to support the similarity comparisons.

3.1.3 Demonstrating Adequacy with Test Data

Uncertainties associated with the accuracy of the various methods of analysis can be reduced through use of data from laboratory and flight test programs. The objective is to permit extrapolation of test results to conditions other than those in which the tests were conducted. This approach requires information to prove that the component to be tested is appropriately representative of the component to be certified and that the internal and external test environments are comparable to those associated with the operating environments. Reasonably accurate comparisons between observations and predictions provide the needed assurance that the methods can be used to extend information to untested conditions and to interpolate between test conditions.

For example, hot air systems for providing component ice protection were discussed in Chapter III, Section 5. In these systems, the heated air flows to the surfaces to be protected through a system of ducts with pressure and flow regulating valves to control the amount of heat provided to each component. Theory is used to predict the amount of heat that is required to provide the desired protection. The heat required is the amount of heat that must be delivered to the surfaces of the component to produce the external surface temperatures required to prevent formation of ice or to completely evaporate impinging water droplets. The amount of heat required for the desired protection can be predicted through use of impingement and heat transfer equations for the appropriate meteorological design icing conditions. The heat provided to the component surfaces is called the heat available. The heat available must equal or exceed the heat required without exceeding limitations established as a result of non-icing considerations, such as avoiding over-heating.

Calculation of the heat available for component ice protection requires determination of the losses that occur during transport of the heat through the duct system, from the heat source to the protected surface. It also requires determination of the amount of residual heat lost to the air flowing through the ducts and exhausted into the airstream. Equations defining the heat transported to the internal surfaces of the component to be protected and for conducting the heat through the component structure to the external surfaces involve a number of factors that can introduce a degree of uncertainty.

The equations used to predict heat required and heat available to provide the desired ice protection can be evaluated through use of test data. Data for this purpose can be obtained from measurements taken with the component located in a wind tunnel, or from measurements taken from an essentially identical component installed on an aircraft. The surface temperatures resulting from exposure to test icing conditions and from measured amounts of heat supplied to the component provide the primary measure of accuracy. The amount of heat supplied to the component can be compared with the amount of heat available from the heat source for the various operating conditions. The observed surface temperatures can be compared with those predicted by the equations.

Location of the temperature observation points can affect the sufficiency of the evaluation, and requires careful consideration. Performance-critical aspects of the installation should be considered

as the basis for locating the temperature measuring points to ensure that the range of temperatures along the surfaces of the test component is covered. Also, test conditions should cover a range of exposures sufficient to provide confidence that the equations can be accepted as a basis for evaluating the performance of the system.

Hot air ice protection systems are often similar in construction to systems used in a previous design for which certification data is available. Differences may involve minor changes in the size and shape of the components, but component materials and the design of the systems for transporting the heat to the surfaces to be protected are essentially the same. It may be permissible in these instances to limit the evaluation tests to a comparison of heat required and heat available, and to omit observation of surface temperatures. An analysis would be required to prove the applicability of the equations used to predict surface temperatures in terms of heat available.

Figure 3-1 illustrates the results of an analysis of the anti-icing requirement for the engine inlet lip of a typical FAR Part 25 transport. The figure shows the total heat release in BTU/hr as a function of altitude for several operating conditions. (The units on the ordinate must be multiplied by 10^4. For example, 8 is 80,000 BTU/hr.) The solid lines represent calculations of the heat required for the various operating conditions. The dashed lines are presented as the actual heat released, but the method for determining these values is not indicated. Additional information would be needed to demonstrate that the method for determining heat requirements actually produces the needed surface temperatures, and data points should be included on the figure to indicate test results. Also, there is no indication that the calculations were made for the performance-critical operating situations in the envelope of design icing conditions, and this aspect of the test results should be covered in the text.

The heat available for the engine inlet lip during the holding operation is illustrated by the dashed line and is shown to vary from 8.5×10^4 BTU/Hr at 5,000 feet to 8.1×10^4 BTU/Hr at 20,000 feet. It is shown to be greater than the amounts of heat required for operation as an evaporative system in continuous maximum icing conditions, and also for operation as a running wet system in intermittent maximum icing conditions.

The heat released during climb and cruise operations is shown to substantially exceed requirements for running wet protection at all altitudes; however, the curves for heat released and for heat required for evaporative protection converge at about 10,000 feet for climb and at about 12,000 feet for cruise (after extrapolation). Figure 3-1 also indicates that an evaluation would be required for the lower altitudes to determine the consequences of ice formations that might develop from run-back water when the system does not provide evaporative protection. Although the heat available for climb and cruise operations is substantially greater than requirements for operation as a running wet system, the presentation would not be sufficient without additional analysis and test data.

V.3.2 AIRCRAFT OPERATION AS AN INTEGRATED SYSTEM

3.2.1 Flight Testing the Aircraft

Flight test programs serve the purpose of establishing that all the components function as intended without adverse interaction or unforeseen problems; also, the test programs naturally insert the pilot in the control system. This provides the operational pilot evaluation of system performance that is not provided during component analyses and testing. Procedures and system controls that prove to require exceptional piloting alertness, skill, or strength, are not acceptable.

3.2.2 Flight Test Illustrations

Illustrative test data for the Generic Model A Aircraft would have to be concocted since the aircraft does not exist. Instead, this discussion makes use of data available from technical papers. Reference 1, "Qualification of Light Aircraft for Flight in Icing Conditions," is a 1971 S.A.E. paper by Paul R. Leckman of Cessna Aircraft Company. The paper presents information concerning the performance of the Cessna Super Skymaster in icing conditions along with comparable information for the Cessna Centurion.

Figure 3-2 is Figure 10B in the S.A.E paper. It illustrates icing effects on brake horsepower as a function of airspeed for the Super Skymaster. The solid line labeled, "CLEAN-NO ICE," represents performance without ice formations on the aircraft. The dashed lines were calculated to fit the observed test points for flight test conditions producing the indicated accumulations of ice. A dashed line was not shown for the 1-inch icing condition labeled "PROP ANTI-ICE ONLY" since the data point fell on the calculated performance line for operation in FAR Continuous Maximum icing conditions with propeller anti-icing system turned on and the wing and tail systems turned off. The agreement between calculated and observed performance confirms the method of calculation and provides the confidence desired when the method is used to calculate performance in other icing conditions.

Data is not shown in Figure 3-2 to indicate performance after the various ice protection systems were operated. Additional information in the paper indicates that about half of the performance loss was recovered when the wing and tail boot systems were operated after the icing encounters.

A curious aspect of icing tests is illustrated by the information shown in Figure 3-2. The wing and tail ice protection systems were not operated during the encounter, and the resulting ice formations produced airspeed losses of 70 to 80 MPH when formation thickness exceeded one inch of ice. The power required for level flight increased from 120 to 200 horsepower. The fact that an aircraft was able to continue flight in design icing conditions without operating the wing and tail protection systems does not, of course, imply that the systems are not needed. The tests, plus the data analysis in such reports, do show that a margin of additional performance is provided by the protection systems in the event that severe icing conditions exceeding the design standard are encountered.

Additional data shown in the report indicate that aircraft rates of climb in FAR Continuous Maximum icing conditions were reduced from approximately 1000 feet per minute at 10,000 feet in clear air to 600 feet per minute in icing conditions with the protection systems operating, and to 150 feet per minute in icing conditions with the systems turned off; also, the aircraft's ceiling as indicated by a 100 foot per minute rate of climb was reduced from about 31,000 feet in clear air to about 24,000 feet in icing conditions with the protection systems operating, and to 16,000 feet in icing conditions when the systems were not used. The ice protection systems on the aircraft substantially improved aircraft performance capability for operation in icing conditions.

3.2.3 Stability and Control

No attempt will be made in this section to develop the equations and analysis techniques needed to evaluate ice formation effects on aircraft stability. It is an important area that requires more attention than can be given to the subject at this time. Its importance is indicated by the icing accidents that occur when pilots are reducing speeds for approach and landing operations. Ice formations affect pitching moments and also the ability of the horizontal and vertical stabilizers to control aircraft attitude. Center of gravity limits can be reduced in some situations, and aircraft stall characteristics can be altered substantially. The effects of ice formations on stability control must include consideration of any special problems resulting from the flap settings used for approach and landing operations. Other considerations involve the potential changes in stability control that could result when power is reduced and when ice formations are removed by turning on the wing and tail protection systems after significant formations have accumulated on the aircraft.

The test data shown in Figure 3-2 does not include information for the 80 to 120 MPH speeds associated with approach and landing operations. Flight tests at these speeds become quite hazardous, and the effects on stability and control are mainly determined by analysis and by the judgment of experienced flight test pilots.

3.2.4 Performance Calculations

The increase in aircraft drag that results when ice forms on aircraft structures is a primary performance consideration. Power has to be increased to maintain flight, and power available is reduced when ice formations affect propeller efficiency. The power required for level flight without ice formations can be expressed by the following equations:

$$D = T = C_D\, q\, S \tag{3-1}$$

$$THP_r = \eta BHP_r = D\left[\frac{V}{550}\right] = C_D\, q\, S\, \left[\frac{V}{550}\right] \tag{3-2}$$

The variables in these equations are:

D	= Drag	(lbs)
T	= Thrust	(lbs)
V	= Airplane True Velocity	(ft/sec)
THP_r	= Thrust Horsepower Required	(hp)
BHP_r	= Brake Horsepower Required	(hp)
n	= Propeller Efficiency	(Dimensionless)
C_D	= Coefficient of Drag	(Dimensionless)
q	= Dynamic Pressure	(lb/ft^2)
S	= Wing Area	(ft^2)

Pilots encountering icing conditions tend to increase power to maintain airspeed and to let airspeed drop after power reaches some arbitrary higher level. The relation between rates of climb and excess power provides an indication of the reduction of climb capability that occurs as power is increased. A typical report of severe icing from a pilot operating a light aircraft often indicates that maximum power is being used to hold altitude.

Reserve power, the excess over the power required, is a measure of the aircraft's ability to overcome the drag effects of ice accumulation by adding more power. Reserve power is also a measure of aircraft ability to climb as indicated by the following equations:

$$\delta THP = THP_a - THP_r = \frac{RC\ W}{33000^*} = \eta BHP_a - \eta BHP_r \tag{3-3}$$

$$\text{and} \qquad RC = \frac{33000\ (\eta BHP_a - \eta BHP_r)}{W} = \frac{\delta THP\ (33000)}{W} \tag{3-4}$$

The variables in these equations are:

δTHP	= Excess Thrust Horsepower	(hp)
THP_a	= Thrust Horsepower Available	(hp)
BHP_a	= Brake Horsepower Available	(hp)
RC	= Rate of Climb	(ft/min)
W	= Aircraft Weight	(lbs)
*	33,000 = 60 x 550, for climb rates in ft/min.	

A ratio of the rate of climb in icing conditions to the rate of climb normally experienced in the same operating circumstances in clear air can be expressed by the following equation:

$$\frac{RC_i}{RC} = \frac{\delta THP_i}{\delta THP} = \frac{\delta\eta BHP_i}{\delta\eta BHP} \qquad (3\text{-}5)$$

where the subscript i is used to indicate parameters associated with icing conditions. Equations 3-3, 3-4, and 3-5 cannot be used for direct comparison when airspeeds are different unless the equations are modified to include an airspeed factor.

Another useful equation for evaluating test data and operational situations relates the coefficient of drag in icing situations to the coefficient of drag in clear air for the same operating situation and to the ratio of true airspeeds and power requirements. This equation is obtained by solving equation 3-2 for C_D and by forming a ratio for iced and non-iced parameters in the equation.

$$\frac{C_{Di}}{C_D} = \left[\frac{V}{V_i}\right]^3 \left[\frac{THP_i}{THP_r}\right] \qquad (3\text{-}6)$$

$$= \left[\frac{V}{V_i}\right]^3 \left[\frac{\eta_i}{\eta}\right] \left[\frac{BHP_i}{BHP_r}\right]$$

$$= \frac{THP_i}{THP_r} = \frac{\eta_i}{\eta} \left[\frac{BHP_i}{BHP_r}\right] \quad \text{(for the same airspeed)}$$

The typical efficiency of constant speed, variable pitch propellers is 0.86 to 0.90 and is assumed to be 0.9 for the full range of operational power settings for the Generic Model A aircraft. Test programs should be conducted to determine the reduction in propeller efficiency in icing conditions with and without operating the anti-icing system.

3.2.5 Estimating Ice Formation Effects on Drag Forces

Estimates of the aerodynamic effects of ice formations are essential to an aircraft icing analysis. The approach outlined in this section requires that drag estimates be made for iced wings and tails and then be combined to estimate the drag for the entire aircraft. More sophisticated methods of analysis using computer codes in an integrated approach are under development but are not discussed here.

Consider an airfoil representing a wing or tail cross section. An ice shape might be estimated for the icing conditions under consideration in one of the following ways:

1. Use an icing wind tunnel to simulate the ice shape for the given conditions.
2. Use an ice accretion computer code such as LEWICE to estimate the ice shape that would accrete at the given conditions. The engineer needs to consult relevant reports concerning the ice accretion computer code used to verify that it is validated or at least calibrated for

the airfoil and conditions in question and also to estimate the uncertainty inherent in its use. Ice accretion computer codes are discussed in Chapter IV, Section 2.

3. Calculate the area of the cross section of the formation that would develop if ice formed in the impingement region. With this approach, the shape of the formation can be adjusted, using relevant experimental data, while keeping the area of the cross section constant.

If an ice shape is estimated, the attendant drag might be estimated by one of the following approaches:

1. Use a computer flow code that is validated or at least calibrated for the type of airfoil and ice shape to be considered. The code must calculate viscous effects and would probably be either a Navier-Stokes solver or an interacting boundary layer code. These codes are discussed in Chapter IV, Section 2.
2. Determine drag force increases from wind tunnel or flight tests with artificial ice formations representing the shapes that have been estimated. If an icing wind tunnel was used to determine the ice shape, the the drag can be measured in the icing wind tunnel for the actual ice accretion rather than using an artificial ice shape.

The following two approaches do not require the estimation of the ice accretion, except that it must be specified as rime or glaze. Unfortunately, it is often very difficult to determine whether either approach is appropriate for a particular problem, and, if it is, to estimate the uncertainty in its use.

1. Use one of the icing drag correlations discussed in Chapter I, Section 2. As noted there, the engineer should study the original report where the correlation appears to determine if it is appropriate to the airfoil and icing conditions that he is studying and to estimate the uncertainty in the use of the correlation.
2. Use the "matching" approach, i.e., match the airfoil in question with another airfoil which has similar impingement characteristics and pressure distribution (at least in the impingement region) and for which adequate experimental data is available.

Of the approaches discussed above, the most attractive from a cost point of view may be the use of an ice accretion computer code to predict the ice shape and then the use of a viscous flow code to precict the coefficient of drag. It is of course essential that the codes be validated or at least calibrated for the airfoil and conditions under study. However, in the rest of this section, the approach that will be used will be the matching approach. This is strictly for convenience in illustration and calculation. The data used is from a NACA wind tunnel investigation of icing effects on the drag of a symmetrical airfoil with an 87.4 inch chord. Information is used concerning component angle of attack, the

calculated weight of water impingement per foot span, and the chord lengths of the components for which the estimates are to be made. It is necessary to determine of the icing conditions would result in a rime ice formation or a ridge type glaze formation. Figure 3-3 presents the data to be employed. The ordinate is the change in drag coefficient, the abscissa is the angle of attack, and the curves show the change in drag coefficient for a range of icing accumulations for rime ice and for ridge-type glaze icing.

Table 3-1 presents steps that may be followed in the estimation of drag for an entire aircraft in an icing encounter. Steps 2 and 3 involve the estimate of drag resulting from ice on the wings, horizontal stabilizer, and vertical stabilizer. These steps assume that all three airfoils can be satisfactorily matched to a NACA 0011 airfoil. This is clearly not a realistic assumption and is made strictly for convenience. In actual practice steps 2 and 3 would likely be replaced by one of the other approaches for estimation of drag on an airfoil as discussed above.

V.3.3 ICE FORMATION EFFECTS ON GENERIC MODEL A PERFORMANCE

3.3.1 The Performance-Critical Holding Problem

3.3.1.1 The Operating Problem

The holding operation for the performance-critical design problem is conducted at 7,000 feet, with 17°F air temperatures, and an equivalent air speed of 125 MPH. LWC is 0.5 g/m^3, MVD is 22, and the droplet distribution is type D. The true airspeed is 136 MPH, which is 200.2 ft/sec. (For such calculations used in this section, refer to table 2-6 in Chapter V, Section 2.) The airplane is assumed to be in the cloud continuously during a 45 minute holding period and to be following a rectangular course. If the analysis shows that the airplane is not capable of withstanding the 45 minute holding operation, a reasonable period may be established for the airplane, but this limitation must be placed in the airplane flight manual.

3.3.1.2 Estimating Drag Increases

The dynamic pressure is 39.98 pounds. The following performance calculations can be made for the Generic Model A airplane:

$$C_L = \frac{4800}{39.98\ (207)} = 0.58 \qquad (3\text{-}7)$$

$$\alpha = \frac{0.58 - 0.387}{.0713} = 2.71^\circ \qquad (3\text{-}8)$$

Equation 2-1 in section 2.0 defined the coefficient of drag for the Generic Model A aircraft as a function of the coefficient of lift for the airplane. With this form of expression, the coefficient of drag defines the drag forces for the entire aircraft and not just for the wing. The total drag force acting on the airplane is the sum of the drag forces acting upon the various components, and a relation

is needed to account for the size effect. The following equation expresses the drag as the sum of the drag forces for the wing, horizontal stabilizer, and the vertical tail. (The drag forces resulting from other components, as well as interference drag, should be included but are ignored for this illustration.)

Total Drag = Drag of (Wing + Horizontal Stabilizer + Vertical Tail)

$$D = C_D\, q\, S = (C_{DW}\, q\, S_W) + (C_{Dh}\, q\, S_h) + (C_{Dt}\, q\, S_t) \qquad (3\text{-}9)$$

$$C_D = \left(C_{DW}\,\frac{S_W}{S}\right) + \left(C_{Dh}\,\frac{S_h}{S}\right) + \left(C_{Dt}\,\frac{S_t}{S}\right)$$

$$= (C_{DW}\,(1)) + \left(C_{Dh}\,\frac{38.8}{207}\right) + \left(C_{Dt}\,\frac{24.4}{207}\right)$$

$$= C_{DW} + .187\, C_{Dh} + .118\, C_{Dt} \quad \text{for Generic Model A} \qquad (3\text{-}10)$$

where equation 3-9 was solved for C_D to obtain equation 3-10. S_W is equal to S, and is the area of the wing, which is 207 ft^2. The area of the horizontal stabilizer is 38.8 ft^2, and the area of the vertical tail is 24.4 ft^2. Therefore, the coefficients of drag force associated with the horizontal stabilizer and the vertical tail are reduced by the ratio of their surface area divided by the area of the wing to obtain the proportional contribution to the total drag force. The ratio is .187 for the horizontal stabilizer and .118 for the vertical tail.

For illustration purposes, the coefficients of drag for the holding problem will be determined for 15 minutes, 30 minutes, and for 45 minutes, and it will be assumed that the formations grow at the same rate throughout the encounter.

The equation for total drag as a function of the coefficient of lift for the Generic Model A aircraft was defined in Chapter V, Section 2 as follows for flight in clear air:

$$C_D = .046\ C_L{}^2 + .03 = .0455 \quad \text{for the holding problem} \qquad (3\text{-}11)$$

Using figure 3-3 for the double ridge ice formation the following drag values are obtained. (Note that the calculation of W_{lb} is illustrated in Chapter V, Section 2.2.4.)

The coefficient of drag = δC_{Di} + C_D = C_{Di}				
15 minutes	W_{lb}	Fig 3-3 x	87.4/MAC x	Area Ratio
Wing	0.60	.0124	.0162	.0162
Hori.Stab	0.43	.0086	.0203	.0038
Vert.Stab.	0.41	.0082	.01	.0016
				.0216 + .0455 = .0671

30 Minutes				
Wing	1.20	.0219	.0286	.0286
Hori.Stab.	0.86	.0157	.0371	.0069
Vert.Stab.	0.82	.0149	.0249	.0029
				.0384 + .0455 = .0839
45 Minutes				
Wing	1.80	.0328	.0428	.0428
Hori.Stab.	1.28	.0233	.0550	.0103
Vert.Stab.	1.23	.0244	.0407	.0048
				.0579 + .0455 = .1034

3.3.1.3 Performance for the Holding Operation

The power requirements clear air and for the 15 minute, 30 minute, and 45 minute holding operations can now be calculated through use of equation 3-2.

$$THP = nBHP = D\left[\frac{V}{550}\right] = C_D\ q\ S\ \left[\frac{V}{550}\right] \qquad (3\text{-}2)$$

The rate of climb can then be calculated through the use of equation 3-4.

$$RC = \frac{33000\ (nBHPa - nBHPr)}{W} = \frac{\delta THP\ (33000)}{W} \qquad (3\text{-}4)$$

The power required in clear air is calculated as follows:

$$D = C_D\ q\ S = .0455(39.98)(207) = 376.6 \text{ pounds}$$

$$THP_r = \frac{D\ V}{550} = \frac{376.6\ (200.2)}{550} = 137 \text{ hp}$$

$$BHP_r = \frac{THP_r}{n} = \frac{137}{0.9} = 152.2 \text{ hp}$$

The rate of climb in clear air is given by:

$$RC = \frac{(296-137)(33000)}{4800} = 1093.1\ \frac{ft}{min}$$

The power required and rate of climb after 15 minutes, 30 minutes, and 45 minutes are calculated in the same way, using the C_D values obtained above. The results are given in the following table. It is assumed that propeller efficiency is not effected by ice formations.

	C_D	Drag (lb)	THP (hp)	BHP (hp)	RC (ft/min)
Clear air	.0455	377	137	152	1093
15 minute hold	.0671	555	202	225	645
30 minute hold	.0839	694	253	281	297
45 minute hold	.1034	856	311	346	-106

Note that sometime between 30 and 45 minutes the aircraft would no longer be able to hold altitude, i.e., it would be forced to descend.

The pilot would have traded speed for altitude if he were unable to change altitude. Suppose that the pilot maintained altitude but reduced speed to an equaivalent airspeed of 105 MPH (a true airspeed of 168 ft/s). For this speed, the maximum available thrust horsepower is 274 hp and the dynamic pressure is 28.21 lb/ft^2. For this dynamic pressure, the coefficient lift is found, as in equation 3-7, to be .82 and the coefficient of drag for clear air is found, as in equation 3-11, to be .064. The values in the table below are calculated just as above.

	C_D	Drag (lb)	THP (hp)	BHP (hp)	RC (ft/min)
Clear air	.064	374	114	127	1100
45 minute hold	.122	712	218	242	388

So at this airspeed the aircraft can still climb after holding for 45 minutes. Note that the 45 minute hold calculation was done using the same value of .0579 for the increment in C_D due to icing, even though less ice would accrete at the slower speed and the value of the increment in C_D would be somewhat reduced. Thus the gain from flying at the slower speed would be greater than shown.

No consideration has been given to the possible loss of power due to propeller icing. Calculations in Section 2 of this Chapter indicated that the outer 11.8 inches of the propeller would be ice free in the 17°F icing conditions and that the performance-critical icing condition for the propeller would be in the colder, higher liquid water content conditions. Losses in propeller efficiency should be determined but typically would not be more than about 5% when the anti-icing system is operating properly. Flight test data would be required to evaluate this aspect of the problem.

3.3.2 Climb-Cruise-Climb Problem

3.3.2.1 The Problem

Table 3-2 presents flight operating data for the climb-cruise-climb operating problem discussed in Section 2 for the Generic Model A aircraft. For this problem it was assumed that the aircraft would encounter FAR 25 Continuous Maximum Icing Conditions at 2,500 feet during climb to a planned 7,000 foot cruising altitude and that icing would continue after level-off. A second climb would begin

after about 3 minutes when permission to climb to 11,000 feet would be obtained from Air Traffic Control. The top of the icing layer was assumed to be at 9,000 feet.

The thickness of the icing layer for the calculations is 6,500 feet. The air temperatures selected for the problem are approximately those associated with the most probable icing condition temperatures for the various altitudes. The climb operation would be performed at an equivalent airspeed of 105 MPH with rates of climb in clear air varying from 1450 feet per minute to 1100 feet per minute in the first climb segment. The pilot would be expected to maintain the same airspeeds during climb after icing is encountered, but rates of climb would be reduced due to the effects of ice formations. A distance of 6.56 miles would normally be traveled during the climb to 7,000 feet.

The true airspeed for the Generic Model A aircraft is normally increased after level-off at 7,000 feet to 205 MPH, and power is cut back to cruise power settings. The aircraft travels an additional distance of 10.01 miles in the 2.93 minutes that elapse before a decision is made and approved to continue the climb. An additional distance of 3.78 miles would normally be traveled during the 1.94 minutes required to climb to the 9,000 foot level at rates of climb that vary from 1100 feet per minute to 960 feet per minute.

3.3.2.2 Estimating Drag Increase

Drag estimates for the Generic Model A aircraft are to be based upon the weight of impingement and a double ridge type of ice formation. The information shown in Figure 3-3, from NACA TN-3564, Reference 2, provides the basis for these estimates. This procedure for estimating the increase in coefficient of drag is assumed to be applicable to the Generic Model A airplane problem. The calculated accumulations of ice that would form on the wings of the Generic Model A aircraft for the climb-cruise-climb problem are shown in Table 3-3. These estimates were developed in Section 2 and represent flight in icing conditions with a 20 micron MVD, a D distribution, and the most probable temperatures for the various flight altitudes. The calculations for the increases in the coefficient of drag associated with the formations are shown in Table 3-4.

3.3.2.3 Climb-Cruise-Climb Performance

Table 3-5 presents the estimated wing icing effects of the performance of the Generic Model A aircraft for the Climb-Cruise-Climb problem. The change in the coefficient of drag for the wing during the climb to 7,000 feet was estimated to be .004. This change would increase power requirements from 114 to 121 THP and reduce rates of climb from 1100 to 1052 feet per minute.

The coefficient of drag when the aircraft begins to accelerate to the intended cruise speed of 205 MPH is shown to be increased by .003 instead of the .004 determined for the climb condition. The difference results because of the angle of attack effect shown in Figure 3-3. Power requirements for initial cruise at 7,000 feet with ice formations from the climb operation are shown in Table 3-5 to increase from 337 to 368 THP. Thrust Horsepower Available is shown to be only 360 ft-lb/sec, and the aircraft would not be able to accelerate to the intended 205 MPH without descending at a rate of 55 FPM.

The coefficients of drag for the wing when the aircraft begins the second climb segment are shown to increase 0.012 for climb at 7,000 feet and to 0.014 for climb at 9,000 feet and 11,000 feet. The rates of climb when the second climb was started at 7,000 feet are shown to be reduced from 1100 to 949 feet per minute at 7,000 feet, from 960 to 790 feet per minute at 9,000 feet, and from 830 to 653 feet per minute at 11,000 feet. The time to climb from 7,000 feet to 9,000 feet would increase from 1.94 minutes to approximately 2.25 minutes as a result of the decreased rates of climb.

The aircraft would not be able to cruise at 11,000 feet at the planned speed of 196 MPH (V_e =167). The thrust horse power available is shown to be 290 as compared to the 352 requirement. The 0.0106 increase in the coefficient of drag would reduce the speed to approximately 179 MPH. Thrust Horsepower available at 11,000 feet is shown to decrease from 290 to 280 ft-lb/sec as a result of the slower speed. The wing ice formations would produce a 17 MPH loss of airspeed for the power setting.

These calculations consider only the effect of ice formations on the wing of the aircraft. There would be additional increases in drag as a result of ice formations on other parts of the aircraft, and a loss of power would be expected even with the propeller ice protection system operating.
The analysis would need to be completed to include drag associated with other components if prepared for FAA certification purposes.

3.3.3 Evaluation Criteria

There are no definitive standards for determining that aircraft performance during climb operations is or is not acceptable when equipment operates properly in design icing conditions and when there is no stability control problem; however, the ability to climb at 11,000 feet at a rate of 653 FPM without deicing the wing surfaces after the climb-cruise-climb performance critical design icing encounter indicates that the Generic Model A aircraft has the reserve performance needed to permit flight into known icing conditions and to escape from any encounter involving the climb-cruise-climb operating situations . For the holding problem, the aircraft was not able to maintain the planned holding speed at 7,000 feet. The calculations indicated that the aircraft should be able to climb at 388.4 ft/min when speed was reduced to its best climb speed at 7,000 feet after accumulating ice formations resulting from the 45 minute holding problem. The performance capability is marginal but may be acceptable depending upon the results of stability control evaluations.

Therefore, the flight handbook would be written to indicate that the aircraft may be flown into known light or moderate icing conditions when all ice protection equipment is functioning properly and that immediate diversion is required when severe icing conditions are encountered.

V.3.4 FLIGHT HANDBOOK

3.4.1 Requirements

FAR Part 23.1419, Ice Protection, indicates that the recommended procedures for the use of the ice protection equipment must be set forth in the Airplane Flight Manual or in approved manual material. FAR Part 23.1416, paragraph (c), requires a means to indicate to the flight crew that the pneumatic de-ice boot system is receiving adequate pressure and is functioning normally. FAR Part 23.1583, paragraph (h), Kinds of Operation, indicates that the kinds of operation (such as VFR, IFR, day, or night) in which the airplane may or may not be used, plus the meteorological conditions under which it many or may not be used, must be furnished. This paragraph also indicates that any installed equipment that affects any operating limitation must be listed and identified as to operation function.

3.4.2 Operating Instructions

No attempt will be made to present flight operating instructions for the Generic Model A airplane. If the instructions were to be prepared, they should include the following points which should be evaluated and modified as necessary as a result of the flight test program:

1. De-icing boots are intended for removal of ice after it has accumulated rather than to prevent its formation. If ice accumulation is slow, best results can be obtained by not using the de-ice system until approximately half an inch of ice has accumulated. The accumulation should be cleared with one or two cycles of operation and the boots should be turned off until another half an inch of ice has accumulated.

2. The boots should not be operated continuously. If ice accumulation is rapid, larger amounts of ice should be allowed to accumulate before cycling the boots. An inch may be recommended depending upon the results of the flight test program.

3. The engines, propellers, and airspeed system should qualify for flight into severe icing conditions. The pilot should be advised to switch the air induction system to alternate air when icing is expected.

4. The airframe systems would qualify the aircraft for flight in rime icing up to and including the continuous and instantaneous maximum conditions, but lack of power limits performance capability when flight is in continuous maximum conditions producing the ridge type of mixed rime and clear icing. If severe icing conditions are those that exceed the continuous maximum, then the aircraft should qualify for flight in known and forecast light and moderate rime icing conditions, and in light mixed rime and clear, or clear icing conditions. The pilot should be required to avoid flight into known or forecast moderate icing conditions whenever possible and to take immediate action to exit severe icing conditions. He should also be required to exit moderate mixed rime and clear icing conditions when ridge type formations are developing.

5. The aircraft will be unable to maintain altitude and airspeed in an extended holding operation in the heavier icing conditions, and action should be taken to avoid such circumstances. If a holding situation develops involving ridge type mixed rime and clear icing conditions, the pilot should request emergency assistance if lower altitudes are not available due to terrain or the traffic situation.

6. An accumulation of 1/2 inch or more of mixed rime and clear icing and the double ridge wing type ice formations will cause a large loss of airspeed and climb capability as well as significant buffet and stall speed increases.

7. Extra airspeed and power should be added during the approach, and the pilot should be prepared for stalling conditions without the usual warning signals. The stall indicator will not provide a reliable warning signal if ice formations are allowed to remain on the wings and tail during the landing operation.

V.3.5 REFERENCES

1. Leckman, Paul R., of Cessna Aircraft Co., SAE Paper 710394, "Qualification of Light Aircraft for Flight in Icing Conditions," Presented at the March 24-26, 1971 National Business Aircraft Meeting, Wichita, Kansas.
2. Bowden, D. T., NACA TN 3564, "Effect of Pneumatic De-Icers and Ice Formations on Aerodynamic Characteristics of an Airfoil," February, 1956.

TABLE V 3-1

PROCEDURE FOR CALCULATING DRAG INCREASE BASED UPON THE WEIGHT OF ICE

1. Determine the wing angle of attack, the accumulation of ice per foot span, and the type of ice formation that is most appropriate.

2. Using figure 3-3, read the drag increase indicated for the component angle of attack and the ice accumulation curve for weight of ice per foot span that is nearest to the weight of the observed ice accumulation.

3. Multiply the resulting number by the ratio of the calculated pounds per foot span of ice accumulation on the component divided by the value associated with the curve which was selected for the comparison.

4. Multiply the adjusted number by another ratio determined by chord length comparison, which in this instance is the 87.4 inch chord associated with the data for the ice accumulation curves, divided by the chord length of the component for which drag force increases are being estimated.

5. The increments of drag must be adjusted by the area ratios determined in equation V 3-10 to determine the appropriate values for use in the equations when the coefficients of drag are expressed as a proportion of the coefficient for total drag.

TABLE V 3-2

GENERIC MODEL A AIRCRAFT CLIMB-CRUISE-CLIMB PERFORMANCE WITHOUT ICE

	Altitude Feet	Temp. °F	Speed-MPH True	V_e	Climb FPM	Time* δt	Distance Miles	Wing C_L	α
Climb	2,500	23	106	105	1450	0.00	0.00	.82228	6.10
Climb	3,000	22	107	105	1400	+0.35	0.62	.82228	6.10
Climb	5,000	19	111	105	1250	+1.51	2.74	.82228	6.10
Climb	7,000	17	115	105	1100	+1.70	3.20	.82228	6.10
						Σ3.56	Σ6.56		
Cruise	7,000	17	205	188	0	+2.93	+10.01	.2570	-1.80
						Σ6.49	Σ16.57		
Climb	7,000	17	115	105	1100	+0.00	+0.00	.82228	6.10
Climb	9,000	15	119	105	960	+1.94	+3.78	.82228	6.10
Climb	11,000	12	123	105	830	_____		.82228	6.10
						Σ8.43	Σ20.35		
Cruise	11,000	12	195	166	0			.35275	-0.83
or									
Cruise	11,000	12	179	153	0			.38874	-0.01

* Time in minutes from climb through the 2500 foot level.

TABLE 3-3

WING ICE ACCUMULATIONS FOR CLIMB-CRUISE-CLIMB PROBLEM

Flight Operating Problem	W_{lb} Pounds H_2O	Volume Cubic Inches	Ice Accumulation Wing δ_i In	Area A_i^2	Meter δ_{ir} In
Climb to 7,000 ft	.1151	3.74	.0626		.24
Accelerate to cruise at 7,000 ft	.1151	3.74	.0626		.24
Begin climb from 7,000 to 11,000 ft	.3415	11.11	.1879		.62
Climbing out of ice at 9,000ft	.3453	11.23	.2240		.76
Begin cruise at 11,000 ft	.4077	13.26	.2240		.76

TABLE V 3-4

AIRFOIL DRAG INCREASE CALCULATIONS FOR CLIMB-CRUISE-CLIMB PROBLEM

1. **Climb to 7,000 feet accumulates 0.1151 pounds of ice per foot span**
   a. Read .008 for .03 pounds at 6.1°
   b. $C_{Di} = C_D + \delta C_D = .064 + .008 \times (.1151 \div .3) \times (87.4 + 67)$
      $= .064 + .004 = .068$

2. **Begin cruise at 7,000 with 0.1151 pounds of ice per foot span**
   a. Read .006 for .03 pounds at -1.8° (use 0° on figure)
   b. $C_{Di} = C_D + \delta C_D = .0330 + .006 \times (.1151 \div .3) \times (87.4 + 67)$
      $= .033 + .003 = .036$

3. **Begin climb to 11,000 feet with 0.3414 pounds of ice per foot span**
   a. Read .008 for .03 pounds at 6.1°
   b. $C_{Di} = C_D + \delta C_D = .064 + .008 \times (.3414 \div .3) \times (87.4 + 67)$
      $= .064 + .0119 = .0759$ Use .012 and .076 for Calculations

4. **Climbing at 9,000 feet with .3414 + (3.78*+6.56*) x .1151=.4077 lb/ft-span**
   a. Read .008 for .03 pounds at 6.1°
   b. $C_{Di} = C_D + \delta C_D = .064 + .008 \times (.4077 + .3) \times (87.4 + 67)$
      $= .064 + .0142 = .0782$, Use .078

*Let the ice accumulation from 7,000 to 9,000 equal a distance traveled fraction of the accumulation resulting from the climb to 7,000 feet.

5. Accelerate to cruise at 11,000 feet with .4077 lb/ft span of ice
   a. Read .006 for .03 pounds at .83°
   b. $C_{Di} = C_D + \delta C_D = .0349 + .006 \times (.4077 + .3) \times (87.4 + 67)$
      $= .0349 + .0106 = .0455$ for attempted cruise at 195 MPH
   c. $C_{Di} = C_D + \delta C_D = .0369 + .0106 = .0475$ for cruise at 179 MPH

TABLE V 3-5

ESTIMATED EFFECTS OF WING ICING ON PERFORMANCE FOR CLIMB PROBLEM

	Without Ice Formation						With Ice Formation					
Alt	C_D	D	THP_r	δTHP	ΣTHP	RC	δC_D	C_{Di}	D	THP_r	δTHP	RC
7,000	.0640	374	114	160	274	1100	.004	.0680	397	121	153	1052
7,000	.0330	617	337	23	360	Cruise	.003	.0360	672	368	-8	-55
7,000	.0640	374	114	160	274	1100	.012	.0760	444	136	138	949
9,000	.0640	374	119	140	259	960	.014	.0780	455	144	115	790
11,000	.0640	374	124	120	244	830	.014	.0780	455	149	95	653
11,000	.0349	509	266	24	290	cruise	.0106	.0455	673	352	-62	-426
11,000*	.0369	456	218	62	280	cruise*	.0106	.0475	586	280	0	0

* True air speed was reduced from 196 MPH to 179 MPH at 11,000 feet. (Equivalent air speed was reduced from 167 to 153 MPH at 11,000 feet.)

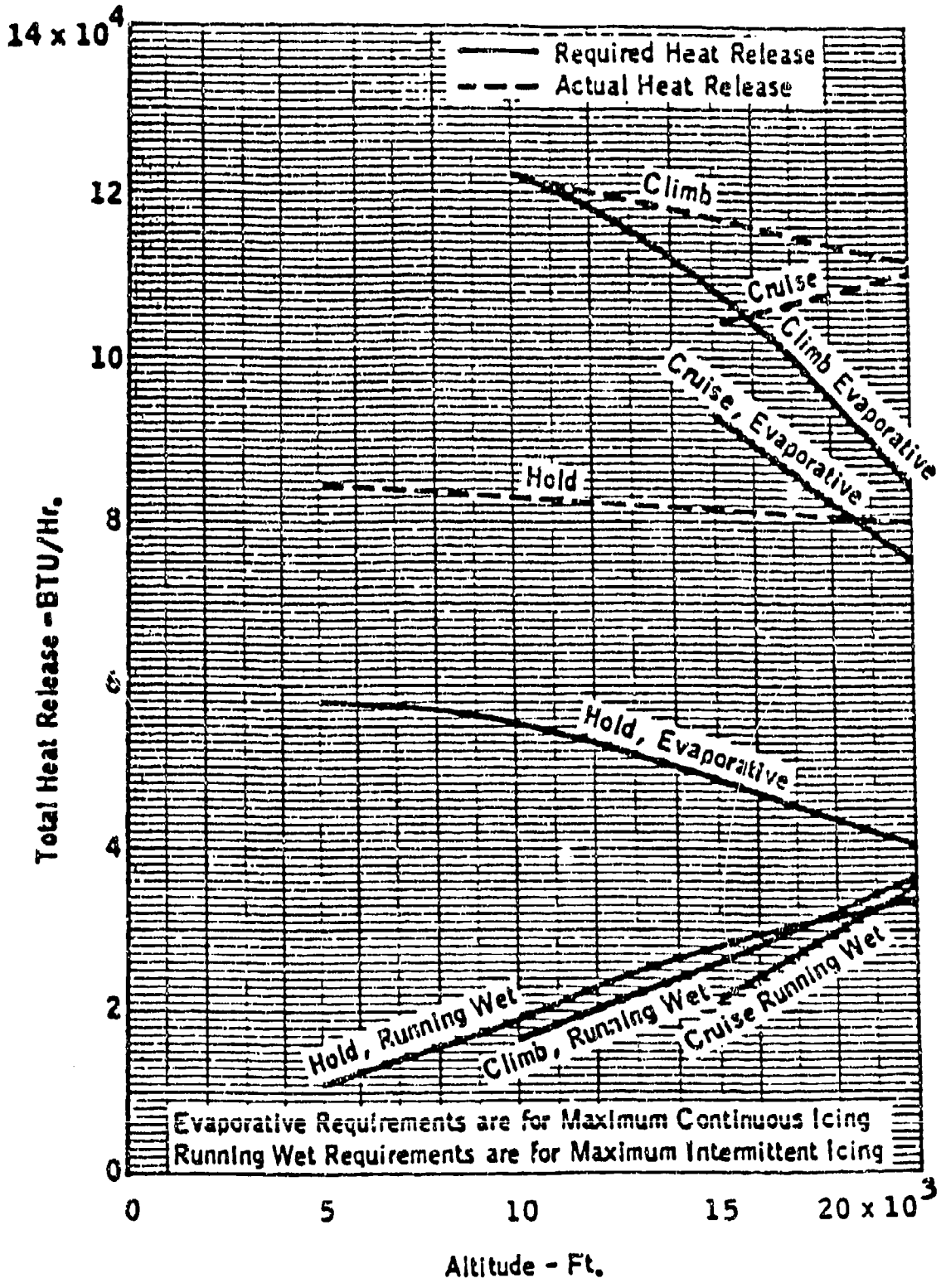

FIGURE 3-1. TYPICAL ENGINE INLET LIP ANTI-ICING HEAT RELEASE ALTITUDE

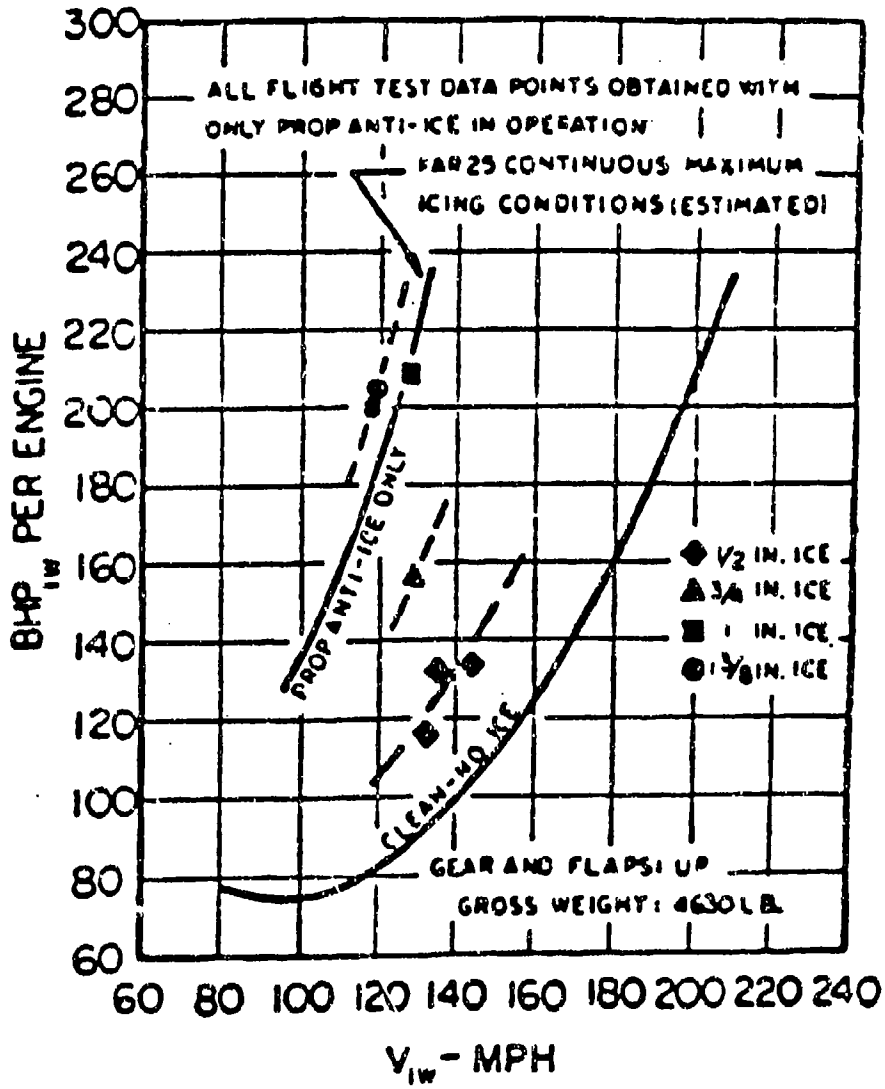

FIGURE 3-2. CORRELATION BETWEEN FLIGHT TEST AND ESTIMATED ICING CRUISE PERFORMANCE DECREMENTS FOR SUPER SKYMASTER

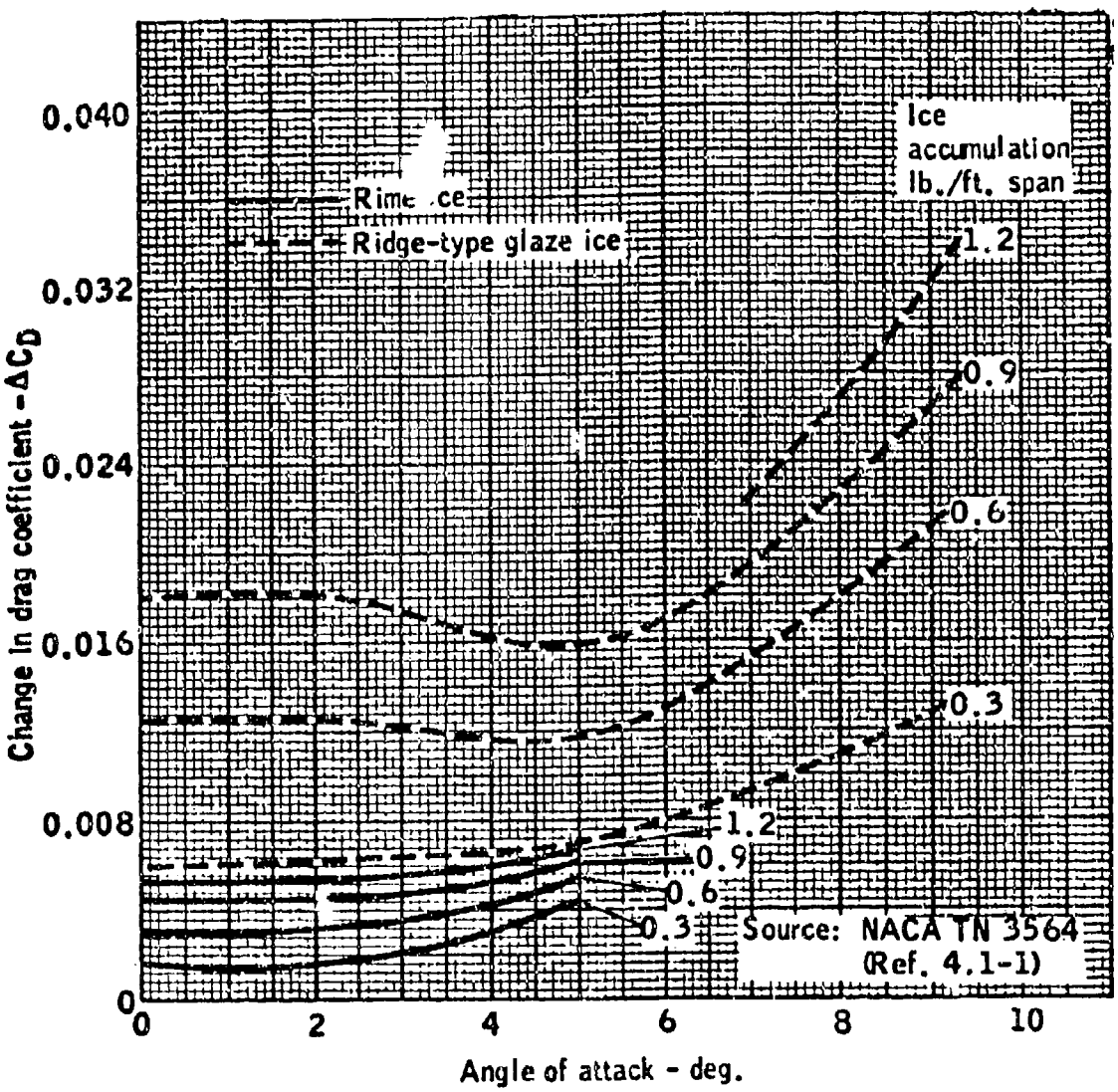

FIGURE 3-3. AIRFOIL SECTION DRAG INCREASE VERSUS ANGLE OF ATTACK FOR RIME ICE AND RIDGE-TYPE GLAZE ICE

CHAPTER V
SECTION 4.0
TESTING TO DEMONSTRATE COMPLIANCE

CHAPTER V - DEMONSTRATING ADEQUACY OF DESIGN
CONTENTS
SECTION 4.0 TESTING TO DEMONSTRATE COMPLIANCE

	page
LIST OF TABLES	V 4-iii
LIST OF FIGURES	V 4-iv
SYMBOLS AND ABBREVIATIONS	V 4-v
GLOSSARY	V 4-viii
V.4.1 INTRODUCTION	V 4-1
V.4.2 TEST PLAN	V 4-1
4.2.1 Test Description	V 4-2
4.2.1.1 Purpose	V 4-3
4.2.1.2 Aircraft Configuration	V 4-3
4.2.1.3 Instrumentation	V 4-3
4.2.1.4 Procedure	V 4-3
4.2.1.5 Data Required	V 4-4
4.2.1.6 Test Points	V 4-4
4.2.1.7 Data Analysis	V 4-4
4.2.2 Proof of Compliance	V 4-4
4.2.2.1 Explanation	V 4-4
4.2.2.2 Procedures	V 4-5
4.2.3 Example Icing Tests	V 4-6
V.4.3 REFERENCES	V 4-6

LIST OF TABLES

		Page
4-1	Example Tests - Fixed Wing Aircraft	V 4-8
4-2	Example Tests - Engine Induction System	V 4-10
4-3	Example Test Procedure for Turbojet Engines	V 4-13
4-4	Summary of Proposed Model X Icing Tests	V 4-14
4-5	Natural Icing Tests	V 4-16
4-6	FAA Flight Test Plan - All Weather Systems	V 4-17
4-7	Airframe Icing Test Program	V 4-20
4-8	Engine Inlet Icing Tests	V 4-24
4-9	Engine Ice Protection Model B - Similarity	V 4-34
4-10	Aircraft and Engine Icing Tests	V 4-36
4-11	Icing Certification Tests - A-6 Engine and B-7 Nacelle	V 4-37
4-12	Engine Nacelle Icing Tests	V 4-42
4-13	All Weather System Compliance Test	V 4-46
4-14	Windshield and Wing Boot Certification	V 4-52
4-15	Large Transport Category Aircraft Icing Certification Test	V 4-55
4-16	Test Schedule - Turboprop Icing Certification	V 4-60

LIST OF FIGURES

		Page
4-1	Ice Shape Cross Section - Inboard Wing	V 4-61
4-2	Ice Shape Installation for Initial Handling Tests	V 4-62
4-3	Ice Shape Installation for FAA Handling Tests	V 4-63
4-4	Natural Dry Air Test of Engine Induction System	V 4-64

SYMBOLS AND ABBREVIATIONS

AC	Advisory Circular
AEDC	Arnold Engineering Development Center
A/R	As Required
°c	Degrees Celsius
C.M.	Continuous Maximum
Cr/Al	Chromel/Alumel thermocouple
CRT	Cathode Ray Tube
Cu/Con	Copper/Constantan thermocouple
Dd	Droplet diameter
DAS	Data Acquisition System
DER	Designated Engineering Representative
ECU	Environmental Control Unit
E.I.	Environmental Intensity
°F	Degrees Fahrenheit
FAA	Federal Aviation Administration
FAR	Federal Aviation Regulation
FPD	Freezing Point Depressant
FTR	Flight Test Request
FTWO	Flight Test Work Order
g/m^3	Grams per cubic meter
IAS	Indicated Airspeed
I.M.	Intermittent Maximum
in.	Inch
ISA	International Standard Atmosphere
ITT	Interstage Turbine Temperature
KCAS	Knots Calibrated Airspeed
KIAS	Knots Indicated Airspeed
KTAS	Knots True Airspeed
kw	Kilowatt
lb.	Pound
LH	Left Hand
LT	Left

LWC	Liquid Water Content
M.C.	Max Continuous power
MED	Median Effective Diameter
Min	Minute
MN	Mach Number
mph	Miles per hour
MVD	Median Volume Diameter
NACA	National Advisory Committee for Aeronautics
Nl	Engine Low Pressure Rotor rpm
N2	Engine High Pressure Rotor rpm
n.mi.	Nautical mile
NRC	National Research Council
OAT	Outside Air Temperature
p	Pressure
psig	Pounds per square inch gage
Ps	Static pressure
pt	Total pressure
RH	Right Hand
rpm	Revolutions per minute
SCW	Supercooled Water
SLS	Sea Level Static
S/N	Serial number
T	Thermocouple or Temperature
TIA	Type Inspection Authorization
TIR	Type Inspection Report
μm	Micrometer (micron)
Vmin	Minimum airspeed
Vmax	Maximum airspeed
Vnor	Normal airspeed
Vs	Stall speed

Subscripts

max	maximum
min	minimum
N	Number
nor	normal
o	ambient condition
s	static
t	total
1	sensor number
2	sensor number
3	sensor number
4	sensor number
5	sensor number

GLOSSARY

liquid water content (LWC) - The total mass of water contained in all the liquid cloud droplets within a unit volume of cloud. Units of LWC are usually grams of water per cubic meter of air (g/m^3).

median effective diameter (MED) - The droplet diameter which divides the total water volume present in the droplet distribution in half, i.e., half the water volume will be in larger drops and half the volume in smaller drops. The value is calculated based on an assumed droplet distribution.

median volumetric diameter (MVD) - The droplet diameter which divides the total water volume present in the droplet distribution in half, i.e., half the water volume will be in larger drops and half the volume in smaller drops. The value is obtained by actual drop size measurements.

micron (μm) - One millionth of a meter.

V.4.0 CERTIFICATION TESTING

V.4.1 INTRODUCTION

After the design, analysis, and development tests of the ice protection system have been completed, additional tests may be required. These tests are to demonstrate to the satisfaction of the FAA Certification Directorate that the ice protection systems are adequate and that the aircraft can operate safely in natural icing conditions. The required tests will vary widely, depending upon the type of system, the amount of previous experience, and the mission and operational requirements of the aircraft. These flight tests are conducted in natural icing. This section does not present the detailed information necessary for a complete certification testing program. Rather, it describes the type of information that should be included in the test plan and test objectives. Facilities, analysis, and test methods along with atmospheric data and instrumentation used to achieve the test objectives are described in Chapters I through IV of this handbook. Early agreement between the applicant and the FAA should be reached on the test plan for compliance.

V.4.2 TEST PLAN

Test programs for an aircraft and its ice protection systems have one primary objective, ie, demonstration of safe flight through natural icing conditions. This objective can be met by conducting tests to show that the systems function properly and that the required performance has been met or exceeded. In cases where ice protection is not provided for all parts of an aircraft, the effect of ice on aircraft performance and handling characteristics must be determined.

Four methods of testing ice protection systems can be used to determine their effectiveness. These are icing tunnel tests, dry air flight tests, natural icing flight tests, and simulated icing flight tests. The method of testing will vary, depending on the aircraft or components under consideration, the design requirements, and the amount of previous data available on the particular aircraft or component (reference 4-1). Natural icing flight tests are required (reference 4-2). One of the other methods or more commonly a combination of methods may be used to demonstrate system effectiveness.

Flight tests in natural icing conditions are costly, and the specific performance-critical conditions needed to demonstrate the adequacy of ice protection systems are difficult to find. The usual procedure is to conduct tests in the maximum severity that can be found, and to use the results from these tests to confirm analysis methods and to extrapolate observed results to the performance - critical design circumstances. Data analysis techniques are discussed in chapter IV and illustrated in section 2 of this chapter.

The certification test plan is a document that is arrived at through the process of proposal by the manufacturer and then negotiation with the FAA Directorate in charge of the certification. Although the list is not intended to be totally comprehensive, the following items should be included in the test plan:

A. Description of the test
B. Purpose of the test
C. Required aircraft configuration
D. Required instrumentation
E. Test procedure
F. Data required
G. Test points
H. Data analysis

Such a plan should be prepared for each item of the aircraft that may be subject to icing where such ice accumulation may contribute to hazardous or unsafe operation of the aircraft. In many cases it is acceptable to arrange the test plan to permit simultaneous testing of multiple ice protection systems. This plan should be submitted to the FAA and agreement reached on procedures before testing is begun (reference 4-3).

4.2.1 Test Description

This section of the test plan should provide a complete description of the required test. It should give details about whether this is to be a scale model test, wind tunnel test, or a flight test, and whether it is to be in artificial or natural icing conditions.

The capabilities of the complete ice protection system to adequately protect the airplane throughout the continuous maximum and intermittent maximum icing envelopes should be demonstrated through analysis combined with instrumented tests in dry air plus artificial and natural icing conditions.

Dry Air Tests

Dry air tests with artificial ice shapes should be accomplished to verify satisfactory handling qualities, stability, stall characteristics and speeds, minimum control speed, and performance capability with the performance - critical ice accumulations predicted for unprotected surfaces and for protected surfaces with the deice mode. Proper operation of the anti-ice system should be verified following prolonged flight or exposure at the minimum operational temperature approved for the airplane to insure that the systems operate properly in the colder temperatures. In addition, it is conceivable that the fluid of a freezing point depressant (FPD) system may freeze on the wing and cause degraded system and airfoil performance.

Artificial Icing Tests

Prior to conducting natural icing tests, the capability of the ice protection system to prevent and/or remove ice accumulation should be evaluated. Using an icing tanker, tunnel, or other device, various sections of the wing and horizontal stabilizer may be immersed in the ice cloud under measured icing envelopes. Additionally, these tests can be used to evaluate the adequacy of the

proposed protection system. During the course of this evaluation, the ability of the system to remove ice that has accumulated prior to system activation should be checked. The trajectory and consequence of ice formations removed from the various components can also be observed and evaluated as part of these tests.

Natural Icing Tests

Instrumented natural icing tests should be conducted to demonstrate the adequacy of the entire airplane ice protection system. Several icing encounters encompassing a variety of atmospheric conditions should be evaluated. Throughout these tests, the observed performance of the system should be compared to that predicted for the existing environment. Ice accumulation on unprotected surfaces is compared to the predicted ice shapes used in dry air tests. The ability of the ice detection system to alert the flight crew of icing conditions prior to accumulation of ice on the airframe should be evaluated. The performance of the ice protection system in actual icing conditions should be consistent with that predicted by analysis.

4.2.1.1 Purpose

This should be a clear statement of why the test is required and the objectives of the test.

4.2.1.2 Aircraft Configuration

This should describe the particular test aircraft that is to be used for the test, including variations from a production configuration that may affect test results, and any special installations or configuration required (e.g., icing measuring instruments, etc.).

4.2.1.3 Instrumentation

This section should contain a complete description of any measuring or photo devices that may be required for the test. Many times a means of observing and photographing ice accretion is needed. Time correlation of photographs with other data is essential. Evaluation of aircraft flight performance in icing requires measurement of airspeed, altitude, ambient temperature, time, angle of attack, and engine performance. Handling qualities may be determined by pilot evaluation plus any special instrumentation deemed necessary. Any test conducted in natural icing conditions will require instrumentation to measure LWC and MVD (reference 4-2). It is imperative that all measuring instrumentation should have calibration checks performed regularly and that the calibration histories be documented for reference purposes.

4.2.1.4 Procedure

This should be a detailed description of the steps to be followed in order to obtain the data required. Where applicable it should reference FAR regulations (references 4-2 and 4-4 through 4-7) and how any required data is to be recorded.

4.2.1.5 Data Required

This is a complete description of all data needed, its accuracy, how recorded, etc. Many times this will be supplemented by hand written comments based on visual observations. In cases where no icing protection is used in specific areas on an aircraft intended for flight through icing, it will be necessary to determine the effects of the maximum likely amount of ice on aircraft performance in terms of increased drag, decreased maximum lift coefficient, increased stall speed, possible damage to components and engines from ice shedding, and general effects on aircraft handling qualities.

4.2.1.6 Test Points

This is a description of the conditions at which data will be recorded. It will contain aircraft flight conditions (e.g., airspeed, altitude, Mach number, attitude, engine power setting) and meteorological conditions (e.g., MVD, LWC, temperature, etc.).

4.2.1.7 Data Analysis

This is a description of how the data that is gathered should be reduced to useful engineering form for demonstrating operational adequacy of the system being tested. It should also include a definition of what constitutes acceptable or unacceptable test results.

4.2.2 Proof of Compliance

4.2.2.1 Explanation

This section provides a degree of latitude for the FAA test team in selecting the combination of tests or inspections required to demonstrate compliance with the regulations. Compliance must be shown for each combination of gross weight, center of gravity, altitude, temperature, airspeed,engine/rotor rpm, MVD, LWC, etc. Engineering tests are designed to investigate the overall capabilities and characteristics of the aircraft throughout its operational envelope. Testing will identify operating limitations, normal and emergency procedures, and performance information to be included in the FAA approved portion of the flight manual. The testing must also provide a means of verifying that the aircraft's actual performance, structural design parameters, propulsion components, and systems operations are consistent with all certification requirements.

Regulations require, in part, that the applicant show compliance with the applicable certification requirements, including flight test, prior to official FAA Type Inspection Authorization (TIA) testing. Compliance in most cases requires systematic flight testing by the applicant. After the applicant has submitted sufficient data to the FAA showing that compliance has been met, the FAA will conduct any inspections, flight, or ground tests required to verify the applicant's test results. FAA compliance may be partially determined from tests conducted by the applicant if the configuration (conformity) of the aircraft can be verified. Compliance may be based on the

applicant's engineering data, and a spot check or validation through FAA flight tests. The FAA testing should obtain validation at critical combinations of proposed flight variables if compliance cannot be inferred using engineering judgment from the combinations investigated.

Performance tests include minimum operating speed (hover in the case of helicopters), takeoff and landing, climb, glide, height - velocity, and power available. Certain other performance tests are conducted to meet specific requirements. Detailed performance test procedures and allowable extrapolation or simulation limits are contained in numerous references (4-3, 4-8 through 4-12, etc.).

(i) For helicopters, hover tests are conducted to determine various combinations of altitude, temperature, and gross weight for both in-ground-effect and, if required, out-of-ground effect conditions. From these data, the hover ceiling may be calculated.

(ii) Takeoff and landing tests are conducted to determine the total distance to takeoff and land at various combinations of altitude, temperature, and gross weight.

(iii) Climb tests establish the variations of rate-of-climb at the best rate-of-climb or published climb airspeed(s) at various combinations of altitude, temperature, and gross weight.

(iv) For helicopters, height-velocity tests are conducted to determine the boundaries of the height versus airspeed envelope within which a safe landing can be accomplished following an engine failure.

(V) Power available tests are conducted to verify or reestablish the calculated installed specification engine performance model on which published performance is based.

The purpose of stability and control tests is to verify that the aircraft possesses the minimum qualitative and quantitative flying qualities and handling characteristics required by the applicable regulations. In order to assess the handling qualities, standardized test procedures must be utilized and the results analyzed by accepted models. Calculation and inference which includes extrapolation and simulation are allowed, but demonstration of controllability, stability, and trim are required. Combinations of both may be used to show compliance to the operating envelope limits. Test methods and equipment are described in other chapters of this handbook.

4.2.2.2 Procedures

Efforts should begin early in the certification program to provide advice and assistance to the applicant to insure coverage of all certification requirements. The applicant should develop a comprehensive test plan which includes the required instrumentation.

The tests and findings specified above are required of the applicant to show basic airworthiness and probable compliance with the minimum requirements specified in the applicable regulations. After these basic findings have been submitted and reviewed, a Type Inspection Authorization, or equivalent, can be issued. The FAA will develop a systematic plan to spot check and confirm that

compliance with the regulations has been shown. The test plan will consider combinations of weight, center of gravity, rpm, and cover the range of altitude, temperature, LWC, MVD, etc., for which certification is requested.

4.2.3 Example Icing Tests

Sample test plans for various compliance test programs are presented in tables 4-1 through 4-8. They do not represent a composite Icing Certification Test Plan and must be treated as only stand-alone examples of some portions of an overall test plan.

V.4.3 REFERENCES

4-1 Bowden, D.T., Gensemer, A.E., and Skeen, C.A., "Engineering Summary of Airframe Icing Technical Data," Federal Aviation Agency, FAA Technical Report ADS-4, 1964.

4-2 "Airworthiness Standards: Transport Category Airplanes," U.S. Department of Transportation, Federal Aviation Administration, Federal Aviation Regulations, FAR Part 25, Washington, D.C.

4-3 "Aircraft Ice Protection," U.S. Department of Transportation, Federal Aviation Administration, AC 20-73, April 21, 1971.

4-4 "Airworthiness Standards: Normal Category Airplanes," U.S. Department of Transportation, Federal Aviation Administration, Federal Aviation Regulations, FAR Part 23, Washington, D.C.

4-5 "Airworthiness Standards: Normal Category Rotorcraft," U.S. Department of Transportation, Federal Aviation Administration, Federal Aviation Regulations, FAR Part 27, Washington, D.C.

4-6 "Airworthiness Standards: Transport Category Rotorcraft," U.S. Department of Transportation, Federal Aviation Administration, Federal Aviation Regulations, FAR Part 29, Washington, D.C.

4-7 "Airworthiness Standards: Aircraft Engines," U.S. Department of Transportation, Federal Aviation Administration, Federal Aviation Regulations, FAR Part 33, Washington, D.C.

4-8 "Certification of Small Airplanes for Flight In Icing conditions," U.S. Department of Transportation, Federal Aviation Administration, Advisory Circular, AC 23.1419-1, September 2, 1986.

4-9 "Certification of Transport Category Rotorcraft," U.S. Department of Transportation, Federal Aviation Administration, Advisory Circular, AC 29-2, September 16, 1987.

4-10 "Airplane De-Ice and Anti-Icing Systems," U.S. Department of transportation, Federal Aviation Administration, Advisory Circular, AC 91-51, September 15, 1977.

4-11 "Certification of Normal Category Rotorcraft," U.S. Department of Transportation, Federal Aviation Administration, Advisory Circular, AC 27-1, August 29, 1985.

4-12 Pfeifer, G.D. and Maier, G.P., "Engineering Summary of Powerplant Icing Technical Data," Federal Aviation administration, Report No. FAA-RD- 77-76, July 1977.

4-13 Jones, Alun R. and Lewis, William, "Recommended Values of Meteorological Factors to be Considered in the Design of Aircraft Ice-Prevention Equipment," NACA TN 1855, 1949.

TABLE 4-1. EXAMPLE TESTS - FIXED WING AIRCRAFT

Brief descriptions of tests designed to provide substantiating data for demonstrating compliance follow.

Dry Air Testing

The impingement limits and the cross sectional area of the maximum expected ice accretion are provided or are calculated by the methods of previous Sections for this example.

Maximum Impingement Limits and Cross Sectional Area

Upper (From Cruise Segment) = 2.25 in.
Lower (From Holding Segment) = 3.00 in.
Total Ice Shape = 6.89 $in.^2$

The shape of the simulated ice is arrived at by drawing various contours and comparing them with photographs of actual ice accumulations on other aircraft. Heavy reliance was given to personal experience plus that of the FAA Western Region Aircraft Engineering Branch. Once a satisfactory contour is determined, it will be drawn to accomodate the required cross sectional area and impingement limits. A planimeter can be used to assist in drawing the shapes to the correct area. (Figure 4-1)

The following process is used in building ice shapes:

1. A 2-ply fiberglass wet lay-up is made to conform to the contour of each area where an ice shape is required.
2. Plywood stiffeners shaped like the ice cross section are attached to the fiberglass base.
3. Additional layers of fiberglass are put over the stiffeners to form the final contour.
4. To create a rough ice-like surface, a thick mixture of fiberglass resin with filler is applied over the finished contour.

Clear Air Testing

The objective of the clear air testing is to determine what effect the ice shapes will have on aircraft handling qualities. To accomplish this, a complete series of handling qualities tests per FAR Part 23 (Reference 4-4) should be conducted with and without ice shapes. These tests included:

Stall Characteristics
Controllability Tests
Stability Tests, Both Static and Dynamic
Trim Tests
Landing Tests
Vibration and Buffeting

All the handling qualities tests are first conducted on the aircraft without ice shapes installed. This will provide a valid baseline with which to compare handling qualities when ice shapes are installed on the unprotected flight surfaces.

TABLE 4-1. EXAMPLE TESTS - FIXED WING AIRCRAFT (Cont'd.)

During initial ice shape tests, the inboard wing sections (see Figure 4-2) will have ice shapes extending the entire distance between the fuselage and engine nacelle. It is anticipated that the previously FAA approved pneumatic wing deice boots, which protected only the outboard wing, would be adequate. It might be noted that a manufacturer can obtain FAA approval to install an ice protection system on an already certified aircraft without obtaining approval for flight into known icing conditions. The only requirements are:

1. The system not create a hazard to flight.
2. It perform its intended function, i.e., remove ice.
3. For small airplanes, a placard must be installed in accordance with FAR 23.1559(b) prohibiting flight into known icing conditions.

An installation, so approved, is considered to provide only minimal protection for a non-anticipated icing encounter and does not allow the pilot to launch a flight into or continue a flight in known icing conditions. To do so would be extremely hazardous, and in direct violation of FAR 23.1419 (Reference 4-4). Because of this, the approved pneumatic wing deice system initially installed did not include inboard wing boots.

The clear air tests with ice shapes should accomplish three objectives:

1. Show where additional ice protection is needed.
2. Help develop operational procedures for flight in an icing environment.
3. Give confidence in the aircraft's capabilities before launching into natural icing encounter tests.

Natural Encoun. r Testing

The parameters that define an icing encounter; air temperature, liquid water content, median volumetric drop diameter, and horizontal extent will be recorded, in addition to airspeed and altitude. An on-board computer will provide real-time data output to a CRT for in-flight "quick look" evaluation of icing conditions. When it is evident that the aircraft is in a useful icing encounter, data will be recorded on magnetic tape for later processing. When a useful encounter is established, an attempt will be made to remain in it as long as possible.

For natural encounter testing, the aircraft will be based in the Pacific Northwest to take advantage of the weather systems prevalent during the winter months. It will be possible to document several data points within both of the FAR Part 25, Appendix C (Reference 4-2) Continuous Maximum and Intermittent Maximum icing envelopes.

TABLE 4-2. EXAMPLE TESTS - ENGINE INDUCTION SYSTEM

Tunnel Icing Testing

The nacelle and inlet were installed in the tunnel with the following tunnel instrumentation.

Icing Tunnel

a. IAS
b. OAT
c. Spray nozzle air pressure
d. Spray nozzle water pressure
e. Spray cloud water flow
f. Barometer
g. Miscellaneous

Test Description - General

The icing tunnel tests involve a supercooled water spray cloud with median moisture droplet diameter 10 to 20 microns. The water content for these tests will be varied from 0.5 grams per cubic meter to 1.8 grams per cubic meter. Tunnel calibration curves will be used in setting water content and droplet size. The temperature should be varied from -15°F to 28°F (and above for thawing and de-icing). NACA TN 1855 (Reference 4-13) and FAR 25 (Reference 4-2) should be used as guides for water content, droplet diameter and temperature. Engine flow will be set with a blower. The engine oil system will be maintained hot during the icing run. When the spray is turned off, the oil system will be allowed to cool.

It is important to have an understanding of the amount of water involved in the icing tests and the correlation to actual atmospheric conditions. In referring to the tunnel operation curves, it can be noted that, to maintain a calibrated spray cloud, the median drop diameter must be between 11 and 20 microns. Reference 4-2 and 4-9 do not include information below 15 microns. Therefore, most of the testing will be limited to 15 to 20 microns. The tunnel cloud water content (grams water per cubic meter of air) is a function of the square root of the difference between the spray nozzle air pressure and water pressure (Delta P). The Delta P was limited to between 10 and 60 psi. At 185 mph, the water content for a calibrated spray cloud must be between 0.7 g/m^3 and 1.8 g/m^3. At 250 mph, the water content limits are 0.5 g/m^3 and 1.3 g/m^3. When looking at atmospheric icing conditions specified in Reference 4-9, it can be seen that the maximum intermittent icing conditions at warm temperatures and the maximum continuous icing at cold temperatures are outside the tunnel limits.

Dry Air Flight Tests

Procedure

The right hand cowl inlet lip is instrumented to read lip temperature (Figure 4-3). A series of flight tests will be conducted at various

altitudes, airspeeds, and power settings. Lip temperatures at each condition, along with the necessary engine parameters, will be recorded.

At each flight condition, a temperature difference (ΔT) between true OAT and coldest hot lip temperature will be measured. Visual and photographic records should be recorded to establish the adequacy of the anti-icing system.

Nacelle Dry Air Similarity Test

The purpose of this test is to demonstrate the adequacy of the engine nacelle anti-icing capability for aircraft B. This will be accomplished by demonstrating the equivalency of the aircraft B nacelle supply bleed air to the aircraft A nacelle supply air in dry air testing. Aircraft A has previously received FAA certification for icing flight.

Summary

Dry air flight testing of the aircraft B nacelle anti-ice system will demonstrate that for equivalent system demand requirements and flight performance conditions, the bleed air supply to the nacelle is equal in pressure and temperature to the aircraft A and is adequate based on system similarity.

Instrumentation

Aircraft B shall be instrumented with temperature and pressure pickups to determine temperature and bleed flow rates in the nacelle anti-icing system on the left nacelle. The pickup locations shall be the same as those used on Aircraft A.

Data Required

The bleed air requirements for aircraft B are different, therefore a survey of bleed requirements shall be performed and the flight condition and operation which produces the most demanding load on the bleed system shall be chosen as a comparison point to the previous aircraft A test data. As an equivalent comparison, altitude, airspeed and engine rpm shall be held as close as possible to the previous tests. The following data will be required:

Aircraft indicated airspeed
LH engine rpm (% of N_1)
RH engine rpm (% of N_1)
Outside air temperature
Altitude
Temperature, pressure and flow rates from instrumentation installed per the appropriate flight test work order.

Test Points

The tests will be conducted on aircraft B at both low and high power settings to duplicate prior test conditions of aircraft A. Sixteen sets of data will be taken for the left nacelle of aircraft B. This compares with eleven sets of data for aircraft A but for both the left and right nacelle.

TABLE 4-2. EXAMPLE TESTS - ENGINE INDUCTION SYSTEM (Concluded)

With all bleed air systems on, record the above data at each of the following LH engine power settings: N_1 = idle, 40%, 60%, 80%, and 90%, for conditions 1 and 2.

1. Altitude = ground level, RH engine shut down.

2. Altitude = ground level, RH engine equals LH engine power setting. (Terminate this test if wing temperatures exceed recommended limits.)

The following test points are to be run with all bleed air systems on:

1. Descent
   Climb to 40,500 feet and stabilize the aircraft for 10 minutes at 75% N_1. Initiate a 2000 ft./min. descent and record data listed above at increments of 1000 feet. Simultaneously reduce power on LH and RH engines as required to maintain 255 KCAS. Terminate descent when an altitude of 4500 feet is obtained.

2. Altitude = 12,000 ft., Airspeed = 195 KCAS
   (a) LH and RH N_1 = 80%; (b) LH and RH N_1 = 94%; (c) with aircraft in clean flight configuration and RH mod valve off, reduce RH engine power to idle and increase LH engine power as required to maintain airspeed to simulate engine out operation.

3. Altitude = 22,000 ft., Airspeed = 125 KCAS
   (a) LH and RH N_1 = 80%; (b) LH and RH N_1 = 94%; (c) with aircraft in clean flight configuration and RH mod valve off, reduce RH engine power to idle and increase LH engine power as required to maintain airspeed to simulate engine out operation; (d) repeat steps (a) and (c) with Airspeed = 170 KCAS.

   NOTE: Flight configuration may be changed to maintain LH N_1 and airspeed specified in condition 2(a), (b) and 3(a), (b). RH N_1 may be deviated if necessary.

Data Analysis

A detail analysis of all of the data will be performed to show that, considering all of the critical flight regimes and bleed flow demands, the nacelle anti-icing systems are equivalent between aircraft A and aircraft B.

TABLE 4-3. EXAMPLE TEST PROCEDURE FOR TURBOJET ENGINES

Reference 4-3 gives these guidelines:

1. The engine should be capable of operating acceptably under the meteorological conditions of Appendix C of FAR 25 over the engine operating envelope and under conditions of ground fog.
2. Experience has indicated that testing to the points set forth in the Table below and the following schedule has been considered a successful means of showing compliance if used in conjunction with the critical conditions determined in the design analysis.

TURBINE ENGINE COMPLIANCE TEST POINTS

Icing Condition	1	2	3*
Liquid Water Content, g/m^3	2.	1.	$\geq$0.3
Atmospheric temperature, °F	23.	-4.	15-30
Droplet Median Volumetric Diameter, (MVD), microns	25.	15.	$\geq$20

*30 minute idle condition

   a. Operate the engine steadily under icing conditions 1 and 2 for at least 10 minutes each at takeoff setting, 75 percent and 50 percent of M.C. and at flight idle setting, then accelerate from flight idle to takeoff. If ice is still building up at the end of 10 minutes, continue running until the ice begins to shed or until the engine will no longer operate satisfactorily.
   b. Operate steadily at ground idle setting for at least 30 minutes under icing condition 3 followed by acceleration to takeoff setting.
   c. While at cruise and flight idle, for engines with icing protection systems, operate for at least one minute in the icing atmosphere prior to turning on the icing protection system.
3. Engine operation in these icing conditions should be reliable, uninterrupted, without any significant adverse effects, and include the ability to continue in operation and accelerate. Some power reduction is acceptable at idle power settings but all other operation should be unaffected.
4. Special consideration and tests should be conducted to adequately substantiate:
   a. Engines with inlet screens.
   b. Engines with air passages which might accumulate snow or ice due to restrictions or contours.
   c. Unprotected surfaces upon which ice may build up in rare instances to significant degrees for longer exposures than specified above.

TABLE 4-4. SUMMARY OF PROPOSED MODEL X ICING TESTS

A summary of proposed icing tests for a jet airplane as presented to the FAA for approval is shown.

REFERENCE: FAA Project Number CT4623-E

The flight test proposal for certification flight testing of the Model X, Report X-2, previously submitted to your office, includes all proposed flight test activity for certification of the subject model. The following data summarizes the portions of X-2, and of the test proposals it lists, that apply to certification testing for icing, and is intended to serve as a guide thru the various documents involved.

1. Proposed Powerplant Icing Protection Tests

   Report X-1, Powerplant Certification Flight Test Proposal, Section 8, page 5, entitled Ice Protection, defines proposed powerplant icing protection tests. Dry air tests will show that inlet flow and temperature are equal to or better than those of the Model R. The NACA scoops for generator cooling will be evaluated by NACA test data and equivalency of the Model X and R. An 'A' revision will be issued to X-1 to include this data.

   In addition to the above noted analysis and dry air testing, the aircraft will be flown behind a tanker to demonstrate that ice shed from all non anti-iced surfaces will not enter the engine inlet in hazardous quantities.

2. Proposed Airframe Ice Protection Tests

   Test Proposal X-4, Proposed Certification Flight Test for Environmental Control System for Model X aircraft, Section 3.6, pages 12-14, entitled Ice Protection, defines proposed airframe ice protection tests. The windshield, radome, pitot static probes, and stall warning vanes will be tested behind the tanker. The aircraft will be fully instrumented and water droplet size and content will be measured.

   The wings will be tested in dry air, using thermocouples on the leading edge to verify that temperatures are adequate to prevent ice from forming on the heated portion of the leading edge.

   The electrically heated horizontal tail will be analyzed to demonstrate that it is equal to or better than the installation on a Model R. Original Model R report data will be presented to verify system adequacy. Report X-5, All Weather Systems Compliance Report, will include this analysis.

3. Aerodynamic Effects of Symmetrical and Unsymmetrical Ice Buildup

   The aerodynamic effects of symmetrical and unsymmetrical ice buildups will be tested per Flight Test Proposal FA-01, FAA Certification Flight

TABLE 4-4. SUMMARY OF PROPOSED MODEL X ICING TESTS (Concluded)

Tests for Performance, Stability and Control Testing for the Model X, Section VI.22, pages 50 and 50(a), entitled Ice Effects. Acceptable handling qualities will be demonstrated with both light and heavy simulated ice shapes in both symmetrical and unsymmetrical arrangements on the unprotected areas of the outboard wing and winglets and on the vertical fin.

It will be demonstrated that the recommended flight manual procedures are satisfactory in the event of an anti-ice failure, by evaluating small ice buildups on the wings and horizontal tail individually and in combination.

4. Natural Ice Testing

The aircraft will be subjected to natural icing as defined by Flight Test Proposal X-4, Section 3.6, page 14. As noted in our letter to the FAA, we proposed the Model X Function and Reliability Evaluation Program. This testing will be conducted in concurrence with accumulation of flight time for the F&R program. The natural icing encounter requirement will be for a moderate uninstrumented encounter, with a 45 minute encounter duration objective.

The documents referenced above have been submitted with form 8110-3 signed by the appropriate DER's, approving or recommending approval of the appropriate data. Your concurrence with this program at an early date is requested, in order that tanker testing may begin in about two weeks with FAA participation beginning about one week thereafter.

TABLE 4-5. NATURAL ICING TESTS

1. Conduct icing test in natural conditions as follows:

   a. Evaluate the performance of the anti-icing equipment during natural icing encounters in as many different combinations of temperature, liquid water content and water droplet size as are accessible. Note individually the windsh eld, wing leading edge, engine inlets, pitot/static probes, total temperature probe and angle of attack sensor. A minimum of three separate ice envelope positions should be evaluated.

   b. Observe and photograph or videotape ice accumulation on the empennage, wing fence, and wing tip. Evaluate accumulations compared to proposed "ice shape" tests.

   c. Evaluate the ice detection capability for night operation. The fuselage mounted ice detection light may be evaluated on the ground by artifically icing the wing and checking effectiveness of the light. Advise the manufacturer on the spot if improved ice detection capability is required (Reference FAR 25.1403).

   d. Observe and photograph or videotape the path of any ice shed from forward portions of the test airplane relative to the engine inlet. In the test plane, note any engine instrument indications of ice ingestion. Shedding is most likely to occur after departing the icing conditions and ascending into warmer air. A minimum of three ice shedding occurrences should be documented.

   e. Evaluate the proposed flight manual, especially in the area of preflight checks and procedures in case of system failures.

   f. Conduct tests per FTR 25 and FTR 26 Section 3.5.3 evaluated for natural ice conditions.

   g. Determine the minimum engine speed for adequate anti-ice system operation.

   h. Investigate airplane slow speed handling qualities by slowing to shaker speed after one significant icing encounter.

   i. Conduct any other natural icing tests deemed necessary.

2. Conduct any other tests deemed necessary.

TABLE 4-6. FAA FLIGHT TEST PLAN - ALL WEATHER SYSTEMS

REFERENCE: FAR Part 25

DESCRIPTION OF TEST REQUESTED

1. PURPOSE

The purpose of this FTR is to present a flight test procedure that will provide data and/or operational characteristics of the All Weather Systems for FAA compliance substantiation.

2. INSTRUMENTATION

The test aircraft shall be instrumented as required so that with this instrumentation and the normally installed aircraft instruments, the data requested in this FTR can be obtained and/or recorded.

3. TEST PROCEDURE

Listed below are the FAR 25 paragraphs and the corresponding test and/or evaluation to be accomplished to show compliance.

Each test condition requested has been selected, using the respective failure analysis for the subject system, to represent a failure condition which corresponds to a level of severity and/or probability specified in the FAR 25 paragraph. The failure analysis for each system will be presented in the compliance report covering each respective FAR 25 paragraph.

In addition to the listed tests, all related flight manual procedures are to be performed.

a. Ice Protection

Perform the following flight tests and all weather systems operational checks to determine that the indicated performance requirements have been accomplished:

NOTE: Flight tests specified by this FTR will obtain data to show compliance with FAR 25.1419 for the airplane nose area (radome and windshield) and the heated area of the wing. Also, evaluate performance for the pitot-static probes and stall vanes.

Previous flight test data were obtained for the heating blanket attached to the horizontal stabilizer. These data will be presented in the Compliance Report. The heating blanket performance will be demonstrated.

TABLE 4-6. FAA FLIGHT TEST PLAN - ALL WEATHER SYSTEMS (Cont'd.)

Flight tests required to show compliance with FAR 25.1419 of the unprotected surfaces are presented in Test Proposal A-1 and for the engine ice protection in Test Proposal A-2.

(1) 25.1419(c)(2) Flight dry air tests of the ice protection system as a whole or of its individual components.

NOTE: Dry air flight test data will be obtained on the heated area of the windshield and heated portion of the wing leading edge. These wing anti-ice system data (these data include 41 temperature locations around the leading edge contour, distributed at 6 spanwise locations on the left wing) and a performance analysis of the wing leading edge anti-ice system will be used to show compliance with FAR 25.1419 of the heated portion of the wing.

TEST: All weather systems operations check (at flight altitude of 22,000 ft.)

a. Select an airspeed and engine power setting representative of a minimum fuel consumption holding pattern.

b. All bleed air systems "ON"; i.e., cabin air, nacelle heat, wing and stab heat, and windshield anti-ice. Maintain condition until temperature data have stabilized.

NOTE: Cabin ventilation airflow. Maintainability of selected cabin pressure altitude. Wing anti-ice airflow (wing temperature indicator). Windshield anti-ice airflow. Stab heat, cycling ammeter reading.

(2) 25.1419(c)(3) Flight tests of the airplane or its components in measured simulated icing conditions.

(3) 25.1419(c)(4) Flight tests of the airplane in measured natural atmospheric icing conditions.

Cloud liquid water and droplet diameter instrumentation will be installed to obtain these data.

Windshield temperature and anti-ice flow data will be recorded continuously while in the natural icing condition. These data will be used with the dry air flight test data as a basis for extrapolation and/or interpolation of data obtained in this test to other conditions within the FAR 25 Appendix C icing condition envelope.

TABLE 4-6. FAA FLIGHT TEST PLAN - ALL WEATHER S' STEMS (Concluded)

NOTE: The purpose of the following test i to obtain data to confirm that the airplane has adequate ice protection required for all weather certification. All anti-icing systems must be turned on prior to entering natural icing condition.

TEST: Operate the airplane in a natural icing encounter at a flight condition representing a sustained holding pattern to simultaneously evaluate the performance of all anti-ice systems. The test objective will be to remain in an icing condition for 45 minutes or until a 2 inch to 3 inch ice build-up has accumulated on the ice "probe", whichever occurs first.

NOTE: To evaluate the pilot windshield alcohol anti-ice system, turn off the windshield heat and turn on the windshield alcohol anti-ice system during the last 10 minutes of the above test condition. Record clear area maintained on pilot's windshield.

4. DATA REQUIRED

Obtain knee-pad data of the observed performance requested for the test conditions requested. The data acquisition system installed in the test airplane should be operated throughout the test conditions to provide a detailed record of the performance of the environmental and all weather systems.

TABLE 4-7. AIRFRAME ICING TEST PROGRAM

1. AIRFRAME ICING PROGRAM

a. Purpose

The test work outlined in this test program is designed to provide sufficient data to demonstrate FAA compliance for flight into known icing conditions. At a meeting with the FAA, the FAA outlined the criteria for acceptable compliance as follows:

- One encounter in either icing envelope per Appendix C, Part 25.
- A flight of 45 minute duration at holding speed in icing conditions.
- A flight with 2 to 3 inch ice build-up.

b. Configuration

(1) The prototype configuration, S/N A-1, equipped with the following de-ice/anti-ice equipment shall be used for these tests.

1. Horizontal stabilizer boots
2. Inboard wing boots
3. Propeller de-ice installation
4. Engine air intake assembly
5. Engine inertial separator installation
6. Wing boots
7. Heated windshields
8. Heated fuel vents
9. Heated stall warning transducer
10. Heated pitot tubes
11. Heated alternate static air source

(2) In order to mount the particle measuring equipment, pylons with heated anti-ice boots shall be installed near each wing tip.

(3) A plexiglass observation window with internal lighting shall be installed on the inboard right engine cowling in place of the cowling panel that covers the inlet screen area.

(4) An observation window shall be installed on right side of aft baggage compartment to allow observation of stabilons and horizontal tail from cabin.

(5) Ice depth gages shall be mounted on each wing tip outboard of the wing de-ice boots. In addition, the right tailette shall be marked to indicate ice depth.

(6) A mirror shall be installed on right nacelle to allow observation from cabin of ice build-up on vortex generator at wing/fuselage junction.

TABLE 4-7. AIRFRAME ICING TEST PROGRAM (Cont'd.)

c. Instrumentation

(1) The following instrumentation shall be required for all the icing flights.

(a) Particle Measuring Systems, Inc., Data Acquisition System, Model DAS-64 used in conjunction with a Pertec T7640-9 magnetic tape recorder to record time history of the following:
1) Altitude (pilot's altimeter)
2) Airspeed (pilot's indicator)
3) OAT
4) Torque (left and right)
5) N_2 (left and right)
6) Particle size
7) Liquid water content
8) Ice flag

(b) Forward scanning spectrometer probe, PMS Model FSSP-100.
(c) Optical array cloud droplet spectrometer probe, PMS Model OAP-200X.
(d) Rosemount Model 871FA Ice Detector
(e) Rosemount Model 102 de-iced total temperature sensor.
(f) Johnson-Williams liquid water content probe.

(2) In addition to the above, a cassette tape recorder and a interphone system wired into the aircrafts COM system shall be used to record pertinent comments by pilot and observer during icing encounters.

(3) A 35mm camera, using VPS vericolor ASA 125 film, shall be used for photographic documentation.

(4) A video camera shall be mounted in aft baggage compartment and aimed through observation window (see 4.2.2.4) to enable viewing stabilons and horizontal tail. A video recorder and color monitor shall also be installed.

d. Procedure

The following tests shall be conducted prior to icing flights:

(1) Structure Dynamics shall conduct ground resonance tests with pylons and PMS equipment installed.
(2) Electrical Lab shall conduct P-Static tests.
(3) All de-ice and anti-ice equipment shall be ground checked for proper operation. Where required, operating voltages, currents or pressures shall be recorded and checked against system requirements.
(4) The pitot-static system shall be functionally checked in flight during rain conditions.

TABLE 4-7. AIRFRAME ICING TEST PROGRAM (Cont'd.)

(5) Deflation rate of boots shall be checked in flight at 25,000 feet in dry air.

The test aircraft shall be flown into icing environments as required to meet acceptable FAA criteria for compliance (see 4.2.1.1).

The following procedures shall be maintained for all flights.

Preflight

(1) A detailed weather briefing shall be obtained by test engineer to determine areas where the desired type of icing is likely to occur and what routes and altitudes to fly in these areas.
(2) Before each flight, personnel from Instrumentation shall preflight the icing test equipment and perform alignment or cleaning of the particle probes, if necessary.

Inflight

(1) During icing encounters, test engineer shall operate recording equipment. He shall also monitor the particle sizes displayed on the DAS-64, the OAT, and the LWC from the Johnson-Williams probe in order to determine the time required to remain in icing conditions.
(2) Photographs shall be taken as necessary prior to de-icing and immediately after.
(3) Test engineer shall voice record the following data on cassette tape at five minute intervals.
Airspeed
Altitude
OAT
Ice Depth
LWC from Johnson-Williams
Average drop size from DAS-64
(4) Pilot shall qualitatively check handling qualities and stall speeds with various degrees of ice build-up.

After Landing

(1) Following landing after each icing encounter, photographs should be taken of exterior of aircraft showing ice build-up on antennas and other unprotected surfaces.

These icing flights will probably necessitate off-site operations. Considerations should be made to provide for support personnel, as required.

FAA personnel will not be required on these icing flights.

TABLE 4-7. AIRFRAME ICING TEST PROGRAM (Concluded)

e. Report

A report shall be prepared documenting the test results and submitted to the FAA for acceptance.

TABLE 4-8. ENGINE INLET ICING TESTS

1. INTRODUCTION

This test is designed to demonstrate the satisfactory operation of the nacelle ice protection system. All testing will be undertaken in a ground level bypassing type facility at the National Research Council, Ottawa, Canada. During the test program, the nacelle will be exposed to supercooled water environments to comply with the specifications detailed in FAR 25.1093 and Advisory Circular AC 20-73.

2. TEST FACILITY DESCRIPTION

The test program for previous tests will be conducted in the number 4 cell at the Engine Laboratory of the NRC. This facility has been utilized for testing of gas turbine engines in icing conditions for many years. A diagram of the facility in side elevation has been included.

a. Refrigeration

Ambient air enters the test cell through three rows of silencing splitters and passes through and 18 foot square refrigeration heat exchanger into an 86 inch dia. icing simulation duct. When necessary, the inlet air is cooled using the refrigeration system which consists of an ammonia vapor compression plant, an ammonia/brine heat exchanger and the brine/air heat exchanger situated in the cell inlet. Control of the level of cooling is exercised by regulating the vapor compression circuit and once the required air temperature is achieved, it can normally be maintained throughout the test run within ±1°C. Ambient air conditions, such as temperature humidity and mass flow rate affected the degree of possible inlet air cooling, a temperature depression of up to -10°C is generally possible.

b. Simulated Forward Speed

Downstream of the 86 in. dia. duct the tunnel contracted through three axisymmetric conical sections to a 30 inch dia. section 78 inches long, which incorprated a manifold of calibrated wall static pressure tappings for airflow velocity indication, and also a series of ports for remote T.V. observation and lighting. The airflow velocity achieved in the 30 inch dia. duct represented the simulated flight velocity, with the value of free stream pressure, temperature, liquid water content obtained at this location being representative of the undisturbed flow ahead of the nacelle in actual flight.

The duct geometry immediately ahead of and surrounding the nacelle inlet section was designed on the basis of a potential flow analysis, with compressibility correction, to produce local airflow conditions representative of the Hold configuration. The ducting designed for the Hold condition is used for all test points.

TABLE 4-8. ENGINE INLET ICING TESTS (Cont'd.)

The hold configuration is the most critical icing condition due to the possibility of extended duration at low power setting in a restricted flight pattern. Operation at flight idle power provides reduced heat supply to the nacelle protection system but as such operation is of limited duration it will result in a less severe total encounter.

Air flow is induced through the test section by the engine itself and also by an auxiliary ejector system, situated in the cell exhaust system, and powered by a 5000 kw plant compressor which provided a primary airflow up to 30 lb./sec. at a maximum pressure of 100 psig. It is thus possible to set the simulated forward speed partially independent of the engine power level. Approach velocities up to M_N 0.3 and M_N .53, respectively, can be achieved at hold and maximum cruise power settings.

c. Icing Simulation Equipment

The water content of the icing environment will be produced by spraying a metered flow of water into the 86 inch dia. icing simulation duct through an array of 36 pneumatic spray nozzles. This array is a permanent feature of the test facility and is situated approximately 34 ft. upstream of the nacelle inlet.

Droplet diameter is controlled by selection of the required atomizing air pressure for the water flow rate, in accordance with established calibration curves. The calibration will be verified by means of the oiled slide sampling technique during the test program.

In order to prevent freeze-out of the water droplets, due to the cooling effect of the adiabatic expansion of the atomizing air, this air is preheated, in accordance with established NRC practice, to a temperature value, in degrees Celsius, equal to twice the atomizing air pressure in psig (Reference 1). The atomizing airflow is determined from previous calibration and the enthalpy increase incurred by preheating this air is taken into account during computation of the tunnel air total head temperature at the reference plane upstream of the nacelle inlet.

Simulation of the snow environment is accomplished by feeding natural snow at predetermined flow rates into a blower which supplied four snow injection chutes located immediately upstream of the water spray mast in the 86 inch dia. duct (Reference Figure 5).

The relative humidity of the ambient air will be determined by means of an Assman type hygrometer located outside of the test building. The possibility of evaporation within the tunnel will be evaluated using the mathematical technique developed by AEDC, Arnold Air Force Station and described in Reference 2.

The water flow rate will be increased to offset predicted evaporation but will not reduced in cases where condensation is predicted.

3. TEST DETAILS

a. Testing Prior to Icing Runs

(1) Ejector Evaluation

Testing will be carried out to evaluate ejector performance in order to ensure the full range of forward speeds necessary for the icing tests.

(2) Thermocouple Evaluation

A series of dry runs will be conducted to ensure that the surface thermocouples are reading the correct values. The test values will be compared with the values predicted using an in house production program.

(3) Water Droplet Checks

The engine will be run at a condition suitable for NRC personnel to carry out water droplet samples for both 15 μm and 25 μm droplet median diameter settings (i.e., oiled slide technique).

(4) Droplet Distribution Check

The engine will be run at a condition suitable for NRC personnel to perform a droplet distribution check (i.e., two steel rods inserted in 30 inch duct normal to each other for ice accumulation comparison).

b. Icing Runs

Carry out the eight icing runs defined in the table labelled Icing Test Conditions. The order of the tests is arranged such that the most critical conditions will be examined first. This will enable us to know if any modifications are required.

(1) Test Condition Description

The test conditions (Table 1) have been prepared to comply with the requirements of FAR 25 and Advisory Circular 20-73.

The ground idle and hold conditions are designed to prove that the icing protection system is satisfactory in low power conditions. Conditions 4) and 5) are supposed to simulate the flight cycle. These tests will show that the nacelle is accep-

table for the complete flight range. The final three tests, 6), 7) and 8), simulate the situation in which the pilot does not immediately engage the icing protection system. In the delayed activation tests the nacelle is in an icing environment for 1 minute at which time the de-icing system is turn on.

4. INSTRUMENTATION

a. Temperatures

There are to be 36 exterior surface temperature thermocouples and 6 interior air temperature thermocouples on the nacelle. These are defined and labelled as follows:

(1) Nacelle Surface Temperatures -Cu/Con (see figure 2)

Section A-A	T101, T102,....T111	(11)
Section B-B	T201, T202,....T211	(11)
Section C-C	T301, T302,....T311	(11)
Section A-A	T121, T122, T123	(3)

(2) Air Temperature (Section A-A) - Cu/Con

air delivery	T11
plenum air	T12
double skin inlet air	T13
double skin air adjacent to front spacer	T14
double skin outlet air	T15
internal air adjacent to ECU	T16
venturi temperature	T17

(3) General

fuel temperature (2)	Cu/Con
I.T.T. T_5	Cr/Al
engine intake T_1	Rosemount

outside air temperature T_0
duct air temperature 4 locations upstream of spray mast
nozzle air temperature for spray mast
water temperature at spray mast
surface temperature (T131) adjacent to heated static tap in 30 inch diameter duct.

Additional Notes

(a) the thermocouple installation is to conform to the memo dated 7 October 1981.

TABLE 4-8. ENGINE INLET ICING TESTS (Cont'd.)

(b) the placement of the thermocouples is to conform to the definition provided by the memo of 1.

(c) for explanation of T131 see note 1) on pressures.

(d) location of T11 - T17 are as previously relayed.

b. Pressures

(1) Air Pressure

Section A-A	P11, P12, P13, P15
Section C-C	P32, P33, P35
delivery piping pressure	P11
plenum pressure	P12, P32
duct inlet pressure	P13, P33
duct outlet pressure	P15, P35

(2) Bleed Air Pressure

calibrated venturi to measure flow to the lip	P17, ΔP
comp. delivery pressure	P3

(3) General

barometric pressure P_0
fan inlet P_1 (from Rosemount)
bypass duct static pressure P_{SD}
spray mast nozzle air pressure
water tank pressure - spray mast
spray mast nozzle water pressure (36)
fuel inlet pressure
statics in 30 inch diameter duct (8) - 7 manifold P130
- 1 single P131 (heated)

Additional Notes

(1) in order to obtain an accurate static pressure reading during the icing condition, the area surrounding one of the statics (P131) has been heated. There are eight statics in this plane, however seven have been manifolded to yield P130 and the remaining one is P131.

(2) the placement of the statics is to conform to the definition provided.

(3) instrumentation and measurement ranges to be as discussed.

TABLE 4-8. ENGINE INLET ICING TESTS (Cont'd.)

c. Miscellaneous

The following quantities must be measured:

N_1

N_2

ambient relative humidity

spraymast water flow rate

vibration	- C.E.C. -1	PL-1-V
	- C.E.C. -2	PL-1-H
	- C.E.C. -3	PL-4-V
	- C.E.C. -4	PL-4-H

fuel flow rate
complete television equipment

Trace Recordings are also required as follows:

CH -1	N_1
CH -2	N_2
CH -3	T_5
CH -4	P_3
CH -5	C.E.C. PL - 1 - V
CH -6	C.E.C. PL - 4 - V
CH -7	Skin Surface Temperature T111
CH -8	Skin Surface Temperature T104

TABLE 4-8. ENGINE INLET ICING TESTS (Cont'd.)

TABLE A. ICING TEST CONDITION

Condition	Velocity (KCAS)	Altitude (Ft.)	T (°F)	D_o (μm)	LWC (g/m^3)	%N_1	Time
1) grd. idle	0	0	29	40	2		60
2) hold	180		-4	15	1		45
3) hold	180		23	25	2		45
Flt. Cycle							
4) grd. idle	0	0	-4	15	1		10
take-off							10
climb	300						10
cruise	350						10
flt. idle	300						10
hold	180						10
5) grd. idle	0	0	23	25	2		10
take-off							10
climb	300						10
cruise	350						10
flt. idle	300						10
hold	180						10
Delayed Act.							
6) flt. idle	300		23	25	2		10
7) hold	180		23	25	2		10
8) cruise	350		23	25	2		10

TABLE 4-8. ENGINE INLET ICING TESTS (Cont'd.)

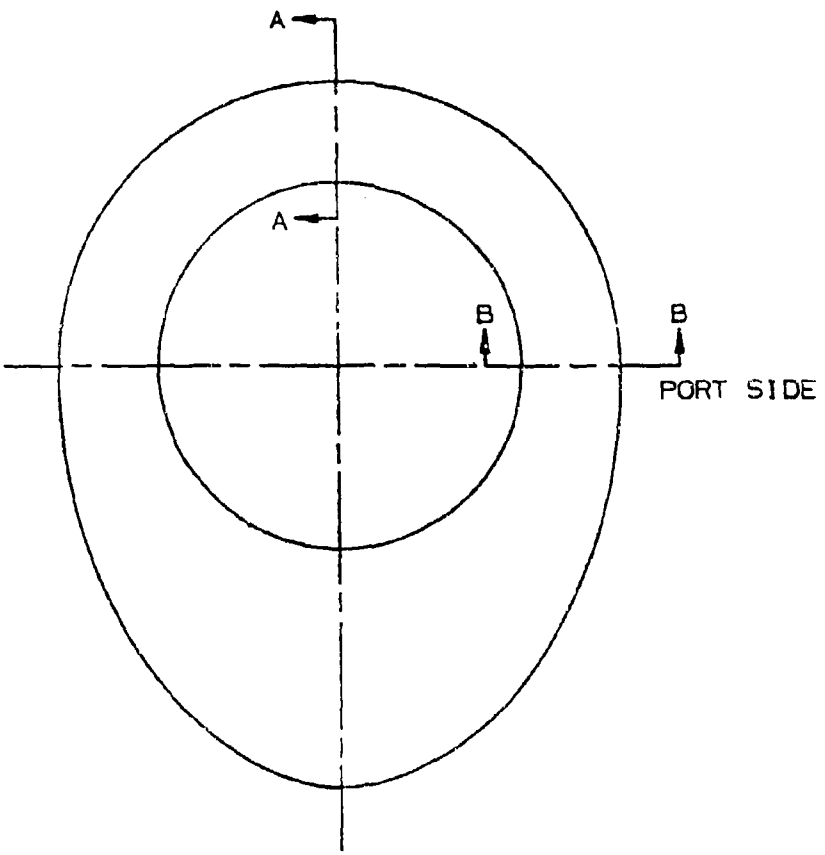

FIGURE A. NACELLE FRONT VIEW LOOKING AFT

TABLE 4-8. ENGINE INLET ICING TESTS (Cont'd.)

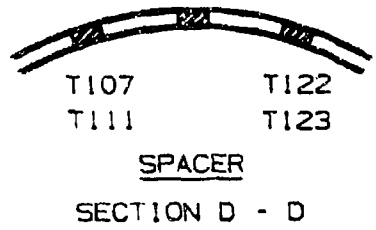

SECTION D - D

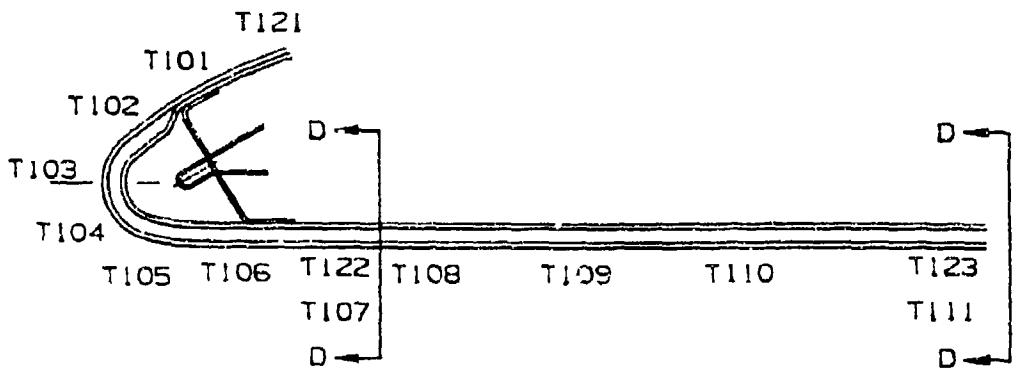

FIGURE B. NACELLE SECTION A - A

TABLE 4-8. ENGINE INLET ICING TESTS (Concluded)

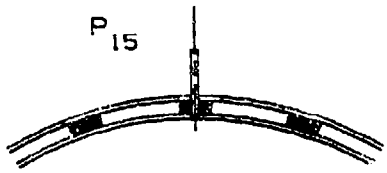

SECTION D - D

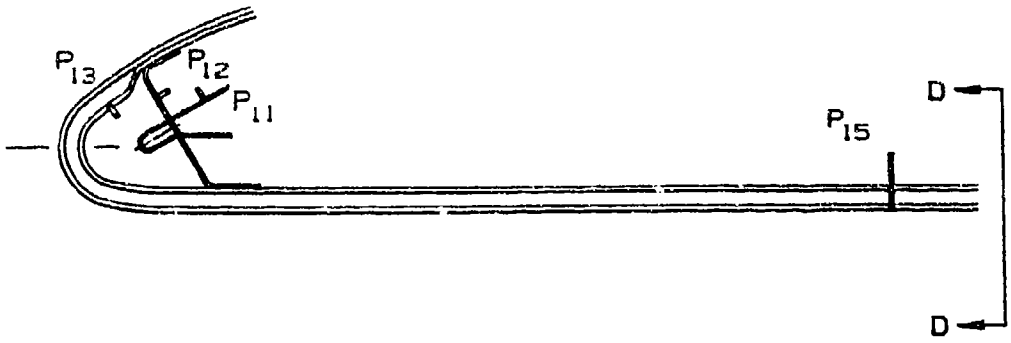

FIGURE C. NACELLE SECTION B - B

TABLE 4-9. ENGINE ICE PROTECTION MODEL B - SIMILARITY

A test plan to show engine inlet anti-ice compliance by means of similarity is shown.

PURPOSE

The purpose of this testing is to obtain the data necessary to verify adequate engine inlet anti-ice performance as required by FAR 25.1093. The intent is to show the anti-ice bleed air flow rate was equal to or greater than on the Model A aircraft and certify the performance by similarity.

AIRCRAFT CONFIGURATION

Experimental aircraft B1 is to be used for this testing. The aircraft will be configured with E-1 engines and thrust reversers. The bleed air pressurization and anti-ice system essentially in production configuration with the exception of engine spinner heat. (Nacelle anti-ice performance with spinner heat installed was checked under FTR A-1 and was also evaluated during natural icing tests under FTR A-2 and A-3.)

INSTRUMENTATION

The left engine inlet anti-ice system was instrumented for pressure and temperature as listed below. (Reference FTWO F-1 and FTR A-2)

a) DP191 anti-ice supply air Pt-Ps
b) PS191 anti-ice supply air Ps
c) T191 anti-ice supply air temp
d) PS191E anti-ice exit air Ps
e) T191E anti-ice exit air temp

Anti-ice flow rate (W191) will be calculated from DP191, PS191 and T191 using the flow calibration attached. Basic aircraft and engine parameters were also recorded as required by the FTR.

TEST CONDITIONS

The test conditions will be as follows:

TABLE 4-9. ENGINE ICE PROTECTION MODEL B - SIMILARITY (Concluded)

FLT NO.	COND NO.	A/S KNOTS	ALT FEET	N_1 LT	N_1 RT	BLEED CONFIG	ANTI-ICE CONFIG	COMMENTS
1	3.1	191	12000	79.8	56.3	Normal	All A/I On	Level Flt
	3.2	197	12000	94.1	69.8	Normal	All A/I On	Level Flt
	3.3	194	12000	73.0	45.6	Rt Bld Off	All A/I On	Level Flt
	4.1	127	22000	80.0	61.2	Normal	All A/I On	Level Flt
	4.2	127	22000	93.9	81.8	Normal	All A/I On	Level Flt
	4.3	129	22000	81.1	60.7	Rt Bld Off	All A/I On	Level Flt
	4.4	171	22000	80.0	84.5	Normal	All A/I On	Level Flt
	4.5	173	22000	80.0	60.7	Rt Bld Off	All A/I On	Level Flt
	14	158	40970	82.4	82.9	Normal	All A/I On	Min Power
	15	188	40850	92.2	94.7	Normal	All A/I On	Descent
	16	235	38890	96.0	97.5	Normal	All A/I On	Descent
	17	260	36660	74.8	75.3	Normal	All A/I On	Descent
	19	267	32750	68.9	69.6	Normal	All A/I On	Descent
	21	262	29040	66.4	67.1	Normal	All A/I On	Descent
	23	258	24930	63.1	63.8	Normal	All A/I On	Descent
	25	258	20911	59.6	60.2	Normal	All A/I On	Descent
	27	254	16230	55.1	55.5	Normal	All A/I On	Descent
	29	257	11920	40.3	40.6	Normal	All A/I On	Descent
	32	252	5240	35.6	35.8	Normal	All A/I On	Descent

DATA

All of the data recorded during this testing will be delivered to Engineering for analysis.

TABLE 4-10. AIRCRAFT AND ENGINE ICING TESTS

A test plan to demonstrate that flight in icing conditions have no adverse effects on aircraft and engine operations is presented.

PURPOSE

Flight testing is required to determine that in-flight icing conditions have no adverse effects on aircraft and engine operation.

LOADING

Optional.

INSTRUMENTATION

In addition to standard aircraft flight and engine instrumentation, the following test instrumentation and items will be installed.

1. One cowl flap motor located aft of each alternate air door. These motors will be positioned to force the alternate air doors open in the event icing conditions block these doors.
2. Micro switches will be located at each alternate air door to indicate when the door is not closed. Lights in the cabin will be wired to illuminate when the respective alternate air door is not closed.

PROCEDURE

The aircraft will be flown in the following icing conditions:

1. Rime ice
2. Clear ice/freezing rain
3. Wet snow

While in icing conditions, all engine power controls will be operated periodically to determine that they have not frozen.

The following data will be recorded:

1. Weather conditions
2. Pressure altitude
3. OAT
4. Power settings: Manifold pressure, RPM, fuel flow
5. IAS
6. Time
7. Alternate air door position: open or closed

Ice build-ups will be photographed with a Polaroid camera when possible.

TABLE 4-11. ICING CERTIFICATION TESTS - A-6 ENGINE AND B-7 NACELLE

A typical test for certification of an engine nacelle combination in an icing tunnel is shown.

1. INTRODUCTION

This request for test defines a schedule of icing tests for certification of the A-6 ice protection system as incorporated in the B-7 aircraft nacelle. Preliminary nacelle calibration and survey testing is defined in RT No. 5.

2. BACKGROUND

The A-6 ice protection system to be incorporated in the B-7 aircraft will include an inertial separator system developed from similar systems. Engine airflow requirements are increased to 10.6 lb/sec. SLS ISA at T.O. power and a retractable No. 2 vane will be incorporated.

The forward nacelle section will be identical to that of the Super King Air models, incorporating an inlet lip section heated by exhaust gas and a movable No. 1 vane which is lowered to effect inertial separation of the icing medium from the engine inlet airflow. This vane is raised in normal operation to optimize inlet performance in the non-icing mode.

The rear nacelle section is similar to that of the Super King Air, with changes incorporated to suit the B-7 installation. This section will incorporate the separator duct, retractable No. 2 vane and bypass duct. The retractable No. 2 vane is normally lowered to close off the bypass flow and minimize inlet pressure losses, it is raised during operation in icing conditions.

An external oil cooler will be installed below the nacelle rear section with a separate air inlet. It is not possible to install the cooler and its fairing in the icing tunnel and thus the nacelle lower contour will be modified to eliminate this feature during the icing test program.

3. TEST SECTION

The nacelle will be installed in the NRC No. 4 cell icing tunnel in the same manner as that for PT6A-41, PT6A-42 and PT6A-50 installations. Airflow will be induced over the nacelle inlet and lower sections with the ejector system situated downstream of the test section. Simulated flight velocities up to 230 KTAS are anticipated. The icing environment for SCW conditions will be supplied using the permanent NRC spraymast, and the blower system will be utilized to inject natural snow into the airstream when required, these two items being situated approximately 33 ft. upstream of the nacelle inlet. Refrigeration of the airstream will be provided using the heat exchanger at tunnel inlet as necessary to achieve the desired air temperature.

As the PT6A-65 engine model is a recent introduction no complete gas generator will be available for this test series. The intake plenum geometry will be maintained with an engine inlet and screen, firewalls, a simulation of the gas generator casing, and all other components required to provide an exact reproduction of the plenum. The engine inlet airflow will be induced with a second ejector system to be specially procured for this program.

4. TEST CONDITIONS

A summary of an analysis to establish critical icing conditions for an inertial separator type ice protection system is included in the reference of item (6).

Two of the most critical icing conditions for this type of system are:

a) Minimum speed, minimum droplet size and maximum engine airflow.
b) Maximum speed, maximum droplet size and maximum engine airflow.

Condition a) is stringent for the engine inlet because at minimum a/c speed and maximum engine airflow the bypass ratio is minimum and hence so is separator efficiency. Minimum droplet size is critical because small droplets are more difficult to separate inertially.

Condition b) is stringent for the bypass duct because of high water catch. Whilst separator efficiency is excellent because of the high bypass ratio and large size of the droplets, separator performance may deteriorate more rapidly due to blockage of the bypass duct.

Icing intercept is obviously important for a system which is to some extent accumulative, as is also the liquid water content. However, temperature is only significant for a system which does not rely on heated surfaces for protection in that it bears a statistical relationship to the LWC and determines the type of ice accretion which will occur.

The hold condition becomes a critical condition in the context of the FAR 25 Appendix C icing environment due to the extended duration in a restricted flight pattern, as it is implied that the range factor cannot be applied to the LWC and values for the standard intercept must be used. For the inertial separator system as used on PT6 installations, this condition has been shown to be one of the most severe.

5. PROPOSED CERTIFICATION TEST SCHEDULE

Based on the summary of para. 4., a schedule of tests applicable to the B-7 engine inlet ice protection system is proposed to demonstrate compliance with the requirements of FAR 33. The proposed schedule is shown in Table A attached.

TABLE 4-11. ICING CERTIFICATION TESTS - A-6 ENGINE AND B-7 NACELLE (Cont'd.)

Droplet sampling and spray distribution checks will be conducted at typical test conditions to demonstrate satisfactory operation of the water spray equipment.

6. **REFERENCES**

PT6A-42 Icing Certification Tests - Winter 1977-78, E.R. No. T21.

TABLE A
A-6 ENGINE/B-7 NACELLE INSTALLATION ICING CERTIFICATION TEST SCHEDULE

Schedule Item #	Simulated Ambient Temp. °F / °C	Stagnation Temp. °F / °C	Icing Medium	Droplet V.M. Dia.	LWC, gm/m³	Simulated Flight Vel. V KIAS	Intercept/Time N.mi./mins	Power Setting	Comments
1	-4/-20†	13.1/-10.5	SCW "	15 15	.06 (C.M.) 1.636(I.M.)	268* "	310 n.mi. 5.2 n.mi.	M.C. M.C.	Cruise (low temperature). Demonstration, severe test for engine inlet protection.
2	6/-14.5	23/-5†	SCW "	25 25	.10 (C.M.) 1.49 (I.M.)	268* "	310 n.mi. 5.2 n.mi.	M.C. M.C.	Cruise. (Severe test for bypass duct blockage.)
3	6/-14.5	23/-5†	SCW "	15 15	.16 (C.M.) 2.49 (I.M.)	268* "	310 n.mi. 5.2 n.mi.	M.C. M.C.	Cruise. (Severe test for engine inlet at high LWC.)
4	17/-8.3	23/-5	SCW "	15 15	.80 (C.M.) 2.93 (I.M.)	160 "	17.4 n.mi./ 2.6 n.mi.	Hold Pwr. Hold Pwr.	Hold in restricted patt. Alternate C.M. & I.M. intercepts for total time of 45 minutes.
5	17/-8.3	23/-5	SCW "	25 25	.50 (C.M.) 1.75 (I.M.)	160 "	17.4 n.mi./ 2.6 n.mi.	Hold Pwr. Hold Pwr.	Hold in restricted patt. Alternate C.M. & I.M. intercepts for total time of 45 minutes.
6	29/-1.7	29.4/-1.4	SCW	40	.60	Static	30 mins.	G.I.	Ground idle in freezing fog.
7	20.1/-6.6	23/-5	SCW "	15 15	.54 (C.M.) 2.49 (I.M.)	110 "	2x10 min. 2x3 min. (6500' vertical intercept)	M.C.	Climb at min.R.O.C. (250 fpm) C.M. icing of 47.7 n.mi. horizontal extent with 2 embedded I.M. intercepts ea of 5.5 n.mi. horizontal extent.

TABLE A (Concluded)

Schedule Item #	Simulated Ambient Temp. °F / °C	Stagnation Temp. °F / °C	Icing Medium	Droplet V.M. Dia.	LWC gm/m^3	Simulated Flight Vel. V KTAS	Intercept/Time N.mi./mins	Power Setting	Comments
8	6/-14.5	23/-5†	SCW	15	2.93 (I.M.)	268*	2 min.	F.I.	Cruise, F.I., 1 min delayed actuation followed by 1 min. with ice protection selected.
9	6/-14.5	23/-5†	SCW	15	2.93 (I.M.)	268*	2 min.	M.C.	Cruise, M.C., 1 min delayed actuation followed by 1 min. with ice protection selected.
10	16 to 23/ -8.9 to -5.0	18.9 to 26.0/ -7.3 to -3.4	Snow	-	2.0	110	10	M.C.	Climb/Cruise operation in falling snow.

NOTES:

1. Test conditions 1-5 and 7-9 are based on FAR 25 Appendix C environment as per FAR 33.
2. LWC for Condition 1 is computed on the basis of droplet dia., ambient temperature, and range factor.
3. LWC for Conditions 2-5 and Condition 7 is the maximum for droplet dia. and range factor, regardless of ambient temperature.
4. LWC for Conditions 8 and 9 is for I.M. concentration and standard intercept, and maximum for droplet dia. regardless of ambient temperature.
5. Test Conditions 6, and 8-10 are based on FAR 33 requirements directly.
6. In the event that the specified LWC is beyond the capacity of the spraymast, the duration will be adjusted to maintain an equivalent icing encounter.
7. Simulated flight velocity indicated thus* is anticipated to exceed the icing tunnel capability. Test will be undertaken at maximum tunnel velocity (= 230 KTAS), intercept and temperature indicated thus † will be maintained.
8. Compensation for any evaporation within the icing tunnel will be in accordance with the procedure described in AEDC-TR-73-140 (AD770069). Basic water content will not be reduced in the event that condensation is observed or predicted.

TABLE 4-12. ENGINE NACELLE ICING TESTS

1. OBJECTIVES OF TEST

This test is designed to demonstrate the satisfactory operation of the nacelle ice protection system. The nacelle will be exposed to supercooled water environments to comply with the specifications detailed in FAR 25.1093 b) and Appendix C.

2. UNIT NUMBER

The engine to be used in these tests is engine 3002/39.

3. FUEL AND OIL

Fuel: Jet A1
Oil: Esso 2380

4. LIMITATIONS

The engine must meet the following operating limitations.

Max. N1	16,540 rpm
Max. N2	31,450 rpm
Max. T5	1440°F
Max. P3	190 psig
Vibration	1.0 in/sec. avg.
Fuel Pressure	1 - 40 psig
Max. Oil Temp.	265°F
Main Oil Press.	78 ±5 psig

5. TEST DETAILS

a. Testing Prior to Icing Runs

(1) Engine Performance Evaluation

Carry out a performance check at the following values of $N_1/\sqrt{\theta}$ (no cabin bleed).

Condition No.	$N_1/\sqrt{\theta}$
1	4,800
2	9,000
3	12,000
4	15,000
5	16,000

The following parameters should be recorded at each test condition:

N_1, N_2, P_3, T_5, P_{50}

TABLE 4-12. ENGINE NACELLE ICING TESTS (Cont'd.)

(2) Ejector Evaluation

Testing should be carried out to evaluate ejector performance to ensure that the full range of forward speeds are achievable.

(3) Thermocouple Evaluation

The engine will be run at a condition suitable to compare the measured values of the surface temperatures with the values predicted using a computer flow field analysis.

(4) Water Droplet Checks

The engine will be run at a condition suitable for NRC personnel to carry out water droplet samples for 15μ, 25μ and 40μ median droplet diameter samples.

(5) Droplet Distribution Check

The engine will be run at a condition suitable for NRC personnel to perform a droplet distribution check.

b. Icing Conditions

Carry out the icing runs listed in Table A. The order of testing is not important except that the extended hold and delayed activation tests should be carried out last. Additional testing may be defined after the results of the above test programs have been studied.

(1) Test Procedure

After start-up, the engine should be run at high power for a sufficient time to stabilize the inlet air temperature. Once stabilized, the engine should be adjusted to the desired operating condition and the necessary computations should be performed to provide the required icing environment. In this stabilized condition, with the icing protection on, a set of dry engine/nacelle operating parameters should be recorded. The water spray will then be initiated and maintained for the required duration of the test. During the test, the instrumentation measurements will be recorded periodically until the test is complete. Once complete, the water, ejectors and engine should be shut off in that order. The top half of the transition duct should then be removed so that NRC can photograph the nacelle inlet and generator scoop. After each test, the duct should be thoroughly cleaned of all ice and water, and an extensive inspection should be performed to ensure that there are no foreign objects in the duct.

The required instrumentation measurements will be specified by aerodynamics.

TABLE A. ENGINE NACELLE ICING TEST TEST PROGRAM

Condition	Velocity (KCAS)	Amb. Temp. (°C)	Dd (μm)	LWC (g/m³)	Time (min)	E.I.[a]	N1 (%)	N1 (rpm)
1. ground idle[2]	50[3]	-2	40	0.60	30			
2. take-off	250	-5	25	0.40	5	C.M.	92.0	14,625
3. take-off	250	-20	15	0.30	5	C.M.	89.1	14,170
4. cruise	250	-5	25	0.40	10	C.M.	94.9	15,090
5. cruise	250	-20	15	0.30	10	C.M.	97.2	15,450
6. flight idle	250	-5	25	0.40	10	C.M.		
7. flight idle	250	-20	15	0.30	10	C.M.		
8. hold	147	-5	15	0.70	6x7[5]	C.M.	61.5	9,770
	147	-5	15	2.73	6x1	I.M.	61.5	9,770
9. hold	147	-5	40	0.13	6x7	C.M.	61.5	9,770
	147	-5	40	0.63	6x1	I.M.	61.5	9,770
10. hold	147	-20	15	0.30	6x7	C.M.	59.9	9,525
	147	-20	15	1.95	6x1	I.M.	59.9	9,525
11. hold	147	-20	40	0.06	6x7	C.M.	59.9	9,525
	147	-20	40	0.40	6x1	I.M.	59.9	9,525
12. flight idle[f]	250	-5	25	0.40	10	C.M.		
13. hold	147	-5	15	0.70	45	C.M.	6.5	9,770
14. hold	147	-5	40	0.13	45	C.M.	61.5	9,770
15. hold	147	-20	15 or 40[7]	-	45	C.M.	59.9	9,525

TABLE A. ENGINE NACELLE ICING TEST (Concluded)

NOTES:

a) Environmental Intensity (E.I.) refers to the intensity of the icing condition (per FAR 25, Appendix C)

C.M. - Continuous Maximum
I.M. - Intermittent Maximum

b) The ground idle will be followed by a momentary operation of take-off thrust.

c) The minimum tunnel speed required to uniformly transport 40μ drops.

d) Operate the engine to a fuel flow at 254 lb/hr.

e) Tests 8) - 11) simulate a holding condition in a restricted pattern. There are 6 cycles per test where a cycle includes 7 minutes of continuous maximum icing and 1 minute of intermittent maximum icing.

f) Test 12) is a delayed actuation test in which the nacelle is in an icing environment for 1 minute before the anti-icing system is engaged.

g) In test 15), 15μ or 40μ will be chosen depending on the results of the previous two tests. The most severe case of tests 13) and 14) will be chosen.

Dd	LWC
15μ	0.30 g/m^3
40μ	0.06 g/m^3

TABLE 4-13. ALL WEATHER SYSTEM COMPLIANCE TEST

TEST COND	ALT 1000 FT	KIAS	% N_1	BLEED SYSTEM IN OPERATION	DATA ACQUISITION RATE (POINTS/MIN)	VALUES TO STABILIZE	DATA LOC. REQUIRED	COMMENTS
200	12		Idle	All	12*	T_{91} & T_{176}	25, 34, 90-199 as shown on schematics	Descent thru given altitude from 5000 ft. above. NOTE: A minimum of 6 minutes is required to stabilize temperature values.
201		V_{min}	54					
202		V_{nor}	70					
203		V_{max} Cruise	87					
204	17		Idle	All	12*	T_{91} & T_{176}	25, 34, 90-199 as shown on schematics	Descent thru given altitude from 5000 ft. above.
205		V_{min}	70					
206		V_{nor}	74					
207		V_{max} Cruise	90					
208	22		Idle	All	12*	T_{91} & T_{176}	25, 34, 90-199 as shown on schematics	Descent thru given altitude from 5000 ft. above.
209		V_{min}	74					
210		V_{nor}	78					
211		V_{max} Cruise	93					
212	Field to 40	A/R	Max Pwr	All	12*	-	25, 34, 90-199 as shown on schematic	Determine that wing overheat indication is provided during max. power climb; Record data at 5000 ft. intervals during climb. Monitor - T_{106} and T_{190}.

*If any system cycles, rerun condition recording continuously

TABLE 4-13. ALL WEATHER SYSTEM COMPLIANCE TEST (Cont'd.)

TEST COND	ALT 1000 FT	KIAS	% N_1	BLEED SYSTEM IN OPERATION	DATA ACQUISITION RATE (POINTS/MIN)	VALUES TO STABILIZE	DATA LOC. REQUIRED	COMMENTS
213	Field to 40	A/R	Max Pwr	All	12*	-	25, 34, 90-199 as shown on schematic: a. At 5000 ft. (to check leading edge press.) b. When wing temp. indicator reaches top of green range. c. When T_{106} reaches maximum stable value. d. When T_{190} reaches maximum stable value.	Max Power Climb: This condition same as 212 except for a simulated failure of the wing anti-ice pressure regulating valve. A simulated failed open valve can be duplicated by disconnecting the wing anti-ice duct pressure sensing line and allowing valve to sense tailcone pressure. Ref. FTWO 4658. Monitor - T_{106} and T_{190}.
214	5	180	A/R	Alcohol System	-	-	Visual and/or dye pattern on windshield.	Descent thru altitude from 1000 feet above and record alcohol flo pattern on windshield.
215	3 to Field	V_{appr}	A/R	Alcohol System	-	-	Visual and/or dye pattern on windshield.	Approach speed and altitude; record alcohol flow pattern on windshield.

TABLE 4-13. ALL WEATHER SYSTEM COMPLIANCE TEST (Cont'd.)

TEST COND	ALT 1000 FT	KIAS	% N_1	BLEED SYSTEM IN OPERATION	DATA ACQUISITION RATE (POINTS/MIN)	VALUES TO STABILIZE	DATA LOC. REQUIRED	COMMENTS
216	22 or below	180	A/R	Alcohol System	-	-	Alcohol quantity used per unit time.	Operate alcohol system for minimum of 15 minutes. (Test to determine available alcohol system duration time.) (See Note below.)
217	5	120	A/R	Cabin & Windshield	12	-	25, 34, 90, 91, 176 thru 199	Determine windshield overheat protection in landing configuration. Monitor - T_{183} and T_{190}. Record at T_{190} stabilized (6 min. minimum) or at windshield overheat.
218	45	180	Climb	Cabin & Windshield	12	-	25, 34, 90, 91, 176 thru 199	Determine windshield overheat protection in high altitude, high power condition. Monitor - T_{183} and T_{190}. Record at T_{190} stabilized (6 min. minimum) or at windshield overheat. NOTE: If complete tank capacity is not used for Condition 216, the usable alcohol quantity must be determined.

TABLE 4-13. ALL WEATHER SYSTEM COMPLIANCE TEST (Cont'd.)

TEST COND	ALT 1000 FT	KIAS	% N_1	BLEED SYSTEM IN OPERATION	DATA ACQUISITION RATE (POINTS/MIN)	VALUES TO STABILIZE	DATA LOC. REQUIRED	COMMENTS
219	5 to Field	Noted	A/R	Windshield	-	-	Visual pattern of windshield clear area.	Evaluate windshield rain removal at 1.6 V_{S1} and lower speeds with flaps retracted; also throughout landing approach, landing, taxi and parking during a heavy rain condition. Determine that the windshield external bleed air anti-ice system maintains the minimum required clear area.
220	Field	-	A/R	Windshield	12	T_{176}	Both engine N_1% 25, 175 thru 199 as shown on schematics at N_1% just below engine speed required to illuminate windshield overheat light.	Determine engine speed required to cause windshield overheat light to illuminate. CAUTION: To prevent windshield overheat monitor T_{183} while slowly increasing N_1%.
221	Field	-	A/R	Wing	12	T_{91} & T_{92}	Both engine N_1% 25 34, 90 thru 161 as shown on schematics at: a. At engine speed required to obtain wing temp. corresponding to top of green range on wing temp. indicator.	Determine engine speed required to cause wing overheat light to illuminate. CAUTION: To prevent wing overheat, monitor T_{106} while slowly increasing N_1%.

TABLE 4-13. ALL WEATHER SYSTEM COMPLIANCE TEST (Cont'd.)

TEST COND	ALT 1000 FT	KIAS	% N_1	BLEED SYSTEM IN OPERATION	DATA ACQUISITION RATE (POINTS/MIN)	VALUES TO STABILIZE	DATA LOC. REQUIRED	COMMENTS
221 Cont'd							b. N_1% just below engine speed required to illuminate wing overheat light.	
222	Field to 22	V_{min}	70 min to 75 max	All	12	-	25, 34, 90-199 as shown on schematics Cloud liquid water content (Gm/M^3) Cloud water droplet mean diameter (microns) Record data continuously while in icing condition. Monitor and record icing probe buildup and anti-iced surfaces for clear condition every 5 minutes.	(This test condition may be accomplished when performing the natural icing test per FTR 1677C) Natural Icing Test These data are required for correlation with dry air flight test data and to provide a basis for extrapolation and/or interpolation of data obtained in this test to other conditions within the FAR 25 Appendix C icing condition envelope. Operate the airplane in a natural icing encounter at a flight condition representing a sustained holding pattern to simultaneously evaluate the performance of all anti-ice systems. The test objective will be to remain in an icing condition for 45 minutes or until a 2

TABLE 4-13. ALL WEATHER SYSTEM COMPLIANCE TEST (Concluded)

TEST COND	ALT 1000 FT	KIAS	% N_1	BLEED SYSTEM IN OPERATION	DATA ACQUISITION RATE (POINTS/MIN)	VALUES TO STABILIZE	DATA LOC. REQUIRED	COMMENTS
222 Cont'd								inch to 3 inch ice build-up has accumulated on the ice "probe", whichever occurs first. NOTE: Anti-ice systems must be turned on prior to entering natural icing condition. NOTE: To evaluate the pilot windshield alcohol anti-ice system, turn off the windshield heat and turn on the windshield alcohol anti-ice system during the last 10 minutes of the above test condition. Record clear area maintained on pilot's windshield.

TABLE 4-14. WINDSHIELD AND WING BOOT CERTIFICATION

A test to demonstrate the adequacy of a hot air system for windshield anti-icing and a pneumatic boot system for a wing leading edge is presented.

FAA Required Icing Tests

The parameters for testing are in accordance with FAR 25, Appendix C, tailored specifically as successfully tested on the Model A with FAA concurrence and approval.

1. **GROUND TESTS**

   a. **Windshield**

      (1) Measure Temps Static

      Normal mode for effectiveness
      Failure mode(s) for overheat protection

2. **FLIGHT TESTS**

   a. **Dry Air Tests**

      (1) Boot Operation

*Alt	IAS	Max Boot Pressure (Look at 1 pump at all Alts)	Time to Reach Max Press	Time to Deflate From Max Pressure	OAT
25000 20000 15000 10000 5000	Max Level Holding Cycle During V_{mo} Descent				

      (2) Windshield Temperatures

Alt	IAS	Pressure	Defrost	Data at Each Condition
5,15, 25	Max Lvl, Holding V_{mo} Descent	On Above 10,000 On and Off Below 10	On and f	(OAT) (16 Windshield Temps) (Temp at inlet to windshield gage valve and heat discharge)

      (3) Windshield De-Ice Capability

      A water tank will be installed in the aircraft with a tube extending to the aircraft nose. Water will be sprayed on the windshield until a layer of ice has accreted on the wind-

TABLE 4-14. WINDSHIELD AND WING BOOT CERTIFICATION (Cont'd.)

shield. (Note: Altitude, and hence temperature, will be varied until ice accretion occurs.) The matrix of temperatures will be recorded. The aircraft will then be flown to -22°F and cold soaked. The windshield de-ice will be turned on and the size of the hole cleared and time required will be measured and photographed. The aircraft will then be descended to -12°F and the size of the hole melted, measured and photographed. This procedure repeated at 10°F increments to +28°F. These tests will be repeated at holding and max cruise speed. The tests will be conducted with water spraying on the windshield when possible (until the exterior plumbing freezes). This is a developmental type test and is not intended to produce direct certification data. The data taken will be used for safety of flight substantiation for icing flights and may be used in analysis for certification.

(4) Vertical Tail Shapes

Shapes simulating the "worst case" ice accretion on the vertical tail have been flown with no adverse effects. The results will be included in the final report.

b. Natural Icing Flight Tests

Instrumentation
Liquid Water Content (Johnson Williams)
OAT
Total Accretion Measurement (Striped Extension on strobe shield with 1/2 in" increments)
Altitude
airspeed
Manifold Pressure
RPM
Droplet Size
Exposure Time

All data will be recorded by hand and by tape recorder.

At least two exposures will be completed, i.e., max. continuous and max. intermittent as defined by FAR 25, Appendix C. During each encounter, the liquid water content obtained will be traded for cloud extent by the method shown in Report 12, Figures 11 thru 14. This method was taken from FAR 25, Appendix C, Figures 3 and 6. Compliance with the 45-minute holding requirement of AC 20-73 will be shown by a linear ratio of water content to time as was done with the Model Q (Ref. Report 10, Figure 13).

All testing in icing conditions will be conducted at the recommended loiter power setting of 24 in. Hg 2200 rpm.

TABLE 4-14. WINDSHIELD AND WING BOOT CERTIFICATION (Concluded)

The results of these tests will be reported in the same basic format as the Model Q tests (Report 10).

TABLE 4-15. LARGE TRANSPORT CATEGORY AIRCRAFT ICING CERTIFICATION TEST

TEST NO.	FAR REF	TEST	GROSS WEIGHT	C.G.	AIRSPEED	ALTITUDE	LANDING GEAR	FLAPS SLATS	ENGINE THRUST	DESCRIPTION OF TEST
3.1		Effect of Engine Bleed Air Extraction	OPT	OPT	Static	Field	DN	UP	Grd Idle to -6D 1.0.	The effects of engine bleed air extraction on engine performance will be demonstrated. The aircraft bleed air systems to be operated during these tests include airconditioning, engine anti-ice, and wing anti-ice.
			OPT	OPT	V_2 to .82 IMM	5,000 to 35,000	As Reqd	As Reqd	60% N_1 to -6D MCT	
88.	25. 1093	Engine Inlet Ice Protection	OPT	OPT	Normal Climb Schedule	Climb	UP	UP	As Reqd	Determine the engine inlet ice protection system performance while operating in dry air.
			OPT	OPT	Holding Speed	15,000	UP	UP	As Reqd	
			OPT	OPT	High Spd Descent	Descent	UP	UP	Flt Idle	
			OPT	OPT	Holding Speed	As Reqd	UP	UP	As Reqd	Demonstrate the engine inlet ice protection system while operating in moisture bearing clouds.
			OPT	OPT	Holding Speed	As Reqd	UP	UP	As Reqd	Demonstrate the engine inlet ice protection system while operating in natural atmospheric icing conditions.

TABLE 4-15. LARGE TRANSPORT CATEGORY AIRCRAFT ICING CERTIFICATION TEST (Cont'd.)

TEST NO.	FAR REF	TEST	GROSS WEIGHT	C.G.	AIRSPEED	ALTITUDE	LANDING GEAR	FLAPS SLATS	ENGINE THRUST	DESCRIPTION OF TEST
101.	25. 1419	Ice Protection	OPT	OPT	Normal schedule	Climb	UP	UP	As Reqd	At the noted conditions in dry air, the engine, windshield and wing ice protection shall be operated. The data obtained will be used to show analytically the adequacy of the ice protection systems.
			OPT	OPT	Holding	15,000	UP	UP	As Reqd	
			OPT	OPT	High Spd Descent	Descent	UP	UP	Flt Idle	
			OPT	OPT	Holding	As Reqd	UP	UP	As Reqd	The ice protection systems shall be demonstrated in moisture bearing clouds. If possible a high speed idle descent will be continued from the top of the cloud through the base of the cloud.

TABLE 4-15. LARGE TRANSPORT CATEGORY AIRCRAFT ICING CERTIFICATION TEST (Cont'd.)

TEST NO.	FAR REF	TEST	GROSS WEIGHT	C.G.	AIRSPEED	ALTITUDE	LANDING GEAR	FLAPS SLATS	ENGINE THRUST	DESCRIPTION OF TEST
101. Cont'd			OPT	OPT	Holding	As Reqd	UP	UP	As Reqd	Under natural atmospheric icing conditions the ice protection systems shall be demonstrated to show adequate protection against ice formation on the windshields, engine inlets, wing, APU inlet and air conditioning ram air inlets. Satisfactory operation of the airspeed system will be demonstrated. Ice will be allowed to build up and then the systems will be turned on to show that sufficient heat is available for ice protection. Ice buildup with the system on will be continued to show that the ice does not affect the operation of the aircraft.
102.	25. 1419	Stall Characteristics with Simulated Ice Shapes	OPT	FWD	1.3 V_S Trim	OPT	UP UP DN	UP/RET 25/EXT 50/EXT	IDLE	Demonstrate stall characteristics under noted conditions with simulated ice shapes installed. During the maneuver record the minimum speed obtained.

TABLE 4-15. LARGE TRANSPORT CATEGORY AIRCRAFT ICING CERTIFICATION TEST (Cont'd.)

TEST NO.	FAR REF	TEST	GROSS WEIGHT	C.G.	AIRSPEED	ALTITUDE	LANDING GEAR	FLAPS SLATS	ENGINE THRUST	DESCRIPTION OF TEST
102.1		Static Longitudinal Stability with Simulated Ice Shapes	OPT OPT LIGHT	FWD FWD FWD	1.4 V_S	10,000	UP DN DN	25/EXT 35/EXT 50/EXT	TFLF IDLE IDLE	Demonstrate static longitudinal stability from 1.1 V_S to 1.8 V_S with simulated ice shapes installed. Conduct free returns from end points.
102.2		Minimum Control Speed-Air, With Simulated Ice Shapes	LIGHT	AFT	---	<5,000	UP	25/EXT	NOTED	Demonstrate the V_{mca} with simulated ice shapes installed is below the normal engine inoperative go-around speed.
102.3		Directional Control Sudden Change in Heading with Simulated Ice Shapes	LDG	AFT	1.4 V_S Trim	OPT	UP	25/EXT	TFLF	Demonstrate sudden change in heading up to 15° in either direction with one wing engine inoperative, while holding wings approximately level with simulated ice shapes installed.
102.4		Low Speed Drag Polars with Simulated Ice Shapes (Drag Increment for Approach Configurations)	OPT	FWD	1.2 V_S 1.25 V_S 1.30 V_S 1.35 V_S 1.40 V_S 1.55 V_S	10,000	UP	T.B.D.	Critical wing eng shutdown opposite wing eng takeoff AOI eng TFLF	Conduct stabilized speed thrust runs at noted conditions.

TABLE 4-15. LARGE TRANSPORT CATEGORY AIRCRAFT ICING CERTIFICATION TEST (Concluded)

TEST NO.	FAR REF	TEST	GROSS WEIGHT	C.G.	AIRSPEED	ALTITUDE	LANDING GEAR	FLAPS SLATS	ENGINE THRUST	DESCRIPTION OF TEST
102.5		Low Speed Drag Polars with Simulated Ice Shapes (Drag Increment for Landing Configuration)	OPT	FWD	1.30 V_S	10,000	DN	50/EXT 35/EXT	TFLF	Conduct stabilized speed thrust runs at noted conditions.
106.	25. 1455	Draining of Fluids Subject to Freezing	OPT	OPT	Cruise	Cruise	UP	UP	TFLF	Demonstrate that the waste water drains are properly located to prevent the formation of ice on the airplane.

TABLE 4-16. TEST SCHEDULE - TURBOPROP ICING CERTIFICATION

COND #	DESCRIPTION	TEMP RANGE °C	DROPLET DIA.	L.W.C. g/m³	DURATION Min.	AIR FLOWS lb/sec			BPR #
						ENGINE	OIL COOLER	BYPASS	
3.1	Cruise	-10 to -5	15	.48 1.64	10.5 1.5				
3.2	Cruise	-10 to -5	25	1.0	10				
3.3	Cruise	-10 to -5	15	1.0	14				
3.4	Holding	-10 to -5	15	1.0	48.5				
3.5	Holding	-10 to -5	25	1.0	30				
3.6	G.I. Fog	-10 to -5	40	1.2	15				
3.7	Climb	-10 to -5	15	.55 2.50	2x10 2x3				
3.8	Delayed actuation descent	-10 to -5	15	3.0	3				
3.9	Delayed actuation descent	-10 to -5	25	3.0	3				

NOTE: A test with snow will not be carried out. Previous icing tests have consistently demonstrated the insignificance of this test.

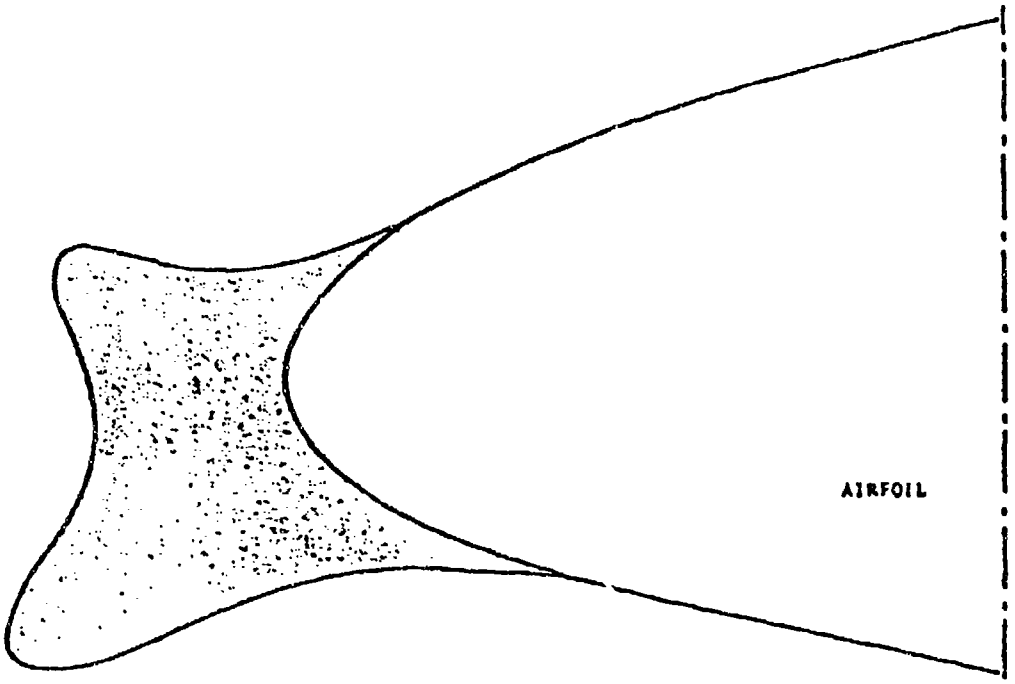

FIGURE 4-1. ICE SHAPE CROSS SECTION - INBOARD WING

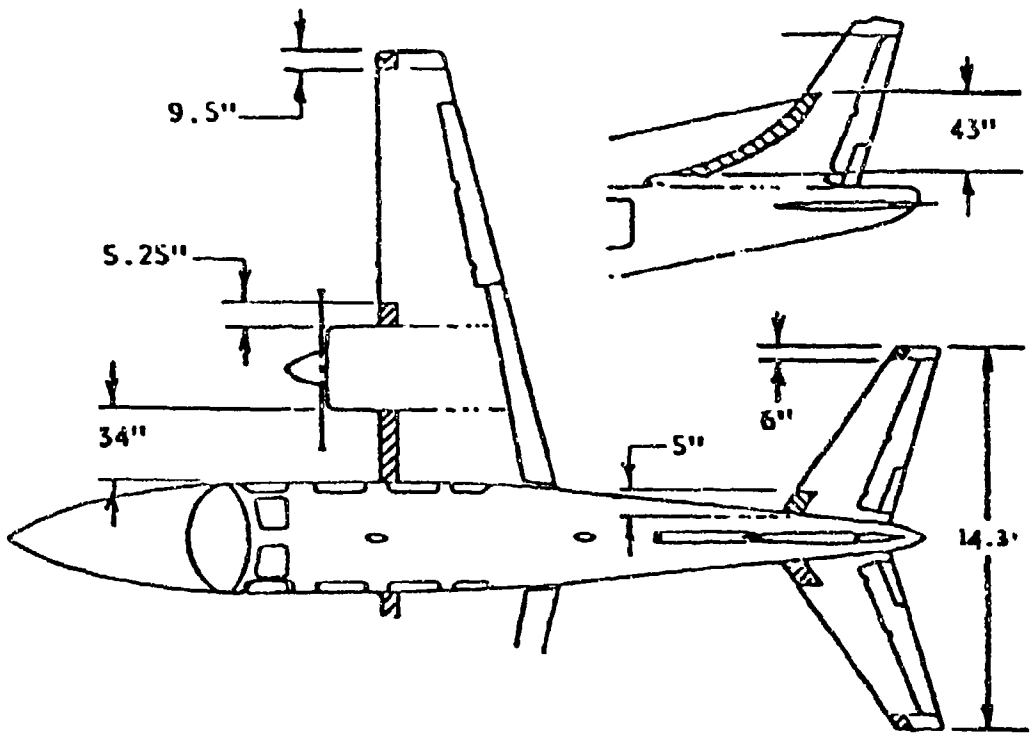

FIGURE 4-2. ICE SHAPE INSTALLATION FOR INITIAL HANDLING TESTS

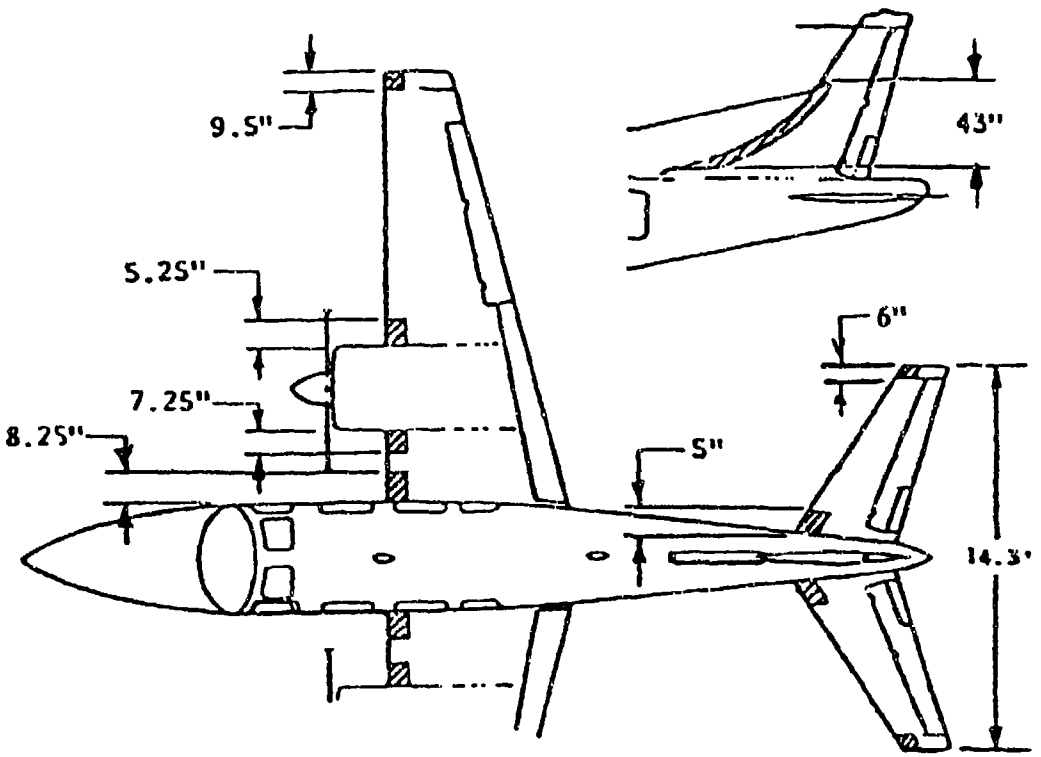

FIGURE 4-3. ICE SHAPE INSTALLATION FOR FAA HANDLING TESTS

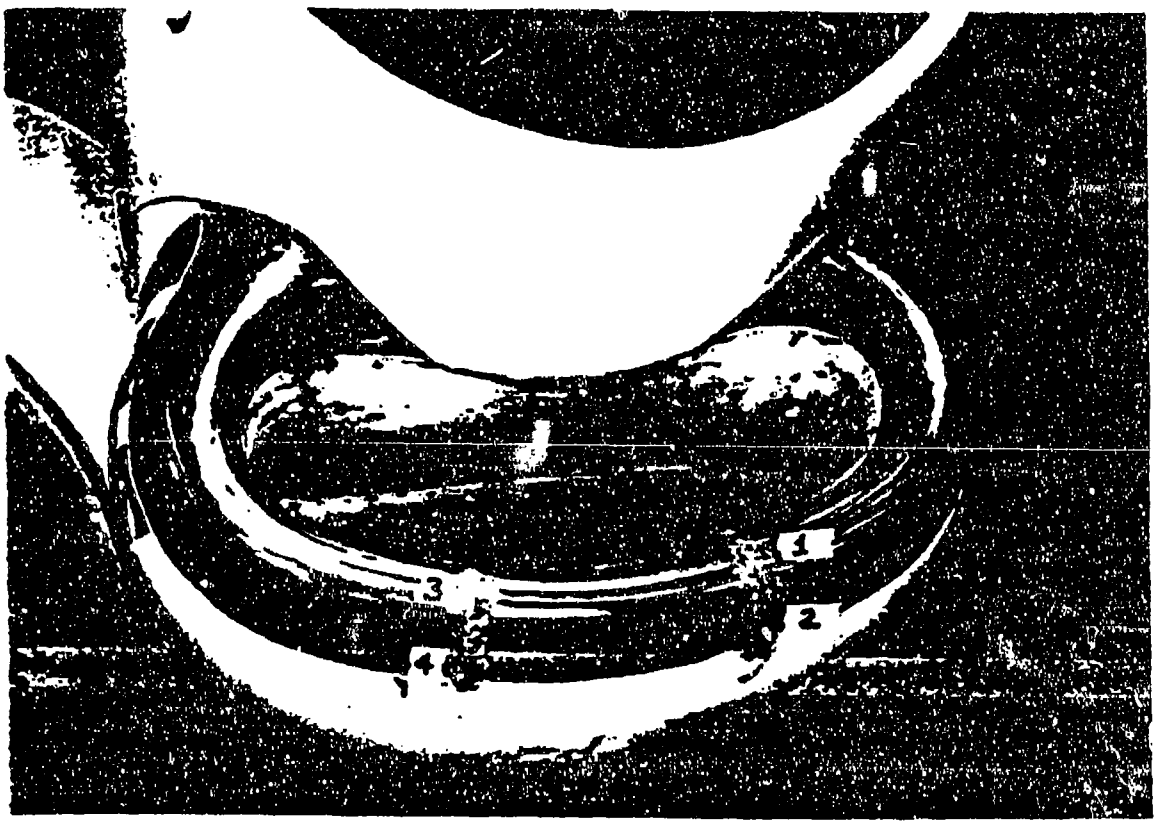

FIGURE 4-4. NATURAL DRY AIR TEST OF ENGINE INDUCTION SYSTEM